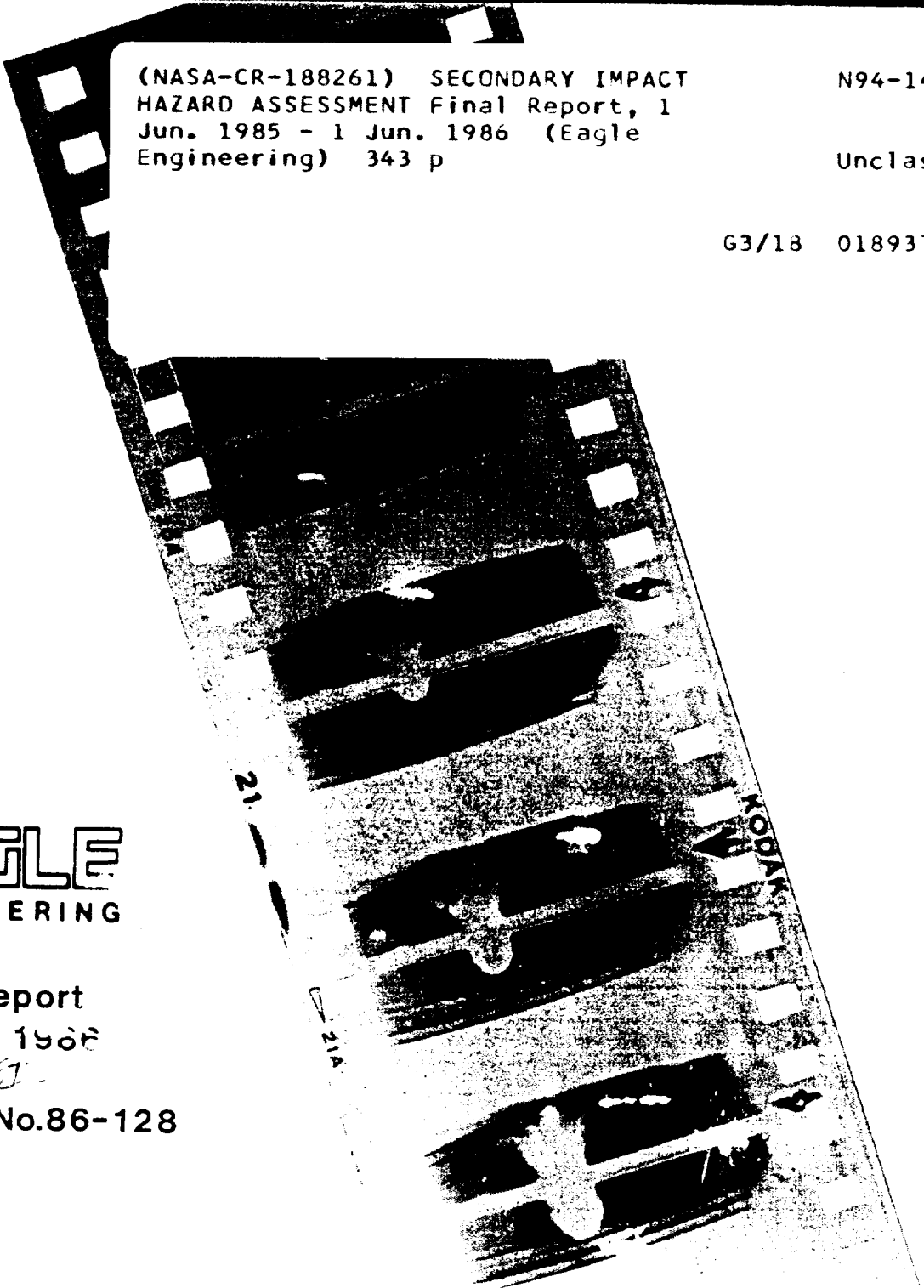


# Secondary Impact Hazard Assessment

5113



(NASA-CR-188261) SECONDARY IMPACT  
HAZARD ASSESSMENT Final Report, 1  
Jun. 1985 - 1 Jun. 1986 (Eagle  
Engineering) 343 p

N94-14483

Unclas

G3/18 0189374

**EAGLE**  
ENGINEERING

Final Report  
June 1, 1986

*EEJ*

Report No.86-128



**Secondary Impact Hazard Assessment**  
**Final Report**  
**Prepared for the Solar System Exploration**  
**Division of the Johnson Space Center by**  
**Eagle Engineering**  
**Houston, Texas**

**Eagle Report No. 86-128**  
**NASA Purchase Order No. T-256M**  
**June 1, 1986**





## Table of Contents

	Page
1.0 Executive Summary-----	1
2.0 Introduction-----	3
3.0 Graphite/Epoxy Targets-----	6
3.1 Semi-Infinite (thick) Targets - Ejecta and Spall Collected-----	10
3.1.1 Discussion of Test Setup-----	10
3.1.2 Shot #883 (1/2 " thick, cloth on front)-	11
3.1.3 Shot #884 (1/2 " thick, no cloth on front)-----	25
3.2 Thin Graphite/Epoxy Targets - Ejecta and Spall Collected-----	38
3.2.1 Discussion of Test Setup-----	38
3.2.2 Shot #894 (0.093" thick, no cloth)-----	38
3.2.3 Shot #917 (0.127" thick, with cloth)----	48
3.2.4 Shot #923 (0.095" thick, no cloth, 30 deg. oblique impact)-----	73
3.3 Thin Graphite/Epoxy Targets - Projectile Density Effects-----	100
3.4 Thin Graphite/Epoxy Targets - Hi Speed Film Data--	102
3.4.1 Shot #972-----	104
3.4.2 Shot #981-----	104
3.4.3 Shot #990-----	104
3.4.4 Discussion of Calculated/Measured Velocity Comparison-----	104
4.0 Aluminum Targets-----	117
4.1 Shot #933 - Ejecta and Spall Collected-----	117



**Table of Contents (Continued)**

	<b>Page</b>
4.2 Shot #975 - High Speed Film Data Shot-----	144
4.3 Shots #979,991, and 992 - Additional Data-----	144
5.0 Derived Relationships from Graphite/Epoxy and Aluminum Impact Data-----	150
5.1 Total Ejecta/Spall Mass Scaled with Projectile Energy-----	150
5.1.1 Graphite/Epoxy Targets-----	152
5.1.2 Aluminum Targets-----	157
5.2 No. of Ejecta/Spall Particles of a Given Mass and Above vs. Total Ejecta/Spall Mass-----	159
5.2.1 Graphite/Epoxy Targets-----	159
5.2.2 Aluminum Targets-----	165
5.3 No. of Ejecta/Spall Particles of a Given Energy and Above-----	165
5.3.1 Graphite/Epoxy Targets-----	167
5.3.2 Aluminum Targets-----	167
5.4 Ejecta/Spall Particle Velocity and Mass-----	180
6.0 Estimate of Damage Potential to the Space Station-----	182
6.1 Damage From Primary Impacts - Meteoroids and Orbital Debris-----	182
6.1.1 Meteoroid Model-----	183
6.1.2 Orbital Debris Model-----	183
6.1.3 Space Station Area Model and Probability of Impact-----	184
6.2 Damage From Secondary Impacts - Ejecta and Spall--	184
6.2.1 Damage Assessment Worksheet-----	185
6.2.2 Model Assumptions and Approximations----	196



## Table of Contents (Continued)

	Page	
6.2.3	Graphs of Results at Various Critical Energies-----	198
6.3	Application of Model to Cases of Interest-----	204
6.3.1	Module Window-----	206
6.3.1.1	Critical Energy Calculation---	206
6.3.1.2	Discussion-----	206
6.3.2	Orbiter Window with Orbiter Docked to Space Station-----	216
6.3.2.1	Critical Energy Calculation---	216
6.3.2.2	Discussion-----	217
6.3.3	Habitat Module-----	225
6.3.3.1	Critical Energy Calculation---	225
6.3.3.2	Discussion-----	225
6.3.4	Solar Panels-----	231
6.3.4.1	Critical Energy Calculation---	231
6.3.4.2	Discussion-----	231
7.0	Conclusions-----	239
8.0	Recommendations-----	239
9.0	References-----	240
Appendix A	- Listing of Shot Data-----	A-1
Appendix B	- Raw Data from Shots with Particle Catchers-----	B-1
Appendix C	- Single Frame Photography Data-----	C-1



## List of Figures

	Page
Figure 3-1, Photos of Target-----	13
Figure 3-2, Ejecta Mass vs. Particle Length (Shot #883)-----	14
Figure 3-3, Ejecta Mass vs. Particle Diameter (Shot #883)---	15
Figure 3-4, Ejecta Particle Mass vs. Theta (Shot #883)-----	16
Figure 3-5, Ejecta Calc. Particle Vel. vs. Theta (Shot #883)	17
Figure 3-6, Ejecta Part. Mass vs. Phi (Shot #883)-----	18
Figure 3-7, Ejecta Part. Velocity vs. Phi (Shot #883)-----	19
Figure 3-8, Ejecta Particle Mass vs. Cone Angle (Shot #883)-	20
Figure 3-9, Ejecta Part. Velocity vs. Cone Angle (Shot #883)	21
Figure 3-10, Ejecta Part. Vel. vs. Part. Mass (Shot #883)---	22
Figure 3-11, Log(No. of part. mass $m_i$ & $>$ ) vs. Log( $m_i/m_{total}$ ) (Shot #883)-----	23
Figure 3-12, Log(No. of part. mass $m_i$ & $>$ ) vs. Log( $m_i/m_{total}$ ) (Shot #883) with Equation Derivation-----	24
Figure 3-13, Photos of Target-----	26
Figure 3-14, Ejecta Mass vs. Particle Length (Shot #884)-----	27
Figure 3-15, Ejecta Mass vs. Particle Diameter (Shot #884)--	28
Figure 3-16, Ejecta Particle Mass vs. Theta (Shot #884)-----	29
Figure 3-17, Ejecta Calc. Particle Vel. vs. Theta (Shot #884)-----	30
Figure 3-18, Ejecta Part. Mass vs. Phi (Shot #884)-----	31
Figure 3-19, Ejecta Part. Velocity vs. Phi (Shot #884)-----	32
Figure 3-20, Ejecta Particle Mass vs. Cone Angle (Shot #884)	33
Figure 3-21, Ejecta Part. Velocity vs. Cone Angle (Shot #884)-----	34
Figure 3-22, Ejecta Part. Velocity vs. Part. Mass (Shot #884)-----	35
Figure 3-23, Log(No. of part. mass $m_i$ & $>$ ) vs. Log( $m_i/m_{total}$ ) (Shot #884) with Equation Derivation-----	36
Figure 3-24, Log(No. of part. mass $m_i$ & $>$ ) vs. Log( $m_i/m_{total}$ ) (Shot #884) with Aluminum Equation Also-----	37
Figure 3-25, Photos of Catcher Box (Shot #894)-----	40
Figure 3-26, Ejecta/Spall Mass vs. Part. Length (Shot #894)-	42
Figure 3-27, Ejecta/Spall Mass vs. Part. Dia. (Shot #894)---	43
Figure 3-28, Log(No. of ejecta part. mass $M_i$ & $>$ ) vs. Log( $M_i/M_{total}$ ejecta) (Shot #894) with Equation Derivation-----	44
Figure 3-29, Log(No. of spall part. mass $M_i$ & $>$ ) vs. Log( $M_i/M_{total}$ spall) (Shot #894) with Equation Derivation-----	45
Figure 3-30, Log(No. of spall &/or ejecta part. mass $M_i$ & $>$ ) vs. Log( $M_i/M_{total}$ spall &/or ejecta) (Shot #894)-----	46
Figure 3-31, Log(No. of spall & ejecta part. mass $M_i$ & $>$ ) vs. Log( $M_i/M_{total}$ spall & ejecta) (Shot #894) with Equation Der. & Aluminum Equation-----	47
Figure 3-32, Photos of Target (Shot #917)-----	50
Figure 3-33, Ejecta Mass vs. Particle Length (Shot #917)----	51
Figure 3-34, Ejecta Mass vs. Particle Diameter (Shot #917)--	52
Figure 3-35, Ejecta Particle Mass vs. Theta (Shot #917)-----	53





**List of Figures (Continued)**

	Page
Figure 3-36, Ejecta Calc. Particle Vel. vs. Theta (Shot #917)-----	54
Figure 3-37, Ejecta Part. Mass vs. Phi (Shot #917)-----	55
Figure 3-38, Ejecta Part. Velocity vs. Phi (Shot #917)-----	56
Figure 3-39, Ejecta Particle Mass vs. Cone Angle (Shot #917)-	57
Figure 3-40, Ejecta Part. Velocity vs. Cone Angle (Shot #917)-----	58
Figure 3-41, Ejecta Part. Velocity vs. Part. Mass (Shot #917)-----	59
Figure 3-42, Log(No. of ejecta part. mass $M_i$ & $>$ ) vs. Log( $M_i/M_{total}$ ejecta) (Shot #917) with Equa. Derivation-----	60
Figure 3-43, Spall Mass vs. Particle Length (Shot #917)-----	61
Figure 3-44, Spall Mass vs. Particle Diameter (Shot #917)---	62
Figure 3-45, Spall Particle Mass vs. Theta (Shot #917)-----	63
Figure 3-46, Spall Calc. Particle Vel. vs. Theta (Shot #884)-----	64
Figure 3-47, Spall Part. Mass vs. Phi (Shot #917)-----	65
Figure 3-48, Spall Part. Velocity vs. Phi (Shot #917)-----	66
Figure 3-49, Spall Particle Mass vs. Cone Angle (Shot #917)-	67
Figure 3-50, Spall Part. Velocity vs. Cone Angle (Shot #917)-----	68
Figure 3-51, Spall Part. Velocity vs. Part. Mass (Shot #917)-----	69
Figure 3-52, Log(No. of spall part. mass $M_i$ & $>$ ) vs. Log( $M_i/M_{total}$ spall), (Shot #917) with Equation Derivation-----	70
Figure 3-53, Log(No. of spall &/or ejecta part. mass $M_i$ & $>$ ) vs. Log( $M_i/M_{total}$ spall &/or ejecta) (Shot #917) equa. only-----	71
Figure 3-54, Log(No. of spall & ejecta part. mass $M_i$ & $>$ ) vs. Log( $M_i/M_{total}$ spall & ejecta) (Shot #917) with Alum. Equa.-----	72
Figure 3-55, Photos of Catcher Box (Shot #923)-----	75
Figure 3-56, Photos of Target (Shot #923)-----	77
Figure 3-57, Ejecta Mass vs. Particle Length (Shot #923)----	78
Figure 3-58, Ejecta Mass vs. Particle Diameter (Shot #923)--	79
Figure 3-59, Ejecta Particle Mass vs. Theta (Shot #923)-----	80
Figure 3-60, Ejecta Calc. Particle Vel. vs. Theta (Shot #923)-----	81
Figure 3-61, Ejecta Part. Mass vs. Phi (Shot #923)-----	82
Figure 3-62, Ejecta Part. Velocity vs. Phi (Shot #923)-----	83
Figure 3-63, Ejecta Particle Mass vs. Cone Angle (Shot #923)	84
Figure 3-64, Ejecta Part. Velocity vs. Cone Angle (Shot #923)-----	85
Figure 3-65, Ejecta Part. Vel. vs. Part. Mass (Shot #923)---	86
Figure 3-66, Log(No. of ejecta part. mass $M_i$ & $>$ ) vs. Log( $M_i/M_{total}$ ejecta) (Shot #923) with Equa. Derivation	87
Figure 3-67, Spall Mass vs. Particle Length (Shot #923)-----	88



**List of Figures (Continued)**

	<b>Page</b>
Figure 3-68, Spall Mass vs. Particle Diameter (Shot #923)---	89
Figure 3-69, Spall Particle Mass vs. Theta (Shot #923)-----	90
Figure 3-70, Spall Calc. Particle Vel. vs. Theta (Shot #923)-----	91
Figure 3-71, Spall Part. Mass vs. Phi (Shot #923)-----	92
Figure 3-72, Spall Part. Velocity vs. Phi (Shot #923)-----	93
Figure 3-73, Spall Particle Mass vs. Cone Angle (Shot #923)-	94
Figure 3-74, Spall Part. Vel. vs. Cone Angle (Shot #923)----	95
Figure 3-75, Spall Part. Velocity vs. Part. Mass (Shot #923)-----	96
Figure 3-76, Log(No. of spall part. mass $M_i$ & $>$ ) vs. Log( $M_i/M_{total}$ spall), (Shot #923) with Equation Derivation-----	97
Figure 3-77, Log(No. of spall &/or ejecta part. mass $M_i$ & $>$ ) vs. Log( $M_i/M_{total}$ spall &/or ejecta) (Shot #923) equa. only-----	98
Figure 3-78, Log(No. of spall & ejecta part. mass $M_i$ & $>$ ) vs. Log( $M_i/M_{total}$ spall & ejecta) (Shot #923) with Alum. Equa.-----	99
Figure 3-79, High Speed Film, Shot #972-----	105
Figure 3-80, High Speed Film, Shot #981-----	107
Figure 3-81, Shot #981 Spall Velocity (from Univ. of Texas)-	111
Figure 3-82, High Speed Film, Shot #990-----	113
Figure 3-83, Ejecta Velocity Comparison, Film-Estimation, Shots #884, 972, and #981-----	115
Figure 3-84, Spall Velocity Comparison, Film-Estimation, Shots #917, 972, and 981-----	116
Figure 4-1, Photos of Target (Shot #933)-----	119
Figure 4-2, Ejecta Mass vs. Particle Length (Shot #933)-----	120
Figure 4-3, Ejecta Mass vs. Particle Diameter (Shot #933)---	121
Figure 4-4, Ejecta Particle Mass vs. Theta (Shot #933)-----	122
Figure 4-5, Ejecta Calc. Particle Vel. vs. Theta (Shot #933)-	123
Figure 4-6, Ejecta Part. Mass vs. Phi (Shot #933)-----	124
Figure 4-7, Ejecta Part. Velocity vs. Phi (Shot #933)-----	125
Figure 4-8, Ejecta Particle Mass vs. Cone Angle (Shot #933)-	126
Figure 4-9, Ejecta Part. Velocity vs. Cone Angle (Shot #933)-----	127
Figure 4-10, Ejecta Part. Velocity vs. Part. Mass (Shot #933)-----	128
Figure 4-11, Log(No. of ejecta part. mass $m$ & $>$ ) vs. Log( $m_{ejecta}/m_{total}$ ejecta) (Shot #933) with Equa. Der.	129
Figure 4-12, Spall Mass vs. Particle Length (Shot #933)-----	130
Figure 4-13, Spall Mass vs. Particle Diameter (Shot #933)---	131
Figure 4-14, Spall Particle Mass vs. Theta (Shot #933)-----	132
Figure 4-15, Spall Calc. Particle Vel. vs. Theta (Shot #933)-----	133
Figure 4-16, Spall Part. Mass vs. Phi (Shot #933)-----	134
Figure 4-17, Spall Part. Velocity vs. Phi (Shot #933)-----	135



## List of Figures (Continued)

	Page
Figure 4-18, Spall Particle Mass vs. Cone Angle (Shot #933)-	136
Figure 4-19, Spall Part. Velocity vs. Cone Angle (Shot #933)-----	137
Figure 4-20, Spall Part. Velocity vs. Part. Mass (Shot #933)-----	138
Figure 4-21, Log(No. of spall part. mass $M_i$ & $>$ ) vs. Log( $M_i/M_{total}$ spall), (Shot #933) with Equation Derivation-----	139
Figure 4-22, Ejecta and Spall Mass vs. Length (Shot #933)---	140
Figure 4-23, Ejecta and Spall Dia. vs. Length (Shot #933)---	141
Figure 4-24, Log(No. of spall &/or ejecta part. mass $M_i$ & $>$ ) vs. Log( $M_i/M_{total}$ spall &/or ejecta) (Shot #933) equa. only-----	142
Figure 4-25, Log(No. of spall & ejecta part. mass $M_i$ & $>$ ) vs. Log( $M_i/M_{total}$ spall & ejecta) (Shot #933) with Ref. 2 Alum. Equa.-----	143
Figure 4-26, High Speed Camera Photos, Shot #975-----	145
Figure 4-27, Measured vs. Cal. Alum. Ejecta Mass and Vel.---	148
Figure 4-28, Measured vs. Cal. Aluminum Spall Mass and Vel.-	149
Figure 5-1, Ejecta and Spall Total Mass vs. Proj. Energy----	151
Figure 5-2, Graphite/Epoxy Ejecta and Spall Total Mass Scaling Curve-----	154
Figure 5-3, Projectile Density Effect-----	155
Figure 5-4, Projectile Shape Effect-----	156
Figure 5-5, Alum. Ejecta and Spall Total Mass Scaling Curve-	158
Figure 5-6, G/E Ejecta Particle Mass Distribution-----	161
Figure 5-7, G/E Spall Particle Mass Distribution-----	162
Figure 5-8, G/E Combined Ejecta and Spall Particle Mass Distribution-----	163
Figure 5-9, G/E With and Without Cloth Particle Mass Distribution-----	164
Figure 5-10, G/E and Aluminum Particle Mass Distribution----	166
Figure 5-11, G/E Combined Ejecta and Spall Particle Energy Distribution-----	168
Figure 5-12, G/E With Cloth Particle Energy Distribution----	169
Figure 5-13, G/E Without Cloth Particle Energy Distribution-	170
Figure 5-14, G/E Ejecta Particle Energy Distribution-----	171
Figure 5-15, G/E Spall Particle Energy Distribution-----	172
Figure 5-16, G/E With and Without Cloth Particle Energy Distribution-----	173
Figure 5-17, G/E Ejecta and Spall Particle Energy Dist.----	174
Figure 5-18, Aluminum Combined Ejecta and Spall Particle Energy Distribution-----	175
Figure 5-19, Aluminum Ejecta Particle Energy Distribution---	176
Figure 5-20, Aluminum Spall Particle Energy Distribution----	177
Figure 5-21, Aluminum Ejecta and Spall Particle Energy Distribution-----	178



## List of Figures (Continued)

	Page
Figure 5-22, Graphite/Epoxy and Aluminum Particle Energy Distribution-----	179
Figure 5-23, Graphite/Epoxy Particle Mass and Velocity-----	181
Figure 6-1, 1990's Average Meteoroid and Orbital Debris Environment-----	187
Figure 6-2, Primary/Secondary Particle Fluxes for Example---	195
Figure 6-3, Primary/Secondary Particle Fluxes with 10 Joule Critical Energy-----	199
Figure 6-4, Primary/Secondary Particle Fluxes with 100 Joule Critical Energy-----	200
Figure 6-5, Primary/Secondary Particle Fluxes with 1000 Joule Critical Energy-----	201
Figure 6-6, Primary/Secondary Particle Fluxes with 10,000 Joule Critical Energy-----	202
Figure 6-7, Primary/Secondary Particle Fluxes for a 5% Secondaries Impact Fraction-----	233
Figure 6-8, International Space Station Configuration-----	204
Figure 6-9, Cupola Window Workstation Concept-----	213
Figure 6-10, Cupola Window Configuration-----	214
Figure 6-11, Primary/Secondary Particle Fluxes for Space Station Window-----	215
Figure 6-12, Orbiter Docked with Space Station-----	218
Figure 6-13, Primary/Secondary Particle Fluxes for Orbiter Window-----	224
Figure 6-14, Primary/Secondary Particle Fluxes for Habitat Module Wall-----	230
Figure 6-15, Primary/Secondary Particle Fluxes for Solar Array-----	238





## List of Tables

	Page
Table 3-1, Graphite/Epoxy Test Specimens Ordered-----	7
Table 3-2, Semi-Infinite and Thin Graphite/Epoxy Shots, Spall and Ejecta Collected-----	9
Table 3-3, Thin Graphite/Epoxy Targets, Projectile Density Effects-----	101
Table 3-4, Velocity Measurement Worksheet, Shot #972-----	103
Table 3-5, Velocity Measurement Worksheet, Shot #981-----	106
Table 3-6, Velocity Measurement Worksheet, Shot #990-----	112
Table 3-7, Velocity Measurement Worksheet, Shot #990-----	114
Table 4-1, Velocity Measurement Worksheet, Shot #975-----	146
Table 6-1, Space Station Surface Area and Impact Probability Calculations-----	188
Table 6-2, Damage Assessment Worksheet Example-----	191
Table 6-3, Space Station Window Critical Energy Calculation-	208
Table 6-4, Space Station Window Damage Assessment Worksheet-	209
Table 6-5, Orbiter Window Critical Energy Calculation-----	219
Table 6-6, Orbiter Window Damage Assessment Worksheet-----	220
Table 6-7, Habitat Module Wall Damage Assessment Worksheet--	226
Table 6-8, Solar Cell Critical Energy Calculation-----	233
Table 6-9, Solar Array Damage Assessment Worksheet-----	234



## **Foreword**

This study was conducted between June 1, 1985 and June 1, 1986 for the Solar System Exploration Division of the Johnson Space Center. The purpose of this study was to make a preliminary assessment of the danger of damage to the Space Station caused by secondary particles (ejecta and spall) from meteoroid and orbital debris impact. A second purpose was to characterize the nature of spall and ejecta from hypervelocity impacts on graphite/epoxy composites.

Ms. Jeanne L. Crews was the NASA technical monitor. Mr. Tommy Thompson (Lockheed) and Mr. Kenny Oser (Lockheed) performed the data shots with the Johnson Space Center Light Gas Gun. Mr. Earl Brownfield (Lockheed) provided photographic support. Valuable advise and other data were provided by Mr. Burton G. Cour-Palais (NASA JSC) and Dr. Ching Yew (Univ. of Texas).

Mr. Bill Stump was the Eagle Project Manager. Mr. Eric Christiansen performed the major part of the Eagle contribution. Mr. Norman Smith, an Eagle Co-op, also assisted.



## 1.0 Executive Summary

A series of light gas gun shots (4 to 7 km/sec) were performed with 5 mg nylon and aluminum projectiles to determine the size, mass, velocity, and spatial distribution of spall and ejecta from a number of graphite/epoxy targets. Similar determinations were also performed on a few aluminum targets. Target thickness and material were chosen to be representative of proposed Space Station structure.

The data from these shots and other information were used to predict the hazard to Space Station elements from secondary particles resulting from impacts of micrometeoroids and orbital debris on the Space Station. This hazard was quantified as an additional flux over and above the primary micrometeoroid and orbital debris flux that must be considered in the design process. In order to simplify the calculations, eject and spall mass were assumed to scale directly with the energy of the projectile. Other scaling systems may be closer to reality.

The secondary particles considered are only those particles that may impact other structure immediately after the primary impact. The addition to the orbital debris problem from these primary impacts was not addressed. Data from this study should be fed into the orbital debris model to see if Space Station secondaries make a significant contribution to orbital debris.

The hazard to a Space Station element from secondary particles above and beyond the micrometeoroid and orbital debris hazard is categorized in terms of two factors: 1) The "view factor" of the element to other Space Station structure or the geometry of placement of the element, and 2) The sensitivity to damage, stated in terms of energy.

Several example cases were chosen, the Space Station module windows, windows of a Shuttle docked to the Space Station, the habitat module walls, and the photovoltaic solar cell arrays. For the examples chosen the secondary flux contributed no more than 10 percent to the total flux (primary and secondary) above a given calculated critical energy. A key assumption in these calculations is that above a certain critical energy, significant damage will be done. This is not true for all structures. Double-walled, bumpered structures are an example for which damage may be reduced as energy goes up. The critical energy assumption is probably conservative, however, in terms of secondary damage.

To understand why the secondary impacts seem to, in general, contribute less than 10 percent of the flux above a given critical energy, consider the case of a meteoroid impact of a given energy on a fixed, large surface. This impact results in a variety of secondary particles, all of which have much less energy than the original impact. Conservation of energy prohibits any other

situation. Thus if damage is linked to a critical energy of a particle, the primary flux will always deliver particles of much greater energy. Even if all the secondary particles impacted other Space Station structure, none would have a kinetic energy more than a fraction of the primary impact energy.

## 2.0 Introduction

This study was a low cost "quick look" with three basic purposes: 1) to assess, in a preliminary manner, the hazards from secondary spall and ejecta from meteoroid and orbital debris impact on the Space Station, 2) to begin to characterize the nature of graphite/epoxy spall and ejecta resulting from hypervelocity impact, and 3) to compare graphite/epoxy and aluminum spall and ejecta in terms of damage potential. In a more basic sense, this study was to search out directions for future work in this area.

In this report, spall is defined as the material that comes off of the back side of an impacted target. Ejecta is defined as the material that comes off of the front side.

The characterization of aluminum and graphite/epoxy spall and ejecta was limited to the following parameters resulting from a single impact:

- a) numbers of particles
- b) size distribution of particles
- c) mass distribution of particles
- d) velocity distribution of particles
- e) energy distribution of particles
- f) angular distribution or angle of dispersion of ejecta/spall particles

These ejecta/spall parameters vary with the following projectile and target parameters. This variation was studied and empirical relationships were developed in some cases.

- a) target types - aluminum (6061-T6) and graphite/epoxy (different layups, with and without cloth, thick and thin)
- b) projectile energy
- c) projectile density
- d) oblique and normal impacts

There are other variables and relationships that could (and perhaps should) be studied also. Equipment and funding limitations on this study required that the number of variables and relationships studied be kept small. The above variables were therefore chosen as the most important.

Orbital debris and micrometeoroids are significant hazards to the Space Station and must be taken into account in its design. Meteoroid or orbital debris impacts have been shown to break off 10 to 100 times their own mass from the target material. Some of this ejected and spalled secondary mass will be traveling at hypervelocity. This study was initiated based on these facts. By themselves, these facts indicate that designers may have to protect against these secondary impacts as well as primary orbital debris and meteoroids. Other factors also play a part however. The

three most important are: 1) the number, velocity, and size of hypervelocity particles generated at an impact, 2) the fraction of these particles that may impact other sensitive Space Station structure, and 3) the sensitivity of Space Station structure to damage from these particles. This study attempts to determine or otherwise quantify these variables.

The dual keel Space Station is predicted to have three major structural components in terms of surface area: the graphite/epoxy truss structure, the modules, and the solar power system. Table 6-1 shows how these break down in terms of area for one design. OTV hangars may also have significant area on a growth Space Station.

The modules will probably have aluminum meteor and orbital debris shields protecting their inner hulls. The bumper material has not been selected as of this date, however, and graphite/epoxy or other non-metallic materials are also in the running. The truss structure will be graphite/epoxy with some type of coating (not selected at present - it may be an aluminum foil). The solar arrays will likely be solar cell material (very thin - 14 mils for cover glass and cell according to one estimate) on a thin flexible substrate or perhaps thicker (1 cm) aluminum honeycomb structure. Solar dynamic reflectors will probably be aluminum. The Space Station configuration and materials are still in the design process at this time, but, as far as impacts are concerned, the two major materials will be aluminum and/or graphite/epoxy.

The first major effort in this study was therefore to acquire data on the spall and ejecta characteristics of graphite/epoxy and aluminum material. Hypervelocity impacts on aluminum have been studied for many years and a number of good references exist (Ref. 1 - 2). More attention has been paid to the spall than to the ejecta however, but some aluminum ejecta data was available in the literature (Ref. 1). Only a few actual aluminum shots were therefore performed as a part of this effort (see section 4.0). On the other hand, no one (to our knowledge) has previously studied the spall and ejecta characteristics of graphite/epoxy, so considerable experimental work was required. Section 3.0 documents the experimental work performed on graphite/epoxy as a part of this effort.

Given experimental data in hand, scaling equations were derived that can be used in an overall prediction of hazards to the Space Station. Section 5.0 describes this work.

Section 6.0 describes the assessment of damage to Space Station elements based on the equations generated in section 5.0. Section 7.0 and 8.0 contain conclusions and recommendations.



Appendix A contains a complete listing of all shots of interest to this study (ordered by shot number) and data associated with them. Appendix B contains the raw data from shots for which particle counts were made. Appendix C contains some single frame photos of graphite/epoxy targets shortly after impact.

### 3.0 Graphite/Epoxy Targets

Table 3-1 lists the graphite/epoxy targets that were ordered from Hercules as a part of this testing effort. The reader should refer to Table 3-1 for a detailed description of the size and properties of the targets used. Some of the targets were used in other test programs and their shots will be documented elsewhere.

The graphite/epoxy shots are divided into four categories: shots into semi-infinite targets (section 3.1) with no camera data, but with ejecta mass collected; shots into thin targets (section 3.2) with no camera data, but with ejecta and spall mass collected; additional shots into thin targets used to determine projectile density effects (section 3.3); and shots for which high speed film data was available (section 3.4).

Table 3-2 summarizes the section 3.1 and 3.2 shots. An aluminum shot (see section 4.0) is also included at the bottom of Table 3-2. Table 3-2 includes all the shots for which ejecta and spall particles were collected, counted, and weighed. Numbers of interest in Table 3-2 include:

- a. the ratio of spall and ejecta mass to projectile mass (average around 35)
- b. average cone angle or angle between the spall or ejecta velocity vectors and a normal to the target surface coming out of the impact point
- c. average calculated particulate velocity (see Appendix B for how this velocity was calculated)
- d. fraction of the secondary mass that was spall or percent spall
- e. fraction of the secondary mass that was dust or percent dust. This is the difference between the total spall and ejecta mass (determined by before and after weighing of the target) and the sum of the masses of particles collected from catcher material and in the chamber. The percent dust represents that fraction of the total secondary mass that disappeared, vaporized, or was crushed to dust too small to recover ( $\ll 0.0001$  gms particles). The percent dust also represents larger particles that may have been lost in handling, and so could probably be arbitrarily reduced 5 or 10 percent

Summary tables with similar information for section 3.3 and 3.4 data are contained at the start of each of those sections.

Table 3-1, Test Specimens Ordered

S/N	MATERIAL	LAY UP	WEIGHT (GM)	THICKNESS (IN)	JSC SHOT #
JSC-01A-001			512.6	.528	900
-002	AS4/3501-6	CLOTH, {0,	513.0	.528	899
-003		+45,-45,90,	508.2	.520	883
-004		90,-45,+45,	504.0	.515	
-005		0}12,CLOTH	508.6	.524	901
-006			508.9	.524	
-007	Al93PW/3501-6		511.7	.528	
-008	CLOTH		508.9	.524	
-009			513.4	.530	
-010			509.8	.525	
JSC-01B-001			502.0	.518	
-002		CLOTH, {0,	503.7	.518	884
-003	AS4/3501-6	+45,-45,90,	503.8	.519	
-004		90,-45,+45,	505.0	.519	
-005		0}12	503.1	.517	
-006	Al93PW/3501-6		502.1	.516	
-007	CLOTH		503.5	.518	
-008			505.7	.520	
-009			502.4	.516	
-010			502.6	.517	
JSC-02A-001			96.4	.105	988
-002		CLOTH, {+45,	101.7	.113	990
-003	AS4/3501-6	-45,0,0,+45,	99.9	.111	
-004	Al93PW/3501-6	-45,0,90}5,	99.7	.111	
-005	CLOTH	CLOTH	97.5	.107	
JSC-02B-001			86.4	.095	889
-002		{+45,-45,0,	85.9	.094	893
-003	AS4/3501-6	0,+45,-45,	85.9	.093	894
-004		0,90}5	86.2	.095	981
-005			86.4	.095	923
JSC-03A-001			114.0	.125	911
-002	AS4/3501-6	CLOTH,0,0,	113.0	.124	909
-003		0,0,0,0,0,	114.3	.127	917
-004	Al93PW/3501-6	+45,-45,90,	116.1	.129	
-005	CLOTH	-45,+45,0,	115.8	.127	
		0,0,0,0,			
		0,0,CLOTH			
JSC-03B-001	AS4/3501-6	0,0,0,0,0,	103.3	.115	895
-002		0,0,+45,-45,	101.3	.112	890
		90,-45,+45,			
		0,0,0,0,0,			
		0,0			
JSC-04A-001	120VOLAN/3501-6	[CLOTH, { [0,	151.7	.157	*
-002	CLOTH	+60,-60]IM6	148.9	.153	
	IM6/3501-6	[-60,+60,			
	S-2/3501-6	0]S2}2]5			
	HYBRID				

Table 3-1, Continued

S/N	MATERIAL	LAY UP	WEIGHT (GM)	THICKNESS (IN)	JSC SHOT #
JSC-05A-001	S-2/3501-6	{CLOTH,0,-60,	113.1	.104	913
-002	120VOLAN/3501-6 CLOTH	+60,0,0,+60, -60,-60,+60, 0}5	113.4	.106	*
JSC-06A-001	IM6/8551	CLOTH,{0,+60,	174.0	.194	910
-002	Al93PW/3501-6 CLOTH	-60}5}4,CLOTH	171.3	.191	912

IM6 - GRAPHITE  
 120VOLAN - GLASS CLOTH  
 S-2 - GLASS  
 AS-4 - GRAPHITE  
 3501-6 - STANDARD RESIN  
 Al93PW - GRAPHITE CLOTH  
 8551 - TOUGHENED RESIN

\*CUT INTO FOUR PIECES

Table 3-2, Shots for Which Particulate Counts Were Made

Data from JSC Light Gas Gun Shots

Projectile vs. Ejecta/Spall Mass Summary

JSC Shot #	Target Description	Projectile Type	Projectile Velocity (ft/sec)	Proj. Mass (mg)	Impact Angle (deg)	Secondary Particle Type	Sec. Mass (g)	(Gamma) Ratio of secondary mass to Projectile Mass	(H) -- # of particles of mass M & greater $M = K \cdot (H / M \text{ Total}) \cdot n$	Average Cone Angle (degrees)	Calc. Part. Velocity (ft/sec)	Percent Spall	Dust Part. Mass (g)	Percent Dust	
883	Graphite/Epoxy Cloth	Nylon	6.42	4.93	0	Ejecta	0.11	22.31	0.0206	-1.143	50.17	0.39	0	0.07391	67.2
884	Graphite/Epoxy No Cloth	Nylon	6.26	4.76	0	Ejecta	0.195	40.97	0.1075	-0.954	57.14	0.84	0	0.06845	35.1
894	Graphite/Epoxy Thin, No Cloth (similar to 889,893,923)	Nylon	4.75	4.94	0	Ejecta Spall Total	0.04803 0.08197 0.13	9.72 16.59 26.32	0.0780 0.0266 0.0192	-1.127 -1.280 -1.325	-	-	63.1	0.02445	18.8
917	Graphite/Epoxy Thin, Cloth (similar to 909,911)	Nylon	5.99	4.86	0	Ejecta Spall Total	0.075164 0.174836 0.25	15.47 35.97 51.44	0.0194 0.0014 0.0038	-1.294 -1.676 -1.502	34.66 41.09	0.269 0.334	69.9	0.093782	37.5
923	Graphite/Epoxy Thin, No Cloth (similar to 889,893,894)	Nylon	7.02	5.80	30	Ejecta Spall Total	0.09407 0.15593 0.25	16.22 26.88 43.10	0.0909 0.2133 0.1499	-1.015 -0.920 -0.965	47.05 49.90	0.266 0.432	62.4	0.057064	22.8
933 A)	Al 6061-T6 Thin	Nylon	6.3	4.98	0	Ejecta Spall Total	0.03457 0.08543 0.12	6.94 17.15 24.10	0.0081 0.8191 0.0873	-1.332 -0.527 -0.997	37.13 18.00	4.33 4.134	71.2	0.0589	49.1

### 3.1 Semi-Infinite (thick) Targets - Ejecta and Spall Collected

When this study was initiated, the high speed camera was not available and the techniques later developed were untried. In addition, other restrictions existed on testing. For these reasons, a number of thick targets which would not be penetrated and produced only ejecta were ordered for testing. The mass of ejecta was easily and reliably determined by weighing the target before and after the shot. This ejected mass was then compared with the mass of material collected in a catcher box attached to the front of the target.

The data from these shots was used in developing the relationship for number of graphite/epoxy ejecta particles with a given energy and greater. The data was not used in the relationship giving total ejecta/spall mass as a function of projectile energy because only ejecta was produced in these tests, resulting in less total particle mass for a given projectile energy than with thin targets which were penetrated.

#### 3.1.1 Discussion of Test Setup

A small styrofoam box was placed on the front of the target, with a hole cut in the center of the end to let the projectile enter. When the target was impacted, much of the ejecta stuck in the styrofoam. The individual ejecta particles were extracted from styrofoam and their location (x,y,z), mass, length, and depth of penetration measured. Mass measurements were accurate to 0.0001 g except where groups of very small particles were counted and weighed together to get an average mass. Distance measurements were accurate to 1 mm. The location (x,y,z coordinates) of the projectile impact was also recorded.

This data allowed an accurate estimate of the total ejected mass, an approximate determination of the particle size distribution and velocity vector direction, and a crude estimate of the velocity of each particle based on the penetration distance into the styrofoam. When the high speed camera was acquired later in the testing this velocity approximation was checked and found to be reasonably accurate for the graphite/epoxy tests (see section 3.4.4). It was somewhat less accurate for the aluminum shots (see section 4.4), though only one aluminum high speed camera shot was available to check against it.

### 3.1.2 Shot #883 ( 1/2" thick, cloth on front)

This target (JSC-01A-003) had a layer of Hercules Al93PW cloth on both front and back sides. The cloth layer on the back was to help prevent spall. The cloth layer on the front reduced the amount of ejecta when compared to the next shot.

Table 3-2 summarizes the basic parameters of this shot. A nylon projectile of roughly 5 mg going 6.42 km/sec impacted a 1/2 inch thick graphite/epoxy (G/E) target in a vacuum chamber (with a vacuum of 200 microns of mercury. The Johnson Space Center (JSC) light gas gun was used. A styrofoam box fixed to the front of the target was used to collect the individual pieces of ejecta.

Following the shot, each piece of ejecta was removed from the styrofoam, weighed, and its location noted. The raw data from this considerable effort is given in appendix B. The difference between the before and after weights and the total mass collected from the styrofoam was assumed to represent vapor or dust. For this shot it was 67.2 percent of the total mass. Some of this may be due to loss of large particles through the projectile entry hole and in handling with this first attempt at particle collection.

Figure 3-1 shows the target front and back after the shot. Compare this with Figure 3-13, a no-cloth shot. The cloth reduces the amount of large ejecta.

Figures 3-2 and 3-3 plot ejecta mass versus length and diameter. Most of the mass of recovered composite ejecta is in the form of long thin slivers of material. The diameters plotted are actually an average calculated value. The length and mass of the slivers were measured, and given the density and assuming a cylindrical particle, an average diameter was calculated.

Figures 3-4 through 3-7 plot ejecta mass and velocity versus theta and phi (see appendix A for a definition of theta and phi).

Figures 3-8 and 3-9 plot ejecta mass and velocity versus cone angle. The cone angle is the angle between a normal to the target face at the impact point and the ejecta particle's velocity vector. The mass distribution (in Figure 3-8) seems to center around a cone angle of 50 to 60 degrees. The velocity distribution does also, but not as clearly.

Figure 3-10 plots mass versus velocity and illustrates that, in general, only small particles travel at high velocities.

Figure 3-11 shows a small scale plot of the Log(number of particles of mass  $M_i$  and larger) versus the Log( $M_i/M_{total}$  ejecta mass). Figure 3-12 shows a least squares fit linear relationship

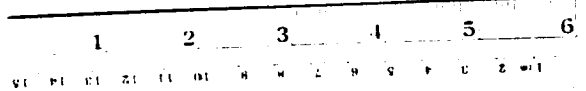
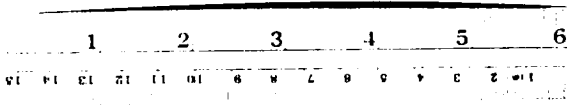
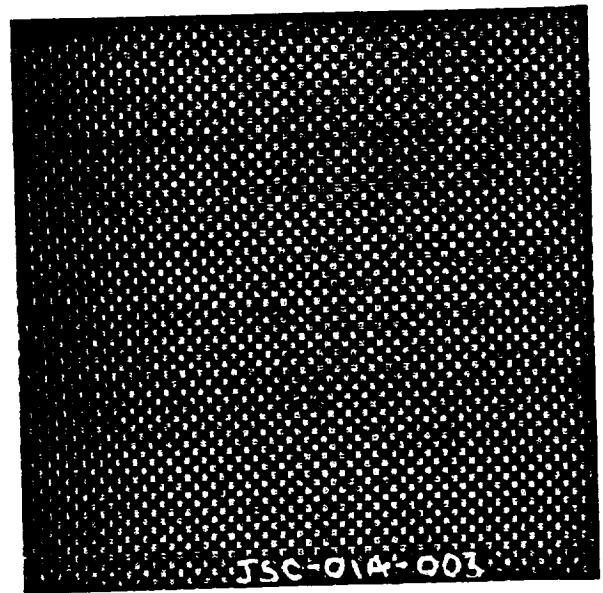
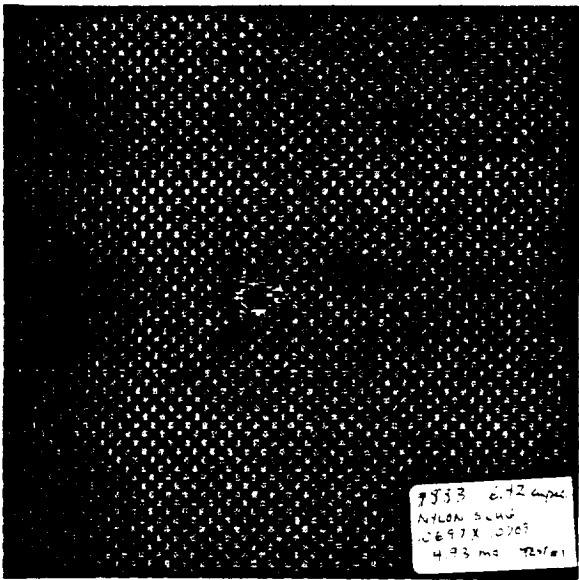
for these two quantities and the derived equation (without the Logs) that results. A similar equation for aluminum taken from reference 1 is also plotted.



Figure 3-1, Photos of Target (Shot #883)  
JSC 01A-003, 1/2 inch thick, graphite/epoxy

Front

Back



ORIGINAL PAGE IS  
OF POOR QUALITY

Figure 3-2

# EJECTA MASS & LENGTH

JSC Shot No. 883 - Cloth

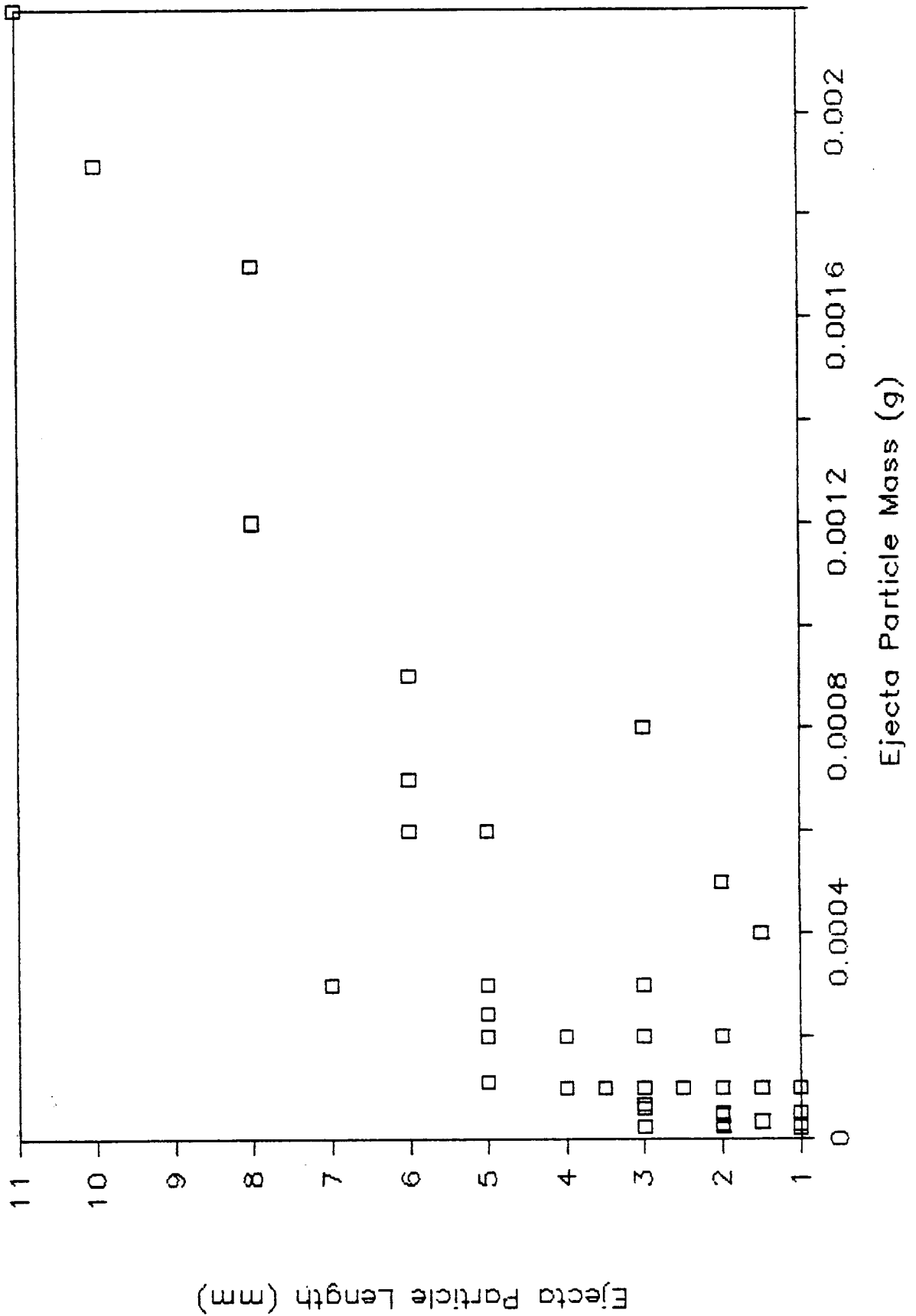


Figure 3-3

# EJECTA MASS & DIAMETER

JSC Shot No. 883 - Cloth

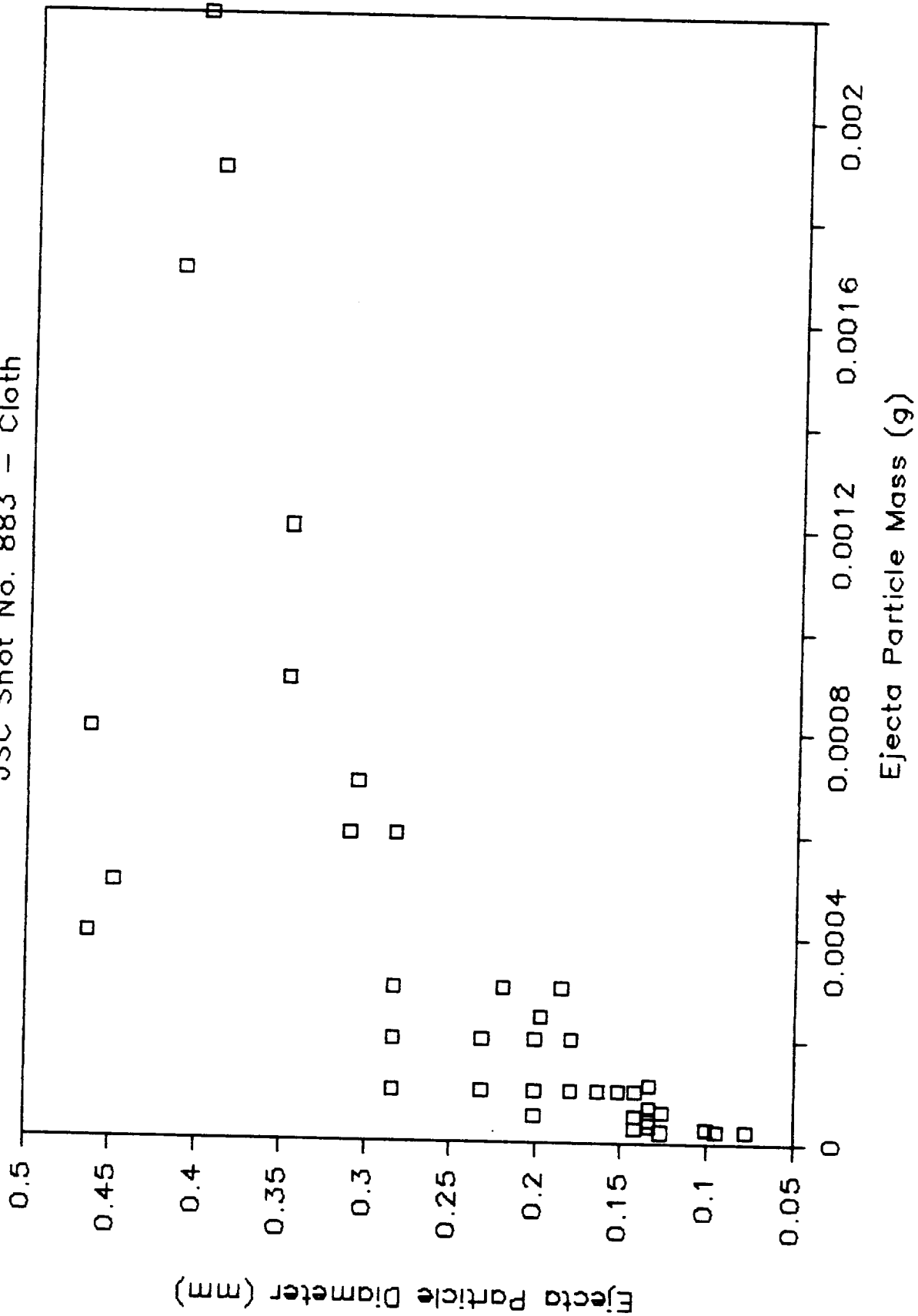


Figure 3-4

# EJECTA MASS DISTRIBUTION

JSC Shot No. 883 - Cloth

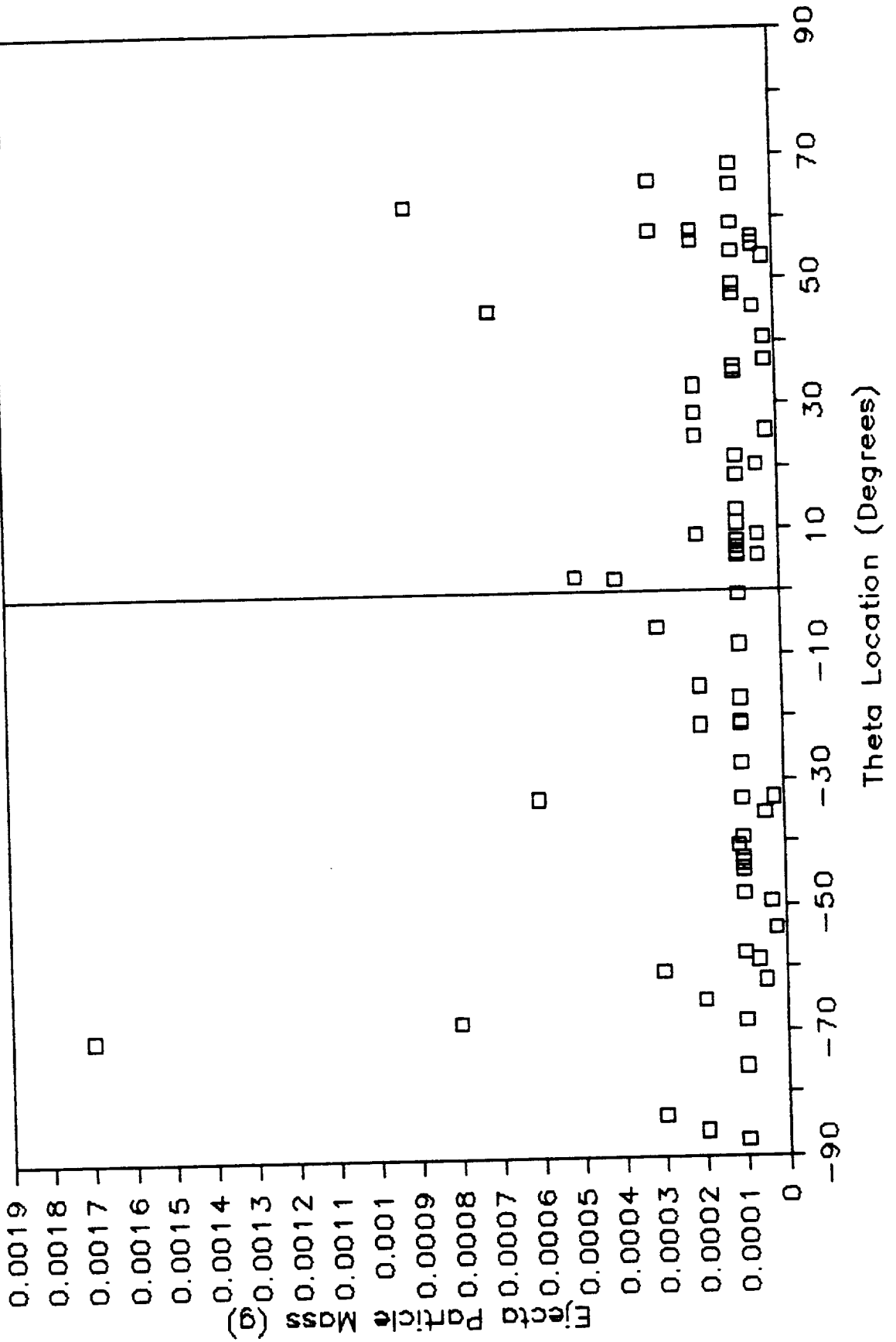


Figure 3-5

# EJECTA VELOCITY DISTRIBUTION

JSC Shot No. 883 - Cloth

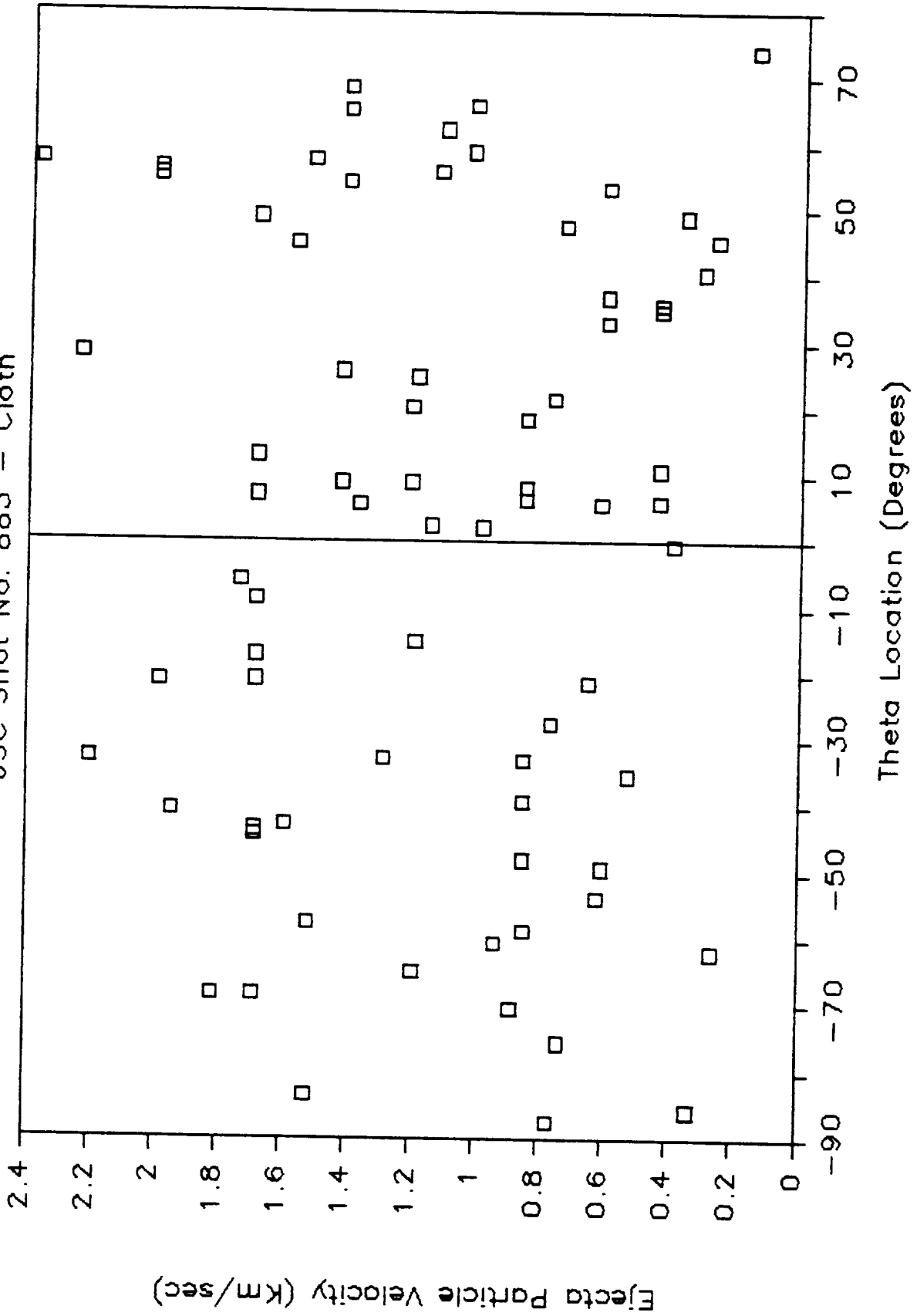


Figure 3-6

# EJECTA MASS DISTRIBUTION

JSC Shot No. 883 - Cloth

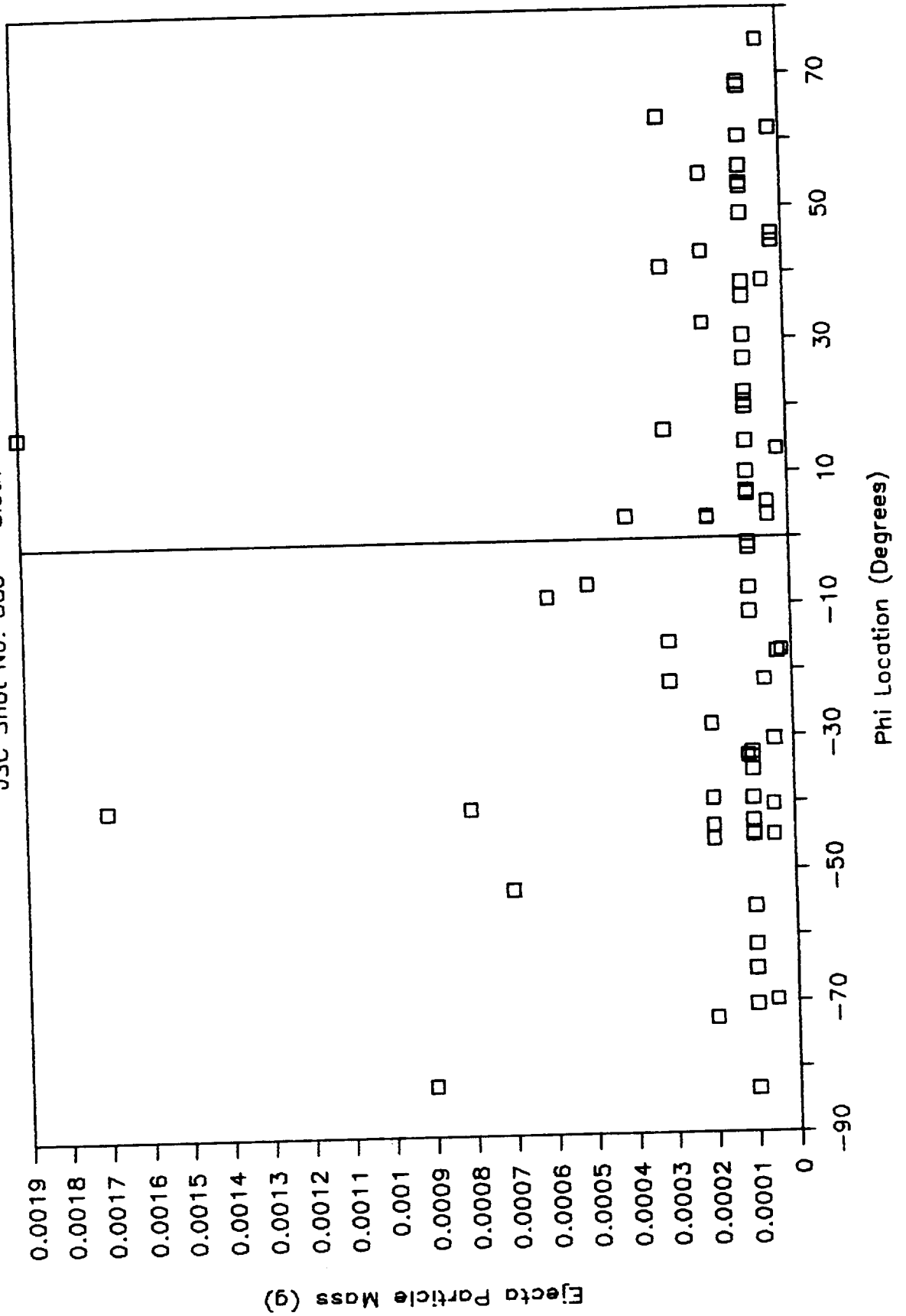


Figure 3-7

# EJECTA VELOCITY DISTRIBUTION

JSC Shot No. 883 - Cloth

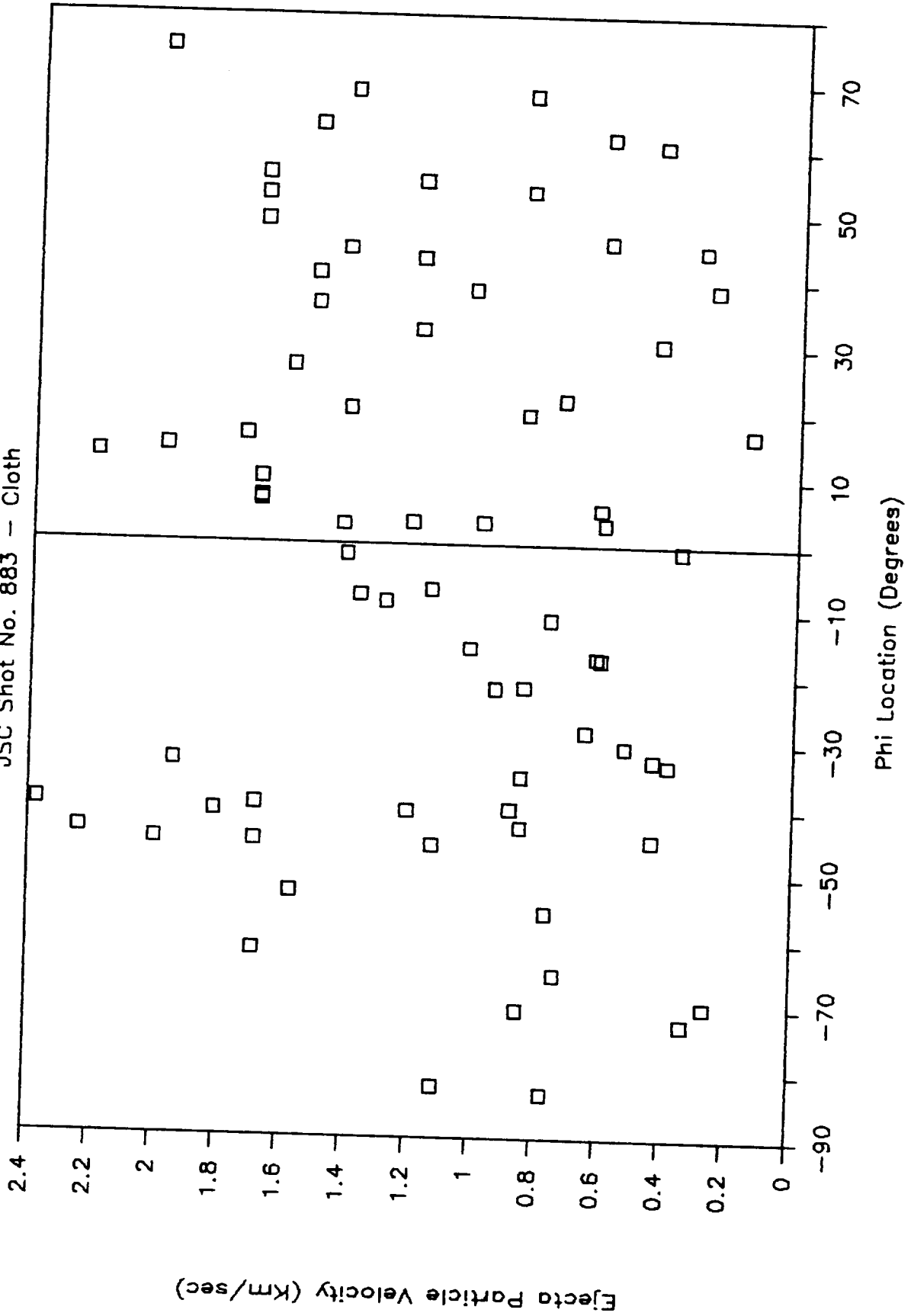


Figure 3-8

# EJECTA MASS DISTRIBUTION

JSC Shot No. 883 - Cloth

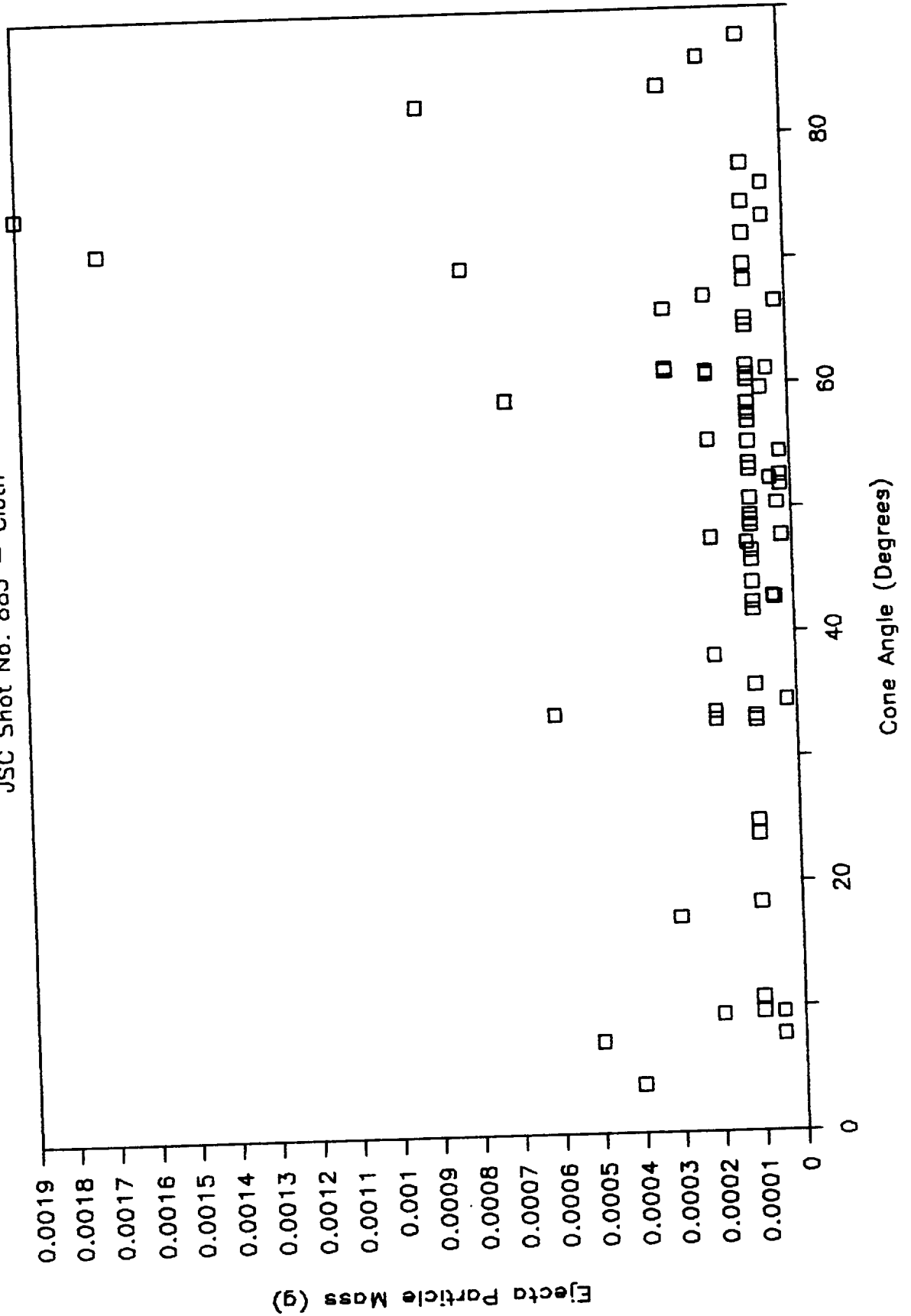




Figure 3-9

# EJECTA VELOCITY DISTRIBUTION

JSC Shot No. 883 - Cloth

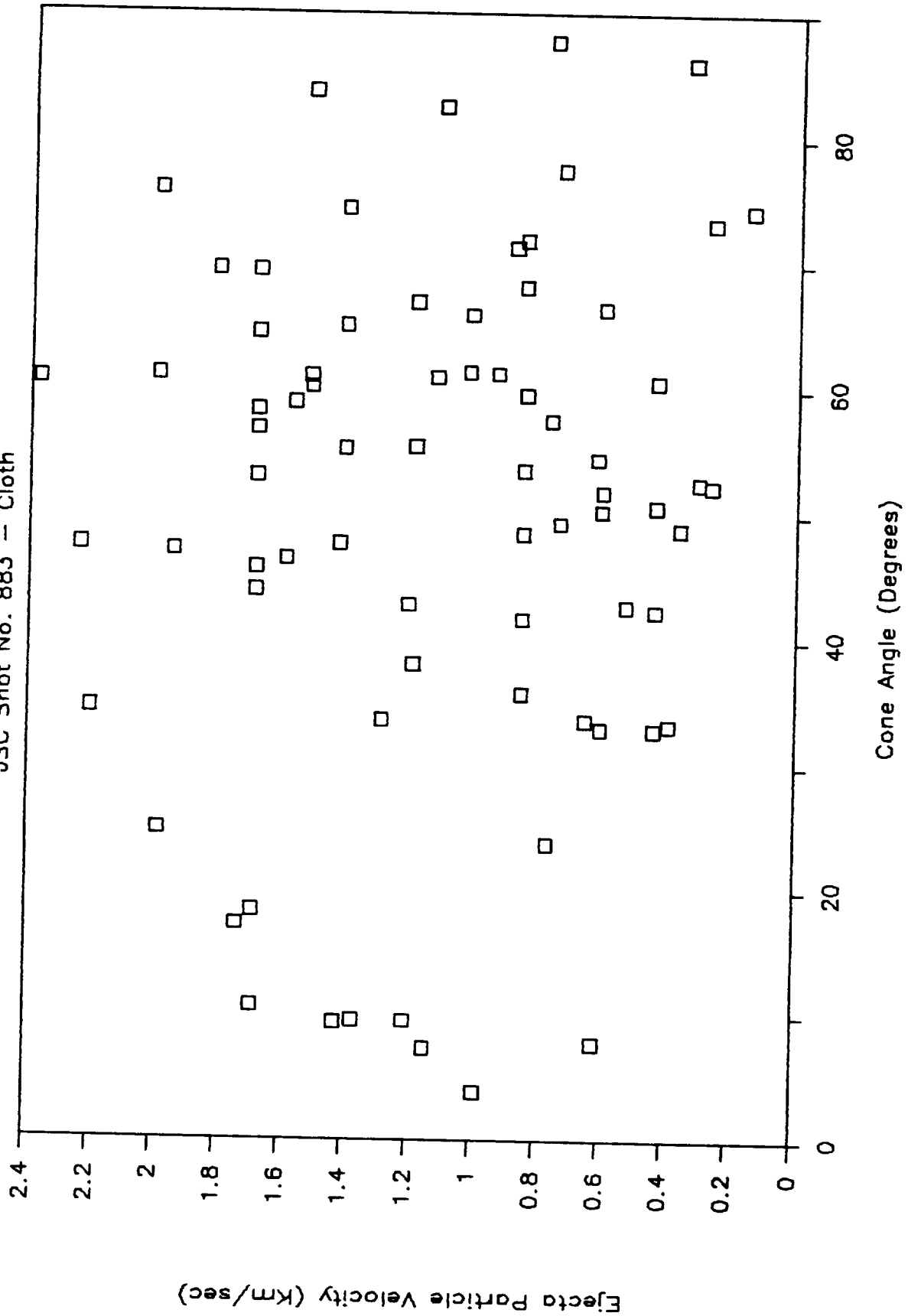


Figure 3-10

# EJECTA MASS & VELOCITY

JSC Shot No. 883 - Cloth

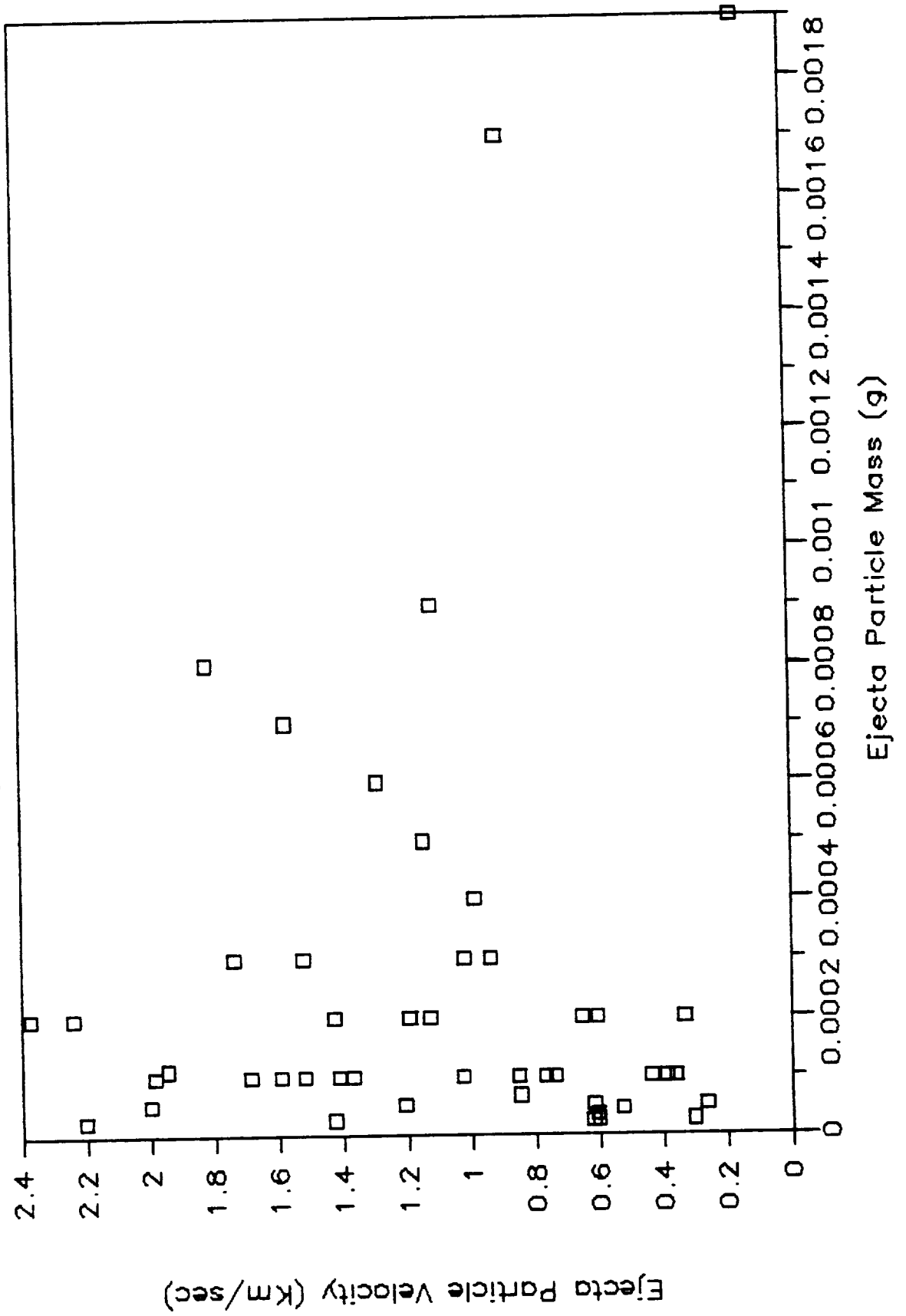


Figure 3-11

# EJECTA MASS AND PARTICLE NUMBER

JSC Shot No. 883 - Cloth

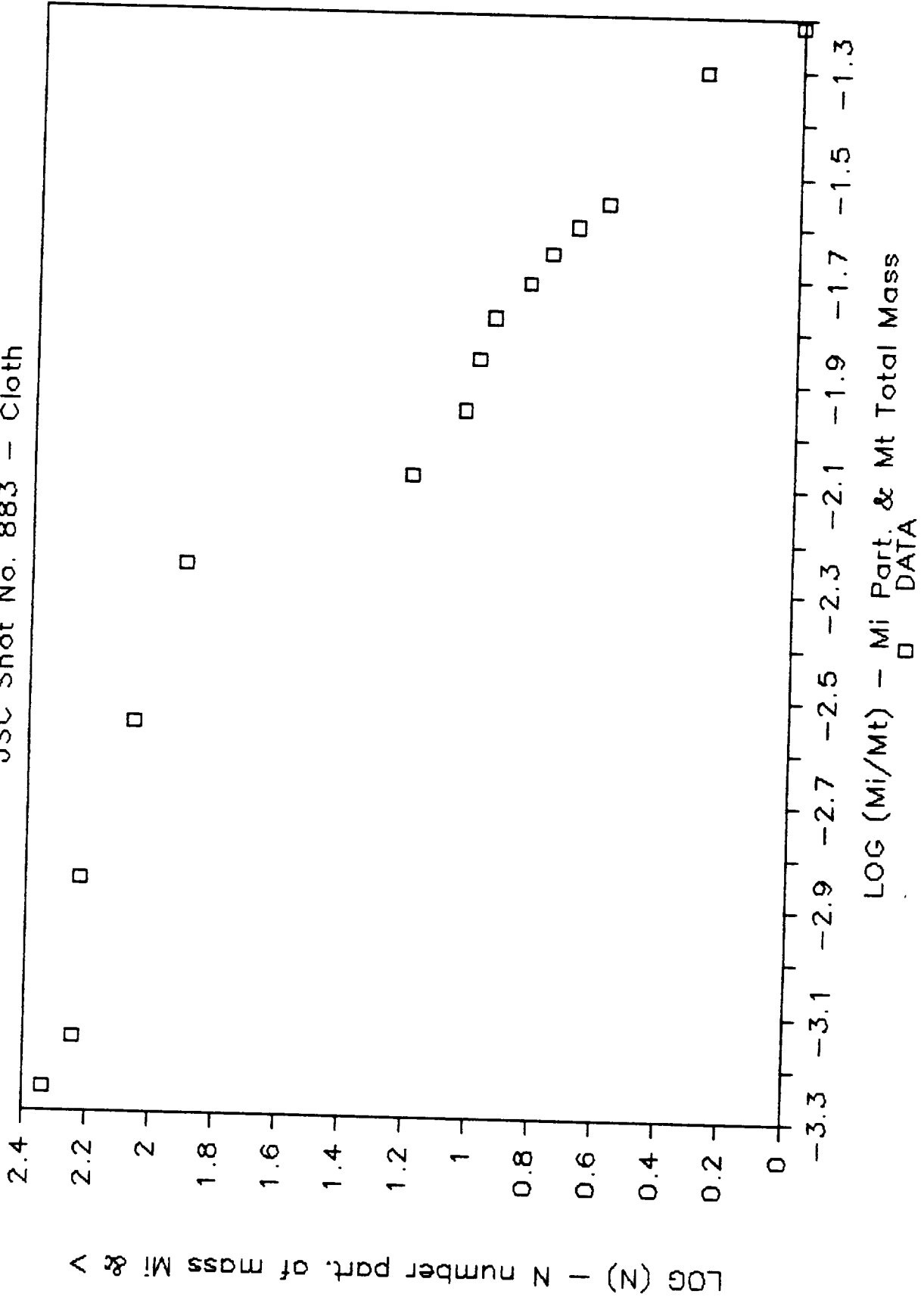
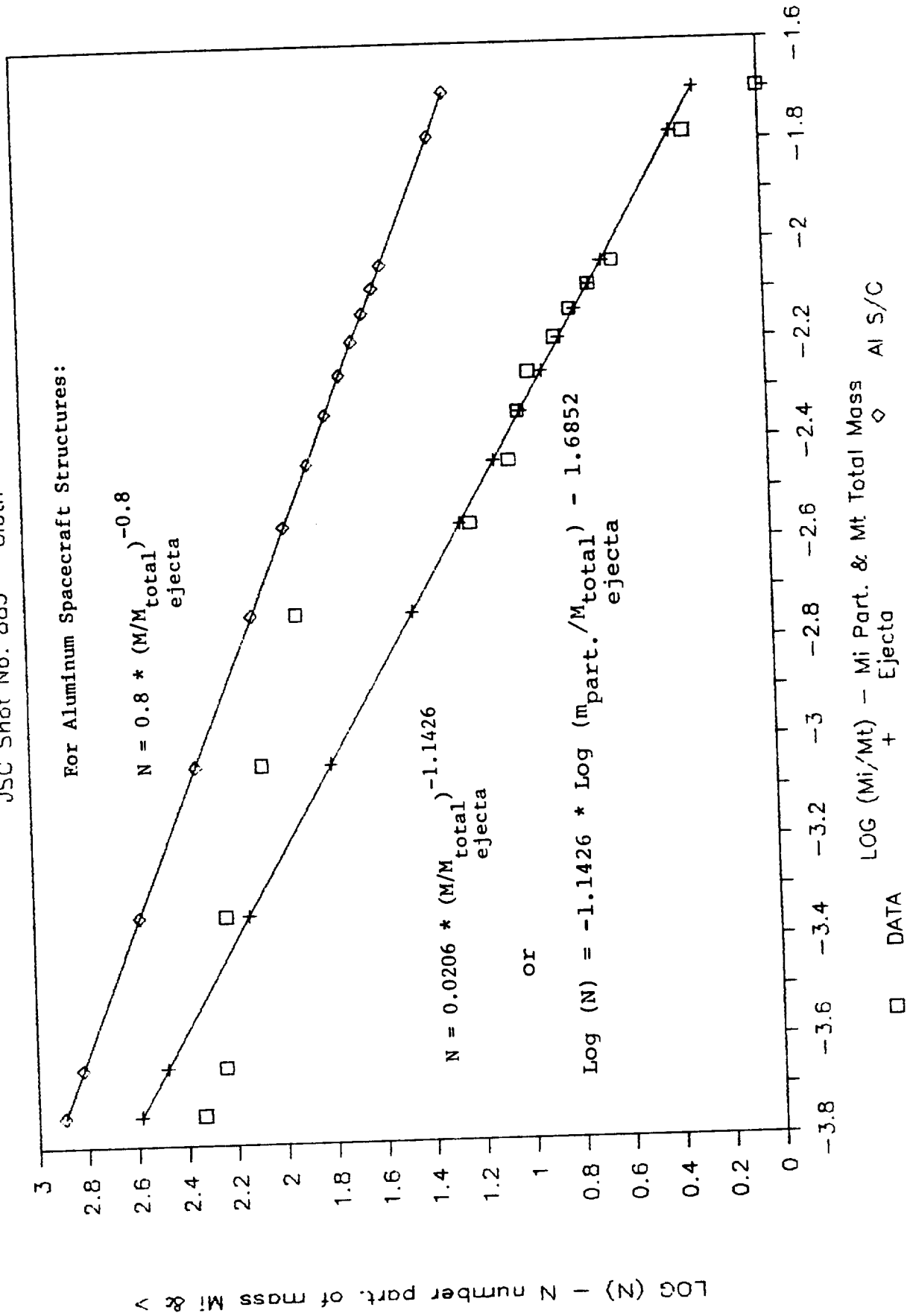


Figure 3-12

# EJECTA MASS AND PARTICLE NUMBER

JSC Shot No. 883 - Cloth



### 3.1.3 Shot #884 (1/2" thick, no cloth on front)

This shot is almost identical to the previous one, except this target (JSC-01B-002) had no cloth on the front surface. This shot was predicted to result in more ejecta.

Table 3-2 summarizes the parameters. A 4.76 mg nylon projectile going 6.26 km/sec impacted a 1/2 inch thick graphite/epoxy target. A styrofoam box fixed to the front of the target was used to collect the individual pieces of ejecta as explained in the previous shot.

Table 3-2 shows, as predicted, that this target, with no cloth on the front, produced almost twice as much total ejecta. There is roughly 50 percent less dust, indicating that much, if not all of this additional ejecta is in the form of large, collectable particles. Figure 3-13 shows the target front and back after the shot. Compare it with Figure 3-1.

Figures 3-14 and 3-15 plot ejecta mass versus length and diameter. A comparison with Figure 3-2 shows that the particle lengths for this shot were almost ten times greater. The masses are also almost ten times larger. The diameters plotted are calculated using the lengths and masses of the slivers and a given density, and an assumed cylindrical particle.

Figures 3-16 through 3-19 plot ejecta mass and velocity versus theta and phi (see figure A-1 in the appendix for a definition of theta and phi). Comparing the velocity versus theta plots (3-5 and 3-17) it is clear that the no cloth shot resulted in many higher calculated-velocity particles. See section 3.4 for a comparison of measured and calculated velocity.

Figures 3-20 and 3-21 plot ejecta mass and velocity versus cone angle. The cone angle is the angle between a normal to the target face at the impact point and the ejecta particle's velocity vector. The mass distribution (in Figure 3-20) seems to center around a cone angle of 60 to 70 degrees, a somewhat greater cone angle than for the previous shot with cloth covering. The velocity distribution also centers around the 60 to 70 degree cone angle, more clearly than the with cloth case.

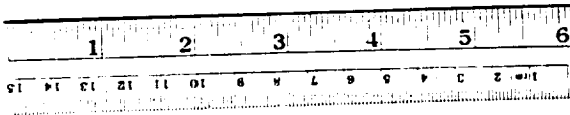
Figure 3-22 plots mass versus velocity. It shows far more clearly than the cloth covered shot, that the small particles are faster than the large particles.

Figure 3-23 shows a small scale plot of the Log(number of particles of mass  $M_i$  and larger) versus the Log( $M_i/M_{total}$  ejecta mass) and a least squares fit linear relationship for these two quantities and the derived equations (with and without the Logs) that results. The same plot, with a similar equation for aluminum taken from reference 1, is also plotted in Figure 3-24.

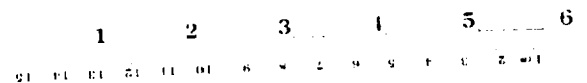
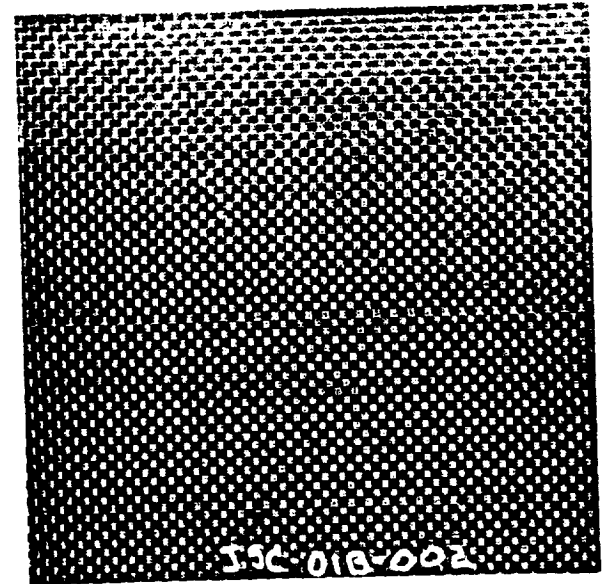
**Figure 3-13, Photos of Target (Shot #884)**

JSC 01A-003, 1/2 inch thick, graphite/epoxy, no cloth on front

Front



Back



ORIGINAL PAGE IS  
OF POOR QUALITY

Figure 3-14

# EJECTA MASS/LENGTH RELATIONSHIP

JSC Shot No. 884 - No Cloth

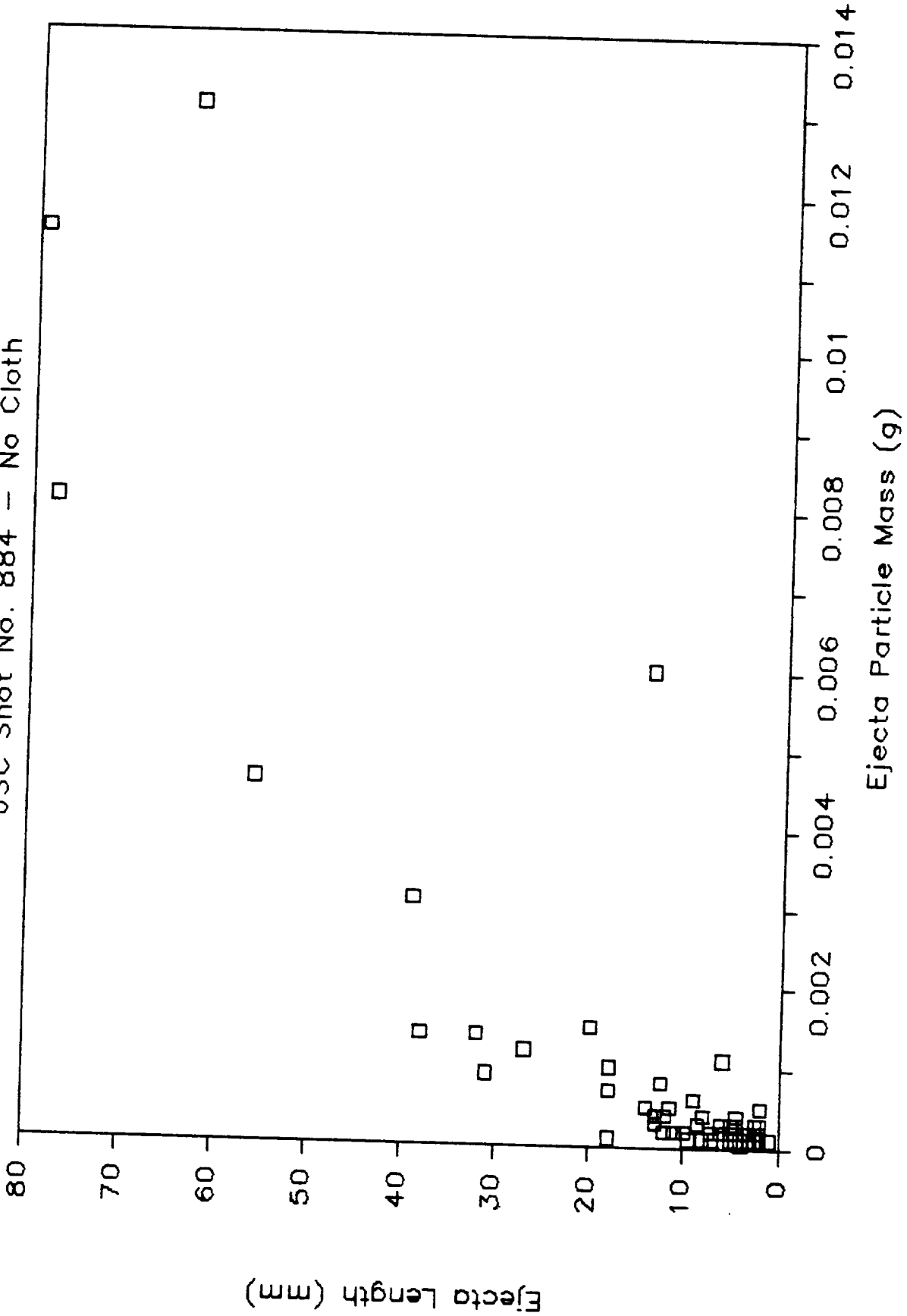


Figure 3-15

# EJECTA MASS/DIAMETER RELATIONSHIP

JSC Shot No. 884 - No Cloth

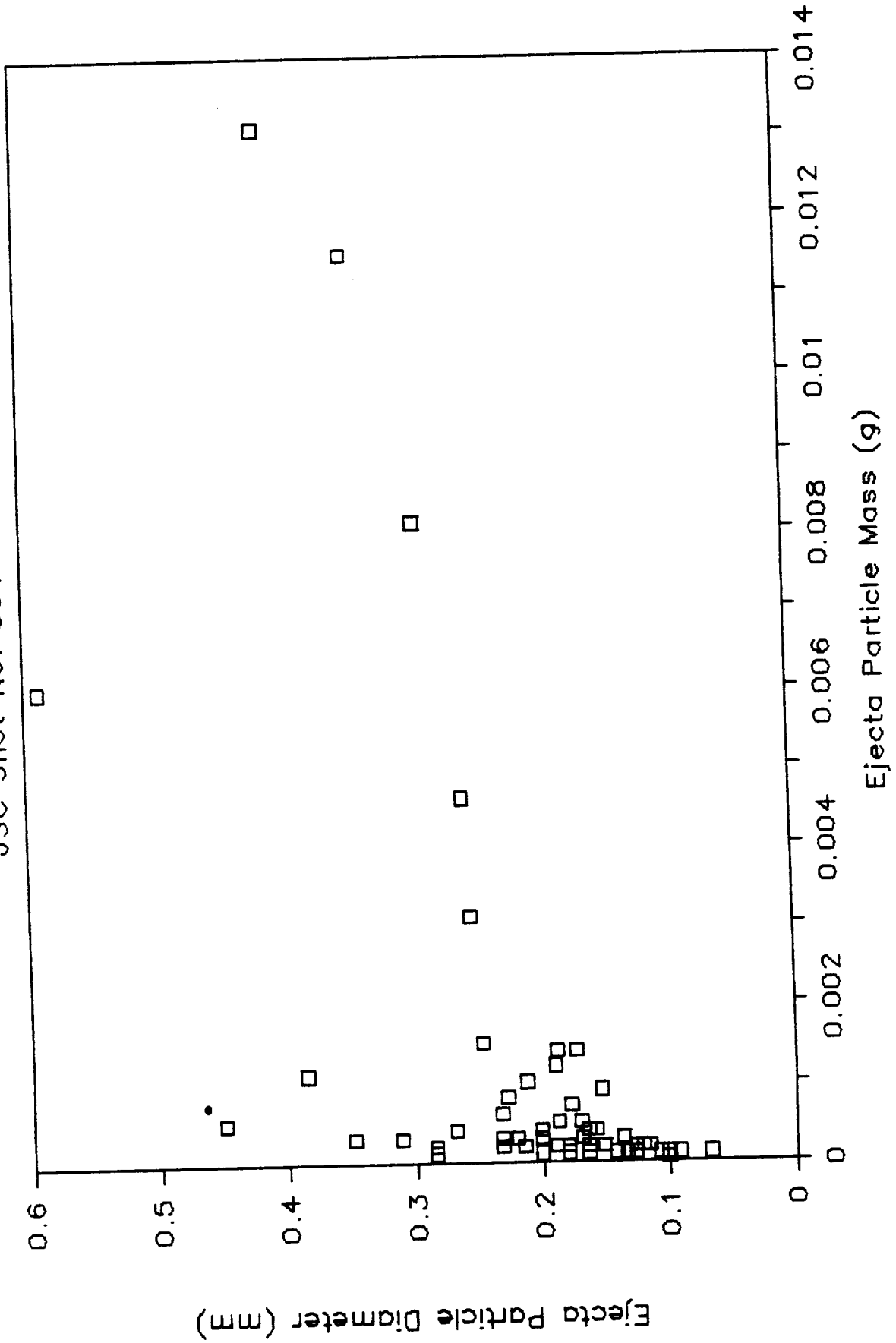




Figure 3-16

# EJECTA MASS DISTRIBUTION

JSC Shot No. 884 - No Cloth

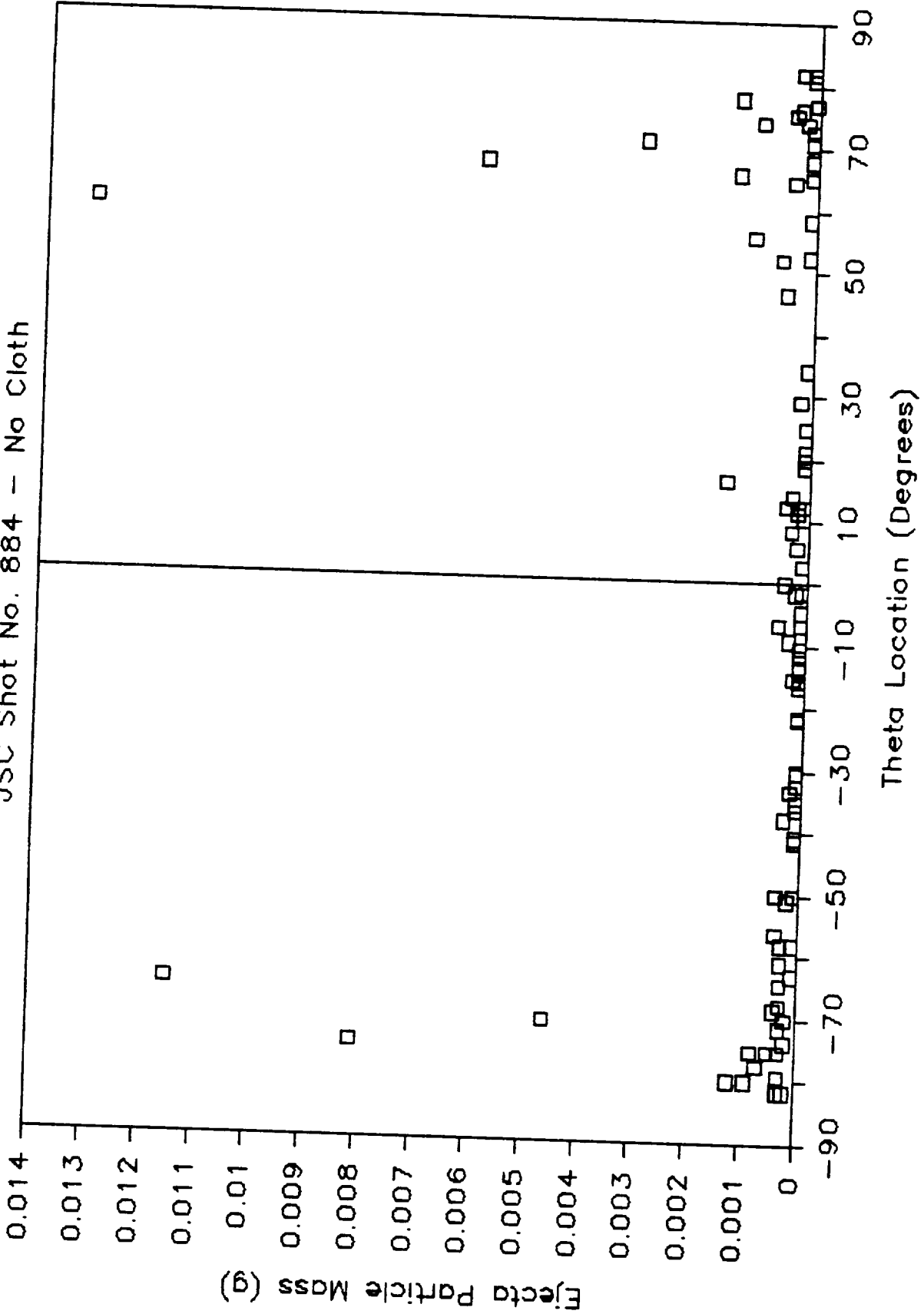


Figure 3-17

# EJECTA VELOCITY DISTRIBUTION

JSC Shot No. 884 - No Cloth

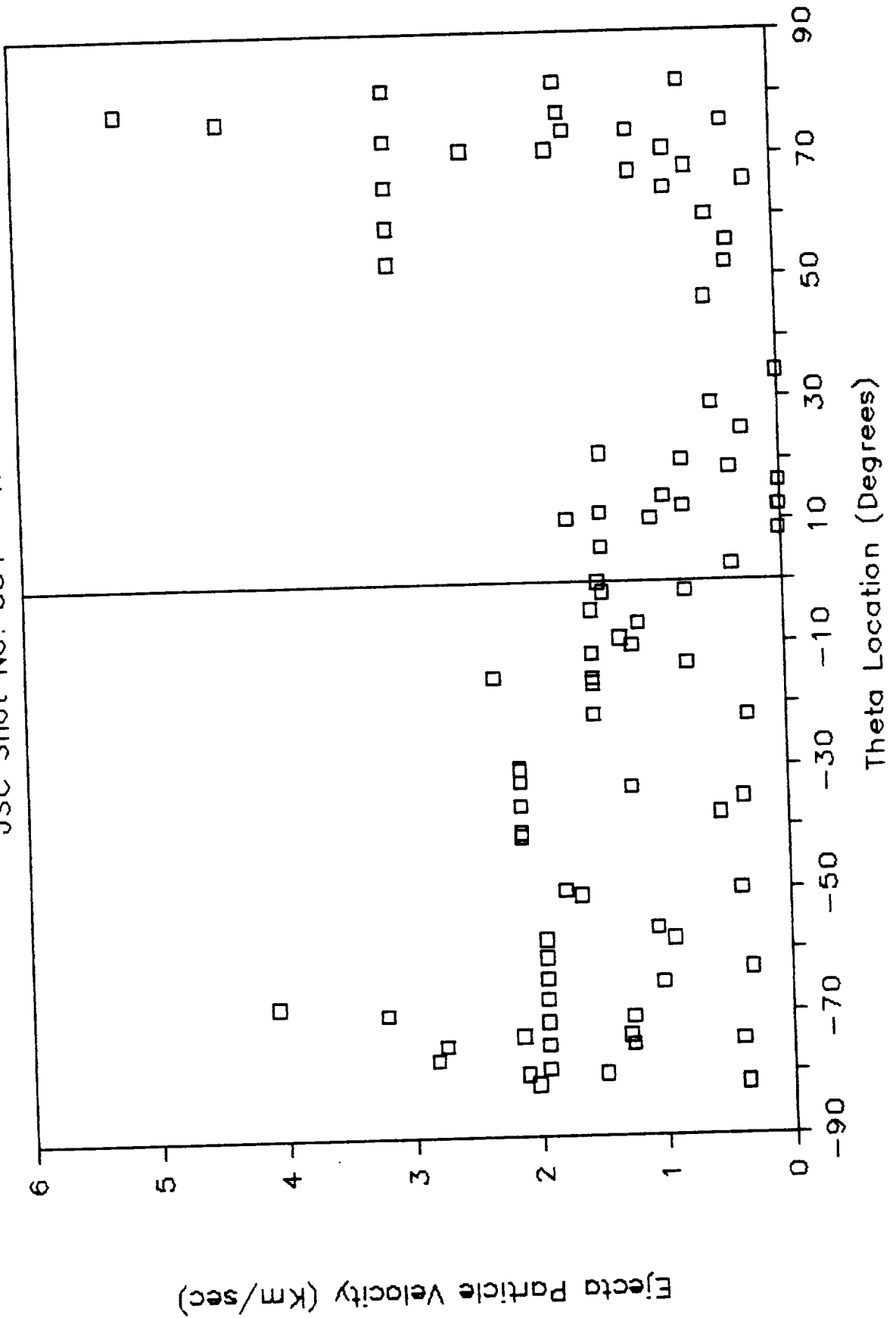


Figure 3-18

# EJECTA MASS DISTRIBUTION

JSC Shot No. 884 - No Cloth

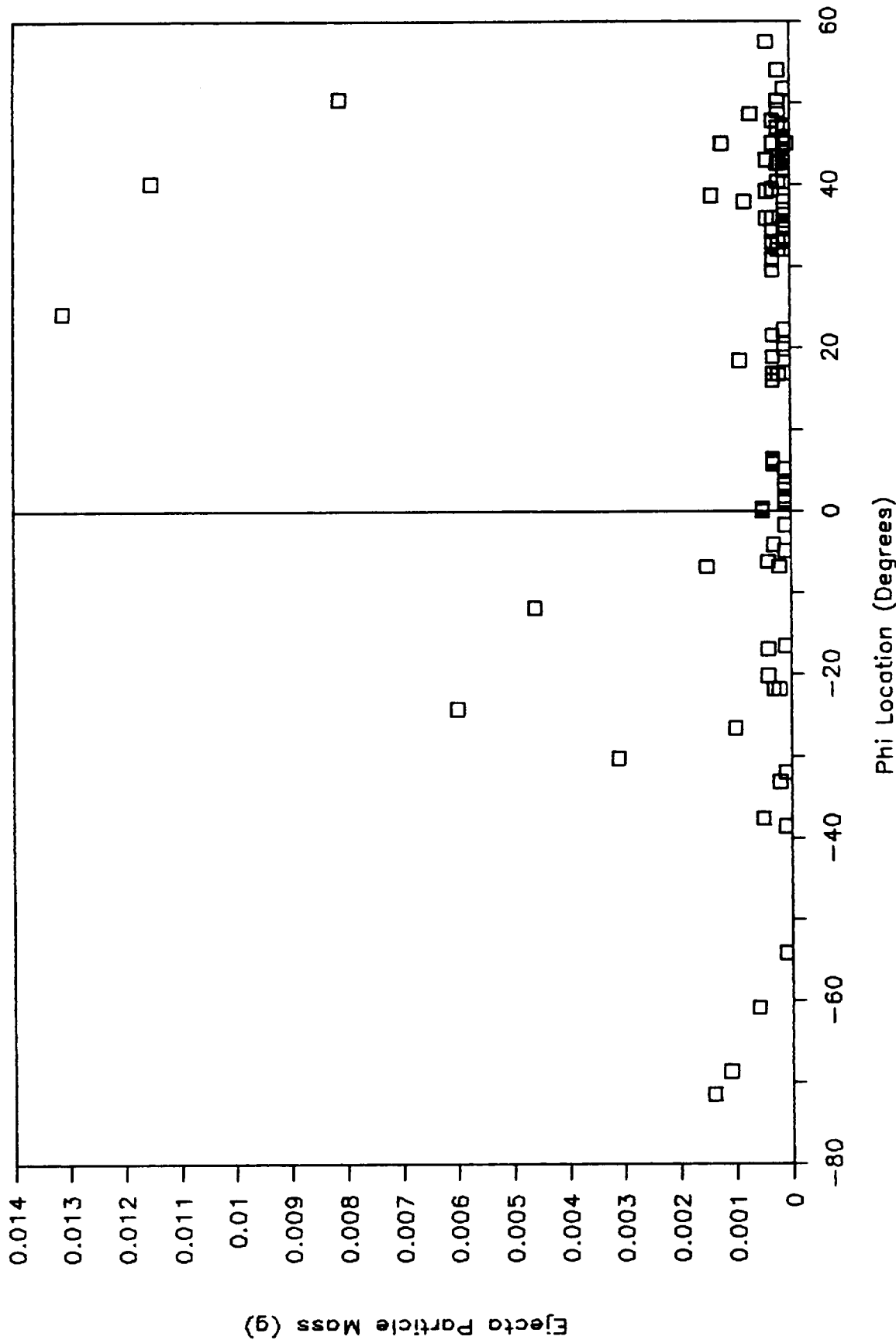


Figure 3-19

# EJECTA VELOCITY DISTRIBUTION

JSC Shot No. 884 - No Cloth

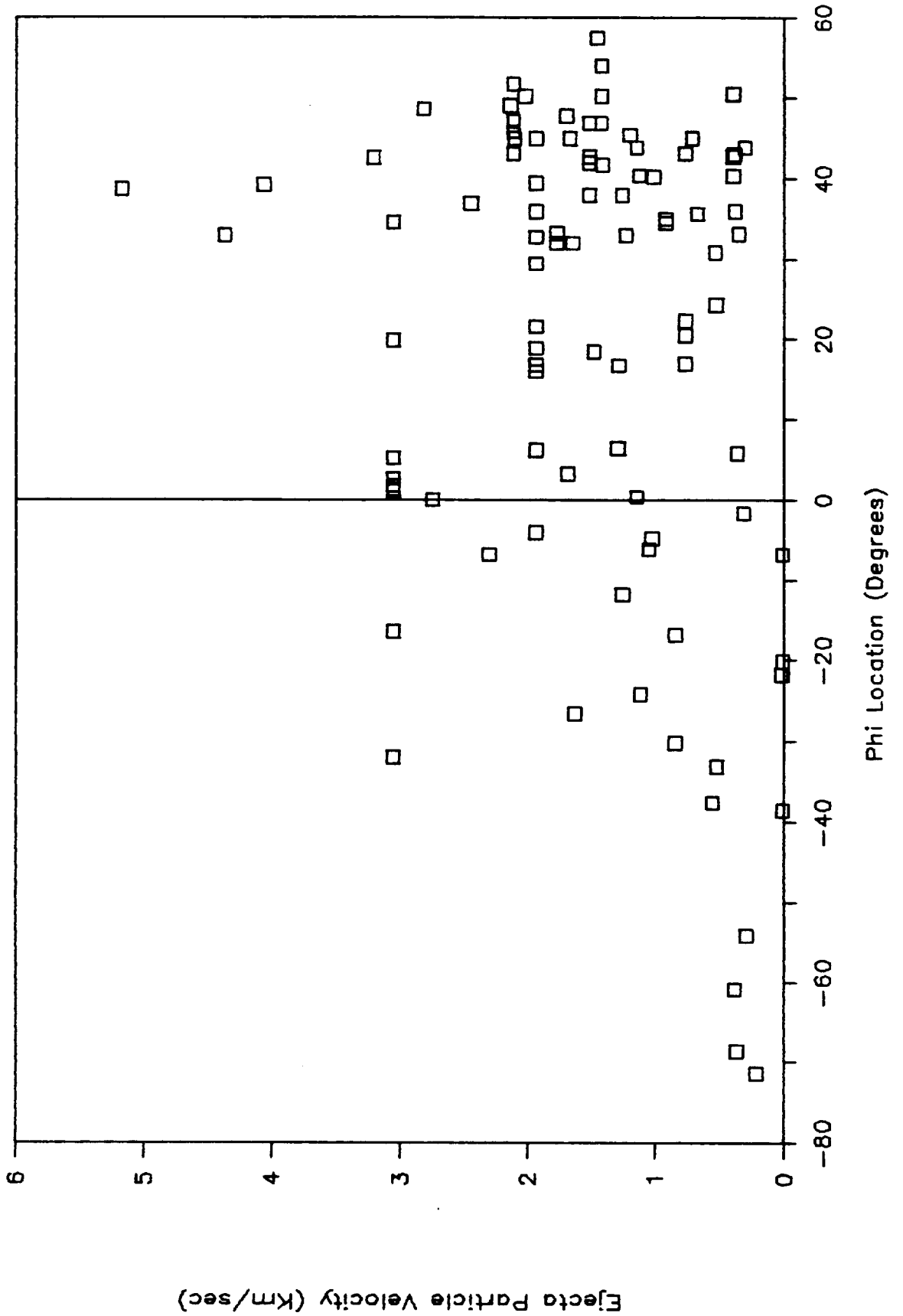


Figure 3-20

# EJECTA MASS DISTRIBUTION

JSC Shot No. 884 - No Cloth

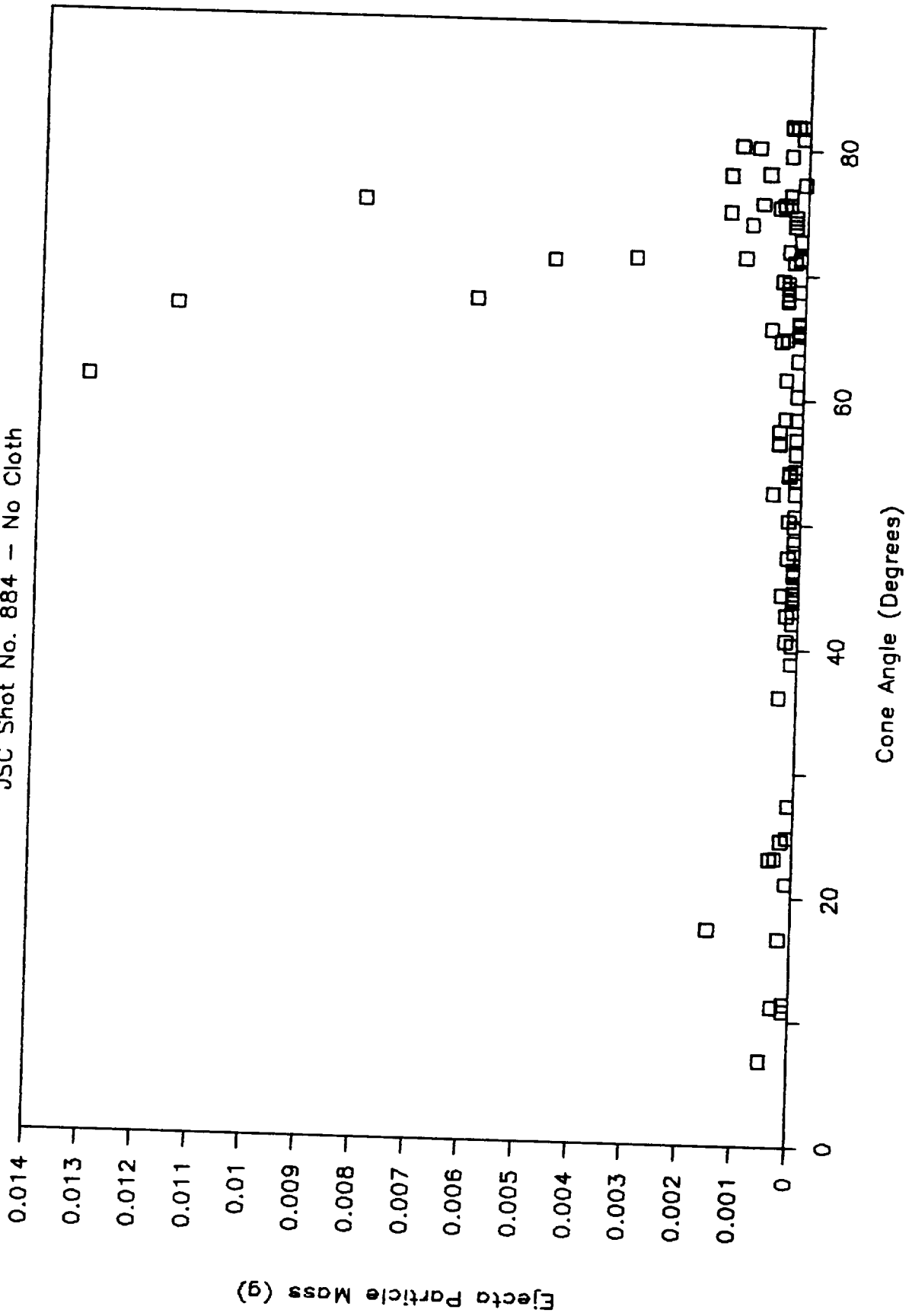


Figure 3-21

# EJECTA VELOCITY DISTRIBUTION

JSC Shot No. 884 - No Cloth

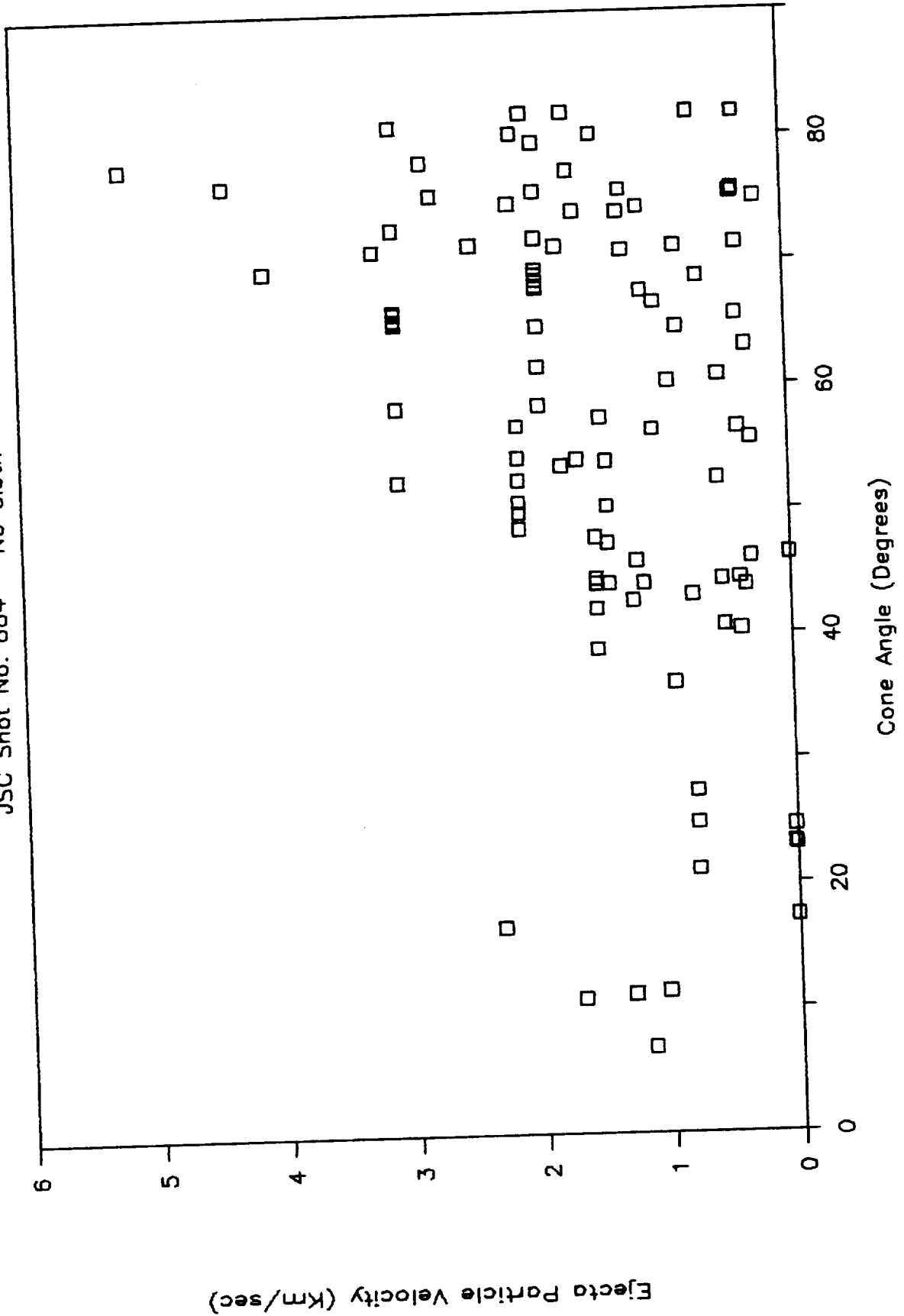


Figure 3-22

# EJECTA MASS/VELOCITY RELATIONSHIP

JSC Shot No. 884 - No Cloth

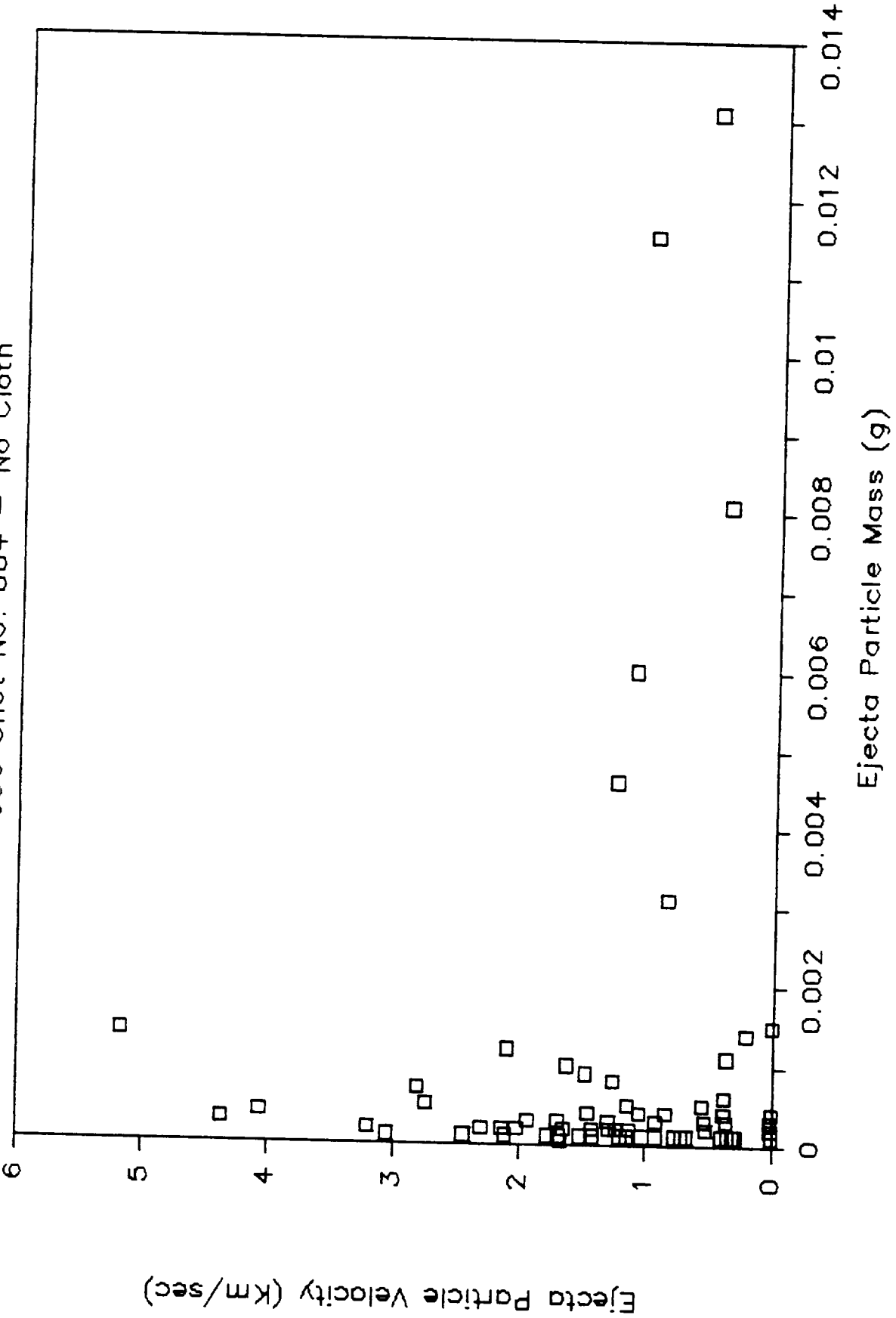


Figure 3-23

# EJECTA MASS AND PARTICLE NUMBER

JSC Shot No. 884 - No Cloth

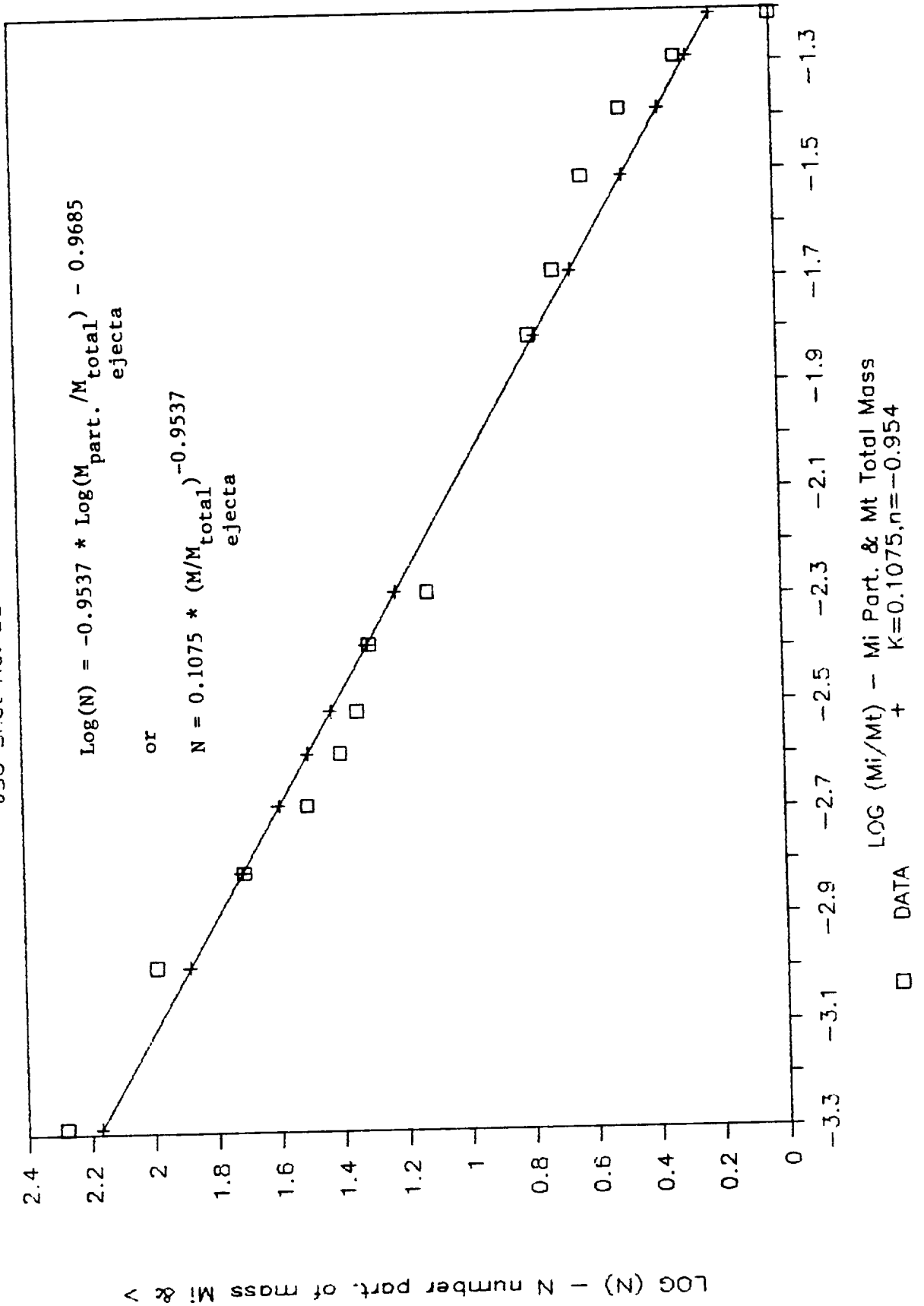
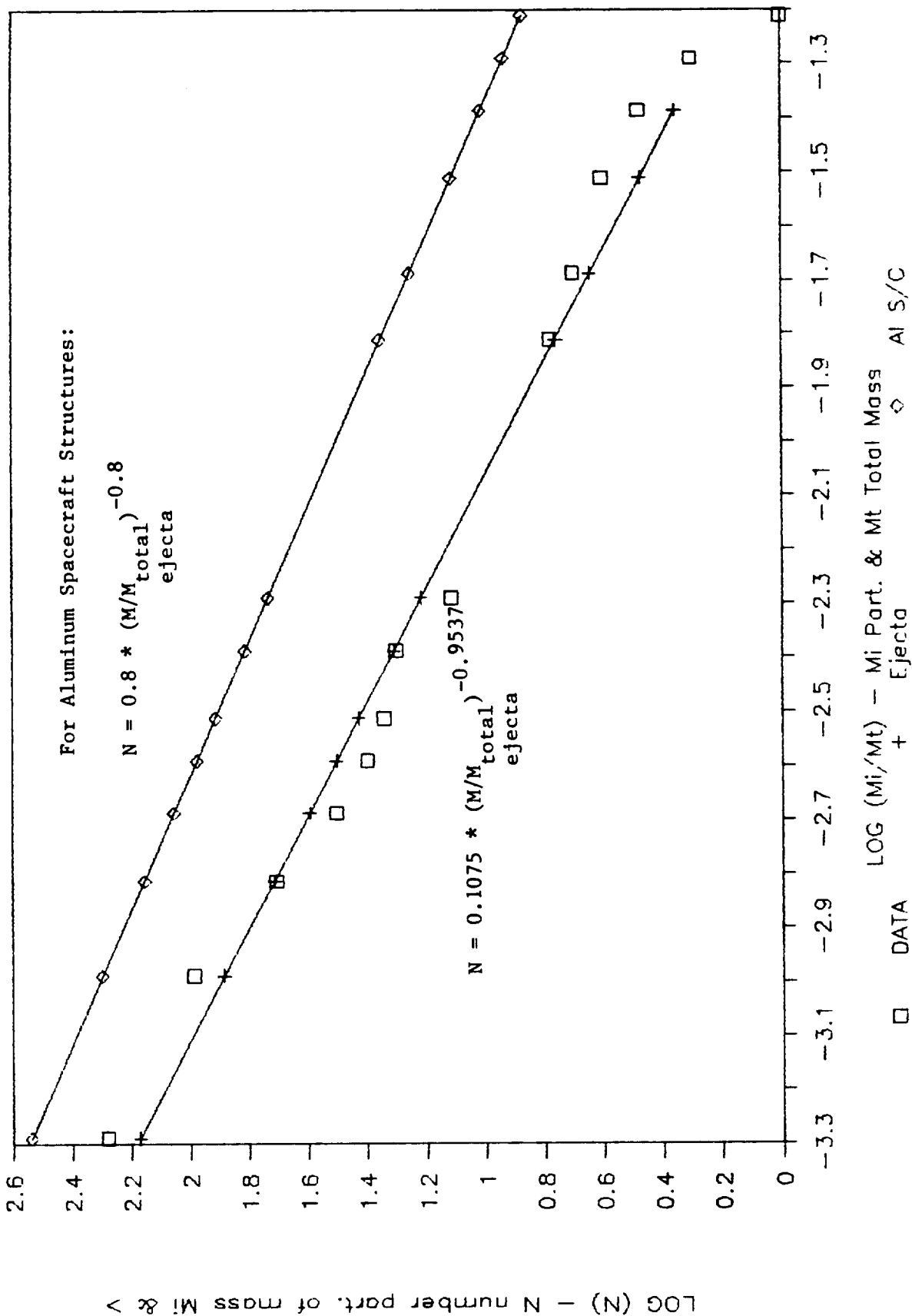




Figure 3-24

# EJECTA MASS AND PARTICLE NUMBER

JSC Shot No. 884 - No Cloth



### **3.2 Thin Graphite/Epoxy Targets - Ejecta and Spall Collected**

Once a capture technique was developed and some other restrictions removed, it was clearly desirable to acquire data on spall as well as ejecta. Thin targets representative of truss element walls and possible module bumpers (.06 to .10 inches thick) were then tested.

This data was used both in developing the particle number/-particle energy relationship and also the total mass/projectile energy relationship.

#### **3.2.1 Discussion of Test Setup**

Shots 894, 917 and 923 used a plexiglass box enclosing the target in the vacuum chamber to catch and separate the ejecta from the spall. Initially, the purpose of this setup was merely to determine the ratio of spall to ejecta for these targets. It was very successful. Some of the photos in Figure 3-55 show the overall setup. In addition to styrofoam, two other catcher materials were tried. For shot 894, a sheet of plastic wool matting was placed at either end of the box to catch some of the ejecta/spall particles. See Figure 3-25. This setup was not as effective as the styrofoam because velocity estimation from depth of penetration was not practical. A flexible sponge-type foam was also tried and had the same problem. They were sufficient to obtain a size & mass distribution of the ejecta and spall, but did not allow even a crude estimation of the particle velocities. In all subsequent shots, styrofoam was used (see Figure 3-55).

For shot 917 and 923, sheets of styrofoam were installed at the ends, along the sides, and on the bottom and top of the box. See Figure 3-55. This worked well for getting the spatial particle distribution as well as size and mass distribution. An approximate particle velocity was calculated from the depth of particle penetration into the styrofoam, particle geometry parameters, and styrofoam shear strength. This allowed the estimation of the particle kinetic energy distribution.

Single frame photography data is available for shots 917 and 894. This data is contained in appendix C.

#### **3.2.2 Shot #894 (0.093" thick, no cloth)**

Table 3-2 summarizes the parameters. A 4.94 mg nylon projectile travelling at 4.75 km/sec impacted a .093 inch thick graphite/epoxy target with no cloth covering (JSC-02B-003). The impact velocity was somewhat lower than the rest of the shots; this should be kept in mind when comparing it with other shots. The velocity is still within the range of interest, however.

Shots 894, 917, and 923, as shown in Table 3-2, represent roughly 5, 6, and 7 km/sec shots with approximately the same conditions. Shot 917 had a cloth covering, while 894 and 923 did not. All shots were into approximately 0.10 inch thick G/E targets.

Figure 3-25 shows the overall setup for catching the spall and ejecta. The target was encased in a plexiglass box to separate spall from ejecta. The projectile enters through a small hole at one end. After the shot, the individual particles of ejecta and spall are collected and weighed. This shot used a woven batting inside the box to try to catch the individual particles where they impacted the box. This batting had been effective previously at catching aluminum particles.

Some approximate velocity data on particles is available from the single frame photograph of this shot (see Appendix C).

Figures 3-26 and 3-27 plot ejecta and spall mass versus particle length and diameter. The length plot, looking at ejecta only, shows about the same results as the semi-infinite shot without a cloth covering (see Figure 3-14, shot #884). The diameters plotted are actually an average calculated value. The length and mass of the slivers were measured, and given the density and assuming a cylindrical partical, an average diameter was calculated.

The cloth batting was only at the ends of the plexiglass box. Most of the particles bounced off at the plexiglass and ended up on the bottom of the box. A spatial estimate (Theta and Phi, etc.) of particle location was therefore not produced.

Figure 3-28 shows a plot of the Log(number of ejecta particles of mass  $M_i$  and larger) versus the Log( $M_i/M_{total}$  ejecta mass) and a least squares fit linear relationship for these two quantities and the derived equations (with and without the Logs) that result. Figure 3-29 shows the same thing for spall. Figure 3-30 shows the spall, ejecta, and total spall plus ejecta plotted together on the same graph. The lines are all close together, indicating they all might be approximated by one curve.

Figure 3-31 shows the total spall and ejecta Log curve with a curve for aluminum (taken from Ref. 1). The aluminum line shows more particles of a given mass and greater once Log( $M_i/M_t$ ) goes above -3.2. In other words, there are more small graphite/epoxy particles, but more medium sized and greater aluminum particles. A form of these equations is used elsewhere in the estimate of hazards to the Space Station.

Figure 3-25, Photos of Catcher Box (Shot #894)

JSC 02B-003, 0.093 inch thick, graphite/epoxy, no cloth on front

Top View



Projectile  
enters here

Side View



Figure 3-25, Continued, Photos of Catcher Box (Shot #894)

JSC 02B-003, 0.093 inch thick, graphite/epoxy, no cloth on front

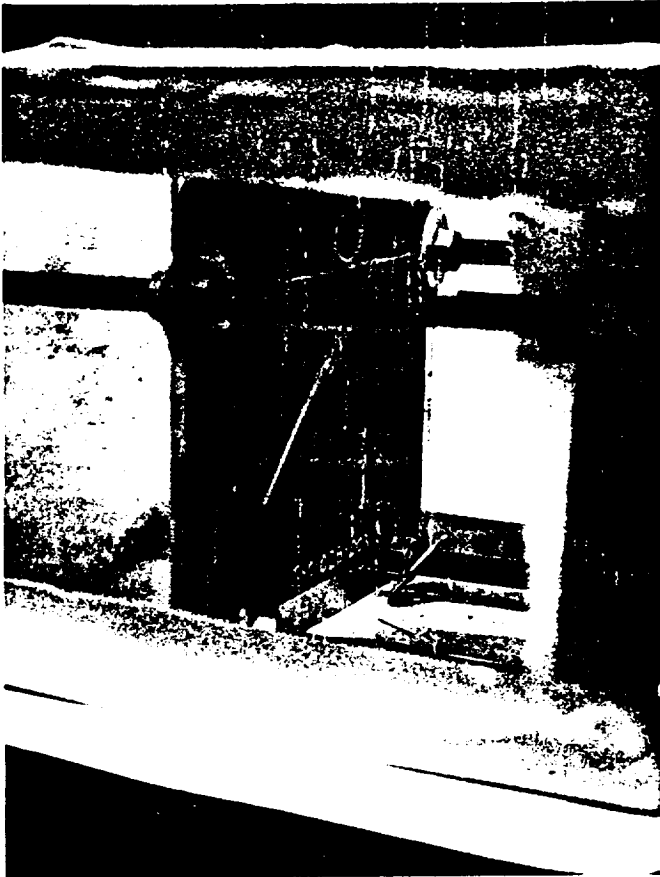


Figure 3-26

# EJECTA/SPALL MASS & LENGTH

JSC Shot No. 894 - Thin Plate

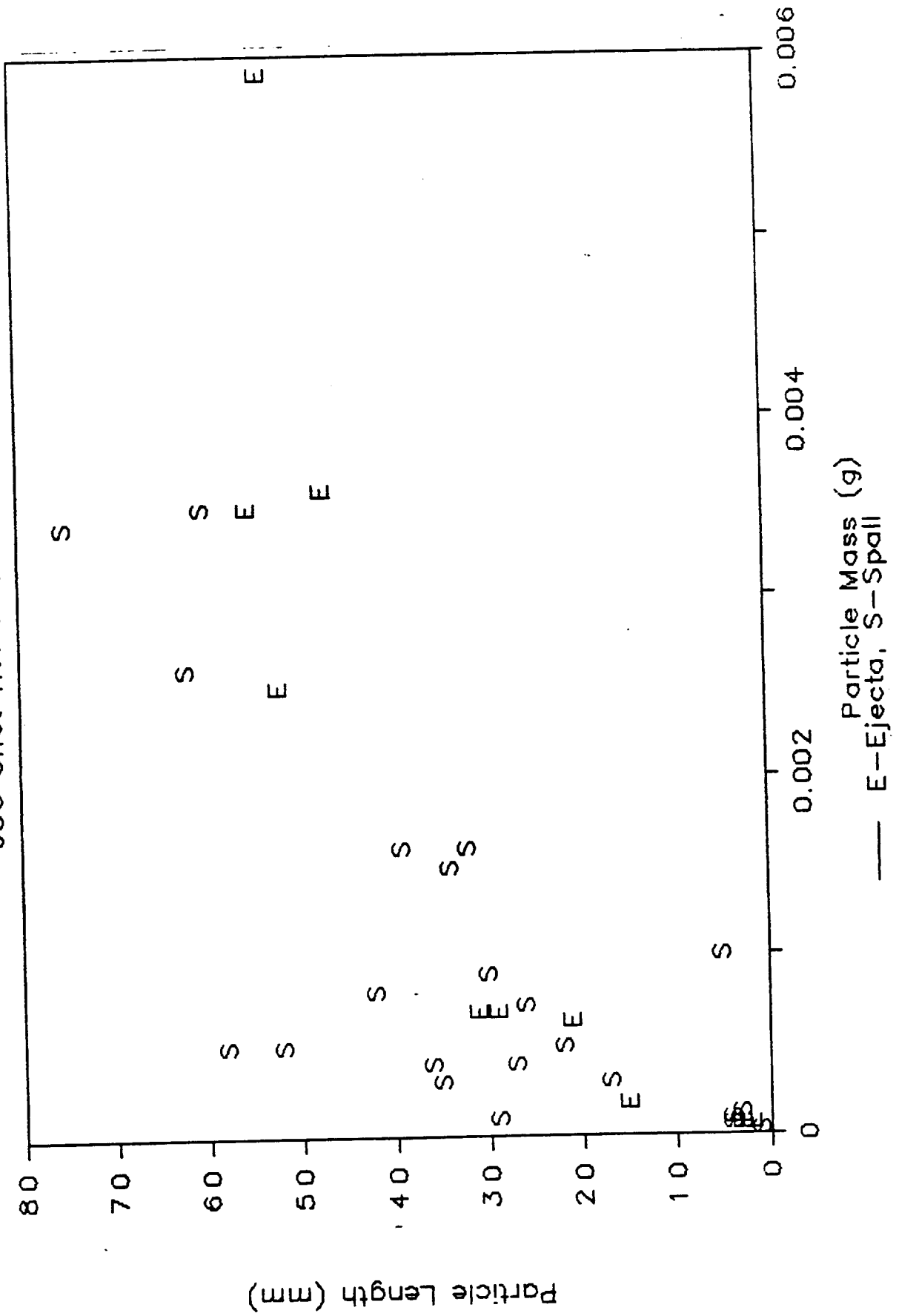


Figure 3-27

# EJECTA/SPALL MASS & DIAMETER

JSC Shot No. 894 - Thin Plate

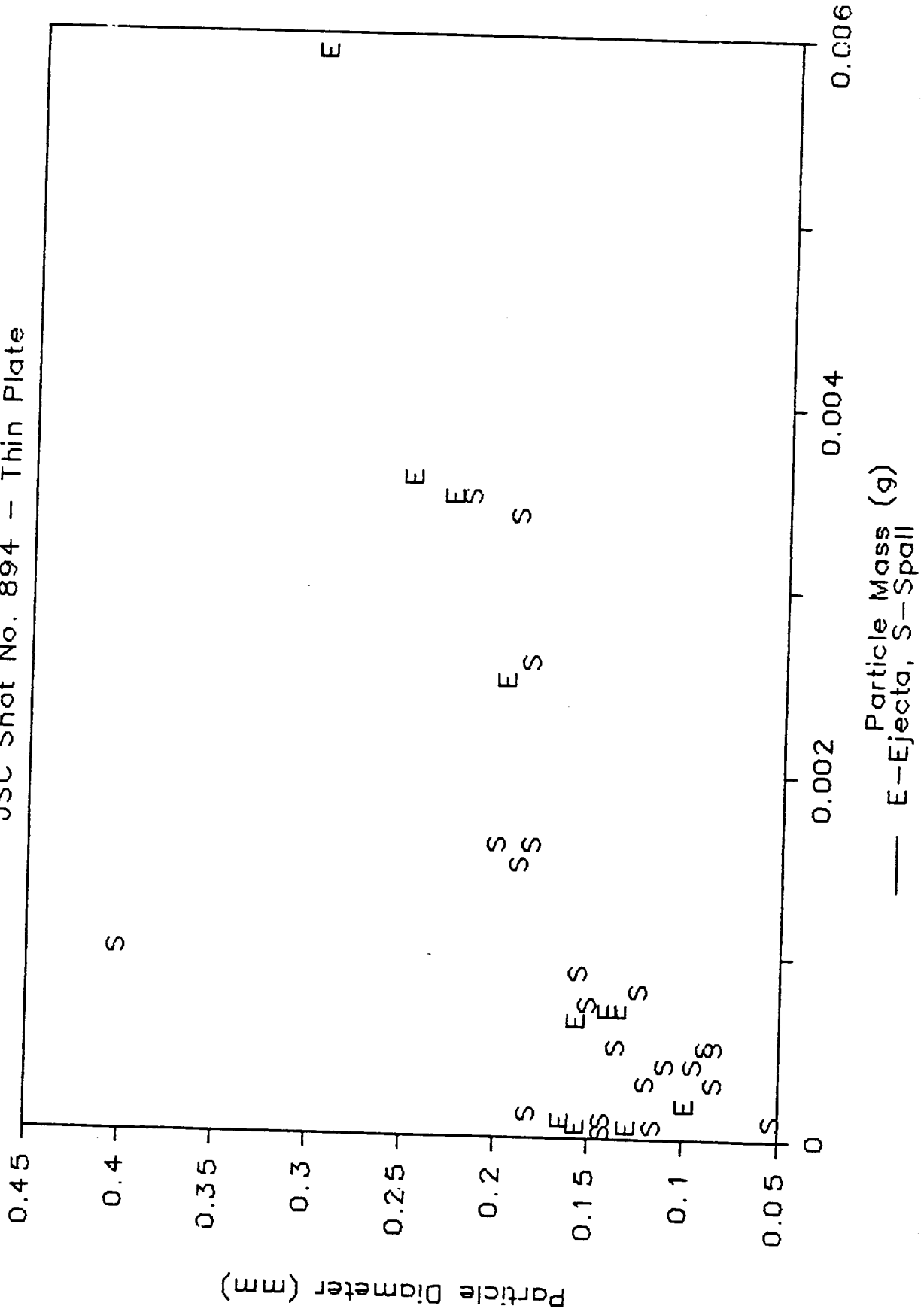


Figure 3-28

# EJECTA MASS AND PARTICLE NUMBER

JSC Shot No. 894 - Thin Plate

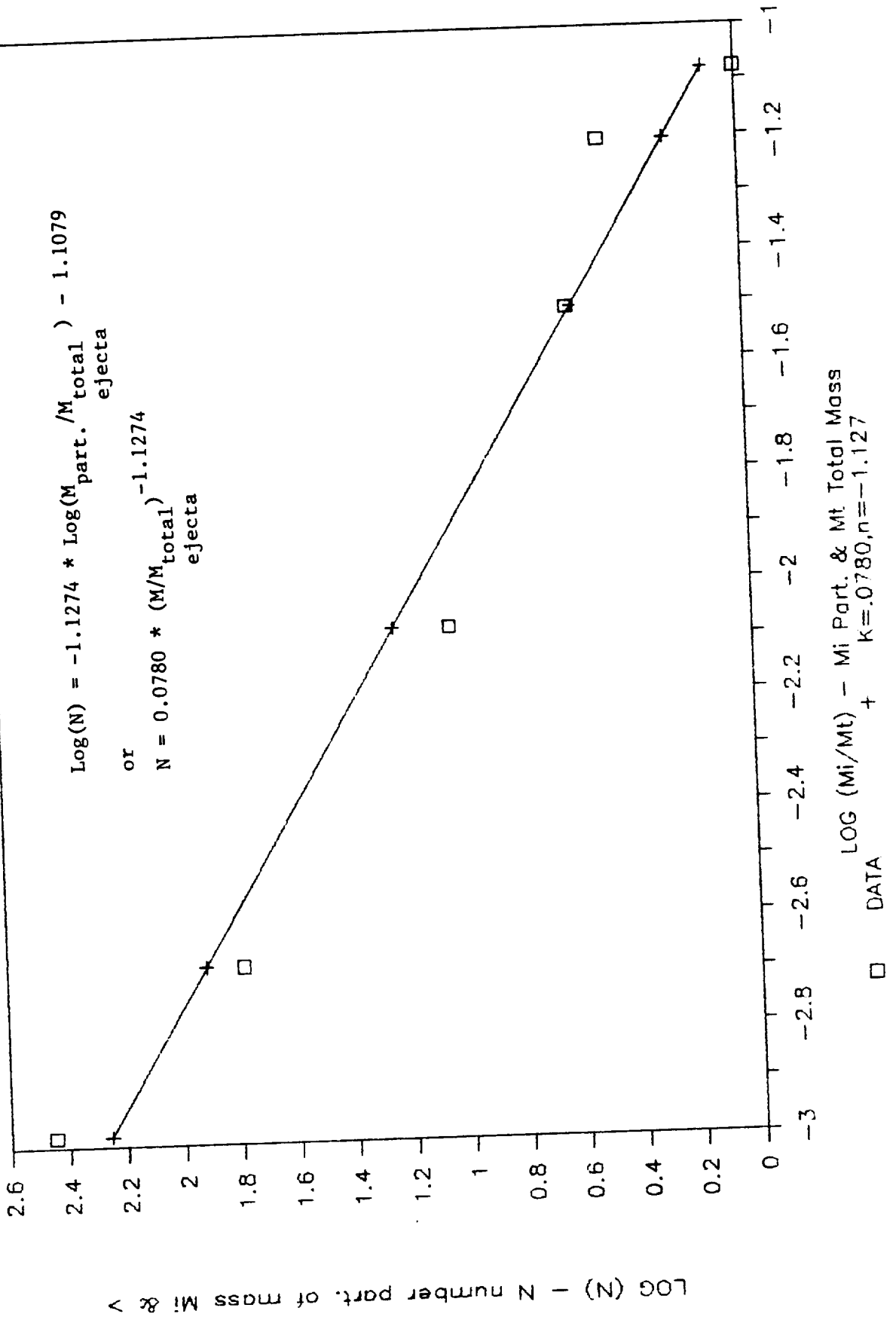




Figure 3-29

# SPALL MASS AND PARTICLE NUMBER

JSC Shot No. 894 - Thin Plate

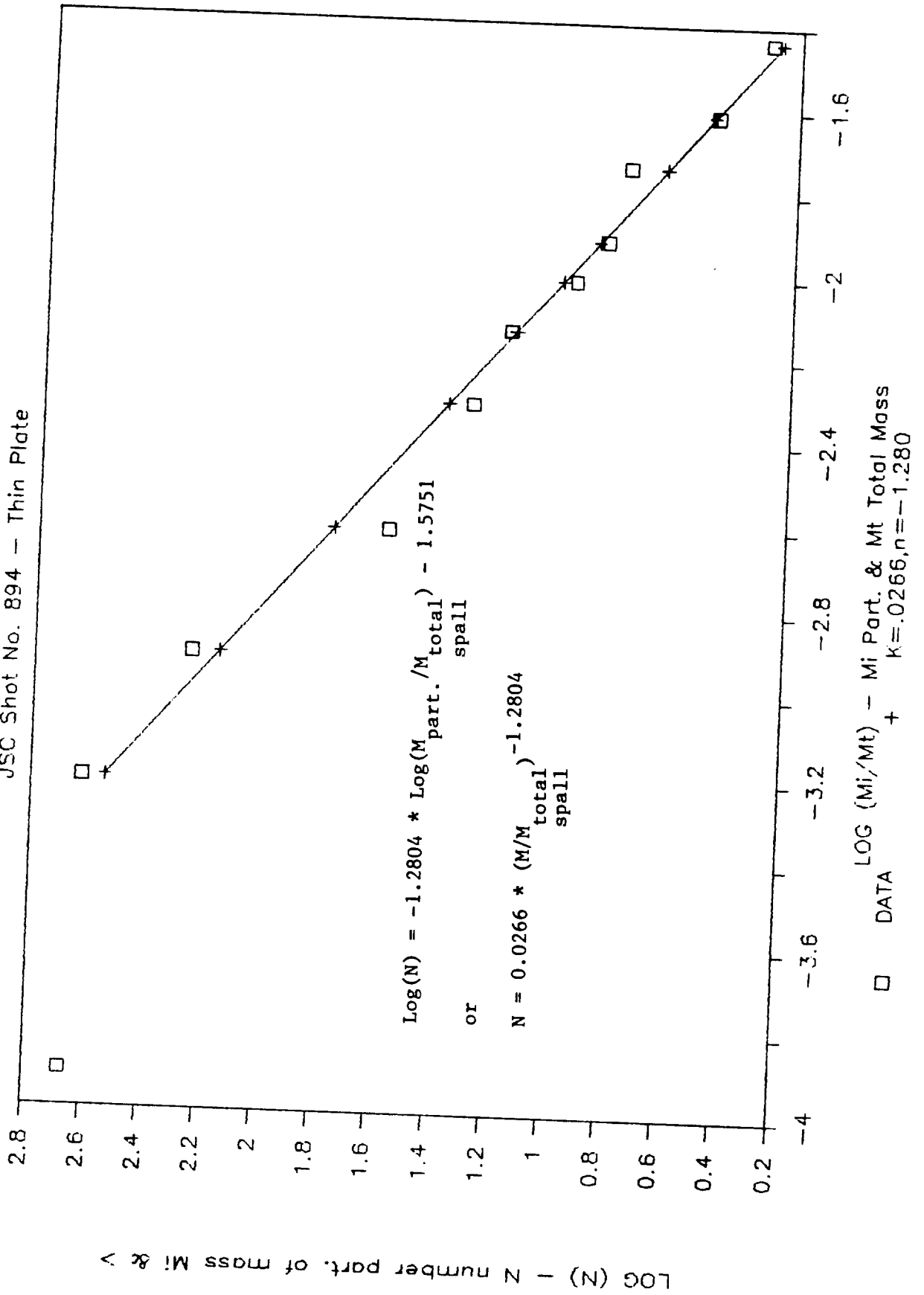


Figure 3-30

# SPALL/EJECTA MASS AND PARTICLE NUMBER

JSC Shot No. 894 - Thin Plate

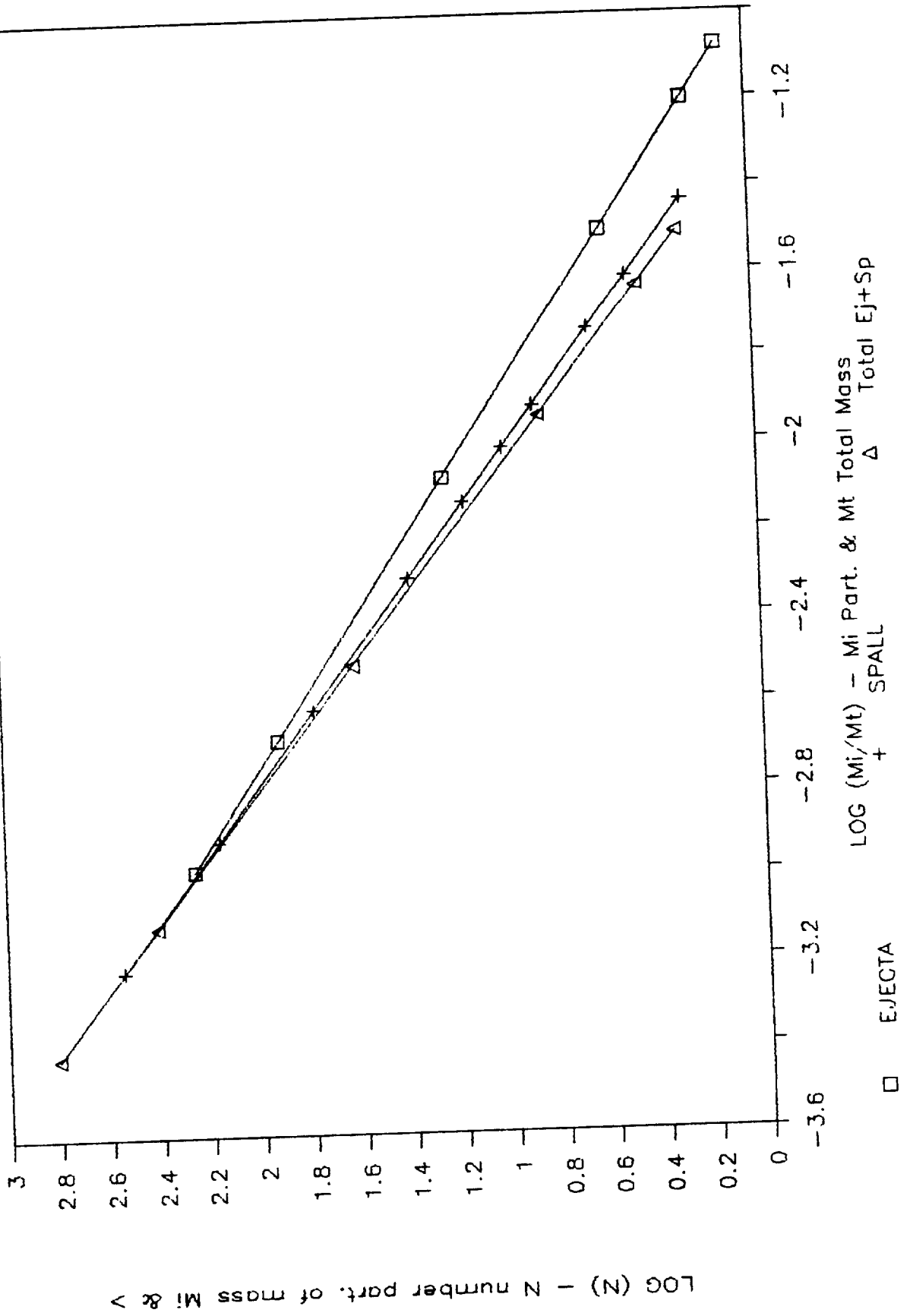
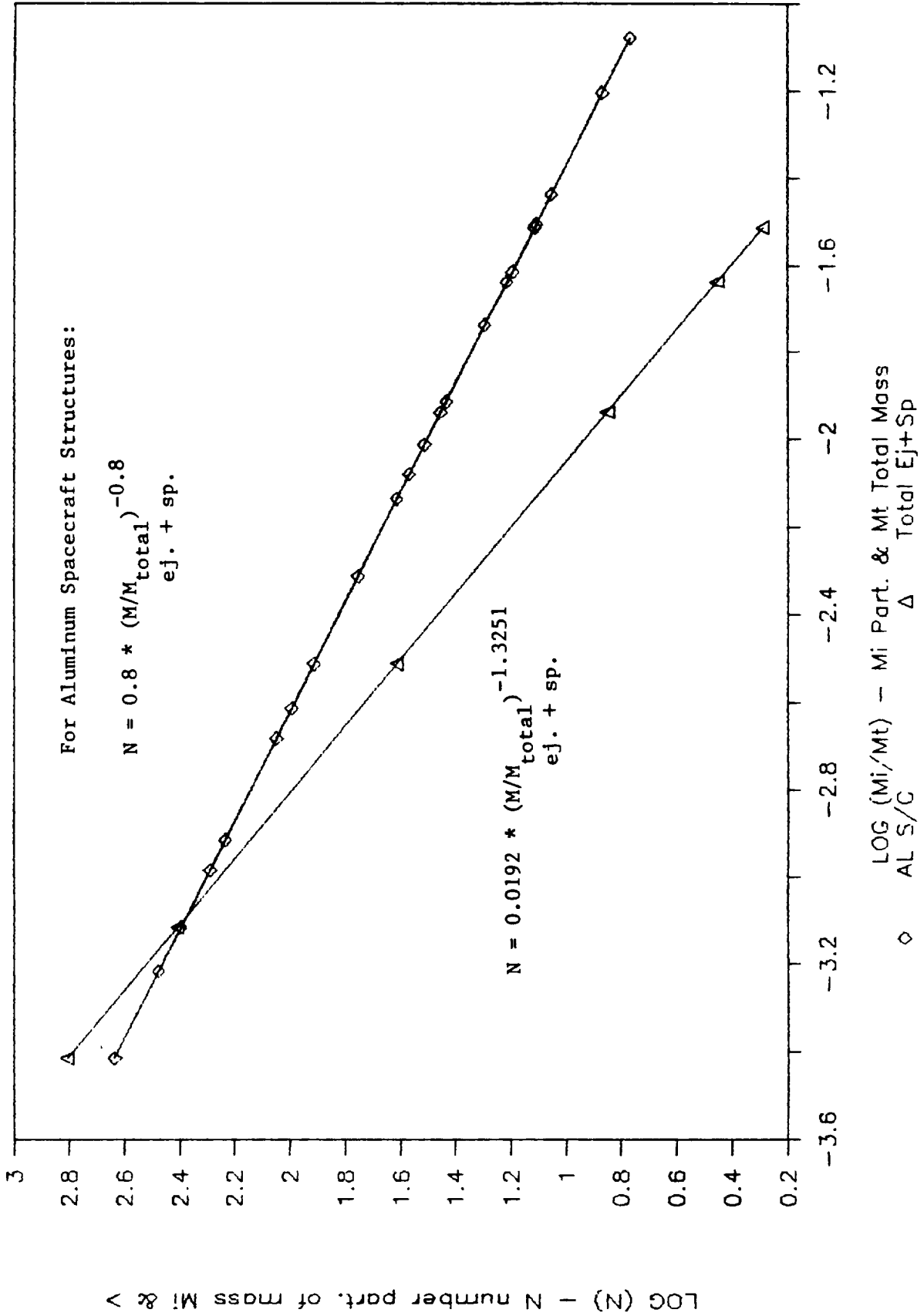


Figure 3-31

# SPALL/EJECTA MASS AND PARTICLE NUMBER

JSC Shot No. 894 - Thin Plate



### 3.2.3 Shot #917 (0.127" thick, with cloth)

This shot is similar to the previous one, except this target (JSC-03A-003) had cloth on the front and back surfaces, predicted to result in less ejecta and spall. This shot was also at a higher velocity (5.99 km/sec versus 4.75 for the previous shot, # 894). Figure 3-32 shows photos of the the target after impact. Compare it to Figure 3-56, from the next shot, with no cloth. The cloth reduces the number of large particles, but not the total mass of ejecta and spall as shown in Table 3-2. This may be due to other factors, such as the velocity difference, however. Another variable that was not easily measured or controlled at this point in the testing is the way in which the non-symmetrical projectile (which is a cylinder) impacts the target. See Figure 5-4.

Table 3-2 summarizes the parameters. A 4.86 mg nylon projectile going 5.99 km/sec impacted a 0.127 inch thick graphite/epoxy target with a cloth covering on the front and back. A plexiglass box with styrofoam placed around the inside (see Figure 3-55) was used to catch the individual pieces of ejecta.

Figures 3-33 and 3-34 plot ejecta mass versus length and diameter. A comparison with Figure 3-26 shows that the largest particle lengths for this shot (with cloth on the front) were almost ten times less than those for the shot with no cloth (#894).

Figures 3-35 through 3-38 plot ejecta mass and calculated velocity versus theta and phi (see figure A-1 in the appendix for a definition of theta and phi). Other approximate velocity data is available from the single frame photo of the impact in Appendix C.

Figures 3-39 and 3-40 plot ejecta mass and velocity versus cone angle. The cone angle, in this case, is the angle between the incoming projectile's velocity vector and the ejecta particle's velocity vector. The mass distribution (in Figure 3-39) seems to center around a cone angle of 30 to 40 degrees, smaller than the 60 to 70 degree averages for semi-infinite shots. Table 3-2, which calculates an average cone angle, also shows this. The velocity distribution shows the same centering, around 40 degrees or so.

In other hypervelocity impacts, evidence is said to exist of very high speed ejecta particles coming off at angles near 90 degrees, almost parallel to the face of the target plate. Our data (including high speed camera photos in later sections) do not show this occurring with graphite/epoxy.

Figure 3-41 plots ejecta mass versus velocity. This plot does not include all particles. It only includes those that were recovered and their velocity estimated, and as such it should be

considered representative of a fraction of the data only. The very small particles, which are likely to be moving at even higher velocities, could not be captured and are thus not shown on this plot.

Figure 3-42 plots the Log(number of ejecta particles of mass  $M_i$  and larger) versus the Log( $M_i/M_{total}$  ejecta mass). A least squares fit linear relationship for these two quantities and the derived equations (with and without the Logs) that result are also shown. These equations are used elsewhere in the estimate of hazards to the Space Station.

Figures 3-43 and 3-44 plot spall mass versus length and diameter. Except for a few large slivers, the data is similar to that for the ejecta.

Figures 3-45 through 3-48 plot spall mass and velocity versus theta and phi (see figure A-1 in the appendix for a definition of theta and phi).

Figures 3-49 and 3-50 plot spall mass and velocity versus cone angle. The cone angle is the angle between a normal to the target face at the impact point and the ejecta particle's velocity vector. The distributions seem somewhat more spread out than in previous plots.

Figure 3-51 plots spall mass versus velocity.

Figure 3-52 plots the Log(number of spall particles of mass  $M_i$  and larger) versus the Log( $M_i/M_{total}$  spall mass). A least squares fit linear relationship for these two quantities and the derived equations (with and without the Logs) are also shown.

Figure 3-53 plots the equations derived from Figures 3-42 and 3-52 and the Log Log plot of total ejecta and spall. The lines are all close together, indicating they could all be approximated by one line.

Figure 3-54 plots the Log-Log total ejecta and spall line along with an aluminum line (from Ref. 1). The results are similar to previous plots. The equations derived will be used to estimate the damage hazard to the Space Station.

Figure 3-32, Photos of Target (Shot #917)

JSC 03A-003, 0.127 inch thick, graphite/epoxy, with cloth

Front

Back

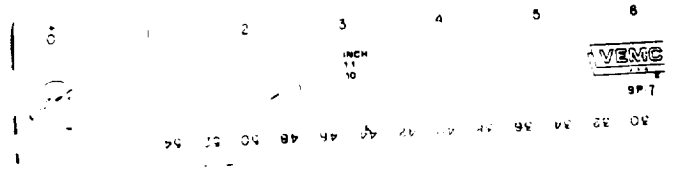
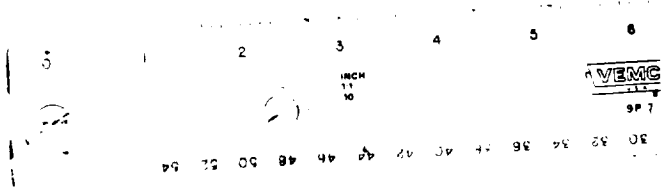
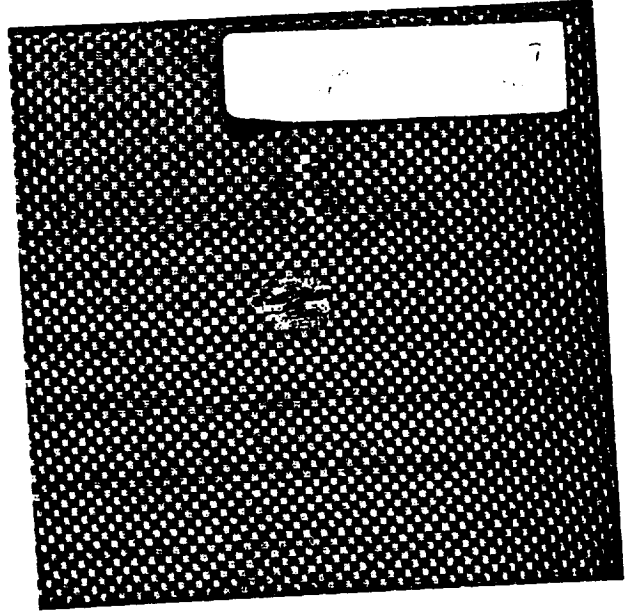
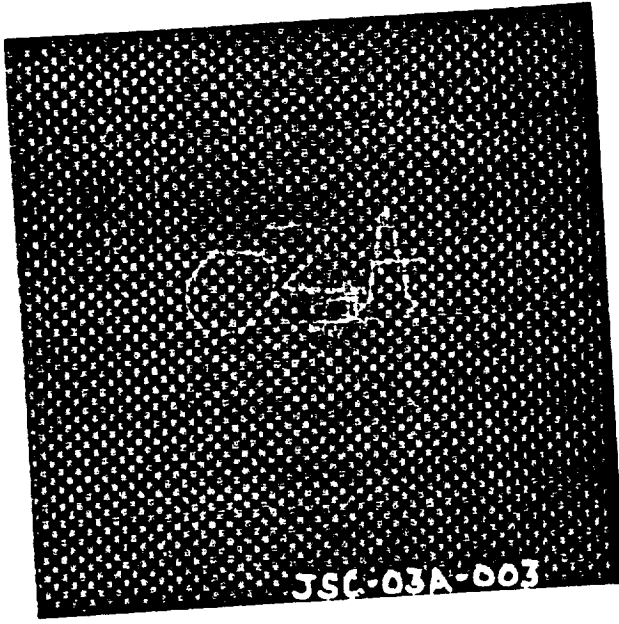


Figure 3-33

# EJECTA MASS & LENGTH

JSC No. 917 - Thin Plate, with Cloth

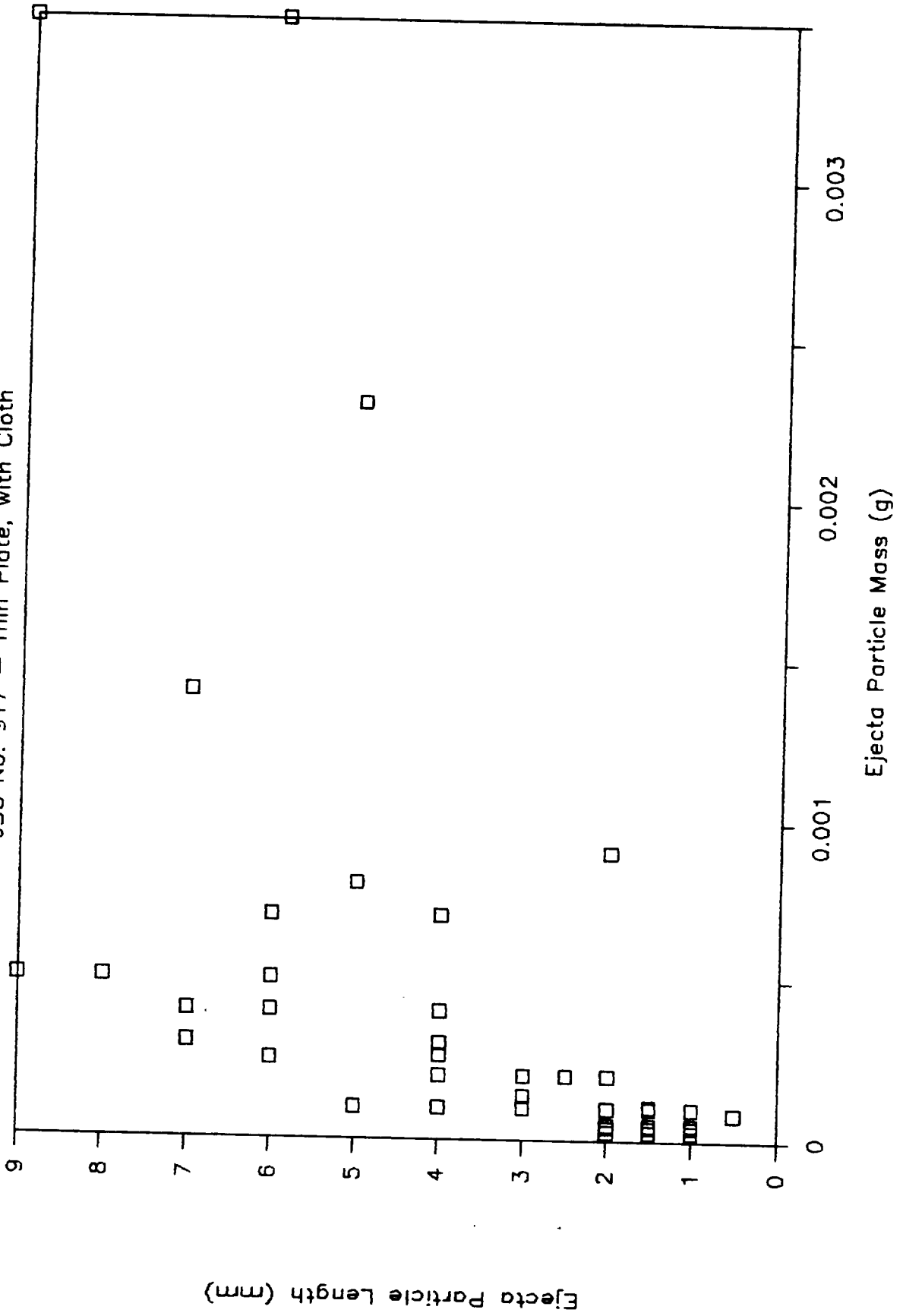


Figure 3-34

# EJECTA MASS & DIAMETER

JSC No. 917 - Thin Plate, with Cloth

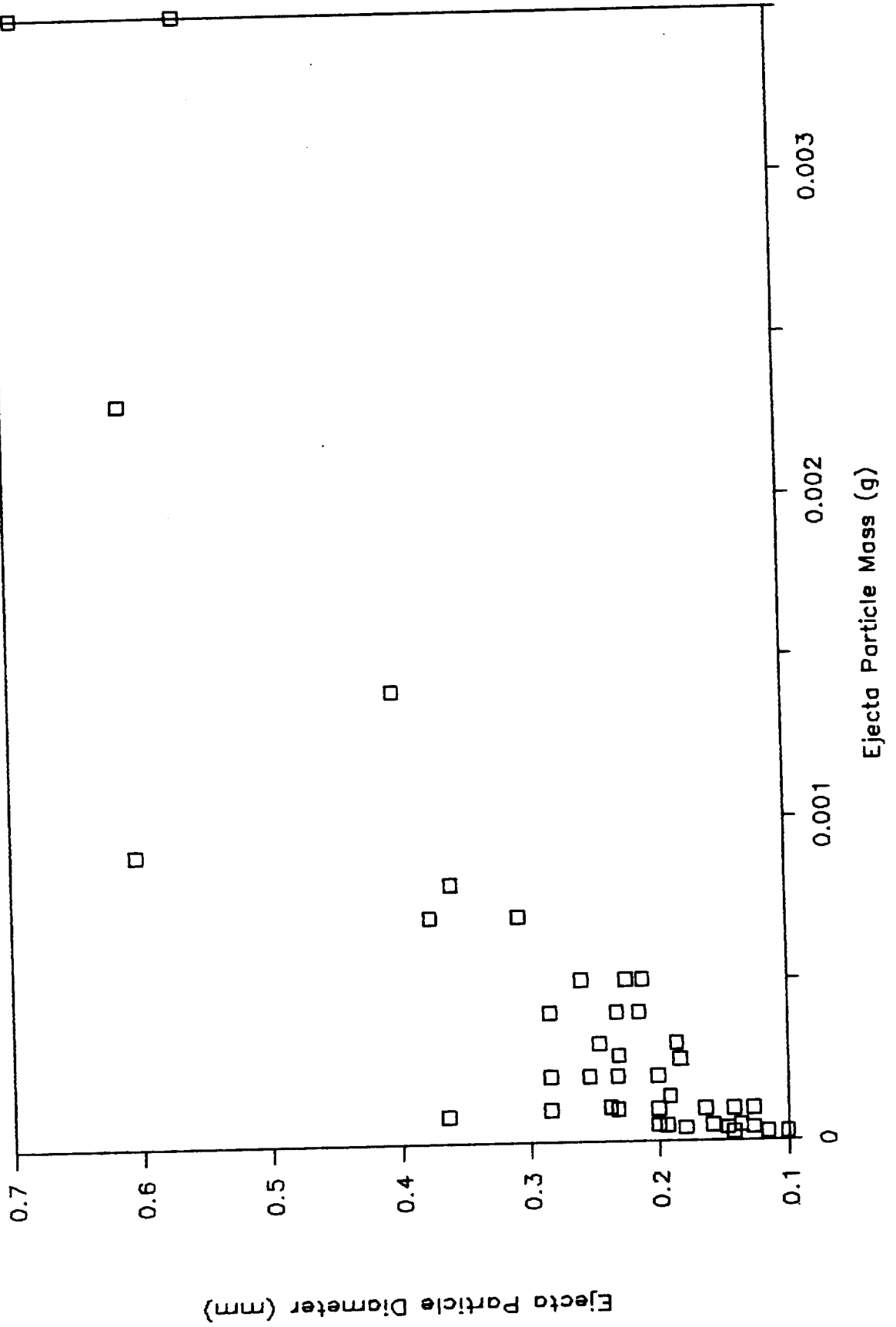




Figure 3-35

# EJECTA MASS DISTRIBUTION

JSC No. 917 - Thin Plate, with Cloth

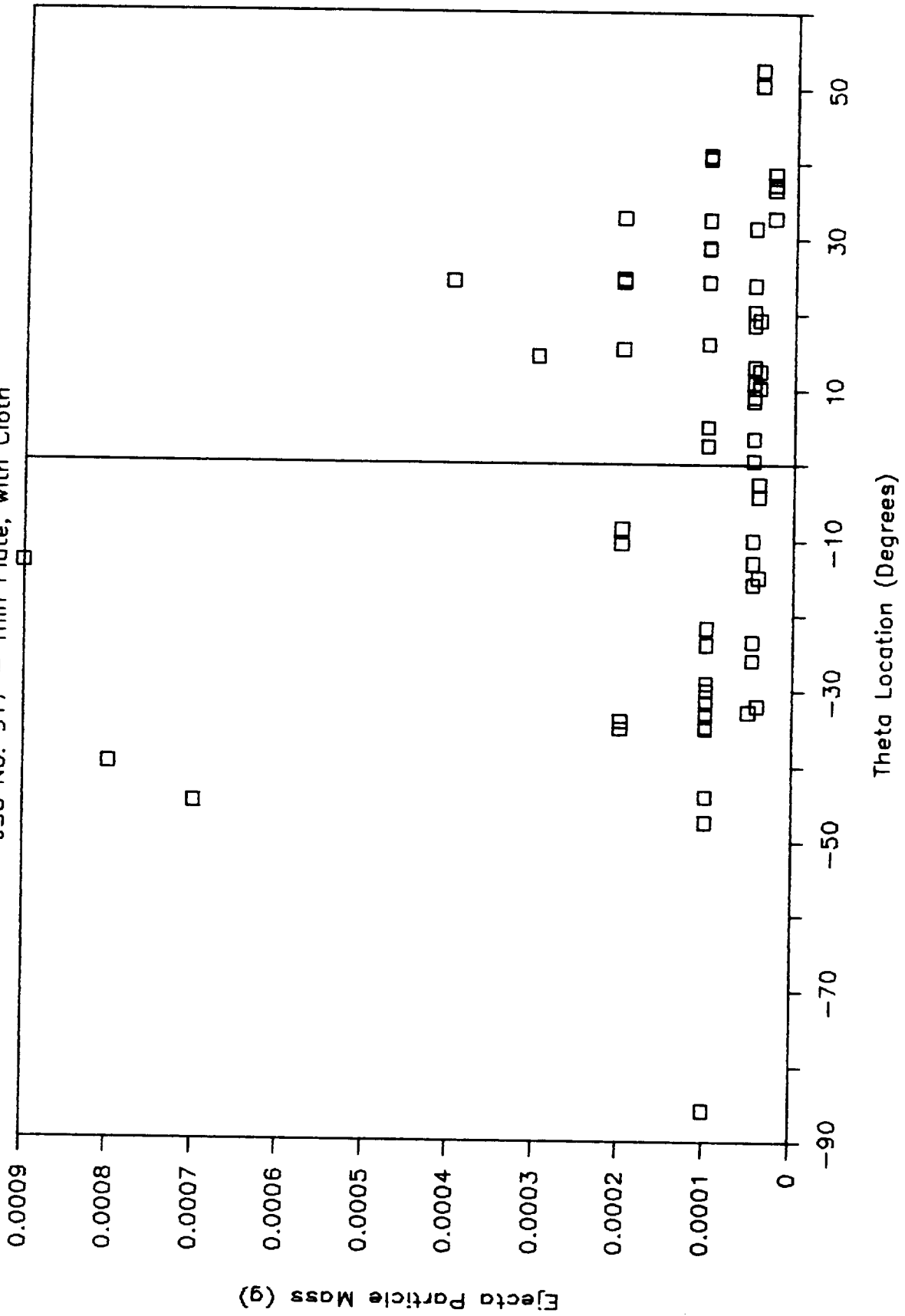


Figure 3-36

# EJECTA VELOCITY DISTRIBUTION

JSC No. 917 - Thin Plate, with Cloth

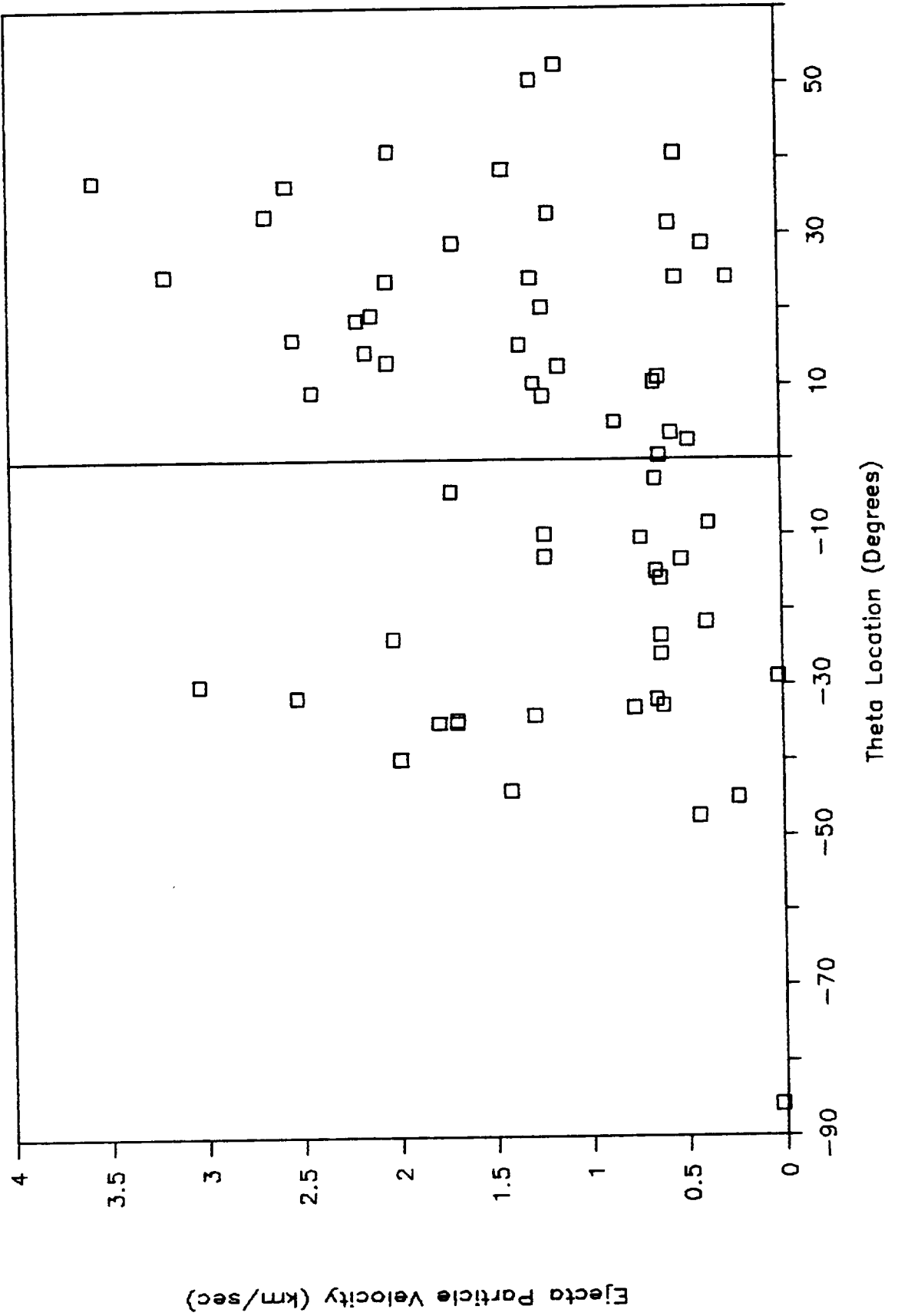


Figure 3-37

# EJECTA MASS DISTRIBUTION

JSC No. 917 - Thin Plate, with Cloth

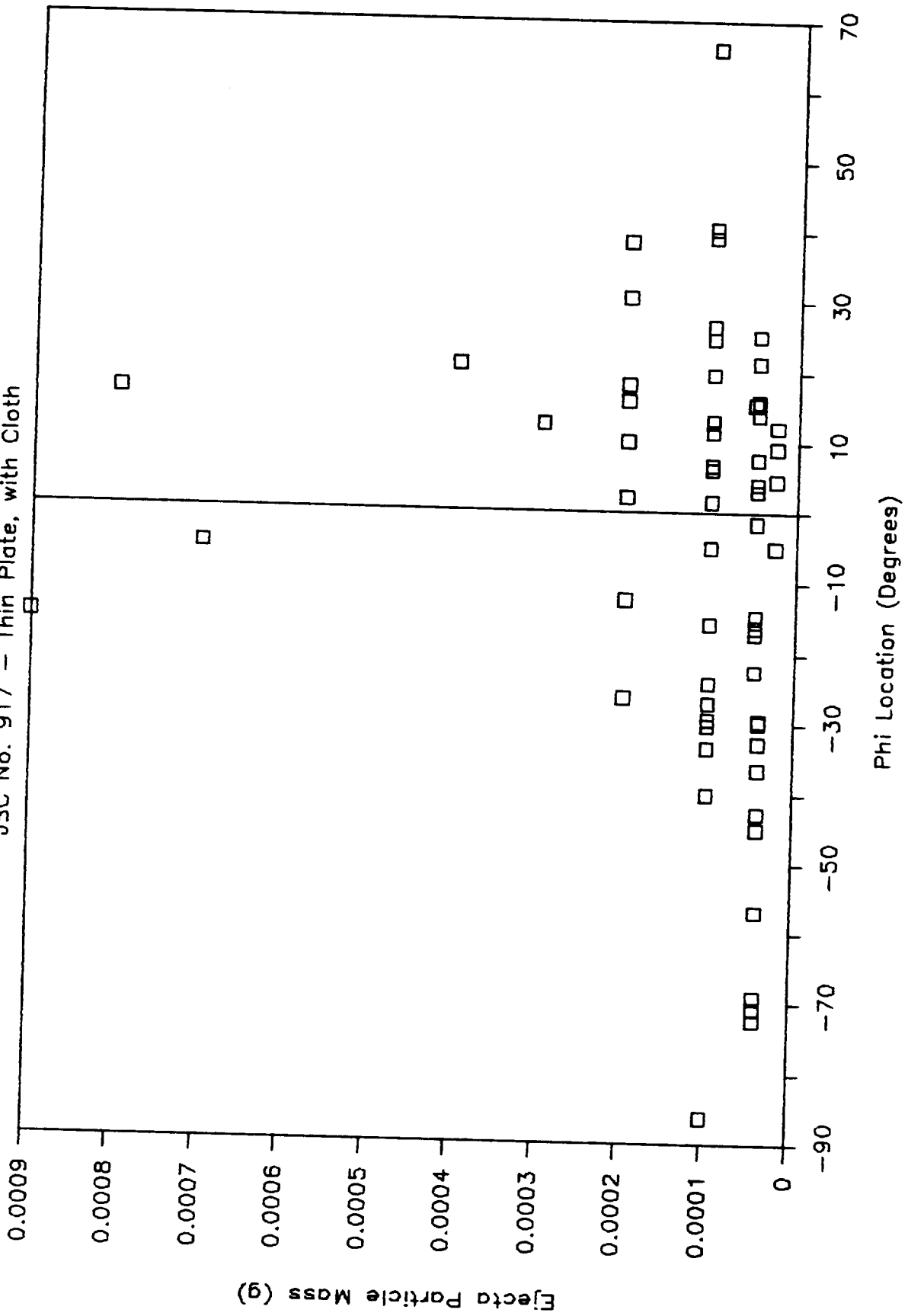


Figure 3-38

# EJECTA VELOCITY DISTRIBUTION

JSC No. 917 - Thin Plate, with Cloth

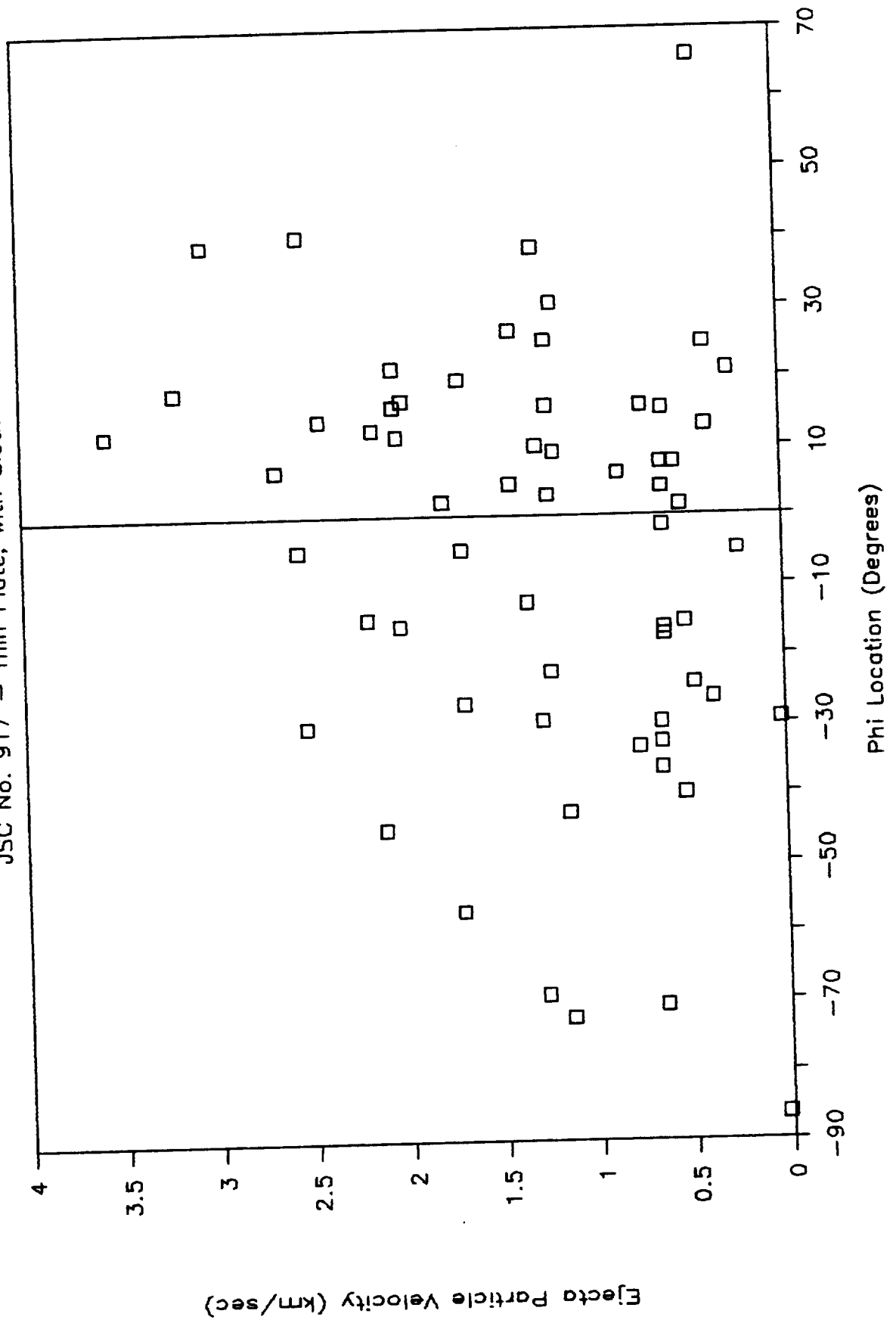


Figure 3-39

# EJECTA MASS DISTRIBUTION

JSC No. 917 - Thin Plate, with Cloth

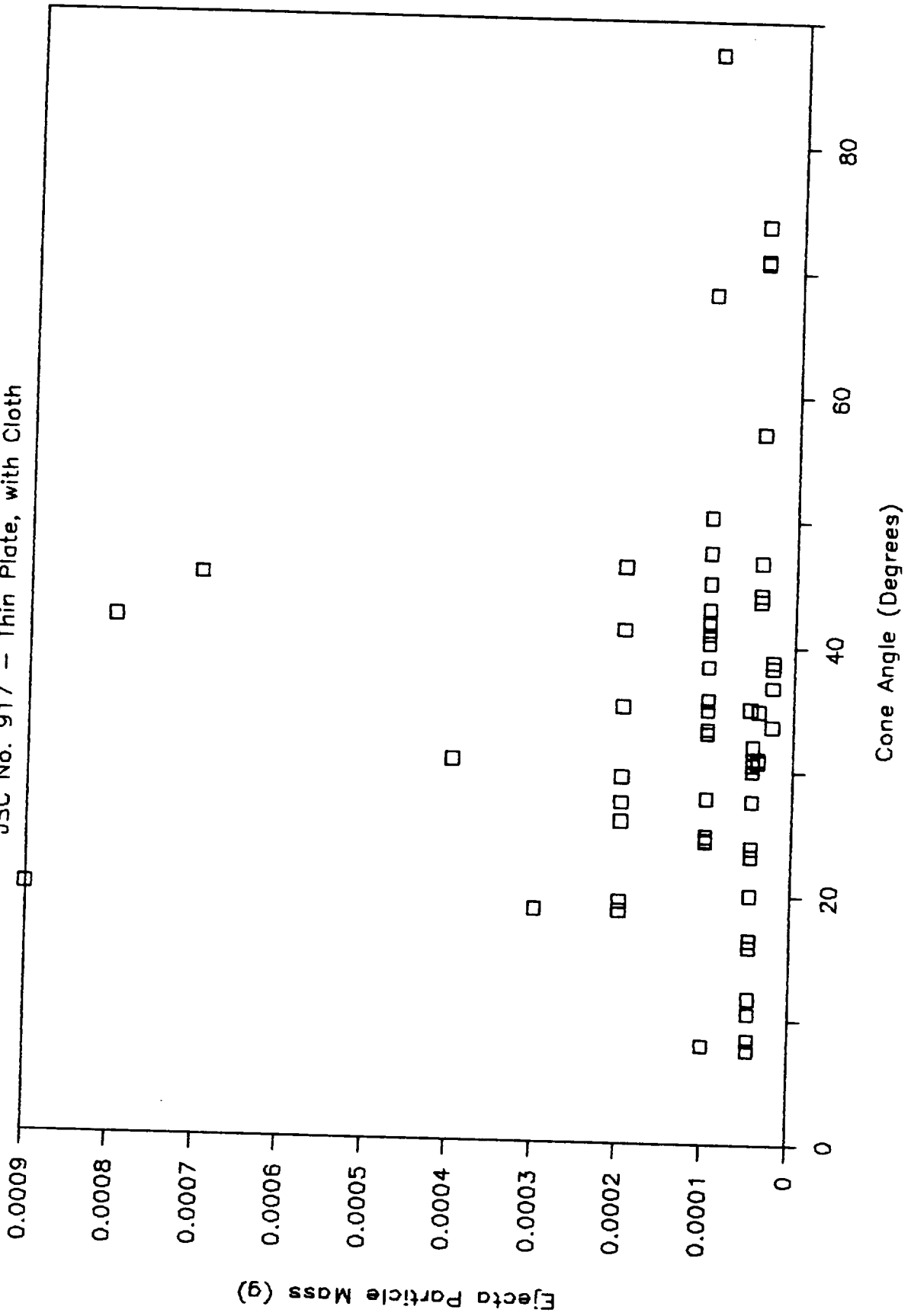


Figure 3-40

# EJECTA VELOCITY DISTRIBUTION

JSC No. 917 - Thin Plate, with Cloth

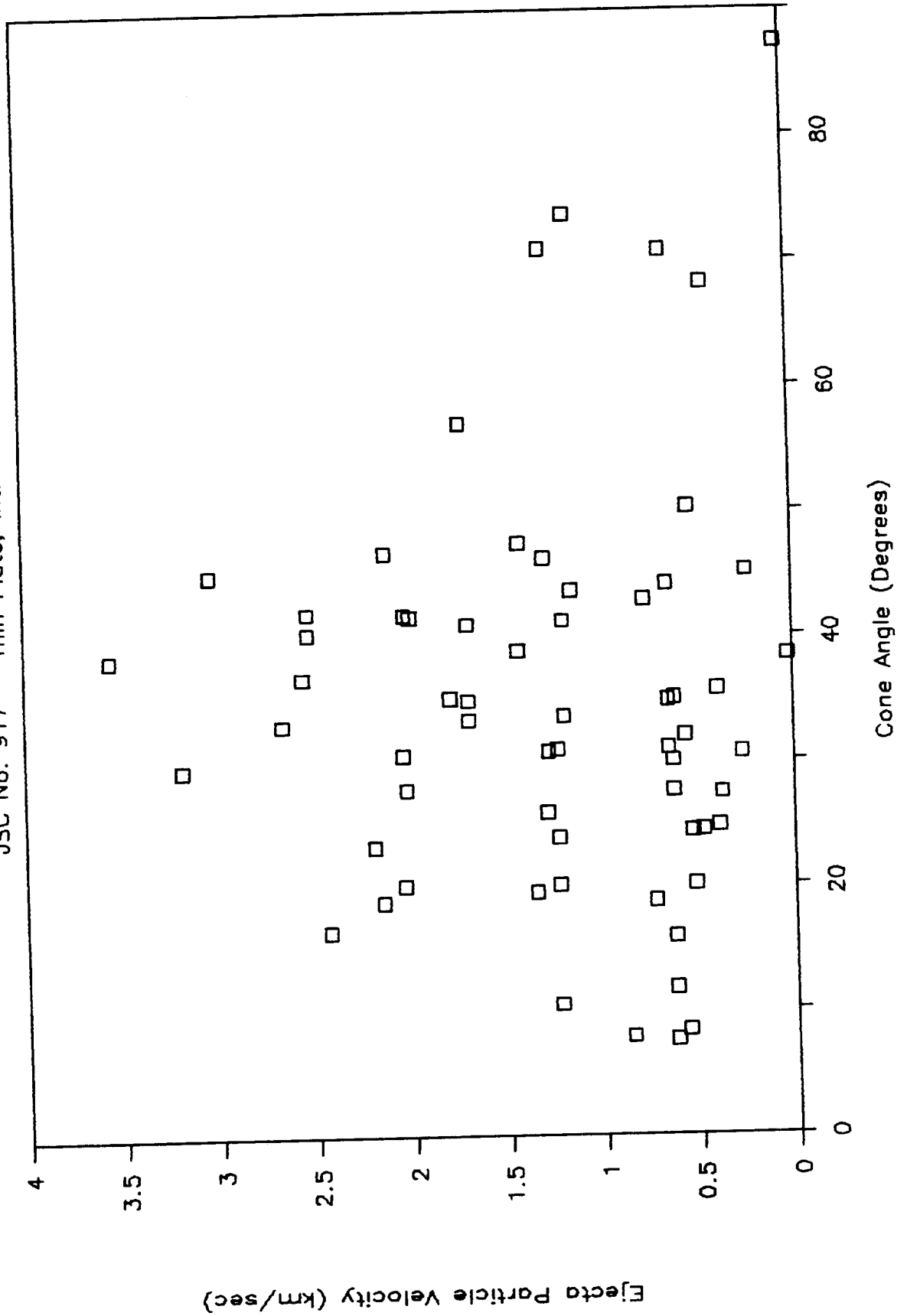


Figure 3-41

# EJECTA MASS & VELOCITY

JSC No. 917 - Thin Plate, with Cloth

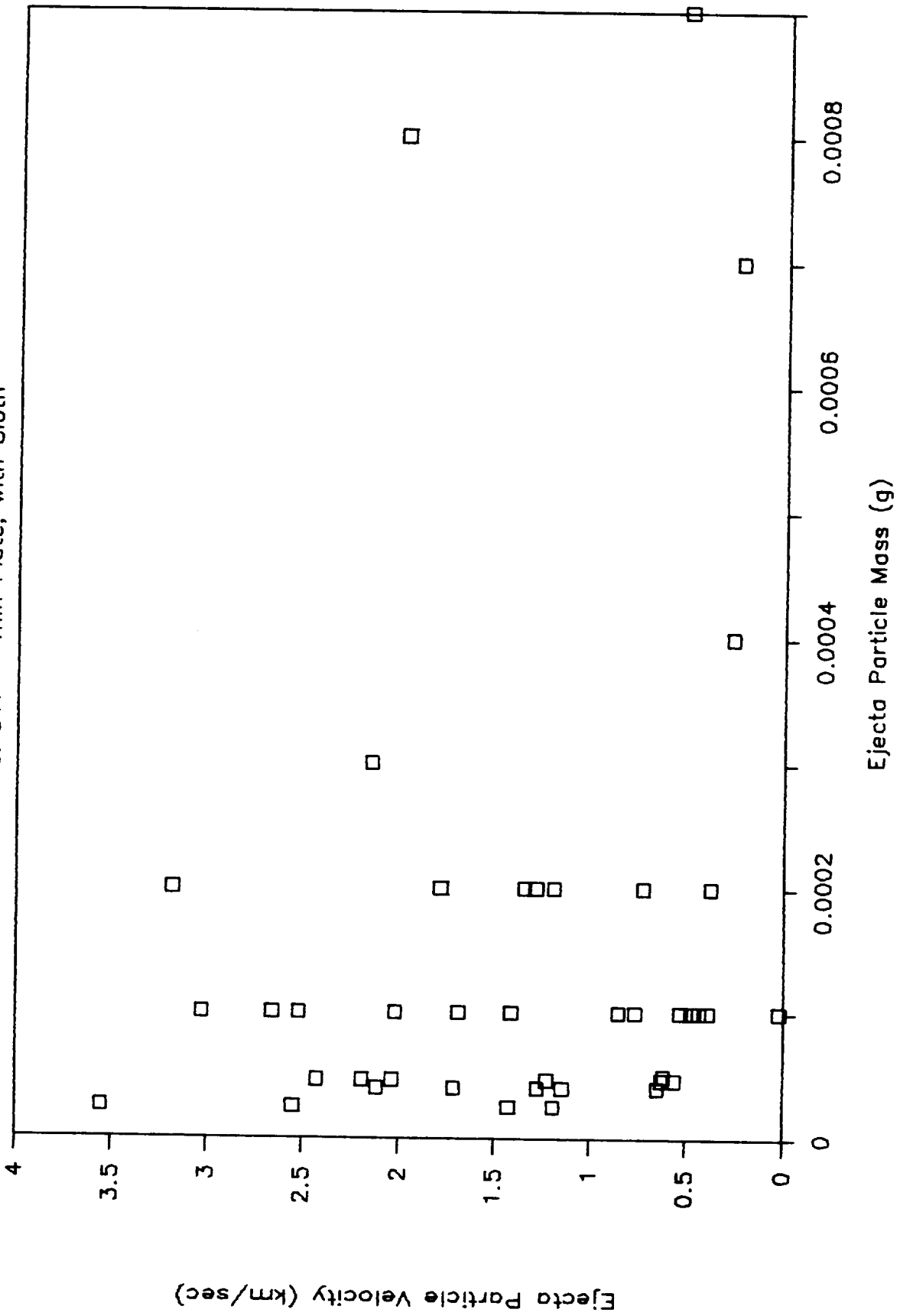


Figure 3-42

# EJECTA MASS AND PARTICLE NUMBER

JSC No. 917 - with Cloth

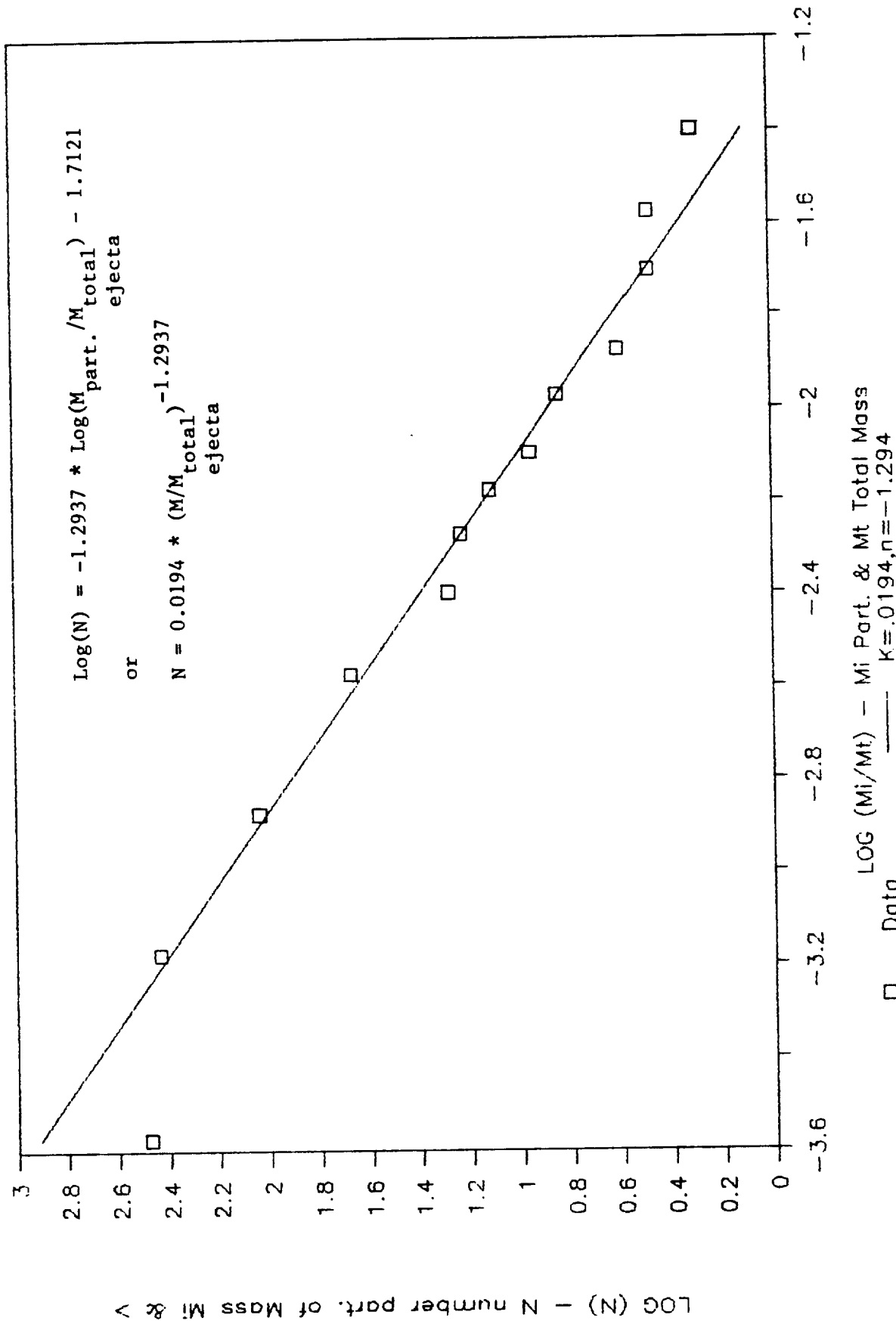




Figure 3-43

# SPALL MASS & LENGTH

JSC No. 917 - Thin Plate, with Cloth

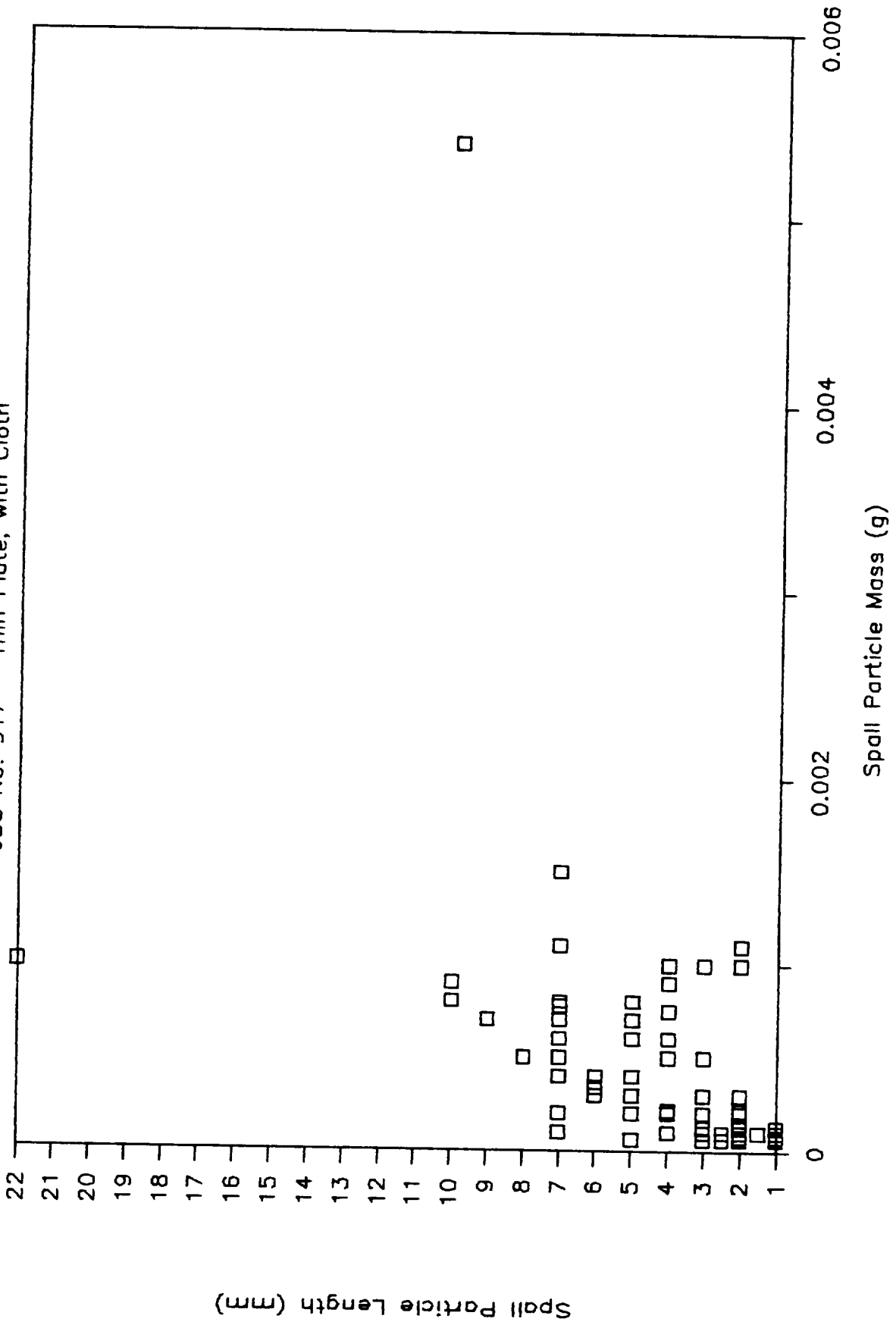


Figure 3-44

# SPALL MASS & DIAMETER

JSC No. 917 - Thin Plate, with Cloth

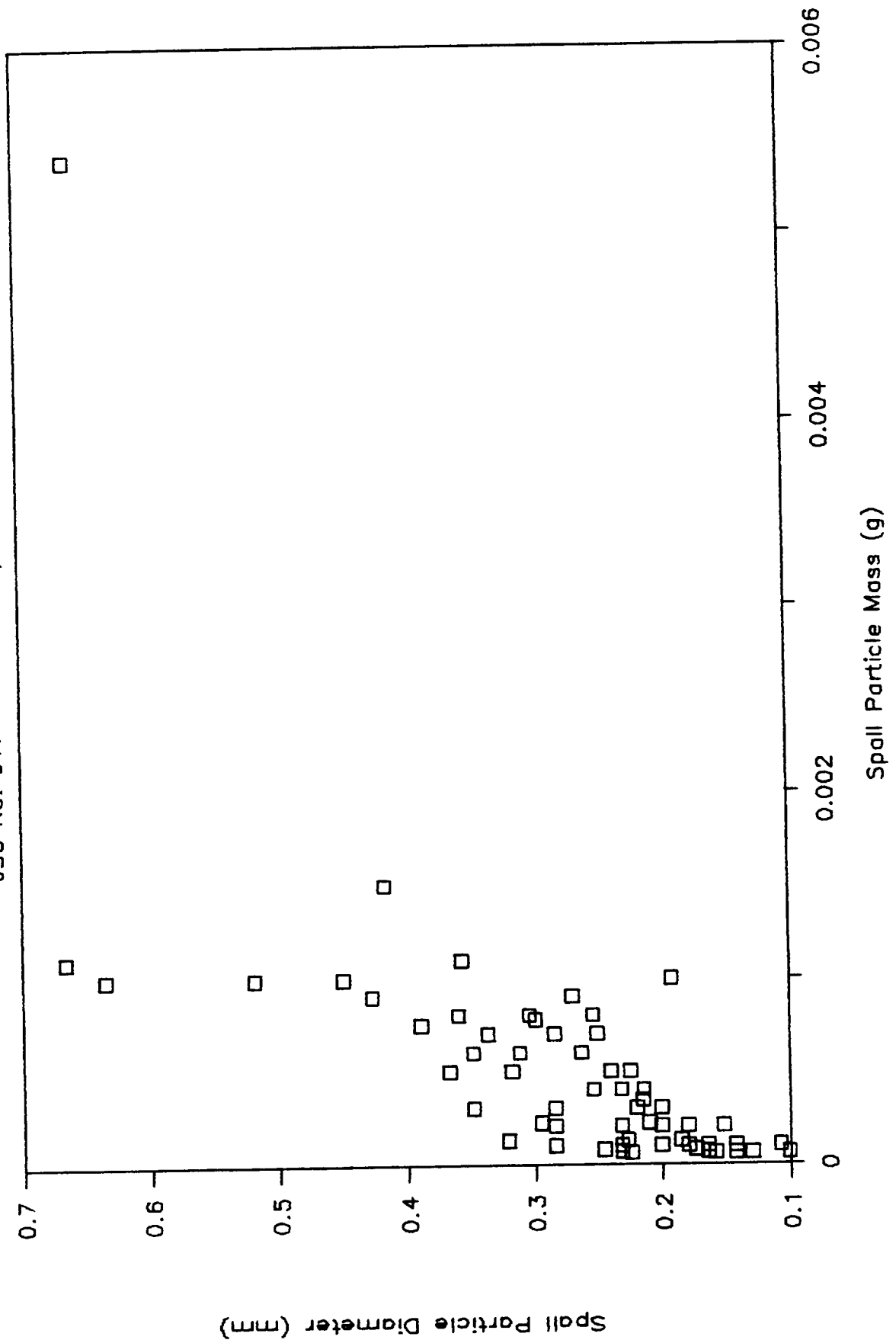


Figure 3-45

# SPALL MASS DISTRIBUTION

JSC No. 917 - Thin Plate, with Cloth

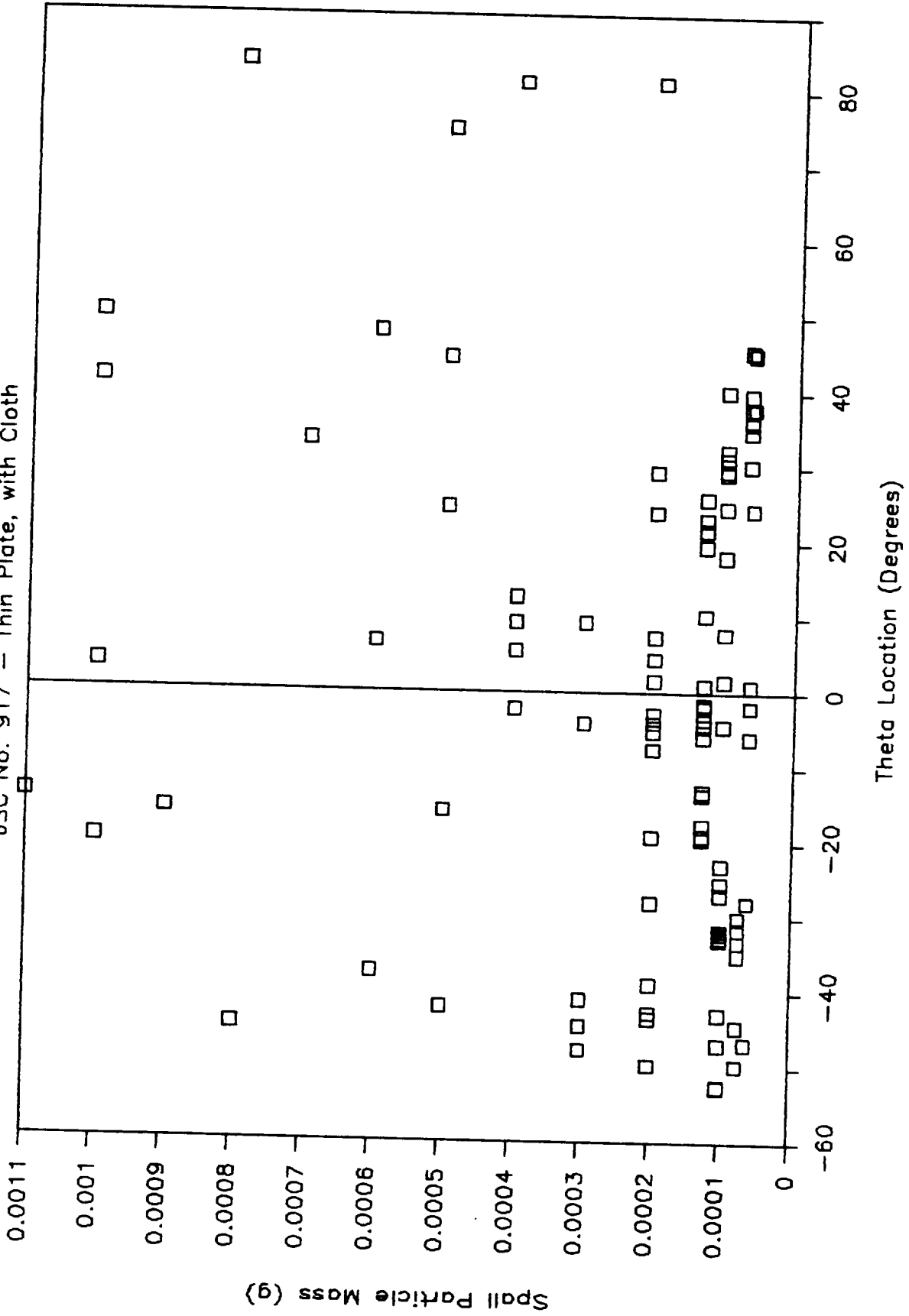


Figure 16

# SPALL VELOCITY DISTRIBUTION

JSC No. 917 - Thin Plate, with Cloth

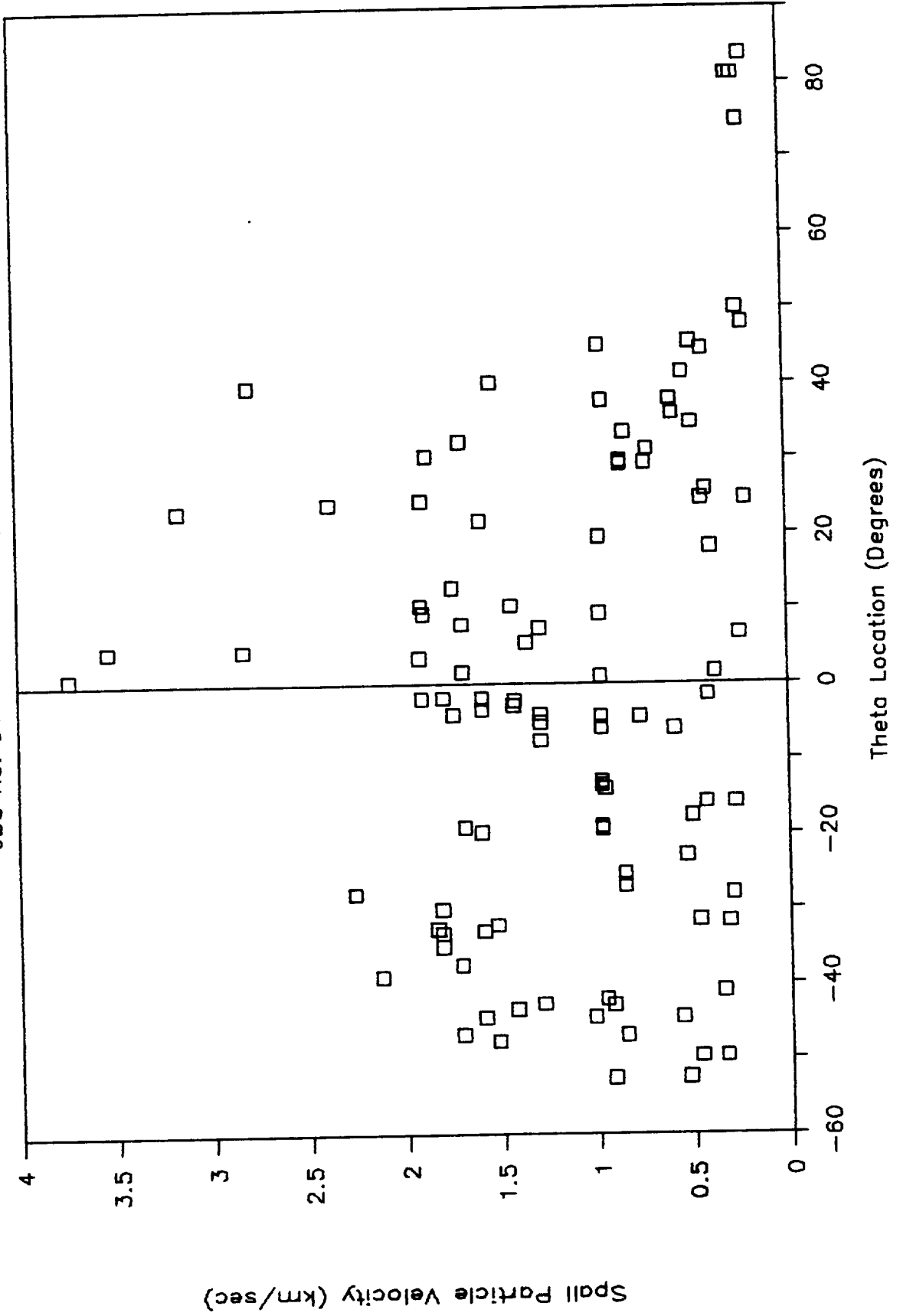


Figure 3-47

# SPALL MASS DISTRIBUTION

JSC No. 917 - Thin Plate, with Cloth

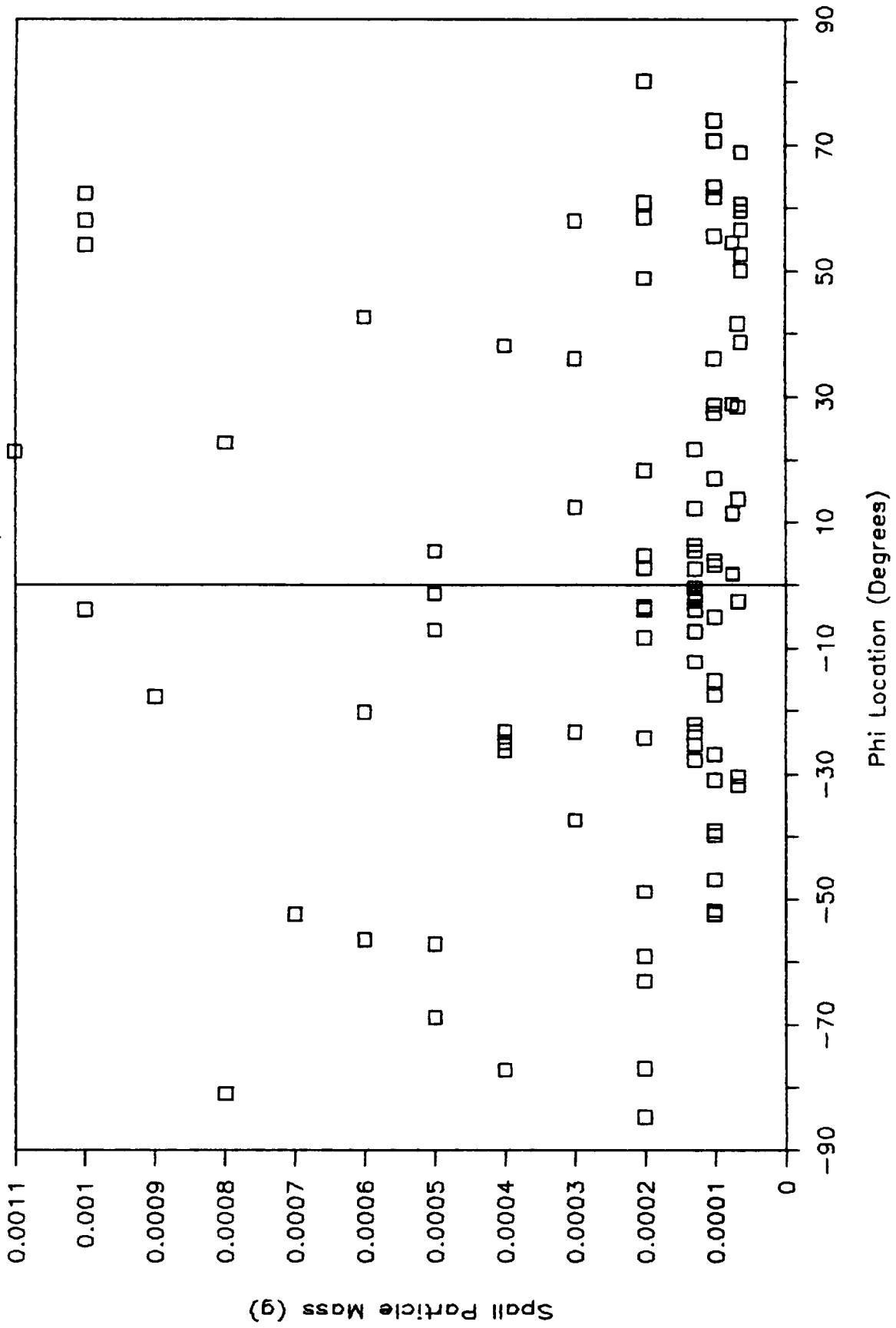


Figure 3-48

# SPALL VELOCITY DISTRIBUTION

JSC No. 917 - Thin Plate, with Cloth

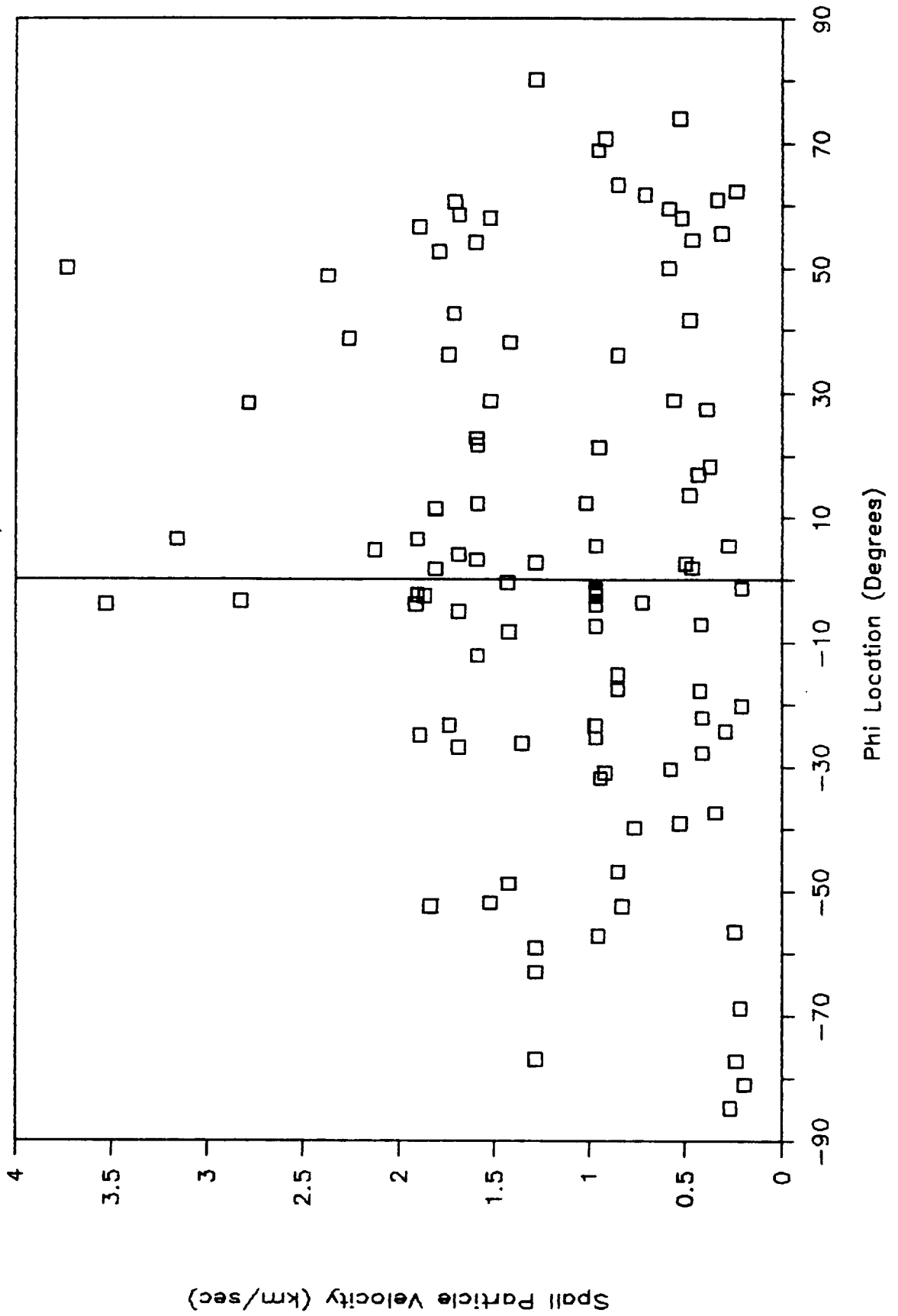


Figure 3-49

# SPALL MASS DISTRIBUTION

JSC No. 917 - Thin Plate, with Cloth

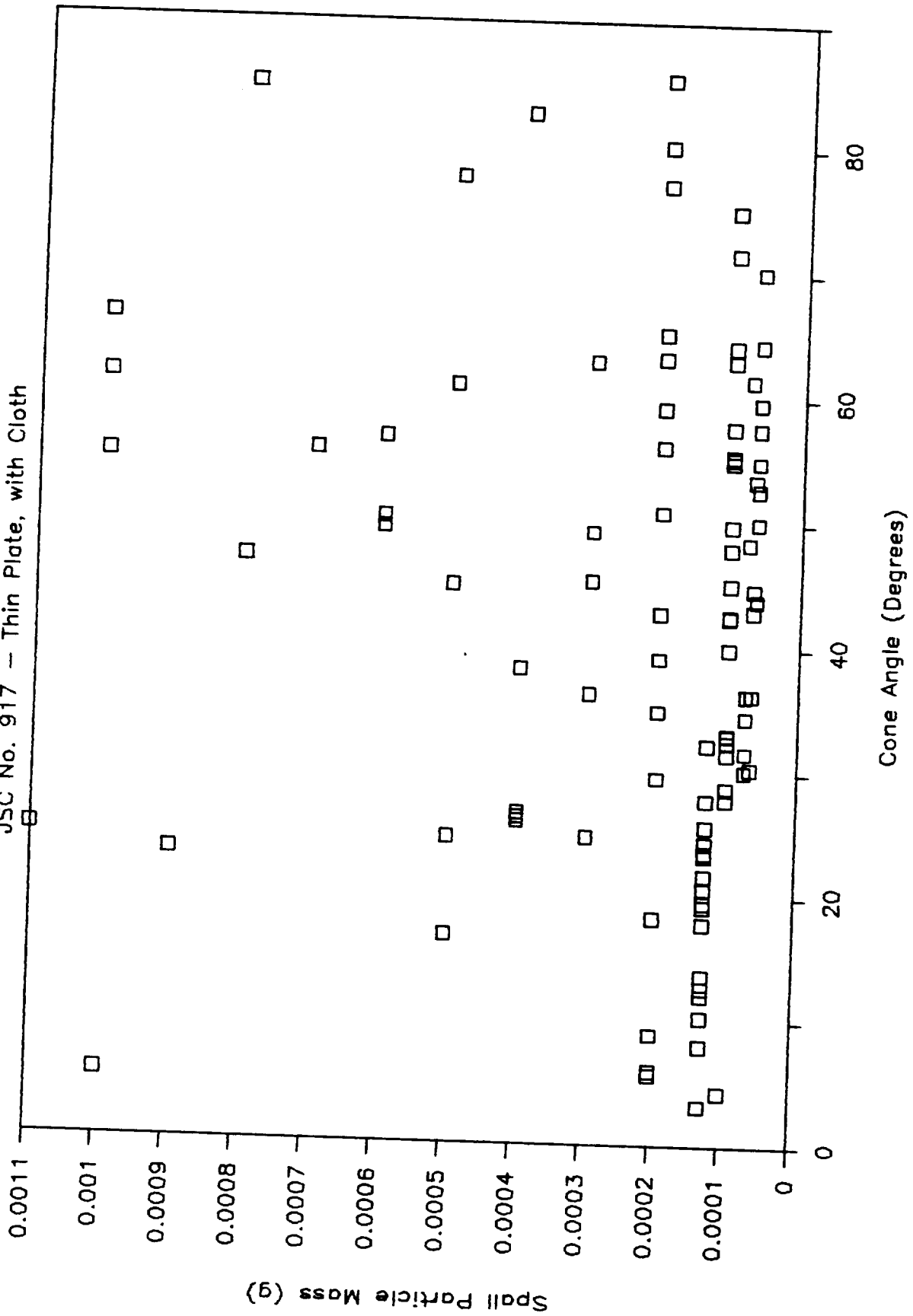


Figure 3-50

# SPALL VELOCITY DISTRIBUTION

JSC No. 917 - Thin Plate, with Cloth

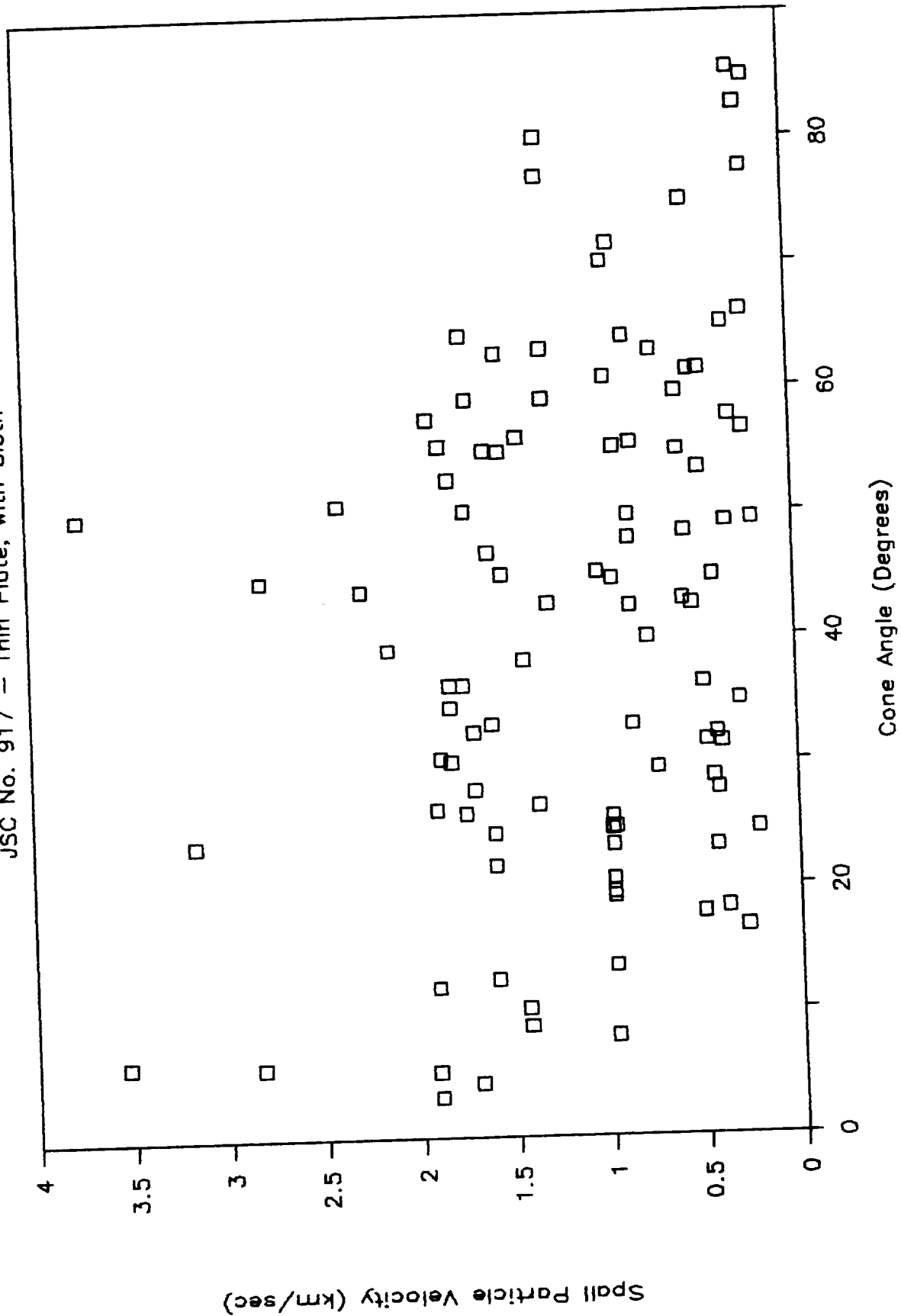




Figure 3-51

# SPALL MASS & VELOCITY

JSC No. 917 - Thin Plate, with Cloth

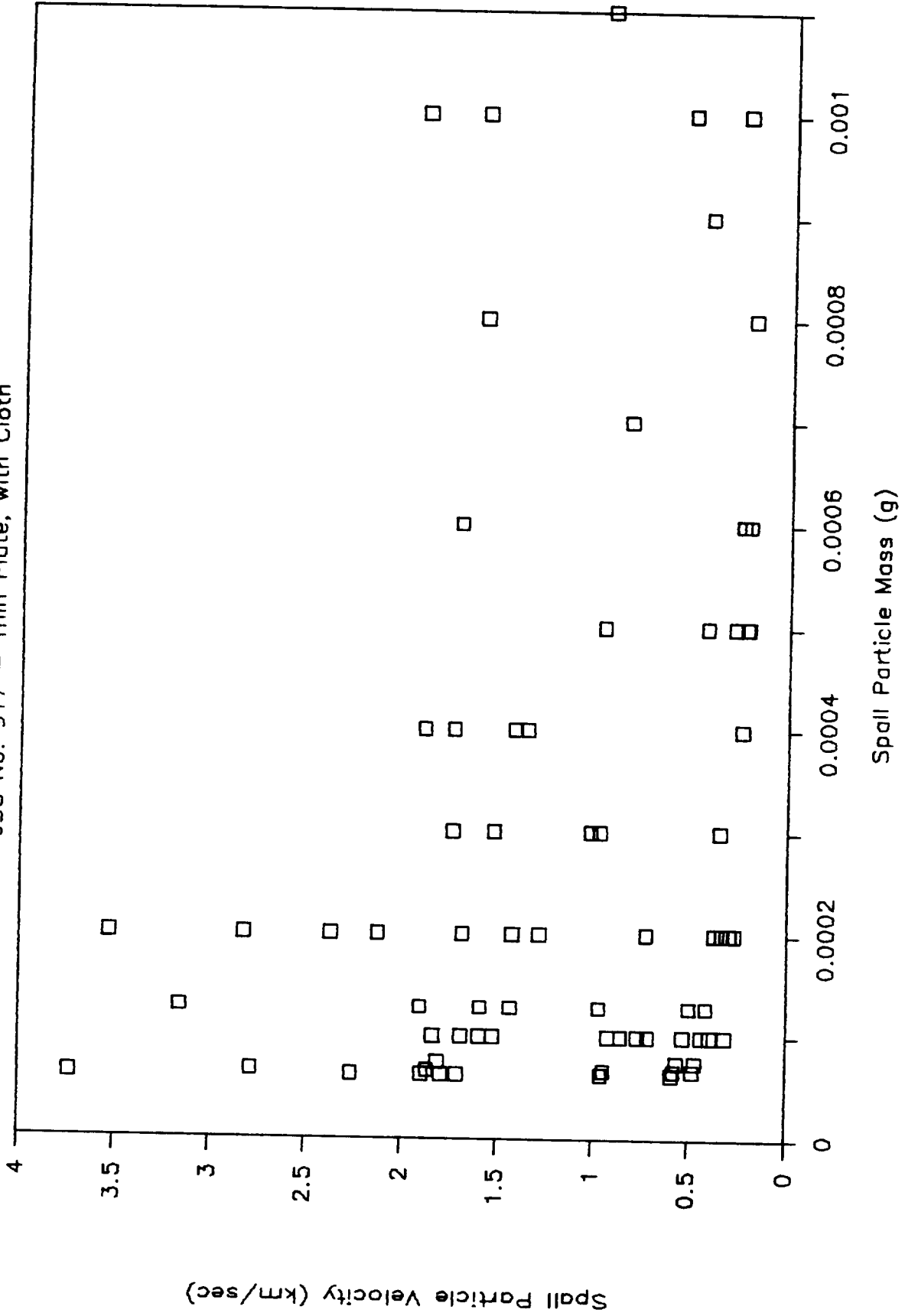


Figure 3-52

# SPALL MASS AND PARTICLE NUMBER

JSC No. 917 - with Cloth

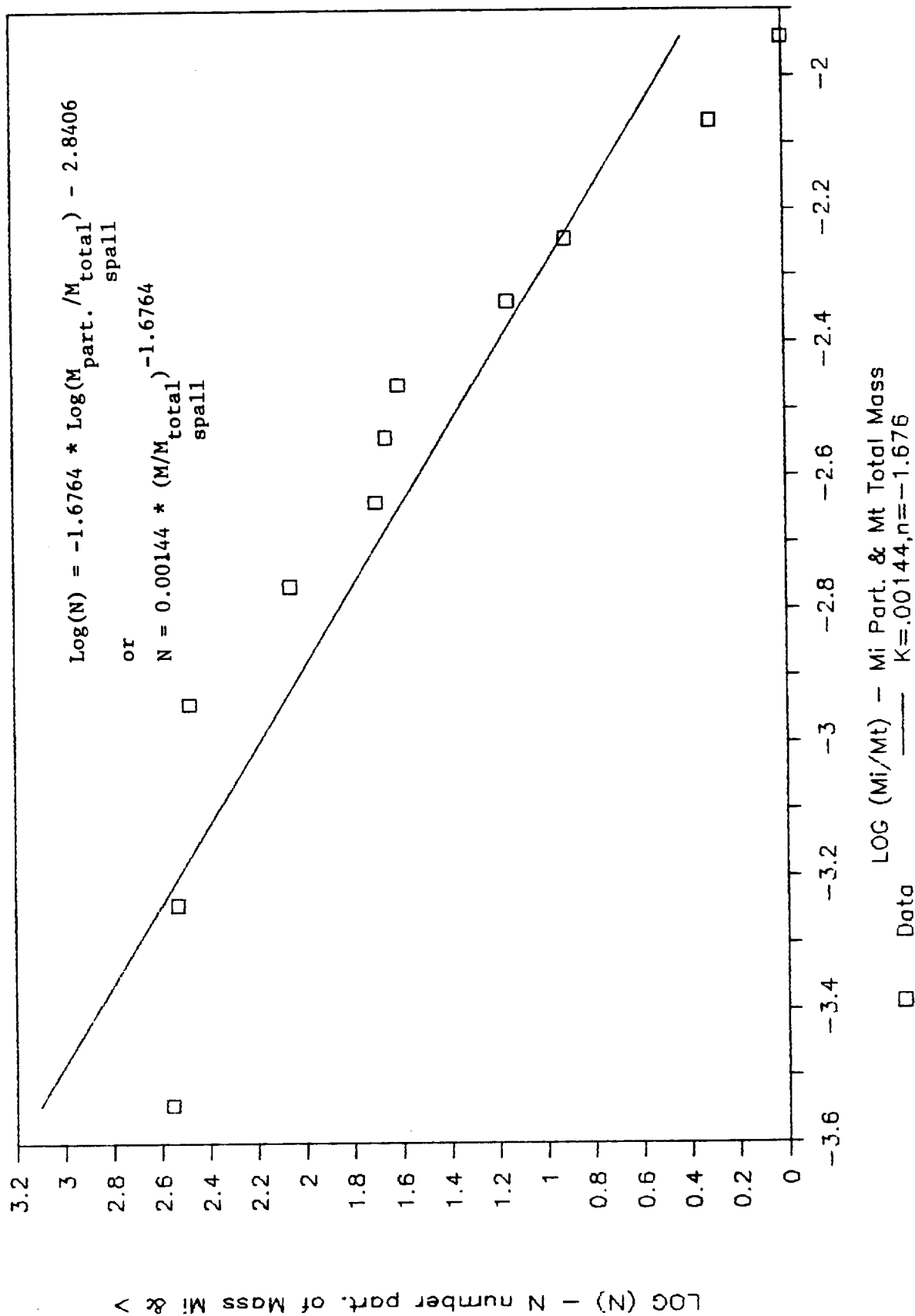


Figure 3-53

# EJECTA/SPALL MASS & PARTICLE NUMBER

JSC No. 917 - with Cloth

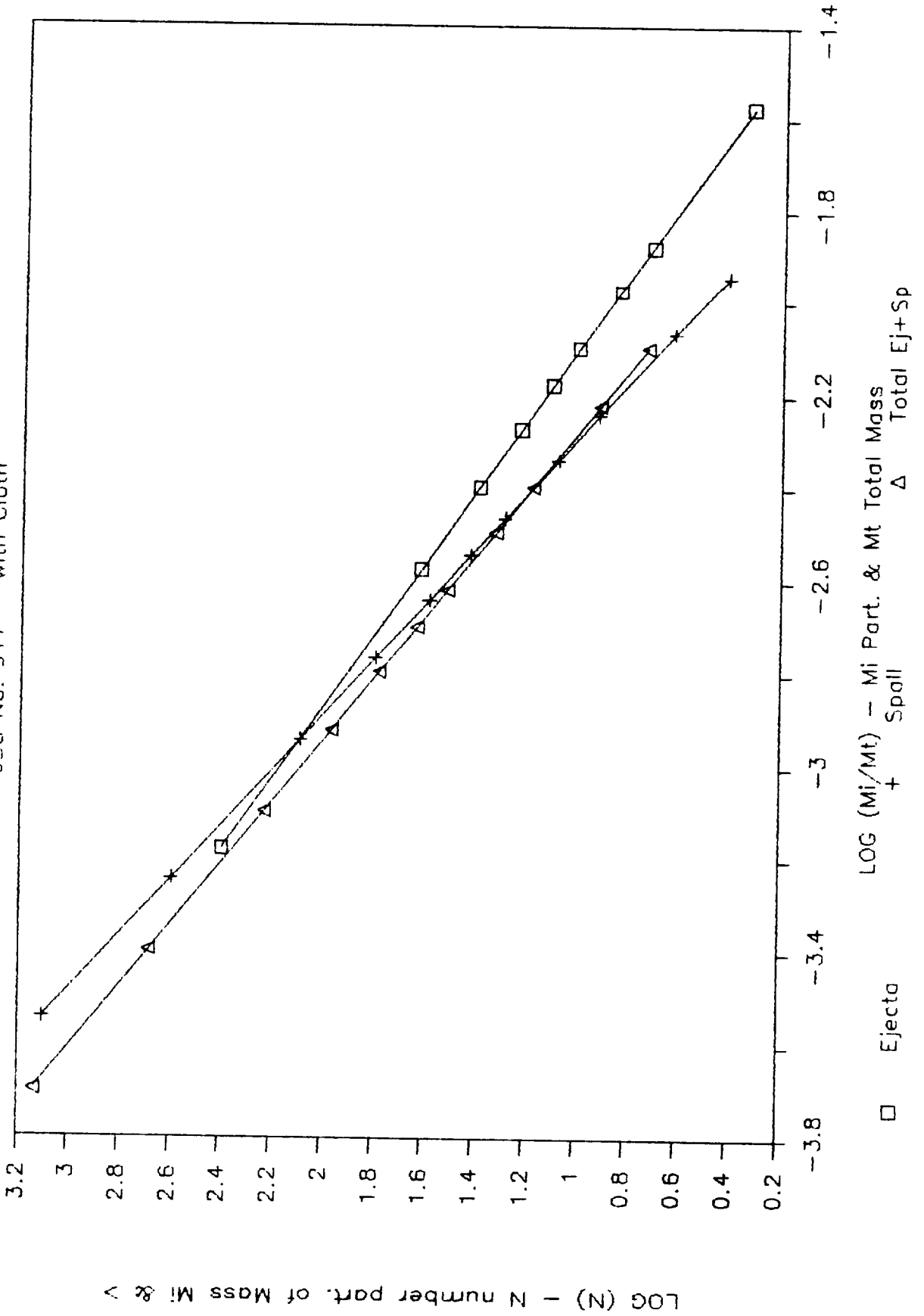
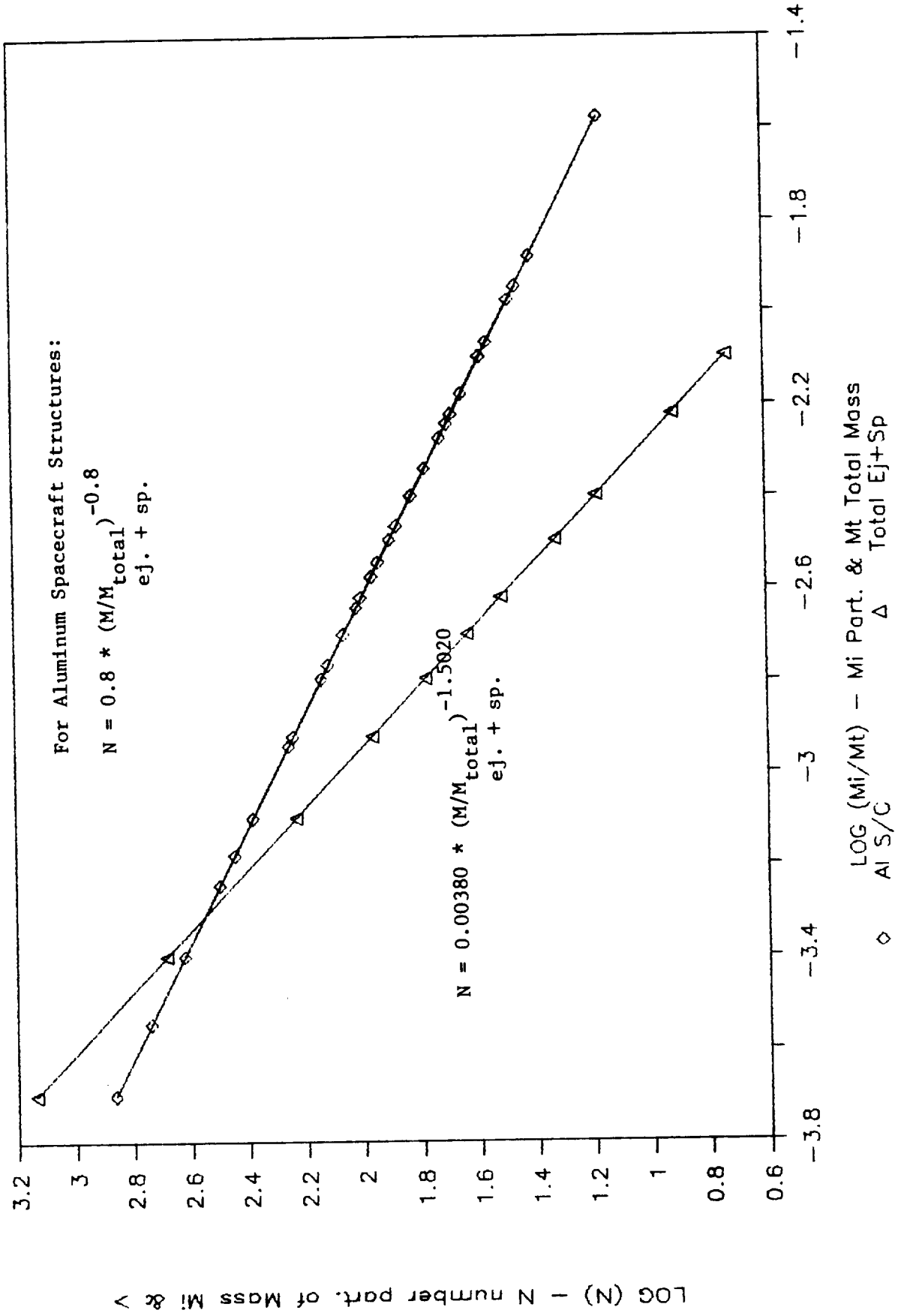


Figure 3-54

# EJECTA/SPALL MASS & PARTICLE NUMBER

JSC No. 917 - with Cloth



### 3.2.4 Shot #923 (0.095", without cloth, 30 deg. oblique impact)

This shot is similar to the previous two, except this target (JSC-02B-005) was angled 30 degrees to the projectile velocity vector and had no cloth covering, predicted to result in more ejecta and spall. This shot was also at a higher velocity (7.02 km/sec versus roughly 5 and 6 km/sec for the previous two thin G/E shots).

Figure 3-55 shows the catcher box made of plexiglass and lined with styrofoam. The large holes in two of the styrofoam side panels were to allow single frame photography, which didn't work on this shot. Appendix C shows some single frames that did work on graphite/epoxy shots. Approximate velocity data can be deduced from the single frame shots.

Figure 3-56 shows photos of the the target after impact. Compare it to Figure 3-32, from the previous shot, with cloth. The cloth reduces the number of large particles, but not the total mass of ejecta and spall as shown in Table 3-2. The total mass ejected and spalled in this shot was exactly the same as for the previous shot, even though the velocity and angle of impact were different. This indicates that cloth covering (and perhaps 1 km/sec velocity and 30 degree angle) do not have large effects on the total mass of ejecta and spall. The factors could be offsetting however, and hidden variables such as projectile impact attitude could also be playing a part. In any event, given the low level of approximation needed in this rough assessment of damage hazard, these factors (30 deg. angle, w/wo cloth, 1 km/sec) are assumed unimportant when equations that describe the spall and ejecta are produced. A many shot program focusing on these factors alone will be needed to see their effects.

Figures 3-57 and 3-58 plot ejecta mass versus length and diameter. A comparison with Figures 3-26 and 3-33 shows that the largest particle lengths for the two no cloth shots are about the same. The no cloth, 30 degree angle shot has the most massive piece of ejecta however, by a factor of three.

Figures 3-59 through 3-62 plot ejecta mass and calculated velocity versus theta and phi (see Appendix B for a definition of theta and phi).

Figures 3-63 and 3-64 plot ejecta mass and velocity versus cone angle. The cone angle, in this case, is the angle between the outgoing ejecta or spall particle's velocity vector and a normal to the plane of the target's face, coming out of the impact point. The mass distribution seems fairly uniform between 20 and 70 degrees. Table 3-2, which calculates an average cone angle, shows an average of 47 degrees.

Figure 3-65 plots ejecta mass versus velocity. This plot shows the small particles going faster than the big ones, fairly clearly.

Figure 3-66 plots the Log(number of ejecta particles of mass  $M_i$  and larger) versus the Log( $M_i/M_{total}$  ejecta mass). A least squares fit linear relationship for these two quantities and the derived equations (with and without the Logs) that result are also shown.

Figures 3-67 and 3-68 plot spall mass versus length and diameter. Compare the plots with Figures 3-57 and 3-58.

Figures 3-69 through 3-72 plot spall mass and velocity versus  $\theta$  and  $\phi$ .

Figures 3-73 and 3-74 plot spall mass and velocity versus cone angle. The cone angle is the angle between a normal to the target surface at the impact point and the ejecta particle's velocity vector.

Figure 3-75 plots spall mass versus velocity.

Figure 3-76 plots the Log(number of spall particles of mass  $M_i$  and larger) versus the Log( $M_i/M_{total}$  spall mass). A least squares fit linear relationship for these two quantities and the derived equations (with and without the Logs) are also shown.

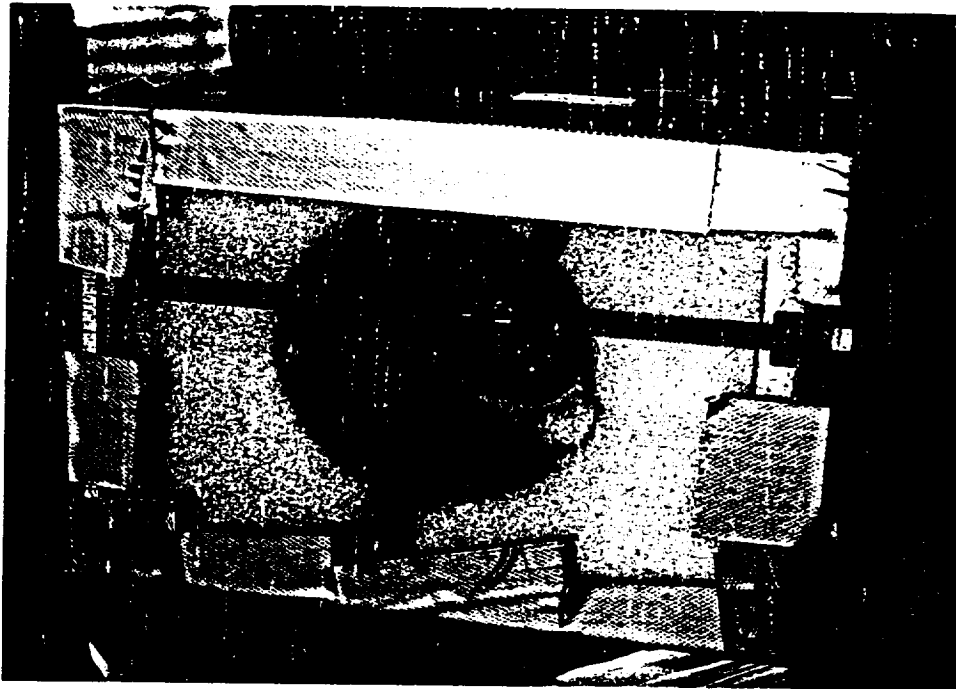
Figure 3-77 plots the equations from Figures 3-66 and 3-76 and the Log Log plot of total ejecta and spall. The lines are all close together, indicating they could all be approximated by one line.

Figure 3-78 plots the Log Log total ejecta and spall line along with an aluminum line (from Ref. 1). The results are similar to previous plots. The equations derived will be used to estimate the damage hazard to the Space Station.

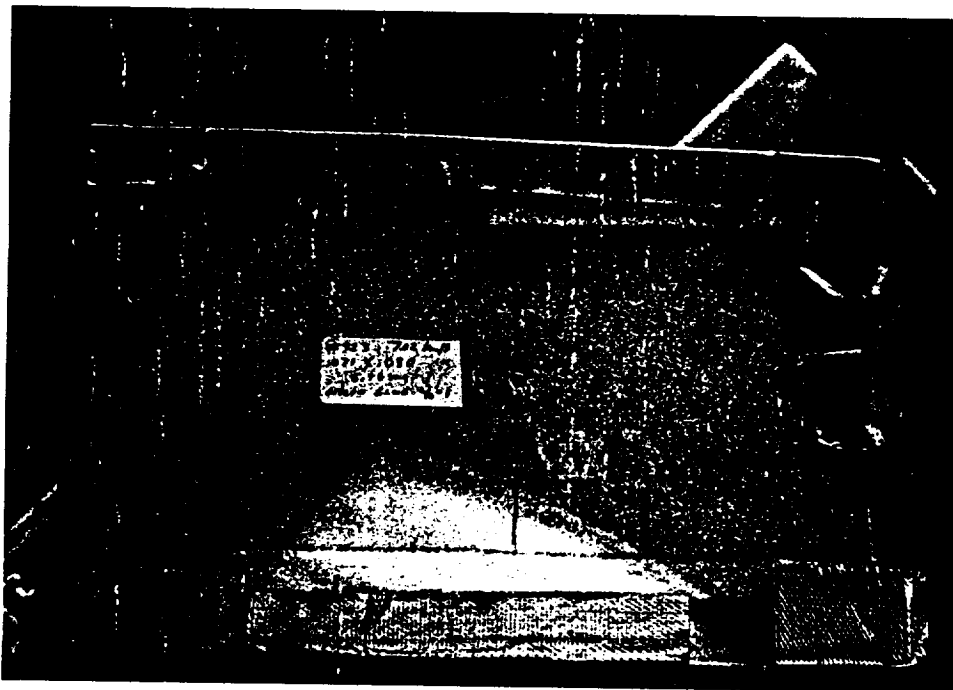
Figure 3-55, Photos of Catcher Box (Shot #923)

JSC 02B-005, 0.095 inch thick, graphite/epoxy, no cloth on front

Projectile  
enters



Side View

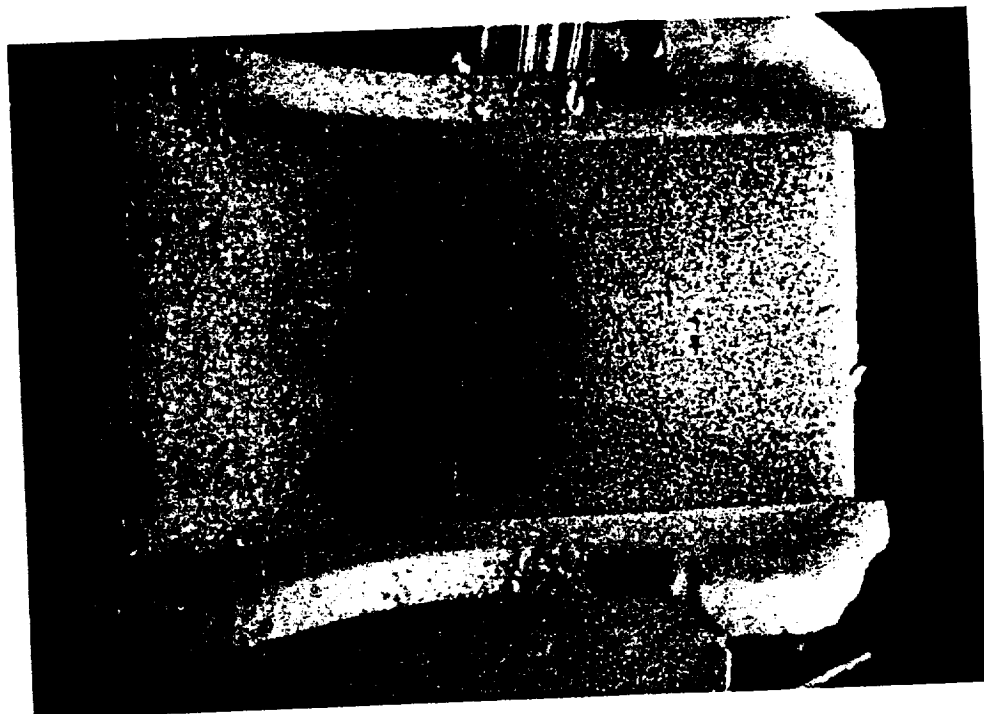


Top View

Figure 3-55, Continued, Photos of Catcher Box (Shot #923)  
JSC 02B-005, 0.095 inch thick, graphite/epoxy, no cloth on front



Top View



Spall on  
back wall



**Figure 3-56, Photos of Target (Shot #923)**

JSC 02B-005, 0.095 inch thick, graphite/epoxy, no cloth on front

Front

Back

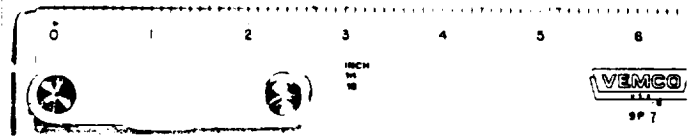
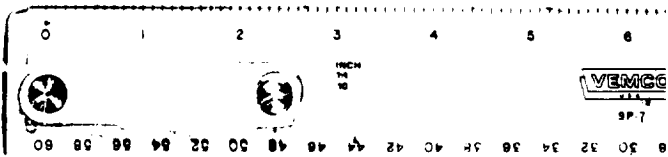
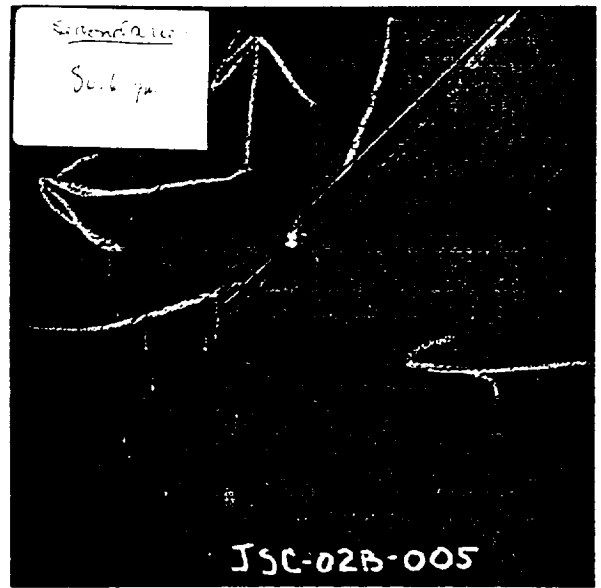
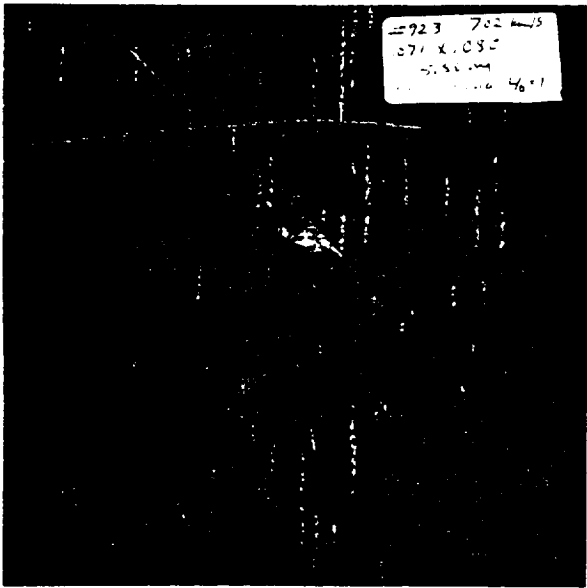


Figure 3-57

# EJECTA MASS & LENGTH

JSC No. 923 - No Cloth, 30 deg Impact

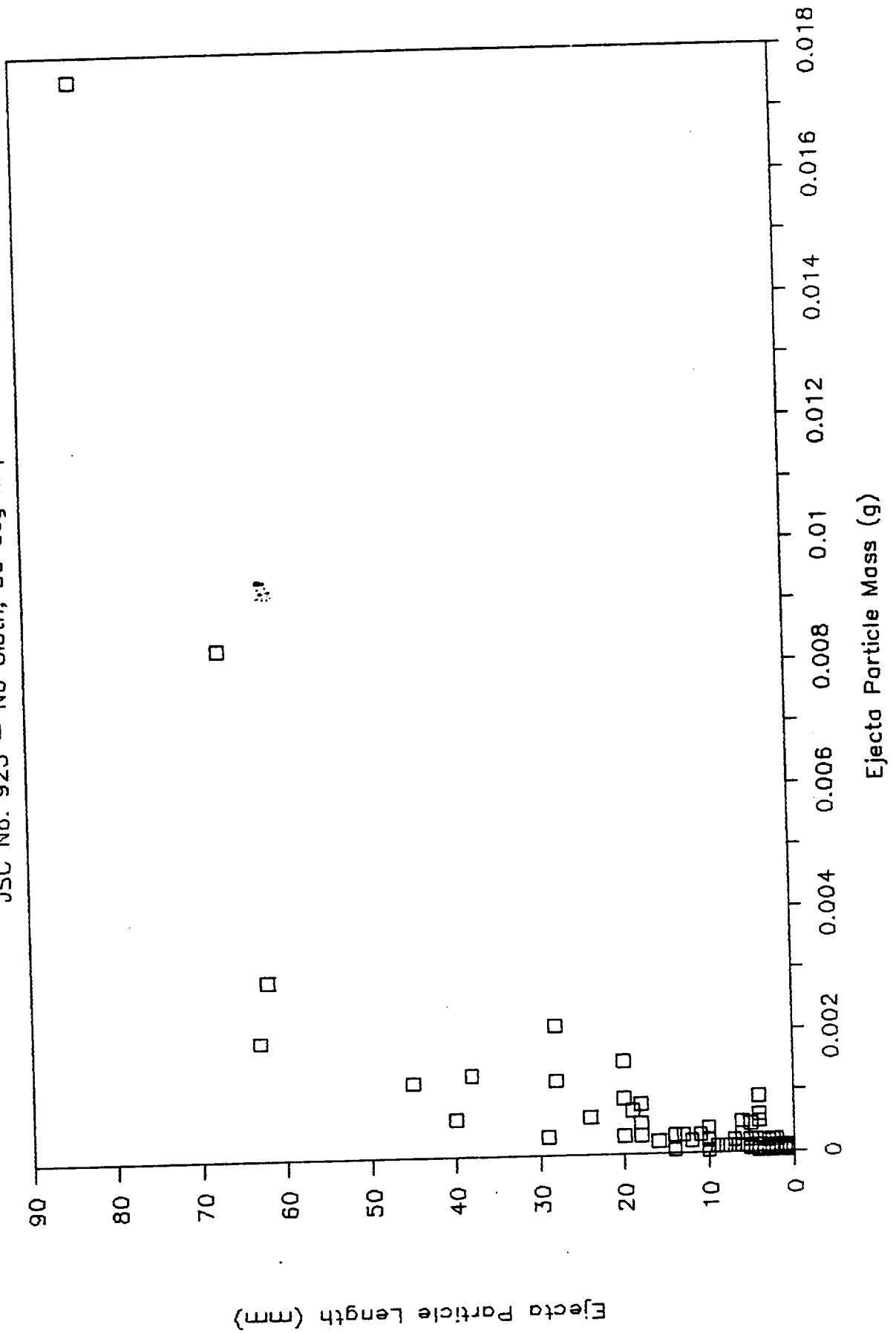


Figure 3-58

# EJECTA MASS & DIAMETER

JSC No. 923 - No Cloth, 30 deg Impact

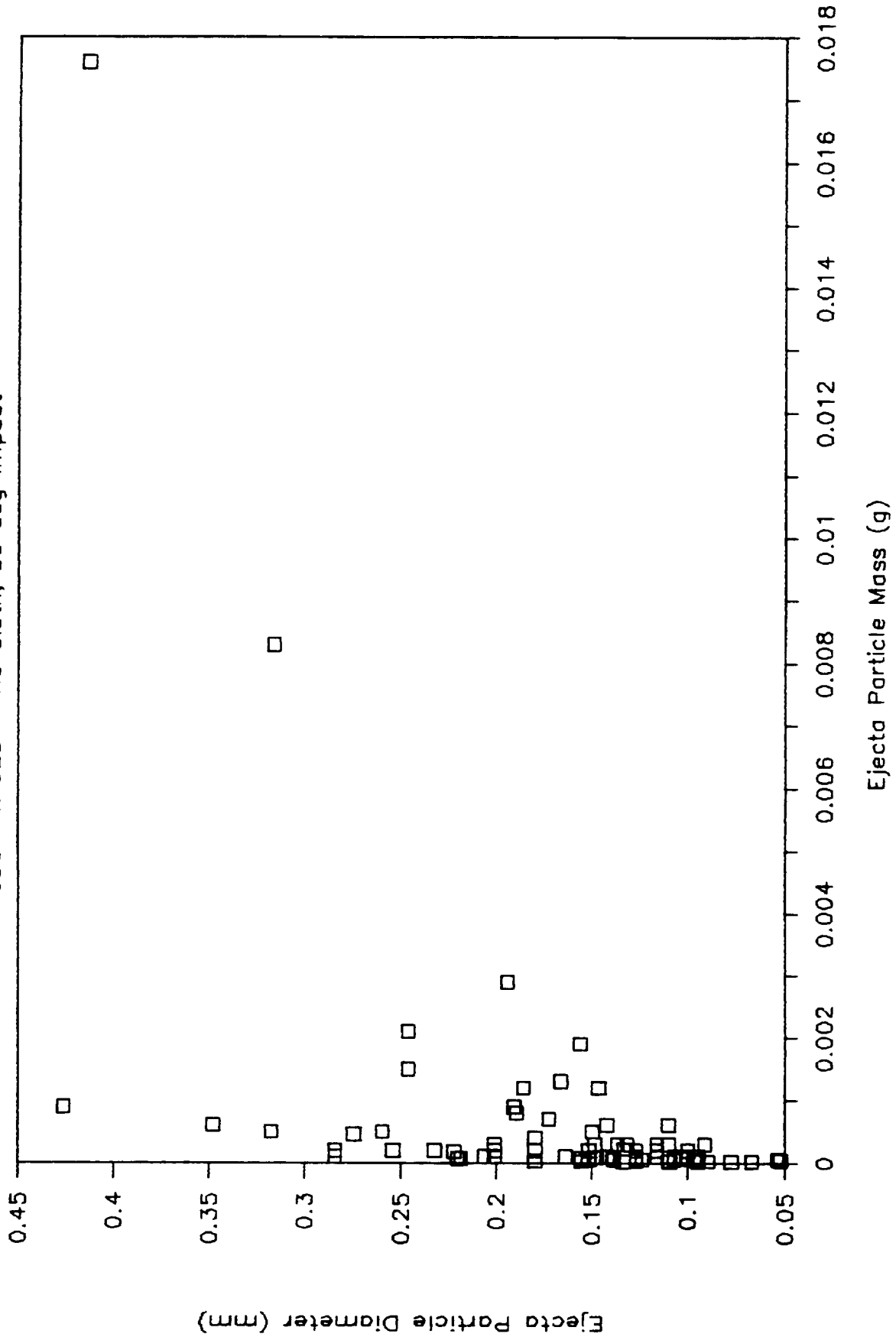


Figure 3-59

# EJECTA MASS DISTRIBUTION

JSC No. 923 - No Cloth, 30 deg Impact

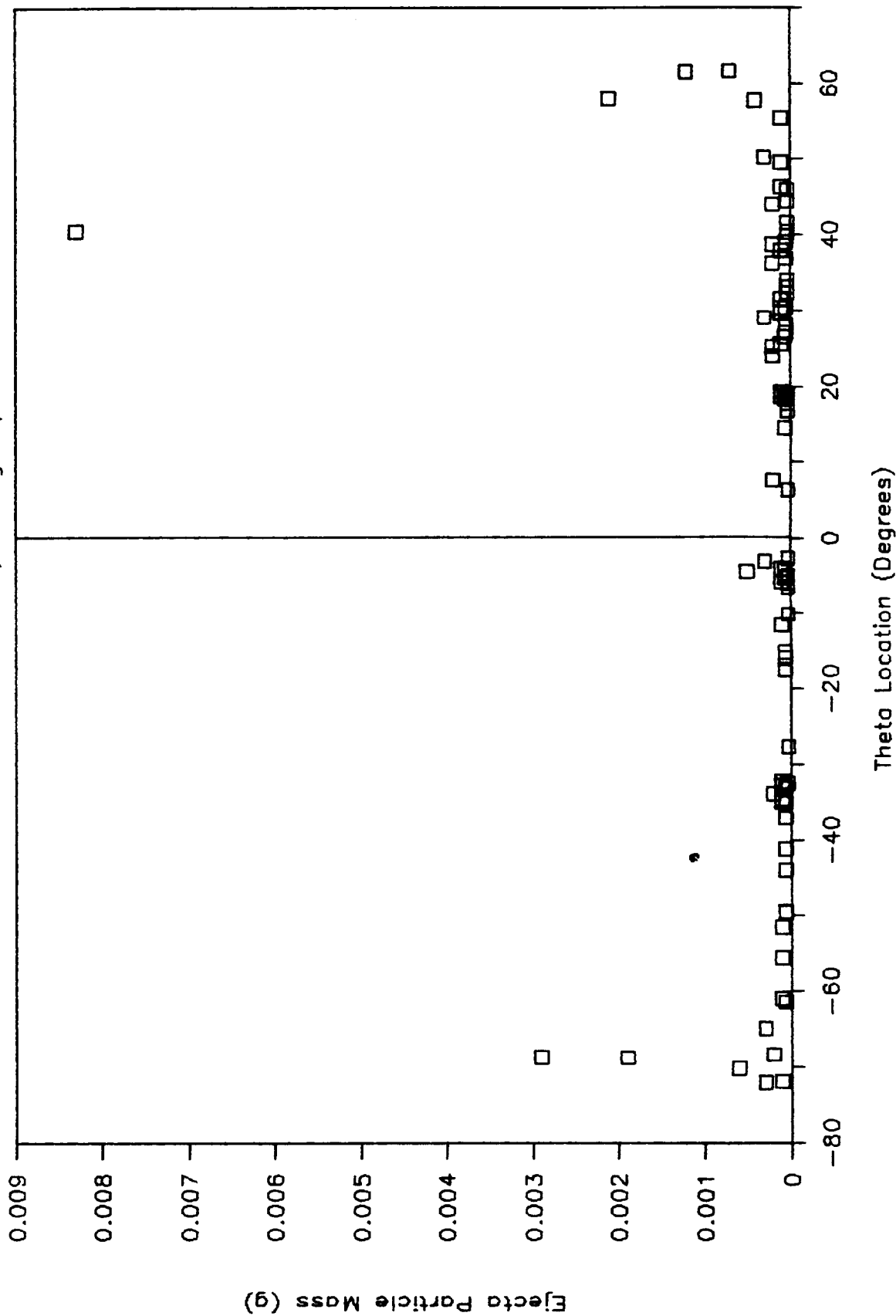


Figure 3-60

# EJECTA VELOCITY DISTRIBUTION

JSC No. 923 - No Cloth, 30 deg Impact

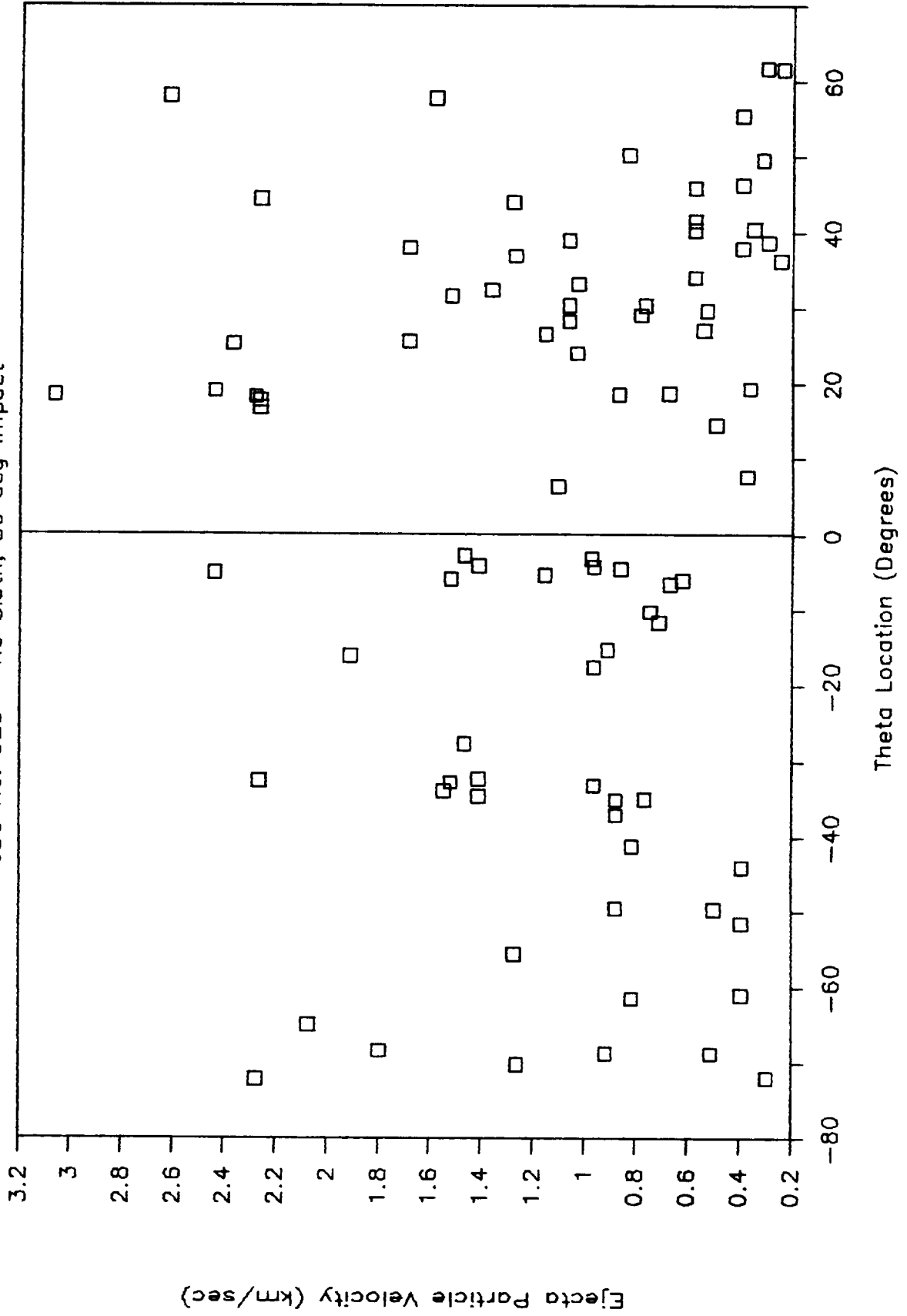


Figure 3-61

# EJECTA MASS DISTRIBUTION

JSC No. 923 - No Cloth, 30 deg Impact

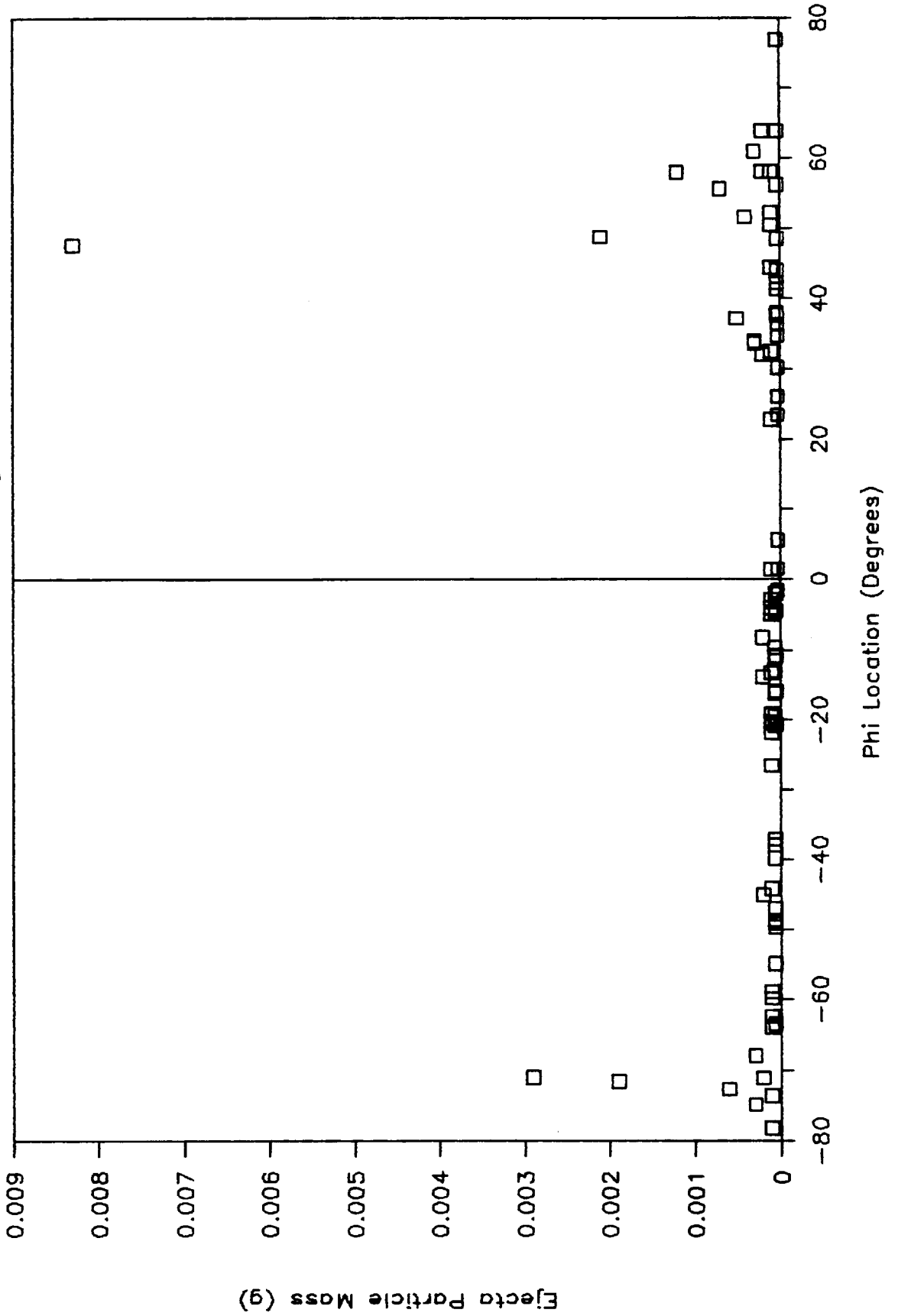


Figure 3-62

# EJECTA VELOCITY DISTRIBUTION

JSC No. 923 - No Cloth, 30 deg Impact

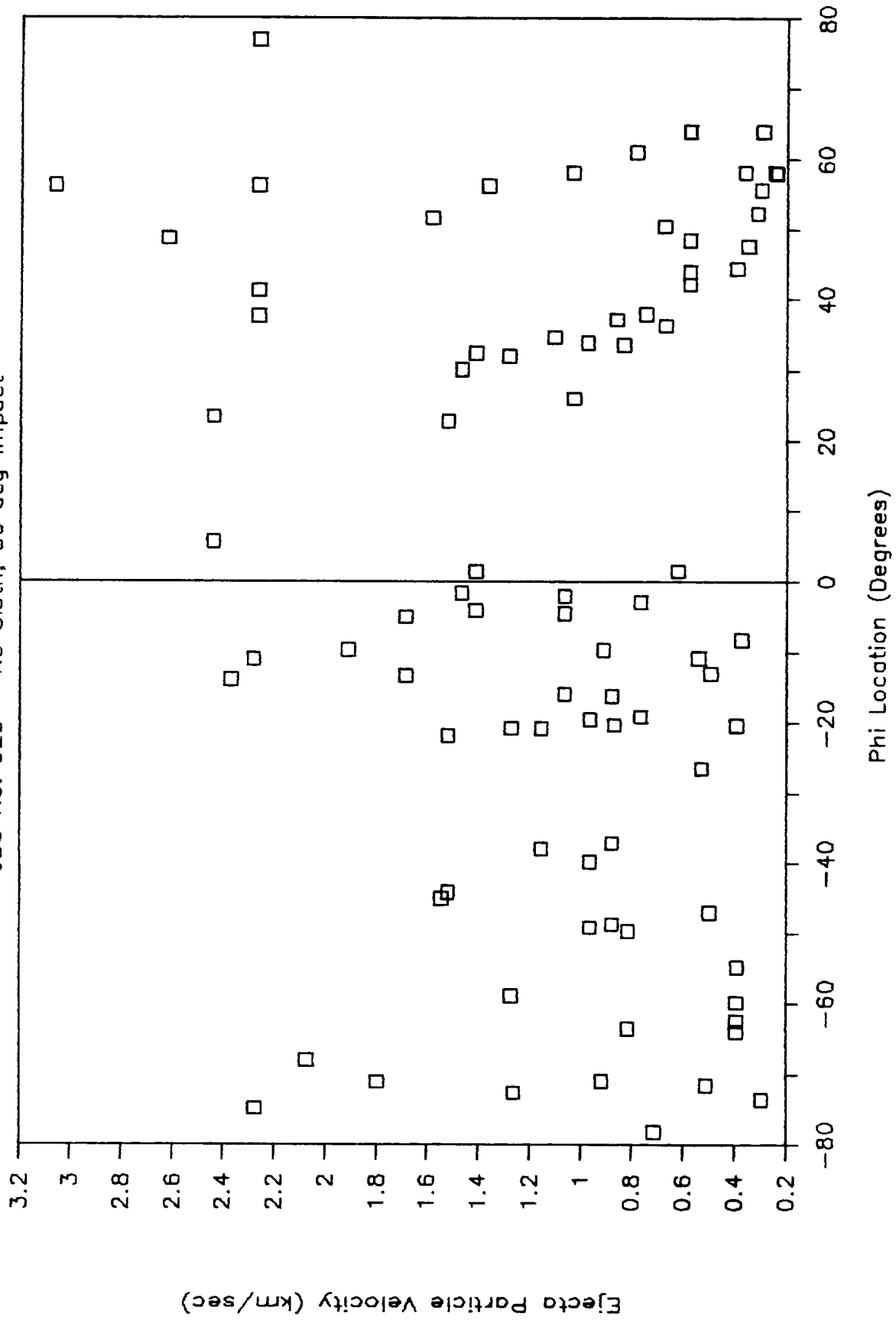


Figure 3-63

# EJECTA MASS DISTRIBUTION

JSC No. 923 - No Cloth, 30 deg Impact

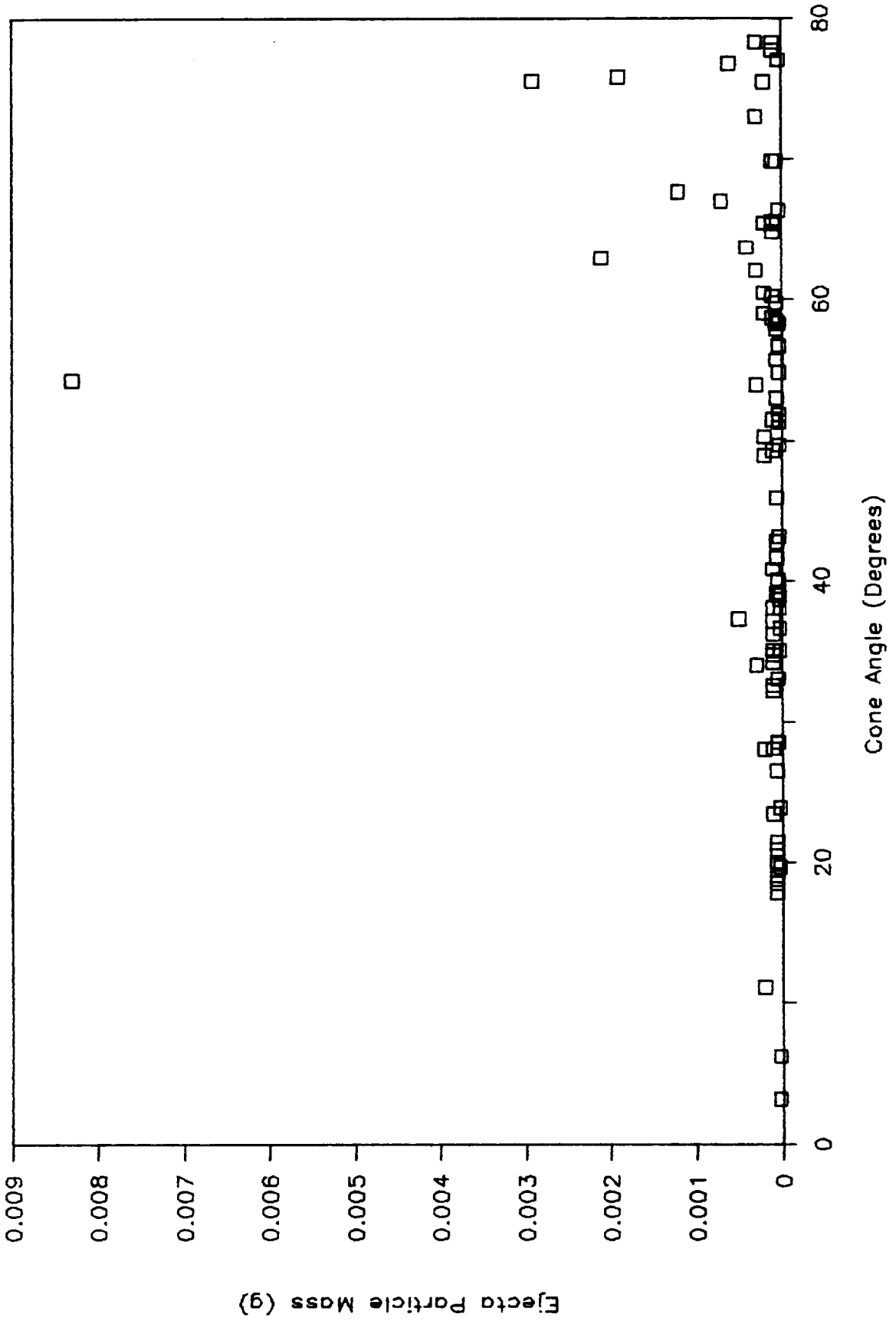




Figure 3-64

# EJECTA VELOCITY DISTRIBUTION

JSC No. 923 - No Cloth, 30 deg Impact

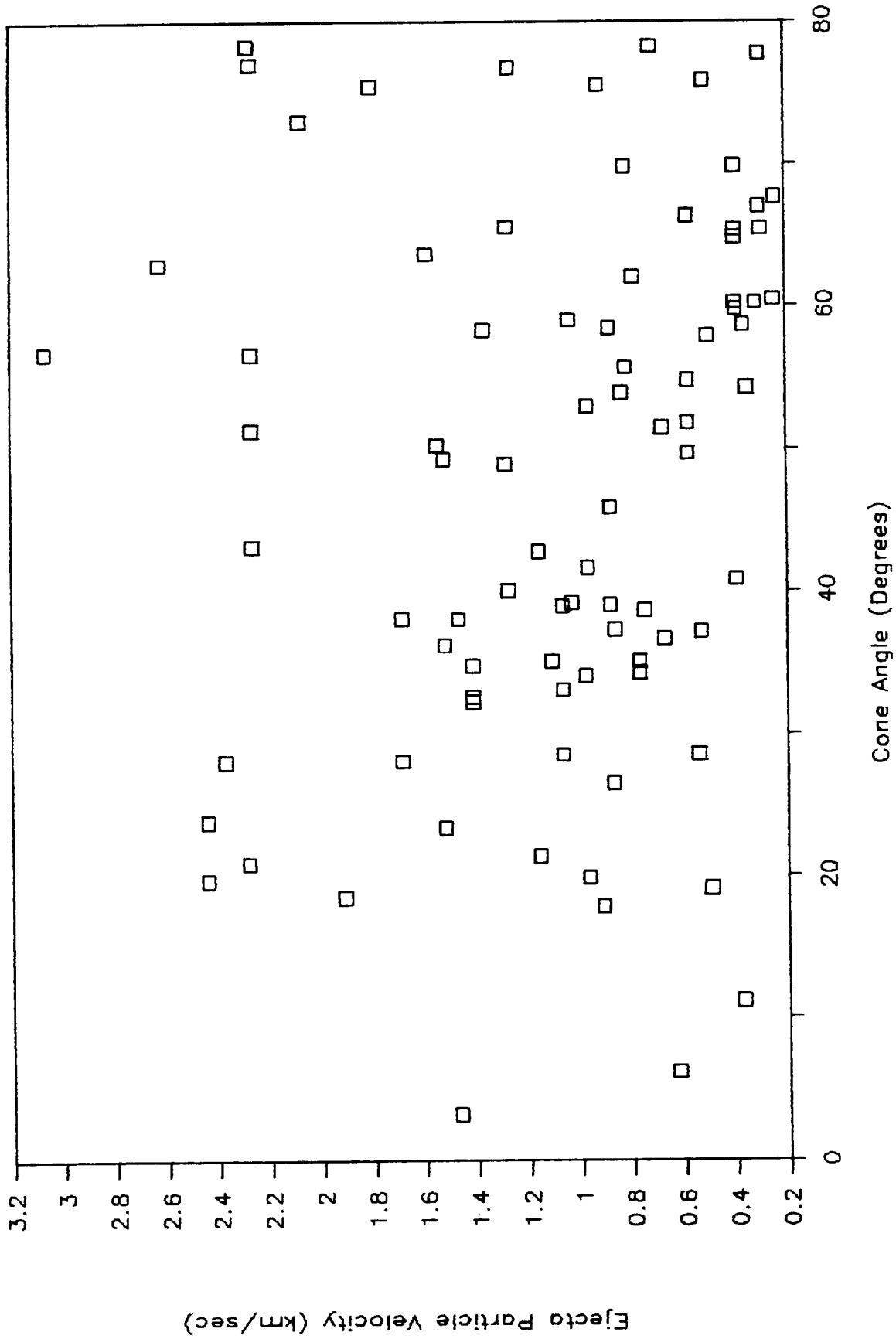


Figure 3-65

# EJECTA MASS & VELOCITY

JSC No. 923 - No Cloth, 30 deg Impact

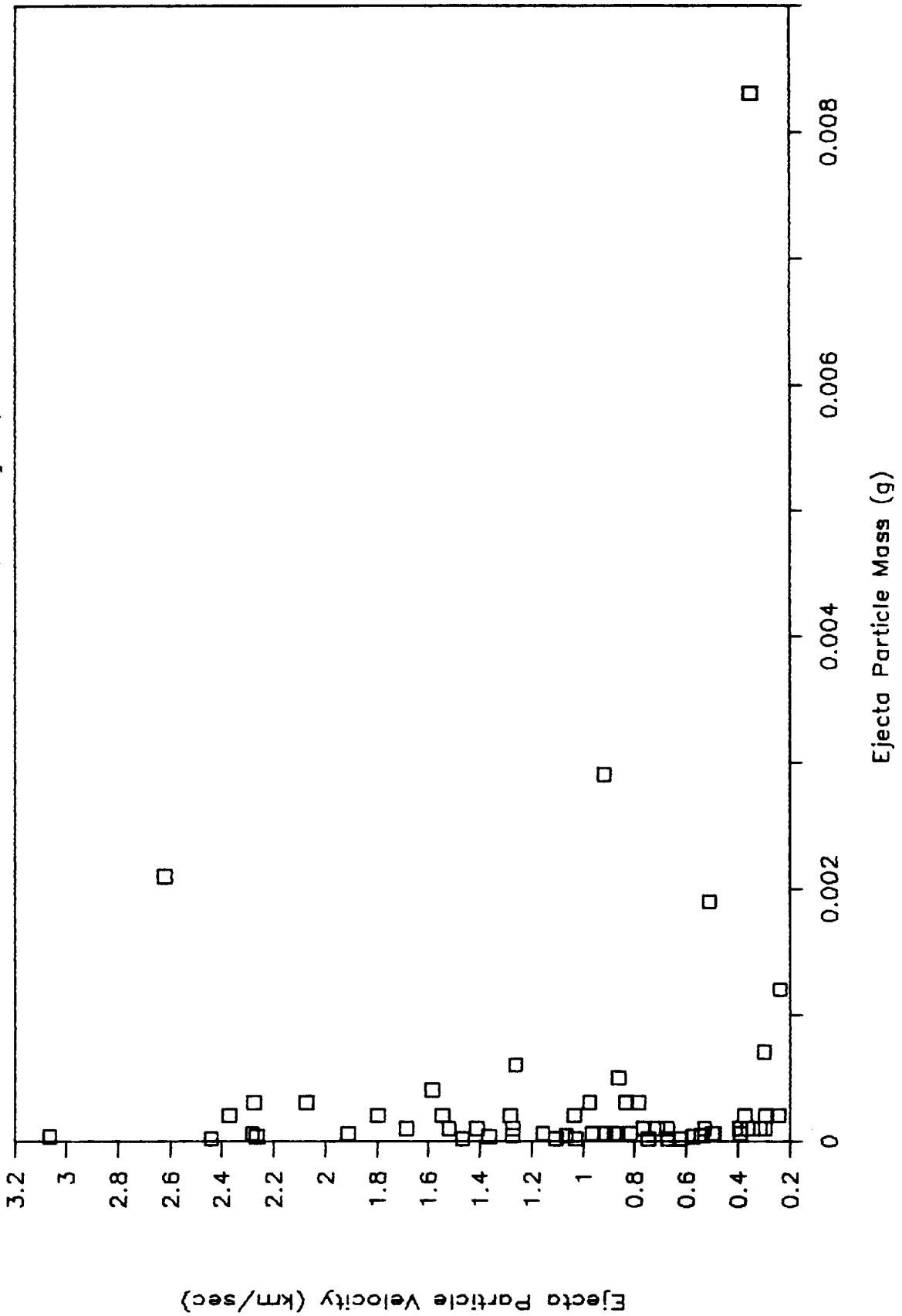


Figure 3-66

# EJECTA MASS AND PARTICLE NUMBER

JSC No. 923 - No Cloth, 30 deg Impact

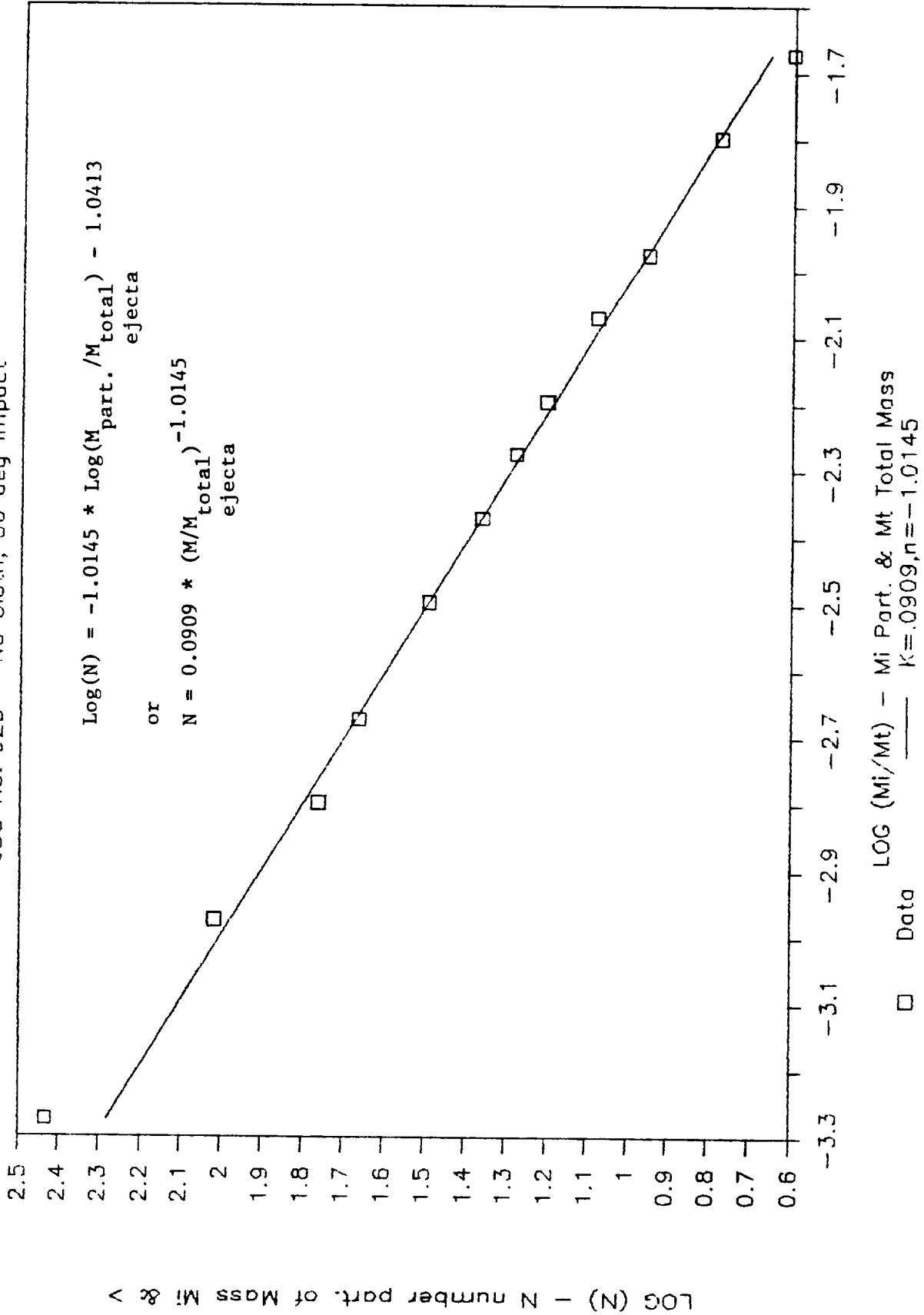


Figure 3-67

# SPALL MASS & LENGTH

JSC No. 923 - No Cloth, 30 deg Impact

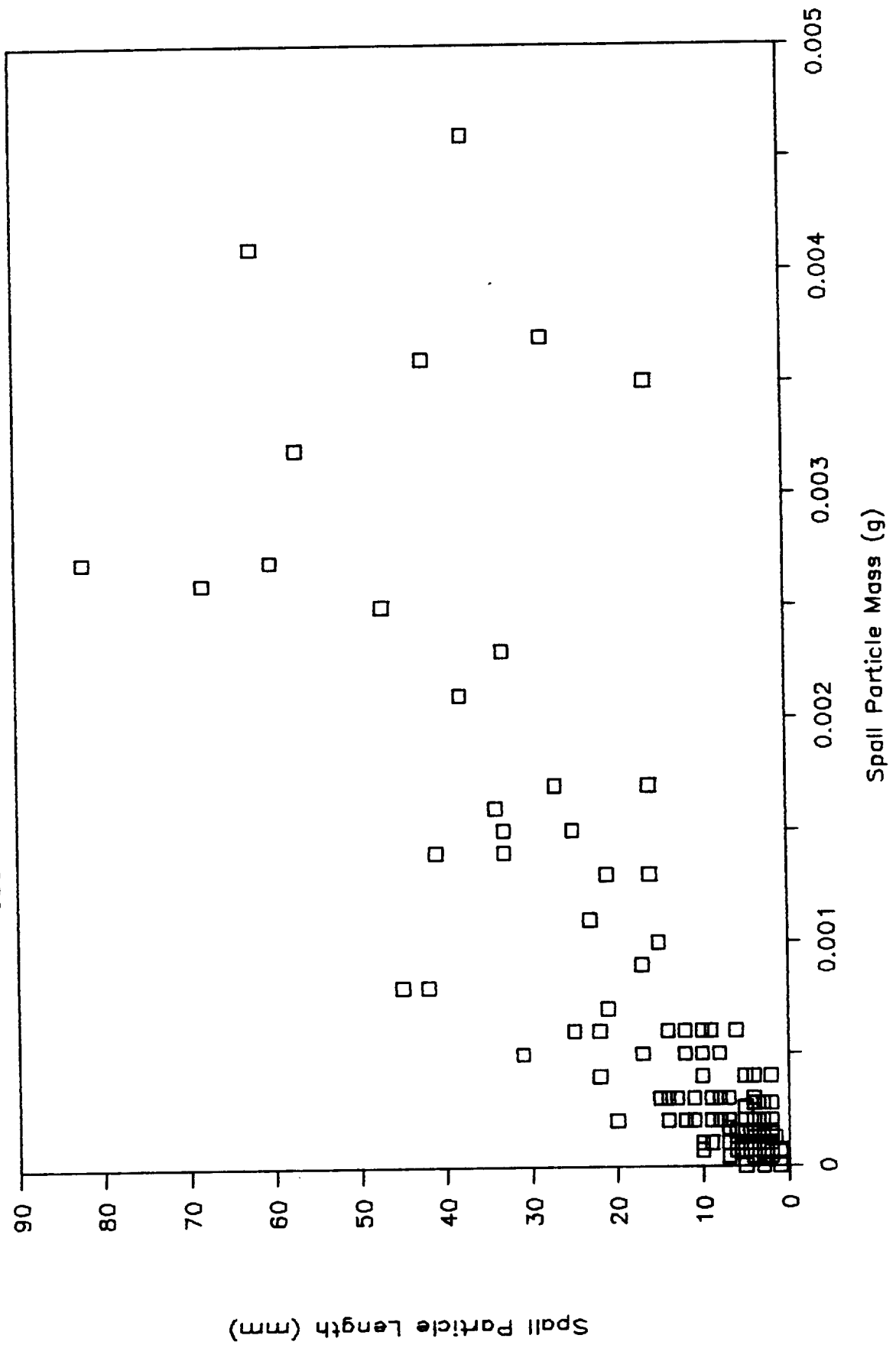


Figure 3-68

# SPALL MASS & DIAMETER

JSC No. 923 - No Cloth, 30 deg Impact

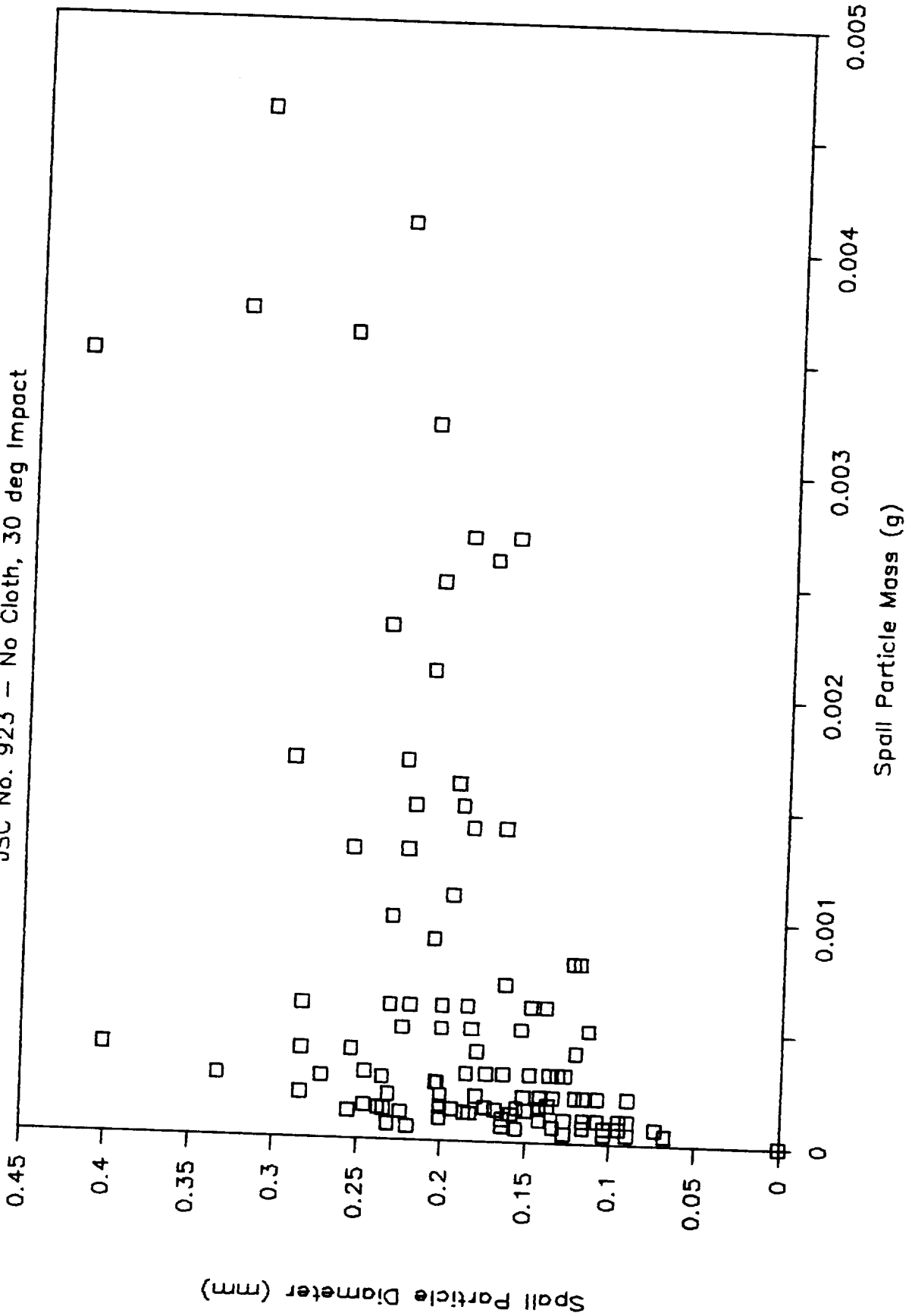


Figure 3-69

# SPALL MASS DISTRIBUTION

JSC No. 923 - No Cloth, 30 deg Impact

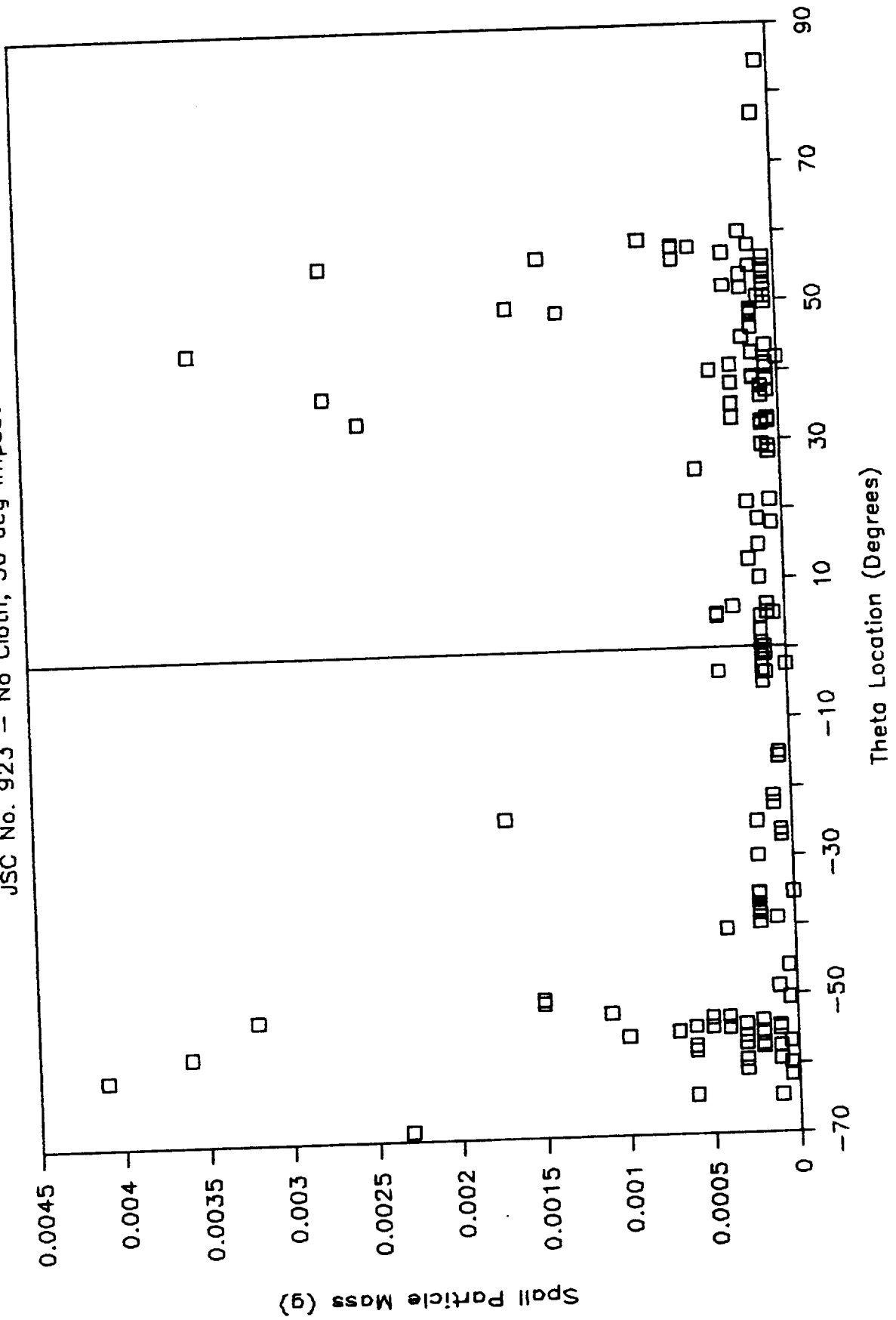


Figure 3-70

# SPALL VELOCITY DISTRIBUTION

JSC No. 923 - No Cloth, 30 deg Impact

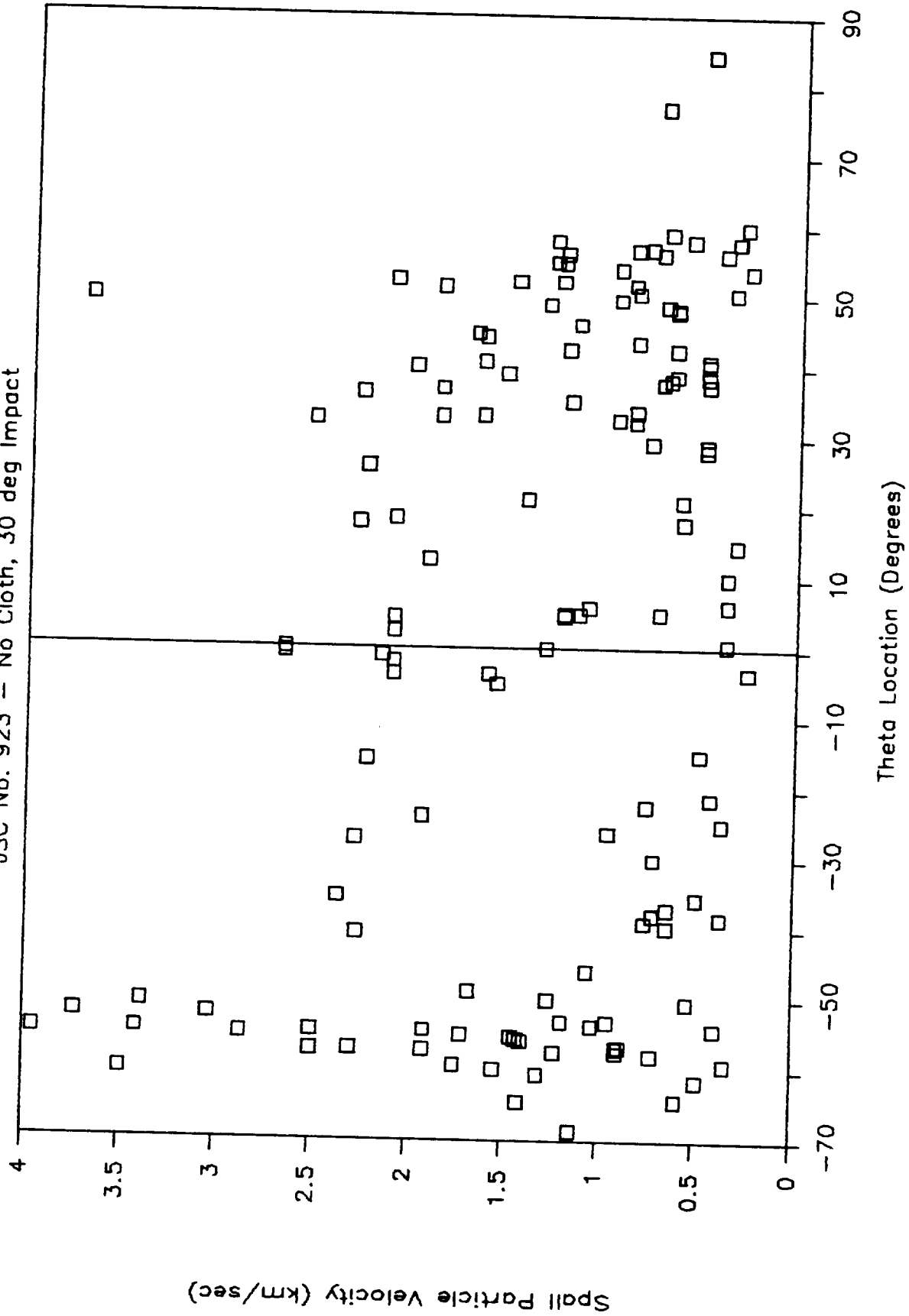


Figure 3-71

# SPALL MASS DISTRIBUTION

JSC No. 923 - No Cloth, 30 deg Impact

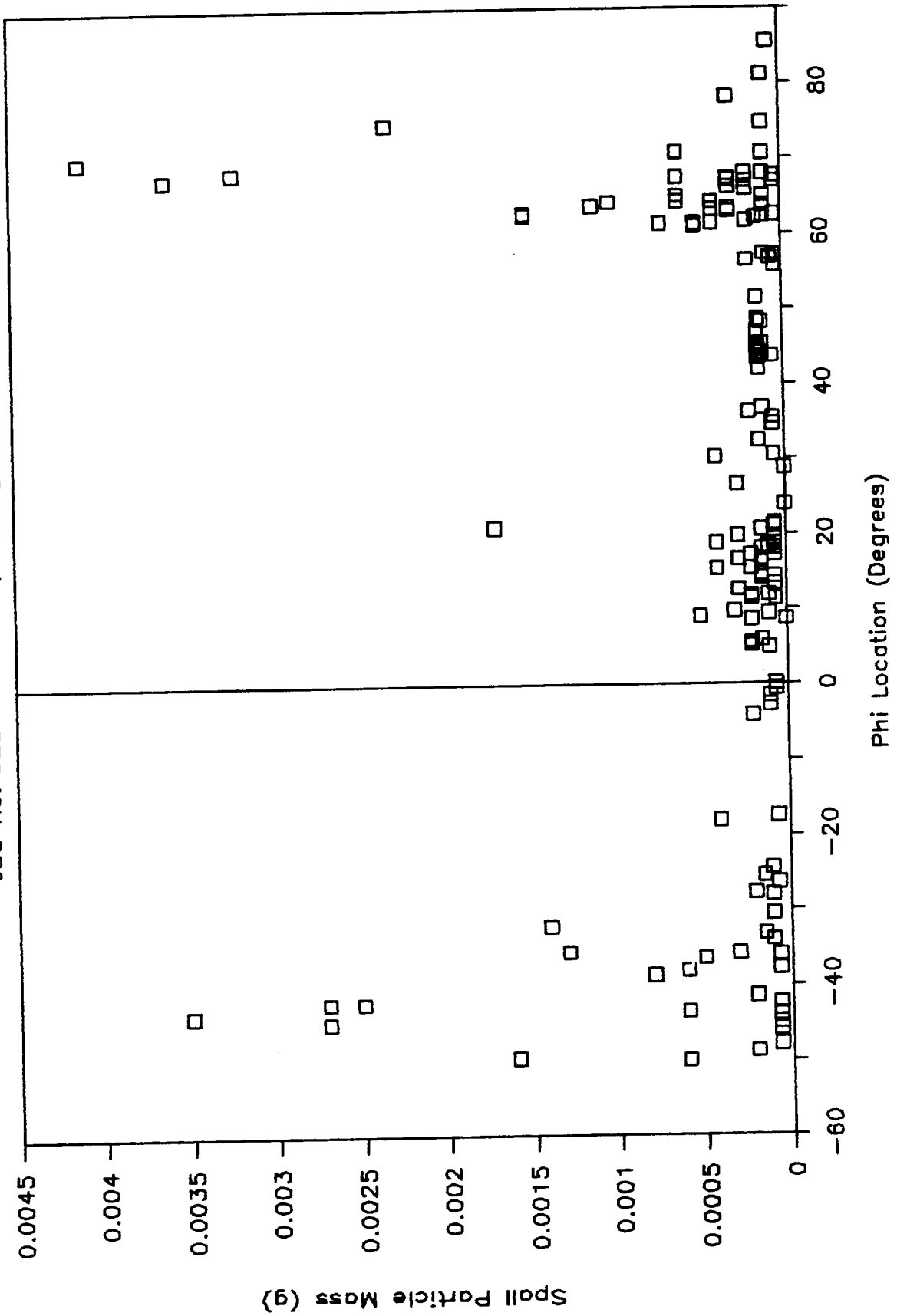




Figure 3-72

# SPALL VELOCITY DISTRIBUTION

JSC No. 923 - No Cloth, 30 deg Impact

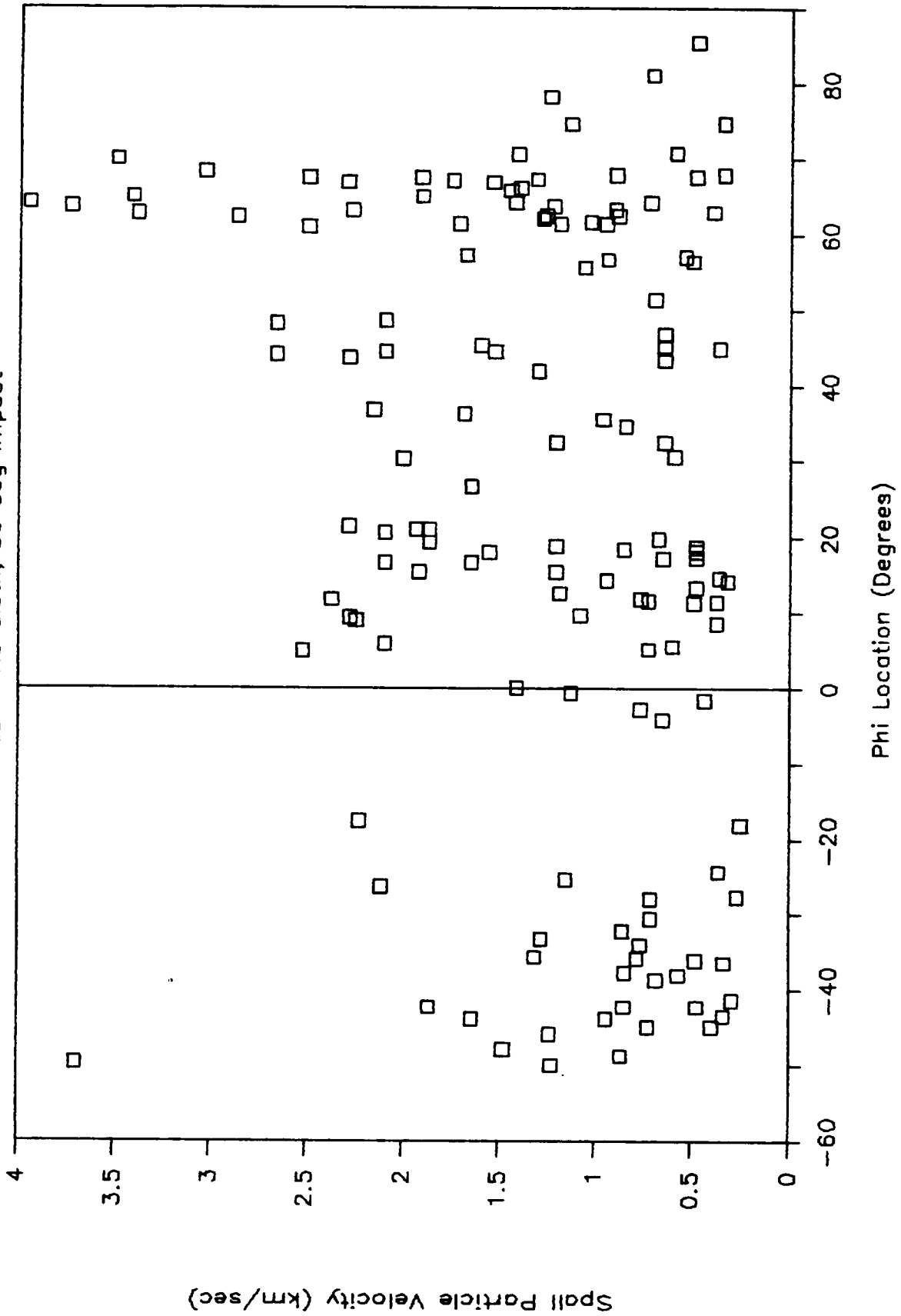


Figure 3-73

# SPALL MASS DISTRIBUTION

JSC No. 923 - No Cloth, 30 deg Impact

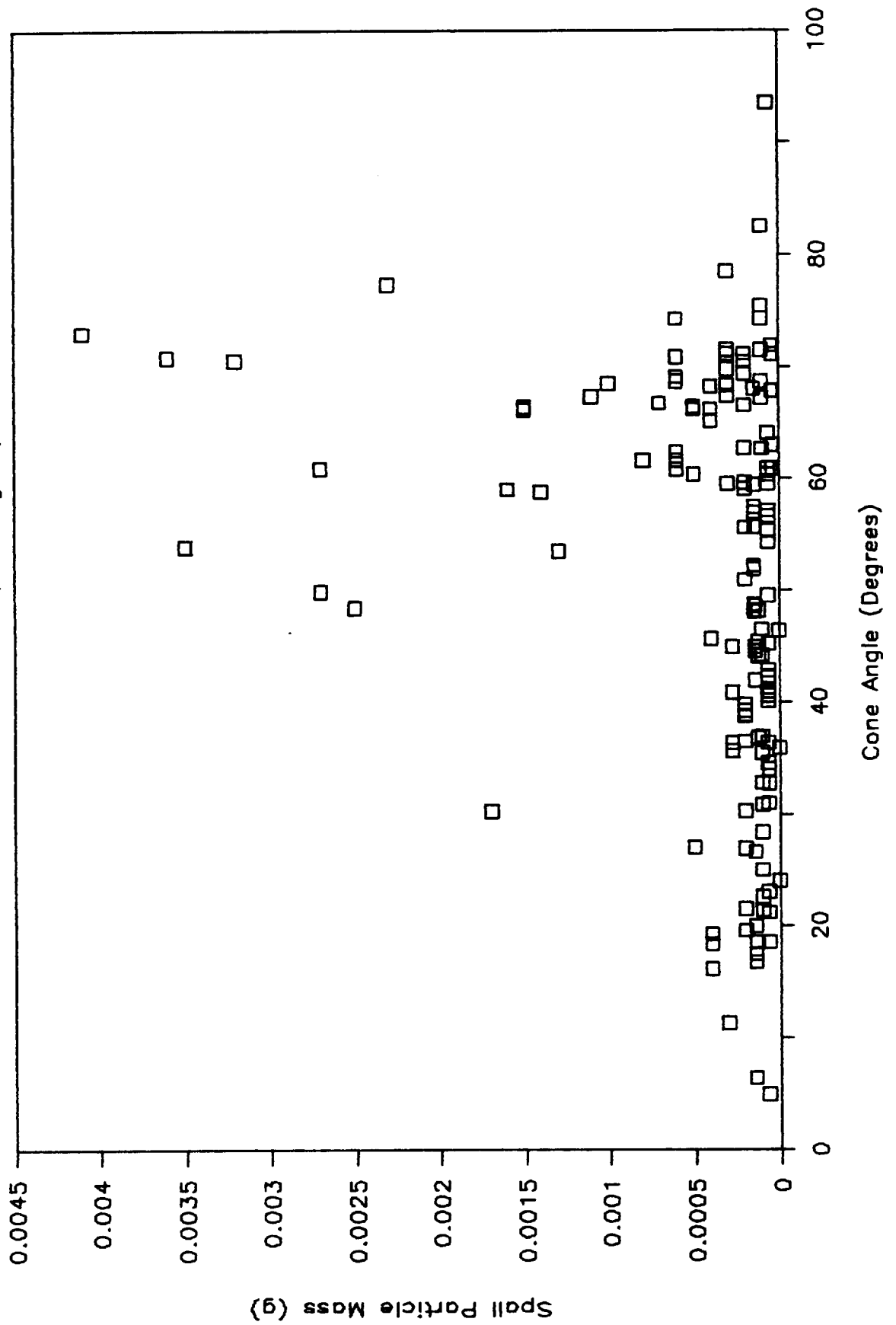


Figure 3-74

# SPALL VELOCITY DISTRIBUTION

JSC No. 923 - No Cloth, 30 deg Impact

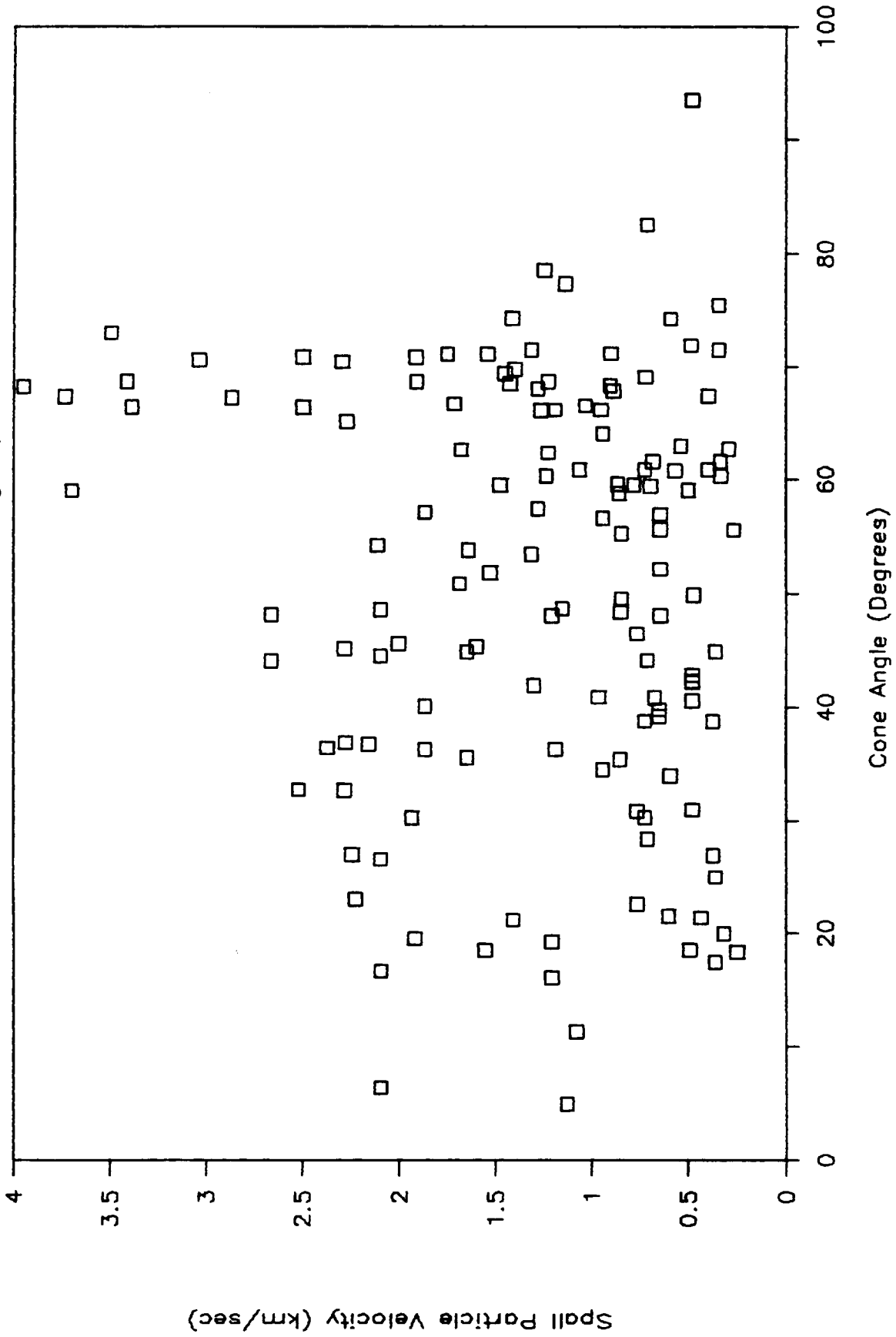


Figure 3-75

# SPALL MASS & VELOCITY

JSC No. 923 - No Cloth, 30 deg Impact

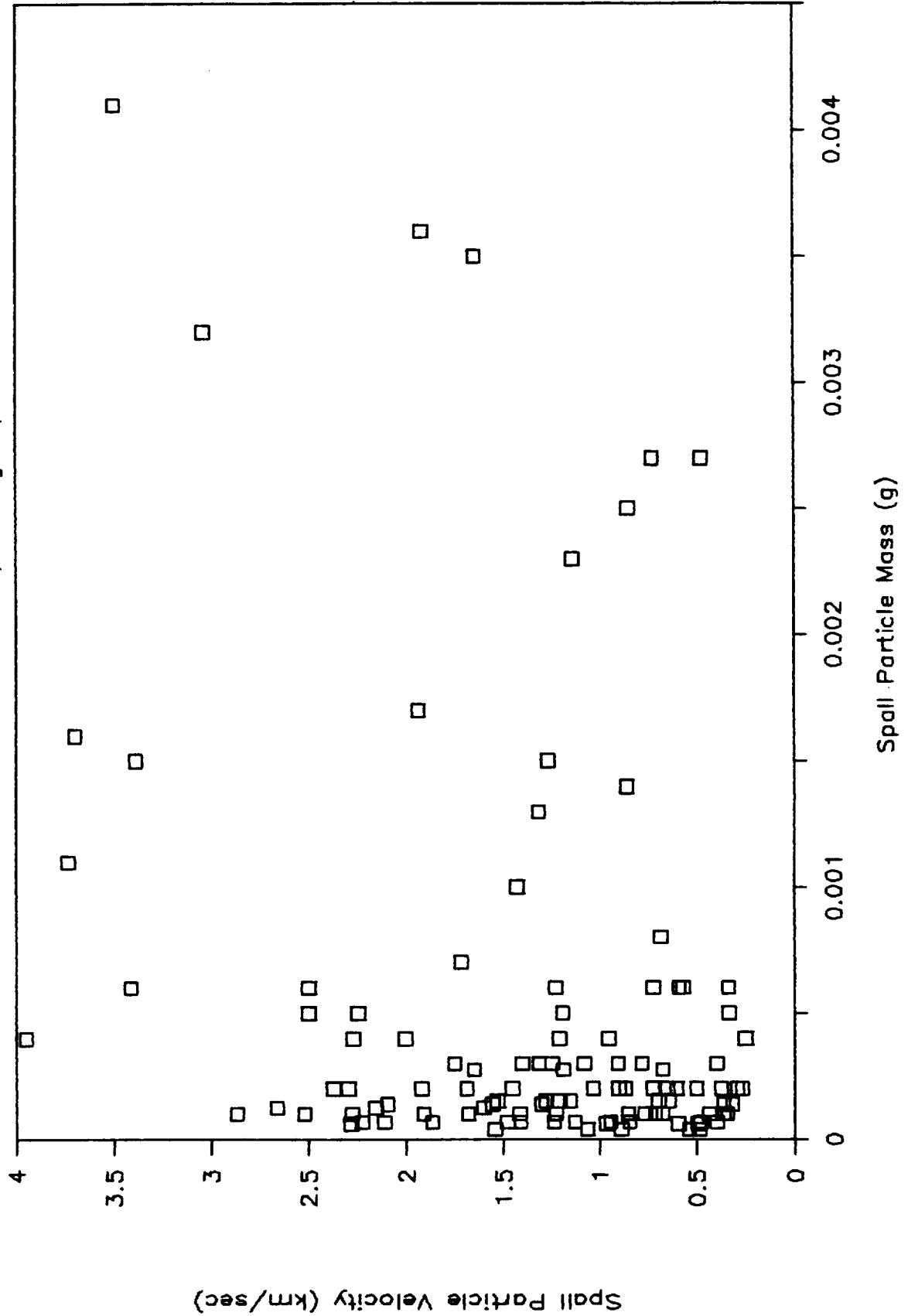
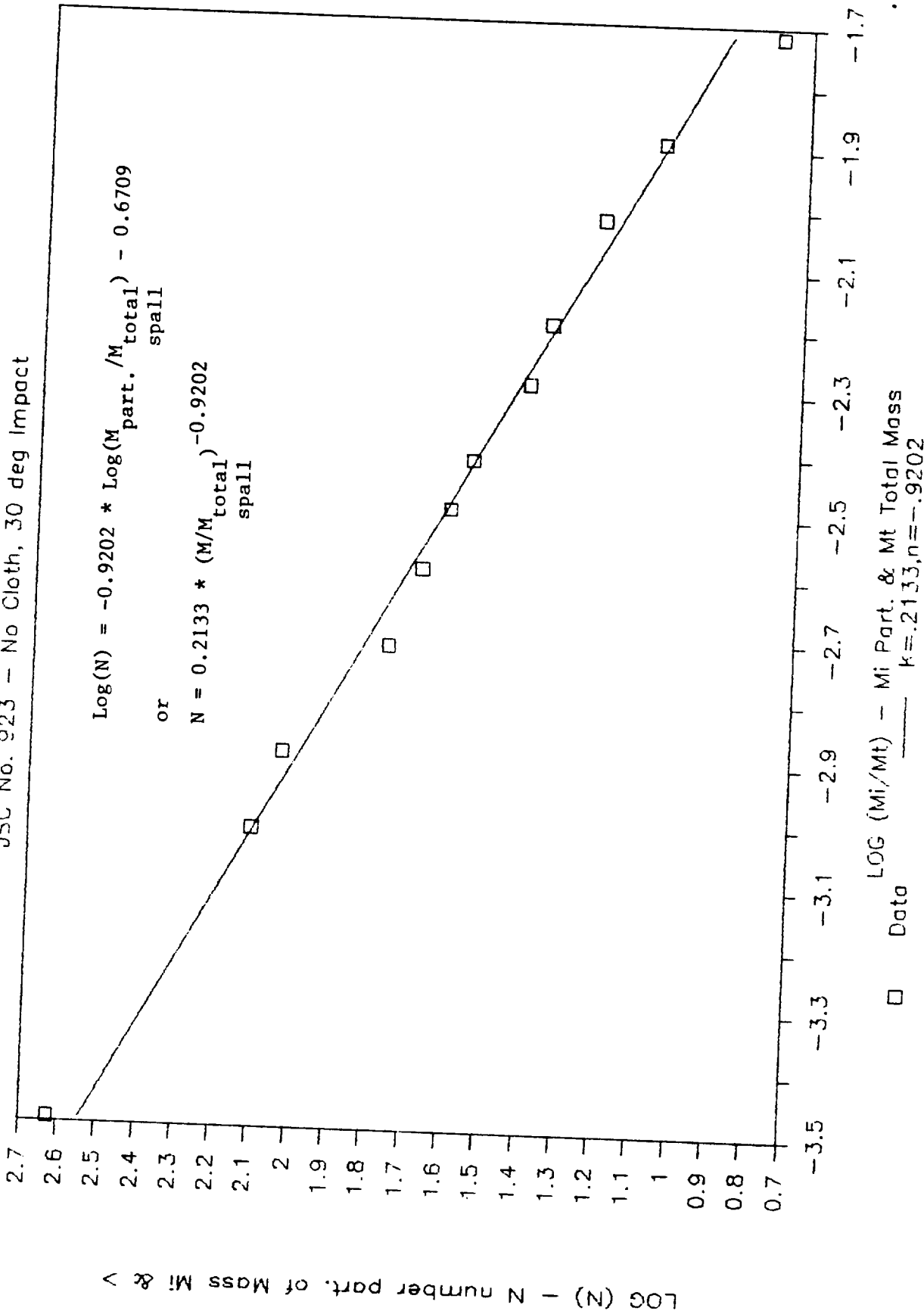


Figure 3-76

# SPALL MASS AND PARTICLE NUMBER

JSC No. 923 - No Cloth, 30 deg Impact



# EJECTA/SPALL MASS & PARTICLE NUMBER

Figure 3-77

JSC No. 923 - No Cloth, 30 deg Impact

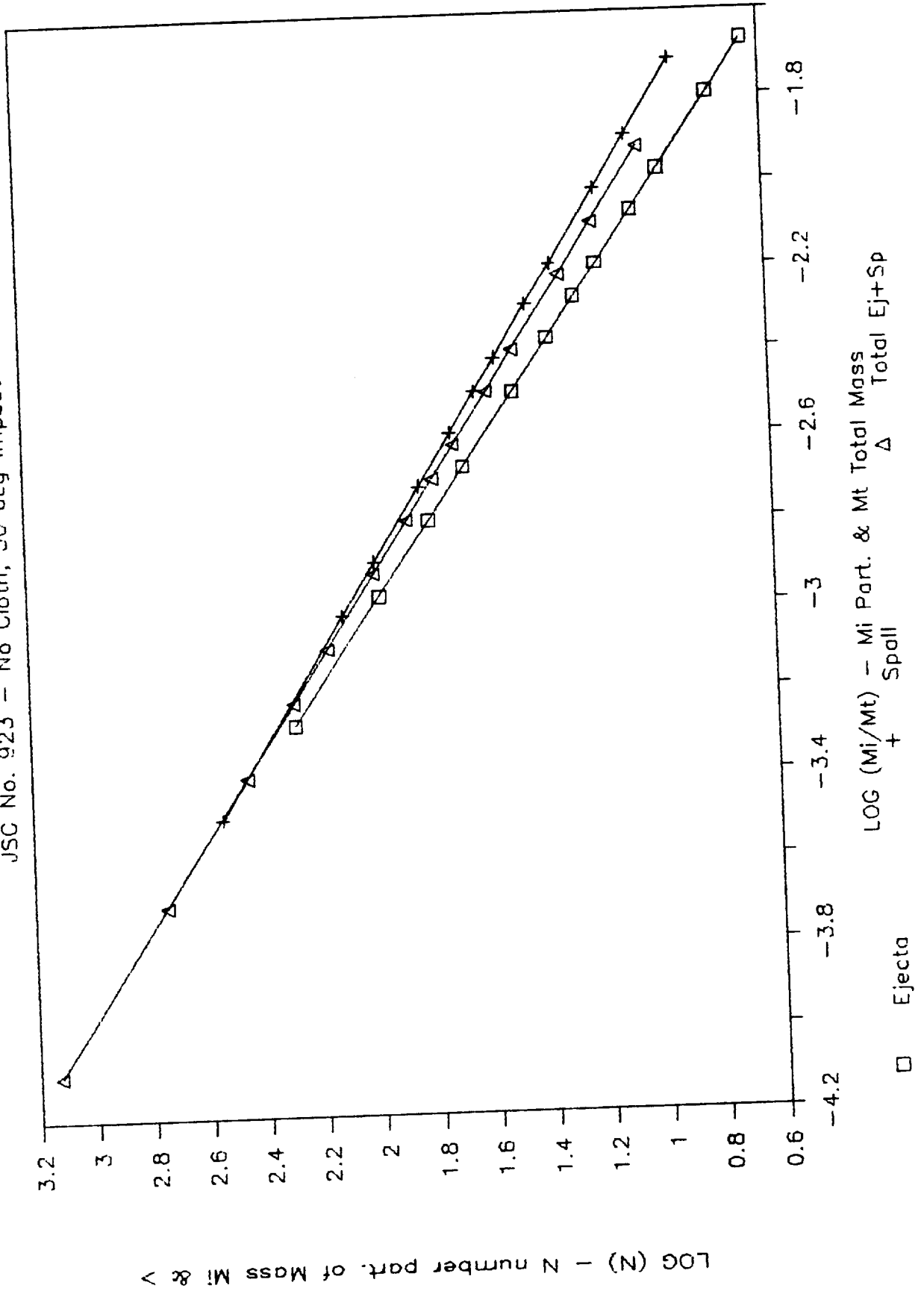
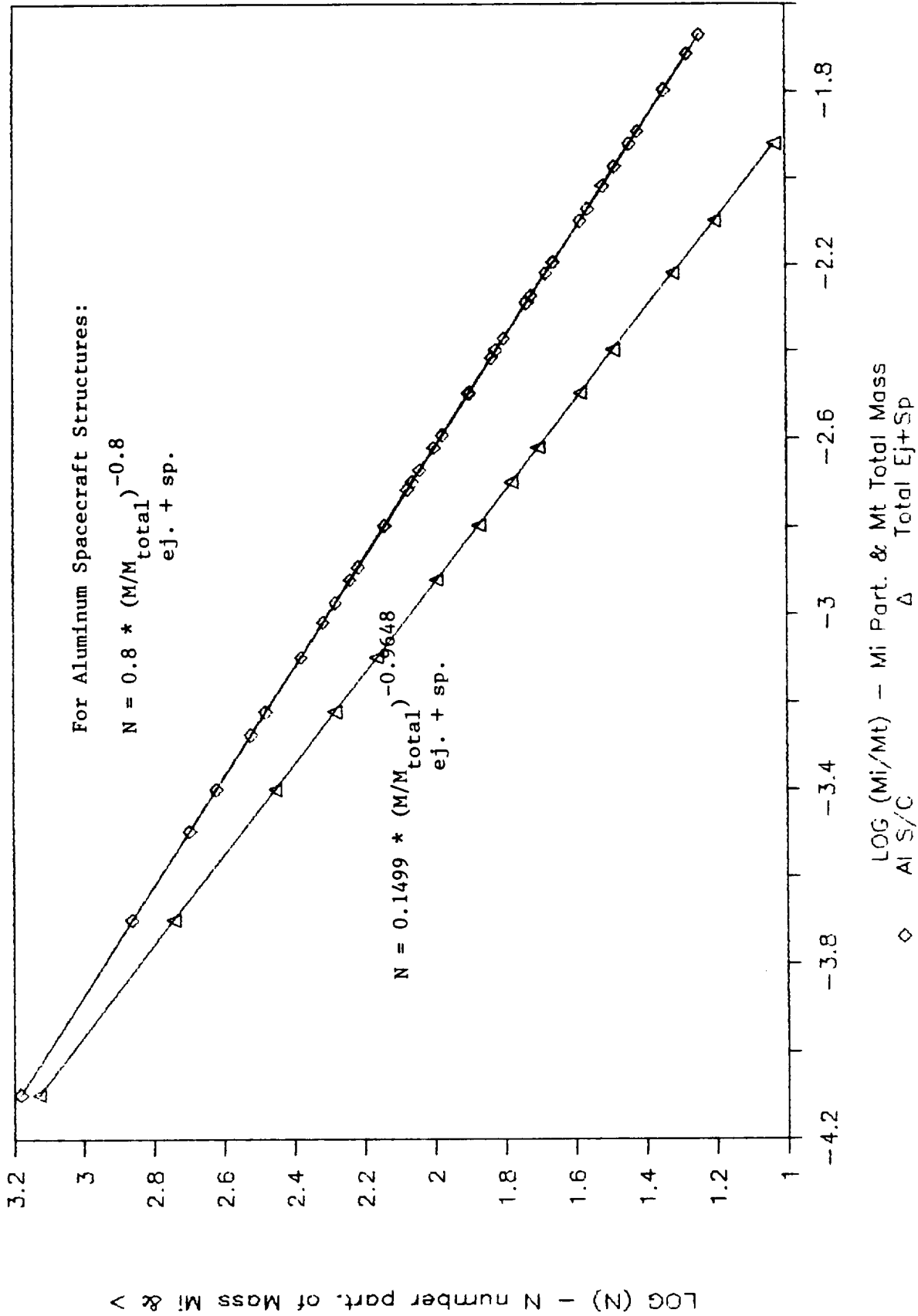


Figure 3-78

# EJECTA/SPALL MASS & PARTICLE NUMBER

JSC No. 923 - No Cloth, 30 deg Impact



### **3.3 Thin Graphite/Epoxy Targets - Projectile Density Effects**

Table 3-3 shows a series of additional shots, some performed in conjunction with a University of Texas effort to determine projectile density effects. Aluminum and nylon projectiles were used at velocities around 5 km/sec. In Shots #889, 890, and 895 ejecta and spall particles were collected separately, but detailed data, as shown previously, was not collected. Some of the shots used a toughened resin system. A shot using a fiberglass target (#913) is also shown for comparison.

More data is needed (at different projectile energies) to conclude decisively, but it appears that the higher density aluminum shots produced more ejecta/spall versus equivalent energy nylon shots. Figure 5-3, taken from Ref. 2 shows the same relationship between projectile density and ejecta/spall mass for aluminum.

From the data shown in Table 3-3 it also appears that toughened resin offers no significant advantage in reducing the mass of ejecta/spall produced from hypervelocity impacts. The toughened resin may have other advantages, however. The data collected in these shots was primarily used in developing the total ejecta/spall mass versus projectile energy relationship.



Table 3-3

Data from additional JSC Light Gas Gun Shots  
 Projectile vs. Ejecta/Spall Mass Summary

JSC Shot #	Target Description	Projectile Type	Velocity (Km/sec)	Proj. Mass (mg)	Impact Angle (deg)	Secondary Particle Type	Sec. Mass (g)	Percent Spall to Projectile Mass	(Gamma) Ratio of secondary to Projectile Mass
889	Graphite/Epoxy Thin, No Cloth (similar to 893,894,923)	Al 6061	5.02	5.00	0	Ejecta Spall Total	0.06 0.24 0.3	80.0	60.00
890	Graphite/Epoxy Thin, Truss layup, No Cloth (similar to 895)	Al 6061	4.5	4.93	0	Ejecta Spall Total	0.04 0.17 0.21	81.0	42.60
893	Graphite/Epoxy Thin, No Cloth (similar to 889,894,923)	Nylon	4.75	4.99	0	Total	0.18		36.07
895	Graphite/Epoxy Thin, Truss layup, No Cloth (similar to 890)	Nylon	4.82	4.96	0	Ejecta Spall Total	0.03 0.10 0.13	76.9	26.21
909	Graphite/Epoxy Thin, Truss layup, Cloth (similar to 911,917)	Nylon	6.20	4.99	0	Total	0.37		74.15
910	Graphite Thin, Cloth, Toughened Resin (similar to 912)	Nylon	6.11	5.00	0	Total	0.28		56.00
911	Graphite/Epoxy Thin, Truss layup, Cloth (similar to 909,917)	Al 6061	5.17	5.00	0	Total	0.22		44.00
912	Graphite Thin, Cloth, Toughened Resin (similar to 910)	Al 6061	4.57	5.00	0	Total	0.16		32.00
913	Fiberglass	Al 6061	4.00	4.98	0	Total	0.1		20.08

### 3.4 Thin Graphite/Epoxy Targets with High Speed Camera

Accurate velocity measurements of ejecta and spall are critical to assessing the hazard to the Space Station. In the first series of shots done in this study, accurate velocity measurement was unavailable. A crude method for estimating the velocity of the larger particles based on their penetration into styrofoam was used and checked with a few single photos and one film. Once the Orbital Debris Lab High Speed Camera became operational it was possible to check the estimates more carefully. The camera data was also used to check the projectile velocity.

Table 3-4 summarizes the shots for which high speed camera data was taken. Three graphite/epoxy targets and one aluminum target were used.

The new camera system is a custom designed, state-of-the-art ultra-high-speed rotating mirror framing camera, utilizing a laser diode for image illumination. The camera is capable of exposing 80 frames of 35mm IR film at  $2 \times 10^6$  frames/sec. Even at that framing rate, conventional illuminating systems (on the order of 10 to 15 nsec.) were not fast enough to "freeze" a 300 micron particle traveling at speeds in excess of 7km/sec. The 860nm, 100 watt laser diode used for this system has a pulse duration of 5 nanosec. The "exposure time" is therefore 5 nanoseconds and there is one microsecond between exposures.

Table 3-4

Data from JSC Light Gas Gun Shots with Hi-Speed Camera

Projectile vs. Ejecta/Spall Mass Summary																
JSC Shot #	Target Description	Projectile Type	Projectile Velocity (ka/sec)	Proj. Mass (mg)	Impact Angle (deg)	Secondary Particle Type	Sec. Mass (g)	Impact Angle (deg)	Percent Spall to Projectile Mass	(Gama)	EJECTA Maximum Cone Angle (degrees)	EJECTA Maximum Measured Velocity (ka/sec)	EJECTA Typical Meas. Large Particle Velocity (ka/sec)	SPALL Maximum Dispersion Angle (degrees)	SPALL Maximum Measured Velocity (ka/sec)	SPALL Typical Meas. Large Particle Velocity (ka/sec)
972	6/E, generic no cloth, 0.078" thickness	Nylon	7.19	5.00	0	Total	0.33	-	66.00	35	5.30	-	-	34	2.71	-
975	Al 6061-T6 0.089" thickness	Nylon	6.66	4.60	0	Total	0.1	-	21.74	31	3.74	0.7	0.7	34	1.44	0.25
981	6/E, no cloth JSC-028-004	Nylon	7.38	4.91	0	Total	0.30	-	61.10	24	2.63	0.8	0.8	27	2.78	-
990	6/E, cloth JSC-02A-003	Nylon	6.29	5.02	30	Total	0.20	-	39.84	66	4.89	-	-	22	0.75	-

### **3.4.1 Shot #972**

Figure 3-79 shows the raw film data. The target used in this test was a generic graphite/epoxy sample, similar to the roughly 0.10 inch samples used in the other shots, but not listed in Table 3-1.

Table 3-5 illustrates how the raw data from the film was turned into velocity estimates.

### **3.4.2 Shot #981**

Figure 3-80 shows the raw film data. The Figure 3-80 photographs and analysis shown in Figure 3-81 were provided by Dr. Ching Yew of the Univ. of Texas.

Figure 3-81 plots the progress of the spall front, indicating a constant velocity consistent with velocities calculated for graphite/epoxy particles.

Table 3-6 is the data worksheet.

### **3.4.3 Shot #990**

Figure 3-82 shows the raw film data. The negative was not high quality, but data could be taken from it.

Table 3-7 is the worksheet.

### **3.4.4 Comparison of Calculated and Measured Velocity**

Figure 3-83 compares measured and estimated ejecta velocities over the range of masses. The plot indicates the calculated values are fairly accurate.

Figure 3-84 compares measured and estimated spall velocities for a range of masses. The two data points fall within the same general range as the calculated values.

Overall, the calculated graphite/epoxy spall and ejecta velocities appear to be roughly accurate.

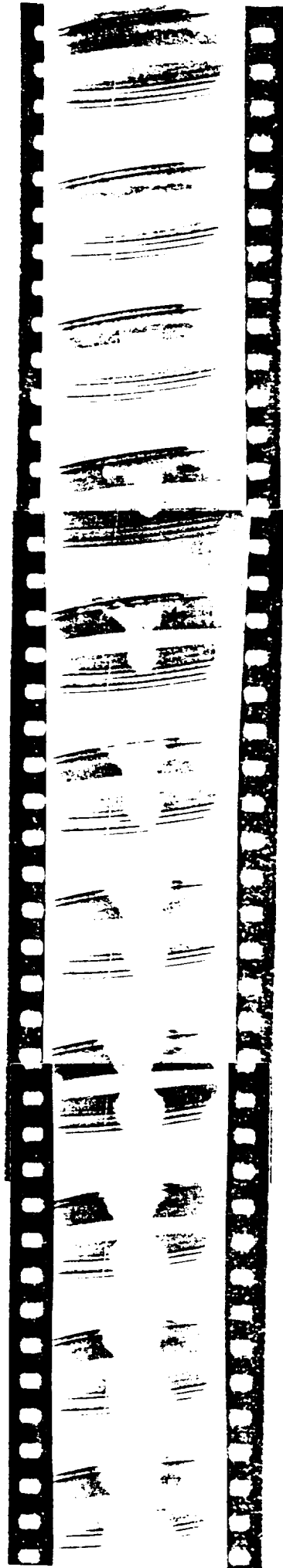
Figure 3-79

High Speed Camera Data for Generic  
Graphite/Epoxy Target (Shot #972)

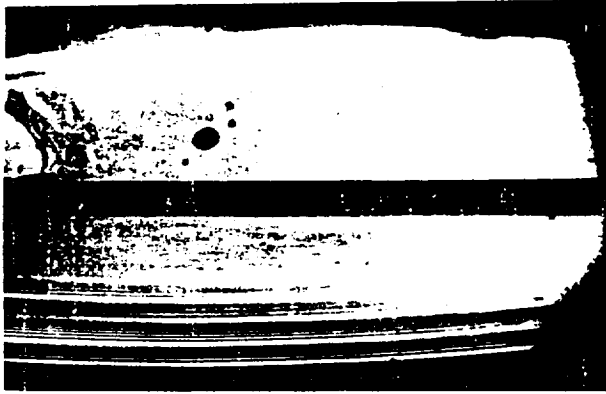
1.13 microseconds between frames  
.0695 inches = projectile diameter

ORIGINAL PAGE IS  
OF POOR QUALITY

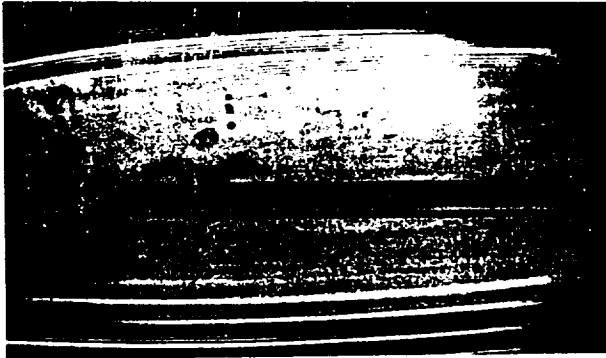
11 | 10 | 9 | 8 | 7 | 6 | 5 | 4 | 3 | 2 | 1



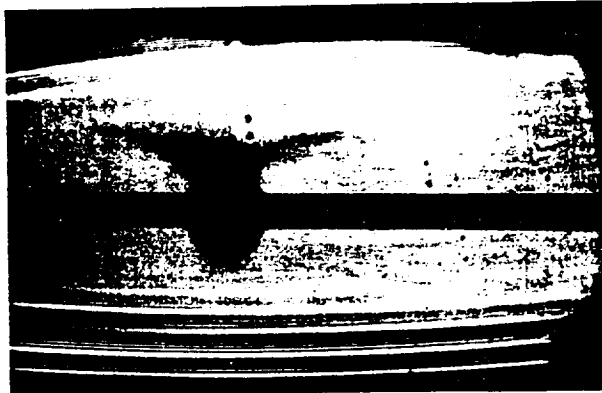




t=0             $\mu$  sec



t=1.0246       $\mu$  sec



t=2.0492       $\mu$  sec

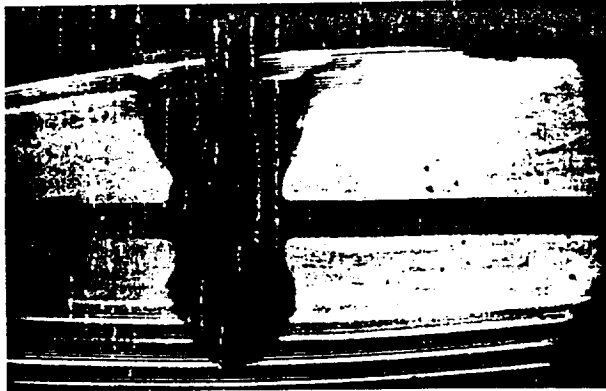


t=3.0738       $\mu$  sec

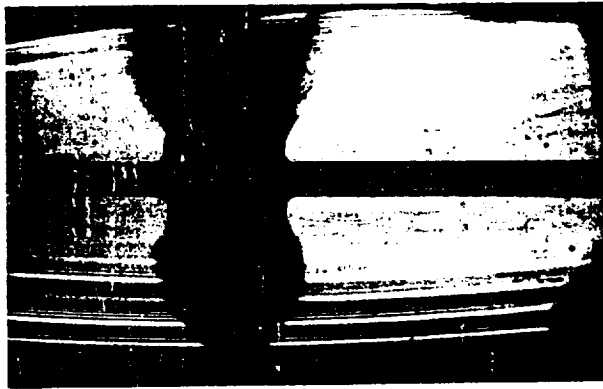
Figure 3-80 (cont'd)



$t=4.0984 \mu \text{ sec}$



$t=5.123 \mu \text{ sec}$



$t=6.1476 \mu \text{ sec}$



$t=7.1722 \mu \text{ sec}$



Figure 3-80 (cont'd)



$t=8.1968 \mu \text{ sec}$



$t=9.2214 \mu \text{ sec}$



$t=13.3198 \mu \text{ sec}$

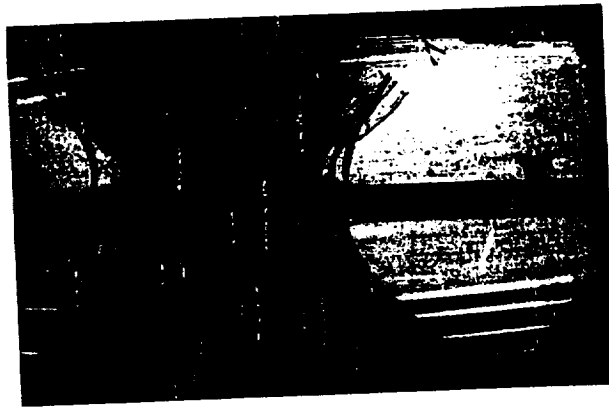
Figure 3-80 (cont'd)



$t=16.3936 \mu \text{ sec}$



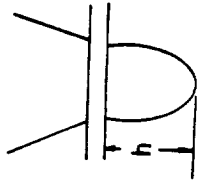
$t=20.492 \mu \text{ sec}$



$t=28.6888 \mu \text{ sec}$

Figure 3-81, Shot 981

(Provided by Dr. Ching Yew, Univ. of Texas)



$$V_0 = 8.3 \times 10^3 \text{ ft/sec} = 2.54 \text{ km/sec}$$

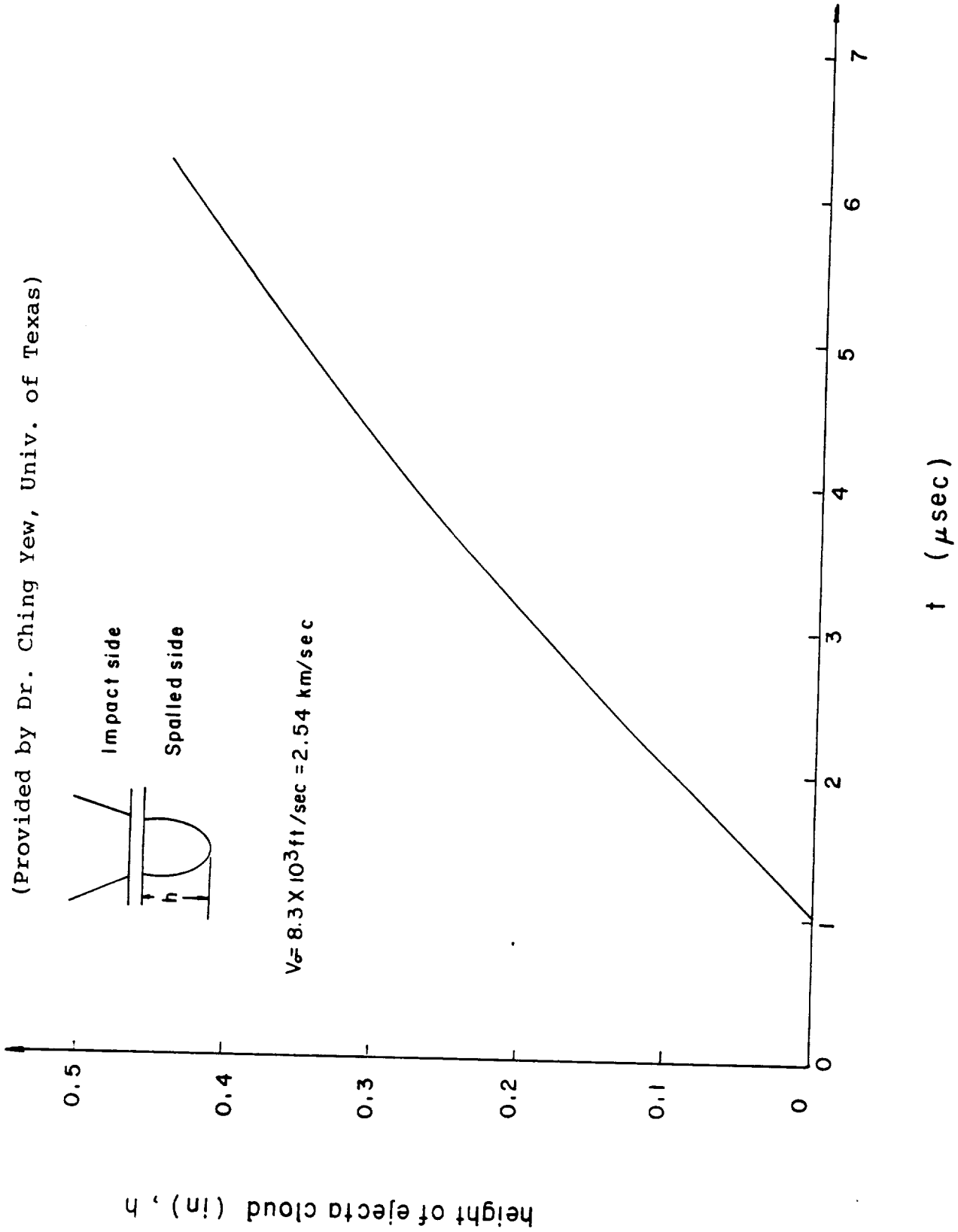


Table 3-6  
Worksheet for Shot # 981

Ejecta and Spall Velocities determined from Hi-Speed Camera

USC Shot #	981
Target type	Gr/Ep
Actual Projectile Diameter (in)	0.0695
Framing Period	245.9
Time between frames (micro-sec)	1.0246
Distance Correction Factor	2.6165
Calc. Proj. Vel. (Kt/sec)	5.07 (inaccurate)

Frame	MEASUREMENTS (uncorrected by distance factor)										CALCULATED VALUES (corrected with distance factor)										
	EJECTA SIDE					SPALL SIDE					EJECTA SIDE					SPALL SIDE					
Proj. diameter (in)	Proj. dist. from plate (in)	Proj. from impact point (perpendicular dist. at zero deg.)	Max. cone angle - normal at zero deg. first front (deg)	Approximate Meas. Particle Length (in)	Correct Velocity (Kt/sec)	Approximate Particle Mass (g)	Width of crater (in)	Width of crater (in)	Max. cone angle (deg)	Perpen-dicular distance from impact point (in)	Incremental Apparent Velocity for cone angle (Kt/sec)	Incremental Velocity corrected for cone angle (Kt/sec)	Overall Apparent Velocity (Kt/sec)	Overall Velocity corrected for cone angle (Kt/sec)	Incremental Velocity for cone angle (Kt/sec)	Incremental Velocity corrected for cone angle (Kt/sec)	Overall Apparent Velocity (Kt/sec)	Overall Velocity corrected for cone angle (Kt/sec)	Incremental Velocity (Kt/sec)	Overall Velocity (Kt/sec)	
1	0.0266	0.0781					0.0625	0.164		0.0047	1.52	1.66	2.53	2.76	1.66	2.53	2.53	2.76	1.66	2.53	3.24
2			0.0234	48.19			0.0938	0.245		0.0547	2.53	2.76	2.79	3.32	2.76	2.79	2.79	3.04	2.76	2.79	2.64
3			0.0625	28.96			0.1094	0.286		0.0859	3.04	3.32	2.87	3.32	3.32	3.32	2.87	3.13	3.32	3.13	2.94
4			0.1094	25.84			0.1250	0.327		0.1406	3.04	1.11	2.61	1.11	1.11	1.11	2.61	2.63	1.11	2.63	2.71
5			0.1563	32.20			0.1406	0.368		0.1719	1.01										2.03
6			0.1719				0.1563	0.409		0.2188											3.04
7							0.1719	0.450	33.56												0.30
8								0.450	27.27												3.24
25																					2.64

Velocities of Large Particles

Ejecta Particle	Number of Frames Used	Measured Distance (in)	Apparent Velocity (Kt/sec)	Correct Velocity (Kt/sec)	Approximate Meas. Particle Length (in)	Approximate Particle Mass (g)
1	6	0.0517	0.709	0.774	0.046875	0.00271
					0.0625	0.00203

Figure 3-82  
High Speed Camera Data (Shot # 990)  
1.04 microseconds between frames

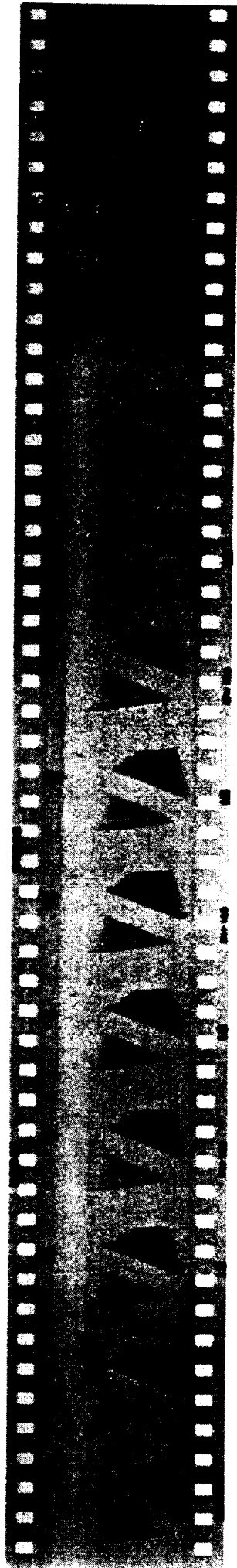
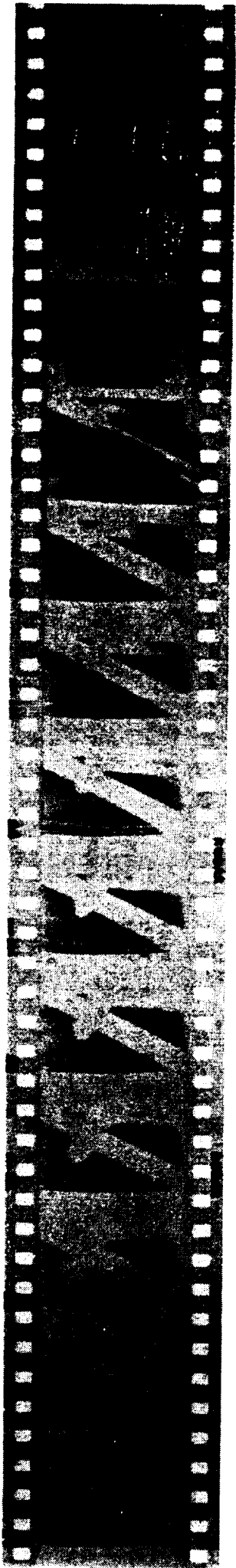


Table 3-7  
Worksheet for Shot # 990

Ejecta and Spall Velocities determined from Hi-Speed Camera

JSC Shot # 990  
 Target type Sr/Ep  
 Actual Projectile Length (in) 0.0711  
 Framing Period 249.7  
 Time between frames (micro-sec) 1.04041666  
 Distance Correction Factor 0.89657752 (est. from crater dimensions)  
 Calc. Proj. Vel. (K/sec) - (uncalculatable)

CALCULATED VALUES (corrected with distance factor)

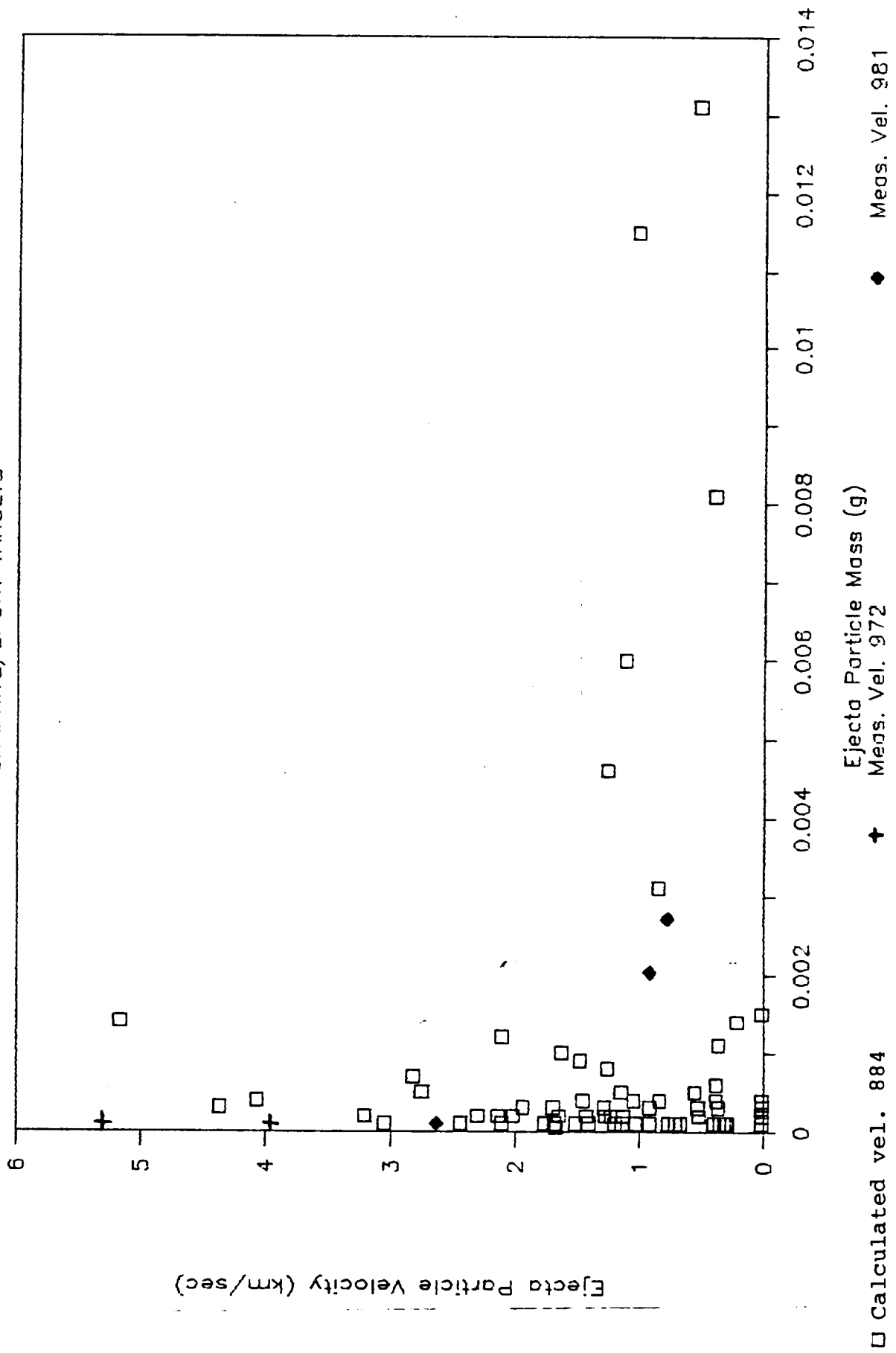
MEASUREMENTS (uncorrected by distance factor)

Frame	EJECTA SIDE				SPALL SIDE				EJECTA SIDE				SPALL SIDE								
	Proj. dist. from plate (in)	Proj. dist. from impact point (in)	Max. cone angle - normal at zero deg. front (deg)	Max. cone angle - normal at zero deg. second front (deg)	Width of crater (in)	Perpen- dicular distance from impact point (in)	Max. cone angle (deg)	Width of crater of crater (in)	Incremental Apparent Velocity (K/sec)	Incremental Velocity corrected for cone angle (K/sec)	Overall Apparent Velocity (K/sec)	Overall Velocity corrected for cone angle (K/sec)	Width of crater (in)	Max. cone angle (deg)	Width of crater of crater (in)	Incremental Apparent Velocity (K/sec)	Incremental Velocity corrected for cone angle (K/sec)	Overall Apparent Velocity (K/sec)	Overall Velocity corrected for cone angle (K/sec)	Incremental Velocity (K/sec)	Overall Velocity (K/sec)
1	0.0703	0.1016	67.75	64.29	0.1094	0.098	20.50	0.098	4.00	5.41	4.89	2.491	0.098	20.50	0.098	4.00	5.41	4.89	4.89	0.17	0.96
2	0.1563	0.1719	67.38	64.44	0.1172	0.105	22.47	0.105	4.89	5.41	4.89	2.469	0.105	22.47	0.105	4.89	5.41	4.89	4.89	0.38	0.67
3				65.73	0.1250	0.112		0.112	1.54	3.74	3.74	2.847	0.112		0.112	1.54	3.74	3.74	3.74	0.86	0.73
4					0.1328	0.0516		0.119	2.22			3.025	0.119		0.119					0.86	0.73
5					0.1406	0.0688		0.126	1.54			3.202	0.126		0.126					0.68	0.72
6					0.1484	0.1078		0.133	1.54			3.380	0.133		0.133					0.89	0.75
7					0.15625	0.1390625		0.140	1.54			3.558	0.140		0.140					0.68	0.74
8					0.1640625	0.1796875		0.147	1.54			3.736	0.147		0.147					0.68	0.74
9					0.171875	0.2109375		0.154	1.54			3.914	0.154		0.154					0.51	0.71
10					0.171875	0.234375		0.154	1.54			4.092	0.154		0.154					0.51	0.71
11					0.1796875	0.2734375		0.161	1.54			4.270	0.161		0.161					0.51	0.71
20					0.203125			0.182	1.54			4.626	0.182		0.182					0.51	0.71
24					0.2109375			0.189	1.54			4.804	0.189		0.189					0.51	0.71

Figure 3-83

# EJECTA MASS & VELOCITY

GRAPHITE/EPOXY TARGETS







## 4.0 Aluminum Targets

A significant fraction, if not most of the Space Station, will be built of aluminum. Some data on aluminum spall and ejecta exists in the literature. The following shots supplement this information.

All of the targets used in these shots were 6 x 6 x 0.089 inch thick 6061 T-6 aluminum. This material is representative of what might be expected in a bumper or outer wall protecting the inner hull of a habitation module.

### 4.1 Shot #933 (0.089 " Thick 6061 T-6 Aluminum)

The test setup for this shot was exactly the same as for the graphite/epoxy shots #917 and 923. The target was inside a plexiglass box, with styrofoam all around to catch the spall and ejecta.

Table 3-2 summarizes the data for this shot. A 4.98 mg nylon projectile impacted a 0.089 inch thick target of 6061 T-6 aluminum traveling at 6.3 km/sec. 0.12 grams of ejecta and spall were collected, making up 50.9 percent of the mass change of the target. 71.2 percent of the collected material was spall.

Figure 4-1 shows the target after the shot.

Figures 4-2 and 4-3 plot ejecta mass versus length and diameter. The length and diameter terms are somewhat misleading holdovers from the graphite/epoxy plots. The aluminum particles are small chips or flakes rather than slivers.

Figures 4-4 through 4-7 plot ejecta mass and calculated velocity versus theta and phi (see appendix B for a definition of theta and phi). The calculated velocities are, in general much higher than for the graphite epoxy shots. The high speed film data (see section 4.2) indicates that while these estimated velocities are in the correct range for the large particles, they may be a factor of two or so too high for the small particles. Thus the highest velocities indicated in these graphs may need to be reduced by a factor of two.

Figures 4-8 and 4-9 plot ejecta mass and velocity versus cone angle. The cone angle, in this case, is the angle between a normal to the target face at the impact point and the ejecta particle's velocity vector.

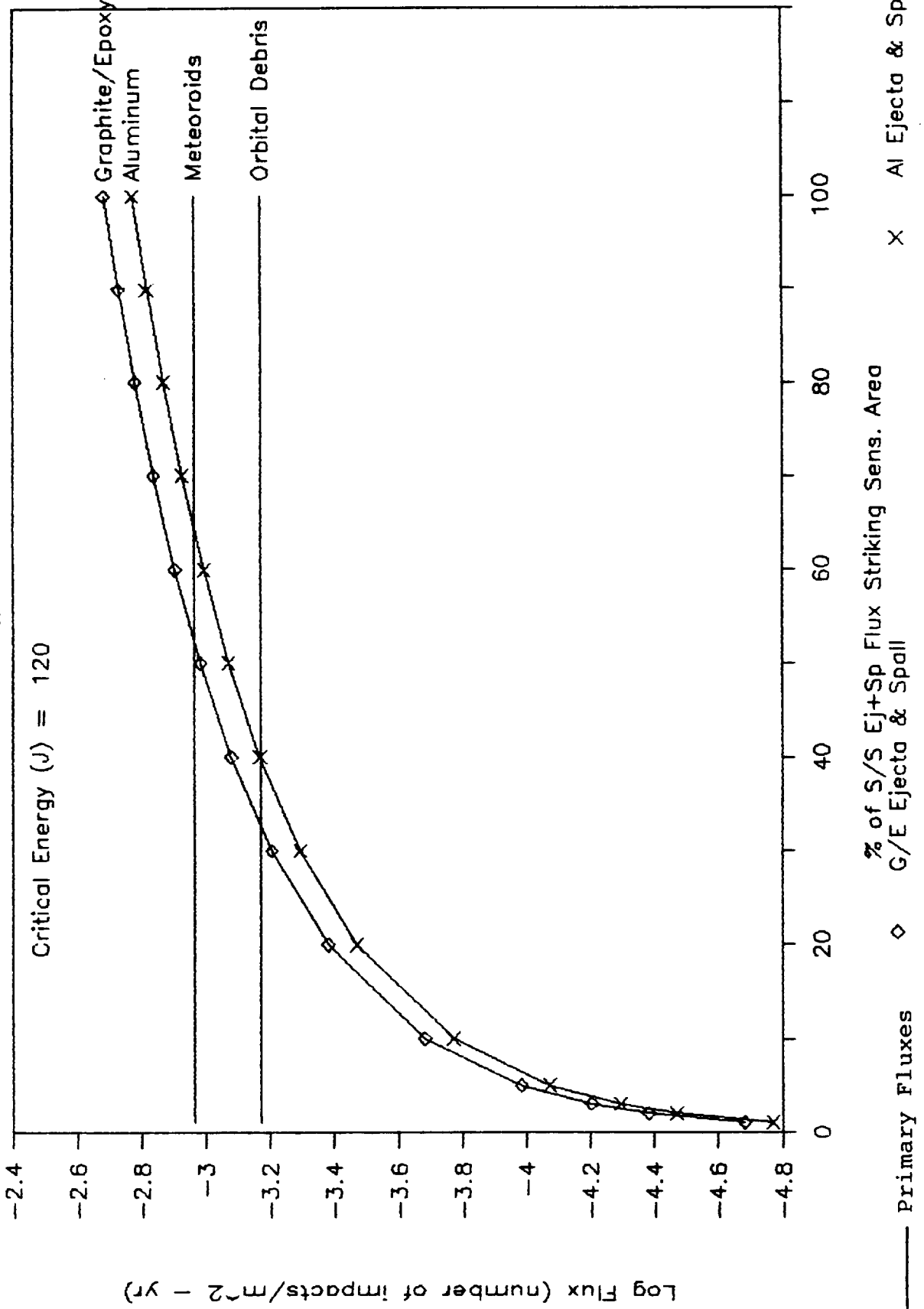
Figure 4-10 plots ejecta mass versus velocity. This plot is estimated to include about half the total ejecta mass.

Figure 4-11 plots the Log(number of ejecta particles of mass  $M_i$  and larger) versus the Log( $M_i/M_{total}$  ejecta mass). A least

Figure 6-2

# Primary and Secondary Particle Fluxes

vs % S/S crit energy ej/sp flux on area



195

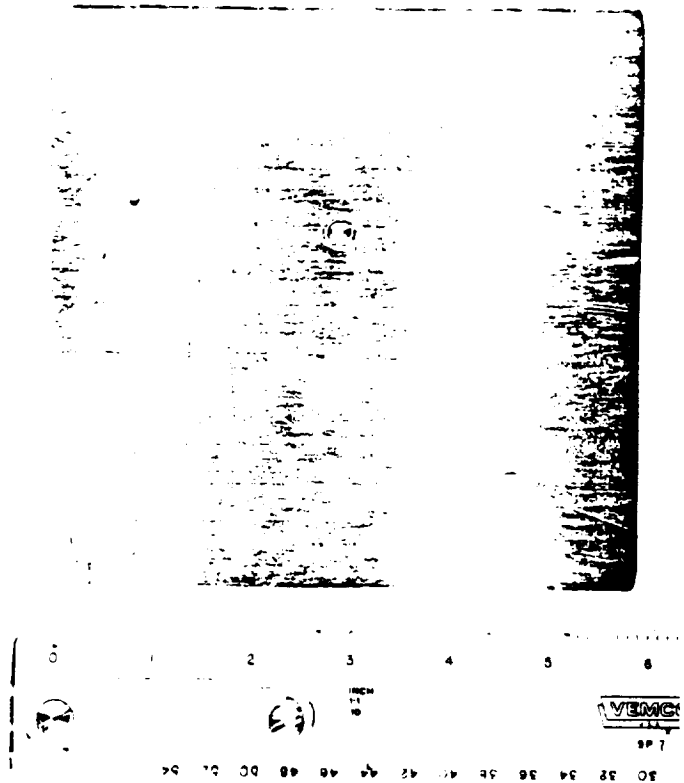
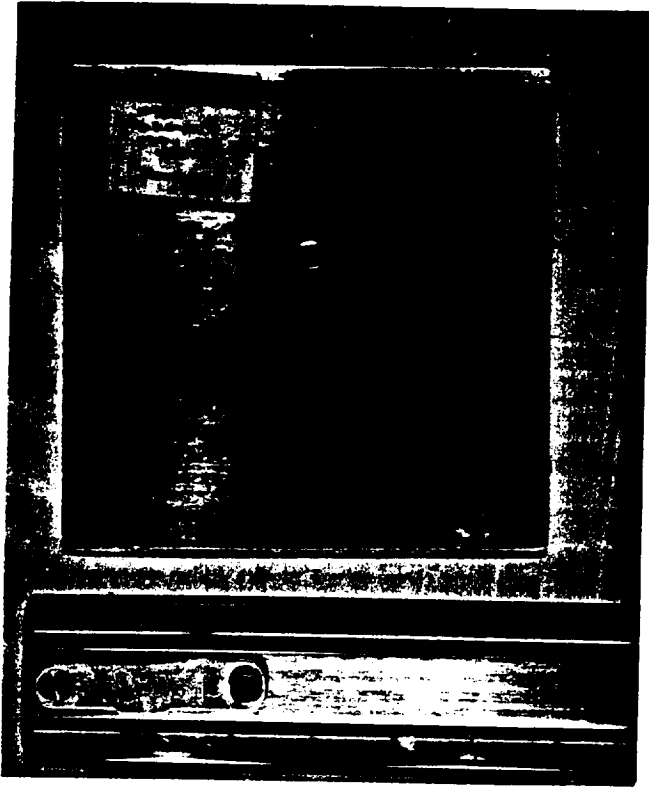
118

**Figure 4-1, Photos of Target (Shot #933)**

0.089 inch thick, 6061 T-6 Aluminum

Front

Back



**ORIGINAL PAGE IS  
OF POOR QUALITY**

*118*  
**PRECEDING PAGE BLANK NOT FILMED**

Figure 4-2

# EJECTA MASS & LENGTH

JSC Shot No. 933 - Al Plate

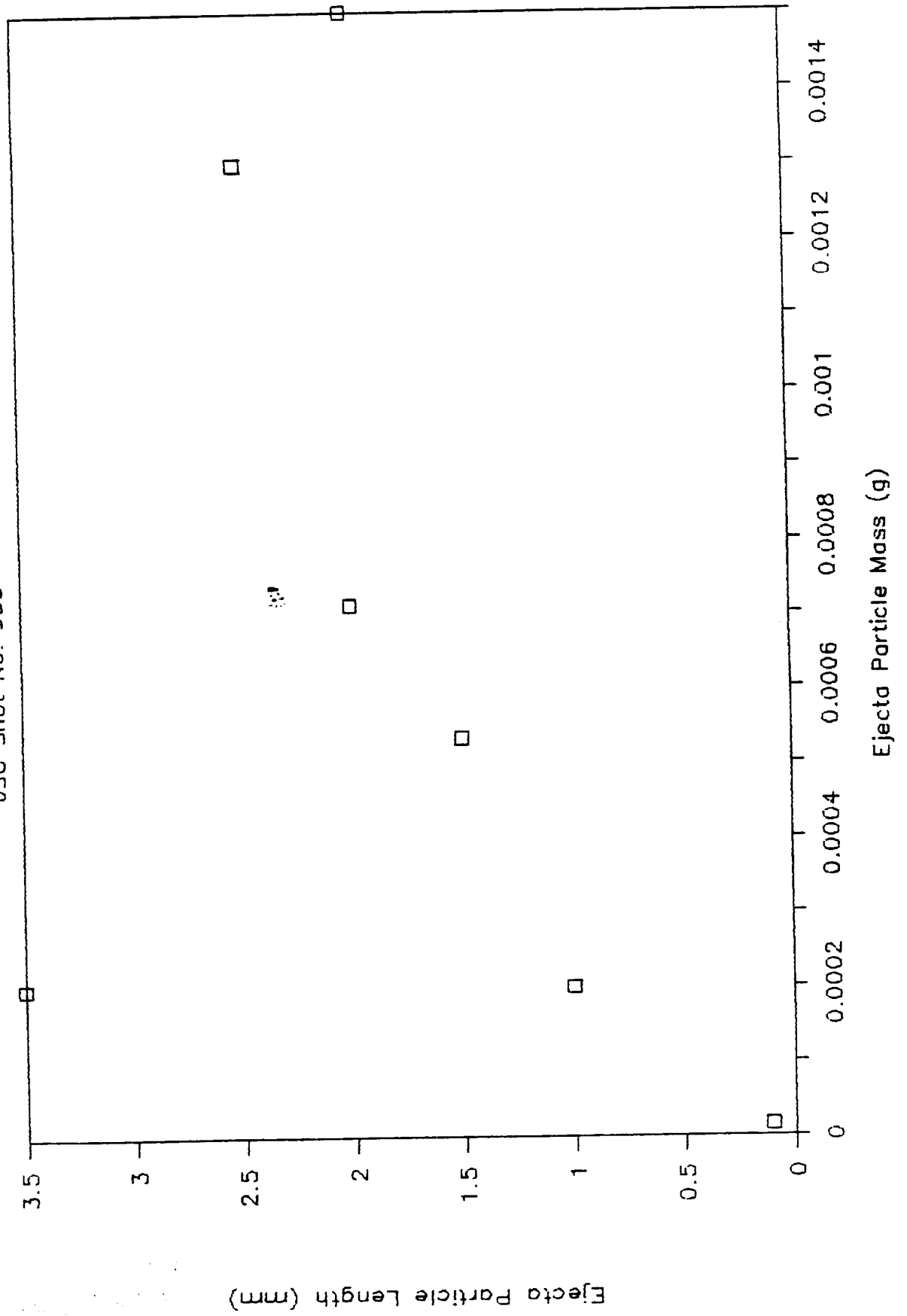


Figure 4-3

# EJECTA MASS & DIAMETER

JSC Shot No. 933 - Al Plate

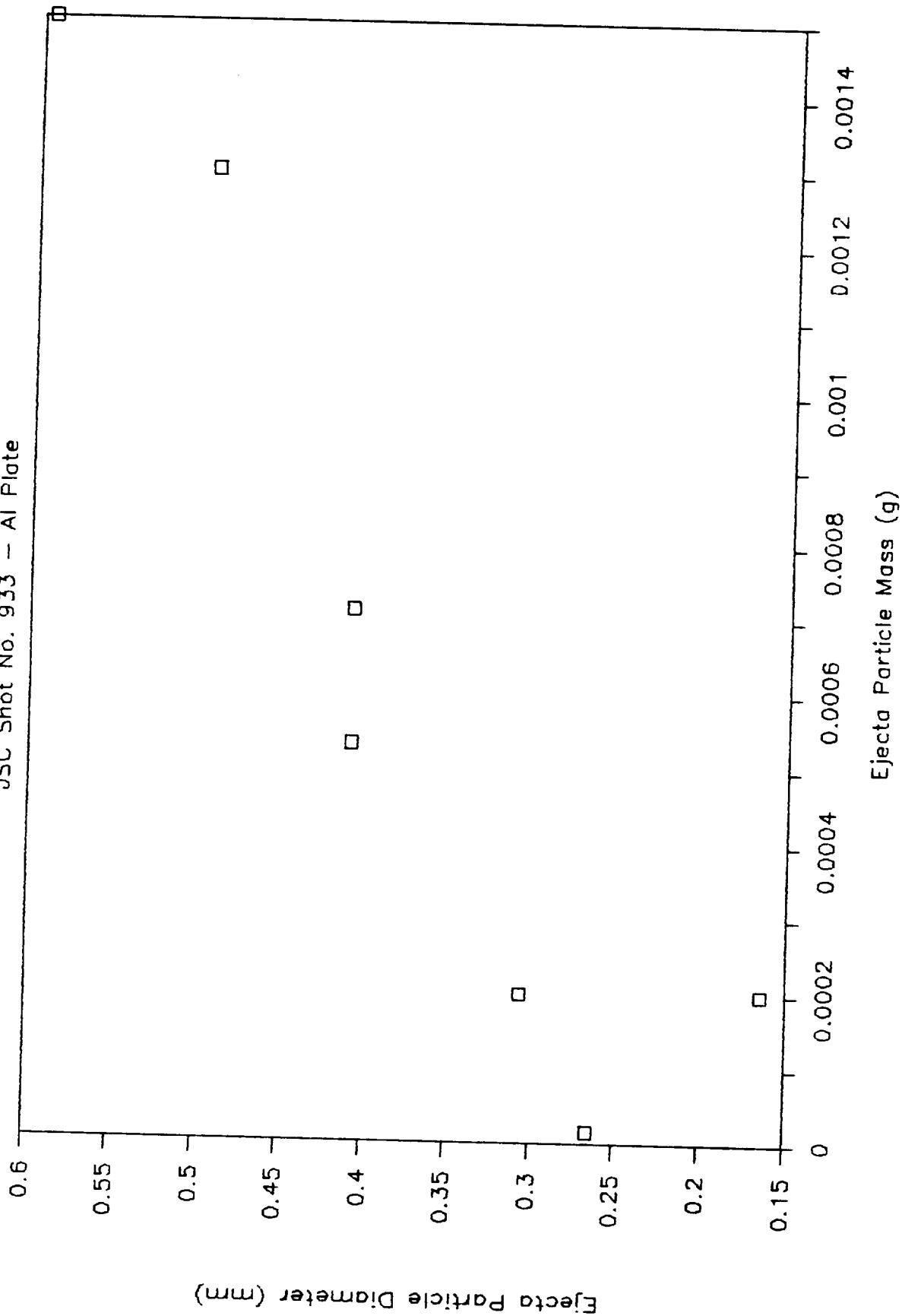


Figure 4-4

# EJECTA MASS DISTRIBUTION

JSC Shot No. 933 - Al Plate

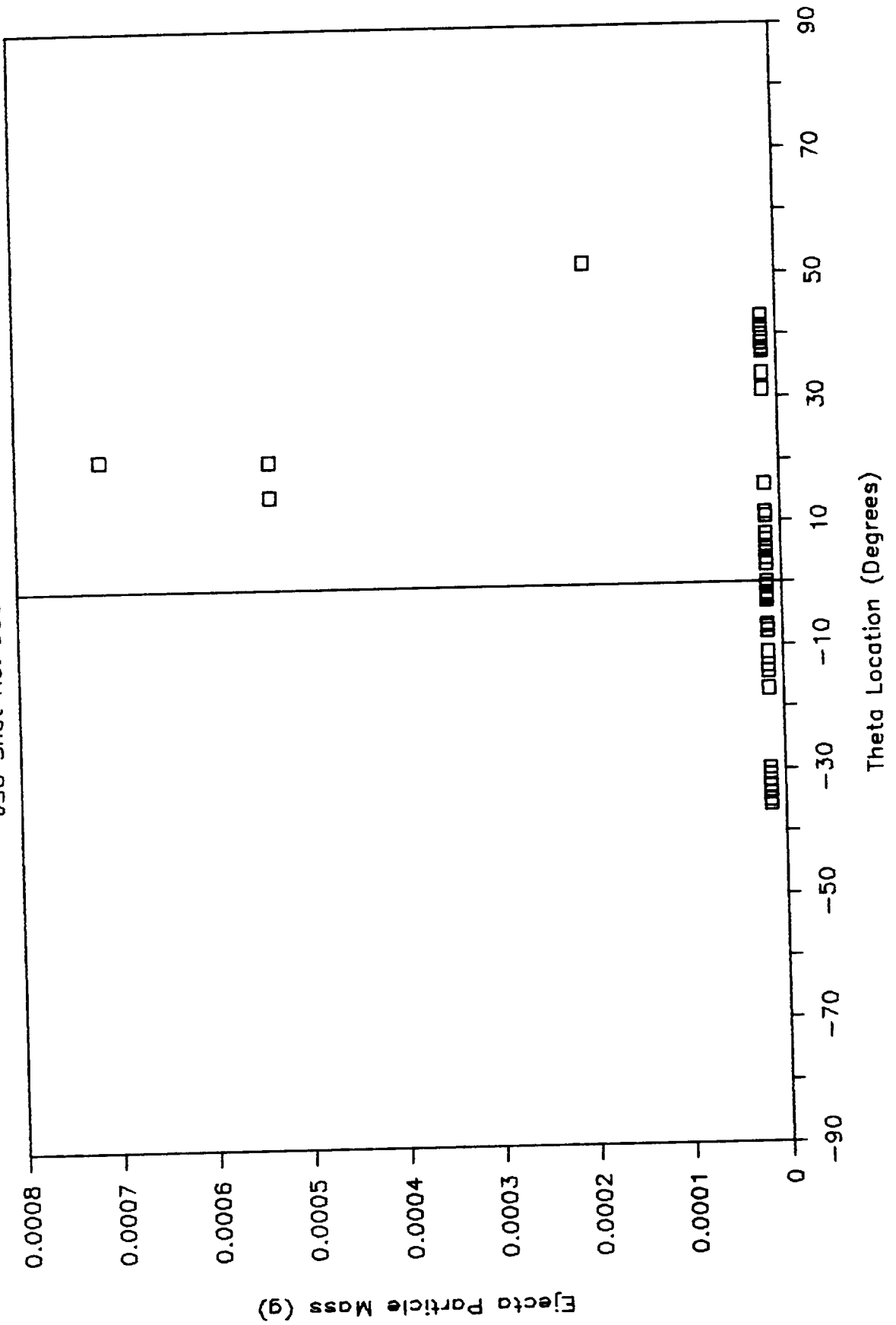


Figure 4-5

# EJECTA VELOCITY DISTRIBUTION

JSC Shot No. 933 - Al Plate

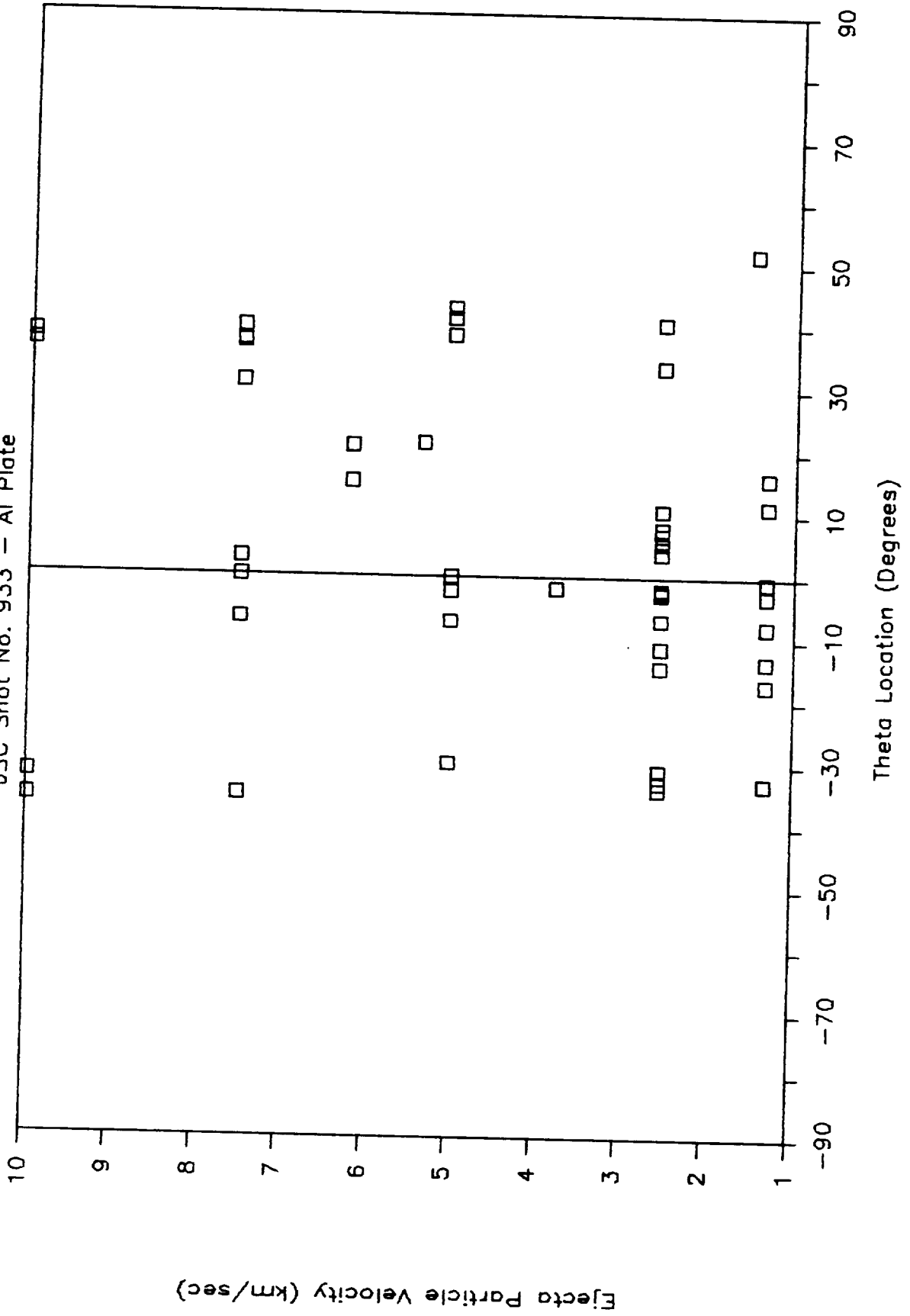


Figure 4-6

# EJECTA MASS DISTRIBUTION

JSC Shot No. 933 - Al Plate

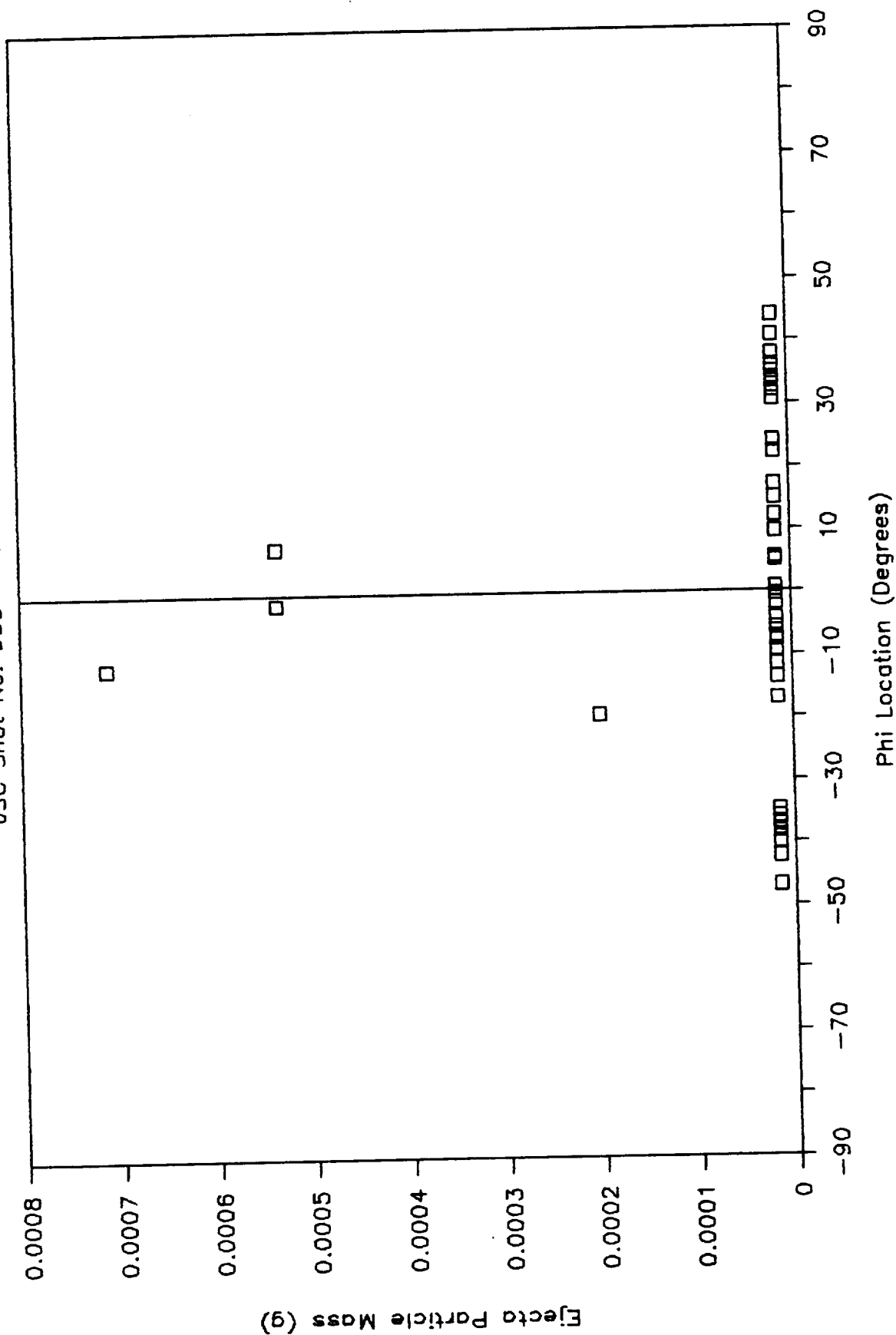




Figure 4-7

# EJECTA VELOCITY DISTRIBUTION

JSC Shot No. 933 - Al Plate

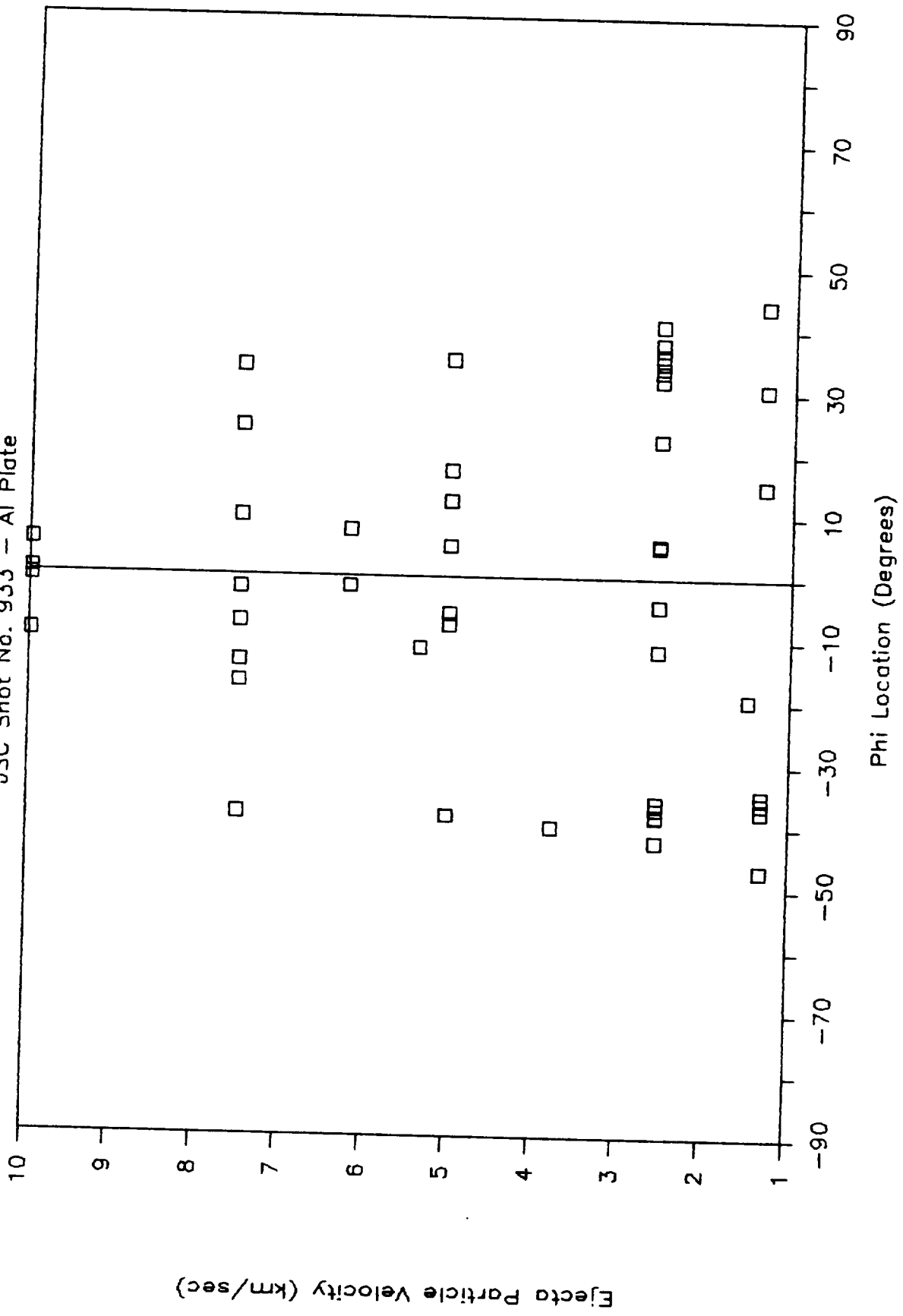


Figure 4-8

# EJECTA MASS DISTRIBUTION

JSC Shot No. 933 - Al Plate

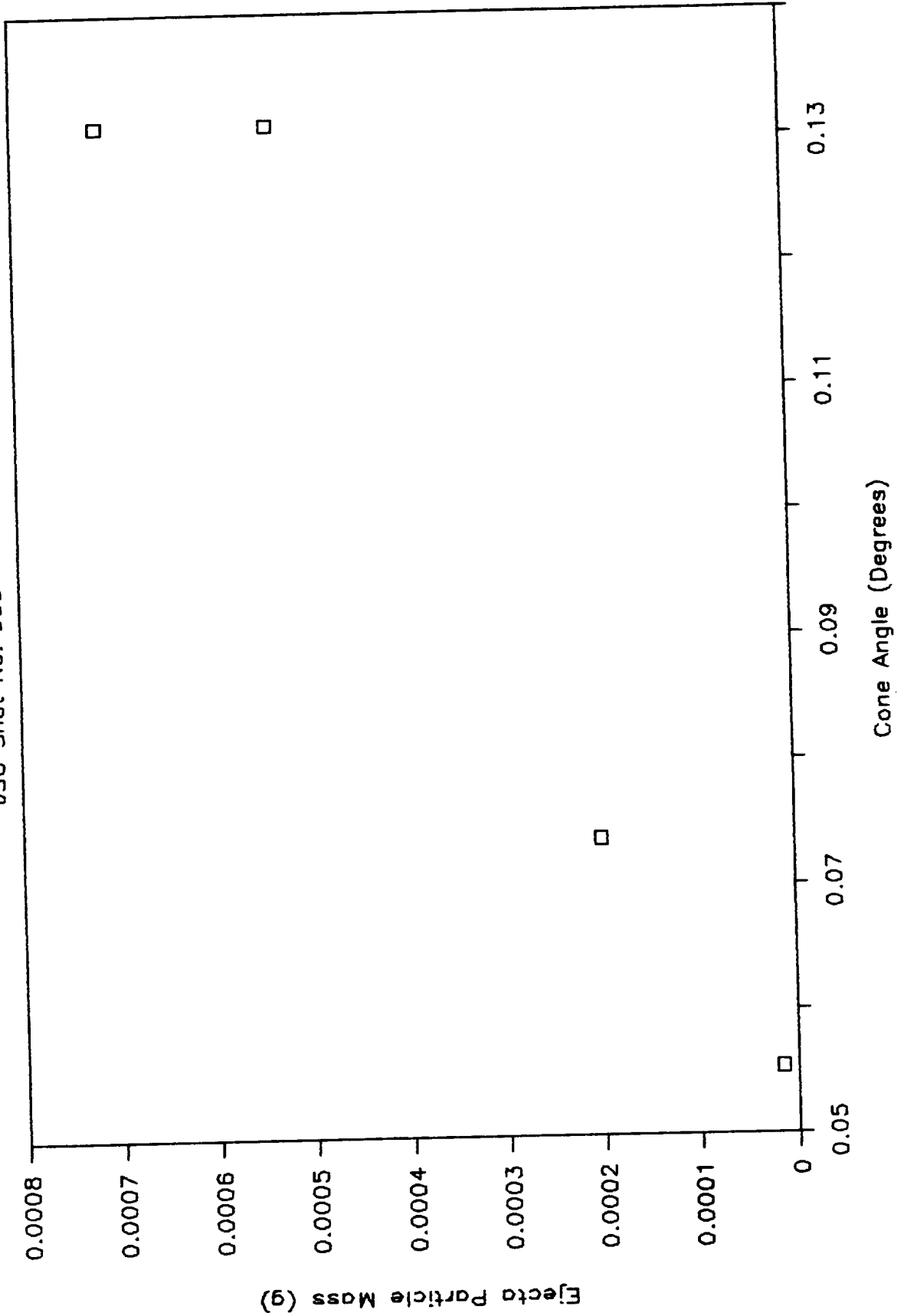


Figure 4-9

# EJECTA VELOCITY DISTRIBUTION

JSC Shot No. 933 - Al Plate

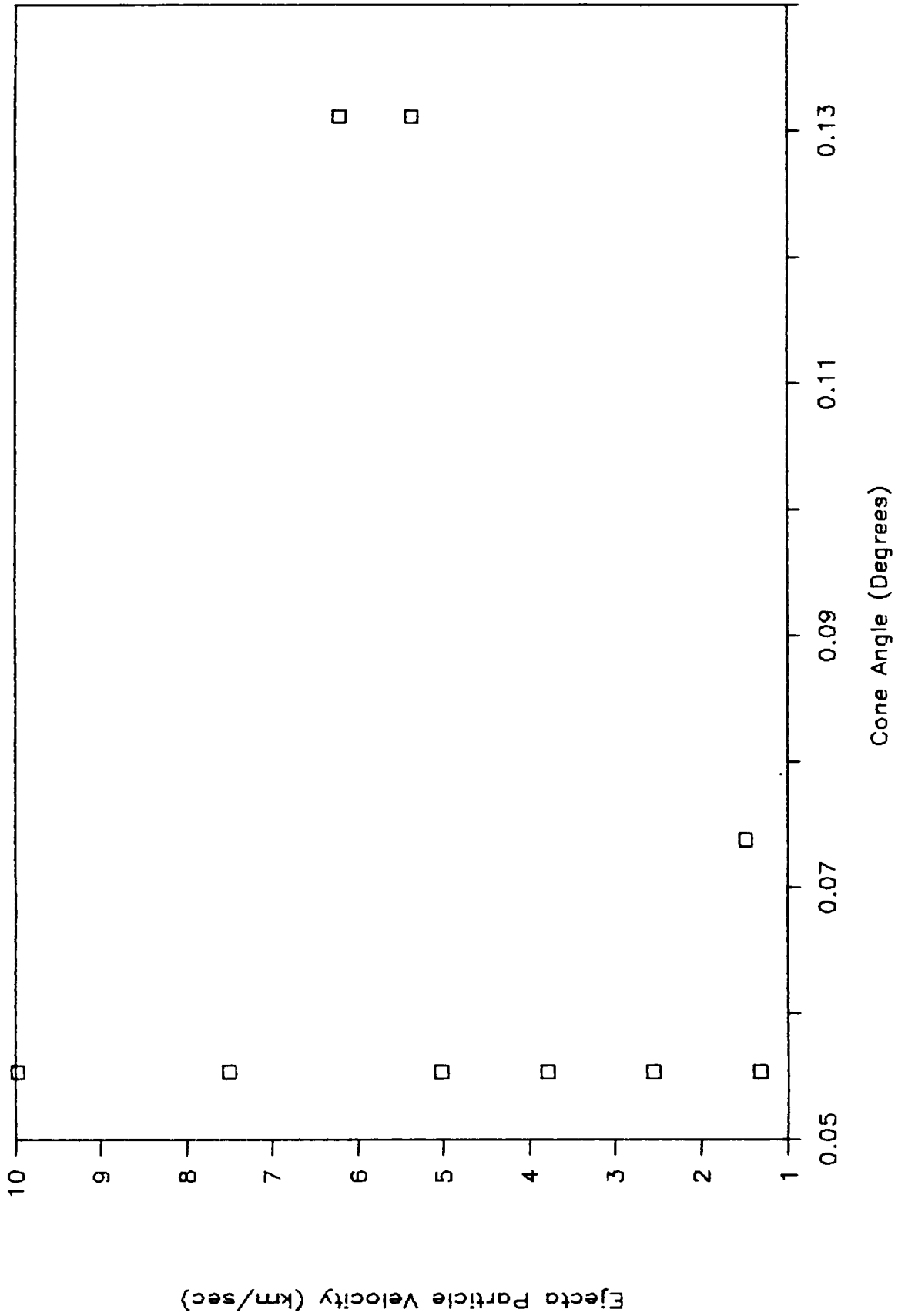


Figure 4-10

# EJECTA MASS & VELOCITY

JSC Shot No. 933 - Al Plate

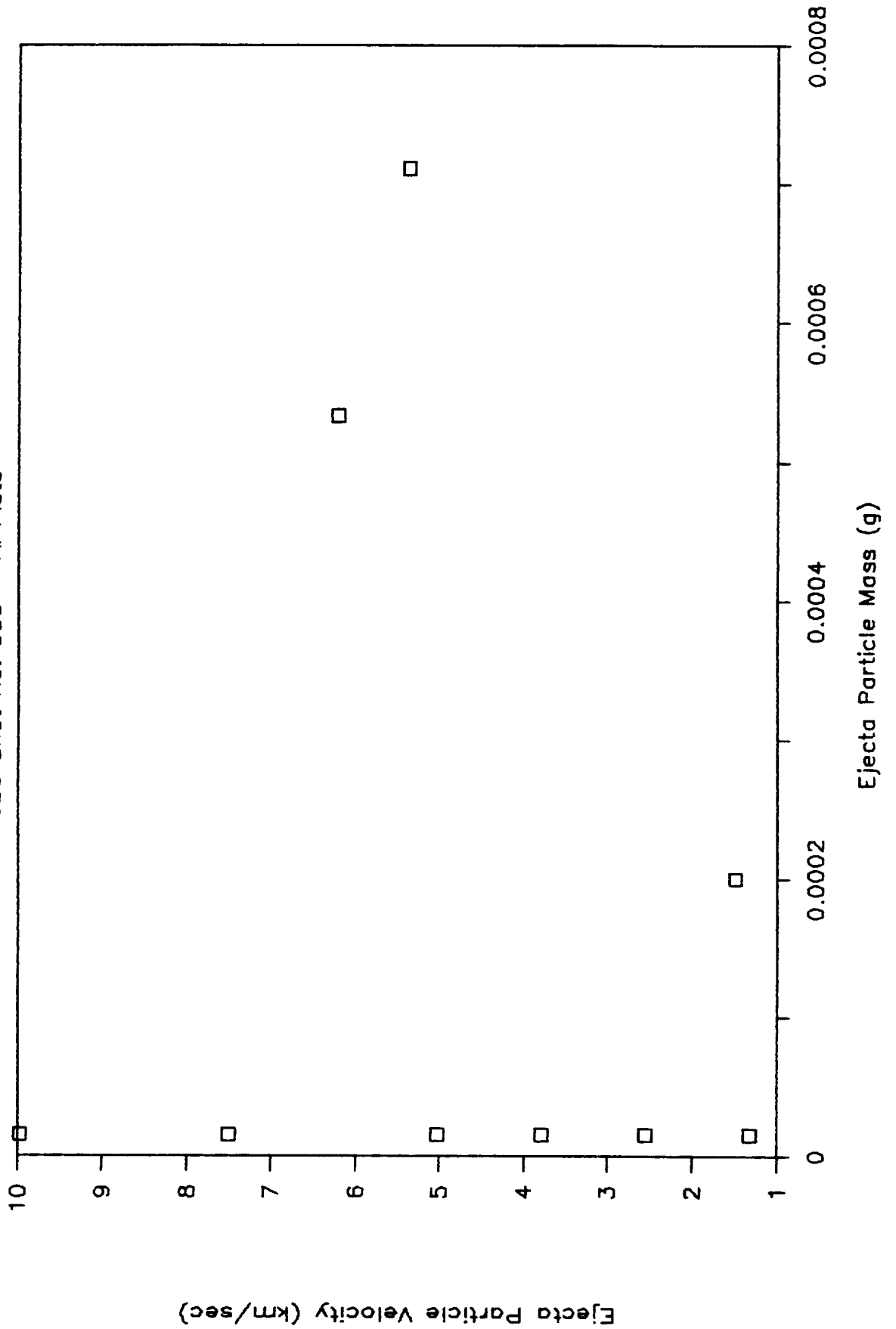


Figure 4-11

# EJECTA MASS AND PARTICLE NUMBER

JSC Shot No. 933 - Thin Al Plate

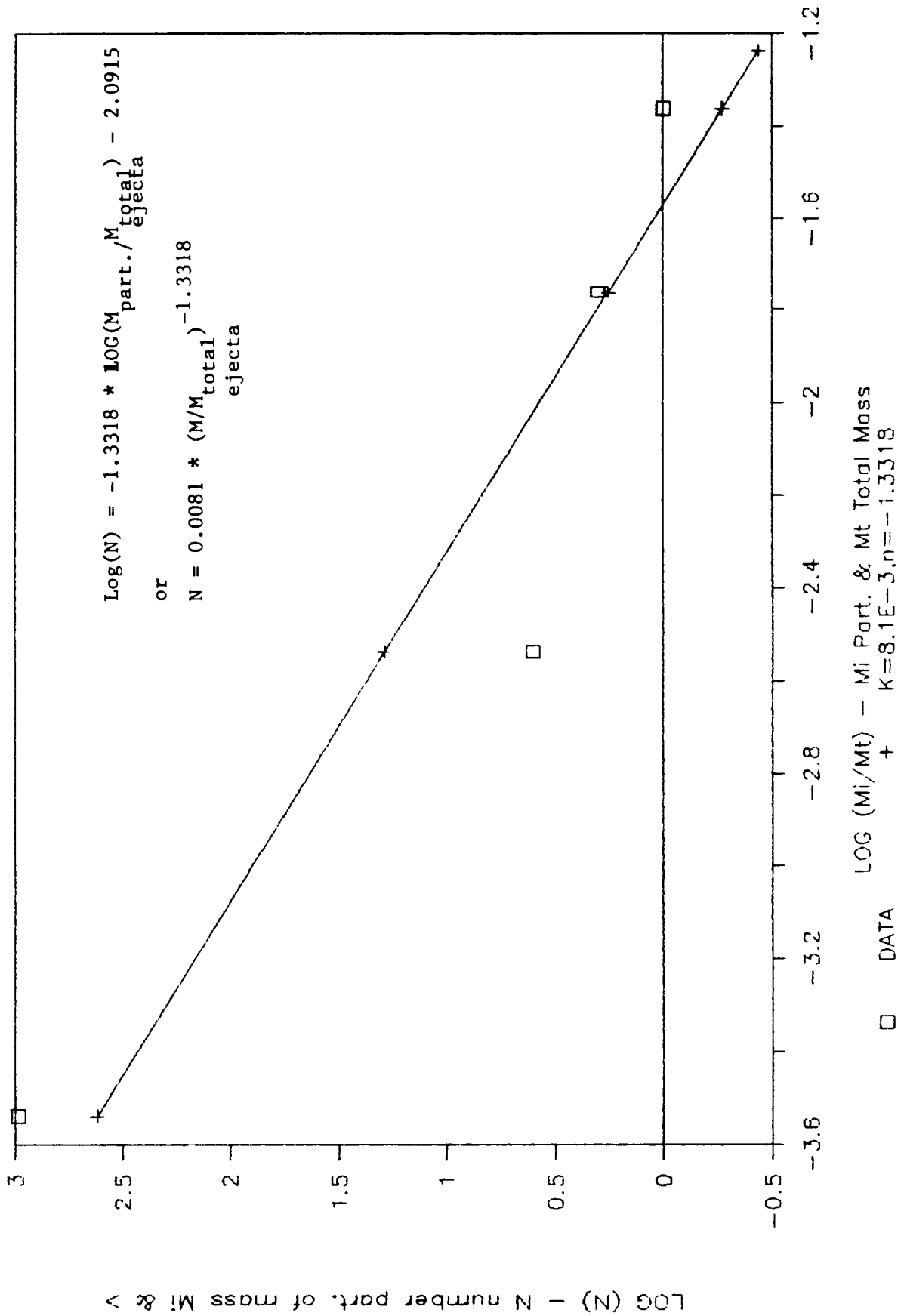


Figure 4-12

# SPALL MASS & LENGTH

JSC Shot No. 933 - Al Plate

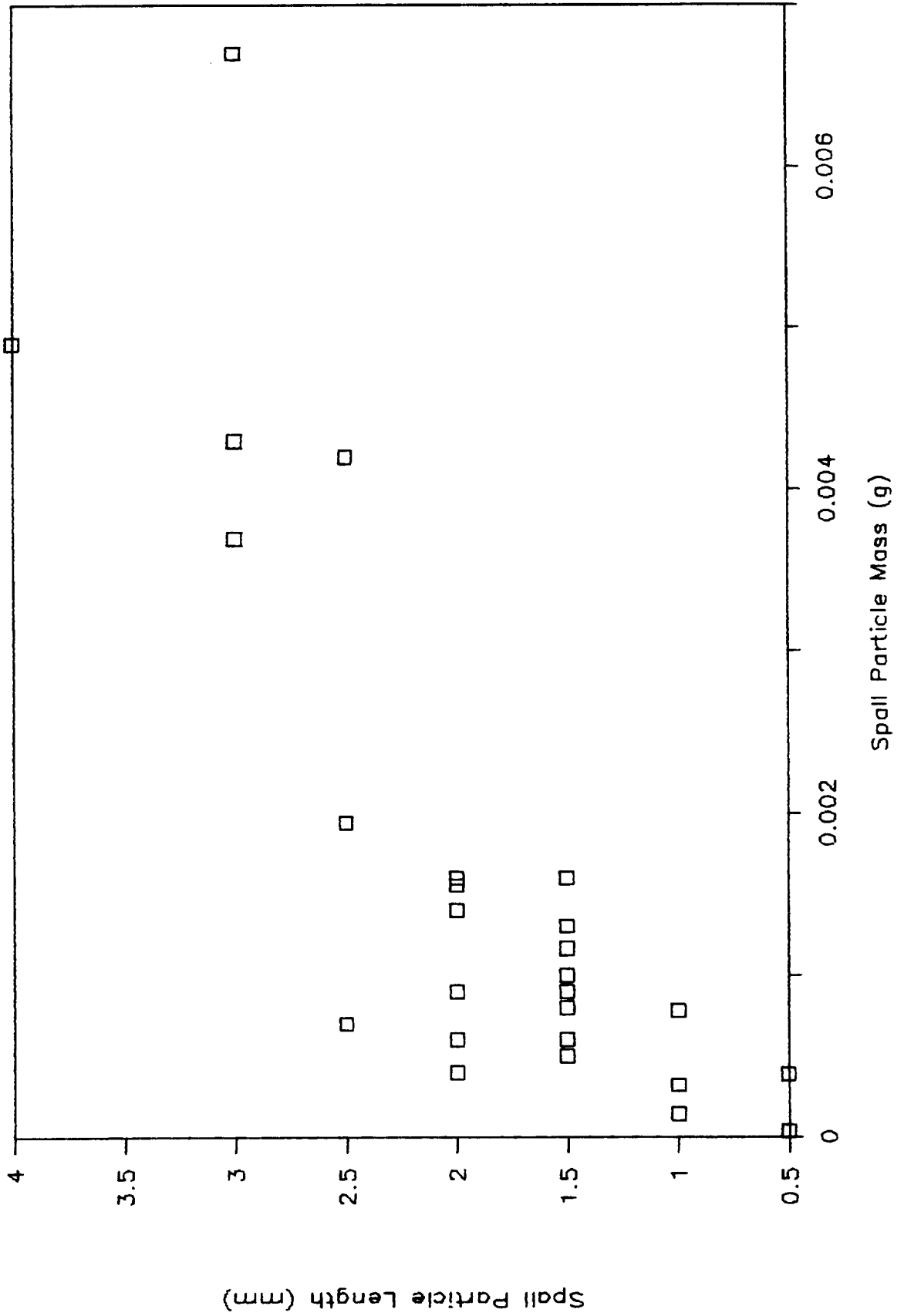


Figure 4-13

# SPALL MASS & DIAMETER

JSC Shot No. 933 - Al Plate

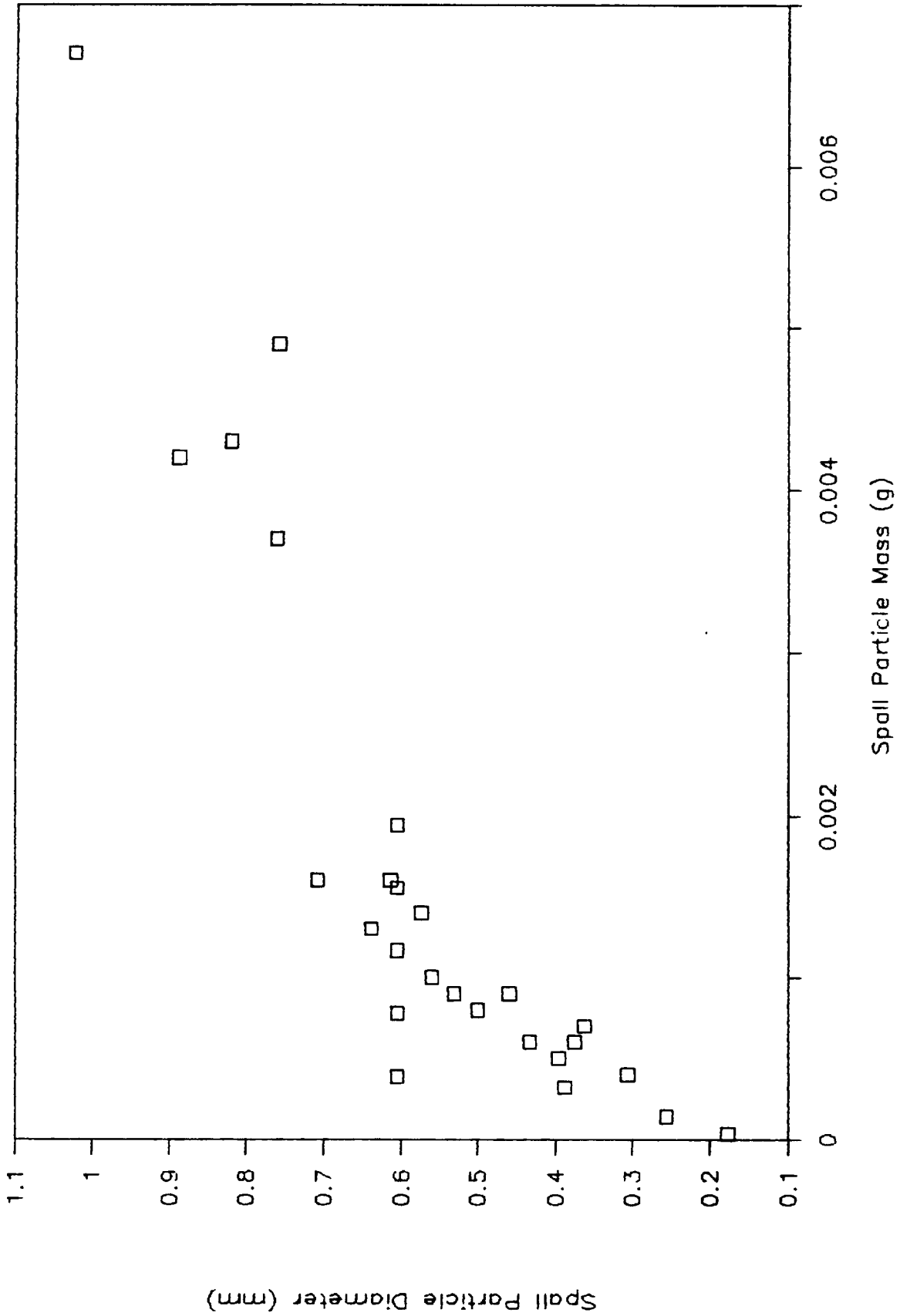


Figure 4-14

# SPALL MASS DISTRIBUTION

JSC Shot No. 933 - Al Plate

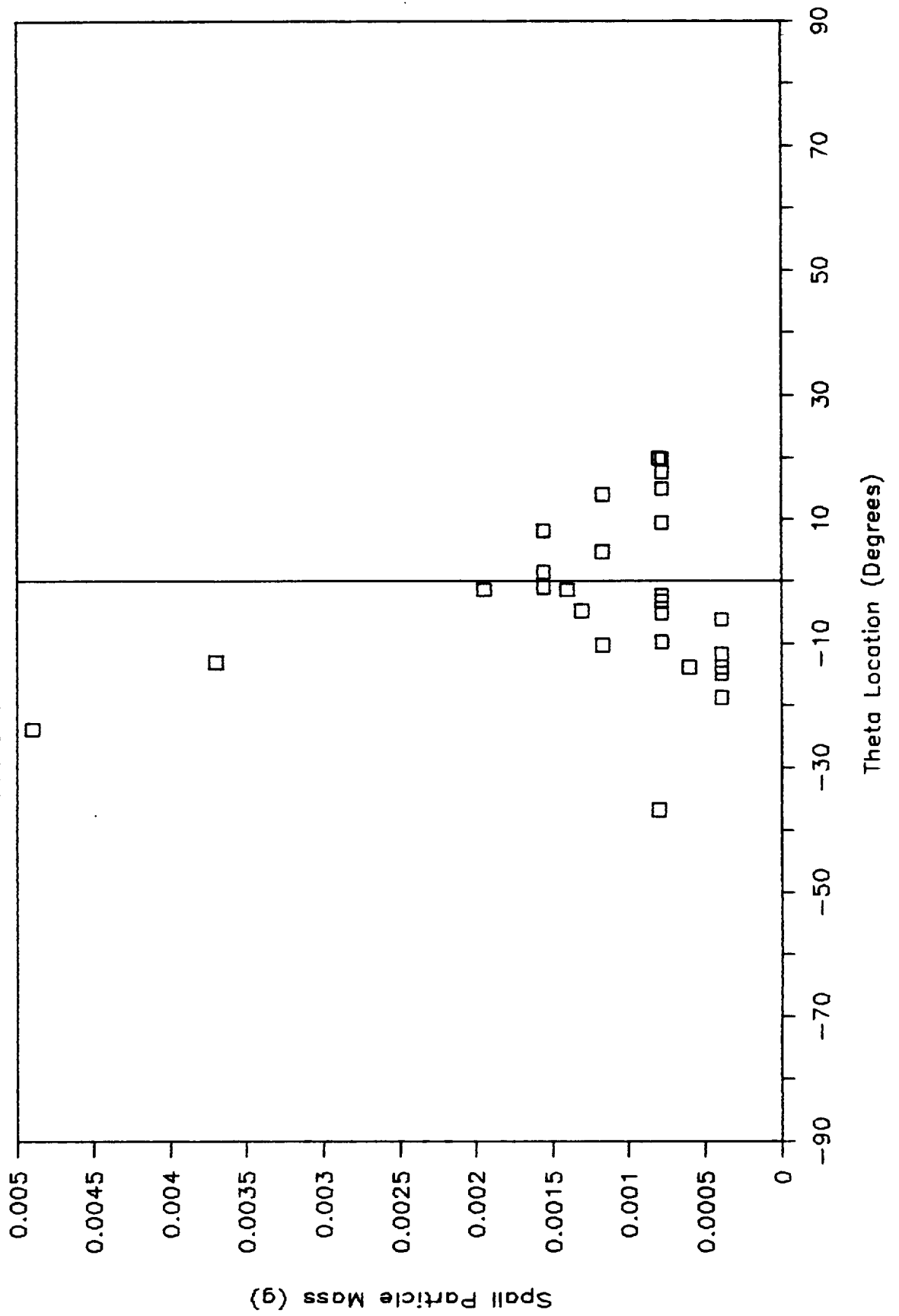




Figure 4-15

# SPALL VELOCITY DISTRIBUTION

JSC Shot No. 933 - Al Plate

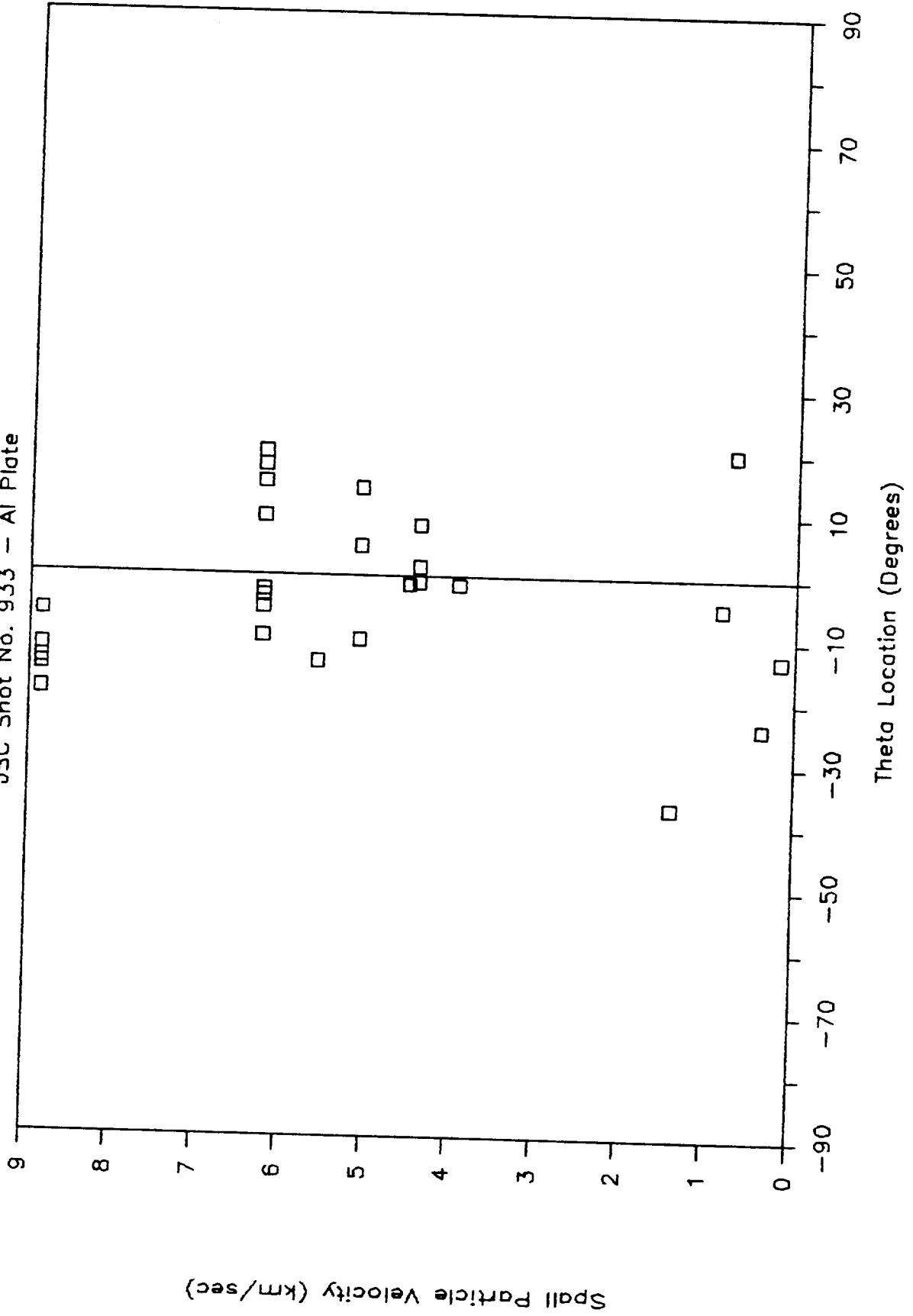


Figure 4-16

# SPALL MASS DISTRIBUTION

JSC Shot No. 933 - Al Plate

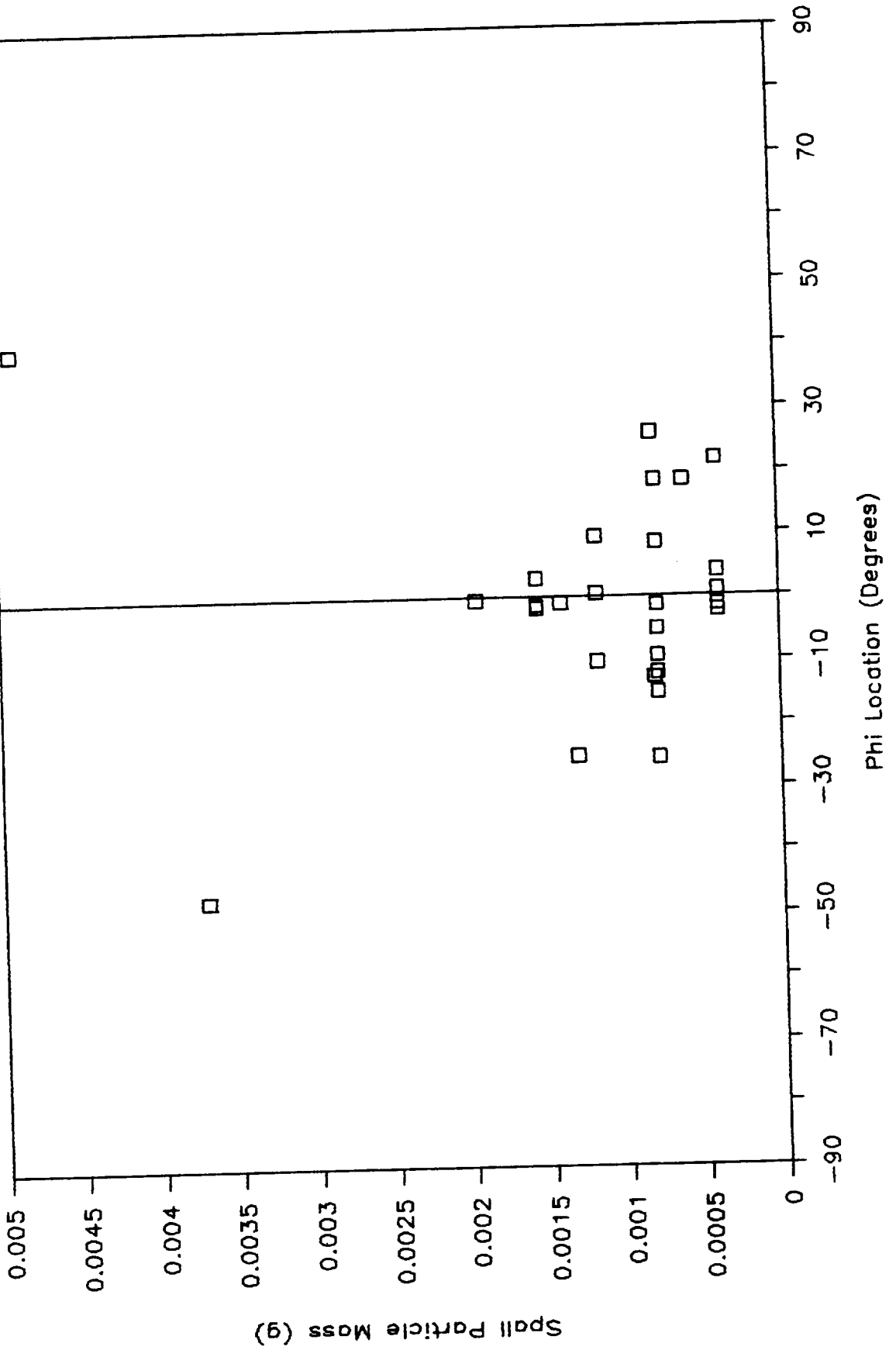


Figure 4-17

# SPALL VELOCITY DISTRIBUTION

JSC Shot No. 933 - Al Plate

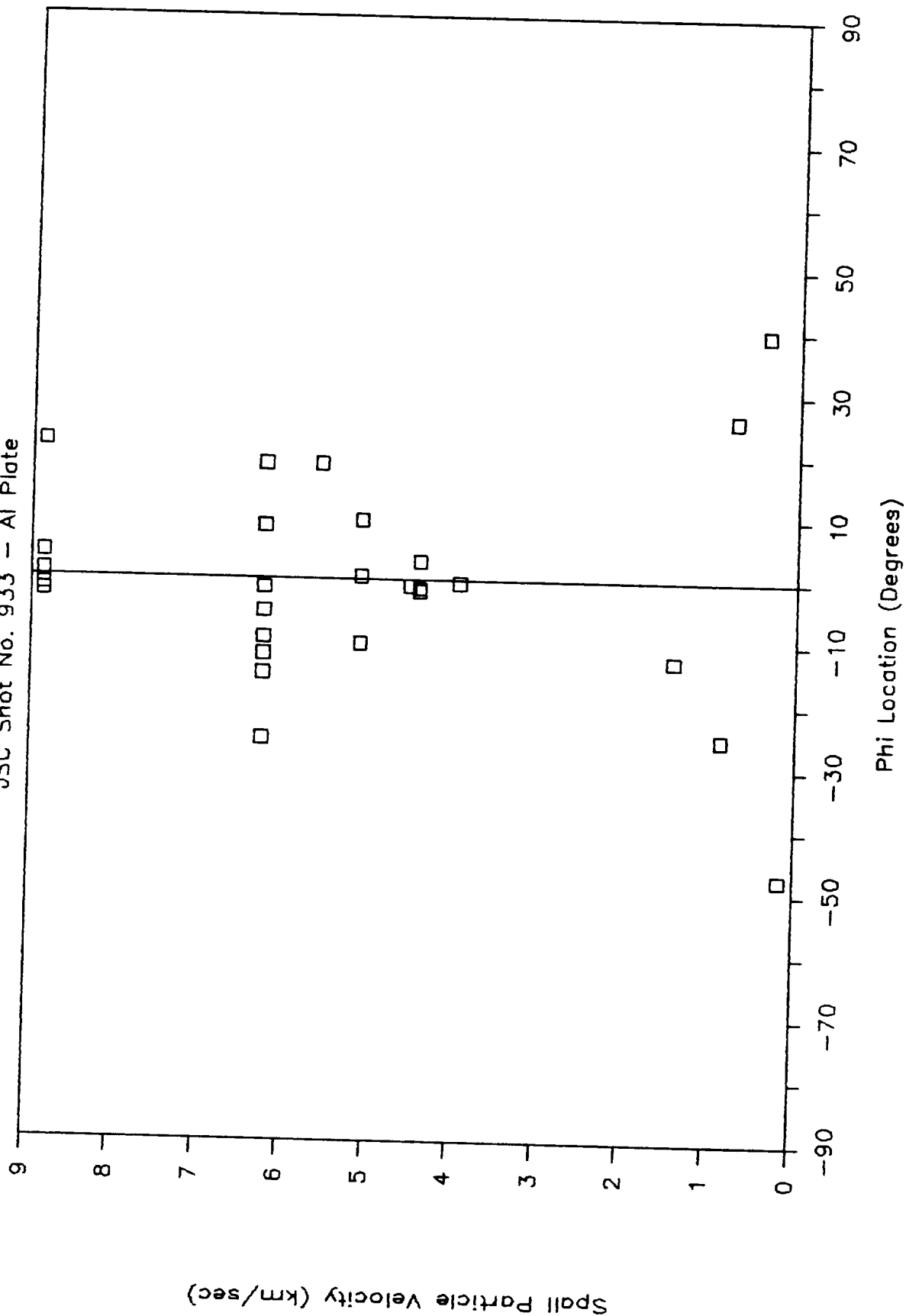


Figure 4-18

# SPALL MASS DISTRIBUTION

JSC Shot No. 933 - Al Plate

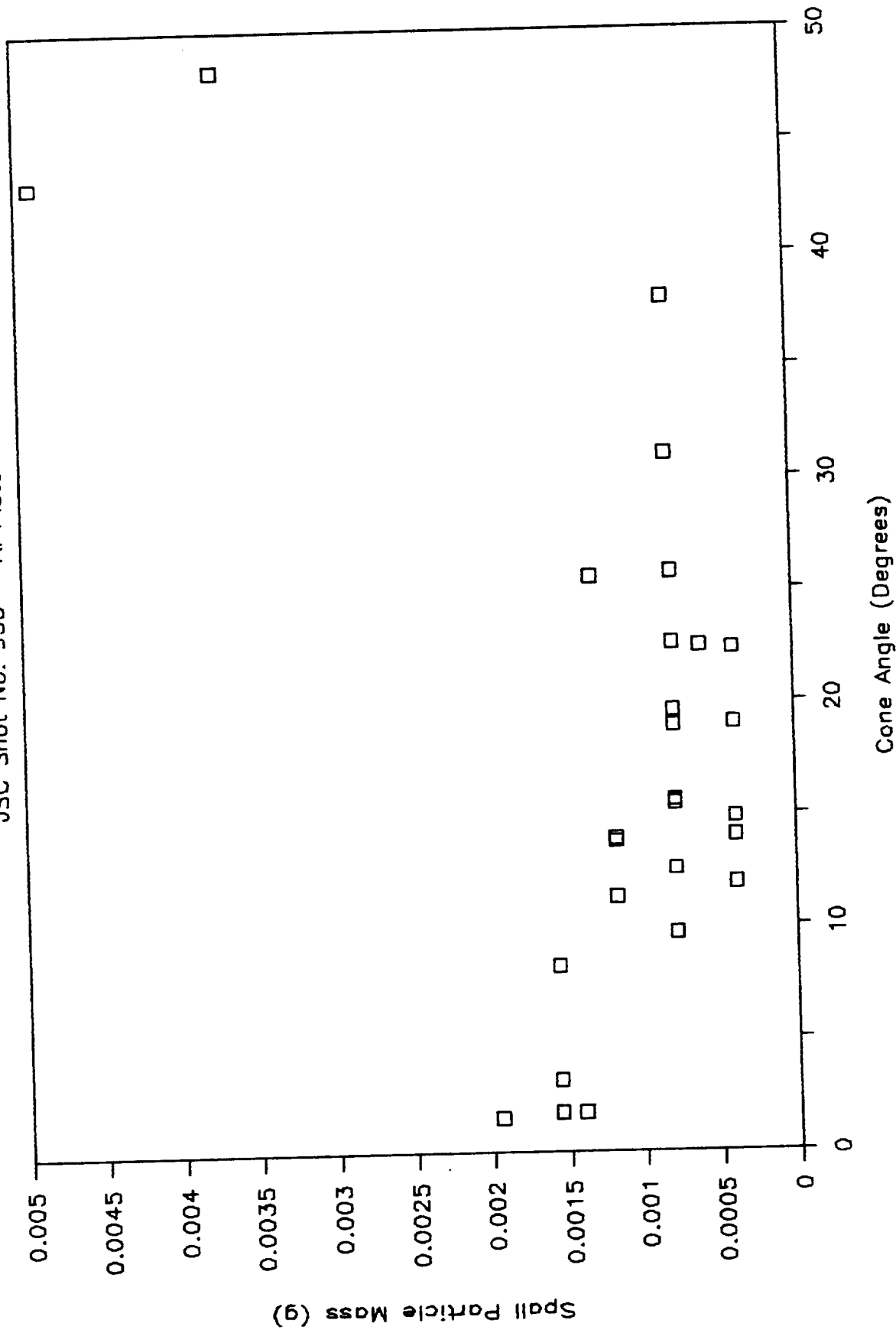


Figure 4-19

# SPALL VELOCITY DISTRIBUTION

JSC Shot No. 933 - Al Plate

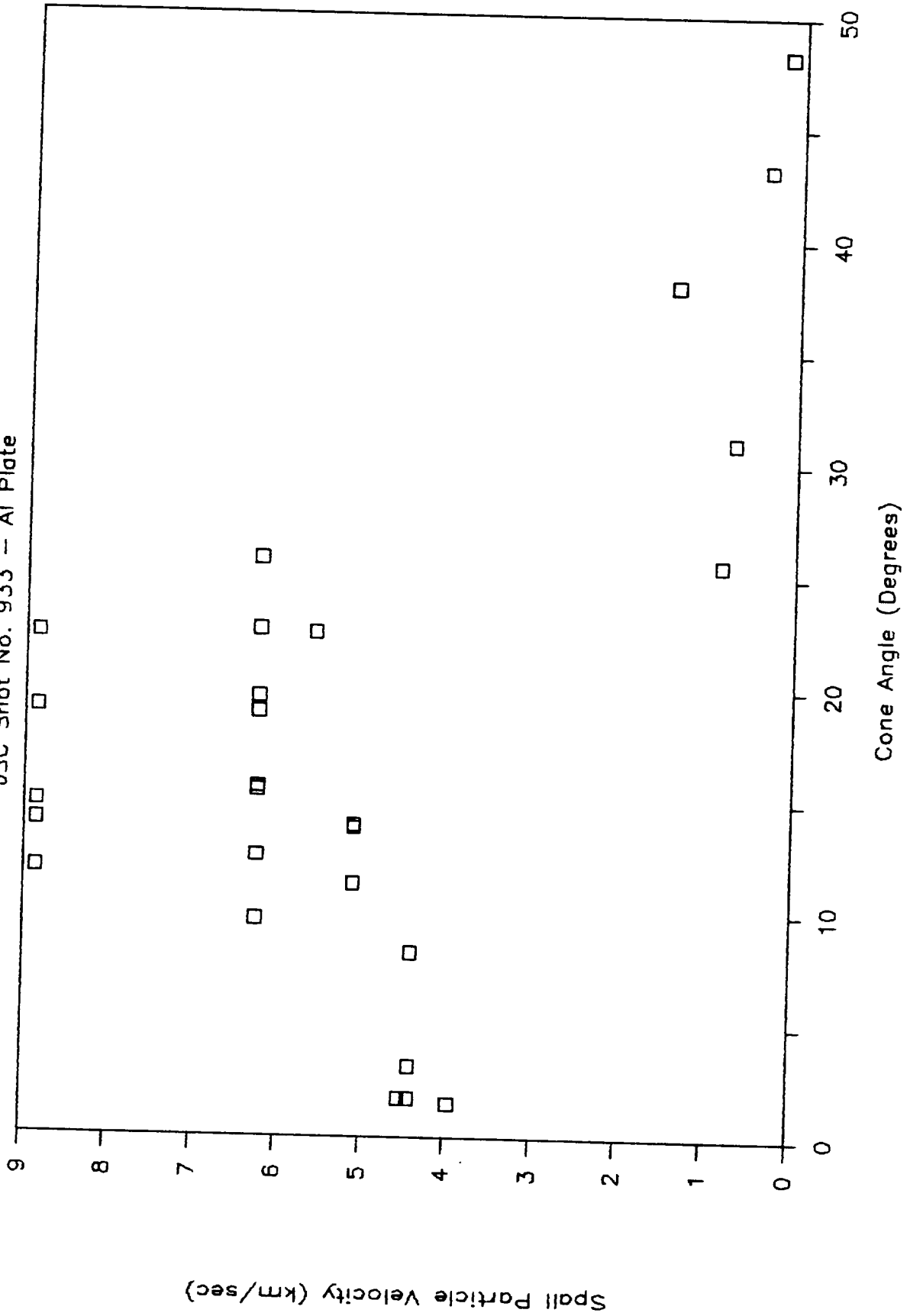


Figure 4-20

# SPALL MASS & VELOCITY

JSC Shot No. 933 - Al Plate

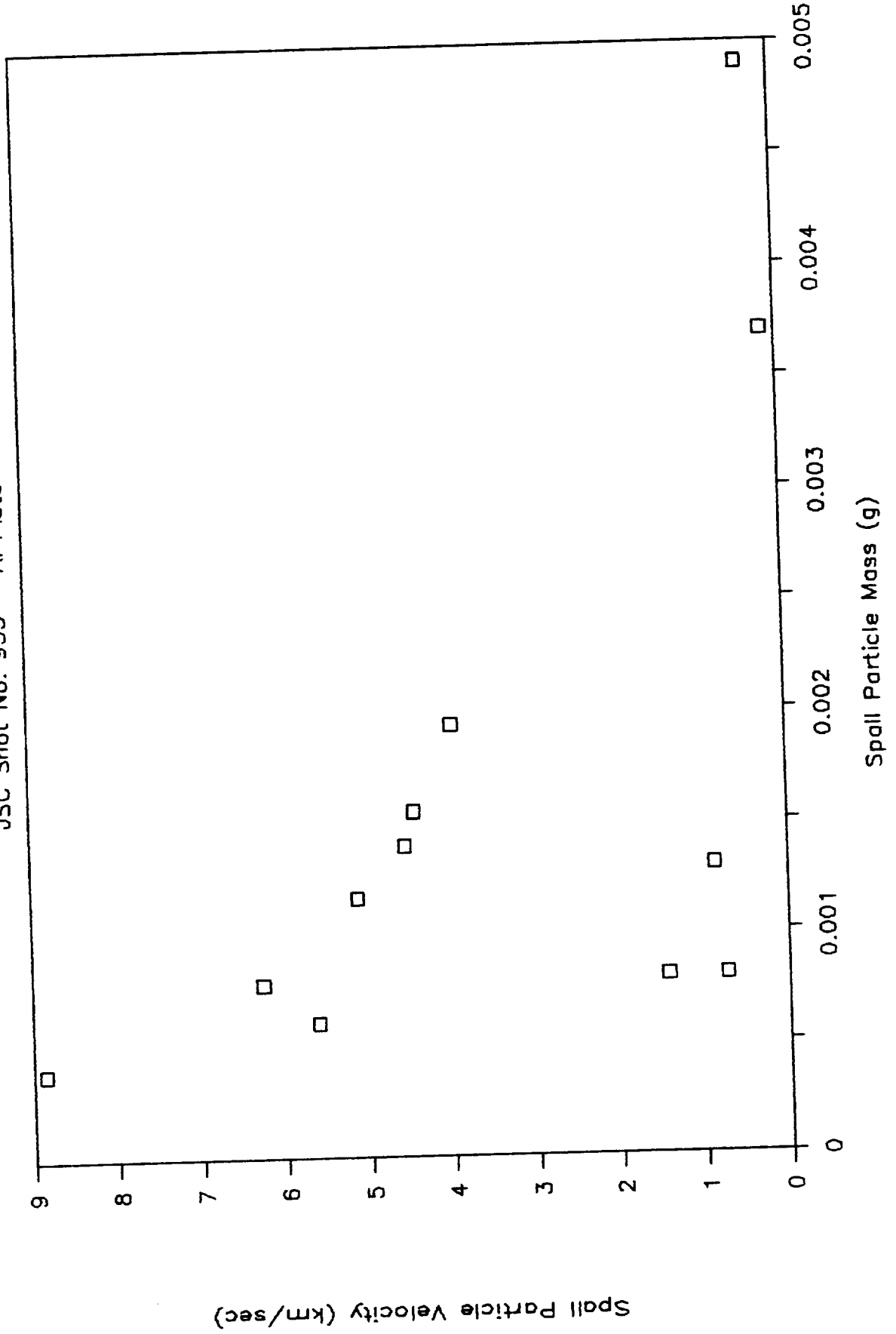


Figure 4-21

# SPALL MASS AND PARTICLE NUMBER

JSC Shot No. 933 - Thin Al Plate

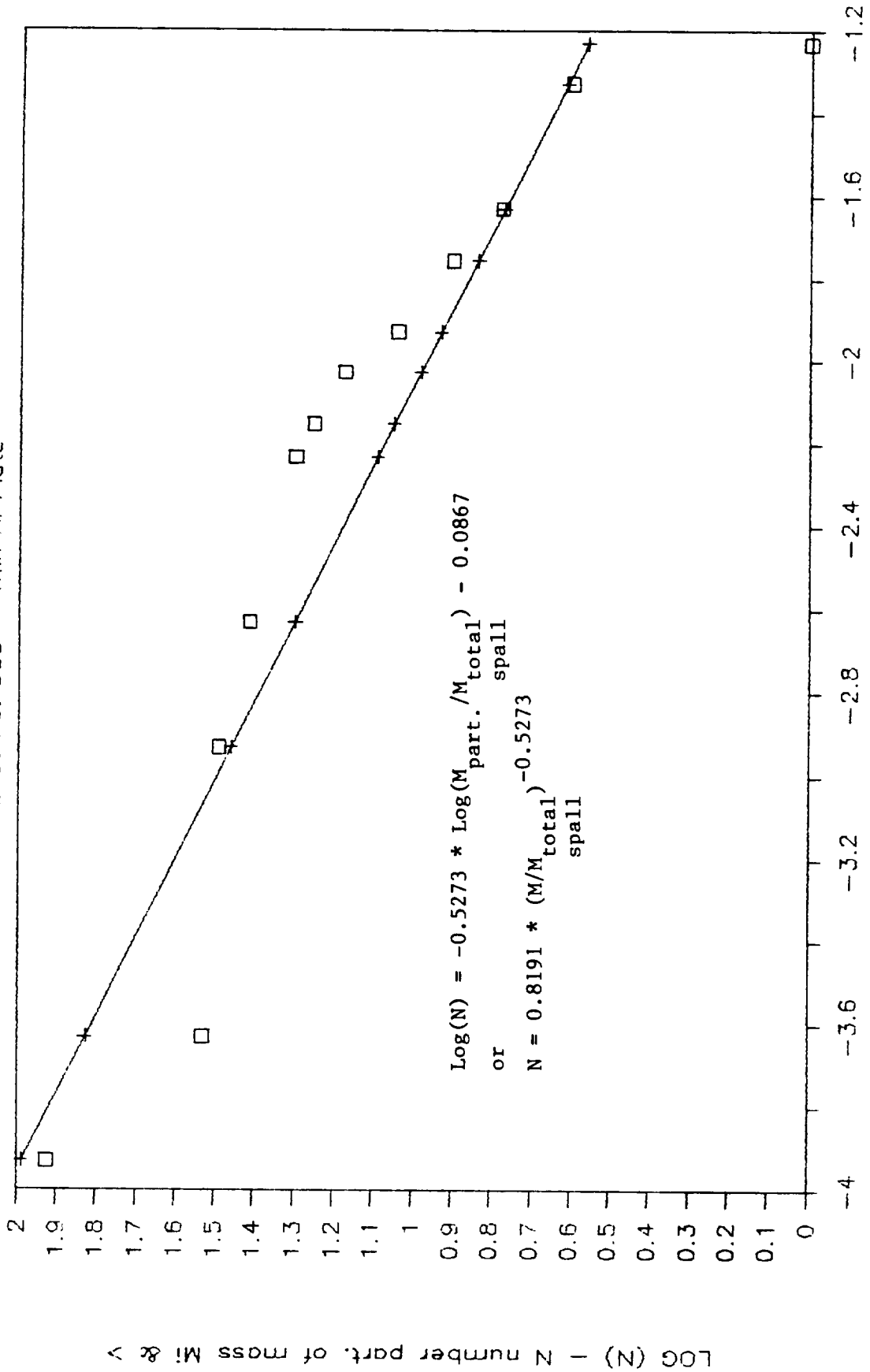


Figure 4-22

# EJECTA/SPALL MASS & LENGTH

JSC Shot No. 933 - Al Plate

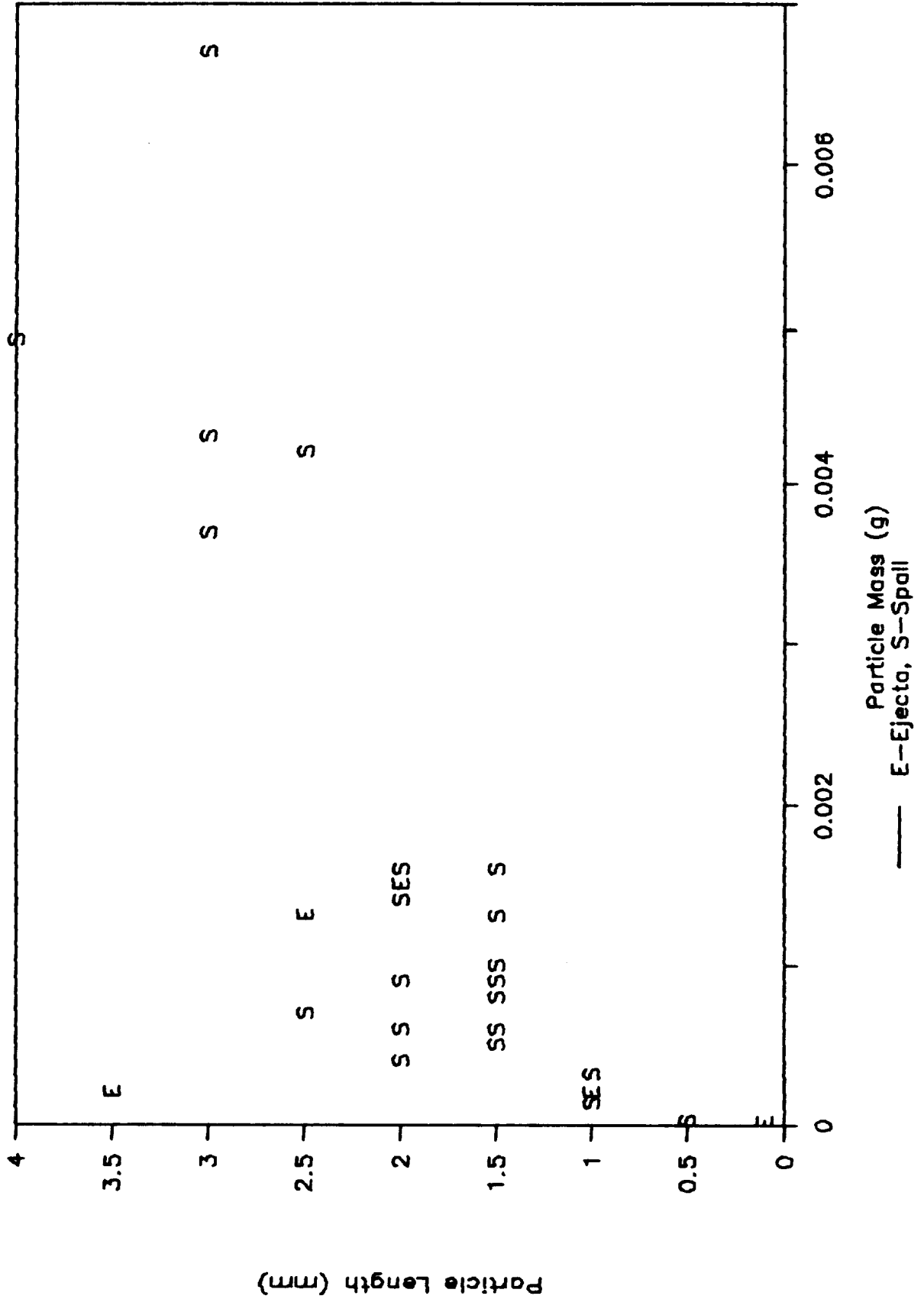




Figure 4-23

# EJECTA/SPALL MASS & DIAMETER

JSC Shot No. 933 - Al Plate

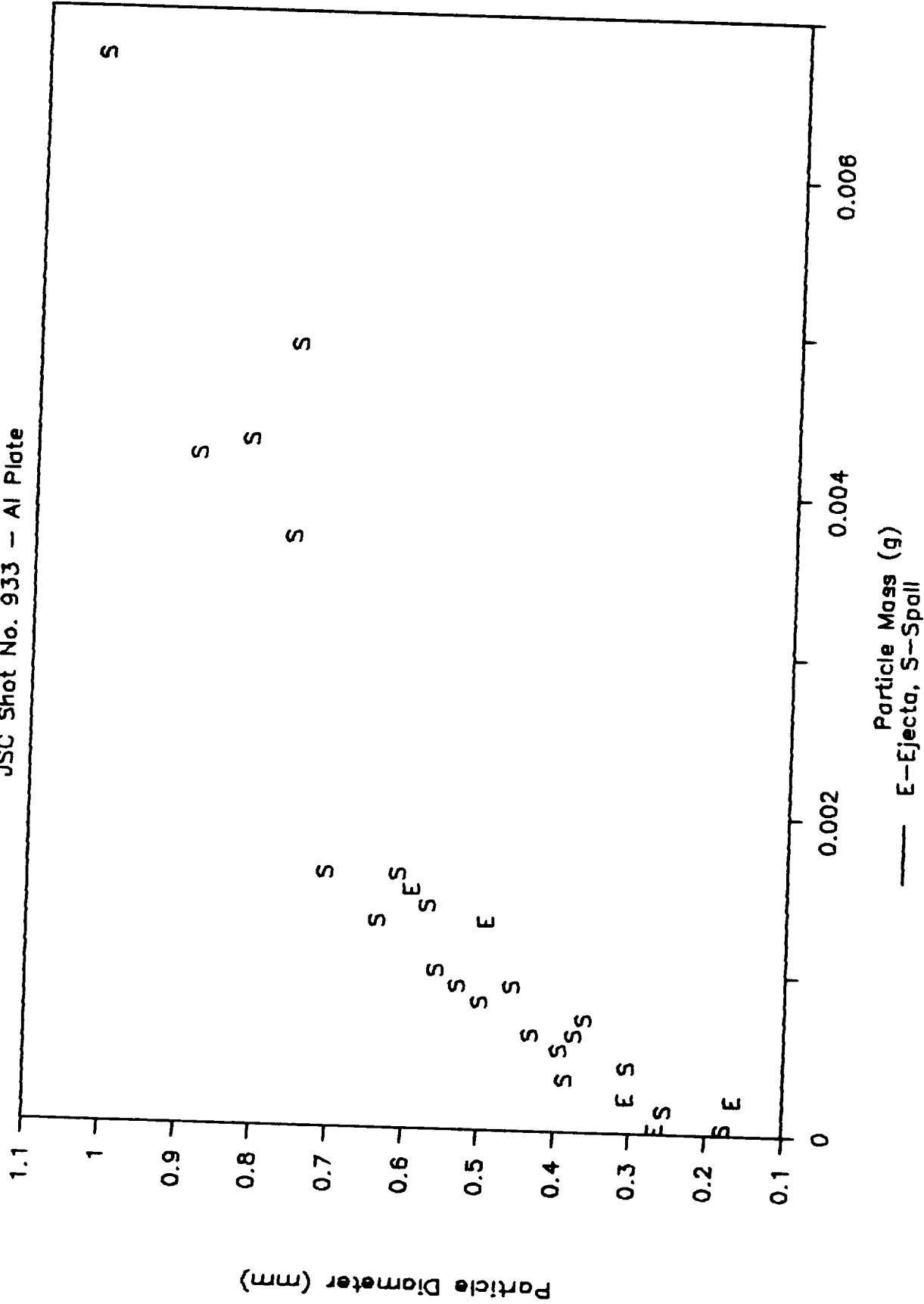


Figure 4-24

# SPALL/EJECTA MASS AND PARTICLE NUMBER

JSC Shot No. 933 - Thin Al Plate

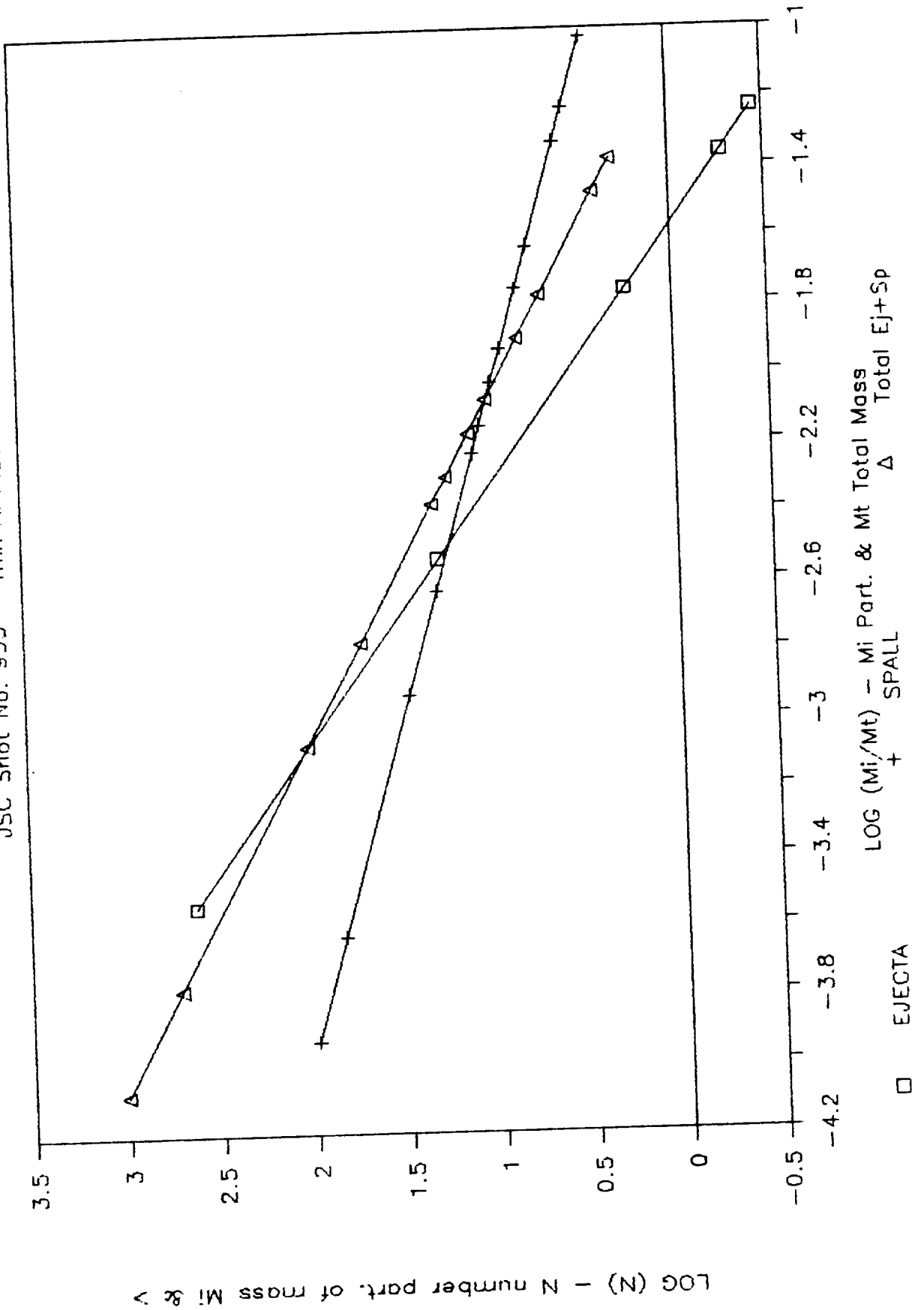
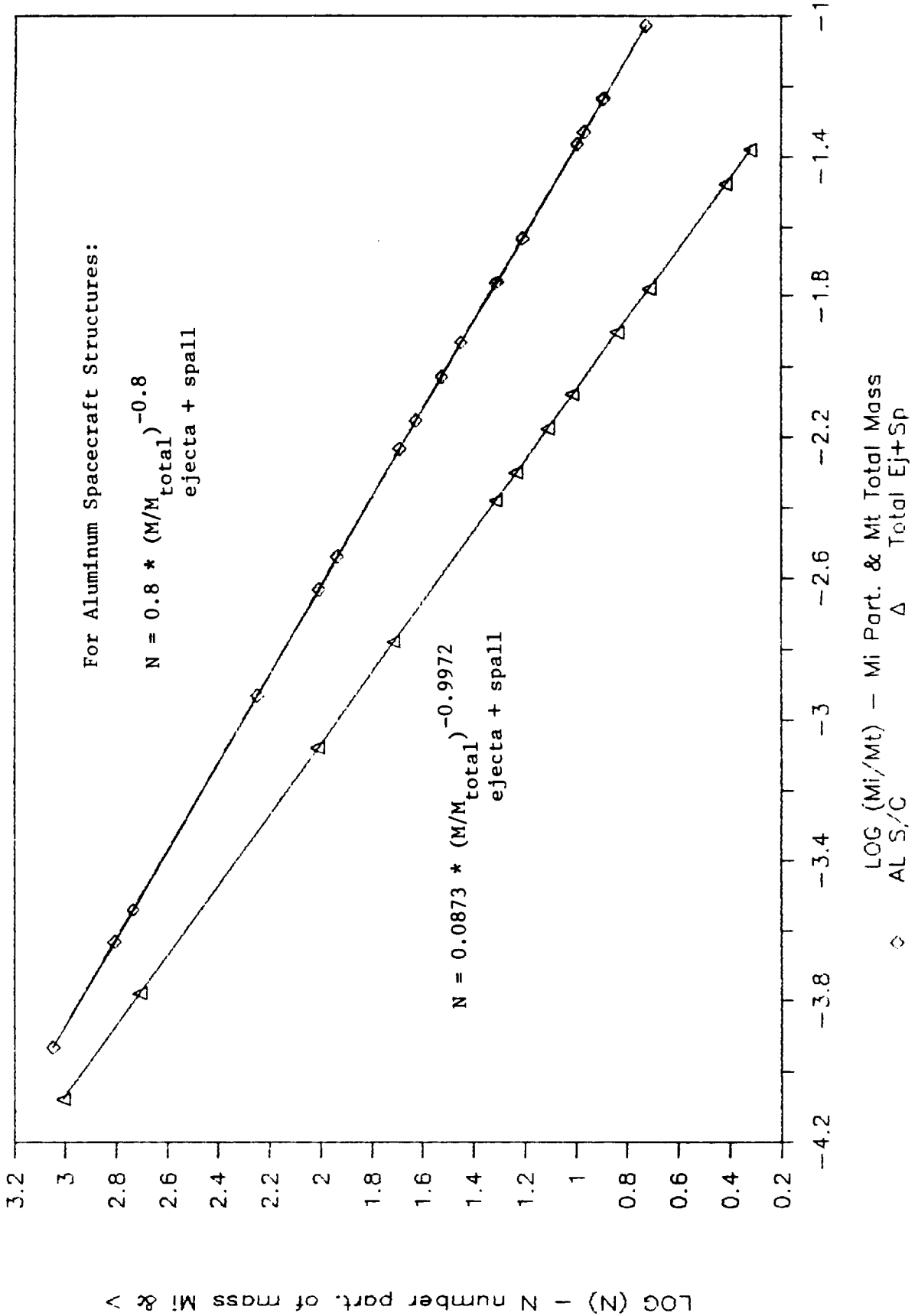


Figure 4-25

# SPALL/EJECTA MASS AND PARTICLE NUMBER

JSC Shot No. 933 - Thin Al Plate



## **4.2 Shot #975 - High Speed Camera Shot**

Shot #975 was performed to determine accurate ejecta and spall particle velocities. A 4.6 mg nylon projectile, traveling at 6.66 km/sec impacted a .089 inch thick, 6061 T-6 aluminum target. 0.10 grams of spall and ejecta were produced as measured by weighing the target before and after the shot. More data on the shot is contained in Appendix A, which lists all the shots and their basic parameters.

Figure 4-26 shows the high speed film raw data.

Table 4-1 shows the worksheet used to calculate the particle velocity.

## **4.3 Shot #979 - Additional Data**

Though no high speed film or particle count data was taken with this shot, the total ejecta and spall and energy were used in later derivations of equations.

A 4.60 mg projectile traveling at an estimated 5.6 km/sec impacted a 6061 T-6 aluminum target and produced a total of 0.07 grams of spall and ejecta. Appendix A documents the shot in more detail.

Figure 4-26

High Speed Camera Data (Shot#975)  
1.015 Microseconds between frames  
0.0297 inches = projectile diameter

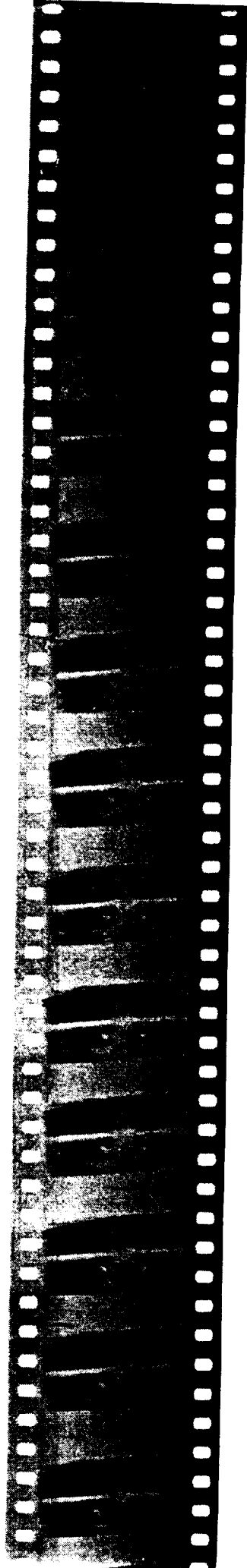
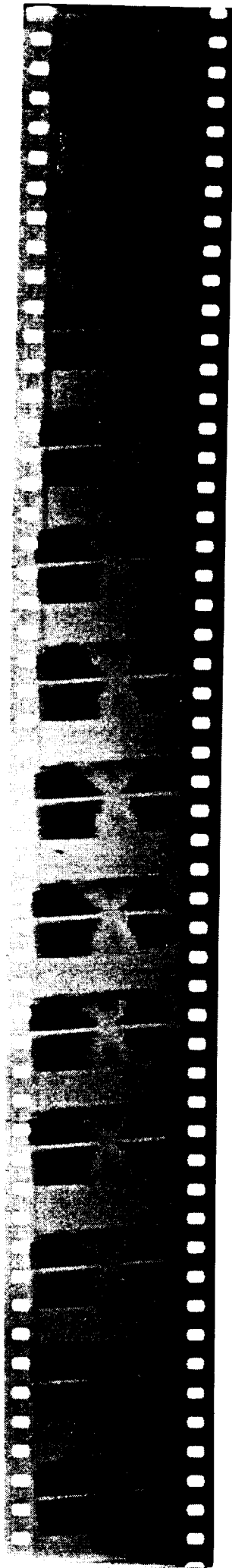
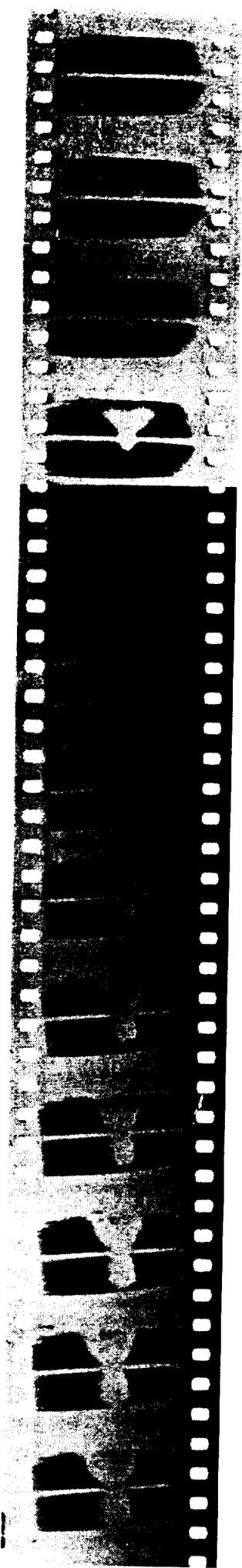


Table 4-1  
Worksheet for Shot # 975

Velocities of Large Particles

Ejecta Particle	Number Frames Used	Measured Distance (in)	Apparent Velocity (K/sec)	Correct Velocity (K/sec)	Approximate Meas. Particle Diameter (in)	Approximate Particle Mass (g)
1	4	0.0469	0.916	1.068	0.0125	0.00468
2	6	0.0781	0.916	1.068	0.0109	0.00313
3	9	0.0781	0.572	0.668	0.0141	0.00666
4	5	0.0469	0.687	0.801	0.0094	0.00197
5	11	0.0625	0.366	0.427	0.0125	0.00468
6	10	0.0547	0.356	0.415	0.0094	0.00197

Spall Particle

Spall Particle	Number Frames Used	Measured Distance (in)	Apparent Velocity (K/sec)	Correct Velocity (K/sec)	Approximate Meas. Particle Diameter (in)	Approximate Particle Mass (g)
1	17	0.0625	0.229	0.275	0.0313	0.07310
2	17	0.0547	0.200	0.240	0.0156	0.00914
3	17	0.0313	0.114	0.137	0.0156	0.00914
4	13	0.0313	0.153	0.183	0.0094	0.00197
5	10	0.0313	0.204	0.244	0.0125	0.00468
6	12	0.0469	0.250	0.300	0.0161	0.00666

CALCULATED VALUES (corrected with distance factor)

Frame	EJECTA SIDE				SPALL SIDE				EJECTA SIDE				SPALL SIDE			
	Proj. Diameter (in)	Projectile distance from impact point (in)	Projectile small particle front perpendicular dist. from impact point (in)	Max. cone angle at zero deg. at small part. front (deg)	Width of crater (in)	Perpen. distance from impact point (in)	Max. angle of cone (deg)	Width of crater (in)	Incremental Velocity for cone angle small part. front (K/sec)	Overall Apparent Velocity (K/sec)	Overall Velocity corrected for cone angle small part. front (K/sec)	Incremental Velocity for cone angle small part. front (K/sec)	Overall Apparent Velocity (K/sec)	Overall Velocity corrected for cone angle small part. front (K/sec)	Incremental Velocity (K/sec)	Overall Velocity (K/sec)
1	0.0297	0.1797	0.0391	31.00	0.0625	0.146	3.716	2.29	2.67	4.12	4.81	4.81	4.81	1.83	1.83	
2	0.0297	0.0625	0.1094	33.56	0.1172	0.274	6.968	4.12	4.81	3.43	4.01	4.01	4.01	1.83	1.83	
3			0.1563	34.30	0.1172	0.274	6.968	2.75	3.21	3.21	3.74	3.74	3.74	0.92	1.37	
4			0.2031	31.00	0.1172	0.274	6.968	2.75	3.21	3.21	3.74	3.74	3.74	1.83	1.83	
5					0.1172	0.274	6.968							1.83	1.60	
6					0.1172	0.274	6.968							1.83	1.65	
7					0.1250	0.293	7.433							1.83	1.65	
8					0.1250	0.293	7.433							0.92	1.53	
9					0.1250	0.293	7.433							0.92	1.53	
10					0.1250	0.293	7.433							0.92	1.53	
11					0.1250	0.293	7.433							0.92	1.53	
12					0.1250	0.293	7.433							0.92	1.53	
13					0.1250	0.293	7.433							0.92	1.53	

#### 4.4 Comparison of Calculated and Measured Velocity Data

Figure 4-27 shows calculated ejecta velocity from shot #933 and measured (with the high speed camera film) velocity from shot #975. The calculated data indicates smaller high speed particles (max velocity = 7.5 km/sec). The measured data shows a single point for the small particles of around 4 km/sec. This single data point represents a maximum velocity for the small particles as measured on the film for shot #975. This indicates the calculated velocities for the small aluminum particles may be high by as much as a factor of two. Since this error is conservative for damage estimation, and since projectiles with densities higher than nylon (which was used in these tests) are likely to occur in the real case, the calculated velocities were used in later damage calculations. Higher density projectiles are predicted to result in more spall and ejecta coming off at higher velocities.

Figure 4-28 shows a similar plot for spall. Once again, the maximum calculated velocities for the small particles are much higher than the maximum measured velocity.

Figure 4-27

# EJECTA MASS & VELOCITY

ALUMINUM 6061-T6, 0.089" TARGETS

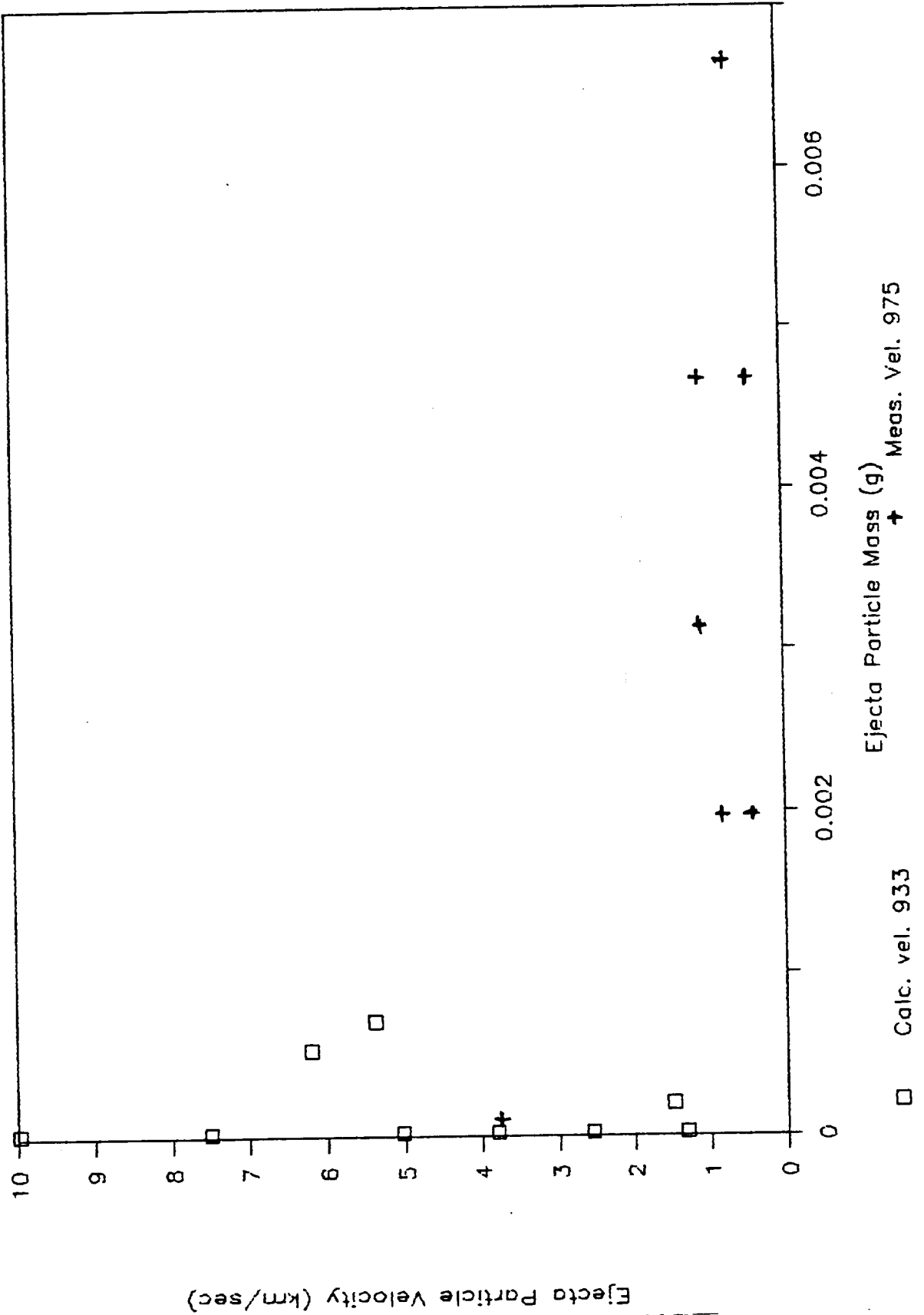
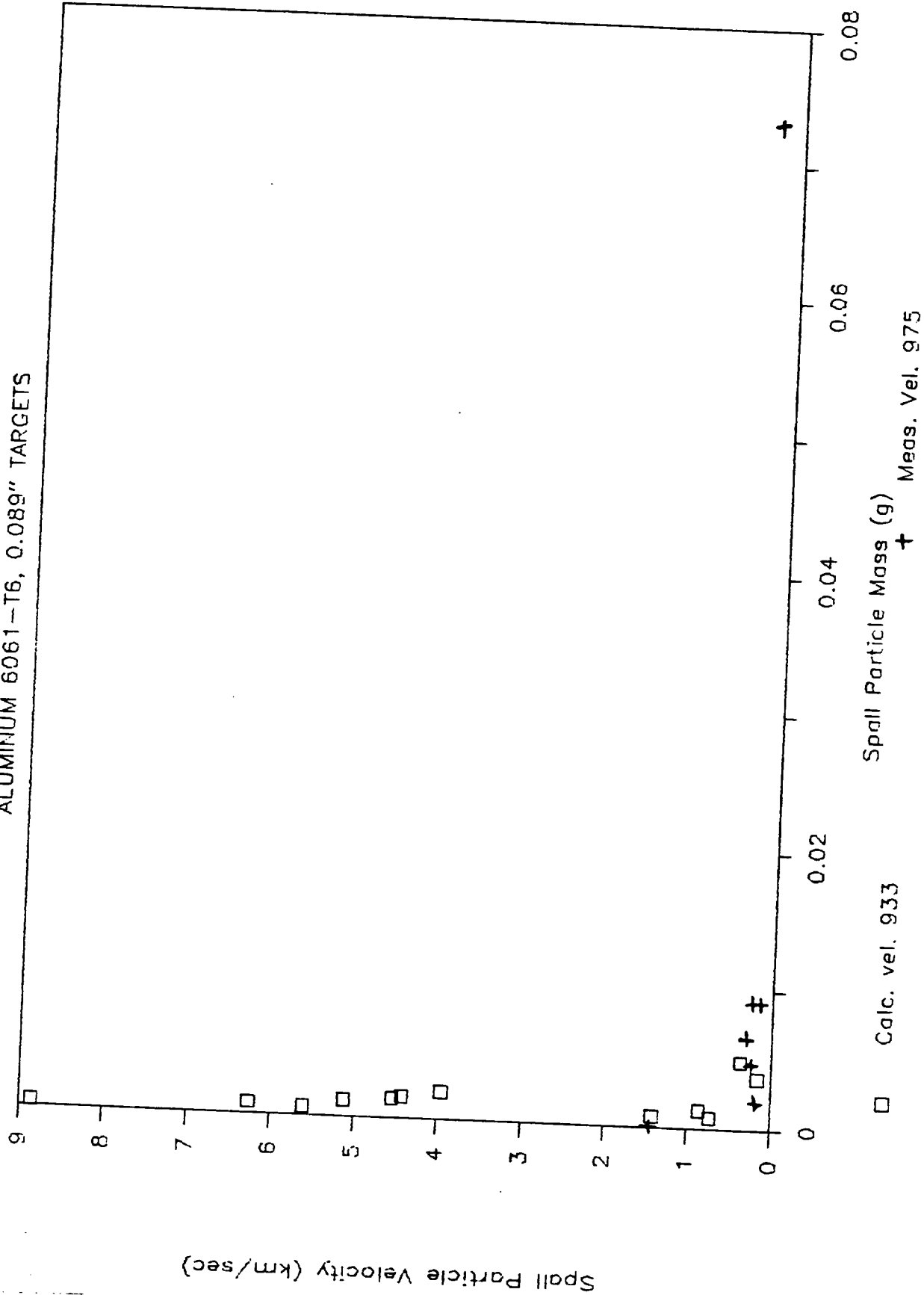




Figure 4-28

# SPALL MASS & VELOCITY

ALUMINUM 6061-T6, 0.089" TARGETS



## **5.0 Derived Relationships from Graphite/Epoxy and Aluminum Impact Data**

Several empirically derived relationships for ejecta/spall were developed to help determine the relative damage potential from secondary impacts. They were generally developed for both graphite/epoxy and aluminum targets by least squares fits of data from the shots described in Sections 3 and 4. Two basic equations used in the damage assessment program (described in Section 6) were developed. One correlated the total mass of the ejecta/spall particles with the energy of the projectile, while the other related the number of ejecta/spall particles of a given energy and above to the total mass of ejecta/spall. These two relationships could have been combined into a single relationship that expresses the number of ejecta/spall particles with a given energy and above to the particle and projectile energies, although this was not done in this study. Both relationships were developed separately for graphite/epoxy and aluminum targets and are therefore valid only for the specific target type.

The following sections describe all relationships developed in the study.

### **5.1 Total Ejecta/Spall Mass Scaled with Projectile Energy**

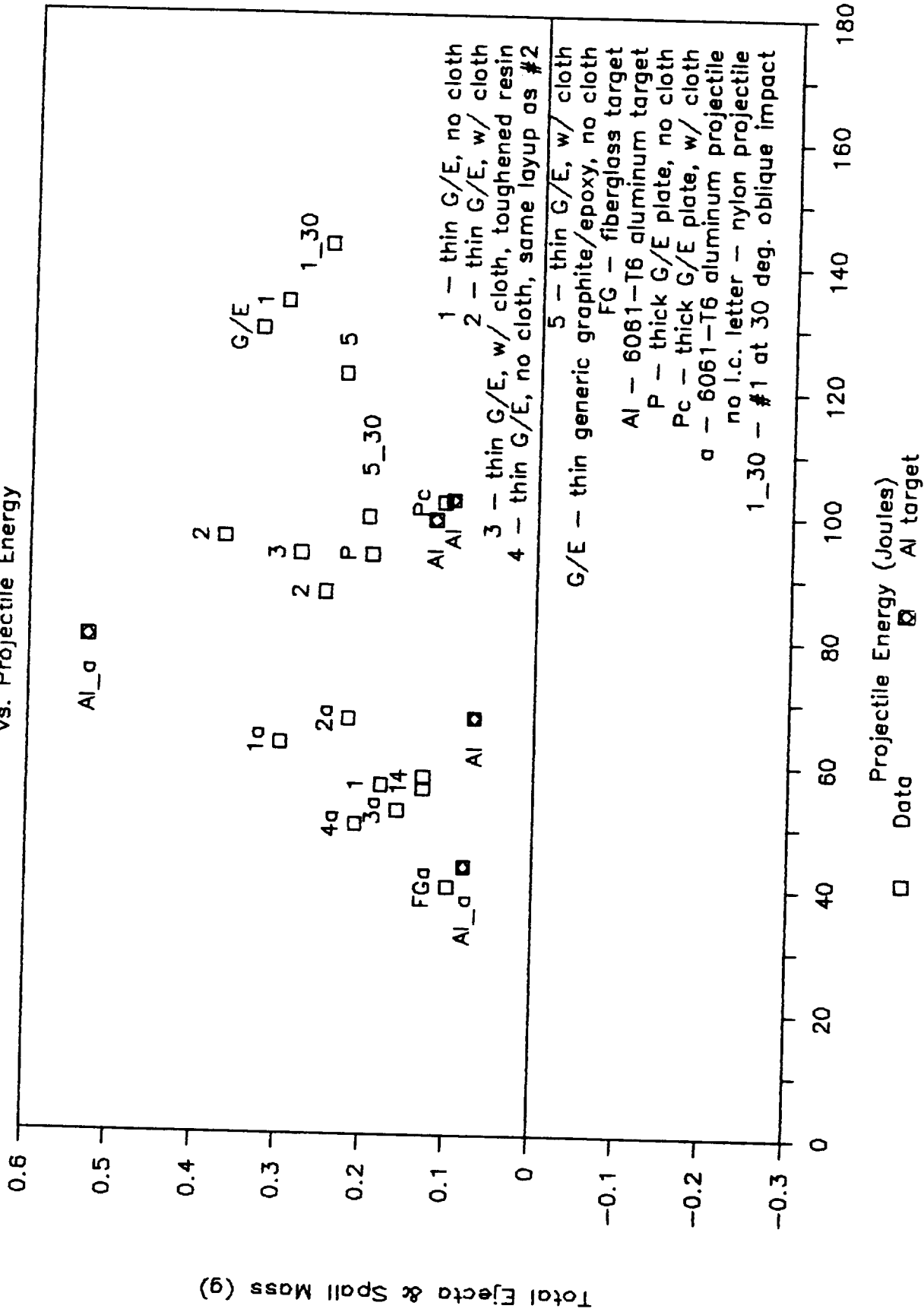
As a rough approximation in this limited study, the total combined mass of ejecta and spall produced from hypervelocity impact was scaled as a function of projectile energy. This approach may be conservative in that the mass of ejecta/spall is probably over-estimated as projectile energy increases.

In Figure 5-1, the total combined ejecta and spall mass is plotted versus projectile energy for all shots with sufficient data listed in Appendix A. The labels indicate whether a target is graphite/epoxy or aluminum, differences in ply orientation, cloth or no-cloth covering, thin or semi-infinite (0.5 in. thick) target, aluminum or nylon projectile, and normal or oblique impact angles. The impact obliquity angle is the angle between the target surface normal and the projectile flight path (30 deg. in the two oblique shots in this study).

Figure 5-1

# Ejecta & Spall Mass

vs. Projectile Energy



### 5.1.1 Graphite/Epoxy Targets

In Figure 5-2, a least-squares linear fit to the thin plate graphite/epoxy data (with and without cloth covering) is given by the equation and line. The equation relates the combined mass of ejecta/spall,  $M_{es}$  (g), to projectile energy,  $E_{proj}$  (J).

$$M_{es} = 0.00357 * E_{proj} - 0.00935$$

This equation is valid for thin (approximately 0.1 in. thick) graphite/epoxy targets. It does not include the effects of projectile density, obliquity angle, or target surface covering. Several shots from late in the study were not included in this earlier formulation but were used for other purposes (primarily ejecta and spall particle velocity verification using the Cardin high speed camera).

Generally, more ejecta/spall was produced from the thin plates than the thick for equal energy projectiles. This effect also seems to play a role in the oblique angle shots on the thin plates; because the projectile passes through the plate at an angle, it "sees" more plate, ie. the plate is relatively thicker for the oblique impacts. In the limited number of oblique shots, the ejecta/spall mass was slightly less for equal energy projectiles. Given more data, ejecta/spall mass versus projectile energy curves could be constructed for different target thickness to projectile diameter ratios.

Slightly more ejecta/spall was produced from equal energy impacts with higher density (2.7 g/cc) aluminum (6061-T6) projectiles than with nylon projectiles (1.14 g/cc) for the thin targets. This phenomenon for semi-infinite targets is illustrated by the increase in crater volume with projectile density in Figure 5-3. The impact velocity for the data plotted in Figure 5-3 was 6.6 km/sec. It has been reported that the influence of projectile density on crater volume and presumably ejecta mass decreases with increasing projectile velocity, and may become negligible at meteoroid velocities (Ref.2, p.467).

The projectile density effect was not quantified for additional reasons. First, for identical shots at nearly equivalent projectile energies (#893 and #894), the ejecta/spall mass varied by 0.05 g or approximately 25 percent. Thus, the apparent increase in ejecta/spall mass with density increases was not appreciably greater than the accuracy of the data. Second, the length to diameter ratio for the aluminum cylindrical projectiles was approximately 0.5 while the nylon projectiles' L/D ratio was approximately 1.0. As the L/D ratio decreases, the crater volume (and perhaps ejecta/spall mass) also decreases as shown in Figure 5-4. Thus, the full effect of higher projectile density was masked by lower projectile L/D ratio. Also, occasionally the projectile will yaw (crater volume is a function of the cosine of

yaw angle). Yaw is especially a problem with the aluminum projectiles with a low L/D. All this results in uncertainties that led us to disregard the projectile density in these approximate calculations.

A cloth covering significantly reduced the amount of ejecta produced from equivalent energy projectiles for thick plates tested in this study (shots #883 and #884). However, the effect of cloth is not nearly as apparent for the thin plate data which was used to generate the above equation. The quantitative advantage of cloth in terms of reducing the mass of ejecta/spall appears to be a function of the target thickness to projectile diameter ratio. More data will be needed to develop the exact relationship.

Figure 5-2  
 Graphite/Epoxy Ejecta and Spall Mass  
 as function of Projectile Energy

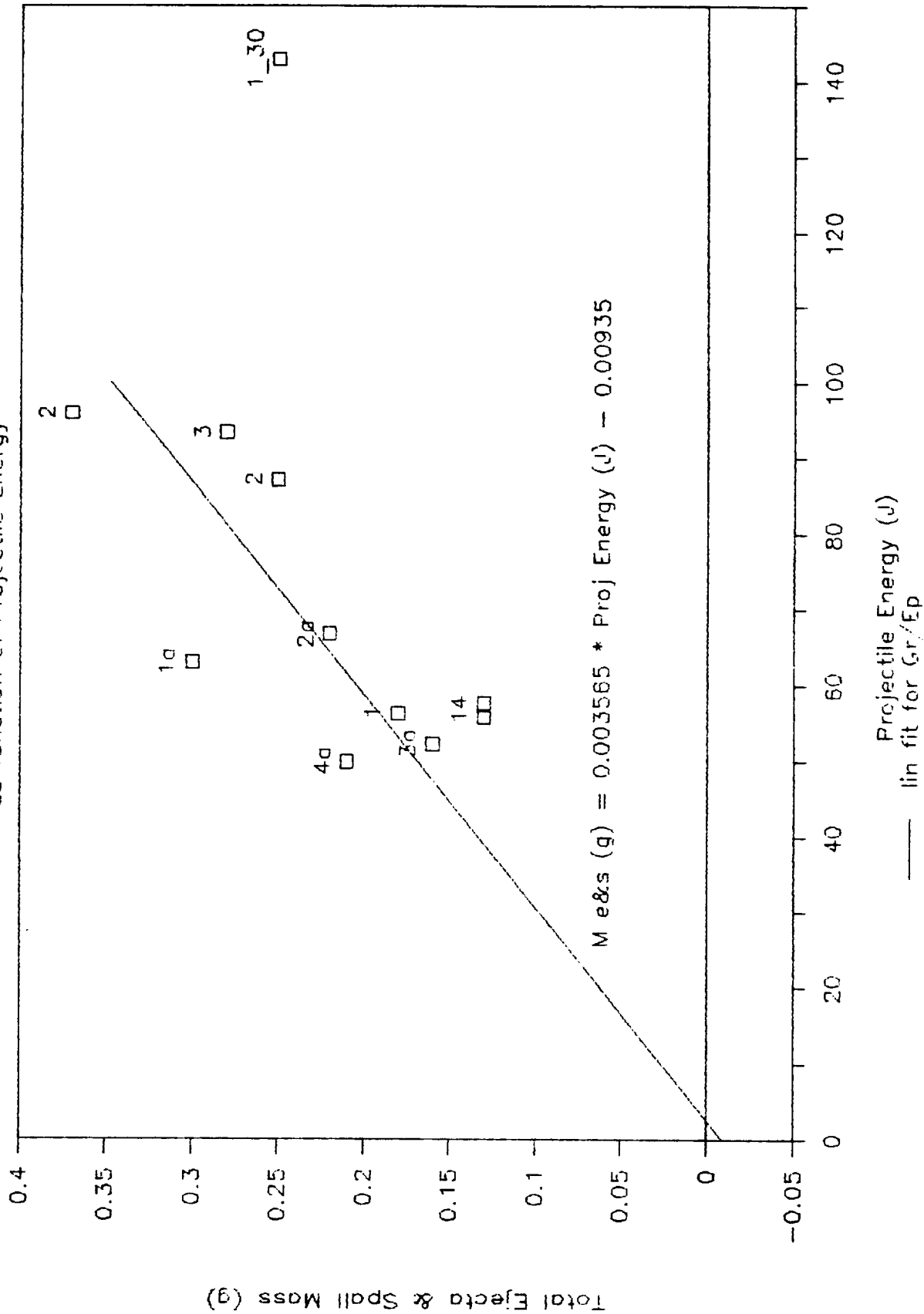
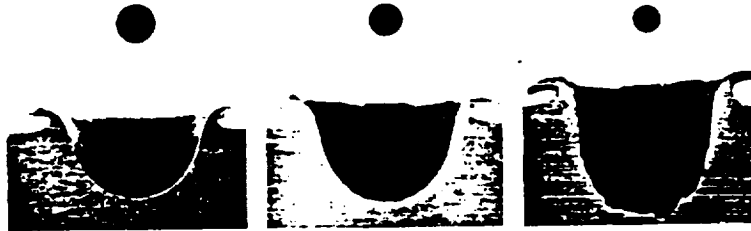
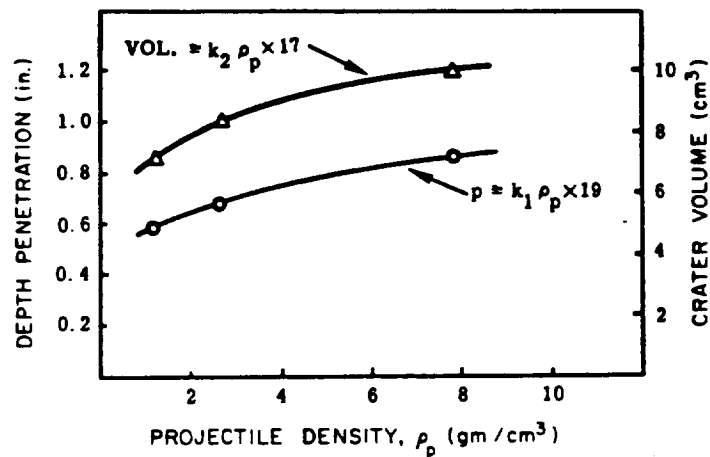


Figure 5-3  
 Projectile Density Effects  
 (Taken from Ref. 2)



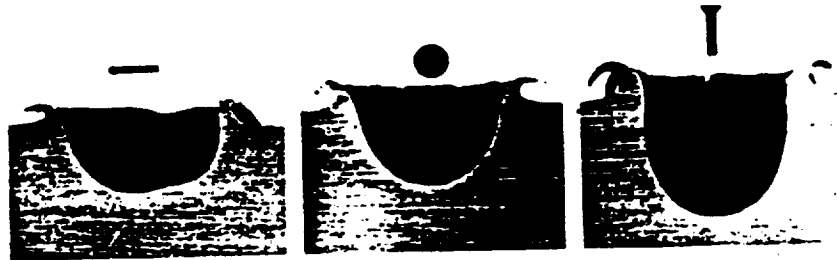
(a)



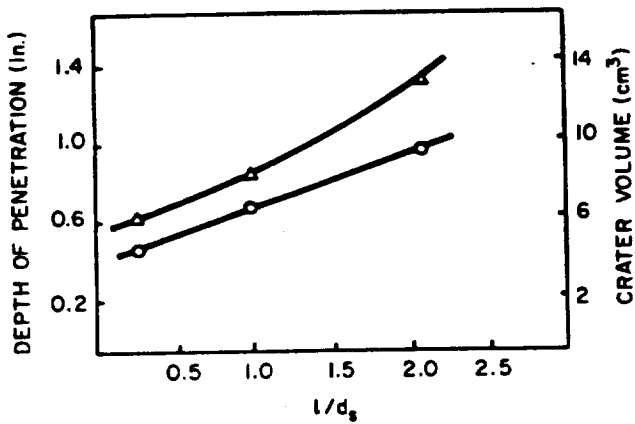
(b)

Crater depth and volume for equal-mass spheres of various densities.  
 (a) Photographic representation; (b) graphical representation: ( $\Delta$ ) volume versus  $\rho_p$ ;  
 ( $\circ$ ) penetration versus  $\rho_p$ . Target: 110-F Al, semiinfinite. Impact velocity: 6.6 km/sec.  
 Projectile: Zelux-type M ( $\rho_p = 1.20$ , diam = 0.313); 2017 Al ( $\rho_p = 2.70$ , diam = 0.240);  
 C1020 steel ( $\rho_p = 7.80$  g/cm, diam = 0.169 in.). All projectiles same mass—0.32 g.

Figure 5-4  
 Projectile L/D Effects  
 (Taken from Ref. 2)



(a)



(b)

Crater depth and volume for projectiles of equal mass and various shapes. (a) Photographic representation; (b) graphical representation versus  $l/d_s$ ; (O) penetration versus  $l/d_s$ ; ( $\Delta$ ) volume versus  $l/d_s$ . Target: 1100-F Al, semiinfinite. Impact velocity: 6.6 km/sec. Projectile: 2017 Al. All projectiles same mass—0.32 g.



### 5.1.2 Aluminum Targets

Figure 5-5 illustrates a linear fit to the 6061-T6 aluminum total ejecta and spall mass versus projectile energy data. The equation relates the combined mass of ejecta/spall,  $M_{es}$  (g), to projectile energy,  $E_{proj}$  (J), for thin (0.089 in. thick) 6061-T6 aluminum targets.

$$M_{es} = 0.00301 * E_{proj} - 0.178$$

When this equation was developed, only two early data points at basically the same projectile energy were available (shots #933 and #975). Therefore, an empirical equation for aluminum developed from experimental results for use at 10 km/sec projectile speeds (Ref. 1, p.2640) was used to generate another point at higher projectile energies. This equation related the ejecta mass to projectile mass.

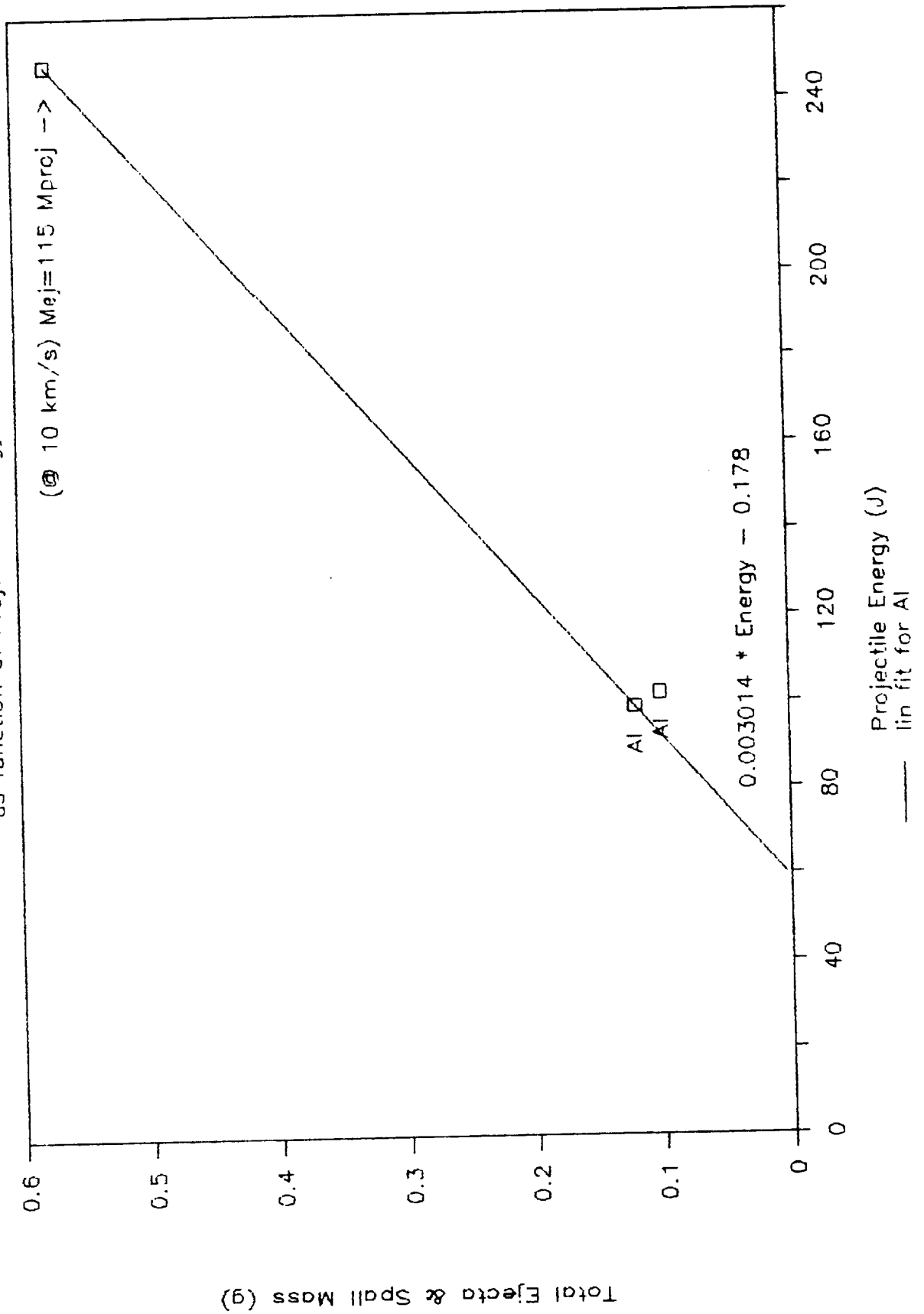
$$M_e = 115 * M_{proj}$$

The linear fit was through these three data points. Shot #979 was an additional later nylon projectile data point that fell near the aluminum linear scaling line. The last two shots (#991 and #992) were with aluminum (6061-T6) projectiles and seem to indicate that the projectile density effect for aluminum targets may be greater than for graphite/epoxy because of the large amounts of ejecta/spall that were produced (especially in shot #991). More data will be necessary to confirm this however.

Figure 5-5

# Aluminum Ejecta and Spall Mass

as function of Projectile Energy



## 5.2 Number of Ejecta/Spall Particles of a Given Mass and Above

From the data of individual ejecta and spall particles, a linear Log-Log relationship was found relating the number of particles of a given mass and greater,  $N$ , to the ratio of the particle mass,  $M$  (g), over the total ejecta/spall mass,  $M_{es}$  (g). The functional form of this equation is useful to get an idea of the mass distribution of the ejecta and spall particles, but was not used as such in the damage assessment model explained in Section 6. The general form of the equation reduces to

$$N = k * (M / M_{es})^n$$

where the constants,  $k$  and  $n$ , for various specific target groups are given in the following sub-sections.

### 5.2.1 Graphite/Epoxy Targets

The least-squares linear fits for the graphite/epoxy ejecta particles given in Figures 3-11, 3-23, 3-28, 3-42, and 3-66 are all plotted in Figure 5-6 together with the overall graphite/epoxy ejecta average. Similarly, the linear fits for the graphite/epoxy spall particles given in Figures 3-29, 3-52, and 3-76 are all plotted in Figure 5-7 with the overall graphite/epoxy spall average. The ejecta and spall average lines as well as the overall graphite/epoxy average are plotted in Figure 5-8. Spall is typically about 60 to 70 percent of the total ejecta and spall mass for the plate thicknesses (approximately 0.1 in.) tested in this study as is indicated in Table 3-2.

From Figure 5-8, it is evident that although there is about twice as much spall mass as ejecta mass, the number of particles of a given particle mass and greater for the same ratio of particle mass to total particle mass (ejecta or spall) is nearly the same for ejecta and spall (for typical particle to total mass ratios of 0.0001 to 0.05). In other words, there are approximately twice as many spall particles as ejecta particles for a given particle mass. (The real factor is  $\frac{1}{2}$  raised to the  $n$  power when total spall mass is twice the ejecta mass which, because  $n$  approximately equals  $-1$ , makes  $N_s = 2 * N_e$ ). The  $k$  and  $n$  constants for the general equation are:

	<u>k</u>	<u>n</u>
G/E Ejecta	0.0276	-1.155
G/E Spall	0.0070	-1.382
G/E Avg.	0.0131	-1.253

In Figure 5-9, the average equation for graphite/epoxy with cloth is plotted with the average equation for graphite/epoxy without cloth. In Section 5.1.1, it was mentioned that for a given energy projectile there was little observable difference between

cloth and no-cloth covered graphite/epoxy in terms of the total ejecta/spall mass. Given that information, it is apparent from Figure 5-9 that, in the typical particle to total mass ratio range of 0.0001 to 0.05, there are more ejecta/spall particles that have large relative masses (particle to total mass ratio of 0.001 and greater) for graphite/epoxy targets without cloth than with cloth. The reverse holds true for ejecta/spall particles of lower relative masses (particle to total mass ratio of less than 0.001). The k and n constants for the general form of the equation are:

	<u>k</u>	<u>n</u>
G/E w/ Cloth	0.0036	-1.426
G/E w/out Cloth	0.0356	-1.157

Figure 5-6  
 Number of Particles of Mass  $M_i$  &  $>$   
 GRAPHITE/EPOXY EJECTA

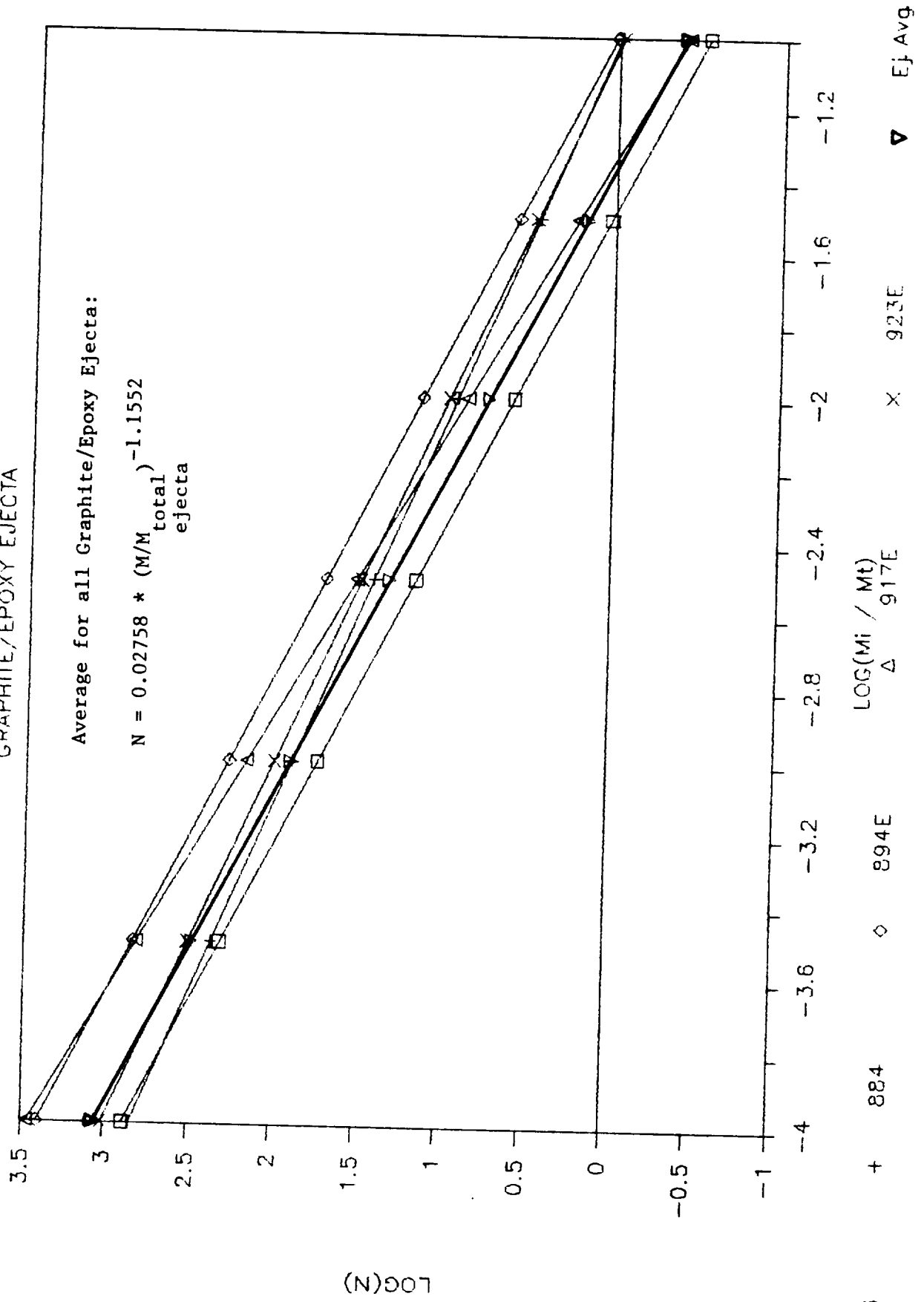


Figure 5-7  
 Number of Particles of Mass  $M_i$  &  $>$   
 GRAPHITE/EPOXY SPALL

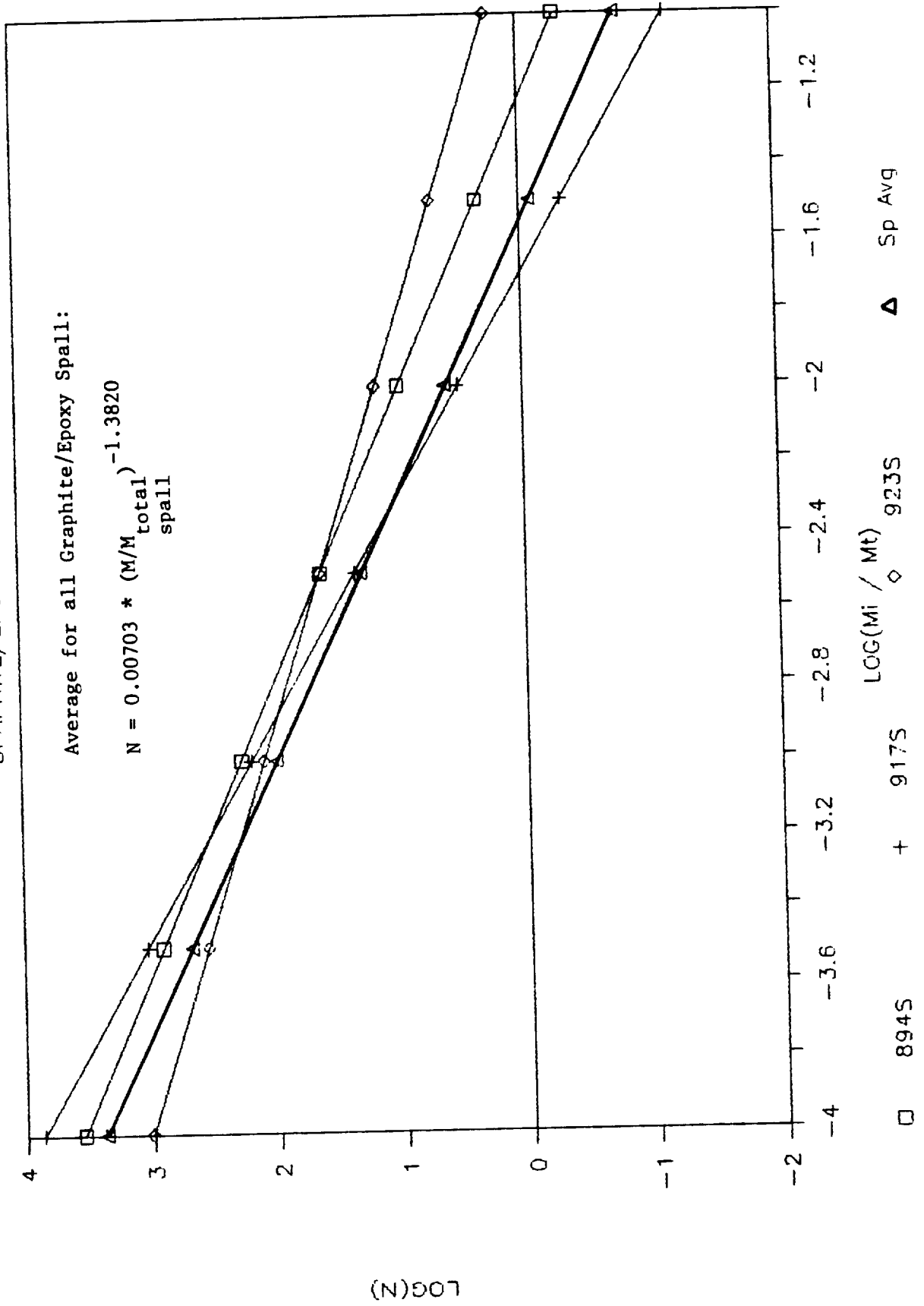


Figure 5-8

# Number of Particles of Mass $M_i$ & $>$

Graphite/Epoxy Composite Averages

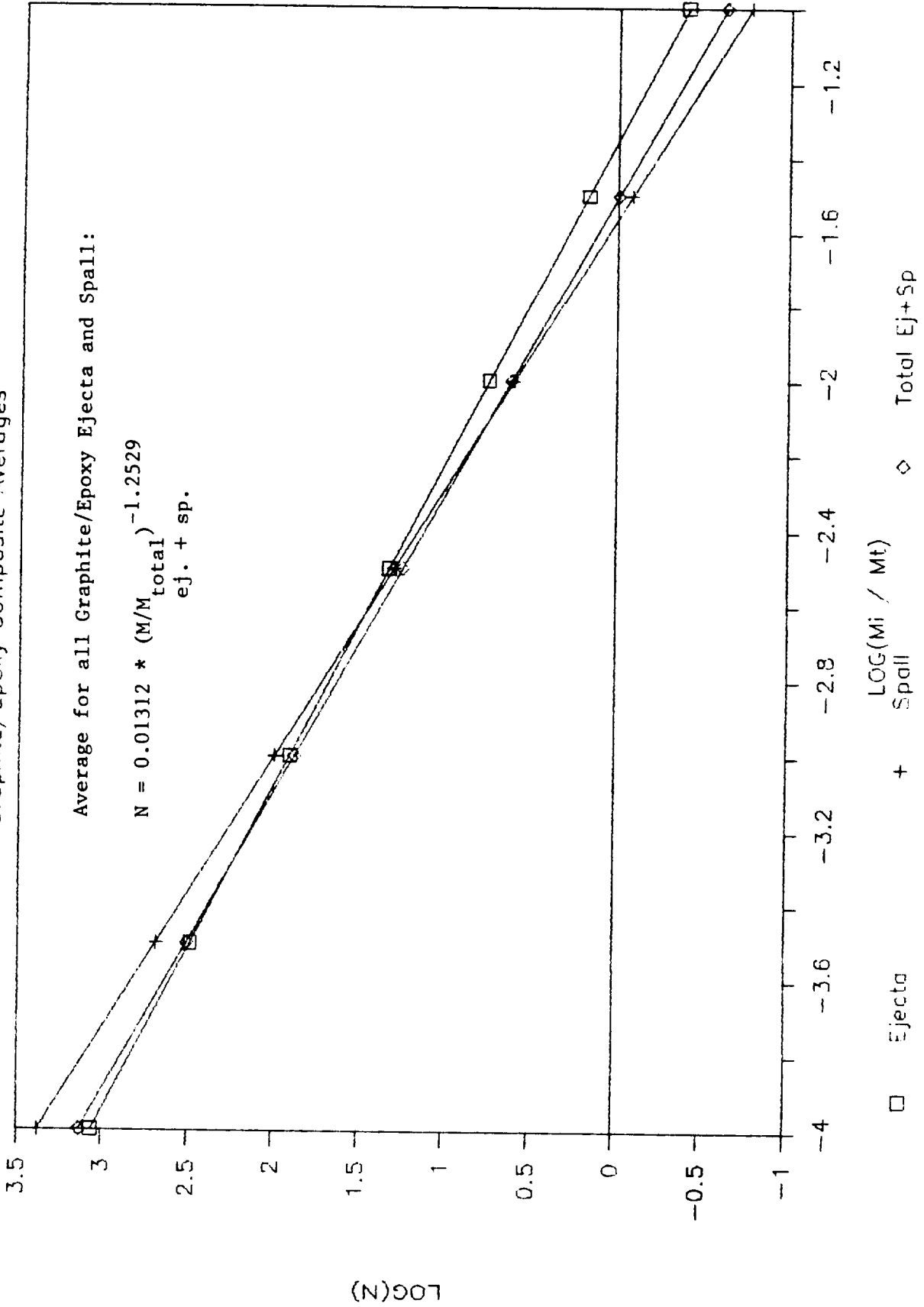
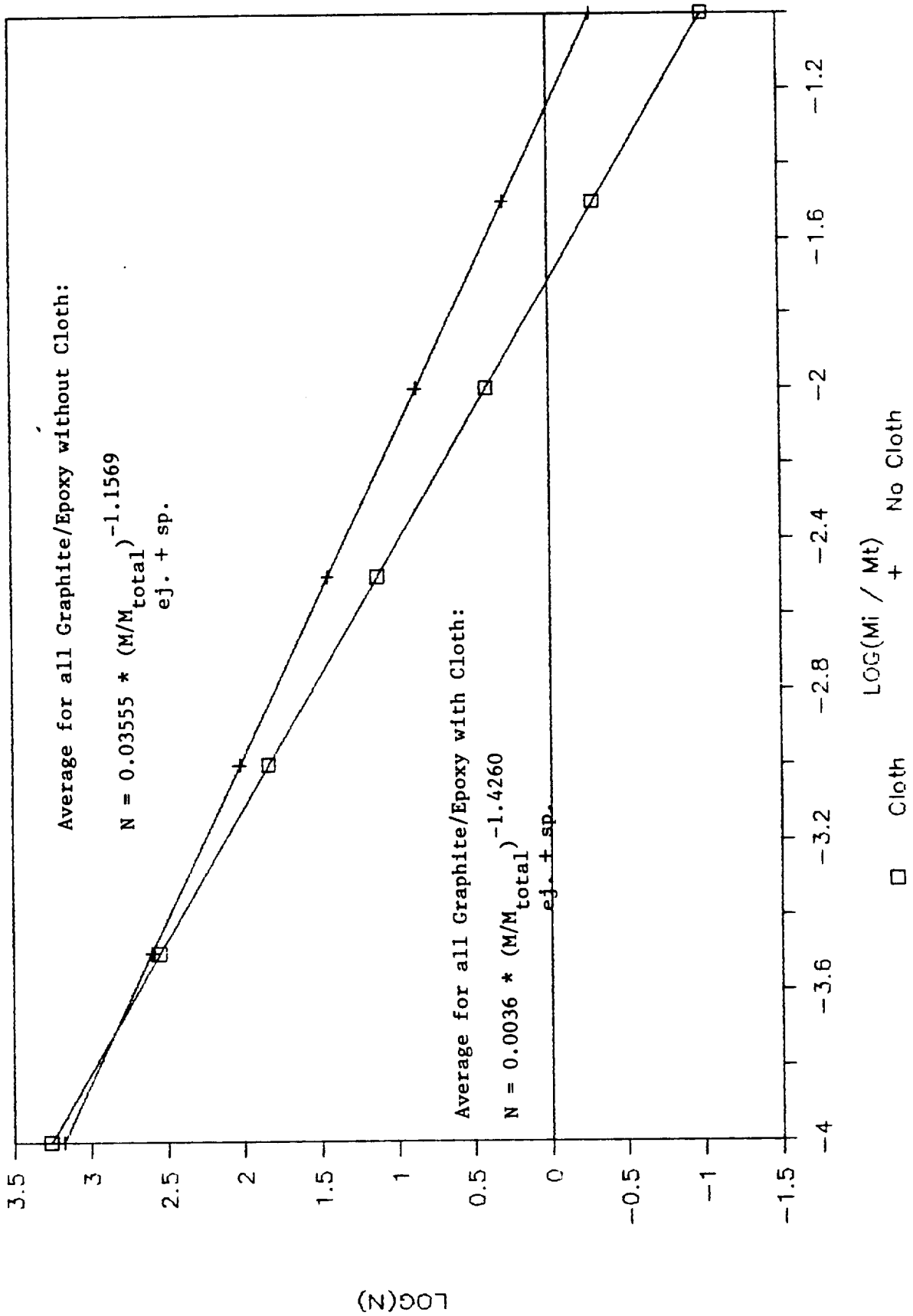


Figure 5-9  
 Number of Particles of Mass  $M_i$  &  $>$   
 Graphite/Epoxy Cloth vs No Cloth





### 5.2.2 Aluminum Targets

In Figure 5-10, the overall average graphite/epoxy equation (from Section 5.2.1) is plotted with the average aluminum equation of Figure 4-24 and a equation from the literature for the mass distribution of particles resulting from a 10 Km/sec impact on an aluminum spacecraft (Ref. 1, p.2640). From Figure 5-10 it is clear that the aluminum test where particle counts were taken (shot #933) resulted in somewhat fewer particles of a given mass and greater than the literature equation for orbital debris impacting into an aluminum spacecraft. This may be due to the lower density for the nylon projectile (1.14 g/cc) used in shot #933 versus the presumed higher projectile density in the tests that resulted in the reported spacecraft particle distribution (typically 2.8 g/cc is used for orbital debris density). The k and n constants for the general form of the equation are:

	<u>k</u>	<u>n</u>
G/E average	0.0276	-1.155
Al average	0.0873	-0.997
Al Spacecraft	0.8	-0.8

### 5.3 Number of Ejecta/Spall Particles of a Given Energy and Above

A key pair of equations developed for the damage assessment model (described in Section 6) relates the number of ejecta and spall particles of a given energy and above to the particle energy and the total ejecta and spall mass for both graphite/epoxy and aluminum (6061-T6) targets. The general form of the equation is:

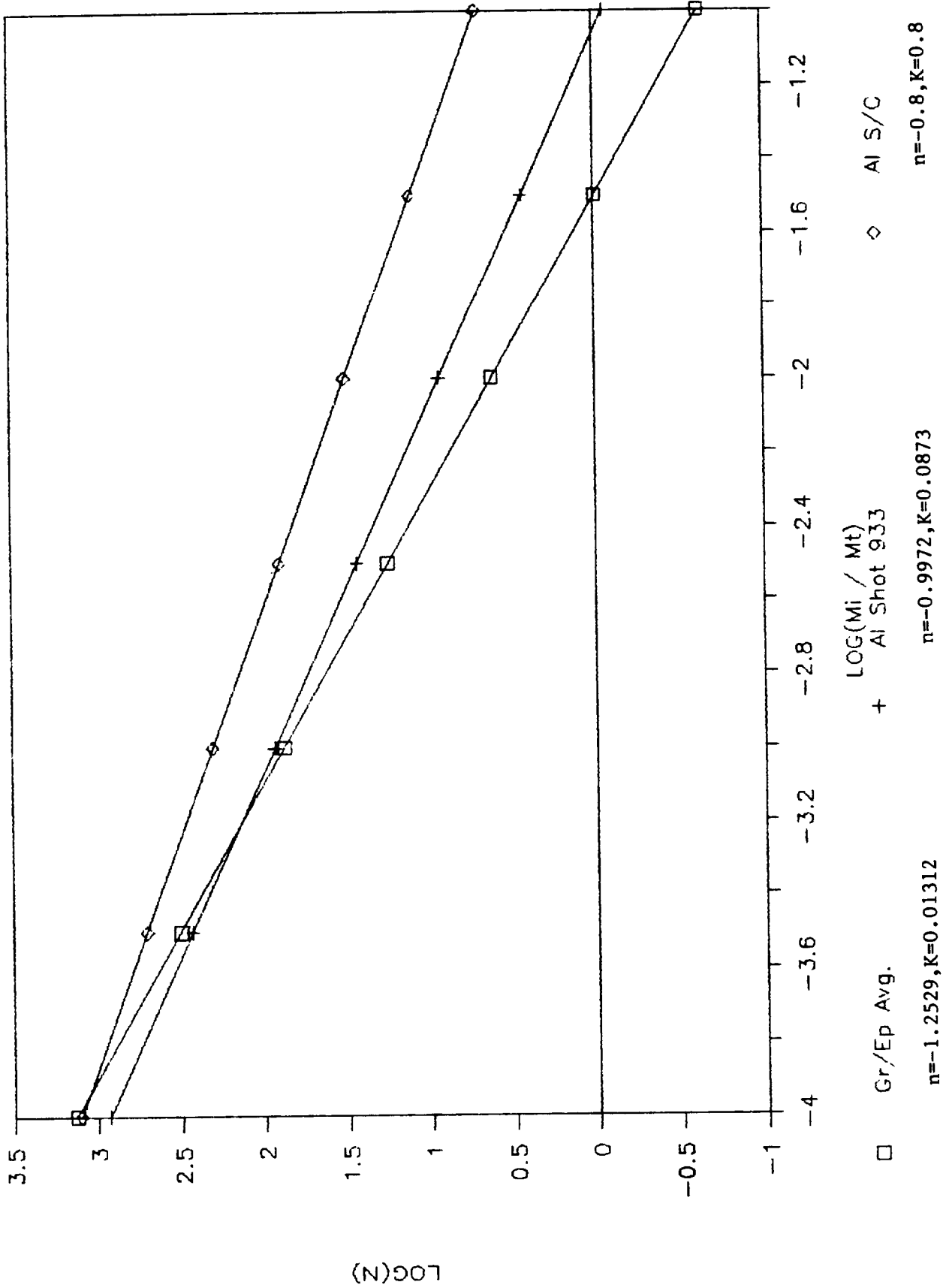
$$\text{Log}(N) = a * (\text{Log}(E / M_{es}))^2 + b * \text{Log}(E / M_{es}) + c$$

where the number, N, of ejecta/spall particles of a given particle energy, E (J), and greater related in a second-order Log-Log expression to the particle energy and total ejecta/spall mass,  $M_{es}$  (g). The total ejecta and spall mass,  $M_{es}$  (g), is related to the projectile energy as explained in section 5.1. The equations and constants (a,b,c) for both graphite/epoxy and aluminum targets are described in the following sections.

Figure 5-10

# Number of Particles of Mass $M_i$ & $>$

Graphite/Epoxy vs Aluminum



### 5.3.1 Graphite/Epoxy Targets

Figure 5-11 shows the least-squares fit to all the graphite/epoxy data for which particle counts were completed (shots #883, #884, #894, #917, and #923). Curve-fits were also developed for graphite/epoxy with and without a cloth covering as given in Figures 5-12 and 5-13, and to describe the graphite/epoxy ejecta and spall particle energies as given in Figures 5-14 and 5-15. The curves for cloth and no-cloth covered graphite/epoxy are compared in Figure 5-16. From this figure it is obvious that a cloth covering reduces the energy of the ejecta/spall particles. As will be seen in section 5.4, this is due to the reduction of the ejecta/spall particle velocity. Ejecta and spall particle energy curves are compared in Figure 5-17. There is not a large difference between ejecta and spall particle energies (on a ratio basis of particle energy to total particle mass; remember that spall mass was found to be approximately twice ejecta mass in this study) but a slight tendency exists for spall to have more higher energy particles and fewer lower energy particles than ejecta (on a ratio basis). The graphite/epoxy coefficients for the general equation (a,b,c) are:

	<u>a</u>	<u>b</u>	<u>c</u>
G/E overall	-0.168	-0.851	+1.695
G/E w/ Cloth	-0.322	-1.227	+1.203
G/E w/out Cloth	-0.163	-0.663	+1.822
G/E Ejecta	-0.218	-0.897	+1.602
G/E Spall	-0.169	-0.674	+1.737

### 5.3.2 Aluminum Targets

Figure 5-18 shows the quadratic form of the ejecta/spall particle energy distribution for aluminum (shot #933). The aluminum ejecta equation and curve appears in Figure 5-19, the aluminum spall equation is in Figure 5-20, and a comparison between them in Figure 5-21. There were significantly more higher energy and less lower energy spall particles than ejecta particles. This was due to the mass distribution of the aluminum ejecta/spall particles, not a difference in observed velocity between ejecta and spall. There were many more large particles (chunks) in the aluminum spall, while the aluminum ejecta was mainly very small particles (less than/equal to 0.0001 g) and dust. A comparison between the overall graphite/epoxy and overall aluminum particle energy curves is given in Figure 5-22. These curves were used in the damage assessment model as discussed in Section 6. Basically, there were significantly more high energy and less low energy aluminum ejecta/spall particles observed than graphite/epoxy ejecta/spall particles for the limited number of shots made during this study.

Figure 5-11

# Num. of Graphite/Epoxy E<sub>j</sub>&S<sub>p</sub> Particles

with Given Energy and Greater

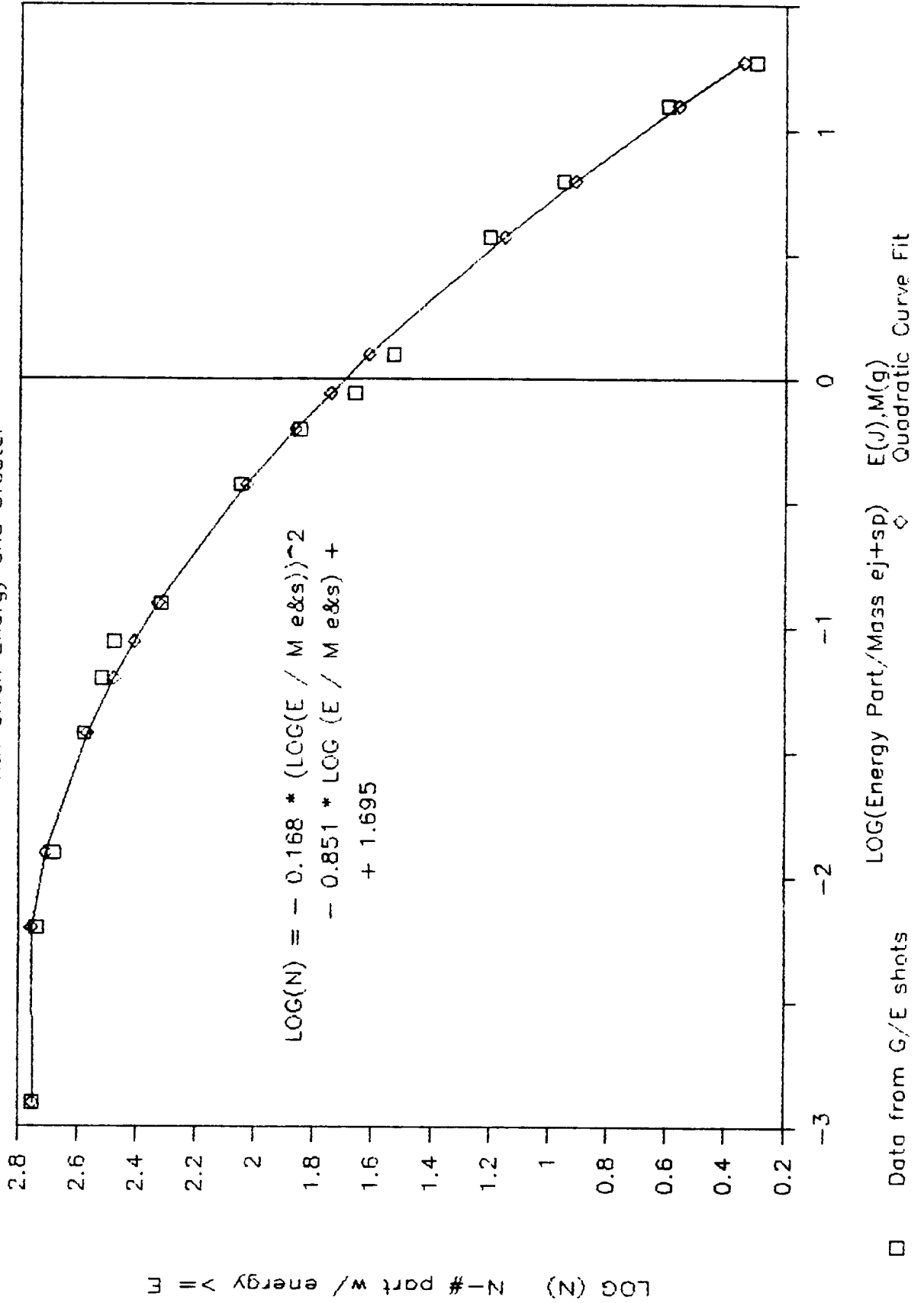


Figure 5-12

# Num. of Gr/Ep (Cloth) Ej&Sp Particles

with Given Energy and Greater

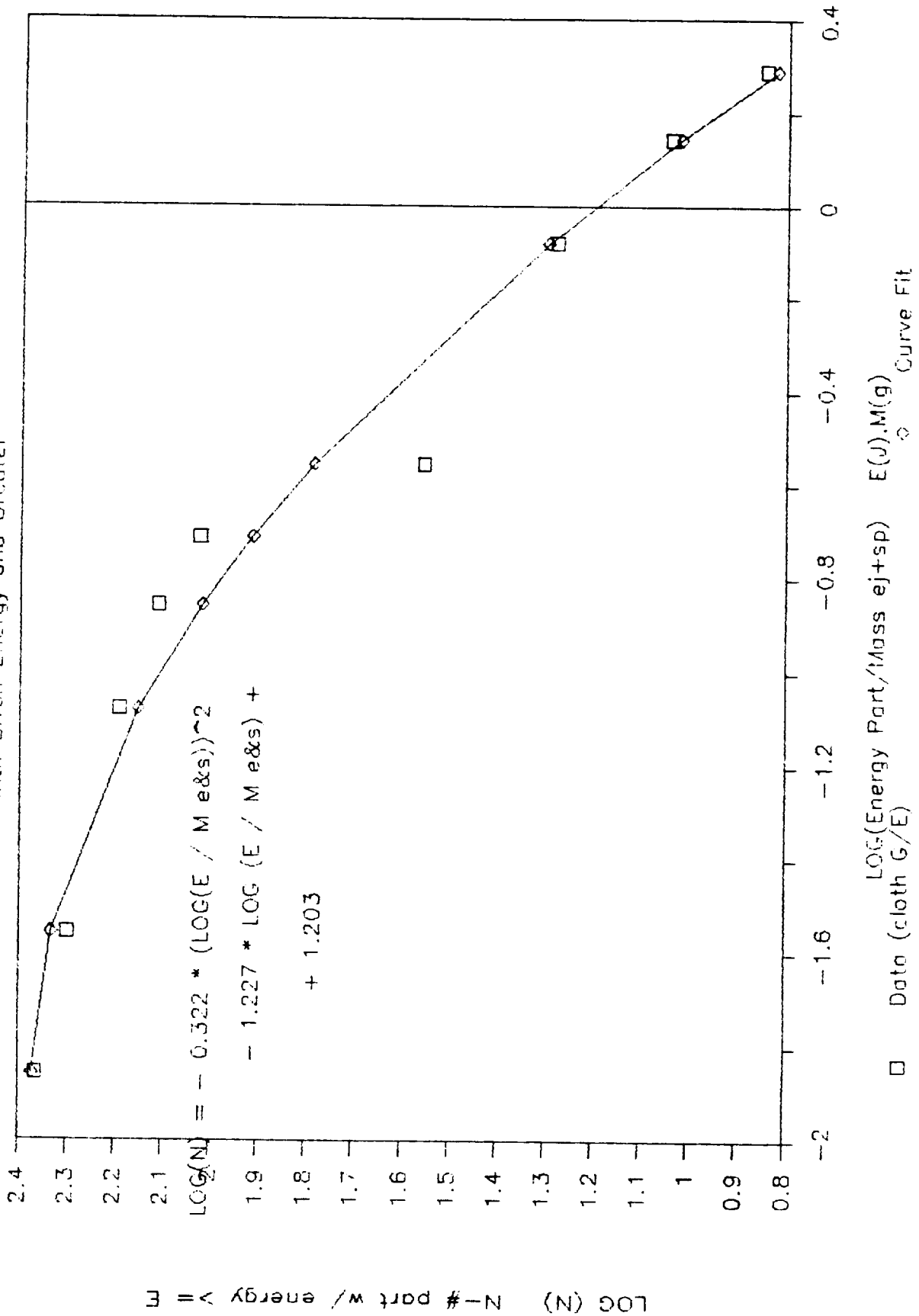


Figure 5-13

Num of Gr/Ep (No Cloth) Ej&Sp Particles  
with Given Energy and Greater

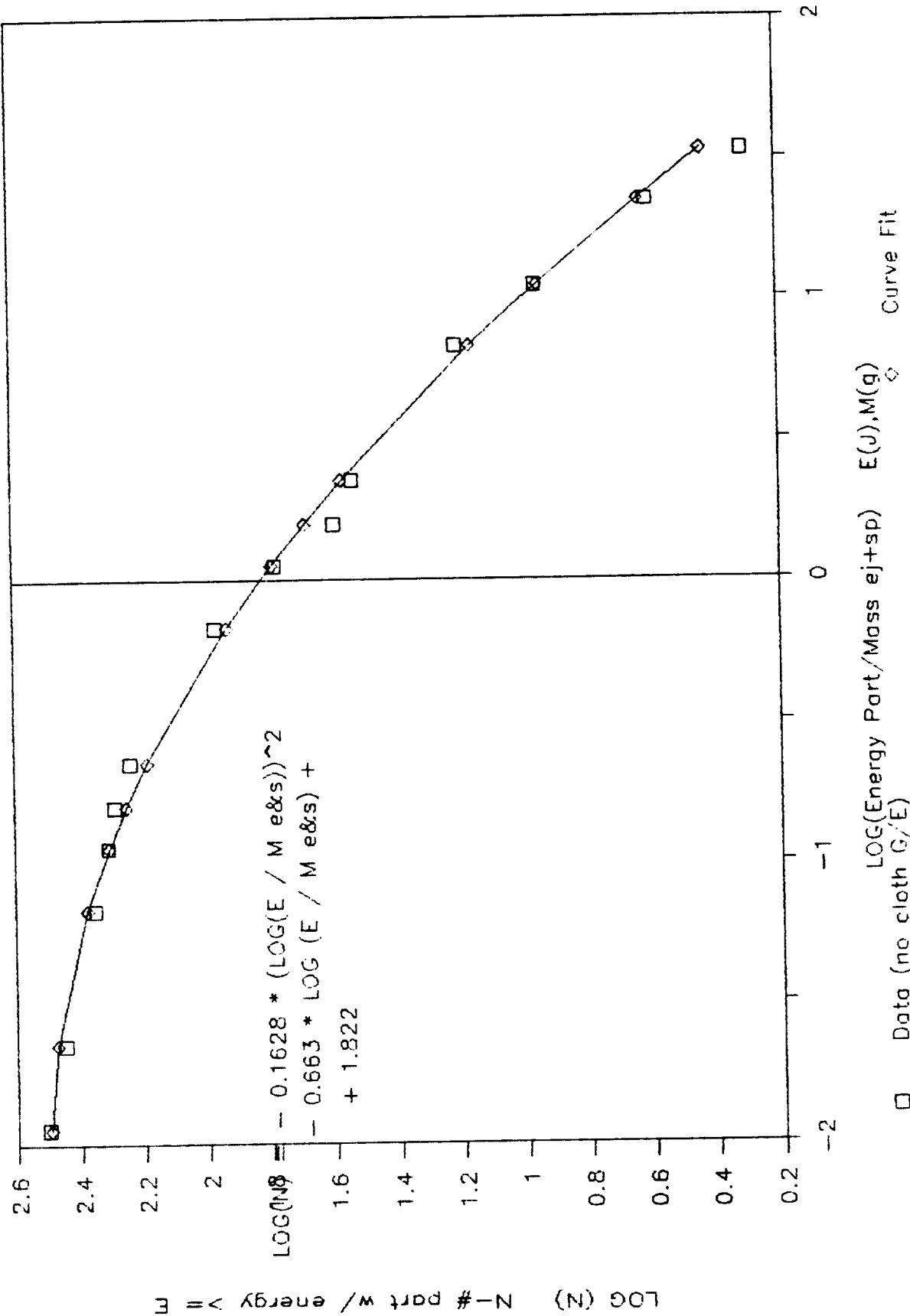


Figure 5-14

# Number of Gr/Ep Ejecta Particles

with Given Energy and Greater

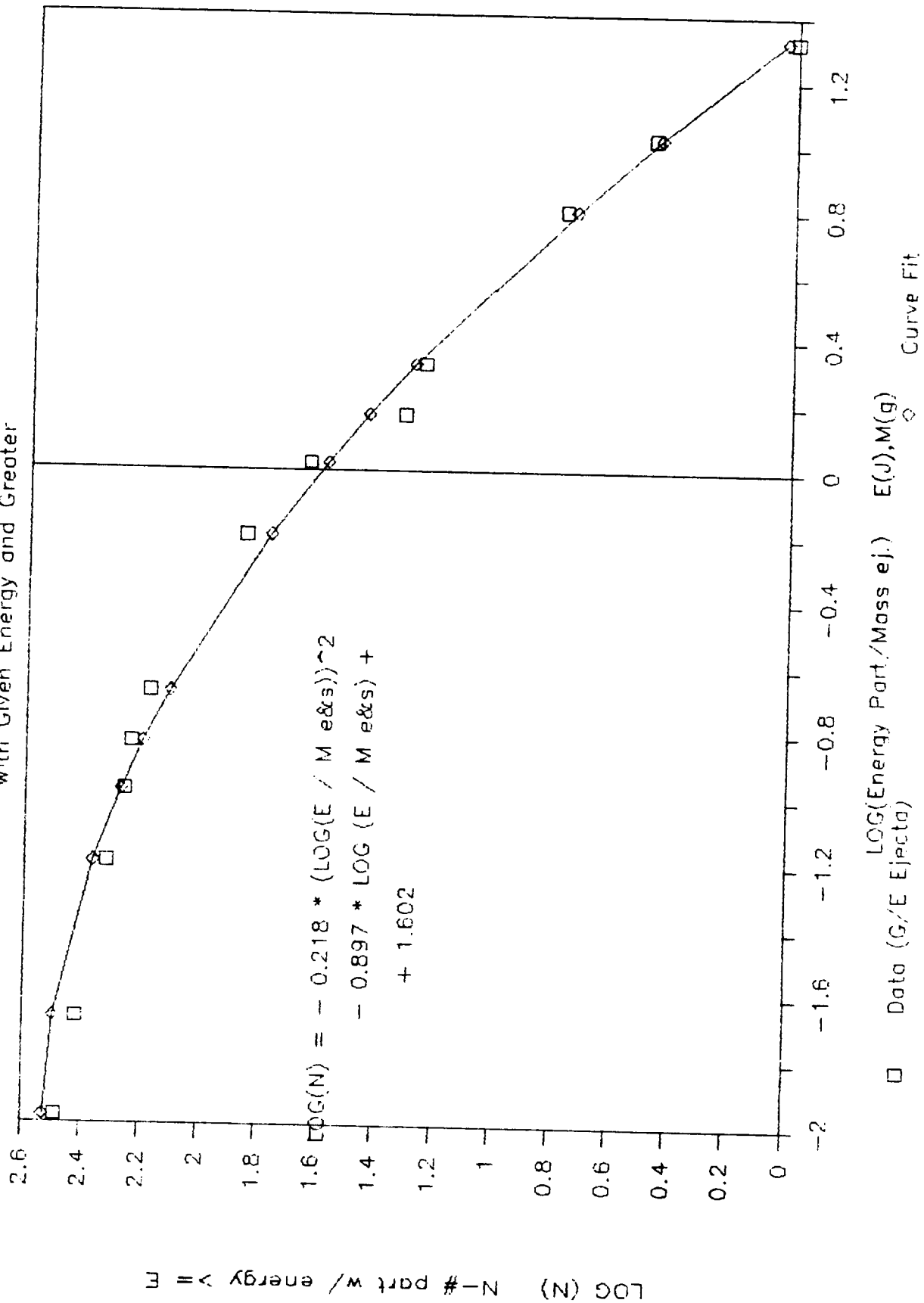


Figure 5-15

# Number of Gr/Ep Spall Particles with Given Energy and Greater

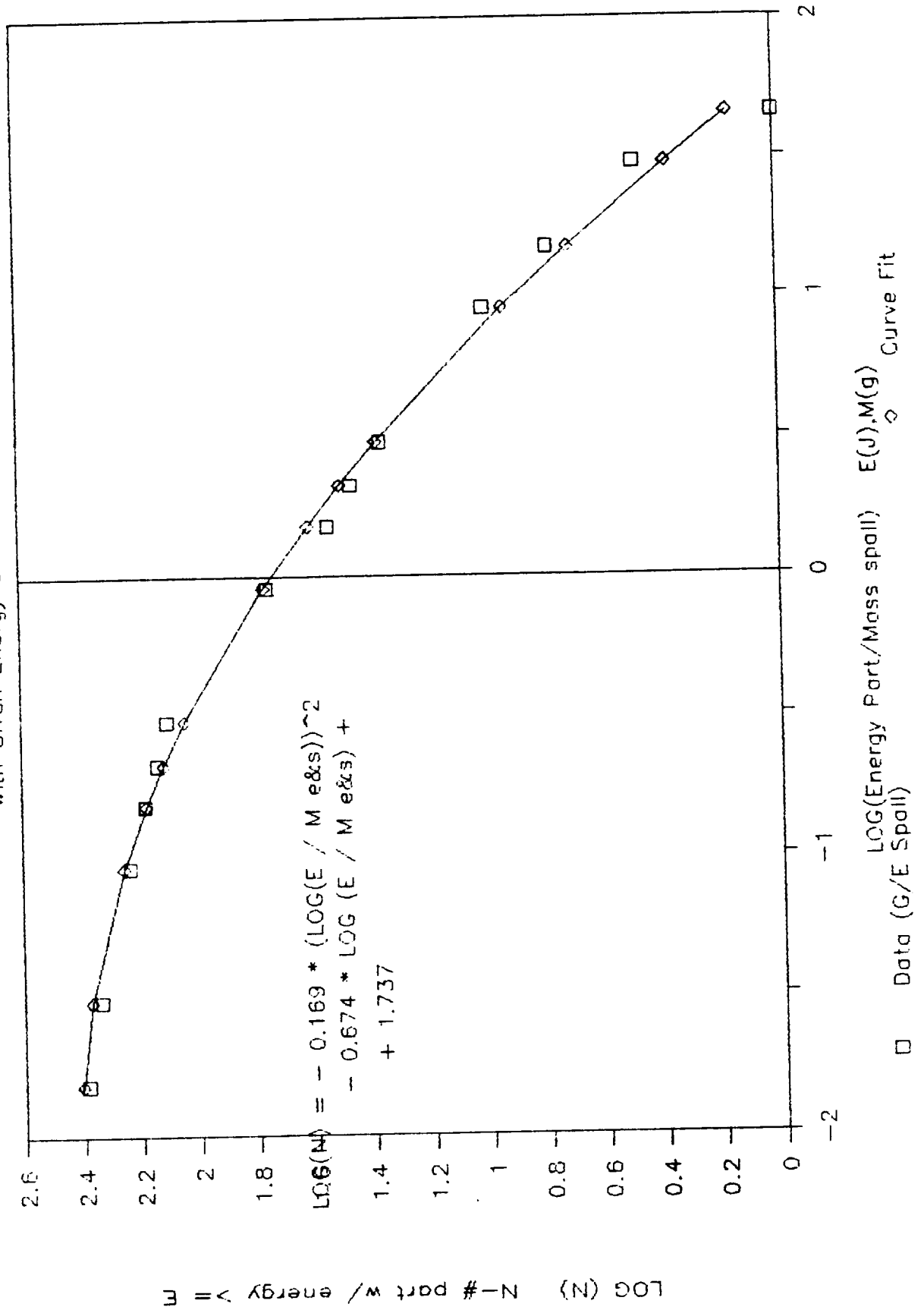




Figure 5-16

# Num. of Graphite/Epoxy Ej&Sp Particles

with Given Energy and Greater

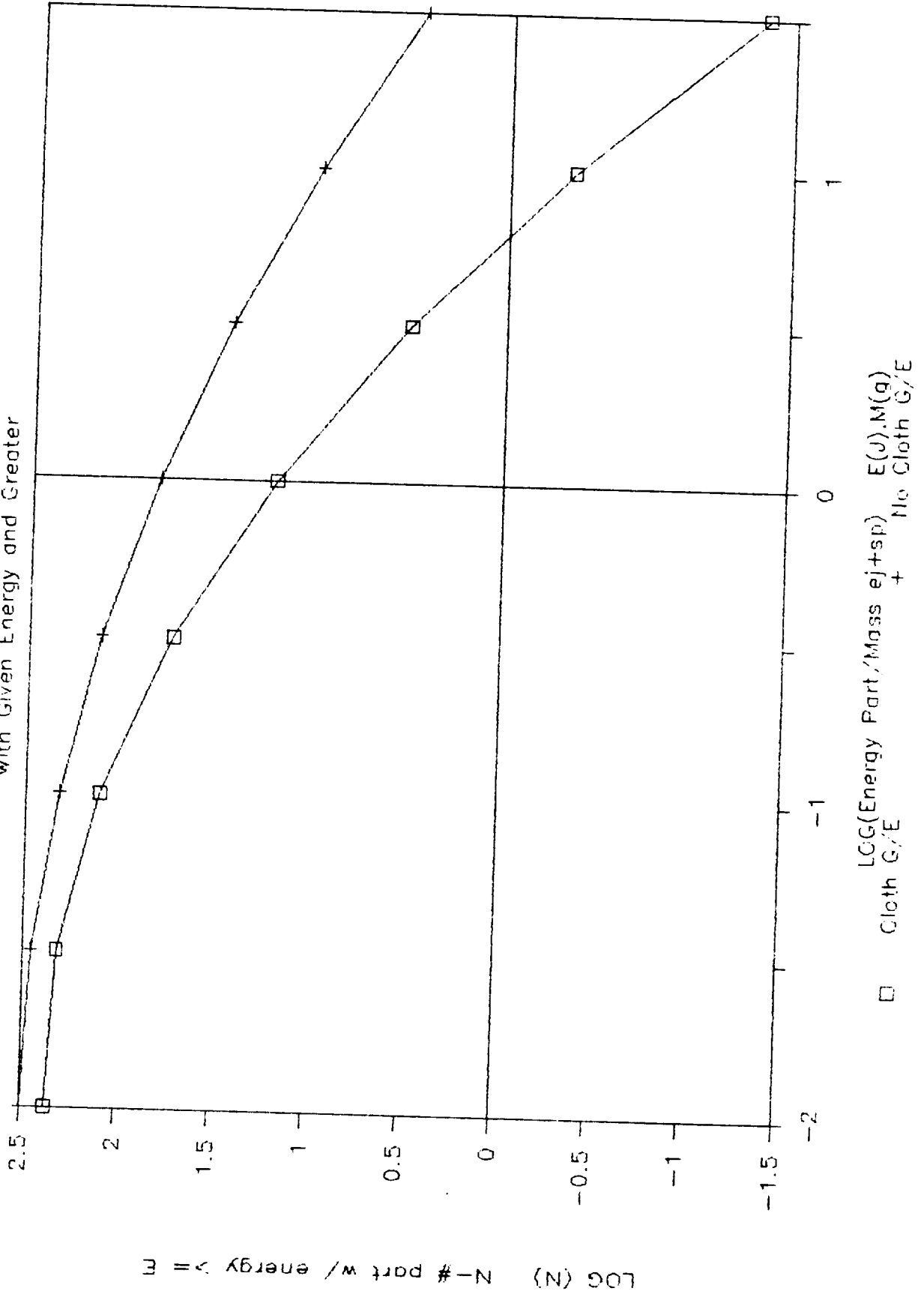


Figure 5-17

# Num. of Graphite/Epoxy Ej&Sp Particles

with Given Energy and Greater

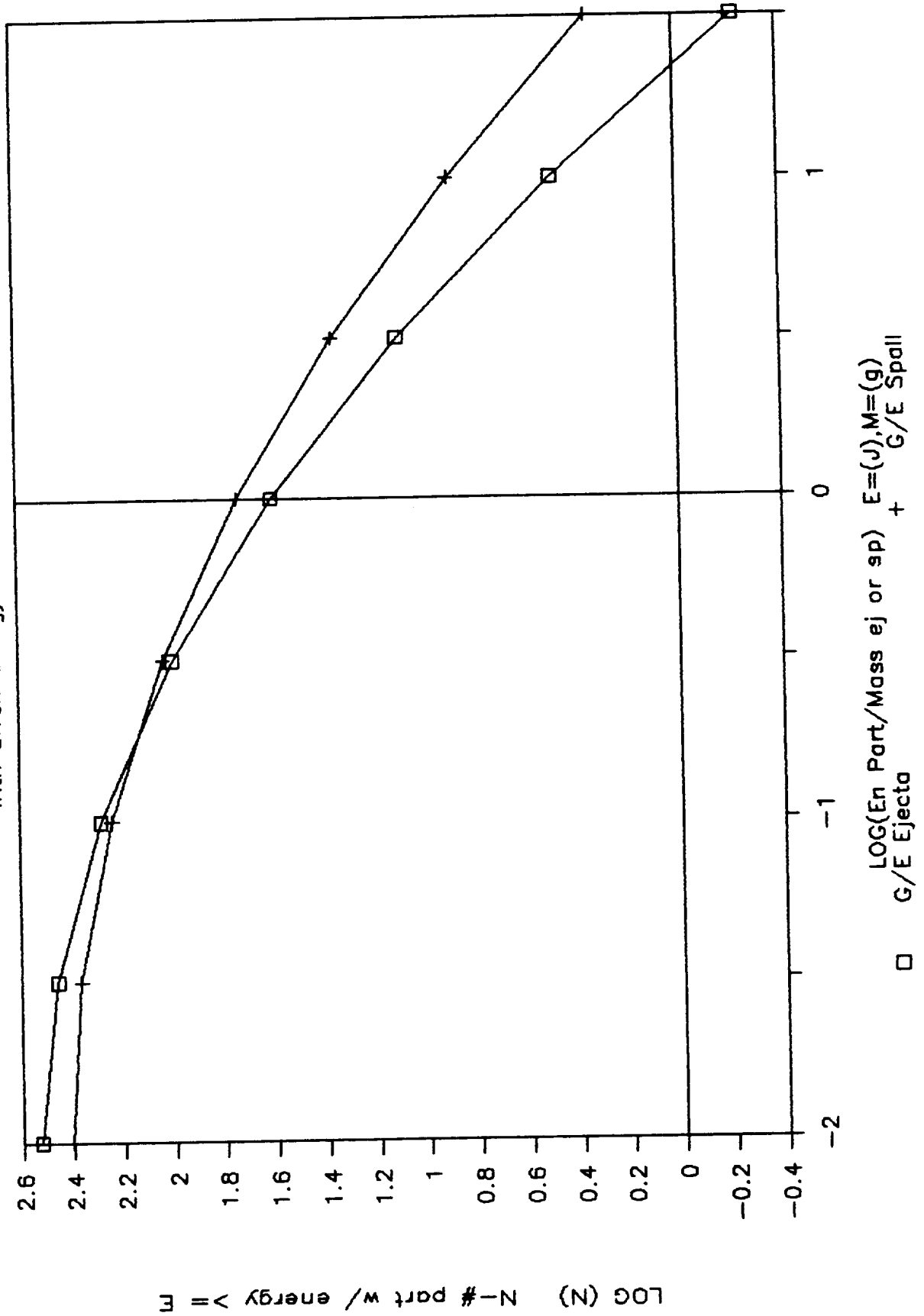


Figure 5-18

# Num. of Aluminum Ej & Sp Particles with Given Energy and Greater

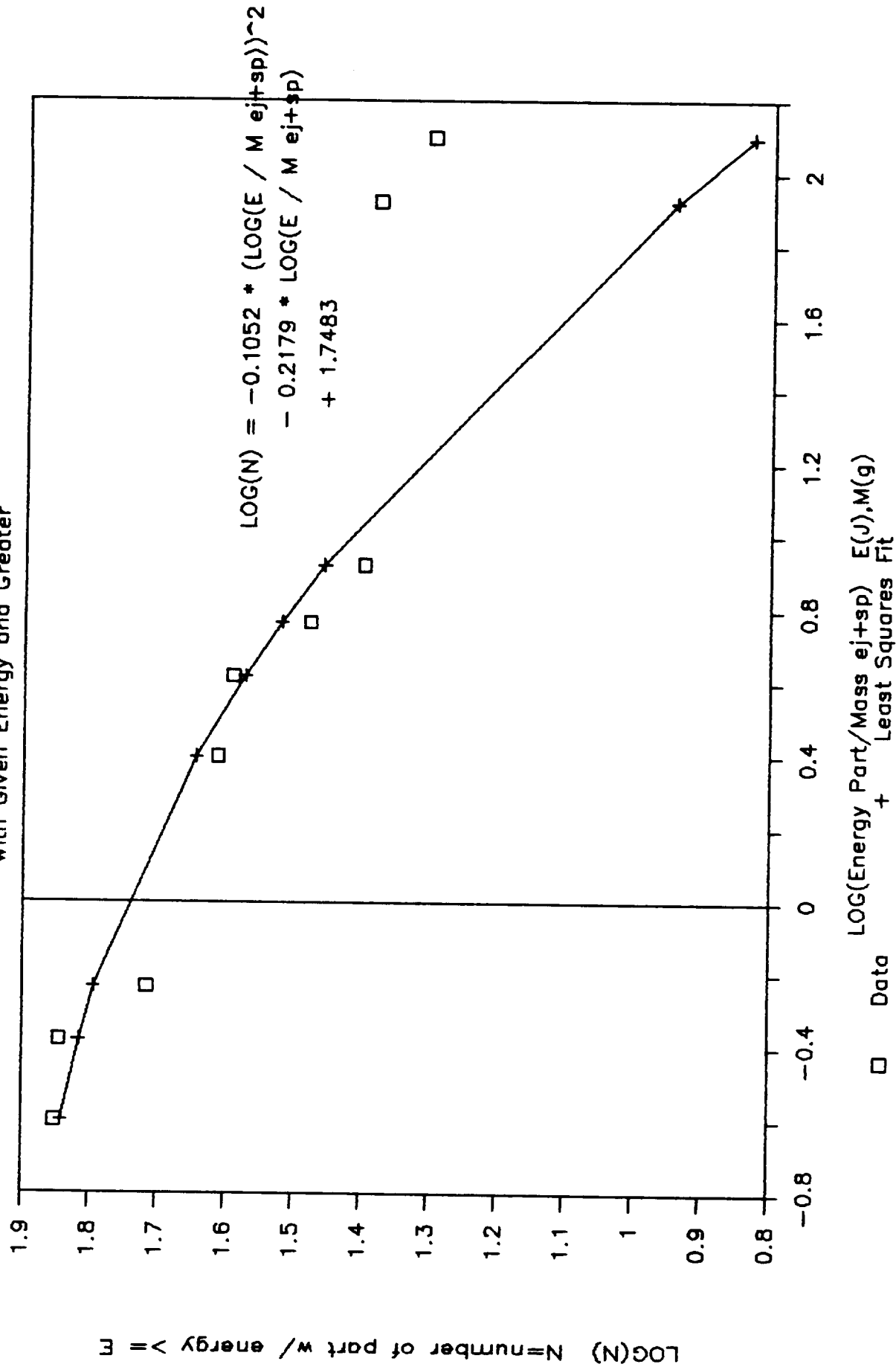


Figure 5-19

# Num. of Aluminum Ejecta Particles with Given Energy and Greater

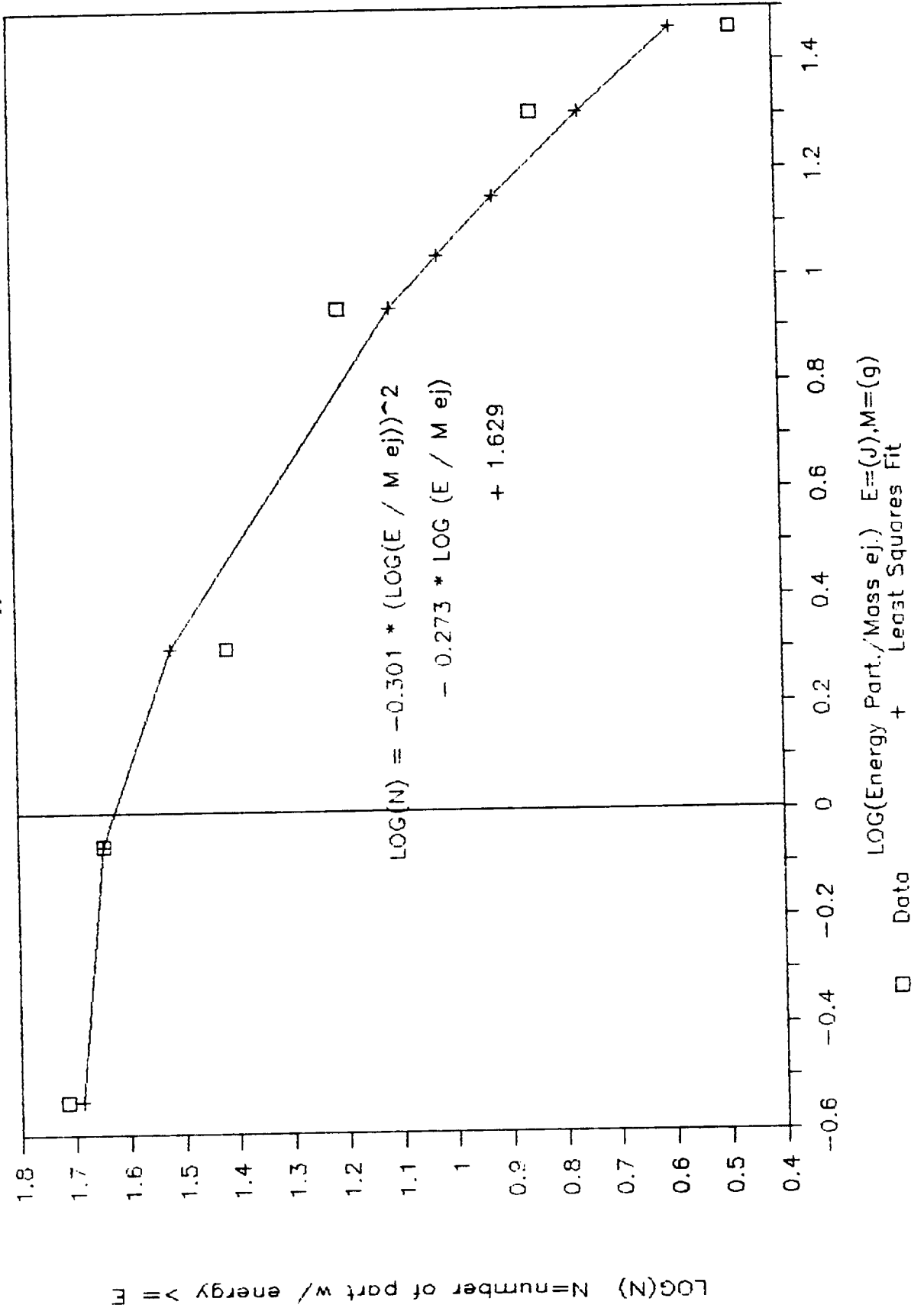


Figure 5-20

# Num. of Aluminum Spall Particles with Given Energy and Greater

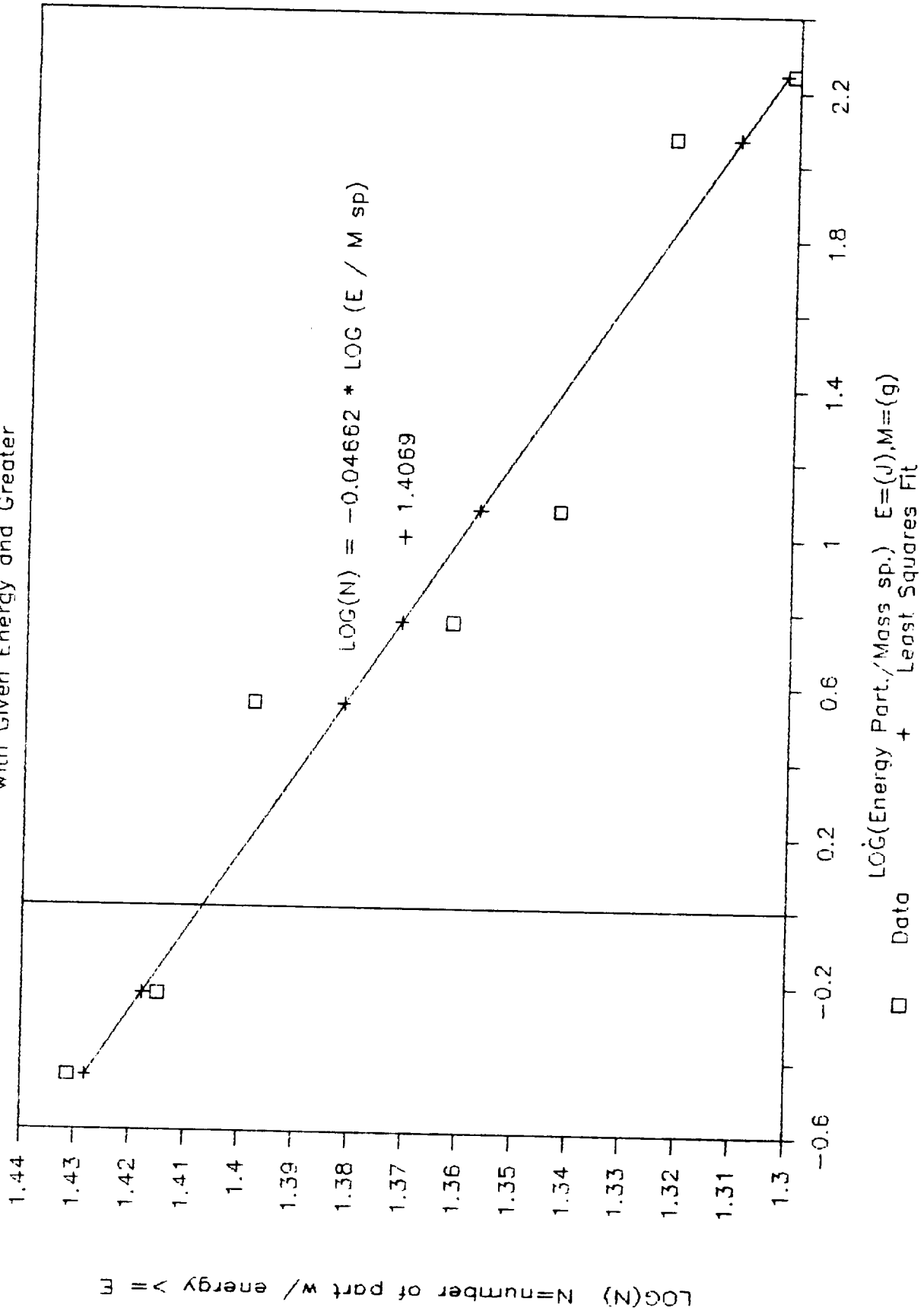


Figure 5-21

# Num. of Aluminum Ej & Sp Particles with Given Energy and Greater

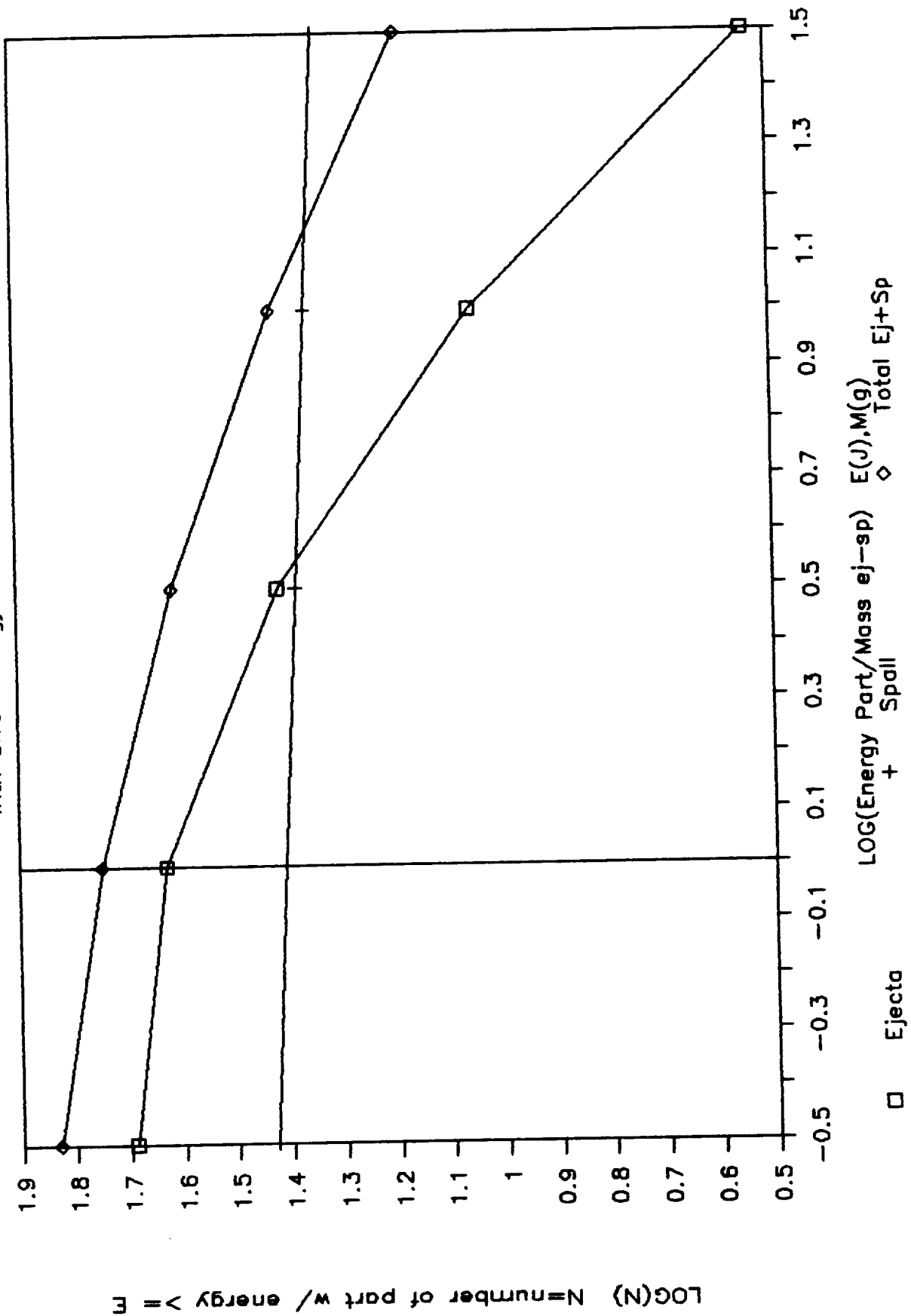
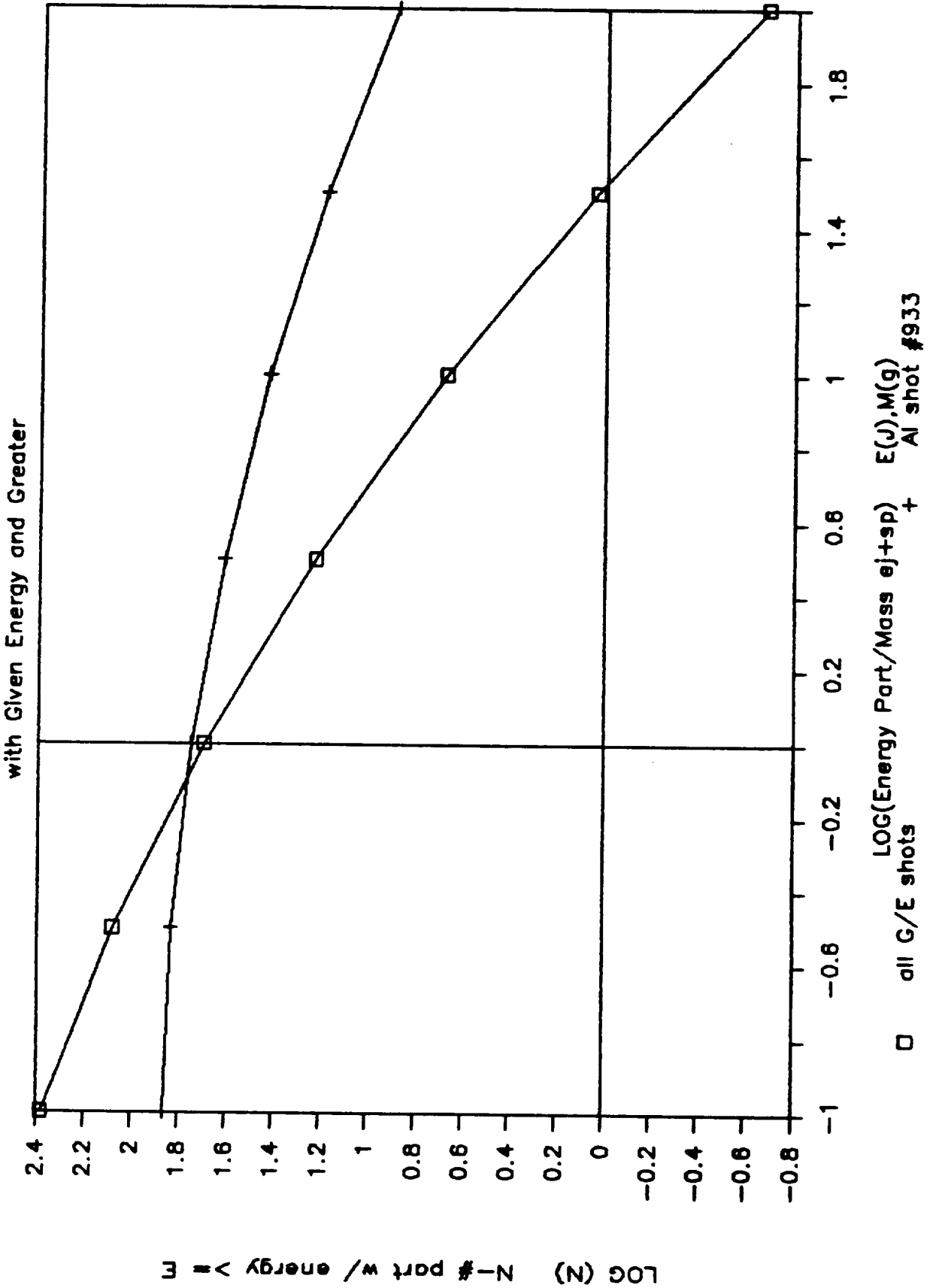


Figure 5-22

# Num. of Gr/Ep or Al Ej&Sp Particles with Given Energy and Greater



#### 5.4 Ejecta/Spall Particle Velocity and Mass

Figure 5-23 is a combination of Figures 3-9, 3-22, 3-41, 3-51, 3-65, and 3-75. It gives an idea of how the calculated particle velocity varies with particle mass. Some of the lower mass ejecta/spall particles can travel relatively fast while all higher mass particles tend to travel slowly. For each individual shot, a line was constructed that delineated the maximum particle velocity boundary. There was little real difference between ejecta and spall particle velocities. However, the particle velocities for cloth covered graphite/epoxy were significantly lower than for graphite/epoxy without cloth. Figure 5-23 shows three lines which are averages of the individual boundaries:

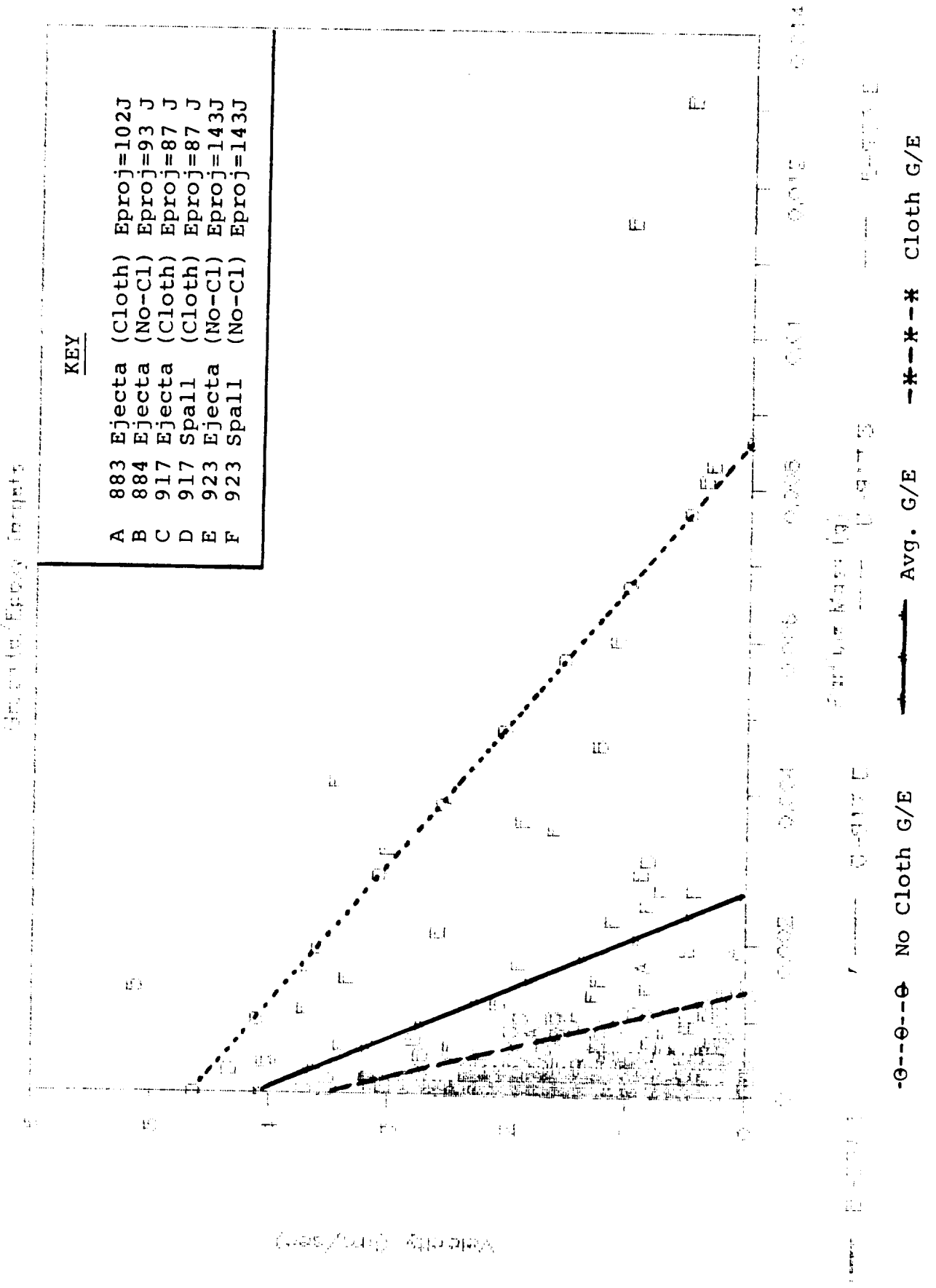
G/E w/out cloth	$V = -540 * M + 4.65$
G/E average	$V = -1543 * M + 4.09$
G/E w/ cloth	$V = -2546 * M + 3.53$

where the maximum ejecta/spall particle velocity,  $V$  (km/sec), is related to particle mass,  $M$  (g). These equations were not used in the damage assessment model described in Section 6, but are presented to indicate calculated particle velocity distributions.



Figure 5-23

# VELOCITY VS. EJECTA/SPALL MASS



## 6.0 Estimate of Damage Potential to the Space Station

Based on the scaling relationships developed in the previous section, a preliminary assessment was made of the relative amounts of damage that can be expected from impacts by ejecta and spall particles on particular Space Station structures. The flux from primary impacts (meteoroids and orbital debris) is compared to the flux from secondary impacts (ejecta and spall) with a given critical kinetic energy that will result in damage to the particular Space Station structure of interest. A spreadsheet program for IBM compatible PC computers was developed to perform the damage assessment calculations.

This section describes the damage assessment model; specifically summarizing the empirical equations used for relating the primary/secondary fluxes and explaining the main model assumptions. Then, the results from applying the model to cases of interest (Station module window, docked Space Shuttle window, habitat module wall, and solar panels) are described.

### 6.1 Damage From Primary Impacts - Meteoroids and Orbital Debris

Spacecraft, space stations, and satellites in Earth orbit are susceptible to potential damage from collisions with both meteoroids and orbital debris. Meteoroids occur naturally while orbital debris (or space junk) originate from man-made objects. Generally, because orbital debris are Earth-orbiting while meteoroids follow interplanetary trajectories, the relative velocities are lower for collisions between orbital debris and spacecraft (average approximately 10 km/sec) than for meteoroid collisions (average approximately 20 km/sec). The average density of orbital debris is approximately that of aluminum, 2.8 g/cc, while cometary meteoroids have a typical density of 0.5 g/cc. Both types of objects are assumed to be spherical.

The level of hazard to a spacecraft from primary impacts depends on the size of the spacecraft, the number and size of primary objects in its operating environment and the time-in-orbit for the spacecraft. The number of impacts,  $N_i$ , over a time period,  $t$  (yrs), is related to the primary flux,  $F$  (impacts/m<sup>2</sup> of surface area - yr), and spacecraft surface area,  $A$  (m<sup>2</sup>), by:

$$N_i = F * A * t$$

### 6.1.1 Meteoroid Model

The NASA recommended meteoroid model (Ref. 7) was used in this study. The average near-Earth meteoroid flux,  $F_{met}$  (impacts/m<sup>2</sup> of surface area - yr), with meteoroid mass,  $M_{met}$  (g), and larger is given by the following equations:

for  $M_{met} \geq 10^{-6}$ ,

$$\text{Log}(F_{met}) = -1.213 * \text{Log}(M_{met}) - 6.871$$

and for  $M_{met} < 10^{-6}$ ,

$$\text{Log}(F_{met}) = -0.063 * (\text{Log}(M_{met}))^2 - 1.584 * \text{Log}(M_{met}) - 6.840$$

This meteoroid flux is assumed to be omnidirectional although recent work (Ref. 8) indicates a directional dependence with most meteoroids coming from the direction of motion. The Earth partially shields the Space Station from meteoroids and the extent of shielding is a function of altitude (Ref. 9). The equation used to multiplicatively compensate the meteoroid flux for this effect is:

$$SF = (R + H + (H^2 + 2RH)^{1/2}) / (2R + H)$$

where SF is the shielding factor which depends on the radius of the Earth, R, and the altitude of the Space Station, H. Because meteoroids are attracted by the Earth's gravity field, the meteoroid flux is also factored by a Earth defocusing factor, DF, which depends on the distance from the Space Station to the center of Earth in units of Earth's radius, r:

$$DF = 0.568 + (0.432/r)$$

### 6.1.2 Orbital Debris Model

Orbital debris are different size particles, fragments, and objects in orbit that result mainly from satellite breakups/explosions and subsequent collisions with operational and nonoperational payloads, rocket casings, etc. Unlike meteoroids which just pass through, orbital debris tends to accumulate (with every launch) and build (from subsequent collisions with other objects) in orbit, especially for frequently used low Earth and geosynchronous orbits. The only natural mechanism for debris removal is atmospheric drag, which acts slowly except at the lowest altitudes. Thus, orbital debris is of particular concern for future space missions (Refs. 2, 10-13). The 1990's predicted orbital debris flux,  $F_{od}$  (impacts/m<sup>2</sup> surface area - yr), with debris mass,  $M_{od}$  (g), and greater for a

Space Station in 30 degree inclination, 500 km circular orbit is given by (Ref. 14):

for  $M_{od} \leq 1.47$  g

$$\text{Log}(F_{od}) = -0.84 * \text{Log}(M_{od}) - 5.320$$

and for  $M_{od} > 1.47$  g,

$$\text{Log}(F_{od}) = 0.0391 * (\text{Log}(M_{od}))^2 - 0.466 * \text{Log}(M_{od}) - 5.384$$

The orbital debris flux is highly directional (essentially only impacting a spacecraft from the direction of flight), but because the above flux equations are expressed in terms of total surface area and the effect of oblique impacts on total ejecta/spall mass was not quantified, flux directionality was not included in this study. An illustration of how quickly the primary fluxes decrease with increasing primary particle size is given in Figure 6-1 (from Ref. 14).

### 6.1.3 Space Station Area Model and Probability of Impact

A model of the dual keel Space Station was developed early in this study to determine the surface area to be used in calculating the total number of primary impacts expected during the Space Station operating lifetime. The total Space Station surface area (including truss, pressurized volumes, solar arrays, radiators, and major payload/experiment packages) as given in Table 6-1 is approximately 11,500 m<sup>2</sup>. The subject of the model was an IOC Space Station reference configuration prior to March 1986 (Ref. 15). Since that time the configuration has further evolved (Ref. 16,17) and this model requires updating. However, it is presented here because the surface area was used in the damage assessment model. Changes in Space Station surface area should not change the relative damage potential between primary and secondary impacts much.

The meteoroid and orbital debris fluxes are calculated using the equations in Sections 6.1.1 and 6.1.2. The sum of the impacts from orbital debris with a diameter of 1 cm and greater and from meteoroids with an equal energy to the 1 cm debris particle is calculated using the equation in Section 6.1. Finally, the probability of no impact,  $P_{ni}$ , during the 30 year assumed lifetime of the Space Station is calculated from Poisson's probability:

$$P_{ni} = \exp(-(F_{met} * SF * DF + F_{od}) * t * A)$$

### 6.2 Damage From Secondary Impacts - Ejecta and Spall

A model was constructed and programmed in a spreadsheet format to estimate the amount of damage that can be expected from secondary impacts. That program is described below.

### 6.2.1 Damage Assessment Worksheet

An example worksheet is given in Table 6-2. A couple of Space Station variables need to be set by the user: station surface area (from Table 6-1) and station lifetime. In addition, several variables need to be set that describe the structure for which the damage assessment is being made.

One of the key variables to be defined is a critical energy for a particle that would result in unacceptable damage to the sensitive area (or structure that is being assessed).

For this particular example, the critical energy was arbitrarily set at 120 joules. Another variable is the sensitive area's surface area which was set at 200 m<sup>2</sup> in this example. This variable is not particularly important because it is only used in the calculation for the total number of impacts on the sensitive surface. An assessment of the relative amount of damage from primary and secondary impacts can be made simply by looking at the fluxes of primary/secondary particles on the sensitive surface. The flux calculation does not involve the sensitive area surface area directly.

However, the surface area is involved indirectly in another important parameter--the fraction of surface area of the Space Station that faces the sensitive area. In other words, this factor gives the fraction of Space Station surface area that produces ejecta/spall that can potentially hit the sensitive surface (ie. the fraction of station area that is within line-of-sight of the sensitive surface). It has to be calculated/estimated by the user based on the geometry of the station and the size of the sensitive surface. Naturally, as the sensitive surface area decreases, less station surface area is within the line-of-sight of the sensitive surface. This factor will be referred to as the "station surface area fraction" or SAF through the remainder of the text.

Another important user supplied factor is the fraction of sky covered by the station as seen from the sensitive surface (using hemispherical geometry). Because it is geometry related, no calculation exists in the present program and it must be calculated/estimated by the user. This factor will be referred to as the "view factor" or VF. The fraction of the ejecta/spall produced by primary impacts on the Space Station that immediately hits the sensitive surface is thus calculated as the product of SAF and VF (this product will be referred to as the secondary impact fraction or SF).

For a given critical energy, the flux of primary particles that have this energy and greater is calculated based on the flux equations in Sections 6.1.1 and 6.1.2, and the average velocities for meteoroids and orbital debris. These fluxes for the example

critical energy of 120 J are given on the first page of Table 6-2 (within the highlighted box). The meteoroid flux is greater in this case but as critical energy increases, the orbital debris flux becomes the more important primary flux.

The ejecta/spall flux of particles having the critical energy and greater is determined by integrating over the entire range of appropriate projectile masses (the model now integrates from 0.001 g and above). For a given projectile mass and velocity (using the averages for orbital debris and meteoroids), the mass of ejecta and spall is calculated from the equations in Section 5.1. Two sets of calculations are made--one for the case of having the entire Space Station made of aluminum (and thus all ejecta/spall produced from primary impacts would be aluminum), and the other set for the case of the Space Station being entirely graphite/epoxy. A comparison is then possible between the relative damage potential of graphite/epoxy ejecta/spall and aluminum ejecta/spall.

If the results from applying this model to sensitive areas of interest indicate that secondary impacts may create as much or more of a problem than primary impacts, then it might be advisable to make the model more realistic by setting it up with different materials for various Space Station structures and calculating a more accurate picture of the amount of secondary damage to expect on the sensitive surface.

After the total ejecta/spall mass is calculated, the equations described in Section 5.3 are applied to determine the number (or flux) of ejecta/spall particles having the critical energy and greater. The secondary impact fraction (SF) is then used to factor the total Space Station secondaries flux having the critical energy and greater to determine the amount of secondaries flux striking the sensitive surface. In the example of Table 6-2, with a SAF of 25% and a VF of 25%, the resulting SF is 0.0625 which results in the ejecta/spall flux being about 7% of the total number of critical energy impacts on the sensitive surface if the Space Station was entirely graphite/epoxy and about 6% if it was aluminum. This example indicates that a designer for the sensitive surface that was concerned about meteoroid/orbital debris damage should factor the total primary flux (sum of meteoroid and orbital debris fluxes) by approximately 1.07 to compensate for damage from secondary impacts.

Figure 6-2 is a graph of the Table 6-2 example that plots the secondary flux versus SF. The graphite/epoxy secondaries flux is slightly above the aluminum secondaries flux primarily because of an assumption that significantly reduced the number of potentially damaging aluminum ejecta/spall particles. This assumption is explained in Section 6.2.2 (letter d).

Figure 6-1 -  
Primary Fluxes (from Ref. 14)

# 1990's AVERAGE ENVIRONMENT

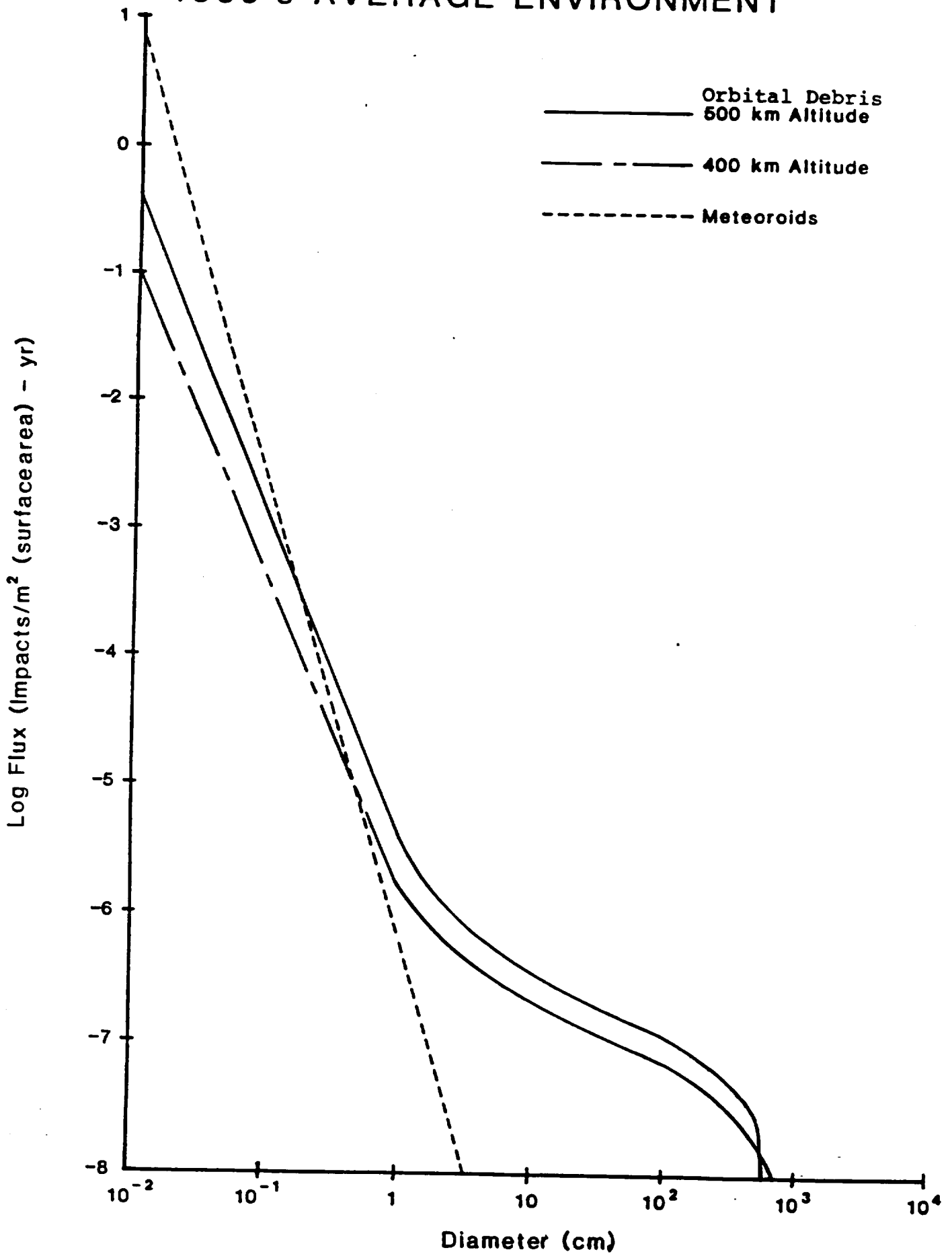


Table 6-1  
(page 1 of 3)

Properties	Value		
Composite density (g/cc)	1.5775	Aluminum den.	
Meteoroid density (g/cc)	0.5	(g/cc)	2.712
Orbital Debris density (g/cc)	2.8		
Meteoroid critical mass (g)	3.6632E-01	Ave. Vel. (km/s)	20
Orbital Debris crit. mass (g)	1.4661E+00	Ave. Vel. (km/s)	10
Space station structure life (yrs)		30	
Logistics module life (yrs)		1	
Ejecta station view factor		0.25	
Meteoroid Energy (J)	73303.8		
Orbital Debris Energy (J)	73303.8		
Kevlar 3501-6 Unidirectional Fiber			
Et (giga Pa)	1.92000	S (giga Pa)	0.12110
Ec (giga Pa)	-2.27000	K (giga Pa)	0.18204
Vt (giga Pa)	0.04216		
Yc (giga Pa)	-0.09308		
Vaporization Energy (J/g)	3578.5		
Vaporization Energy (J/g)	12059.0		
Al 2219-T8 yield stress (giga Pa)	0.317159		



Table 6-1, Continued  
(page 2 of 3)

SPACE STATION  
SURFACE AREA TABULATION

DUAL KEEL REFERENCE CONFIGURATION

ITEM	SHAPE	LENGTH	WIDTH OR	DEPTH	SURFACE	NUMBER	TOT. SURF.	MATERIAL	SKIN	TOTAL	TIME
		FT	DIAMETER	FT							
		FT	FT	FT	FT SQRD.		FT SQRD.	TYPE	INCHES	METERS SQ.	
Common Module	Cylinder	42	14	-	2,155.1	4	8,620.5	Aluminum	0.06	800.87	30
CDM 1202	Cylinder	21	14	-	1,231.5	1	1,231.5	Aluminum	0.06	114.41	30
Logistics Mod.	Cylinder	38	13.2	-	1,849.5	1	1,849.5	Composite	0.1	171.82	1
Solar Arrays	Flat Plate	80	32.5		5,200.0	8	41,600.0	Ceramic		3,864.77	30
Radiators (Module)	Flat Plate	50	24		2,400.0	2	4,800.0	Metallic		445.93	30
Radiators (Par sys.)	Flat Plate	50	6		600.0	2	1,200.0	Metallic		111.48	30
Hangar (TDM 2570)	Box	60	27	25	7,590.0	1	7,590.0	Composite		705.13	30
SAT Instr. Stor.	Box	45	10	10	2,000.0	1	2,000.0	Composite		185.81	30
SAA 0004	Box	20	10	10	1,000.0	1	1,000.0	Composite		92.90	30
TDM 2010	Box	10	10	10	600.0	1	600.0	Composite		55.74	30
SAA 0025	Box	15	10	10	800.0	1	800.0	Composite		74.32	30
SAA 0207	Box	10	10	10	600.0	1	600.0	Composite		55.74	30
SAA 0009	Box	15	12	10	900.0	1	900.0	Composite		83.61	30
SAT Stor. Bay	Box	70	30	30	10,200.0	1	10,200.0	Composite		947.61	30
SAT SVC Bay	Box	70	30	30	10,200.0	1	10,200.0	Composite		947.61	30
TDM 2200	Box	32	6	6	840.0	1	840.0	Composite		78.04	30
Refueling Bay	Box	70	30	30	10,200.0	1	10,200.0	Composite		947.61	30
Truss Elements											
(in a 16.4042 foot cube truss, there is app. 255.3029 linear feet of 2 inch OD tubes.)											
		Boon Len. (ft)	Lin. ft of truss	Width (ft)							
Dual Keel	Cylinder	311.7	4,850.8	0.167	2,539.9	2	5,079.7	Composite	0.1	471.92	30
Upper Boon	Cylinder	147.6	2,297.7	0.167	1,203.1	1	1,203.1	Composite	0.1	111.77	30
Lower Boon	Cylinder	147.6	2,297.7	0.167	1,203.1	1	1,203.1	Composite	0.1	111.77	30
Mid Boon	Cylinder	114.8	1,787.1	0.167	935.7	1	935.7	Composite	0.1	86.93	30
Transv. Boon (inboard and outboard)	Cylinder	147.6	2,297.7	0.167	1,203.1	2	2,406.2	Composite	0.1	223.54	30
Module Support Boon Elements	Cylinder	213.3	3,318.9	0.167	1,737.8	1	1,737.8	Composite	0.1	161.45	30
Truss Total							12,565.6			1,167.38	30
DMV	Cylinder	3	15	-	141.4	2	282.7	Aluminum	0.06	26.27	30
Airlocks	Cylinder	10	7	-	219.9	2	439.8	Aluminum	0.06	40.86	30
Antenna (TDM 2060/2070)	Dish	-	100	-	7,854.0	1	7,854.0	Composite/Metal		729.66	30
Station Total							125,373.6			11,647.58	30

Table 6-1, Continued  
(page 3 of 3)

IMPACT PROBABILITY CALCULATIONS

ITEM	DEBRIS CRIT. MASS GRAMS	DEBRIS AVE. VOL. (CC)	DEBRIS AVE. DIA. (CM)	DEBRIS FLUX ABOVE CRIT. MASS #/M <sup>2</sup> /YR	NO DEBRIS IMPACT PROBABILITY CRIT. MASS OR GREATER	METEOROID AVE. DIA. (CM)	EARTH DEFOCUSING FACTOR	EARTH SHIELDING FACTOR	METEOROID FLUX ABOVE CRIT. MASS #/M <sup>2</sup> /YR	NO MET. IMPACT PROBABILITY CRIT. MASS OR GREATER	COMBINED NO IMPACT PROB. CRIT. MASS OR GREATER	LIFETIME IMPACTS Crit. Mass & Greater MET. DEBRIS	
Common Module	1.4661	5.24E-01	1.000	3.597E-06	0.91720	1.12E+00	0.9675	0.717	4.185E-07	0.9930	9.11E-01	0.0070	0.08...
CDM 1202	1.4661	5.24E-01	1.000	3.597E-06	0.98773	1.12E+00	0.9675	0.717	4.185E-07	0.9990	9.87E-01	0.0010	0.0127
Logistics Mod.	1.4661	5.24E-01	1.000	3.597E-06	0.99938	1.12E+00	0.9675	0.717	4.185E-07	1.0000	9.99E-01	0.0000	0.00
Solar Arrays	1.4661	5.24E-01	1.000	3.597E-06	0.65895	1.12E+00	0.9675	0.717	4.185E-07	0.9669	6.37E-01	0.0337	0.4171
Radiators (Module)	1.4661	5.24E-01	1.000	3.597E-06	0.95301	1.12E+00	0.9675	0.717	4.185E-07	0.9961	9.49E-01	0.0039	0.04
Radiators (Pwr sys.)	1.4661	5.24E-01	1.000	3.597E-06	0.98804	1.12E+00	0.9675	0.717	4.185E-07	0.9990	9.87E-01	0.0010	0.0120
Hangar (TDM 2570)	1.4661	5.24E-01	1.000	3.597E-06	0.92672	1.12E+00	0.9675	0.717	4.185E-07	0.9939	9.21E-01	0.0061	0.07
SAT Instr. Stor.	1.4661	5.24E-01	1.000	3.597E-06	0.98015	1.12E+00	0.9675	0.717	4.185E-07	0.9984	9.79E-01	0.0016	0.0201
SAA 000e	1.4661	5.24E-01	1.000	3.597E-06	0.99002	1.12E+00	0.9675	0.717	4.185E-07	0.9992	9.89E-01	0.0008	0.01
TDM 2010	1.4661	5.24E-01	1.000	3.597E-06	0.99400	1.12E+00	0.9675	0.717	4.185E-07	0.9995	9.94E-01	0.0005	0.0060
SAA 0005	1.4661	5.24E-01	1.000	3.597E-06	0.99201	1.12E+00	0.9675	0.717	4.185E-07	0.9994	9.91E-01	0.0006	0.007
SAA 0207	1.4661	5.24E-01	1.000	3.597E-06	0.99400	1.12E+00	0.9675	0.717	4.185E-07	0.9995	9.94E-01	0.0005	0.00...
SAA 0009	1.4661	5.24E-01	1.000	3.597E-06	0.99102	1.12E+00	0.9675	0.717	4.185E-07	0.9993	9.90E-01	0.0007	0.0090
SAT Stor. Bay	1.4661	5.24E-01	1.000	3.597E-06	0.90279	1.12E+00	0.9675	0.717	4.185E-07	0.9918	8.95E-01	0.0083	0.10...
SAT SVC Bay	1.4661	5.24E-01	1.000	3.597E-06	0.90279	1.12E+00	0.9675	0.717	4.185E-07	0.9918	8.95E-01	0.0083	0.1023
TDM 2260	1.4661	5.24E-01	1.000	3.597E-06	0.99161	1.12E+00	0.9675	0.717	4.185E-07	0.9993	9.91E-01	0.0007	0.001
Refueling Bay	1.4661	5.24E-01	1.000	3.597E-06	0.90279	1.12E+00	0.9675	0.717	4.185E-07	0.9918	8.95E-01	0.0083	0.1023
Dual Keel	1.4661	5.24E-01	1.000	3.597E-06	0.95034	1.12E+00	0.9675	0.717	4.185E-07	0.9959	9.46E-01	0.0041	0.0500
Upper Boom	1.4661	5.24E-01	1.000	3.597E-06	0.98801	1.12E+00	0.9675	0.717	4.185E-07	0.9990	9.87E-01	0.0010	0.017
Lower Boom	1.4661	5.24E-01	1.000	3.597E-06	0.98801	1.12E+00	0.9675	0.717	4.185E-07	0.9990	9.87E-01	0.0010	0.012
Mid Boom	1.4661	5.24E-01	1.000	3.597E-06	0.99066	1.12E+00	0.9675	0.717	4.185E-07	0.9992	9.90E-01	0.0008	0.009
Transv. Boom (inboard and ou	1.4661	5.24E-01	1.000	3.597E-06	0.97616	1.12E+00	0.9675	0.717	4.185E-07	0.9981	9.74E-01	0.0019	0.024
Module Support Boom Elements	1.4661	5.24E-01	1.000	3.597E-06	0.98273	1.12E+00	0.9675	0.717	4.185E-07	0.9986	9.81E-01	0.0014	0.017
Truss Total	1.4661	5.24E-01	1.000	3.4674E-06	8.8565E-01	1.12E+00	0.9675	0.717	4.185E-07	0.9899	8.77E-01	0.0102	0.121
DMV	1.4661	5.24E-01	1.000	3.597E-06	0.99717	1.12E+00	0.9675	0.717	4.185E-07	0.9998	9.97E-01	0.0002	0.002
Airlocks	1.4661	5.24E-01	1.000	3.597E-06	0.99560	1.12E+00	0.9675	0.717	4.185E-07	0.9996	9.95E-01	0.0004	0.004
Antenna (TDM 2060/2070)	1.4661	5.24E-01	1.000	3.597E-06	0.92427	1.12E+00	0.9675	0.717	4.185E-07	0.9937	9.18E-01	0.0064	0.078
Station Total	1.4661	5.24E-01	1.000	3.597E-06	2.8449E-01	1.12E+00	0.9675	0.717	4.185E-07	9.0353E-01	2.57E-01	0.1014	1.25

Table 6-2, Damage Assessment Worksheet  
(page 1 of 4)

Flux of Ejecta/Spall Particles of Critical Energy and Greater on a Sensitive Area of Space Station

Surface Area of Station (m <sup>2</sup> )	11416.1	Fraction of surface area of Station facing sensitive area	0.25	Earth's radius (km)	6378.145
Orbital Life (yrs)	30	Fraction of sky covered by Station as seen from sensitive area (hemispherical View Factor)	0.25	Station orbital altitude (km)	500
Critical Energy to damage sensitive surface (Joules)	120	Fraction of Station Ejecta & Spall striking the sensitive area (Station SA fraction & view factor)	0.0625	Altitude in Earth radii	1.078392
Surface Area of critical surface (m <sup>2</sup> )	200	Particle	Flux with critical energy and greater on sens. area (Number impacts/m <sup>2</sup> -yr)	Earth defocusing factor	0.968596
Drb. Debris Average Velocity (km/sec)	9.3	Meteoroids	1.09E-03	Earth shielding factor	0.713070
Drb. Debris Density (g/cc)	2.8	Drb. Debris	6.71E-04	Percent of total impacts on sensitive area if S/S ej. & sp. all Aluminum	58.35%
Meteoroid Average Velocity (km/sec)	20	Ejecta/Spall (if S/S all graphite/epoxy)	1.30E-04	Percent of total impacts on sensitive area if S/S ej. & sp. all Aluminum	35.99%
Meteoroid Density (g/cc)	0.5	Ejecta/Spall (if S/S all aluminum)	1.06E-04	Percent of total impacts on sensitive area if S/S ej. & sp. all Aluminum	6.86%
Velocity above which Al targets vaporize (km/sec)	7	Average Graphite-Epoxy Ejecta/Spall velocity (km/sec)	0.5	Probability of no impact on sens. area with critical energy & greater (percent)	1.10%
		Average Aluminum Ejecta/Spall velocity (km/sec)	4.232		1.78%
		Orbital Debris Fraction below vaporization velocity	0.235359		45.93%
		Drb. Debris Average Vel. (km/sec) below vaporization velocity	4.837984		53.07%

Projectile Mass (g)	0.001	0.01	0.02	0.04	0.06	0.08	0.1	0.2	0.3	0.4	0.5	0.6	0.7	0.8	0.9	1	1.1	1.2	1.3	1.4	1.5	
Orbital Debris Parameters																						
Drb. Deb. Dia. (cm)	0.0680	0.1896	0.2389	0.3010	0.3446	0.3793	0.4086	0.5148	0.5893	0.6486	0.6987	0.7424	0.7816	0.8172	0.8499	0.8803	0.9087	0.9354	0.9607	0.9847	1.0077	
Orbital Debris Flux (if of impacts of given mass & greater per m <sup>2</sup> surface - year)	1.58E-03	2.29E-04	1.28E-04	7.14E-05	5.08E-05	3.99E-05	3.31E-05	1.85E-05	1.31E-05	1.03E-05	8.58E-06	7.34E-06	6.45E-06	5.77E-06	5.22E-06	4.78E-06	4.41E-06	4.10E-06	3.84E-06	3.60E-06	3.43E-06	
Probability of no impacts on Station	0.000%	0.000%	0.000%	0.000%	0.000%	0.000%	0.001%	0.178%	1.108%	2.914%	5.332%	8.085%	10.974%	13.873%	16.710%	19.445%	22.056%	24.535%	26.882%	29.100%	30.873%	
Incremental Orbital Debris Flux	1.35E-03	1.01E-04	5.64E-05	2.06E-05	1.09E-05	6.82E-06	1.46E-05	5.33E-06	1.74E-06	1.22E-06	8.92E-07	6.45E-07	5.43E-07	4.42E-07	3.68E-07	3.11E-07	2.67E-07	2.32E-07	1.73E-07	1.73E-07	3.43E-06	

Table 6-2, Continued  
(page 2 of 4)

<p>18 of impacts of given avg. mass plus or minus 0.004 when proj. mass (= 0.01 g, 0.005 for 0.01 &lt; proj. mass &lt; 0.02, 0.01 g for 0.02 &lt; proj. mass &lt; 0.1g, and 0.05 g when proj. mass &gt;= 0.1 g per m<sup>2</sup> - year)</p>																						
Average Debris Mass (g) for incremental calcs.	0.0055	0.015	0.03	0.05	0.07	0.09	0.15	0.25	0.35	0.45	0.55	0.65	0.75	0.85	0.95	1.05	1.15	1.25	1.35	1.45	1.5	
Number of Impacts from Orbital Debris	463.881	34.594	19.326	7.061	3.735	2.336	5.000	1.827	0.966	0.604	0.416	0.305	0.234	0.186	0.152	0.126	0.107	0.091	0.079	0.057	0.057	1.175
<p>Peteoroid Parameters</p>																						
Peteoroid Dia. (cm)	0.1563	0.3368	0.4243	0.5346	0.6120	0.6736	0.7756	0.9142	1.0464	1.1518	1.2407	1.3184	1.3880	1.4511	1.5092	1.5632	1.6136	1.6611	1.7060	1.7487	1.7874	
Peteoroid Flux (8 of impacts of given mass & greater per m <sup>2</sup> surface - year)	5.86E-04	3.59E-05	1.55E-05	6.48E-06	4.08E-06	2.88E-06	2.20E-06	9.48E-07	5.80E-07	4.09E-07	3.12E-07	2.50E-07	2.07E-07	1.76E-07	1.53E-07	1.35E-07	1.20E-07	1.08E-07	9.79E-08	8.94E-08	8.23E-08	
Probability of no impacts on Station	0.0002	0.0212	2.5712	20.6152	38.0732	50.6012	59.4722	79.9182	87.1902	90.7832	92.8892	94.2582	95.2192	95.9142	96.4492	96.8682	97.2052	97.4812	97.7122	97.9062	98.0732	
Incremental Met. Flux (8 of impacts of given avg. mass plus or minus 0.004 when proj. mass (= 0.01 g, 0.005 for 0.01 < proj. mass < 0.02, 0.01 g for 0.02 < proj. mass < 0.1g, and 0.05 g when proj. mass >= 0.1 g per m <sup>2</sup> - year)	5.50E-04	2.04E-05	8.80E-06	2.59E-06	1.20E-06	6.83E-07	1.25E-06	3.68E-07	1.71E-07	9.69E-08	6.19E-08	4.26E-08	3.10E-08	2.35E-08	1.83E-08	1.47E-08	1.20E-08	9.98E-09	8.41E-09	7.18E-09	8.23E-09	
Average Met. Mass (g) for incremental calcs.	0.0055	0.015	0.03	0.05	0.07	0.09	0.15	0.25	0.35	0.45	0.55	0.65	0.75	0.85	0.95	1.05	1.15	1.25	1.35	1.45	1.5	
Number of Impacts from Meteoroids	130.100	4.826	2.082	0.613	0.284	0.162	0.295	0.087	0.040	0.0229	0.0146	0.0101	0.0073	0.0055	0.0043	0.0035	0.0028	0.0024	0.0020	0.0017	0.0195	
<p>If Ejecta/Spall all from Carbon-Graphite Composite Structures</p>																						
<p>For Impacts from Orbital Debris</p>																						
Mass ejecta & spall per orbital debris impact (g)	0.85	2.31	4.62	7.70	10.78	13.86	23.11	38.51	53.92	69.32	84.73	100.14	115.54	130.95	146.35	161.76	177.16	192.57	207.97	223.38	231.08	
Number of ejecta & spall particles of critical energy and greater per impact from orbital debris of given average mass within mass range.	0.12	0.55	1.43	2.76	4.17	5.62	10.00	17.13	23.93	30.38	36.52	42.37	47.97	53.34	58.50	63.47	68.27	72.91	77.40	81.75	85.88	
<p>Number of critical particles created from orbital debris impacts over lifetime of station.</p>																						
Number of critical energy particles per m <sup>2</sup> - year.	56.55	19.02	27.60	19.48	15.58	13.12	50.00	31.30	23.13	18.36	15.20	12.94	11.25	9.92	8.86	8.00	7.27	6.66	6.14	4.83	58.59	
<p>Flux of critical energy particles of critical energy and greater from orbital debris impacts</p>																						
	1.55E-07	1.19E-03	1.13E-03	1.05E-03	9.98E-04	9.51E-04	9.12E-04	7.66E-04	6.75E-04	6.07E-04	5.54E-04	5.09E-04	4.72E-04	4.39E-04	4.10E-04	3.84E-04	3.61E-04	3.39E-04	3.20E-04	3.02E-04	2.88E-04	

Table 6-2, Continued  
(page 3 of 4)

For Impacts from Meteoroids																					
Mass ejecta & spall per meteoroid impact (g)	3.92	19.89	21.39	35.65	49.91	64.17	106.95	178.25	249.55	320.84	392.14	463.44	534.74	606.04	677.34	748.64	819.94	871.24	962.53	1033.83	1069.48
Number of ejecta & spall particles of critical energy and greater per impact from meteoroids of given average mass within mass range.	1.15	4.13	9.19	15.83	22.19	28.26	44.88	68.60	88.86	106.65	122.56	136.99	150.21	162.42	173.76	184.35	194.29	203.66	212.52	220.91	224.95
Number of critical particles created from meteoroid impacts over lifetime of station.																					
Number of critical energy particles per m <sup>2</sup> - year.	4.11E-05	2.67E-05	1.93E-05	5.61E-05	2.53E-05	1.52E-05	7.58E-06	5.84E-06	4.66E-06	3.81E-06	3.19E-06	2.71E-06	2.33E-06	2.03E-06	1.79E-06	1.59E-06	1.48E-06	1.38E-06	1.29E-06	1.21E-06	1.15E-06
Flux of critical energy particles of critical energy and greater from meteoroid impacts																					
Ejecta/Spall Flux from both orbital debris and meteoroid impacts	2.07E-03	1.47E-03	1.36E-03	1.22E-03	1.14E-03	1.08E-03	1.02E-03	8.39E-04	7.30E-04	6.52E-04	5.91E-04	5.41E-04	4.94E-04	4.64E-04	4.37E-04	4.04E-04	3.79E-04	3.56E-04	3.35E-04	3.16E-04	3.01E-04
If Ejecta/Spall all from Aluminum Structures																					
For Impacts from Orbital Debris																					
Mass ejecta & spall per impact (g)	0.62	0.35	0.88	1.59	2.29	3.00	5.11	8.64	12.17	15.70	19.23	22.76	26.28	29.81	33.34	36.87	40.40	43.92	47.45	50.98	52.75
Number of ejecta & spall particles of critical energy and greater per impact from projectiles of given average mass within mass range.	0.21	3.32	6.36	9.28	11.55	13.46	17.87	23.01	26.78	29.76	32.24	34.36	36.21	37.84	39.31	40.64	41.85	42.97	44.00	44.95	45.40
Number of critical particles created from impacts over lifetime of station.																					
Number of critical energy particles per m <sup>2</sup> - year.	4.56E-05	2.97E-05	2.16E-05	6.14E-05	2.89E-05	1.78E-05	1.24E-05	9.22E-06	7.21E-06	5.83E-06	4.84E-06	4.09E-06	3.52E-06	3.06E-06	2.70E-06	2.40E-06	2.18E-06	1.98E-06	1.83E-06	1.73E-06	1.67E-06
Flux of critical energy particles of critical energy and greater																					
Ejecta/Spall Flux from both orbital debris and meteoroid impacts	5.29E-04	4.61E-04	3.83E-04	2.98E-04	2.23E-04	2.02E-04	1.40E-04	1.12E-04	9.37E-05	8.14E-05	7.22E-05	6.49E-05	5.91E-05	5.43E-05	5.02E-05	4.67E-05	4.38E-05	4.09E-05	3.85E-05	3.67E-05	3.57E-05
For Impacts from Meteoroids																					
Mass ejecta & spall per meteoroid impact (g)	0.23	0.93	2.04	3.52	4.99	6.47	10.90	18.29	25.67	33.06	40.45	47.83	55.22	62.60	69.99	77.38	84.76	92.15	99.54	106.92	110.61
Number of ejecta & spall particles of critical energy and greater per impact from meteoroids of given average mass within mass range.	2.38	6.60	10.79	14.68	17.65	20.07	25.53	31.62	35.91	39.20	41.87	44.10	46.01	47.68	49.15	50.46	51.64	52.71	53.69	54.59	55.01

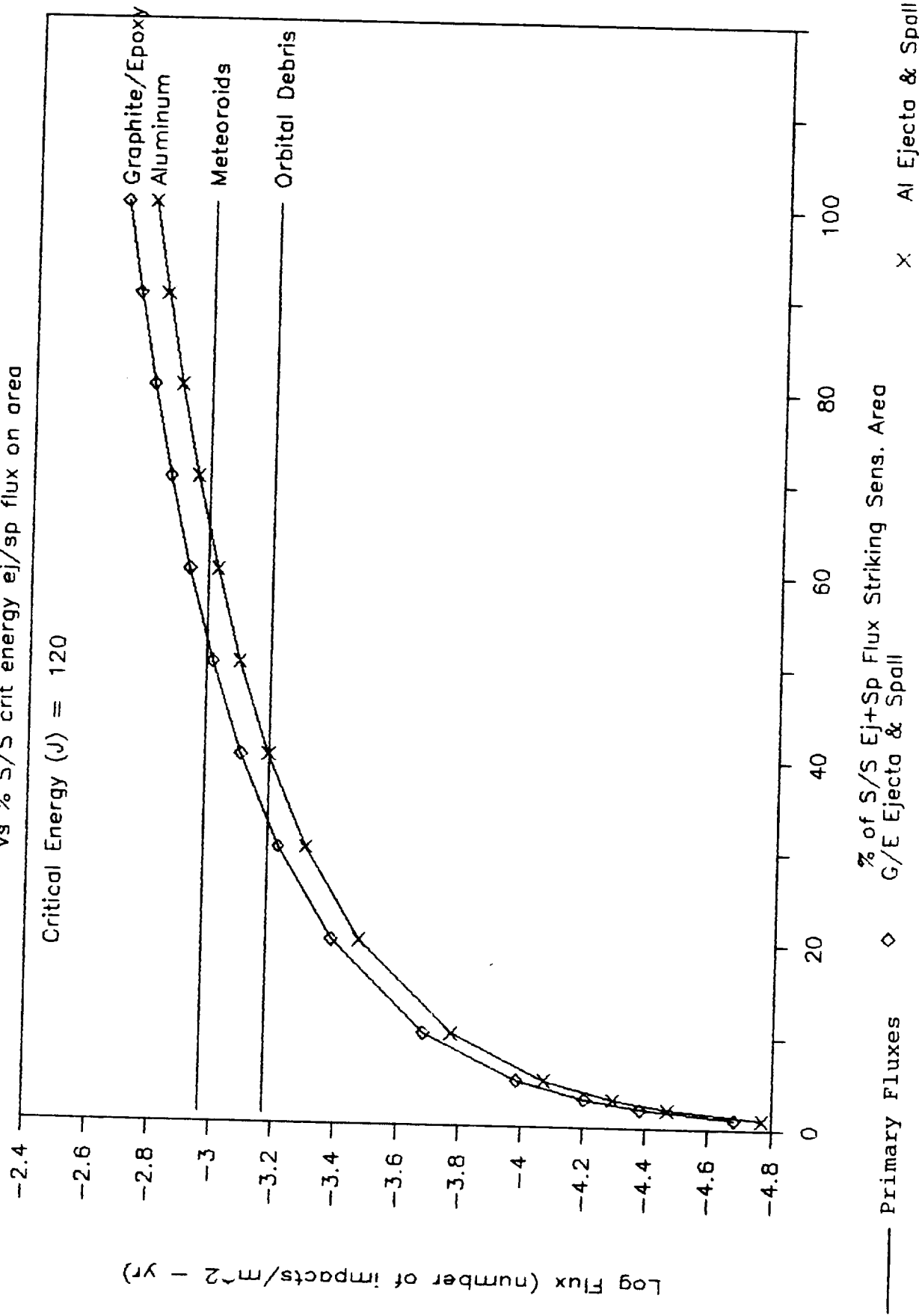
Table 6-2, Continued  
(page 4 of 4)

Number of critical particles created from asteroid impacts over lifetime of station.	309.61	31.85	22.46	9.01	5.02	3.24	7.54	2.75	1.45	0.90	0.61	0.44	0.34	0.26	0.21	0.18	0.15	0.12	0.11	0.09	1.07
Number of critical energy particles per m <sup>2</sup> - year.	1.31E-03	1.35E-04	9.49E-05	3.81E-05	2.12E-05	1.37E-05	3.19E-05	1.16E-05	6.13E-06	3.80E-06	2.59E-06	1.88E-06	1.43E-06	1.12E-06	9.01E-07	7.41E-07	6.20E-07	5.26E-07	4.52E-07	3.92E-07	4.53E-06
Flux of critical energy particles of critical energy and greater from meteoroid impacts	1.68E-03	3.71E-04	2.37E-04	1.42E-04	1.04E-04	8.24E-05	6.88E-05	3.67E-05	2.51E-05	1.90E-05	1.52E-05	1.26E-05	1.07E-05	9.28E-06	8.16E-06	7.26E-06	6.51E-06	5.90E-06	5.37E-06	4.92E-06	4.53E-06
Ejecta/Spall Flux from both Orbital Debris and Meteoroid impacts	1.69E-03	7.18E-04	5.46E-04	3.96E-04	3.25E-04	2.80E-04	2.49E-04	1.66E-04	1.29E-04	9.19E-05	8.08E-05	7.23E-05	6.55E-05	5.99E-05	5.52E-05	5.12E-05	4.77E-05	4.46E-05	4.19E-05	3.98E-05	

Figure 6-2

# Primary and Secondary Particle Fluxes

vs % S/S crit energy  $e_j/sp$  flux on area



## 6.2.2 Model Assumptions and Approximations

The worksheet model included a number of assumptions/approximations which are explained below. The specific model applications described in Section 6.3 were all determined using these assumptions.

- a) The model includes both ejecta and spall in the mass and number of secondary particles produced from primary impacts. Because some of the spall produced in an impact might be contained and prevented from further impacts on other surfaces, this assumption contributes to increasing the estimate of potential damage from secondary impacts. The location of the specific sensitive area relative to the rest of the station will determine if it is subject to secondary ejecta, spall, or both. When using the tables generated, this can be taken into account by choice of SF.
- b) The user must supply a "critical energy" that will result in damage to a surface of interest. There may be more appropriate parameters than kinetic energy to scale on.
- c) The flux of ejecta/spall particles having the critical energy and above is determined using empirical equations developed in this study. These equations are necessarily extrapolated beyond the bounds of the tests run in this study (due to the tremendous velocities of meteoroids/debris which we are trying to model) which implies that an unknown amount of uncertainty is introduced into the calculation.
- d) It was assumed that aluminum vaporizes with projectile velocities above 7 km/sec (Ref.2, p.489--the user can easily change this variable) and above this velocity, impacts on aluminum structures will not produce any damaging ejecta/spall particles (only vapor or very small particles which would be a problem to structures only a relatively few inches away from the impact point). This limit acts to reduce the total (secondary producing) flux of orbital debris on aluminum to about a quarter of its original. This 25% factor is calculated within the model from the orbital debris velocity distribution (Ref. 14) and is equal to the orbital debris fraction with velocities less than 7 km/sec. This limit also reduces the average orbital debris velocity that will produce any damaging ejecta/spall from the actual average (9.3 km/sec) to the average below 7 km/sec (or approximately 4.2 km/sec). This assumption also nearly eliminates meteoroids as a source of damaging ejecta/spall on aluminum structures because of the high relative meteoroid velocities.

Because no information was available on meteoroid velocity distributions when this part of the study was developed, the meteoroid relative velocity for aluminum structures was taken as the assumed aluminum vaporization velocity, ie. 7



km/sec. No corresponding vaporization velocity is assumed for graphite/epoxy targets, pushing the aluminum-graphite/epoxy comparison toward aluminum's favor.

- e) The slopes of the mass distribution curves (Section 5.2) are assumed to not change significantly at higher impact velocities. From reported results of fragmentation distributions due to different energy explosions (Ref. 18), this is probably not quite true (higher energy impacts may produce relatively more small particles and less large particles).
- f) The Space Station nominal altitude was assumed at 500 km (270 nm). Recently, the baseline operating altitude was reduced to 463 km (250 nm) to lower launch costs (Ref. 19). This change will result in somewhat reduced orbital debris flux.
- g) Self-shielding of various Space Station elements is not considered--the entire Space Station surface area is assumed exposed to orbital debris/meteoroid damage.
- h) The program under-estimates the secondaries damage potential at very low critical energies because the lower projectile mass limit in the secondaries flux integration (presently set at 0.001 g) is not low enough.
- i) It is assumed that if ejecta or spall particles hit the sensitive surface, they will do so immediately after being produced. No attempt is made to calculate through orbital mechanics whether any secondary collisions are possible several orbits after the primary impact event.

Figure 6-4

# Primary and Secondary Particle Fluxes

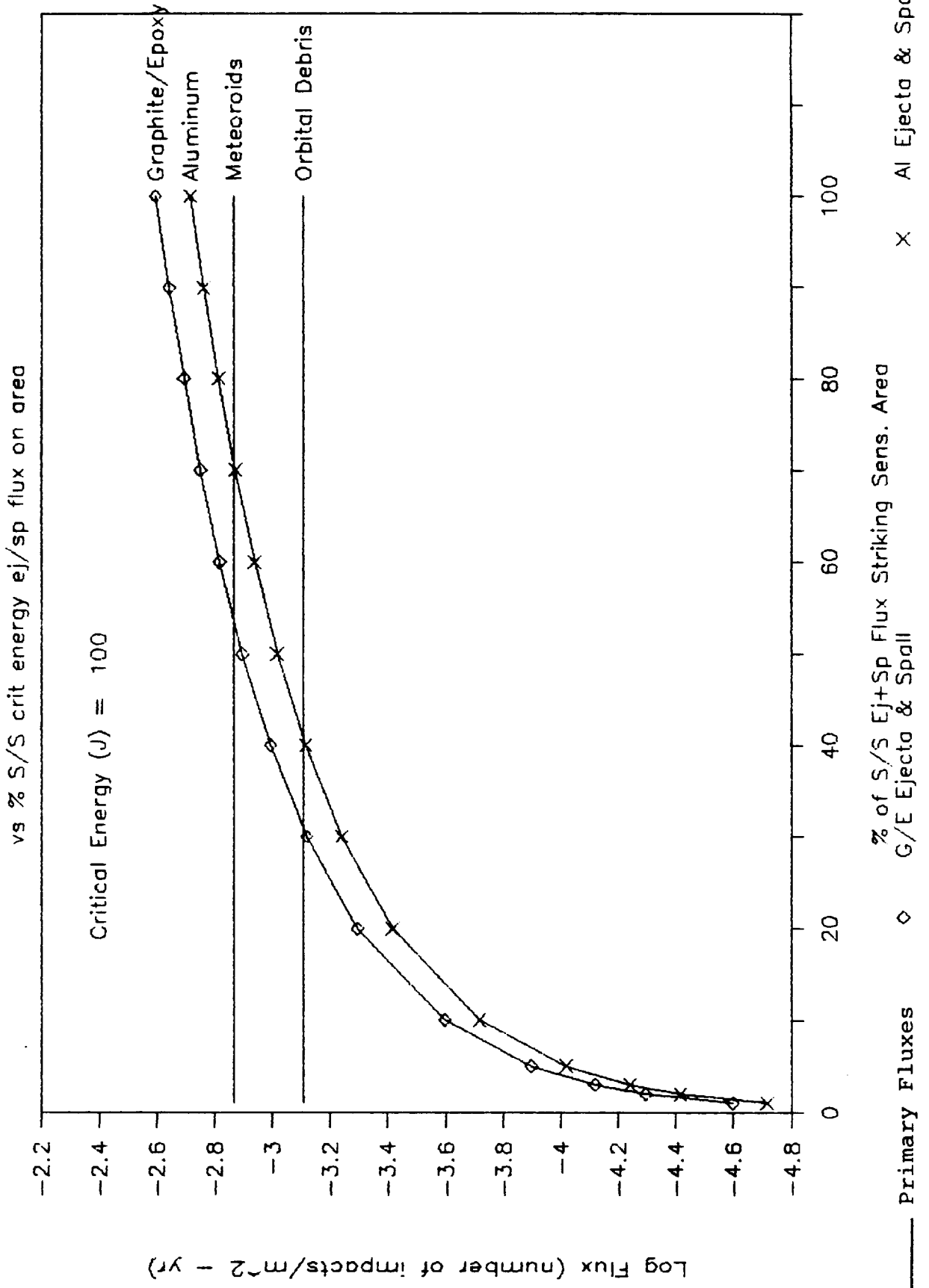


Figure 6-3

# Primary and Secondary Particle Fluxes

vs % S/S crit energy  $e_j/sp$  flux on area

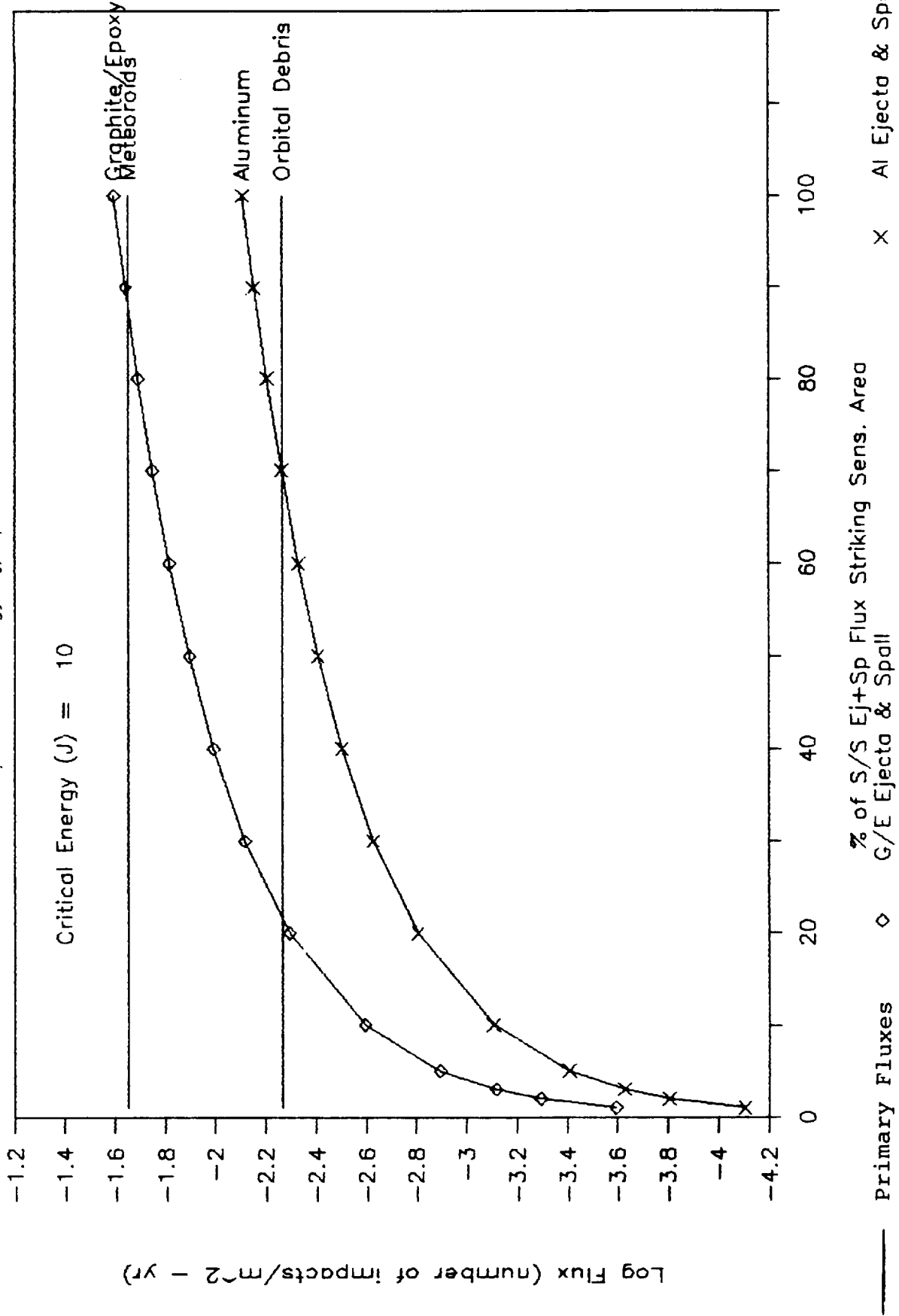


Figure 6-6

# Primary and Secondary Particle Fluxes

vs % S/S crit energy ej/sp flux on area

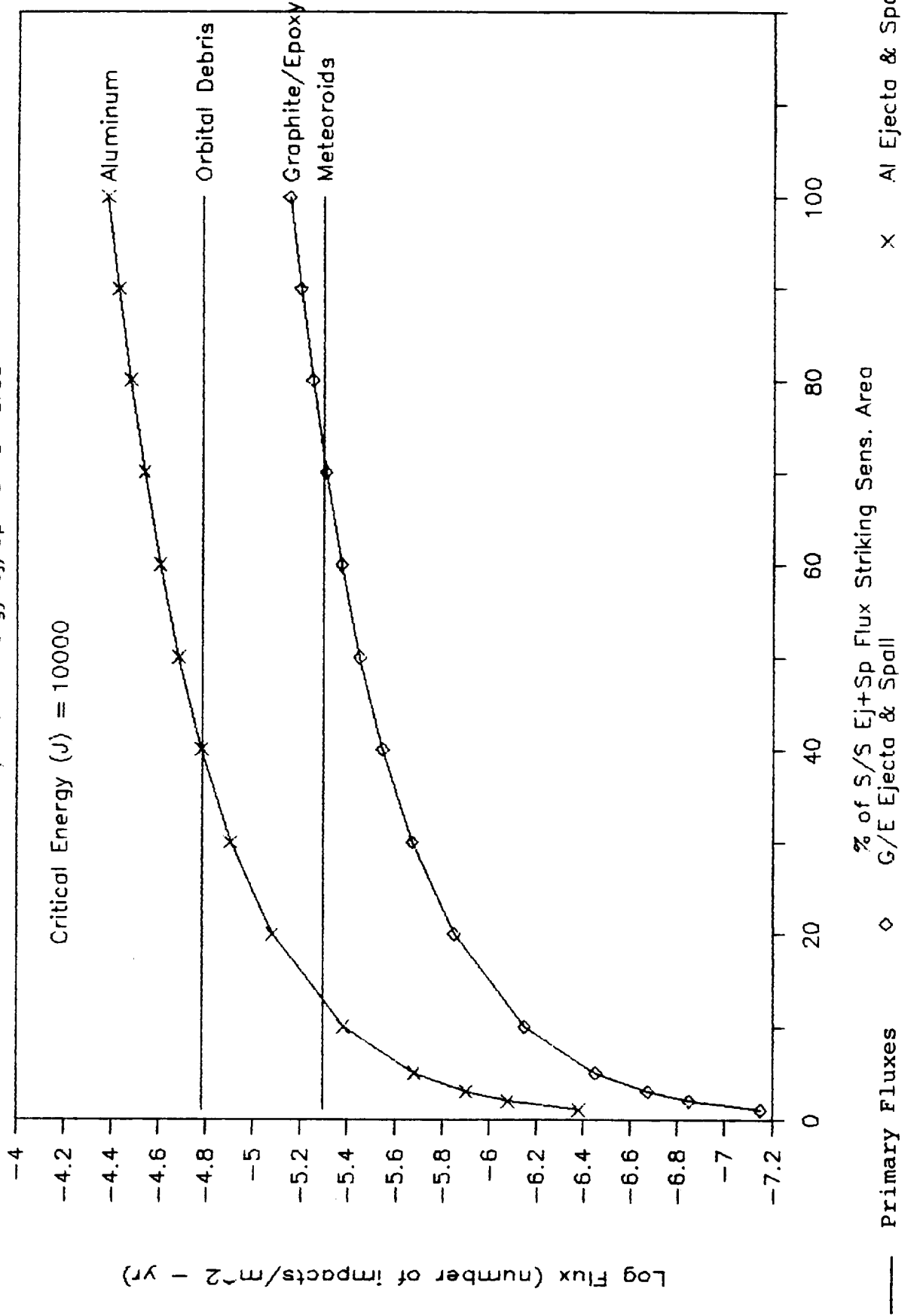
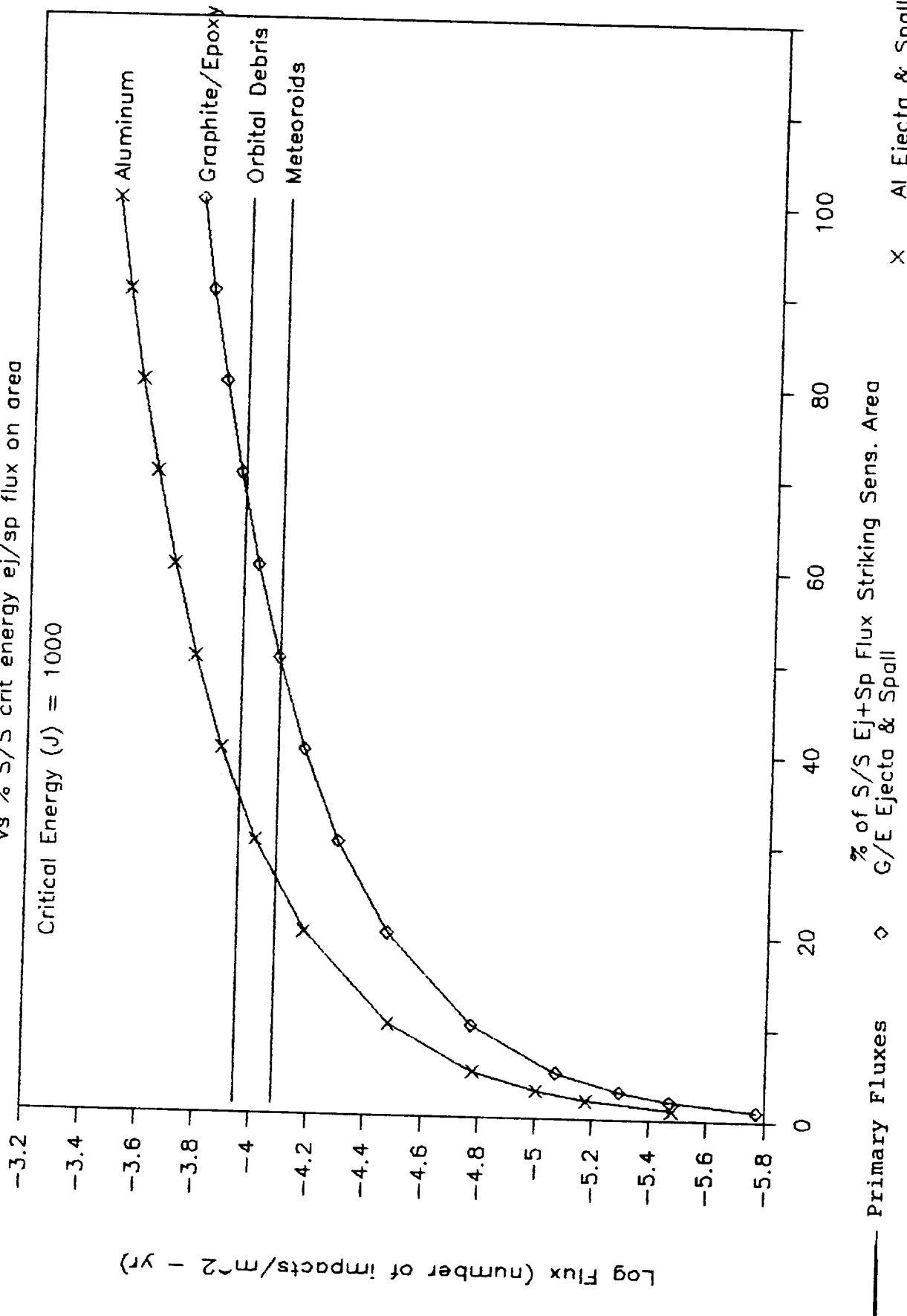


Figure 6-5

# Primary and Secondary Particle Fluxes

vs % S/S crit energy ej/sp flux on area

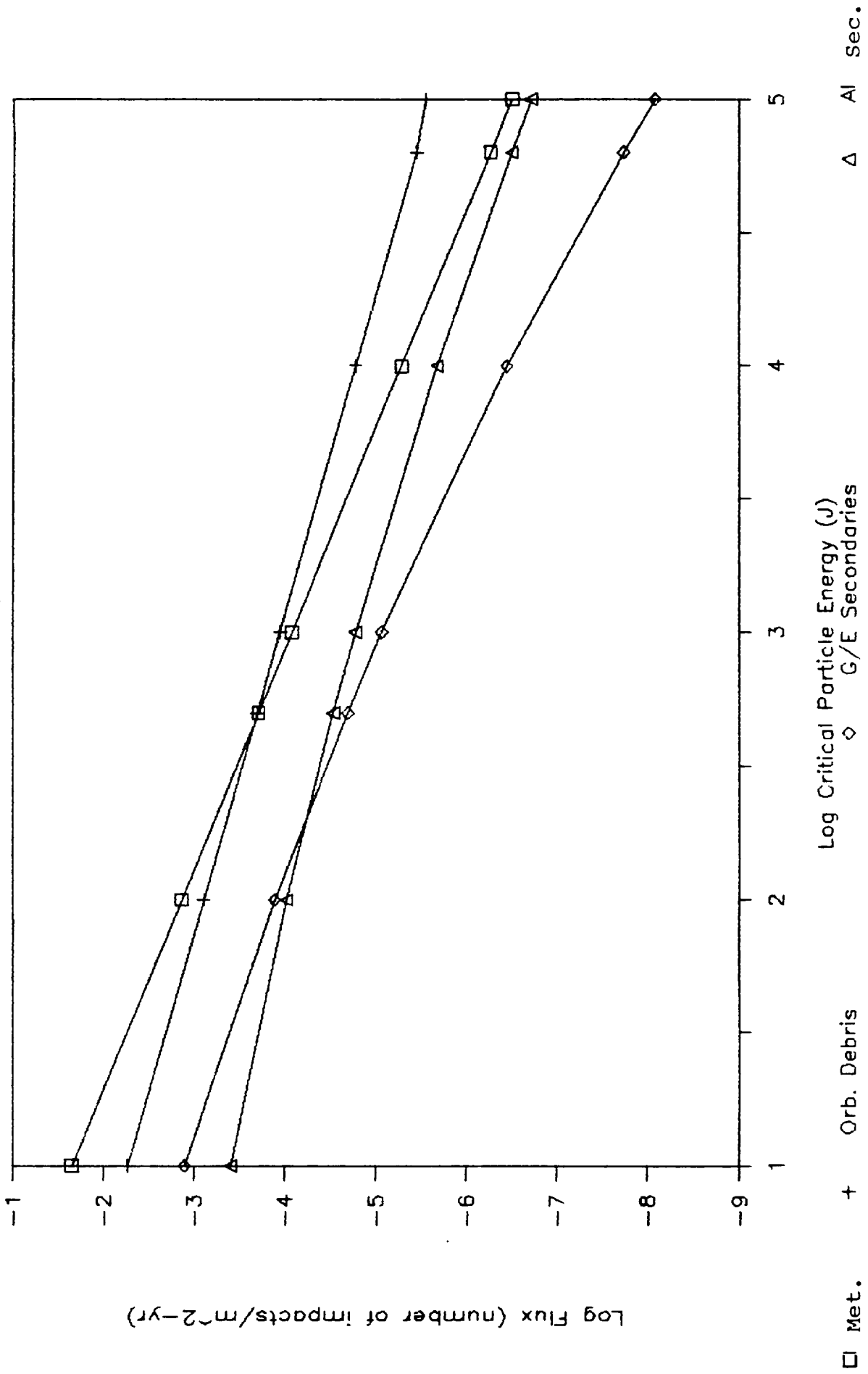


### **6.3 Application of Model to Cases of Interest**

The damage assessment model was applied to several common cases for Space Station operations: a habitat module window, a window of a docked Shuttle, a habitat module wall, and solar panels. Refer to Figure 6-8 for a current International Space Station (ISS) configuration (Ref.17, p.82) that can be used to visualize general geometry and view factors.

Figure 6-7

# Primary and Secondary Particle Fluxes For A 5% Secondaries Impact Fraction



### 6.3.1 Module Window

The module window design discussed in this section was taken from a NASA white paper (Ref. 22). Current window/viewing requirements are under review (Ref. 25) but the window damage assessment technique discussed here could certainly be applied to new window designs. Primary and secondary fluxes are calculated for one of four windows in a module; each window being 16 inches in diameter, double pane, with a 1 inch thick pane of fused silica glass.

Several impacts on previous space station (Skylab, Salyut) windows have been recorded (Ref.23,24). For instance a Soviet Salyut 7 space station window was struck on July 27, 1983 causing a loud crack heard by the two-man cosmonaut crew. The Soviets characterized the impact as "an unpleasant surprise," although the 0.15 in. diameter crater on the window did not threaten the pressure integrity of the pane (Ref.24, p.125).

#### 6.3.1.1 Critical Energy Calculation

The critical energy calculation given in Table 6-3 utilizes a penetration equation developed for Apollo windows and a criterion to prevent spallation (Ref.26). The penetration equation related crater depth, P (cm), to projectile density, p (g/cc), projectile diameter, D (cm), and to projectile velocity, V (km/sec).

$$P = 0.53 * p^{0.5} * D^{1.06} * V^{0.67}$$

The no-spall criterion related the minimum window thickness to prevent spallation, t (cm), to the crater depth.

$$t = 7 * P$$

From the penetration equation and failure criterion, the window pane thickness of 1 in., and known orbital debris/meteoroid density and velocity, the critical size and energy of the projectiles was calculated as given in Table 6-3. From the fluxes of orbital debris and meteoroids having this critical size and greater (equations given in Section 6.1.1 and 6.1.2), the weighted average critical energy for failure of a 1 inch thick glass pane was calculated as approximately 100 joules.

#### 6.3.1.2 Discussion

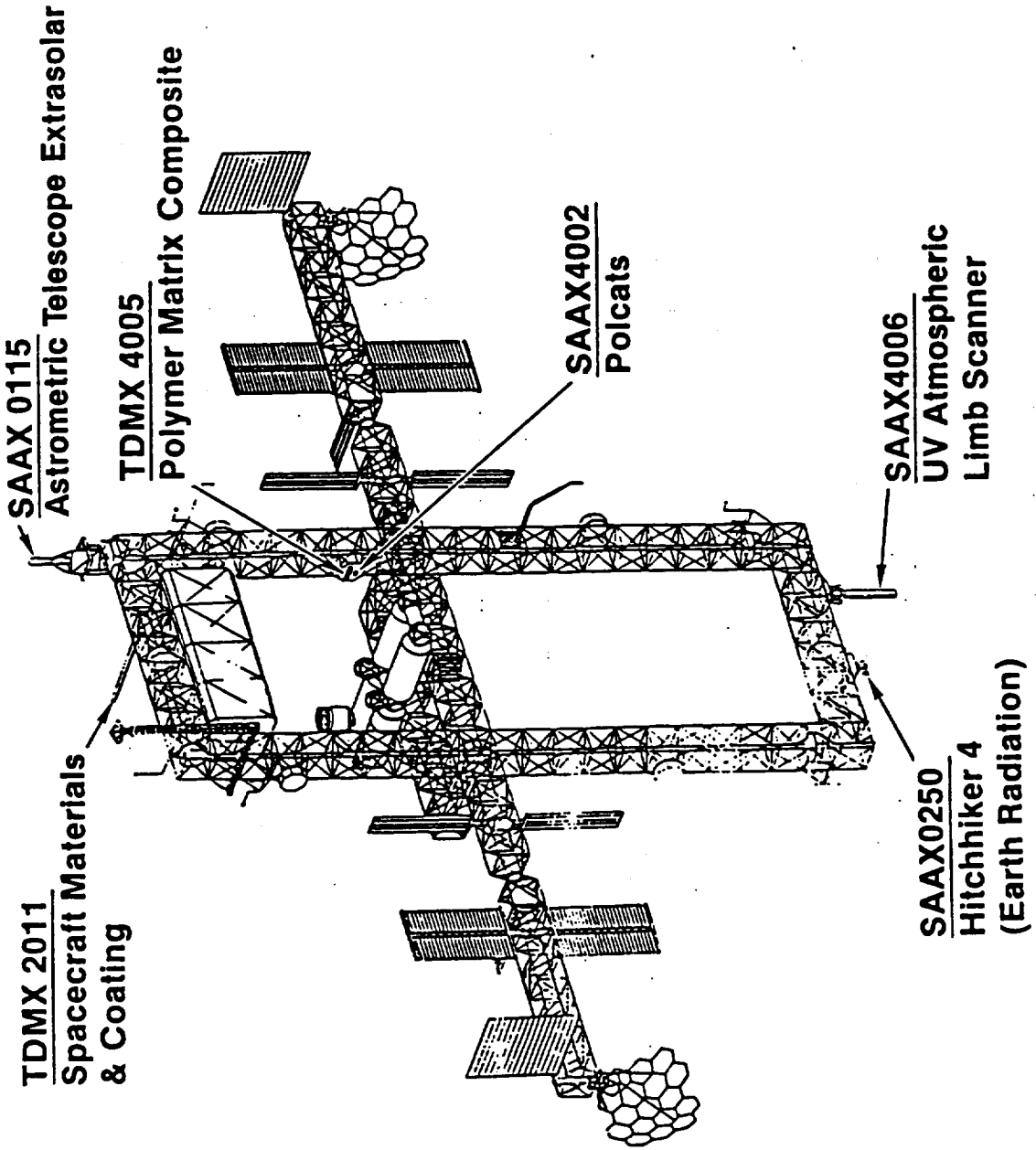
Table 6-4 is the output of the one module window damage assessment program. The window critical energy of 100 J and surface area of 0.13 m<sup>2</sup> has been entered. A SAF factor of 25% was calculated/estimated and a VF of only 10% was estimated because the module window for this analysis was oriented facing away from the other modules (facing mainly truss, radiators and solar arrays). With these factors a very low SF of 0.025 was



Figure 6-8  
(taken from Ref. 17)

VHW031

# ISS CONFIGURATION WITH REPRESENTATIVE PAYLOADS



McDonnell Douglas • Honeywell • IBM • Lockheed • RCA

**SPACE  
STATION**

Table 6-3, Window Worksheet

Spacecraft Window Critical Energy Determination

Glass Thickness (cm) (outer of two panes)	2.54	
	Meteoroid	Debris
Particle Density (g/cc)	0.5	2.8
Particle Velocity (km/s)	20	9.3
Particle Critical Diameter (cm) to avoid spall on silica glass panes (from Cour-Palais)	0.1460	0.1051
Particle Mass (g)	8.15E-04	1.70E-03
Particle Energy (J)	163.03	73.65
Particle Flux (#/m <sup>2</sup> -yr) with critical diameter and greater	5.19E-04	1.01E-03
Percent Flux	33.87	66.13
Average Critical Energy (J) above which results in spalling of the first glass pane from Meteoroid & Orbital Debris Impacts	103.92	

calculated. The important output is within the highlighted block on the first page of the table. Given the low SF, ejecta/spall adds only 2-3% to the total critical energy flux expected on the window. The design factor for compensating the primary flux would be 1.03 in this case.

However, viewing requirements may require that some of the pressurized volume viewing ports have unrestricted views of a large part of the station. For instance, some recent designs call for a 5-window-sided workstation cupola positioned at a Space Station node hatch (Ref.25, pp.2B-25,2B-39,2B-40) which would be designed for good station viewing (Figure 6-9 and 6-10). If the VF went as high as 50% and SAF decreases to 20% (the SAF decreases as VF goes up because less of the total station is seen by the sensitive surface), the SF would be 0.1. From Figure 6-11, a 10% SF would increase the ejecta/spall fraction of the total critical energy flux on the cupola windows to about 0.09. Thus, a design factor of 1.1 should be applied to the primary flux on the cupolas to compensate for the secondaries flux.

Table 6-4, Continued  
(page 2 of 4)

<p>(# of impacts of given avg. mass plus or minus 0.004 when proj. mass <math>\leq</math> 0.01 g, 0.005 for 0.01 &lt; proj. mass <math>\leq</math> 0.02, 0.01 g for 0.02 &lt; proj. mass <math>\leq</math> 0.1g, and 0.05 g when proj. mass <math>&gt;</math> 0.1 g per m<sup>2</sup> - year)</p>																							
Average Debris Mass (g) for incremental calcs.	0.0055	0.015	0.03	0.05	0.07	0.09	0.15	0.25	0.35	0.45	0.55	0.65	0.75	0.85	0.95	1.05	1.15	1.25	1.35	1.45	1.5		
Number of Impacts from Orbital Debris	463.881	34.594	19.326	7.061	3.735	2.336	5.000	1.827	0.966	0.604	0.416	0.305	0.234	0.186	0.152	0.126	0.107	0.091	0.079	0.059	0.059	1.175	
<b>Meteoroid Parameters</b>																							
Meteoroid Dia. (cm)	0.1563	0.3368	0.4243	0.5346	0.6120	0.6736	0.7256	0.9182	1.0464	1.1518	1.2407	1.3184	1.3880	1.4511	1.5092	1.5632	1.6136	1.6611	1.7060	1.7487	1.7894		
Meteoroid Flux (# of impacts of given mass & greater per m <sup>2</sup> surface - year)	5.86E-04	3.59E-05	1.55E-05	6.68E-06	4.08E-06	2.88E-06	2.20E-06	9.40E-07	5.80E-07	4.09E-07	3.12E-07	2.50E-07	1.78E-07	1.35E-07	1.35E-07	1.35E-07	1.20E-07	1.08E-07	9.79E-08	8.94E-08	8.23E-08		
Probability of no impacts on Station	0.0001	0.0217	2.5712	20.6151	39.0731	50.6011	59.4721	79.9181	87.1901	90.7831	92.8891	94.2581	95.2141	95.9141	96.4491	96.8681	97.2051	97.4811	97.7121	97.9061	98.0731		
Incremental Met. Flux (# of impacts of given avg. mass plus or minus 0.004 when proj. mass $\leq$ 0.01 g, 0.005 for 0.01 < proj. mass $\leq$ 0.02, 0.01 g for 0.02 < proj. mass $\leq$ 0.1g, and 0.05 g when proj. mass $>$ 0.1 g per m <sup>2</sup> - year)	5.50E-04	2.04E-05	8.80E-06	2.59E-06	1.20E-06	6.83E-07	1.25E-07	3.68E-07	1.71E-07	9.69E-08	6.19E-08	4.26E-08	3.10E-08	2.35E-08	1.83E-08	1.47E-08	1.20E-08	9.98E-09	8.41E-09	7.18E-09	6.23E-09		
Average Met. Mass (g) for incremental calcs.	0.0055	0.015	0.03	0.05	0.07	0.09	0.15	0.25	0.35	0.45	0.55	0.65	0.75	0.85	0.95	1.05	1.15	1.25	1.35	1.45	1.5		
Number of Impacts from Meteoroids	130.100	4.826	2.082	0.613	0.284	0.162	0.295	0.087	0.040	0.0229	0.0146	0.0101	0.0073	0.0056	0.0043	0.0035	0.0028	0.0024	0.0020	0.0017	0.0017	0.0195	
<b>If Ejecta/Spall all from Carbon-Graphite Composite Structures</b>																							
For Impacts from Orbital Debris																							
Mass ejecta & spall per orbital debris impact (g)	0.85	2.31	4.62	7.70	10.78	13.86	23.11	38.51	53.92	69.32	84.73	100.14	115.54	130.95	146.35	161.76	177.16	192.57	207.97	223.38	231.08		
Number of ejecta & spall particles of critical energy and greater per impact from orbital debris of given average mass within mass range.	0.16	0.71	1.81	3.46	5.18	6.93	12.17	20.58	28.48	35.92	42.94	49.60	55.94	62.00	67.80	73.36	78.72	83.88	88.87	93.69	96.04		
Number of critical particles created from orbital debris impacts over lifetime of station.	75.17	24.61	35.06	24.42	19.35	16.19	60.86	37.59	27.53	21.71	17.87	15.15	13.12	11.54	10.27	9.24	8.39	7.66	7.05	5.54	112.87		
Number of critical energy particles per m <sup>2</sup> - year.	2.19E-04	7.19E-05	1.02E-04	7.13E-05	5.65E-05	4.73E-05	1.78E-04	1.10E-04	8.04E-05	6.34E-05	5.22E-05	4.42E-05	3.83E-05	3.37E-05	3.06E-05	2.70E-05	2.45E-05	2.24E-05	2.06E-05	1.82E-05	3.30E-04		
Flux of critical energy particles of critical energy and greater from orbital debris impacts	1.64E-03	1.42E-03	1.35E-03	1.24E-03	1.17E-03	1.12E-03	1.07E-03	8.92E-04	7.82E-04	7.02E-04	6.39E-04	5.86E-04	5.42E-04	5.04E-04	4.70E-04	4.40E-04	4.13E-04	3.89E-04	3.66E-04	3.46E-04	3.30E-04		

Table 6-4, Critical Energy Calculation for Module Windows  
(page 1 of 4)

Flux of Ejecta/Spall Particles of Critical Energy and Greater on a Sensitive Area of Space Station

Surface Area of Station (m<sup>2</sup>) 11416.1 Fraction of surface area of Station facing sensitive area 0.25 Earth's radius (km) 6378.145  
 Orbital Life (yrs) 30 Fraction of sky covered by Station as seen from sensitive area (hemispherical View Factor) 0.1 Altitude in Earth radii 500  
 Critical Energy to damage sensitive surface (Joules) 100 Fraction of Station Ejecta & Spall striking the sensitive area (Station SA fraction x view factor) 0.025 Earth defocusing factor 0.968596  
 Surface Area of critical surface (m<sup>2</sup>) 0.13 Earth shielding factor 0.713070

Particle	Flux with critical energy and greater on sens. area (Number impacts/m <sup>2</sup> -yr)	Number of impacts on sensitive area with critical energy and greater over Station lifetime	Percent of total impacts on sensitive area if S/S ej. & sp. all Al/Aluminum	Percent of total impacts on sensitive area if S/S ej. & sp. all Aluminum	Probability of no impact on sens. area with critical energy & greater (percent)
Meteoroids	1.36E-03	0.005296	61.62%	62.06%	99.63%
Orb. Debris	7.83E-04	0.003051	35.50%	35.75%	99.70%
Ejecta/Spall (if S/S all graphite/epoxy)	6.33E-05	0.000246	2.87%		99.98%
Ejecta/Spall (if S/S all aluminum)	4.79E-05	0.000186		2.19%	99.98%

Velocity above which Al targets vaporize (ft/sec) 7  
 Average Graphite-Epoxy Ejecta/Spall velocity (km/sec) 0.5  
 Average Aluminum Ejecta/Spall velocity (km/sec) 4.232  
 Orbital Debris Fraction below vaporization velocity 0.235359  
 Orb. Debris Average Vel. (km/sec) below vaporization velocity 4.837984

Projectile Mass (g)	0.001	0.01	0.02	0.04	0.06	0.08	0.1	0.2	0.3	0.4	0.5	0.6	0.7	0.8	0.9	1	1.1	1.2	1.3	1.4	1.5 & >	
Orbital Debris Parameters																						
Orb. Deb. Dia. (cm)	0.0680	0.1896	0.2389	0.3010	0.3446	0.3793	0.4086	0.5148	0.5893	0.6486	0.6987	0.7424	0.7816	0.8172	0.8499	0.8803	0.9087	0.9354	0.9607	0.9847	1.0077	
Orbital Debris Flux (lb of impacts of given mass & greater per m <sup>2</sup> surface - year)	1.58E-03	2.29E-04	1.28E-04	7.14E-05	5.08E-05	3.99E-05	3.11E-05	1.85E-05	1.31E-05	1.03E-05	8.56E-06	7.34E-06	6.45E-06	5.77E-06	5.22E-06	4.78E-06	4.41E-06	4.10E-06	3.84E-06	3.60E-06	3.43E-06	
Probability of no impacts on Station	0.000%	0.000%	0.000%	0.000%	0.000%	0.000%	0.001%	0.178%	1.108%	2.914%	5.332%	8.085%	10.974%	13.873%	16.710%	19.445%	22.056%	24.535%	26.882%	29.100%	30.873%	
Incremental Orbital Debris Flux	1.35E-03	1.01E-04	5.64E-05	2.06E-05	1.09E-05	6.82E-06	1.46E-05	5.33E-06	2.87E-06	1.76E-06	1.22E-06	8.92E-07	6.85E-07	5.43E-07	4.42E-07	3.68E-07	3.11E-07	2.67E-07	2.32E-07	1.71E-07	3.43E-06	

Table 6-4, Continued

(page 4 of 4)

Number of critical particles created from meteoroid impacts over lifetime of station.	357.07	35.88	24.97	9.93	5.50	3.54	8.16	2.95	1.55	0.95	0.65	0.47	0.36	0.28	0.22	0.18	0.15	0.13	0.11	0.10	0.11	1.11
Number of critical energy particles per m <sup>2</sup> - year.	1.51E-03	1.52E-04	1.06E-04	4.20E-05	2.33E-05	1.50E-05	3.45E-05	1.25E-05	6.53E-06	4.03E-06	2.74E-06	1.98E-06	1.50E-06	1.10E-06	9.45E-07	7.76E-07	6.40E-07	5.49E-07	4.71E-07	4.08E-07	4.71E-06	
Flux of critical energy particles of critical energy and greater from meteoroid impacts	1.92E-03	4.11E-04	2.59E-04	1.54E-04	1.12E-04	8.84E-05	7.34E-05	3.90E-05	2.65E-05	1.99E-05	1.59E-05	1.32E-05	1.12E-05	9.68E-06	8.50E-06	7.56E-06	6.78E-06	6.14E-06	5.59E-06	5.12E-06	4.71E-06	
Ejecta/Small Flux from both Orbital Debris and Meteoroid Impacts	1.92E-03	7.94E-04	5.99E-04	4.30E-04	3.51E-04	3.02E-04	2.68E-04	1.77E-04	1.37E-04	1.13E-04	9.72E-05	8.54E-05	7.63E-05	6.91E-05	6.31E-05	5.81E-05	5.39E-05	5.02E-05	4.69E-05	4.41E-05	4.19E-05	

Table 6-4, Continued  
(page 3 of 4)

For Impacts from Meteoroids

Mass ejecta & spall 3.92 10.69 21.39 35.65 49.91 64.17 106.95 178.25 249.55 320.84 392.14 463.44 534.74 606.04 677.34 748.64 819.94 891.24 962.53 1033.83 1069.48  
per meteoroid impact (g)

Number of ejecta & spall particles of critical energy and greater per impact from meteoroids of given average mass within mass range.

Number of critical particles created from meteoroid impacts over lifetime of station. 190.27 24.76 23.32 11.69 7.53 5.41 15.50 6.89 4.10 2.78 2.03 1.55 1.23 1.01 0.84 0.71 0.61 0.53 0.47 0.41 4.81

Number of critical energy particles per m<sup>2</sup> - year. 8.01E-04 1.05E-04 9.86E-05 4.94E-05 3.18E-05 2.29E-05 6.55E-05 2.91E-05 1.73E-05 8.56E-06 6.56E-06 5.21E-06 4.26E-06 3.55E-06 3.00E-06 2.58E-06 2.24E-06 1.97E-06 1.75E-06 2.03E-05

Flux of critical energy particles of critical energy and greater from meteoroid impacts 1.30E-03 4.91E-04 3.86E-04 2.88E-04 2.38E-04 2.07E-04 1.84E-04 1.18E-04 8.91E-05 7.18E-05 6.00E-05 5.15E-05 4.49E-05 3.97E-05 3.54E-05 3.19E-05 2.89E-05 2.63E-05 2.41E-05 2.21E-05 2.03E-05

Ejecta/Spall Flux from both Orbital Debris and Meteoroid Impacts 2.53E-03 1.76E-03 1.61E-03 1.44E-03 1.34E-03 1.26E-03 1.20E-03 9.74E-04 8.44E-04 7.52E-04 6.80E-04 6.22E-04 5.73E-04 5.31E-04 4.95E-04 4.62E-04 4.33E-04 4.07E-04 3.83E-04 3.61E-04 3.44E-04

If Ejecta/Spall all from Aluminum Structures

For Impacts from Orbital Debris

Mass ejecta & spall per impact (g) 0.02 0.35 0.88 1.59 2.29 3.00 5.11 8.64 12.17 15.70 19.23 22.76 26.28 29.81 33.34 36.87 40.40 43.92 47.45 50.98 52.75

Number of ejecta & spall particles of critical energy and greater per impact from projectile's of given average mass within mass range.

Number of critical particles created from impacts over lifetime of station. 27.95 30.93 32.64 17.21 11.27 8.17 23.03 10.74 6.57 4.55 3.38 2.64 2.13 1.76 1.49 1.28 1.11 0.98 0.87 0.66 13.23

Number of critical energy particles per m<sup>2</sup> - year. 8.16E-05 9.03E-05 9.53E-05 5.03E-05 3.29E-05 2.39E-05 6.72E-05 3.14E-05 1.92E-05 1.33E-05 9.88E-06 7.70E-06 6.22E-06 5.15E-06 4.35E-06 3.73E-06 3.24E-06 2.85E-06 2.53E-06 2.36E-05

Flux of critical energy particles of critical energy and greater 5.72E-04 5.10E-04 4.20E-04 3.24E-04 2.74E-04 2.41E-04 2.17E-04 1.50E-04 1.19E-04 9.95E-05 8.62E-05 7.63E-05 6.86E-05 6.24E-05 5.72E-05 5.29E-05 4.92E-05 4.59E-05 4.31E-05 4.05E-05 3.86E-05

For Impacts from Meteoroids

Mass ejecta & spall per meteoroid impact (g) 0.23 0.93 2.04 3.52 4.99 6.47 10.90 18.29 25.67 33.06 40.45 47.83 55.22 62.60 69.99 77.38 84.76 92.15 99.54 106.92 110.64

Number of ejecta & spall particles of critical energy and greater per impact from meteoroids of given average mass within mass range.

Figure 6-10 (from Ref. 25)

### NODE CUPOLA VIEWING



- 50in HEIGHT
- 80in BASE
- 15° FACET INCLINATION

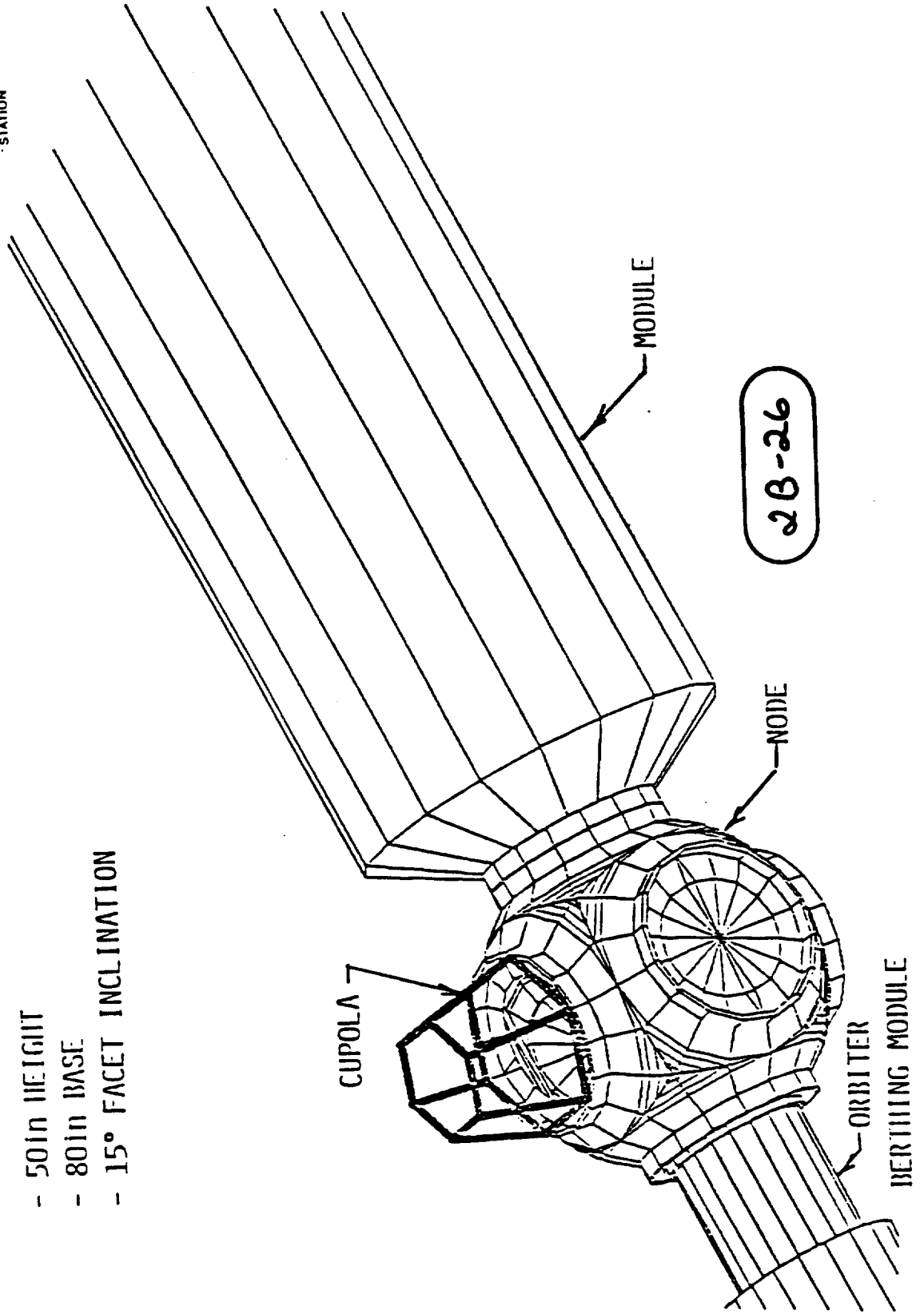


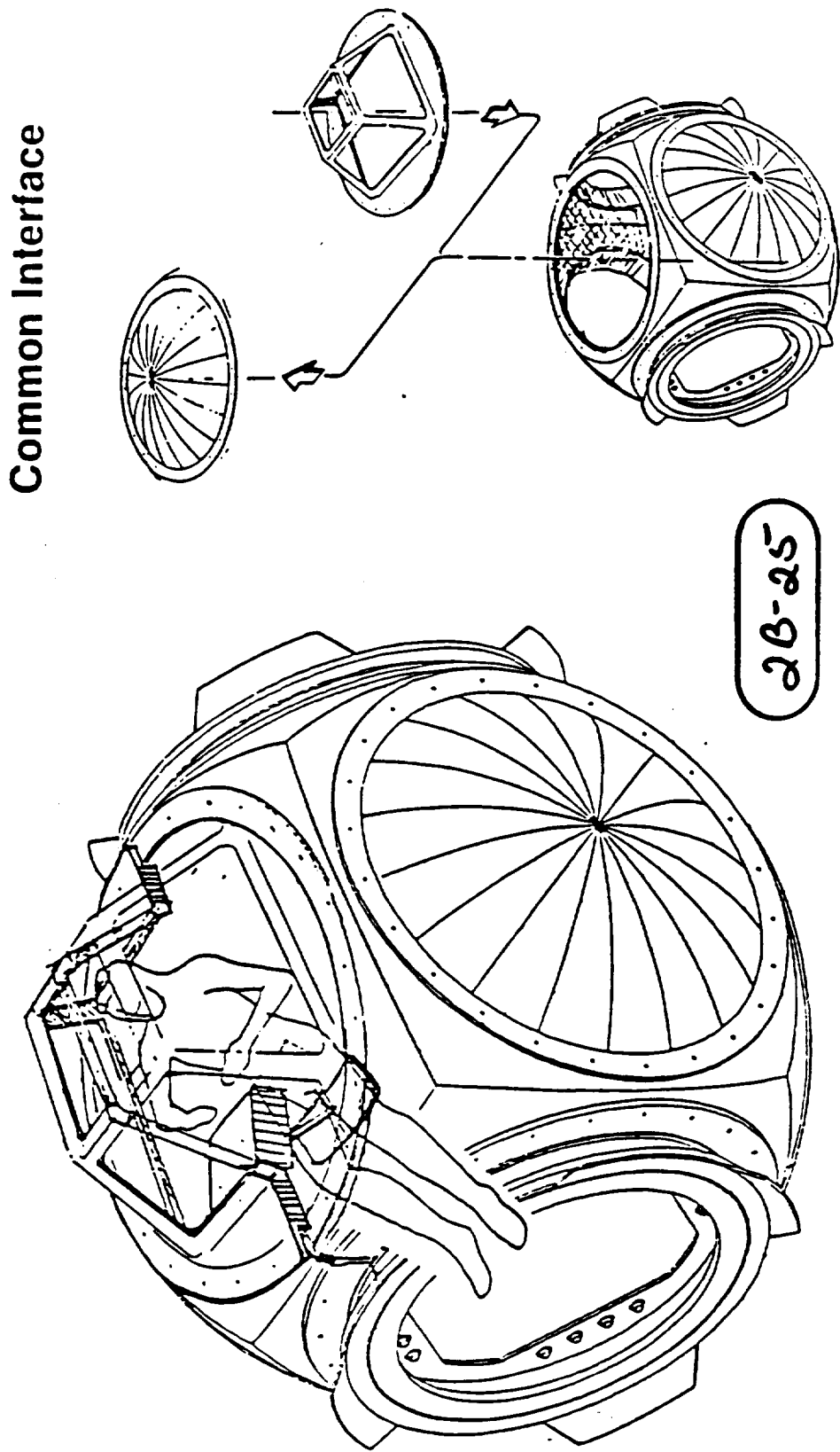


Figure 6-7 (from Ref. 25)

# TRADE 1: CUPOLA VS NODE WINDOW

## CUPOLA WINDOW WORKSTATION CONCEPT

VHQ820



**MCDONNELL DOUGLAS** | **IBM** | **Honeywell** | **NSA** | **Lockheed** | **SPACE STATION PROGRAM**

### 6.3.2 Orbiter Window with Orbiter Docked to Space Station

Figure 6-12 illustrates an orbiter docked to a Space Station module (Ref.25, 2B-39). The orbiter windows comprise three panes with the outer pane being 5/8 inch thick silica glass. The two underlying panes provide a primary and secondary cabin pressure integrity seal. Impact incidents involving the shuttle have happened before. In June 1983, a micrometeorite or debris particle struck Challenger's right-hand middle windshield (window no.5) during STS-7. The crater measured 0.0178 in. deep by 0.0892 in. diameter. Including flaws in the glass, the total damaged area was 0.2 in. wide. Although the pressure integrity of the pane was not compromised, the window was replaced due to fears the damage could expand to dangerous levels when subjected to aerodynamic and heating loads during a later launch or re-entry (Ref.24, p.125).

#### 6.3.2.1 Critical Energy Calculation

The failure criterion and penetration equation for orbiter windows was taken from a study on solid rocket product impingement on shuttle surfaces (Ref.28). The penetration equation was very similar to Cour-Palais (described in Section 6.3.1.1). The crater diameter (with spall),  $D_c$  (cm), is related to the projectile diameter,  $D$  (cm), projectile density,  $p$  (g/cc), and projectile velocity,  $V$  (km/sec).

$$D_c = 2.1 * D * p^{0.5} * v^{0.6}$$

Applying this equation with orbital debris/meteoroid average velocity and density parameters to the size crater that resulted in replacement of the STS-7 window, enabled the calculation of the approximate energy of the impacting object (which differs between orbital debris and meteoroids):

	<u>Dia. (cm)</u>	<u>Mass (g)</u>	<u>Energy (J)</u>
Meteoroids	0.0207	2.32E-6	0.465
Orbital Debris	0.0146	4.54E-6	0.196

The proposed failure criterion for orbiter windows (Ref.28, pp.3-16,6-15) was influenced by experimental evidence on the size of a flaw that would continue to spread after the impact event due to internal stress relief and thermal stress during entry. The failure criterion is in terms of the projectile diameter,  $D$  (cm), and velocity,  $V$  (km/sec). Above this value, an impacting projectile will have enough energy to make it necessary to replace the orbiter's window.

$$D * v^{0.67} \geq 11$$

Figure 6-11

# Primary and Secondary Particle Fluxes

vs % S/S crit energy ej/sp flux on area

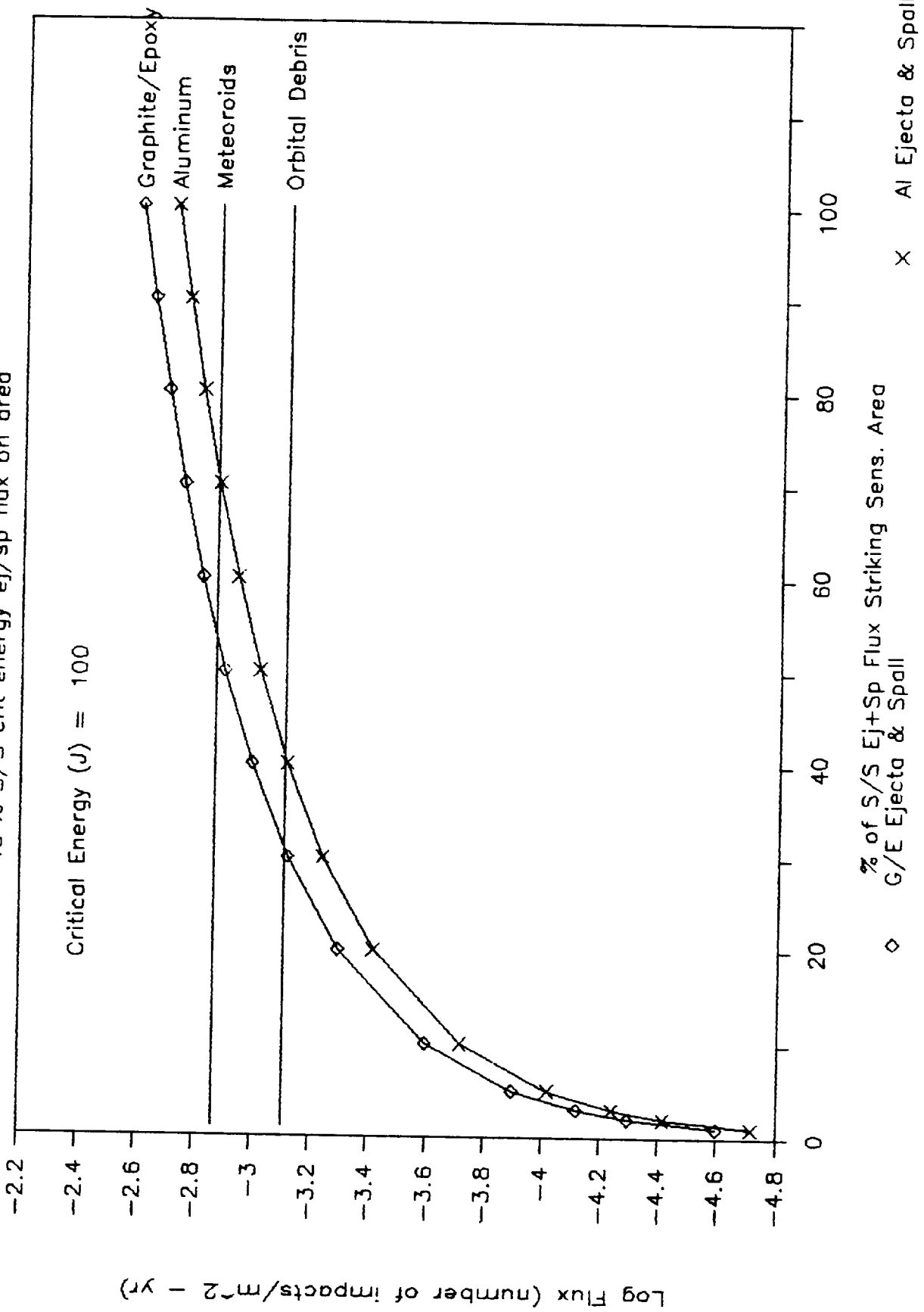
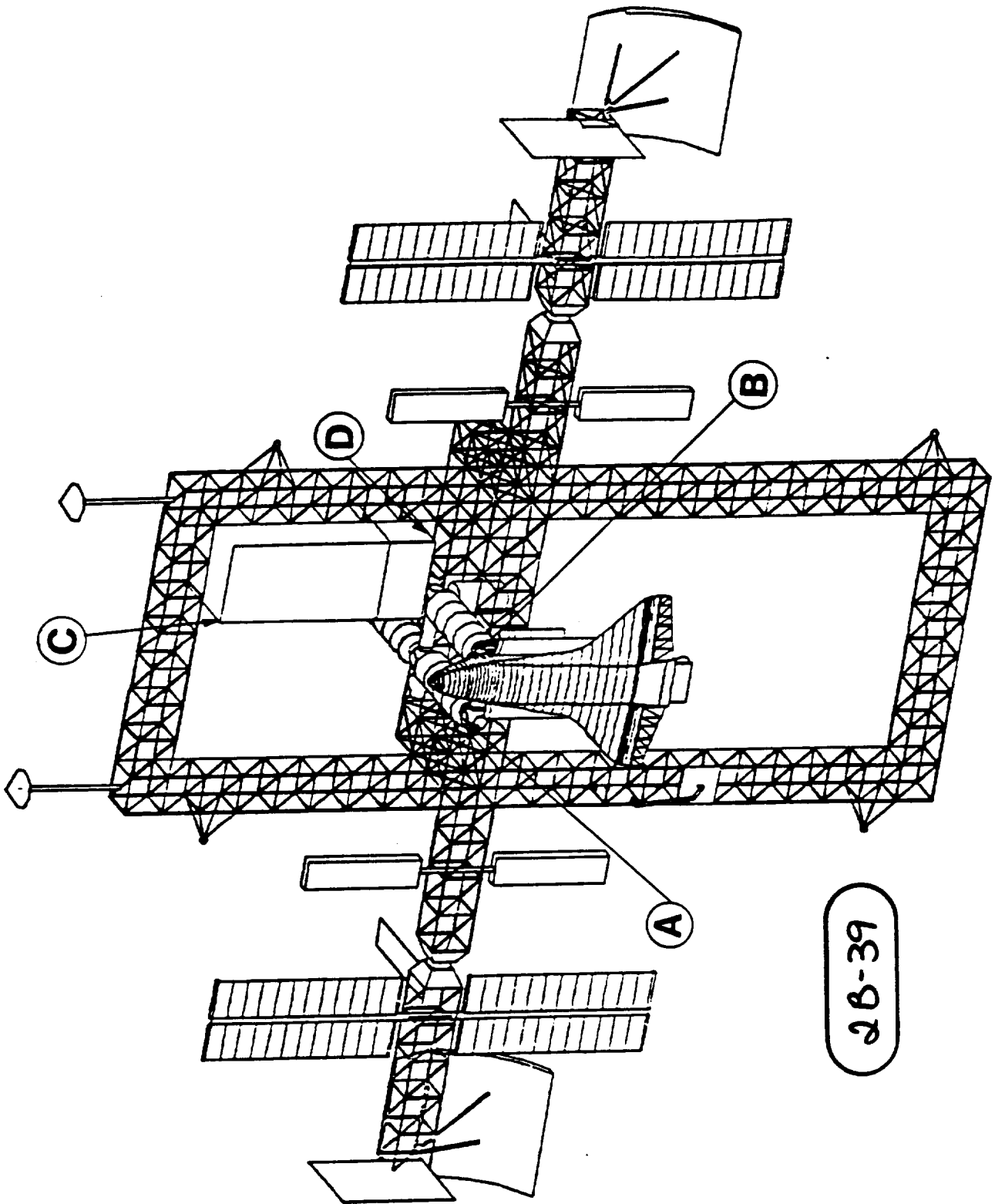


Figure 6-12 (from Ref. 25)



26-39

As given in Table 6-5, this failure criterion results in a critical energy of  $8.72\text{E-}7$  joules which is too low for the model in its present state to accept without significantly underestimating the ejecta/spall effect (see Section 6.2.2, assumption h ). Therefore, a critical energy equal to 0.2 joules was used in for this calculation.

#### 6.3.2.2 Discussion

The orbiter window critical energy (0.2 J), surface area for one window ( $0.15\text{ m}^2$ ), and docking period (0.019 yrs or 7 days) were input into the model as given in Table 6-6. The SAF factor was estimated as only 10% (because the orbiter is so close to the Space Station when docked to a module) while the VF was 50% resulting in a SF of 0.05. At the low critical energy of the orbiter window, graphite/epoxy ejecta/spall particles having the critical energy and greater are more numerous than aluminum. However, the secondary flux in this case is less than a percent of the total critical energy flux, whether the secondary flux is graphite/epoxy or aluminum. Therefore, a flux design factor for hazard assessment studies on the orbiter windows while docked to the Space Station would be approximately 1.01. Figure 6-13 illustrates the dependence of the secondary fluxes on the SF factor.

Table 6-6, Orbiter Window Damage Assessment Worksheet  
(page 1 of 4)

Flux of Ejecta/Spall Particles of Critical Energy and Greater on a Sensitive Area of Space Station

Surface Area of Station (m<sup>2</sup>) 11416.1 Fraction of surface area of Station facing sensitive area 0.1 Earth's radius (km) 6378.145  
 Orbital Life (yrs) 0.019178 (7 days) Fraction of sky covered by Station as seen from sensitive area (hemispherical View Factor) 0.5 Station orbital altitude (km) 500  
 Altitude in Earth radii 1.078392  
 Earth defocusing factor 0.968596  
 Earth shielding factor 0.713070

Particle	Flux with critical energy and greater on sens. area (Number impacts/m <sup>2</sup> -yr)	Number of impacts on sensitive area with critical energy and greater over Station lifetime	Percent of total impacts on sensitive area if S/S e.j. & sp. all Aluminum	Percent of total impacts on sensitive area if S/S e.j. & sp. all Aluminum	Probability of no impact on sens. area with critical energy & greater (percent)
Meteoroids	2.55E+00	0.007103	93.91%	94.57%	99.51%
Orb. Debris	1.45E-01	0.000402	5.33%	5.36%	99.96%
Ejecta/Spall (if S/S all graphite/epoxy)	2.07E-02	0.000057	0.76%	0.76%	99.99%
Ejecta/Spall (if S/S all aluminum)	1.75E-03	0.000004	0.06%	0.06%	100.00%

Average Graphite-Epoxy Ejecta/Spall velocity (km/sec) 0.5  
 Average Aluminum Ejecta/Spall velocity (km/sec) 4.232  
 Orbital Debris Fraction below vaporization velocity 0.235359  
 Orb. Debris Average Vel. (km/sec) below vaporization velocity 4.837984

Projectile Mass (g) 0.001 0.01 0.02 0.04 0.06 0.08 0.1 0.2 0.3 0.4 0.5 0.6 0.7 0.8 0.9 1 1.1 1.2 1.3 1.4 1.5 &gt;

Orbital Debris Parameters

Orb. Deb. Dia. (cm) 0.0680 0.1896 0.2389 0.3010 0.3446 0.3793 0.4086 0.5148 0.5893 0.6486 0.6987 0.7424 0.7816 0.8172 0.8499 0.8803 0.9087 0.9354 0.9607 0.9847 1.0077  
 Orbital Debris Flux 1.58E-03 2.29E-04 1.28E-04 7.14E-05 5.08E-05 3.99E-05 3.31E-05 1.65E-05 1.31E-05 1.03E-05 8.56E-06 7.34E-06 6.45E-06 5.77E-06 4.78E-06 4.41E-06 4.10E-06 3.84E-06 3.60E-06 3.43E-06  
 18 of impacts of given mass & greater per m<sup>2</sup> surface - year)

Probability of no impacts on Station 70.705% 95.113% 97.240% 98.448% 98.894% 99.130% 99.278% 99.596% 99.713% 99.774% 99.813% 99.839% 99.859% 99.874% 99.886% 99.893% 99.903% 99.910% 99.916% 99.921% 99.925%

Incremental Orbital Debris Flux 1.35E-03 1.01E-04 5.64E-05 2.06E-05 1.09E-05 6.82E-06 1.46E-05 5.33E-06 1.74E-06 1.22E-06 8.92E-07 6.85E-07 5.63E-07 4.42E-07 3.68E-07 3.11E-07 2.67E-07 2.32E-07 1.73E-07 3.43E-06

Table 6-6, Continued  
(page 3 of 4)

For Impacts from Meteoroids																						
Mass ejecta & spall per meteoroid impact (g)	3.92	10.69	21.39	35.45	49.91	64.17	106.95	178.25	249.55	320.84	392.14	463.44	534.74	606.04	677.34	748.64	819.94	891.24	962.53	1033.83	1069.48	
Number of ejecta & spall particles of critical energy and greater per impact from meteoroids of given average mass within mass range.	327.01	461.67	537.69	575.21	588.96	593.01	584.49	554.57	524.66	497.99	474.52	453.78	435.33	418.78	403.83	390.22	377.78	366.33	355.75	345.94	341.29	
Number of critical particles created from meteoroid impacts over lifetime of station.	27.20	1.42	0.72	0.23	0.11	0.06	0.11	0.03	0.01	0.01	0.00	0.00	0.00	0.00	0.00	0.00	0.00	0.00	0.00	0.00	0.00	0.00
Number of critical energy particles per m <sup>2</sup> - year.	1.80E-01	9.42E-03	4.73E-03	1.49E-03	7.08E-04	4.05E-04	7.30E-04	2.04E-04	8.96E-05	4.83E-05	2.94E-05	1.93E-05	1.35E-05	9.83E-06	7.41E-06	5.73E-06	4.53E-06	3.66E-06	2.99E-06	2.48E-06	2.81E-05	
Flux of critical energy particles of critical energy and greater from meteoroid impacts	1.98E-01	1.80E-02	8.54E-03	3.80E-03	2.31E-03	1.60E-03	1.20E-03	4.69E-04	2.65E-04	1.75E-04	1.27E-04	9.76E-05	7.82E-05	6.47E-05	5.49E-05	4.75E-05	4.17E-05	3.72E-05	3.36E-05	3.06E-05	2.81E-05	
Ejecta/Spall Flux from both Orbital Debris and Meteoroid Impacts	4.15E-01	9.37E-02	6.12E-02	3.82E-02	2.85E-02	2.30E-02	1.94E-02	7.67E-03	5.94E-03	4.86E-03	4.12E-03	3.59E-03	3.18E-03	2.86E-03	2.60E-03	2.39E-03	2.22E-03	2.07E-03	1.94E-03	1.85E-03		
If Ejecta/Spall all from Aluminua Structures																						
For Impacts from Orbital Debris																						
Mass ejecta & spall per impact (g)	0.02	0.35	0.88	1.59	2.29	3.00	5.11	8.64	12.17	15.70	19.23	22.76	26.28	29.81	33.34	36.87	40.40	43.92	47.45	50.98	52.75	
Number of ejecta & spall particles of critical energy and greater per impact from projectile's of given average mass within mass range.	24.22	62.42	69.98	72.30	72.62	72.28	70.23	66.56	63.40	60.73	58.43	56.43	54.65	53.07	51.84	50.33	49.14	48.03	47.01	46.06	45.61	
Number of critical particles created from impacts over lifetime of station.	1.69	0.32	0.20	0.08	0.04	0.03	0.05	0.02	0.01	0.01	0.00	0.00	0.00	0.00	0.00	0.00	0.00	0.00	0.00	0.00	0.01	
Number of critical energy particles per m <sup>2</sup> - year.	7.72E-03	1.40E-03	9.29E-04	3.51E-04	1.86E-04	1.16E-04	2.41E-04	8.36E-05	4.21E-05	2.52E-05	1.67E-05	1.18E-05	8.81E-06	6.79E-06	5.30E-06	4.36E-06	3.60E-06	3.02E-06	2.56E-06	1.87E-06	3.68E-05	
Flux of critical energy particles of critical energy and greater	1.13E-02	3.56E-03	2.08E-03	1.15E-03	7.96E-04	6.10E-04	4.94E-04	2.53E-04	1.69E-04	1.27E-04	1.02E-04	8.51E-05	7.32E-05	6.44E-05	5.76E-05	5.22E-05	4.79E-05	4.43E-05	4.13E-05	3.87E-05	3.68E-05	
For Impacts from Meteoroids																						
Mass ejecta & spall per meteoroid impact (g)	0.23	0.93	2.04	3.52	4.99	6.47	10.90	18.29	25.67	33.06	40.45	47.83	55.22	62.60	69.99	77.38	84.76	92.15	99.54	106.92	110.61	
Number of ejecta & spall particles of critical energy and greater per impact from meteoroids of given average mass within mass range.	57.61	70.28	72.61	71.86	70.36	68.77	64.47	59.01	54.95	51.74	49.12	46.90	45.00	43.32	41.84	40.51	39.31	38.21	37.20	36.28	35.84	

Table 6-5

## Orbiter Window Critical Energy Determination

Glass Thickness (cm) (outer of three panes)	0.9525	
	Meteoroid	Debris
Particle Density (g/cc)	0.5	2.8
Particle Velocity (km/s)	20	9.3
Particle Critical Diameter (cm)	0.00018729	0.000248
	(from Ref.28 study)	
Particle Mass (g)	1.72E-12	2.26E-11
Particle Energy (J)	3.44E-07	9.76E-07
Particle Flux (#/m <sup>2</sup> -yr) with critical diameter and greater	8.22E+02	4.20E+03
Percent Flux	16.38	83.62
Average Critical Energy (J)	8.72E-07	
above which results in unacceptable damage to the first glass pane from Meteoroid & Orbital Debris Impacts		





Figure 6-13

# Primary and Secondary Particle Fluxes

vs % S/S crit energy ej/sp flux on area

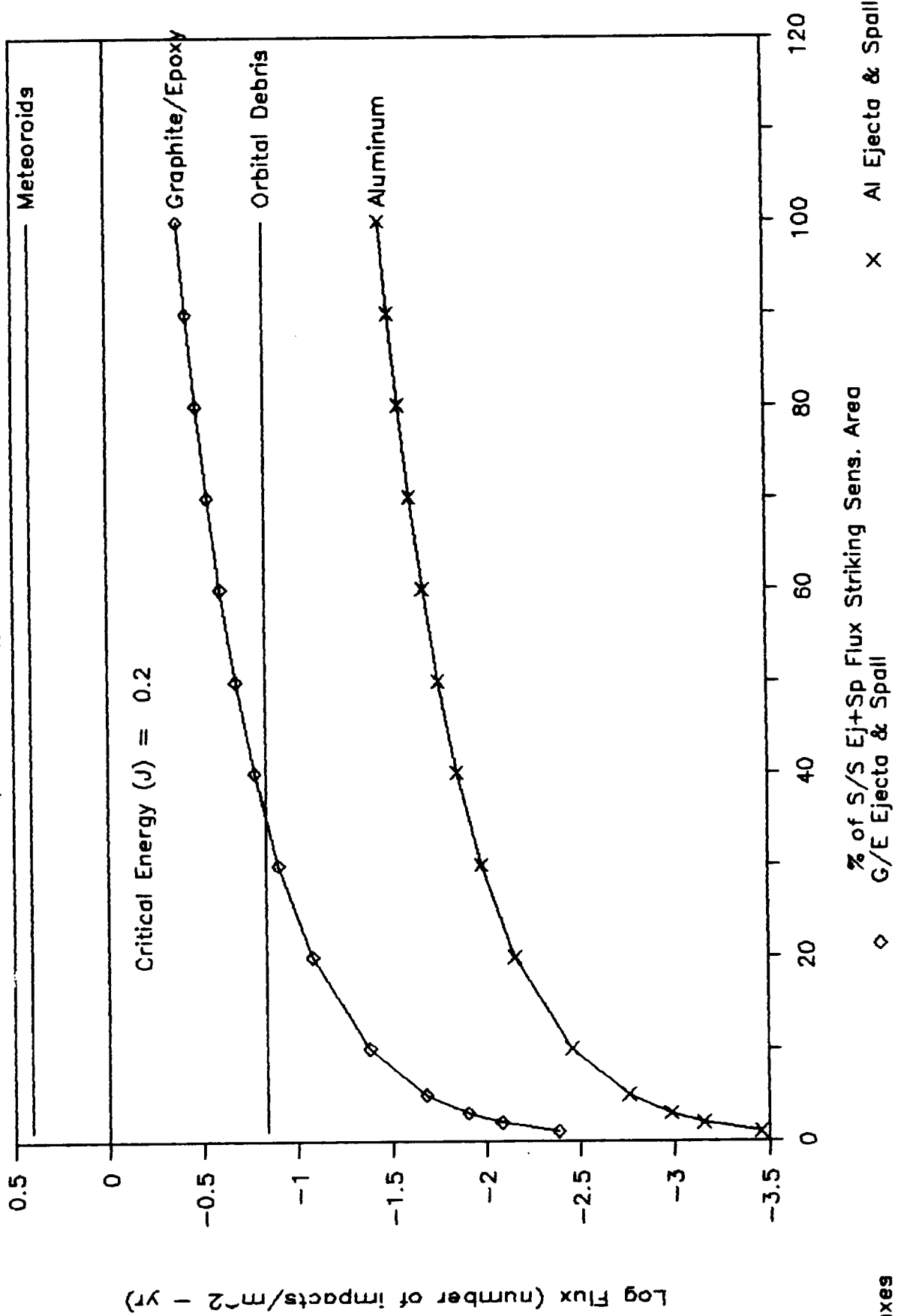


Table 6-6, Continued

(page 4 of 4)

Number of critical particles created from meteoroid impacts over lifetime of station.	4.79	0.22	0.10	0.03	0.01	0.01	0.00	0.00	0.00	0.00	0.00	0.00	0.00	0.00	0.00	0.00	0.00	0.00	0.00	0.00	0.00	0.00	0.00	
Number of critical energy particles per m <sup>2</sup> - year.	3.17E-02	1.43E-03	6.39E-04	1.86E-04	8.46E-05	4.70E-05	8.05E-05	2.17E-05	9.38E-06	5.02E-06	3.04E-06	2.00E-06	1.40E-06	1.02E-06	7.67E-07	5.95E-07	4.72E-07	3.81E-07	3.13E-07	2.60E-07	2.95E-06			
Flux of critical energy particles of critical energy and greater from meteoroid impacts	3.42E-02	2.52E-03	1.09E-03	4.48E-04	2.61E-04	1.77E-04	1.30E-04	4.93E-05	2.76E-05	1.82E-05	1.32E-05	1.01E-05	8.15E-06	6.75E-06	5.74E-06	4.97E-06	4.37E-06	3.90E-06	3.52E-06	3.21E-06	2.95E-06			
Ejecta/Spall Flux from both Orbital Debris and Meteoroid Impacts	3.49E-02	5.30E-03	2.83E-03	1.46E-03	9.77E-04	7.32E-04	5.80E-04	2.87E-04	1.88E-04	1.40E-04	1.11E-04	9.21E-05	7.88E-05	6.91E-05	6.16E-05	5.57E-05	5.09E-05	4.70E-05	4.37E-05	4.09E-05	3.89E-05			

Table 6-7, Habitat Module Wall Damage Assessment Worksheet  
(page 1 of 4)

Flux of Ejecta/Spall Particles of Critical Energy and Greater on a Sensitive Area of Space Station

Surface Area of Station (m <sup>2</sup> )	11416.1	Fraction of surface area of Station facing sensitive area	0.5	Earth's radius (km)	6378.145																				
Orbital Life (yrs)	30	Fraction of qty covered by Station as seen from sensitive area (hemispherical View Factor)	0.1	Station orbital altitude (km)	500																				
				Altitude in Earth radii	1.078392																				
				Earth defocusing factor	0.768576																				
				Earth shielding factor	0.713070																				
Critical Energy to damage sensitive surface (Joules)	63400	Fraction of Station Ejects & Spall striking the sensitive area (Station SA fraction & view factor)	0.05	Percent of total impacts on sensitive area if S/S	12.53%																				
Surface Area of critical surface (m <sup>2</sup> )	350	Particle Flux with critical energy and greater on sens. area (Number impacts/m <sup>2</sup> -yr)		Percent of total impacts on sensitive area if S/S e.j. & sp. all Aluminium	80.15%																				
Orb. Debris Average Velocity (km/sec)	9.3	Meteoroids	5.42E-07	0.005891	13.46%																				
Orb. Debris Density (g/cc)	2.8	Orb. Debris	3.47E-06	0.036395	86.08%																				
		Ejecta/Spall (if S/S all graphite/epoxy)	1.83E-08	0.000192	0.46%																				
Meteoroid Average Velocity (km/sec)	20	Ejecta/Spall (if S/S all aluminium)	3.17E-07	0.003325	7.37%																				
Meteoroid Density (g/cc)	0.5																								
Velocity above which Al targets vaporize (km/sec)	7	Average Graphite-Epoxy Ejecta/Spall velocity (km/sec)			0.5																				
		Average Aluminium Ejecta/Spall velocity (km/sec)			4.232																				
		Orbital Debris Fraction below vaporization velocity			0.235359																				
		Orb. Debris Average Vel. (km/sec) below vaporization velocity			4.837984																				
Projectile Mass (g)	0.001	0.02	0.01	0.01	0.02	0.04	0.06	0.08	0.1	0.2	0.3	0.4	0.5	0.6	0.7	0.8	0.9	1	1.1	1.2	1.3	1.4	1.5		
Orbital Debris Parameters																									
Orb. Deb. Dia. (cm)	0.0880	0.1896	0.2389	0.3010	0.3446	0.3793	0.4086	0.5148	0.5893	0.6486	0.6987	0.7424	0.7816	0.8172	0.8499	0.8803	0.9087	0.9354	0.9607	0.9847	1.0077				
Orbital Debris Flux (# of impacts of mass & greater per m <sup>2</sup> surface - year)	1.58E-03	2.29E-04	1.28E-04	7.14E-05	5.08E-05	3.99E-05	3.31E-05	1.65E-05	1.31E-05	8.54E-06	7.34E-06	6.45E-06	5.77E-06	5.22E-06	4.78E-06	4.41E-06	4.10E-06	3.84E-06	3.60E-06	3.43E-06					
Probability of no impacts on Station	0.0602	0.0002	0.0002	0.0002	0.0002	0.0002	0.0002	0.0002	0.0002	0.0002	0.0002	0.0002	0.0002	0.0002	0.0002	0.0002	0.0002	0.0002	0.0002	0.0002					
Incremental Orbital Debris Flux	1.35E-03	1.01E-04	5.64E-05	2.06E-05	1.09E-05	6.82E-06	1.44E-05	5.33E-06	2.87E-06	1.76E-06	1.22E-06	8.92E-07	4.65E-07	5.43E-07	4.42E-07	3.68E-07	3.11E-07	2.67E-07	2.32E-07	1.73E-07	3.43E-06				

### **6.3.3 Habitat Module Wall**

It is likely that all pressurized volumes will be the most protected places on Space Station in terms of resistance to meteoroid/orbital debris penetration. The habitat module wall, therefore, is an example of the damage assessment model using a high critical energy.

#### **6.3.3.1 Critical Energy Calculation**

The module double wall system may likely have to resist penetration from a 1 cm diameter orbital debris particle (density 2.8 g/cc, velocity 9.3 km/sec) which has an average kinetic energy of approximately 60,000 joules (Ref.27).

#### **6.3.3.2 Discussion**

Table 6-7 gives the relative contribution of ejecta/spall to the total critical energy flux on two modules. Two 42 ft. long, 14 ft. diameter modules will have approximately 350 m<sup>2</sup> surface area. Since the modules are situated at the center of the Space Station, the SAF was estimated at 50%. The VF was calculated at approximately 10% which results in a SF of 0.05. The effect of different SF's on the calculated primary and secondary fluxes can be checked in Figure 6-14.

The contribution of graphite/epoxy ejecta/spall to the total critical energy flux was practically negligible. However, because aluminum targets produce many more large, high energy ejecta/spall particles, the aluminum secondary flux contributed a surprisingly large fraction of the total critical energy flux or about 7%. If the Space Station was primarily aluminum, then module wall designers may want to multiply the combined orbital debris/meteoroid flux by a 1.075 factor in their hazards analysis calculations to compensate for the secondaries flux.

Table 6-7, Continued  
(page 3 of 4)

For Impacts from Meteoroids																					
Mass ejecta & spall per meteoroid impact (g)	3.92	10.69	21.39	35.65	49.91	64.17	106.95	178.25	249.55	320.84	392.14	463.44	534.74	606.04	677.34	748.64	819.94	891.24	962.53	1033.83	1069.48
Number of ejecta & spall particles of critical energy and greater per impact from meteoroids of given average mass within mass range.	0.00	0.00	0.00	0.00	0.00	0.00	0.01	0.03	0.05	0.07	0.10	0.13	0.16	0.20	0.23	0.27	0.31	0.35	0.39	0.43	0.45
Number of critical particles created from meteoroid impacts over lifetime of station.																					
Number of critical energy particles per m <sup>2</sup> - year.	7.51E-09	2.51E-09	4.55E-09	3.69E-09	3.26E-09	2.97E-09	1.30E-08	9.90E-09	8.09E-09	6.94E-09	6.12E-09	5.49E-09	4.99E-09	4.58E-09	4.24E-09	3.95E-09	3.69E-09	3.47E-09	3.28E-09	3.11E-09	3.74E-08
Flux of critical energy particles of critical energy and greater from meteoroid impacts	1.43E-07	1.36E-07	1.33E-07	1.29E-07	1.25E-07	1.22E-07	1.19E-07	1.05E-07	9.53E-08	8.72E-08	8.03E-08	7.42E-08	6.87E-08	6.37E-08	5.91E-08	5.49E-08	5.09E-08	4.72E-08	4.38E-08	4.05E-08	3.74E-08
Ejecta/Spall Flux from both Orbital Debris and Meteoroid Impacts																					
	3.67E-07	3.61E-07	3.59E-07	3.54E-07	3.51E-07	3.47E-07	3.44E-07	3.25E-07	3.10E-07	2.95E-07	2.81E-07	2.68E-07	2.54E-07	2.44E-07	2.32E-07	2.21E-07	2.10E-07	1.99E-07	1.88E-07	1.78E-07	1.69E-07
If Ejecta/Spall all from Aluminum Structures																					
For Impacts from Orbital Debris																					
Mass ejecta & spall per impact (g)	0.02	0.35	0.88	1.59	2.29	3.00	5.11	8.64	12.17	15.70	19.23	22.76	26.28	29.81	33.34	36.87	40.40	43.92	47.45	50.98	52.75
Number of ejecta & spall particles of critical energy and greater per impact from projectile's of given average mass within mass range.	0.00	0.00	0.02	0.03	0.05	0.07	0.12	0.22	0.31	0.39	0.48	0.56	0.64	0.72	0.80	0.87	0.95	1.02	1.09	1.16	1.20
Number of critical particles created from impacts over lifetime of station.																					
Number of critical energy particles per m <sup>2</sup> - year.	1.73E-08	1.18E-07	2.14E-07	1.60E-07	1.30E-07	1.10E-07	4.24E-07	2.71E-07	2.03E-07	1.63E-07	1.37E-07	1.18E-07	1.03E-07	9.22E-08	8.32E-08	7.57E-08	6.95E-08	6.42E-08	5.94E-08	4.73E-08	9.89E-07
Flux of critical energy particles of critical energy and greater	3.63E-06	3.61E-06	3.49E-06	3.28E-06	3.17E-06	2.99E-06	2.88E-06	2.45E-06	2.18E-06	1.98E-06	1.82E-06	1.68E-06	1.56E-06	1.46E-06	1.37E-06	1.29E-06	1.21E-06	1.14E-06	1.08E-06	1.07E-06	9.89E-07
For Impacts from Meteoroids																					
Mass ejecta & spall per meteoroid impact (g)	0.23	0.93	2.04	3.52	4.99	6.47	10.90	18.29	25.67	33.06	40.45	47.83	55.22	62.60	69.99	77.38	84.76	92.15	99.54	106.92	110.61
Number of ejecta & spall particles of critical energy and greater per impact from meteoroids of given average mass within mass range.	0.00	0.02	0.04	0.08	0.12	0.16	0.27	0.46	0.63	0.79	0.95	1.10	1.25	1.39	1.53	1.66	1.79	1.92	2.04	2.16	2.22



Figure 6-14

# Primary and Secondary Particle Fluxes

vs % S/S crit energy  $e_j/sp$  flux on area

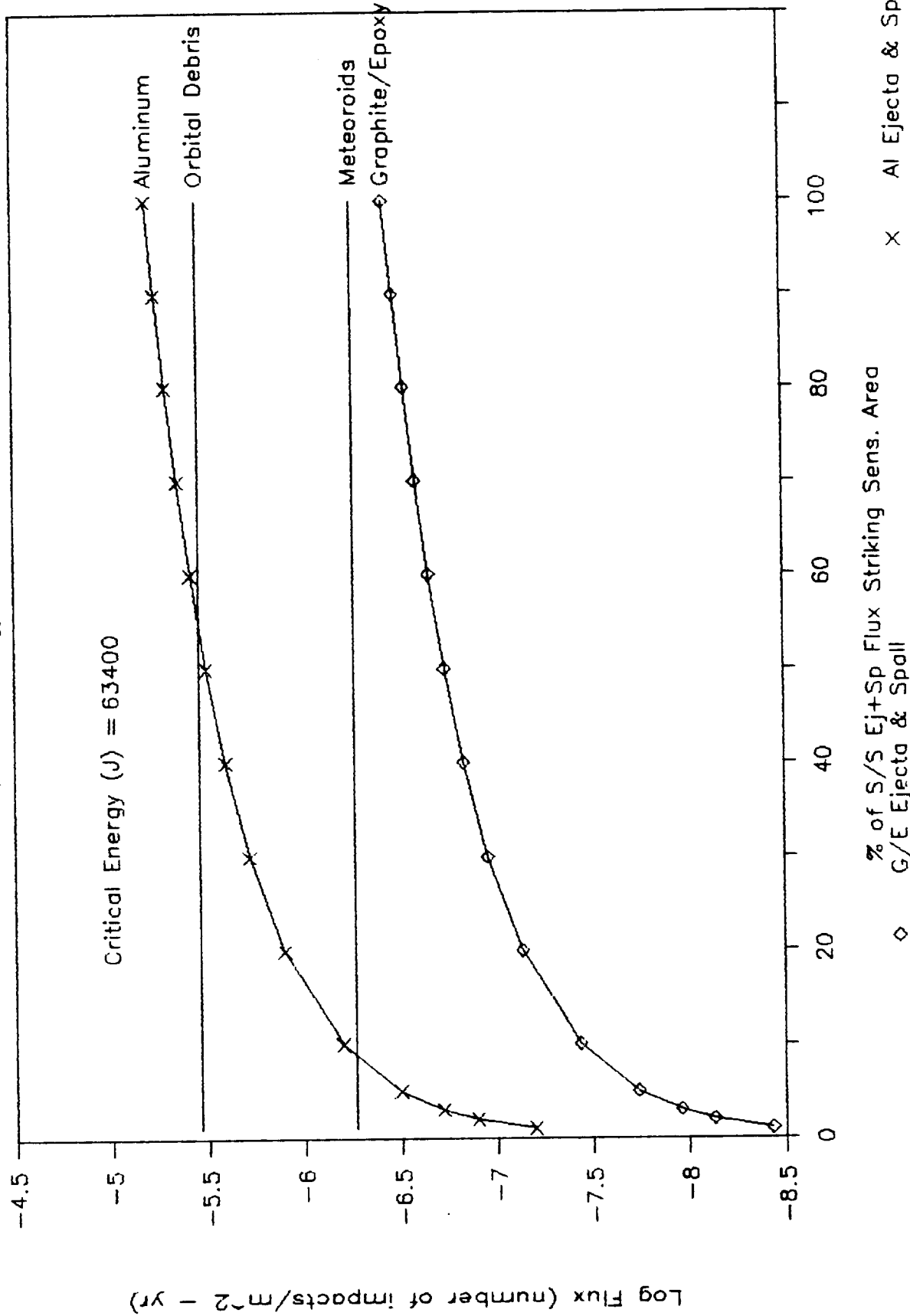




Table 6-7, Continued

(page 4 of 4)

Number of critical particles created from asteroid impacts over lifetime of station.	0.36	0.08	0.09	0.05	0.03	0.03	0.08	0.04	0.03	0.02	0.01	0.01	0.01	0.01	0.01	0.01	0.01	0.01	0.01	0.00	0.00	0.04
Number of critical energy particles per m <sup>2</sup> - year.	1.53E-06	3.52E-07	3.89E-07	2.13E-07	1.45E-07	1.09E-07	3.41E-07	1.68E-07	1.07E-07	7.68E-08	5.88E-08	4.70E-08	3.87E-08	3.26E-08	2.80E-08	2.44E-08	2.15E-08	1.91E-08	1.72E-08	1.55E-08	1.55E-08	1.83E-07
Flux of critical energy particles of critical energy and greater from asteroid impacts	3.91E-06	2.39E-06	2.03E-06	1.65E-06	1.43E-06	1.29E-06	1.18E-06	8.37E-07	6.70E-07	5.62E-07	4.86E-07	4.27E-07	3.80E-07	3.41E-07	3.08E-07	2.80E-07	2.56E-07	2.35E-07	2.15E-07	1.98E-07	1.98E-07	1.83E-07
Ejecta/Spall Flux from both Orbital Debris and Meteoroid Impacts	6.33E-06	5.26E-06	4.90E-06	4.47E-06	4.11E-06	3.88E-06	3.69E-06	3.03E-06	2.65E-06	2.37E-06	2.15E-06	1.98E-06	1.83E-06	1.70E-06	1.58E-06	1.48E-06	1.39E-06	1.30E-06	1.22E-06	1.15E-06	1.15E-06	1.09E-06

material. Including secondary impacts, the number of critical impacts on one solar array would climb to about 35,000. Over a 10 year design lifetime, a solar array would receive about 11,500 critical impacts. A solar array covered with the large area silicon cells that are 5.9 cm by 5.9 cm (Ref.4, p.409) has about 64,000 solar cells. Each impact that completely penetrates the solar array probably has the potential of causing a solar cell to fail. If each penetrating impact did cause a solar cell to fail, approximately 18 percent of the solar cells in a solar array would be inoperative after 10 years. Thus, the solar arrays may potentially need to be replaced every 5 years if only a 10 percent degradation in solar array performance is allowed.

#### 6.3.4 Solar Panels

The International Space Station configuration (Fig. 6-8) has four photovoltaic solar arrays. Each array measures 80 ft. by 32.5 ft. (Ref.4, p.407). The Space Station reference description stated that solar cell performance is expected to degrade by 10 percent over 10 years (Ref.4, p.409) and solar array components would necessarily need to be changed-out.

##### 6.3.4.1 Critical Energy Calculation

An early design for the solar cells called for a 0.008 in. thick silicon cell with a 0.006 in. thick cover glass. The penetration equation by Cour-Palais (Ref.26 - same as Section 6.3.1) was used to calculate the size of orbital debris/meteoroid particles that would penetrate the solar array. The penetration equation related crater depth, P (cm), to projectile density, p (g/cc), projectile diameter, D (cm), and to projectile velocity, V (km/sec).

$$P = 0.53 * p^{0.5} * D^{1.06} * V^{0.67}$$

As given in Table 6-8, the diameter of the orbital debris/meteoroid particles that would create a crater with a depth equal to the total thickness of the solar cell (0.014 in.) was calculated. This failure criterion does not take into account spall effects which can be several times the crater depth and is therefore considered a high estimate. It is also assumed that silicon has similar penetration resistance as silica glass. The solar cell critical energy was calculated from a weighted average of the orbital debris/meteoroid critical energies as 0.21 joules.

##### 6.3.4.2 Discussion

The 0.21 J critical energy and 446 m<sup>2</sup> surface area of one solar array (front and back surfaces) was used in the damage assessment model given in Table 6-9. Because of the large area of the solar array, the SAF factor was estimated as 50% while the VF factor was calculated as approximately 25%. This gave a SF of 0.125. The calculated contribution of graphite/epoxy secondary flux was about 2% of the total primary and secondary flux having the critical energy and above. Because fewer numbers of aluminum particles were counted in this study's tests, the calculated contribution from aluminum secondary flux was less at the low critical energy of the solar cells than graphite/epoxy secondary flux. Thus, a primary flux design factor of 1.02 would include the effects of secondary impacts. Figure 6-15 gives the effect of SF on the calculated secondary fluxes.

Over the 30 year Space Station lifetime, one solar array will likely receive over 34,000 primary impacts from orbital debris and meteoroids that will completely penetrate the solar array

Table 6-9, Solar Array Damage Assessment Worksheet  
(page 1 of 4)

Flux of Ejecta/Spall Particles of Critical Energy and Greater on a Sensitive Area of Space Station

Surface Area of Station (m<sup>2</sup>) 11416.1  
 Orbital Life (yrs) 30  
 Fraction of surface area of Station facing sensitive area 0.5  
 Fraction of sky covered by Station as seen from sensitive area (hemispherical View Factor) 0.25  
 Earth's radius (km) 6378.145  
 Station orbital altitude (km) 500  
 Altitude in Earth radii 1.078392  
 Earth defocusing factor 0.968576  
 Earth shielding factor 0.713070

Particle	Flux with critical energy and greater on sens. area (Number impacts/m <sup>2</sup> -yr)	Number of impacts on sensitive area with critical energy and greater over Station lifetime	Percent of total impacts on sensitive area if S/S all Al	Percent of total impacts on sensitive area if S/S all Aluminum	Probability of no impact on sens. area with critical energy & greater (percent)
Meteoroids	2.40E+00	32190.53	92.69%	94.38%	0.00%
Orb. Debris	1.39E-01	1859.710	5.36%	5.45%	0.00%
Ejecta/Spall (if S/S all graphite/epoxy)	5.06E-02	677.3892	1.95%	0.00%	0.00%
Ejecta/Spall (if S/S all aluminum)	4.31E-03	57.72133	0.17%	0.00%	0.00%

Average Graphite-Epoxy Ejecta/Spall velocity (km/sec) 0.5  
 Average Aluminum Ejecta/Spall velocity (km/sec) 4.232  
 Orbital Debris Fraction below vaporization velocity 0.235359  
 Orb. Debris Average Vel. (km/sec) below vaporization velocity 4.837984

Projectile Mass (g)	0.001	0.01	0.02	0.04	0.06	0.08	0.1	0.2	0.3	0.4	0.5	0.6	0.7	0.8	0.9	1	1.1	1.2	1.3	1.4	1.5 & >	
Orbital Debris Parameters																						
Orb. Deb. Dia. (cm)	0.0880	0.1896	0.2389	0.3010	0.3446	0.3793	0.4066	0.5148	0.5893	0.6486	0.6987	0.7424	0.7816	0.8172	0.8499	0.8803	0.9087	0.9354	0.9607	0.9847	1.0077	
Orbital Debris Flux (of impacts of given mass & greater per m <sup>2</sup> surface - year)	1.58E-03	2.29E-04	1.28E-04	7.14E-05	5.08E-05	3.99E-05	3.31E-05	1.85E-05	1.31E-05	1.03E-05	8.56E-06	7.34E-06	6.45E-06	5.77E-06	5.22E-06	4.78E-06	4.41E-06	4.10E-06	3.84E-06	3.60E-06	3.43E-06	
Probability of no impacts on Station	0.000%	0.000%	0.000%	0.000%	0.000%	0.000%	0.001%	0.178%	1.108%	2.914%	5.332%	8.065%	10.974%	13.873%	16.710%	19.445%	22.056%	24.535%	26.882%	29.100%	30.873%	
Incremental Orbital Debris Flux	1.35E-03	1.01E-04	5.64E-05	2.06E-05	1.09E-05	6.82E-06	1.46E-05	5.33E-06	2.82E-06	1.78E-06	1.22E-06	8.92E-07	6.85E-07	5.43E-07	4.42E-07	3.68E-07	3.11E-07	2.67E-07	2.32E-07	1.73E-07	1.73E-07	3.43E-06

Table 6-8

## Solar Cell Critical Energy Determination

Glass Thickness (cm) (8 mil silicon cell with 6 mil cover glass)	0.03556	
	Meteoroid	Debris
Particle Density (g/cc)	0.5	2.8
Particle Velocity (km/s)	20	9.3
Particle Critical Diameter (cm) for crater depth to completely penetrate silica glass (from Ref.26)	0.0163	0.0117
Particle Mass (g)	1.14E-06	2.38E-06
Particle Energy (J)	0.23	0.10
Particle Flux (#/m <sup>2</sup> -yr) with critical diameter and greater	1.51E+00	2.53E-01
Percent Flux	85.61	14.39
Average Critical Energy (J) above which results in complete penetration of the solar cell from Meteoroid & Orbital Debris Impacts	0.21	

Table 6-9, Continued  
(page 3 of 4)

For Impacts from Meteoroids																					
Mass ejecta & spall per meteoroid impact (g)	3.92	10.69	21.39	35.65	49.91	64.17	106.95	178.25	249.55	320.84	392.14	463.44	534.74	606.04	677.34	748.64	819.94	891.24	962.53	1033.83	1069.48
Number of ejecta & spall particles of critical energy and greater per impact from meteoroids of given average mass within mass range.	320.37	455.54	533.18	572.46	587.54	592.65	586.26	558.27	529.44	503.42	480.38	459.94	441.68	425.27	410.41	396.87	384.46	373.03	362.46	352.64	347.98
Number of critical particles created from meteoroid impacts over lifetime of station.																					
Number of critical energy particles per m <sup>2</sup> - year.	41680.67	2198.26	1109.87	351.19	167.13	95.73	173.24	48.62	21.38	11.54	7.03	4.64	3.24	2.36	1.78	1.38	1.09	0.88	0.72	0.60	6.77
Number of critical energy particles created from meteoroid impacts																					
Flux of critical energy particles of critical energy and greater from meteoroid impacts	1.74E-01	9.29E-03	4.69E-03	1.48E-03	7.07E-04	4.05E-04	7.32E-04	2.04E-04	9.04E-05	4.88E-05	2.97E-05	1.96E-05	1.37E-05	9.98E-06	7.53E-06	5.83E-06	4.61E-06	3.72E-06	3.05E-06	2.55E-06	2.86E-05
Flux of critical energy particles of critical energy and greater from meteoroid impacts																					
Ejecta/Spall Flux from both Orbital Debris and Meteoroid Impacts	1.94E-01	1.78E-02	8.49E-03	3.80E-03	2.32E-03	1.61E-03	1.21E-03	4.74E-04	2.68E-04	1.78E-04	9.92E-05	7.94E-05	6.59E-05	5.59E-05	4.84E-05	4.25E-05	3.79E-05	3.42E-05	3.12E-05	2.86E-05	
Ejecta/Spall Flux from both Orbital Debris and Meteoroid Impacts																					
If Ejecta/Spall all from Aluminum Structures	4.05E-01	9.23E-02	6.05E-02	3.79E-02	2.94E-02	2.29E-02	1.93E-02	1.09E-02	7.70E-03	5.97E-03	4.89E-03	4.15E-03	3.61E-03	3.20E-03	2.88E-03	2.62E-03	2.41E-03	2.23E-03	2.08E-03	1.96E-03	1.86E-03
For Impacts from Orbital Debris																					
Mass ejecta & spall per impact (g)	0.02	0.35	0.88	1.59	2.29	3.00	5.11	8.64	12.17	15.70	19.23	22.76	26.28	29.81	33.34	36.87	40.40	43.92	47.45	50.98	52.75
Number of ejecta & spall particles of critical energy and greater per impact from projectile's of given average mass within mass range.	23.69	61.90	69.69	72.19	72.63	72.38	70.49	66.76	63.88	61.26	58.99	57.81	55.26	53.69	52.26	50.97	49.77	48.68	47.66	46.71	46.25
Number of critical particles created from impacts over lifetime of station.																					
Number of critical energy particles per m <sup>2</sup> - year.	2586.39	504.03	316.97	119.97	63.85	39.79	82.96	28.79	14.53	8.71	5.78	4.10	3.05	2.33	1.86	1.51	1.25	1.05	0.89	0.65	12.79
Flux of critical energy particles of critical energy and greater																					
Flux of critical energy particles of critical energy and greater from meteoroids of given average mass within mass range.	1.11E-02	3.55E-03	2.08E-03	1.15E-03	8.00E-04	6.13E-04	4.97E-04	2.55E-04	1.71E-04	1.28E-04	8.61E-05	7.42E-05	6.53E-05	5.84E-05	5.30E-05	4.86E-05	4.49E-05	4.19E-05	3.93E-05	3.74E-05	
For Impacts from Meteoroids																					
Mass ejecta & spall per meteoroid impact (g)	0.23	0.93	2.04	3.52	4.99	6.47	10.90	18.29	25.67	33.06	40.45	47.83	55.22	62.60	69.99	77.38	84.76	92.15	99.54	106.92	110.61
Number of ejecta & spall particles of critical energy and greater per impact from meteoroids of given average mass within mass range.	57.02	70.01	72.59	72.01	70.61	69.10	64.93	59.57	55.55	52.37	49.76	47.55	45.65	43.97	42.49	41.16	39.95	38.85	37.84	36.91	36.47



Figure 6-15

# Primary and Secondary Particle Fluxes

vs % S/S crit energy ej/sp flux on area

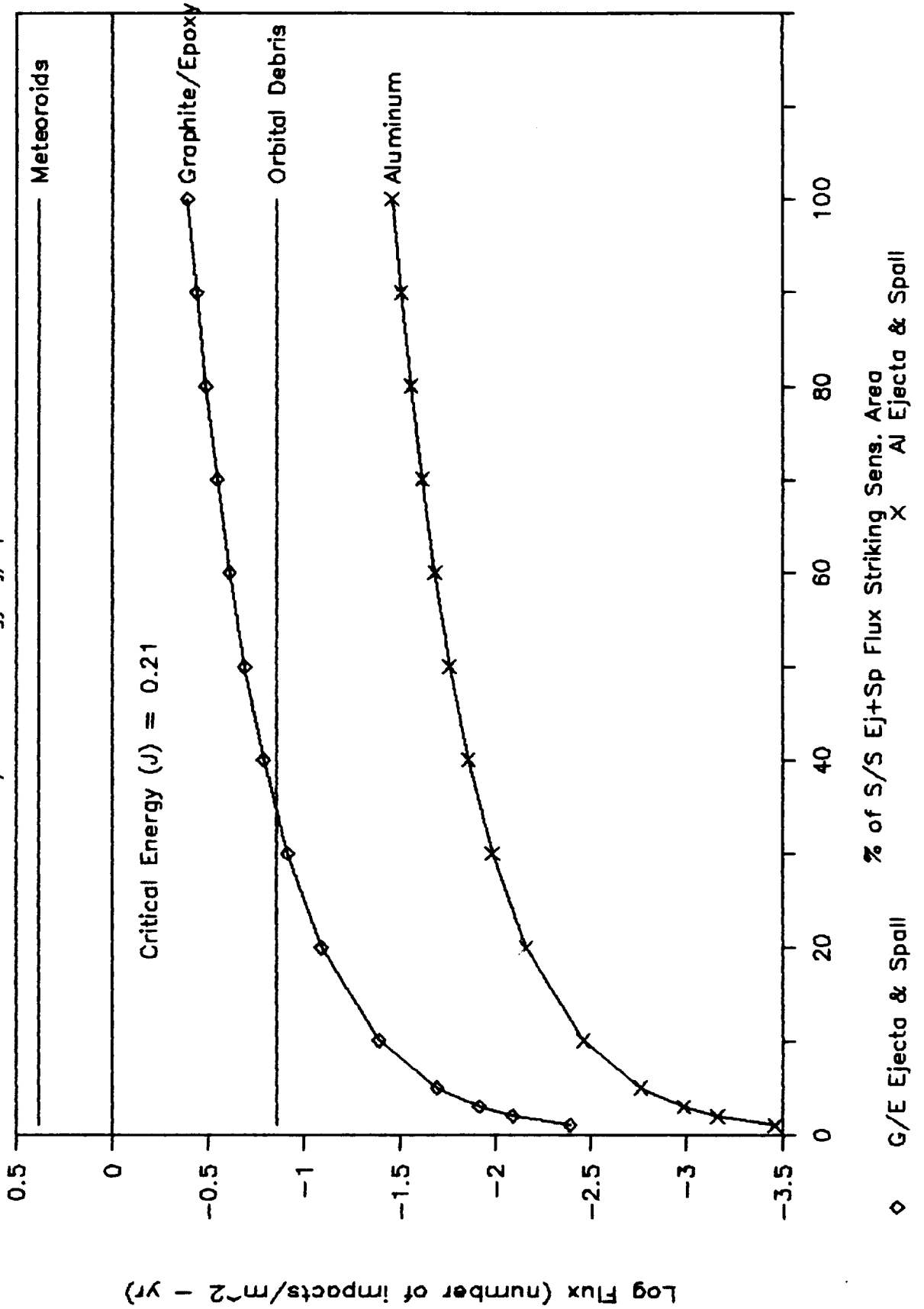




Table 6-9, Continued  
(page 4 of 4)

Number of critical particles created from asteroid impacts over lifetime of station.	7418.84	337.84	151.09	44.17	20.09	11.16	19.19	5.19	2.24	1.20	0.73	0.48	0.33	0.24	0.18	0.14	0.11	0.09	0.08	0.06	0.71
Number of critical energy particles per m <sup>2</sup> - year.	3.14E-02	1.43E-03	6.39E-04	1.87E-04	8.49E-05	4.72E-05	8.11E-05	2.19E-05	9.48E-06	5.08E-06	3.08E-06	1.42E-06	1.03E-06	7.79E-07	6.04E-07	4.80E-07	3.88E-07	3.18E-07	2.65E-07	3.00E-06	
Flux of critical energy particles of critical energy and greater from asteroid impacts	3.39E-02	2.52E-03	1.09E-03	4.50E-04	2.43E-04	1.78E-04	1.31E-04	4.99E-05	2.79E-05	1.85E-05	1.03E-05	8.28E-06	6.87E-06	5.83E-06	5.05E-06	4.43E-06	3.97E-06	3.58E-06	3.28E-06	3.00E-06	
Ejecta/Spall Flux from both Orbital Debris and Meteoroid Impacts	3.45E-02	5.29E-03	2.83E-03	1.46E-03	9.81E-04	7.36E-04	5.88E-04	2.89E-04	1.90E-04	1.41E-04	1.17E-04	9.33E-05	7.99E-05	6.24E-05	5.45E-05	5.16E-05	4.77E-05	4.43E-05	4.15E-05	3.94E-05	

secondary flux, whether from aluminum or graphite/epoxy will be significantly less than primary fluxes having the critical energy or greater. A conservative rule of thumb would be to add 10 percent to meteoroid and orbital debris flux to account for secondary impacts.

## 9.0 References

1. Kessler, D.J. and Cour-Palais, B.G.: Collision Frequency of Artificial Satellites: The Creation of a Debris Belt. *Journal of Geophysical Research*, Vol. 83, No. A6, June 1978, p. 2637.
2. Kinslow, R., ed.: *High-Velocity Impact Phenomena*. Academic Press, Inc. 1970.
3. Thompson, A.B.: Spacecraft Probability of No Meteoroid Penetration Program. April 1978. Included in Appendix C: Composite Space Station Habitation Module Design Approach. Stump, W.R. and Davis, J.I., Eagle Engineering Report No. 83-69, September 1983.
4. Space Station Reference Configuration Description. JSC-19989, August 1984.
5. Vaughan, W.W.: Natural Environment Design Criteria for the Space Station Program Definition Phase. NASA TM-82585, July 1984.
6. Vaughan, W.W.: Natural Environment Design Criteria for the Space Station Definition and Preliminary Design (First Revision). NASA TM-86460, September 1984.
7. Vaughan, W.W. and Green, C.E.: Natural Environment Design Criteria Guidelines for the Space Station Definition and Preliminary Design (Second Revision). NASA TM-86498, 1985.
8. Kessler, D.J.: Meteoroid Velocity Distribution. SN3-86-82, March 1986.
9. Kessler, D.J.: A Guide to Using Meteoroid-Environment Models for Experiment and Spacecraft Design Applications. NASA TN D-6596, March 1972.
10. Kessler, D.J.: Orbital Debris Issues. *Advanced Space Research*, Vol.5, No.2, 1985, pp.3-10.
11. Reynolds, R.C.; Rice, E.E.; and Edgecombe, D.S.: Man-Made Debris Threatens Future Space Operations. *Physics Today*, Vol.35, No.9, 1982.

## 7.0 Conclusions

1. Spall mass made up approximately 70% of the total mass of ejecta/spall particles (for the thin, 0.1 inch thick, targets used in this study).
2. Total ejecta/spall mass was 20-100 times more than projectile mass (with projectile energy ranging from 50-120 Joules). Ejecta/spall mass increased as projectile energy increased (with constant projectile mass). Higher target density and lower projectile density reduced total ejecta/spall mass.
3. Some small ejecta/spall particles are fast while all large ejecta/spall particles are slow.
4. Aluminum structures produce more high energy but fewer low energy ejecta/spall particles than graphite epoxy structures for a given energy impact.
5. For thick graphite/epoxy targets, a cloth covering significantly reduced (by almost 50%) the total ejecta mass. However, it was not apparent that a cloth covering significantly reduced the total ejecta/spall mass for thin graphite/epoxy targets.
6. For most structural elements of interest on the International Space Station, the secondary flux from ejecta/spall particles will contribute no more than 10% to the total flux (primary and secondary) having a given critical energy or greater. Thus, in hazards assessment analysis, designers should multiply the total primary flux by 1.1 to compensate for secondary impact effects.
7. It is predicted that over 35,000 primary and secondary impacts will have sufficient energy to completely penetrate each 80 ft. by 32.5 ft. solar array over the 30 year Space Station lifetime. It has been reported that the solar array performance should degrade only 10 percent before replacement. If each complete penetration causes a solar cell to fail, the solar arrays may need to be replaced every 5 years.

## 8.0 Recommendations

Further work needs to be done to assess the effect of hypervelocity impacts on solar cells. Depending on the sensitivity of the cells to impact damage, significant loss of power could occur over long time periods (10-30 years).

Designers need only include effects (flux) of secondary impacts on surfaces that have high exposure to ejecta/spall produced from the rest of the Space Station. Even on very sensitive surfaces (ones with low critical energy of projectiles that result in damage), unless the exposure fraction is high, the

25. Cooke, D.R.; Lewis, J.; and Byrd, W.J.: Window Viewing Requirements--Presentation to Systems Integration Board (SIB) Review. April 30, 1986.
26. Cour-Palais, B.G.: Hypervelocity Impact Investigations and Meteoroid Shielding Experience Related to Apollo and Skylab. NASA Conf. Pub. 2360, July 1982, p.272.
27. Elfer, N.: Presentation on Space Debris and Meteoroid Protection - IRAD Project M-01S, March 31, 1986.
28. Burris, R.A.: Orbiter Surface Damage Due to SRM Plume Impingement. McDonnell Douglas, NAS9-15550, December 18, 1978.
29. Beer, F.P. and Johnston, E.R.: Mechanics of Materials. McGraw-Hill Book Co., 1981, p. 585.

12. Wolfe, M.; Chobotov, V.; Kessler, D.J.; and Reynolds, R.C.: Man-Made Debris - Does it Restrict Free Access to Space? AIAA Paper No. IAA-81-256, 1981.
13. Reynolds, R.C., Fischer, N.H.; and Edgecombe, D.S.: A Model for the Evolution of On-Orbit Man-Made Debris Environment. NASA Conf. Pub. 2360, July 1982, p.102.
14. Kessler, D.J.: Orbital Debris Environment for Space Station. JSC 20001, 1984.
15. Aaron, J.: Space Station Program Update. Presentation to Committee on Science and Technology, U.S. House of Representatives, February 10, 1986.
16. Space Station Configuration Baseline for Preliminary Design (Initial Draft). McDonnell Douglas, MDAC-5401D, March 1986.
17. Space Station Definition and Preliminary Design, Contract Management Review Documentation and Monthly Status Report (DR-14). McDonnell Douglas Astronautics Company, May 6, 1986.
18. Humes, D.H.; Brooks, D.R.; Alvarez, J.M.; and Bess, T.D.: Manmade Orbital Debris Studies at NASA Langley. NASA Conf. Pub. 2360, July 1982, p.63.
19. Foley, T.M.: NASA Approves Competition of Station Phase C/D Contracts. Aviation Week and Space Technology, May 12, 1986, pp.63-64.
20. Louviere, A.J.: Design Approach to Meteoroid/Debris Protection for Space Station. Johnson Space Center PB3-86-029M, March 24, 1986.
21. Kissinger, D.: Preliminary Memo for Space Station Change Request Proposal BM010028--Meteoroid/Debris Damage, May 1986.
22. Kavanaugh, H.C. and Miller, G.J.: Preliminary Structural Design and Analysis of a Shuttle Launched Space Station Manned Habitable Module. Space Station Subsystem White Paper, June 1984.
23. Clanton, U.S.; Zook, H.A.; and Schultz, R.A.: Hypervelocity Impacts on Skylab IV/Apollo Windows. NASA Conf. Pub. 2360, July 1982, p.177.
24. Raasch, R.F.; Peercy, R.L.; and Rockoff, L.A.: Space Station Crew Safety Alternatives Study - Final Report, Vol II. NASA Contractor Report 3855, NAS1-17242, June 1985.

Target Data on JSC Light Gas Gun Shots

JSC Shot #	Date	Target						Damage Notes	
		Target type	Material	Thickness (inches)	Length (inches)	Width (inches)	Mass before (grams)		Mass after (grams)
756	09-Jul-85	Bumper	Fiberglass (suit)	0.076	4	4			Small hole, elliptical delamination, 1" diameter. Little damage. No bumps on back of inner wall. No large craters on inner wall front.
		Inner Wall	Aluminum (6061-T6)	0.032	6	5.25			
		Standoff Distance	3.875						
		Bumper Mass/unit area =	0.00543 lbm/in <sup>2</sup>						
861	12-Nov-85	Thick plate	Aluminum with paper backing.	0.250	4	4			Perforated. Circular 8 mm dia. crater on front surface with petaling. Rear crater is 2.5 mm diameter and raised. Slight secondary surface marks on front.
			Mass/unit area = 0.0245 lbm/in <sup>2</sup>						
862	12-Nov-85	Thick plate	Graphite/Epoxy (generic).	0.416	6	6			Did not perforate plate. Large spall on back surface. Circular crater on front surface 4mm dia. Peelings in vertical orientation both front and back surfaces. Slight secondary surface marks on front.
			Mass/unit area = 0.0237 lbm/in <sup>2</sup>						
863	13-Nov-85	Thick plate	Graphite/Epoxy (generic).	0.239	6	6			Perforated plate. Circular crater on front 6 mm dia. Peelings on front surface in +45 deg phi, -90 deg theta; -45 deg phi, +90 deg theta orientation. Rear surface in +45 phi, +80 theta; -45 phi, -90 theta orientation.
			Mass/unit area = 0.0136 lbm/in <sup>2</sup>						
865	14-Nov-85	Thick plate	Graphite/Epoxy (generic).	0.191	6	4			Perforated plate. Elliptical crater on front 2 mm long, 1 mm wide; on back circular 4 mm diameter crater. Peelings on front surface in +45 deg phi, +90 deg theta; -45 deg phi, -90 deg theta orientation. Rear surface in +45 phi, -90 theta; -45 phi, +90 theta orientation.
			Mass/unit area = 0.0109 lbm/in <sup>2</sup>						

Other Data on JSC Light Gas Gun Shots

JSC Shot #	Projectile				Other			
	Projectile Material	Mass (milligrams)	Diameter (inches)	Length (inches)	Velocity (km/sec)	Impact Photo?	Doc. Photo?	Purpose of Shot
756	Nylon	5.16	0.0692	0.0731	6.55	No	Yes	To test a fiberglass bumper.
861	304 S/S (Stainless-Steel)	15.3	0.0695	0.0324	3.5	No	Yes	Test to check ability to shoot steel projectile. Also for UT model verification.
862	304 S/S (Stainless-Steel)	13.91	0.0695	0.0335	3.29	No	Yes	Test ability to shoot steel projectile. Also for UT model verification.
863	304 S/S (Stainless-Steel)	14.59	0.0693	0.035	3.58	No	Yes	Test ability to shoot steel projectile. Also for UT model verification.
865	304 S/S (Stainless-Steel)	14.54	0.0695	0.034	3.02	No	Yes	Test ability to shoot steel projectile. Also for UT model verification.

Target Data on JSC Light Gas Gun Shots

JSC Shot # Date

Target

Target type	Material	Thickness (inches)	Length (inches)	Width (inches)	Mass before (grams)	Mass after (grams)	Damage Notes
No Cloth.	JSC-01B-002 Mass/unit area = 0.0313 lbm/in <sup>2</sup>						peelings (2.5 - 3") horizontally (0 deg phi, +90 & -90 deg theta) from crater. No penetration (tape on back - no spall), slightly raised behind impact point.
889 10-Dec-85 Thin. No cloth	Graphite/ Epoxy, AS4/3501-6 JSC-02B-001 WN3 Mass/unit area = 0.0053 lbm/in <sup>2</sup>	0.095	6	6	86.6	86.3 Ejecta wt. = .06g	
890 11-Dec-85 Truss simulator. No cloth. Thin.	Graphite/ Epoxy, AS4/3501-6 JSC-03B-002 WN5 Mass/unit area = 0.0062 lbm/in <sup>2</sup>	0.112	6	6	101.61	101.4 Ejecta wt. = .04g?	
893 12-Dec-85 Thin. No cloth.	Graphite/ Epoxy, AS4/3501-6 JSC-02B-002 WN4 Mass/unit area = 0.0053 lbm/in <sup>2</sup>	0.094	6	6	86.08	85.9	
894 13-Dec-85 Thin (truss-type) Plate. Replacement for WN4.	Graphite/ Epoxy, AS4/3501-6 JSC-02B-003 Mass/unit area = 0.0053 lbm/in <sup>2</sup>	0.093	6	6	85.92	85.79	Complete penetration. Surface delaminations (peelings) on both sides. On ejecta side peelings in +45 deg phi, -90 deg theta; -45 deg phi, +90 deg theta. On spall side peelings in +45 deg phi, +90 deg theta; -45 deg phi, -90 deg theta orientation.
895 16-Dec-85 Truss simulator. No cloth. Thin.	Graphite/ Epoxy, AS4/3501-6 JSC-03B-001 WN6 Mass/unit area = 0.0063 lbm/in <sup>2</sup>	0.115	6	6	103.64	103.41 Ejecta wt. = .03g	
900 18-Dec-85 Thick. Cloth on both sides.	Grphite/ Epoxy, Graphite cloth, AS4/A193PW/ 3501-6 JSC-01A-001 WN2 Mass/unit area = 0.0314 lbm/in <sup>2</sup>	0.528	6	6	512.6		



Other Data on JSC Light Gas Gun Shots

JSC Shot #	Projectile				Velocity (km/sec)	Impact Photo?	Doc. Photo?	Purpose of Shot
	Projectile Material	Mass (milligrams)	Diameter (inches)	Length (inches)				
873	Nylon	5.0	0.0686	0.072	6.32	Yes	No	Impact photograph used to estimate ejecta velocity.
878	Aluminum 6061-T6	5.1	0.0703	0.0336	6.19	No	Yes	To test another fiberglass bumper.
879	Aluminum 6061-T6	4.43	0.0704	0.0317	4.3	No	Yes	To test fiberglass/composite hybrid bumper.
881	Aluminum 6061-T6	4.84	0.0704	0.0344	6.08	No	Yes	To test another fiberglass bumper.
883	Nylon	4.93	0.0697	0.0709	6.42	No, Styro-foam box (completely closed) used to collect ejecta	Yes	Generic shot to characterize ejecta. Compare results for target with cloth to Shot No. 884 (without cloth).
884	Nylon	4.76	0.0696	0.0682	6.26	No, Styro-foam box	Yes	Generic shot to characterize ejecta. Compare results for

Target Data on JSC Light Gas Gun Shots

JSC Shot #	Date	Target						Damage Notes
		Target type	Material	Thickness (inches)	Length (inches)	Width (inches)	Mass before (grams)	
901	18-Dec-85	Thick. Cloth on both sides.	Graph./Epoxy Graphite cloth. AS4/A193PW/3501-6 JSC-01A-005 WN2 Mass/unit area = 0.0311 lbm/in <sup>2</sup>	0.524	6	6	508.6	
909	30-Dec-85	Thin. Cloth on both sides.	Graphite/Epoxy. AS4/3501-6 JSC-03A-002 WN8 Mass/unit area = 0.0069 lbm/in <sup>2</sup>	0.124	8	6	113.29	112.92 Blow out
910	31-Dec-85	Thin. Toughened resin.	Graphite IM6/8551 JSC-06A-001 WN10 Mass/unit area = 0.0107 lbm/in <sup>2</sup>	0.194	6	6	174.1	173.82
911	02-Jan-86	Thin. Cloth on both sides.	Graphite/Epoxy. AS4/3501-6 JSC-03A-001 WN7 Mass/unit area = 0.0070 lbm/in <sup>2</sup>	0.125	6	6	114.24	114.02
912	03-Jan-86	Thin. Toughened resin.	Graphite IM6/8551 JSC-06A-002 WN7 Mass/unit area = 0.0105 lbm/in <sup>2</sup>	0.191	6	6	171.42	171.26
913	03-Jan-86	Thin. Fiberglass with cloth.	Fiberglass. S-2/3501-6 JSC-05A-001 WN11 Mass/unit area = 0.0069 lbm/in <sup>2</sup>	0.104	6	6	113.3	113.2
917	13-Jan-86	Thin (truss-type) plate. Cloth on both sides.	Graphite/Epoxy, AS4/3501-6 JSC-03A-003 Mass/unit area = 0.0070 lbm/in <sup>2</sup>	0.127	6	6	114.75	114.5 Complete penetration. Elliptical crater on front surface 3mm in vertical 4mm in horizontal 114.31 On back surface, circular crater approx. 5mm in diam. On front surface, checkerboard square delaminations on top and bottom edges of crater; cloth ripped off and horizontal delaminations run 8mm to right of crater(facing plate front) and 6mm to left On rear surface, checkerboard

Other Data on JSC Light Gas Gun Shots

JSC Shot #	Projectile				Velocity (km/sec)	Impact Photo?	Doc. Photo?	Purpose of Shot	Other
	Material	Mass (milligrams)	Diameter (inches)	Length (inches)					
889 Al 6061	5	0.0703	0.033	5.02	No			target without cloth to Shot No. 883 (with cloth).	
890 Al 6061	4.93	0.0703	0.032	4.5	No			Test shot for Dr. Yew's model (The University of Texas).	
893 Nylon	4.99	0.0696	0.0754	4.75	No			Test shot for Dr. Yew's model (The University of Texas).	
894 Nylon	4.94	0.0695	0.0718	4.75	Yes (30-35 micro-sec. after impact).	Yes		Generic shot to characterize mass and particle size distribution for both ejecta and spall. No cloth, normal impact. Also used as a test shot for Dr. Yew's model (The University of Texas).	
895 Nylon	4.96	0.0696	0.0713	4.82	No			Test shot for Dr. Yew's model (The University of Texas).	
900 Nylon	5.02	0.0696	0.0717	6	No			Test shot for Dr. Yew's model (The University of Texas).	

Target Data on JSC Light Gas Gun Shots

JSC Shot #	Date	Target						Damage Notes	
		Target type	Material	Thickness (inches)	Length (inches)	Width (inches)	Mass before (grams)		Mass after (grams)
923	21-Jan-86	Thin (truss-type) plate. No cloth.	Graphite/Epoxy, AS4/3501-6 JSC-02B-005 Mass/unit area = 0.0053 lbm/in <sup>2</sup>	0.095	6	6	86.6	86.35	Complete penetration. Surface delaminations (peelings) on both sides. On ejecta side peelings in +45 deg phi, +90 deg theta; -45 deg phi, -90 deg theta. On spall side peelings in +45 deg phi, -90 deg theta; -45 deg phi, +90 deg theta orientation. Elliptical crater 5 mm long, 4mm wide measured on front surface; 6mm long and 5mm wide (horizontal) on rear surface. Surface not raised around crater.
933	29-Jan-86	Thin (bumper-type) plate.	Aluminum 6061-T6 Mass/unit area = 0.0086 lbm/in <sup>2</sup>	0.089	6	6	139.62	139.5	Complete penetration with approx. 6mm diameter circular crater. Petaling on front surface. Only slightly raised lip on rear surface. Obvious circular ejecta spray pattern in styrofoam catcher for front surface. Only random aluminum fragments imbedded in styrofoam catcher for rear surface spall.
969	14-Apr-86	Semi-Infinite Plate.	Graphite/Epoxy, No cloth (Generic) Mass/unit area = 0.0147 lbm/in <sup>2</sup>	0.276	6	6	240.6	240.45	Approx. 3mm dia. surface crater that does not penetrate plate (approx. 1.5mm deep). Some spall off back.
972	15-Apr-86	Bumper  Inner Wall	Graphite/Epoxy, No cloth (Generic) Mass/unit area = 0.0051 lbm/in <sup>2</sup> Al 6061-T6 0.032	0.078	4	4	36.94	36.61	Complete penetration, 5.6mm dia. circular hole. Multiple small craters on back-up sheet, but not penetrated. 0.31g ejecta/spall collected.

Other Data on JSC Light Gas Gun Shots

JSC Shot #	Projectile				Velocity (km/sec)	Impact Photo?	Doc. Photo?	Other
	Projectile Material	Mass (milligrams)	Diameter (inches)	Length (inches)				
901 Nylon	5.07	0.0697	0.0709	6.19	No		Test shot for Dr. Yew's model (The University of Texas).	
909 Nylon	4.99	0.0693	0.0739	6.2	No		Test shot for Dr. Yew's model (The University of Texas).	
910 Nylon	5	0.0698	0.0736	6.11	No		Test shot for Dr. Yew's model (The University of Texas).	
911 Al 6061	5	0.0705	0.034	5.17	No		Test shot for Dr. Yew's model (The University of Texas).	
912 Al 6061	5	0.0706	0.034	4.57	No		Test shot for Dr. Yew's model (The University of Texas).	
913 Al 6061	4.98	0.0706	0.0354	4	No		Test shot for Dr. Yew's model (The University of Texas).	
917 Nylon	4.86	0.0716	0.0676	5.99	Yes (of spall 30 micro-sec after impact)	Yes	Secondary shot to quantify ejecta and spall characteristics (mass, size, distribution, velocity). With cloth, normal impact.	

Target Data on JSC Light Gas Gun Shots

JSC Shot #	Date	Target							Damage Notes
		Target type	Material	Thickness (inches)	Length (inches)	Width (inches)	Mass before (grams)	Mass after (grams)	
		Standoff Distance		4.000					
975	16-Apr-86	Bumper	Al 6061-T6 Mass/unit area = 0.0085 lbm/in <sup>2</sup>	0.089	6	6	138.32	138.22	Complete penetration of bumper, 6mm dia. circular hole. Multiple craters on backup front surface with dimpling on back, but did not penetrate. 0.09g ejecta/spall collected.
		Inner Wall	Al 6061-T6	0.032	5.75	5.75	45.51	45.50	
		Standoff Distance		4.000					
979	18-Apr-86	Bumper	Al 6061-T6 Mass/unit area = 0.0085 lbm/in <sup>2</sup>	0.089	6	6	138.25	138.25	Complete penetration of bumper, 5.2mm dia. circular hole. A few small craters on backup front surface with some dimpling on back, but did not penetrate. 0.02g ejecta/spall collected.
		Inner Wall	Al 6061-T6	0.032	5.75	5.75	43.21	43.2	
		Standoff Distance		4.000					
981	22-Apr-86	Bumper	Graphite/ Epoxy, AS4/3501-6 JSC-02B-004 (no cloth) Mass/unit area = 0.0053 lbm/in <sup>2</sup>	0.095	6	6	86.3	86.0	Complete penetration of bumper with 6mm dia. hole. Numerous very small craters on surface of backup plate but no dimpling or penetration. 0.2g ejecta/spall collected (slight amount of aluminum contained in ej/sp)
		Inner Wall		0.032	5.75	5.75	44.24	44.21	
		Standoff Distance		4.000					
988	29-Apr-86	Bumper	Graphite/ Epoxy, AS4/3501-6 JSC-02A-001 (cloth) Mass/unit area = 0.0059 lbm/in <sup>2</sup>	0.105	6	6	96.75	96.52	Complete penetration of bumper with 5mm dia. hole. Numerous very small craters and shallow short cuts on surface of backup plate. 4-5 small dimples on back of backup but no penetration. 0.1g ejecta/spall collected.
		Inner Wall		0.032	5.75	5.75	48.08	46.09	
		Standoff Distance		4.000					
990	30-Apr-86	Bumper (30 deg. oblique impact)	Graphite/ Epoxy, AS4/3501-6 JSC-02A-001 (cloth) Mass/unit area = 0.0059 lbm/in <sup>2</sup>	0.111	6	6	96.8	96.6	Complete penetration of bumper with 4.5mm dia. hole. Numerous very small craters and shallow short cuts on surface of backup plate, but no small dimples on back of backup
		Inner Wall		0.032	5.75	5.75	45.3	45.3	

Other Data on JSC Light Gas Gun Shots

JSC Shot #	Projectile				Velocity (km/sec)	Impact Photo?	Doc. Photo?	Other
	Projectile Material	Mass (milligrams)	Diameter (inches)	Length (inches)				
923 Nylon	5.8	0.071	0.080	7.02	No	Yes	Secondary shot to quantify ejecta and spall characteristics (mass, size, distribution, velocity). No cloth, oblique impact (-30 deg phi from front surface normal).	
933 Nylon	4.98	0.0714	0.0705	6.3	No	Yes	Secondary shot to quantify ejecta and spall characteristics (mass, size, distribution, velocity). Normal impact. This shot on aluminum target is for comparison purposes with composite targets.	
969 Al 6061	4.86	0.0695	0.031	5.12	No	No	University of Texas test to check for projectile in ejecta/spall. 0.01 g ejecta/spall collected.	
972 Nylon	5.00	0.0695	0.072	7.19	Yes (High-Speed Camera)	No	Test shot to check new high-speed camera.	

Target Data on JSC Light Gas Gun Shots

JSC Shot #	Date	Target							Damage Notes	
		Target type	Material	Thickness (inches)	Length (inches)	Width (inches)	Mass before (grams)	Mass after (grams)		
		Standoff Distance		4.000						
991 01-May-86		Bumper	Al 6061-T6 Mass/unit area = 0.0085 lbm/in <sup>2</sup>	0.089	6	6	138.85	137.32	Complete penetration of bumper, 4.8mm dia. circular hole. 40-50 craters on backup front surface with some dimpling on back, 3-4 near penetrations, 1 did penetrate. 0.02g ejecta and spall collected.	
		Inner Wall	Al 6061-T6	0.032	5.75	5.75	45.21	45.21		
		Standoff Distance		4.000						
992 02-May-86		Bumper	Al 6061-T6 Mass/unit area = 0.0085 lbm/in <sup>2</sup>	0.089	6	6	137.32	137.3	Complete penetration of bumper, 3.5mm dia. circular hole. 30-40 craters on backup front surface with some dimpling on back, but no penetrations or near penetrations. 0.06g ejecta and spall collected.	
		(exactly same as 991)								
		Inner Wall	Al 6061-T6	0.032	5.75	5.75	45.35	45.36		
		Standoff Distance		4.000						



Other Data on JSC Light Gas Gun Shots

JSC Shot #	Projectile					Other		
	Projectile Material	Mass (milligrams)	Diameter (inches)	Length (inches)	Velocity (km/sec)	Impact Photo?	Doc. Photo?	Purpose of Shot
991 Al 6061		4.87	0.0719	0.0297	5.72	No (missed impact)	No	Secondaries test of low energy impact with aluminum projectile on aluminum target using the high-speed camera.
992 Al 6061		5.08	0.0719	0.0309	4.12	No (missed impact)	No	Secondaries test of low energy impact with aluminum projectile on aluminum target using the high-speed camera.



**Appendix A - Listing of All Shots with Characteristics and Notes**

Target Data on JSC Light Gas Gun Shots

JSC Shot #	Date	Target						Damage Notes	
		Target type	Material	Thickness (inches)	Length (inches)	Width (inches)	Mass before (grams)		Mass after (grams)
873	20-Nov-85	Thick plate	Graphite/ Epoxy (generic). Mass/unit area = 0.0380 lbm/in <sup>2</sup>	0.667	6	6			
878	25-Nov-85	Bumper	Fiberglass B86-1, JSC-05A-002	0.094	2.875	2.875	26.04		Small hole, delamination on front-.75"dia., back-1"dia. Small raised bumps on back of plate. Plate was almost penetrated. Some deep craters on front.
		Inner Wall	Aluminum (6061-T6)	0.032	6	5.75			
		Standoff Distance	4.000 Bumper Mass/unit area = 0.0069 lbm/in <sup>2</sup>						
879	26-Nov-85	Bumper	Hybrid Comp. B86-2, JSC-04A-001	0.158	2.875	2.875	34.83		Small hole, visible delamination (.5" dia.). Almost no damage, less than fiberglass only. No craters or bumps.
		Inner Wall	Aluminum (6061-T6)	0.032	6	5.25			
		Standoff Distance	4.000 Bumper Mass/unit area = 0.0093 lbm/in <sup>2</sup>						
881	27-Nov-85	Bumper	Fiberglass(suit) B86-3	0.075	2.875	2.875			Small hole, elliptical delamination,.75" dia. front & back. Some small raised bumps on back, not as many as 878, worse than 765.
		Inner Wall	Aluminum (6061-T6)	0.032	6	5.75			
		Standoff Distance	4.000 Mass/unit area = 0.00529 lbm/in <sup>2</sup>						
883	02-Dec-85	Semi-infinite Plate. Cloth.	Graphite/ Epoxy, AS4/3501-6 JSC-01A-003 Mass/unit area = 0.0315 lbm/in <sup>2</sup>	0.5	6	6	513.69		Circular crater (0.16" dia, 0.15" deep). Front surface noticeably raised around crater, no peelings, small checker-board areas broken away from surface around crater. No penetration (taped back - no spall), slightly raised behind impact point.
884	03-Dec-85	Semi-infinite Plate.	Graphite/ Epoxy, AS4/3501-6	0.5	6	6	510.32		Slightly rectangular crater(0.16 x 0.2" and 0.14" deep). Long

Other Data on JSC Light Gas Gun Shots

JSC Shot #	Projectile				Velocity (km/sec)	Impact Photo?	Doc. Photo?	Other
	Material	Mass (milligrams)	Diameter (inches)	Length (inches)				
975 Nylon	4.60	0.0695	0.066	6.66	Yes (High-Speed Camera)	No	Secondaries test for high-speed film on aluminum target.	
979 Nylon	4.60	0.0694	0.0716	5.4 (Est.)	No	No	Secondaries test to get low energy impact data on aluminum target. High-speed film did not capture impact.	
981 Nylon	4.91	0.0695	0.0696	7.38	Yes High-speed film	No	Secondaries test of high energy impact on this type graphite/epoxy target with high-speed camera capability.	
988 Nylon	4.97	0.0708	0.0747	7.01 (but starts after impact)	Yes High-speed film	No	Secondaries test of high energy impact on this type graphite/epoxy target with high-speed camera capability. Also baselines this type composite.	
990 Nylon	5.02	0.0715	0.0711	6.29	Yes High-speed film	No	Secondaries test of high energy impact on this type graphite/epoxy target at 30 deg. oblique impact, with high-speed camera capability.	



**Appendix B - Raw Data for shots 883,884,894,917,923,933**

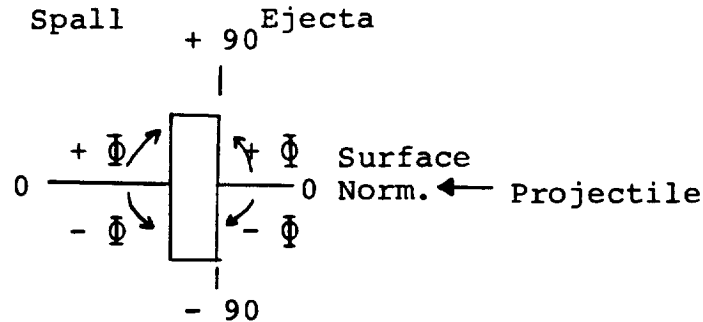
(also includes calculations for theta,phi,  
cone angle, diameter, velocity, energy)

3. Phi angle, Phi (deg), is the angle from the impact point to the ejecta/spall particle in the vertical plane (see diagram). The following equation is for an ejecta particle with the position origin in the lower left-hand corner of a thin plate.

$$\text{Phi} = \text{asin} ((Y - Y_0) / ((Z - Z_0)^2 + (Y - Y_0)^2)^{0.5}) * 180/\text{pi}$$

Side View  
of Target

Y-Z Plane



4. Cone angle, CA (deg), is the angle from the impact point to the ejecta/spall particle. Zero degree cone angle is normal to surface at impact point.

$$\text{CA} = \text{acos} ((Z - Z_0) / R) * 180/\text{pi}$$

5. Particle diameter, D (mm), is determined from the particle density, p (g/cc), and assuming cylindrical particle geometry.

$$D = 2 * (M * 1000 / (\text{pi} * L * p))^{0.5}$$

6. Particle cross-sectional area, A (mm<sup>2</sup>).

$$A = (D/2)^2 * \text{pi}$$

7. Particle velocity, V (km/sec), is derived from particle kinetic energy considerations.

$$V = ( (2 * S_s * (A + (\text{pi} * D * P)) * P / M)^{0.5} ) / 1000$$

8. Particle kinetic energy, KE (joules).

$$\text{KE} = 0.5 * M * V^2 * 1000$$















Measured Values

Calculated Values

Particle No.	X location of impact (origin at *)		Y location of impact (origin at *)		Z location of impact (origin at *)		Penetration Depth	Length of Particle	Mass	R location of impact (origin at **)		Theta location of impact (origin at **)		Phi location of impact (origin at **)		Cone Angle (from normal to surface) (origin at **)	Average Diameter	Average Area	Velocity
	mm	mm	mm	mm	mm	mm				mm	mm	mm	mm	mm	mm				
1	0	73	10	0.8	8.5	0.0003	69.73	-81.75	5.71	81.75	0.17	0.02	0.56						
2	0	76	12	6.1	31	0.0009	70.15	-80.13	18.43	80.15	0.15	0.02	1.48						
3	0	72	18	8	14	0.0005	71.31	-75.38	0.00	75.38	0.17	0.02	2.75						
4	0	67	24	9	56	0.0046	73.23	-70.82	-11.77	70.87	0.26	0.05	1.76						
5	0	84	12	9	27	0.0012	71.06	-80.13	45.00	80.28	0.19	0.03	2.11						
6	0	84	10	4.5	12	0.0002	70.75	-81.75	50.19	81.87	0.12	0.01	2.02						
7	0	86	18	9.5	12.5	0.0008	72.67	-75.38	37.87	75.66	0.23	0.04	1.26						
8	0	89	15	9.5	18	0.0007	72.63	-77.74	48.58	78.08	0.18	0.02	2.82						
9	0	95	19	3.5	77.5	0.0081	75.17	-74.60	50.44	75.36	0.29	0.07	0.39						
10	0	99	32	10	79	0.0115	80.71	-65.12	40.16	66.64	0.34	0.09	1.02						
11	0	102	43	1.5	7	0.0001	86.66	-58.07	34.90	60.25	0.11	0.01	0.31						
12	0	71	35	0.5	7	0.0001	77.38	-63.10	-1.64	63.11	0.11	0.01	0.31						
13	0	67	46	2.5	8	0.0004	83.08	-56.31	-6.20	56.38	0.20	0.03	1.05						
14	0	95	25	7	11	0.0002	76.91	-70.08	42.61	71.03	0.12	0.01	3.21						
15	0	107	56	3.5	10	0.0002	95.51	-50.94	32.01	54.10	0.13	0.01	1.65						
16	0	110	58	3	8	0.0001	97.82	-49.95	33.23	53.64	0.10	0.01	1.77						
17	0	126	58	1	12	0.0004	105.08	-49.95	42.95	56.50	0.16	0.02	0.39						
18	0	136	98	0.5	4.5	0.0001	135.87	-35.15	33.15	43.84	0.13	0.01	0.35						
19	0	125	89	1	4.5	0.0003	124.46	-37.79	30.77	44.35	0.23	0.04	0.53						
20	0	94	27	11	13	0.0004	77.29	-68.63	39.17	69.55	0.16	0.02	4.07						
21	69	144	46	3	4.5	0.0004	85.44	0.00	57.43	57.43	0.27	0.06	1.46						
22	39	144	75	0.5	8	0.0001	108.21	-21.80	43.83	46.12	0.10	0.01	0.30						
23	67	144	77	1	3	0.0001	105.44	-1.49	43.08	43.09	0.16	0.02	0.77						
24	46	144	78	2	3	0.0001	108.61	-16.43	42.71	44.19	0.16	0.02	1.52						
25	28	144	70	3	4	0.0001	108.47	-30.36	45.81	49.81	0.14	0.02	2.11						
26	60	144	75	1.5	3	0.0001	104.36	-6.84	43.83	44.05	0.16	0.02	1.14						
27	95	144	78	0.5	3	0.0001	109.29	18.43	42.71	44.46	0.16	0.02	0.39						
28	100	144	81	2	4	0.0001	112.72	20.94	41.63	44.06	0.14	0.02	1.41						
29	73	144	85	0.5	3	0.0001	111.47	2.69	40.27	40.31	0.16	0.02	0.39						
30	95	144	105	1.5	2.5	0.0003	129.94	13.91	34.44	36.09	0.31	0.08	0.92						
31	56	144	71	1.5	2.5	0.0001	101.95	-10.38	45.40	45.86	0.18	0.03	1.20						
32	0	140	105	2	3.5	0.0002	142.86	-33.31	32.93	42.70	0.21	0.04	1.23						
33	138	83	10	3.5	6	0.0003	70.58	81.75	47.73	81.86	0.20	0.03	1.70						
34	138	84	15	24	32	0.0014	71.62	77.74	38.66	77.91	0.19	0.03	5.17						
35	138	90	40	5	63	0.0131	81.76	59.90	24.23	60.71	0.41	0.13	0.53						
36	138	58	24	5	39	0.0031	74.38	70.82	-30.26	71.18	0.25	0.05	0.85						
37	138	62	33	2	8	0.0004	77.14	64.44	-16.86	64.67	0.20	0.03	0.84						
38	138	62	20	6	18	0.001	72.53	73.84	-26.57	73.99	0.21	0.04	1.63						
39	138	59	29	6	14	0.006	75.97	67.20	-24.15	67.56	0.59	0.27	1.12						
40	138	21	66	1.5	11.5	0.0005	108.25	46.27	-37.69	52.43	0.19	0.03	0.55						
41	122	0	24	1	38	0.0014	92.57	65.64	-71.57	74.97	0.17	0.02	0.21						
42	110	0	28	1	6	0.0011	87.46	55.67	-68.75	71.33	0.38	0.12	0.36						
43	93	0	52	0.5	9.5	0.0001	92.00	74.78	-54.16	55.58	0.09	0.01	0.29						
44	110	55	142	0.01	20	0.0015	148.77	16.11	-6.83	17.36	0.25	0.05	0.01						







Measured Values

Calculated Values

Particle No.	X location of impact (origin at s)	Y location of impact (origin at s)	Z location of impact (origin at s)	Penetration Depth	Length of Particle	Mass	R location of impact (origin at ss)	Theta location of impact (origin at ss)	Phi location of impact (origin at ss)	Diameter Ave. Area
no	no	no	no	no	no	gas	no	Degrees	Degrees	no squared
EJECTA										
1	(Loose on bottom)					47				0.249
2						55				0.227
3						53				0.300
4						31				0.135
5						29				0.140
6		(average of 5)				21				0.157
7						21				0.157
8						21				0.157
9						21				0.157
10						21				0.157
11			(average of approx. 180)			3				0.129
12						3				0.129
13						3				0.129
14						3				0.129
15						3				0.129
16						3				0.129
17						3				0.129
18						3				0.129
19						3				0.129
20						3				0.129
21						3				0.129
22						3				0.129
23						3				0.129
24						3				0.129
25						3				0.129
26						3				0.129
27						3				0.129
28						3				0.129
29						3				0.129
30						3				0.129
31						3				0.129
32						3				0.129
33						3				0.129
34						3				0.129
35						3				0.129
36						3				0.129
37						3				0.129
38						3				0.129
39						3				0.129
40						3				0.129
41						3				0.129

Target 152 x 152 x 2 mm (JSC-02B-003)

Measured Values

Calculated Values

Particle No.	X location of impact (origin at e)			Y location of impact (origin at e)			Z location of impact (origin at e)			Penetration Depth	Length of Particle	Mass	R location of impact (origin at ee)			Theta location of impact (origin at ee)			Phi location of impact (origin at ee)			Cone Angle (from normal to surface) (origin at ee)	Average Diameter	Average Area	Velocity
	mm	mm	mm	mm	mm	mm	mm	mm	mm				mm	mm	mm	mm	mm	mm	mm	mm	mm				
179	.	.	.	.	.	.	.	.	.	.	3.5	0.00015	0.00	-90.00	-90.00	0	0.19	0.03	0.00	0.00	0.00	0.00	0.00	0.00	0.00
180	.	.	.	.	.	.	.	.	.	.	3.5	0.00015	0.00	-90.00	-90.00	0	0.19	0.03	0.00	0.00	0.00	0.00	0.00	0.00	0.00
181	.	.	.	.	.	.	.	.	.	.	3.5	0.00015	0.00	-90.00	-90.00	0	0.19	0.03	0.00	0.00	0.00	0.00	0.00	0.00	0.00
182	.	.	.	.	.	.	.	.	.	.	3.5	0.00015	0.00	-90.00	-90.00	0	0.19	0.03	0.00	0.00	0.00	0.00	0.00	0.00	0.00
183	.	.	.	.	.	.	.	.	.	.	3.5	0.00015	0.00	-90.00	-90.00	0	0.19	0.03	0.00	0.00	0.00	0.00	0.00	0.00	0.00
184	.	.	.	.	.	.	.	.	.	.	3.5	0.00015	0.00	-90.00	-90.00	0	0.19	0.03	0.00	0.00	0.00	0.00	0.00	0.00	0.00
185	.	.	.	.	.	.	.	.	.	.	3.5	0.00015	0.00	-90.00	-90.00	0	0.19	0.03	0.00	0.00	0.00	0.00	0.00	0.00	0.00
186	.	.	.	.	.	.	.	.	.	.	3.5	0.00015	0.00	-90.00	-90.00	0	0.19	0.03	0.00	0.00	0.00	0.00	0.00	0.00	0.00
187	.	.	.	.	.	.	.	.	.	.	3.5	0.00015	0.00	-90.00	-90.00	0	0.19	0.03	0.00	0.00	0.00	0.00	0.00	0.00	0.00
188	.	.	.	.	.	.	.	.	.	.	3.5	0.00015	0.00	-90.00	-90.00	0	0.19	0.03	0.00	0.00	0.00	0.00	0.00	0.00	0.00
189	.	.	.	.	.	.	.	.	.	.	3.5	0.00015	0.00	-90.00	-90.00	0	0.19	0.03	0.00	0.00	0.00	0.00	0.00	0.00	0.00
190	.	.	.	.	.	.	.	.	.	.	3.5	0.00015	0.00	-90.00	-90.00	0	0.19	0.03	0.00	0.00	0.00	0.00	0.00	0.00	0.00
191	.	.	.	.	.	.	.	.	.	.	3.5	0.00015	0.00	-90.00	-90.00	0	0.19	0.03	0.00	0.00	0.00	0.00	0.00	0.00	0.00
192	.	.	.	.	.	.	.	.	.	.	3.5	0.00015	0.00	-90.00	-90.00	0	0.19	0.03	0.00	0.00	0.00	0.00	0.00	0.00	0.00
193	.	.	.	.	.	.	.	.	.	.	3.5	0.00015	0.00	-90.00	-90.00	0	0.19	0.03	0.00	0.00	0.00	0.00	0.00	0.00	0.00
194	.	.	.	.	.	.	.	.	.	.	3.5	0.00015	0.00	-90.00	-90.00	0	0.19	0.03	0.00	0.00	0.00	0.00	0.00	0.00	0.00

Total = 0.09655

Combined measured (less circled particles) 0.0861

Combined measured (compensated for circled particles) 0.0923

Total from mass of target before & after 0.195

Ejecta collected at bottom of target chamber 0.030

Total expected in styrofoam catcher 0.165

Total calc. small particles (dust) 0.06845

35.1% Percent of Total

Origin e, At lower left hand corner of box on the open end.

Origin ee, At center of open end  
 X, mm 69  
 Y, mm 72  
 Z, mm 0

Shear Strength (Estimated) used in velocity calculation, M Pascals 55

Particle No.	Measured Values					Calculated Values					
	X location of impact (origin at s)	Y location of impact (origin at s)	Z location of impact (origin at s)	Penetration Depth	Length of Particle	Mass	R location of impact (origin at s)	Theta location of impact (origin at s)	Phi location of impact (origin at s)	Diameter Ave. Area	
86	00	00	00	00	00	3 0.0000616667	00	00	00	0.129	0.013
87	00	00	00	00	00	3 0.0000616667	00	00	00	0.129	0.013
88	00	00	00	00	00	3 0.0000616667	00	00	00	0.129	0.013
89	00	00	00	00	00	3 0.0000616667	00	00	00	0.129	0.013
90	00	00	00	00	00	3 0.0000616667	00	00	00	0.129	0.013
91	00	00	00	00	00	3 0.0000616667	00	00	00	0.129	0.013
92	00	00	00	00	00	3 0.0000616667	00	00	00	0.129	0.013
93	00	00	00	00	00	3 0.0000616667	00	00	00	0.129	0.013
94	00	00	00	00	00	3 0.0000616667	00	00	00	0.129	0.013
95	00	00	00	00	00	3 0.0000616667	00	00	00	0.129	0.013
96	00	00	00	00	00	3 0.0000616667	00	00	00	0.129	0.013
97	00	00	00	00	00	3 0.0000616667	00	00	00	0.129	0.013
98	00	00	00	00	00	3 0.0000616667	00	00	00	0.129	0.013
99	00	00	00	00	00	3 0.0000616667	00	00	00	0.129	0.013
100	00	00	00	00	00	3 0.0000616667	00	00	00	0.129	0.013
101	00	00	00	00	00	3 0.0000616667	00	00	00	0.129	0.013
102	00	00	00	00	00	3 0.0000616667	00	00	00	0.129	0.013
103	00	00	00	00	00	3 0.0000616667	00	00	00	0.129	0.013
104	00	00	00	00	00	3 0.0000616667	00	00	00	0.129	0.013
105	00	00	00	00	00	3 0.0000616667	00	00	00	0.129	0.013
106	00	00	00	00	00	3 0.0000616667	00	00	00	0.129	0.013
107	00	00	00	00	00	3 0.0000616667	00	00	00	0.129	0.013
108	00	00	00	00	00	3 0.0000616667	00	00	00	0.129	0.013
109	00	00	00	00	00	3 0.0000616667	00	00	00	0.129	0.013
110	00	00	00	00	00	3 0.0000616667	00	00	00	0.129	0.013
111	00	00	00	00	00	3 0.0000616667	00	00	00	0.129	0.013
112	00	00	00	00	00	3 0.0000616667	00	00	00	0.129	0.013
113	00	00	00	00	00	3 0.0000616667	00	00	00	0.129	0.013
114	00	00	00	00	00	3 0.0000616667	00	00	00	0.129	0.013
115	00	00	00	00	00	3 0.0000616667	00	00	00	0.129	0.013
116	00	00	00	00	00	3 0.0000616667	00	00	00	0.129	0.013
117	00	00	00	00	00	3 0.0000616667	00	00	00	0.129	0.013
118	00	00	00	00	00	3 0.0000616667	00	00	00	0.129	0.013
119	00	00	00	00	00	3 0.0000616667	00	00	00	0.129	0.013
120	00	00	00	00	00	3 0.0000616667	00	00	00	0.129	0.013
121	00	00	00	00	00	3 0.0000616667	00	00	00	0.129	0.013
122	00	00	00	00	00	3 0.0000616667	00	00	00	0.129	0.013
123	00	00	00	00	00	3 0.0000616667	00	00	00	0.129	0.013
124	00	00	00	00	00	3 0.0000616667	00	00	00	0.129	0.013
125	00	00	00	00	00	3 0.0000616667	00	00	00	0.129	0.013
126	00	00	00	00	00	3 0.0000616667	00	00	00	0.129	0.013
127	00	00	00	00	00	3 0.0000616667	00	00	00	0.129	0.013
128	00	00	00	00	00	3 0.0000616667	00	00	00	0.129	0.013
129	00	00	00	00	00	3 0.0000616667	00	00	00	0.129	0.013

Measured Values

Calculated Values

Particle No.	Measured Values				Calculated Values						
	X location of impact (origin at *)	Y location of impact (origin at *)	Z location of impact (origin at *)	Penetration Depth	Length of Particle	Mass	R location of impact (origin at *)	Theta location of impact (origin at *)	Phi location of impact (origin at *)	Diameter Ave. Area	
42	00	00	00	00	00	gms	00	00	00	0.129	0.013
43	00	00	00	00	00	3 0.0000616667	00	00	00	0.129	0.013
44	00	00	00	00	00	3 0.0000616667	00	00	00	0.129	0.013
45	00	00	00	00	00	3 0.0000616667	00	00	00	0.129	0.013
46	00	00	00	00	00	3 0.0000616667	00	00	00	0.129	0.013
47	00	00	00	00	00	3 0.0000616667	00	00	00	0.129	0.013
48	00	00	00	00	00	3 0.0000616667	00	00	00	0.129	0.013
49	00	00	00	00	00	3 0.0000616667	00	00	00	0.129	0.013
50	00	00	00	00	00	3 0.0000616667	00	00	00	0.129	0.013
51	00	00	00	00	00	3 0.0000616667	00	00	00	0.129	0.013
52	00	00	00	00	00	3 0.0000616667	00	00	00	0.129	0.013
53	00	00	00	00	00	3 0.0000616667	00	00	00	0.129	0.013
54	00	00	00	00	00	3 0.0000616667	00	00	00	0.129	0.013
55	00	00	00	00	00	3 0.0000616667	00	00	00	0.129	0.013
56	00	00	00	00	00	3 0.0000616667	00	00	00	0.129	0.013
57	00	00	00	00	00	3 0.0000616667	00	00	00	0.129	0.013
58	00	00	00	00	00	3 0.0000616667	00	00	00	0.129	0.013
59	00	00	00	00	00	3 0.0000616667	00	00	00	0.129	0.013
60	00	00	00	00	00	3 0.0000616667	00	00	00	0.129	0.013
61	00	00	00	00	00	3 0.0000616667	00	00	00	0.129	0.013
62	00	00	00	00	00	3 0.0000616667	00	00	00	0.129	0.013
63	00	00	00	00	00	3 0.0000616667	00	00	00	0.129	0.013
64	00	00	00	00	00	3 0.0000616667	00	00	00	0.129	0.013
65	00	00	00	00	00	3 0.0000616667	00	00	00	0.129	0.013
66	00	00	00	00	00	3 0.0000616667	00	00	00	0.129	0.013
67	00	00	00	00	00	3 0.0000616667	00	00	00	0.129	0.013
68	00	00	00	00	00	3 0.0000616667	00	00	00	0.129	0.013
69	00	00	00	00	00	3 0.0000616667	00	00	00	0.129	0.013
70	00	00	00	00	00	3 0.0000616667	00	00	00	0.129	0.013
71	00	00	00	00	00	3 0.0000616667	00	00	00	0.129	0.013
72	00	00	00	00	00	3 0.0000616667	00	00	00	0.129	0.013
73	00	00	00	00	00	3 0.0000616667	00	00	00	0.129	0.013
74	00	00	00	00	00	3 0.0000616667	00	00	00	0.129	0.013
75	00	00	00	00	00	3 0.0000616667	00	00	00	0.129	0.013
76	00	00	00	00	00	3 0.0000616667	00	00	00	0.129	0.013
77	00	00	00	00	00	3 0.0000616667	00	00	00	0.129	0.013
78	00	00	00	00	00	3 0.0000616667	00	00	00	0.129	0.013
79	00	00	00	00	00	3 0.0000616667	00	00	00	0.129	0.013
80	00	00	00	00	00	3 0.0000616667	00	00	00	0.129	0.013
81	00	00	00	00	00	3 0.0000616667	00	00	00	0.129	0.013
82	00	00	00	00	00	3 0.0000616667	00	00	00	0.129	0.013
83	00	00	00	00	00	3 0.0000616667	00	00	00	0.129	0.013
84	00	00	00	00	00	3 0.0000616667	00	00	00	0.129	0.013
85	00	00	00	00	00	3 0.0000616667	00	00	00	0.129	0.013

Measured Values

Calculated Values

Particle No.	Measured Values					Calculated Values					
	X location of impact (origin at s)	Y location of impact (origin at s)	Z location of impact (origin at s)	Penetration Depth	Length of Particle	Mass	R location of impact (origin at s)	Theta location of impact (origin at s)	Phi location of impact (origin at s)	Diameter Ave. Area	
	mm	mm	mm	mm	mm	gms	mm	Degrees	Degrees	mm	mm squared
174	.	.	.	.	.	3 0.0000616667	0.129	0.013	0.129	0.013	
175	.	.	.	.	.	3 0.0000616667	0.129	0.013	0.129	0.013	
176	.	.	.	.	.	3 0.0000616667	0.129	0.013	0.129	0.013	
177	.	.	.	.	.	3 0.0000616667	0.129	0.013	0.129	0.013	
178	.	.	.	.	.	3 0.0000616667	0.129	0.013	0.129	0.013	
179	.	.	.	.	.	3 0.0000616667	0.129	0.013	0.129	0.013	
180	.	.	.	.	.	3 0.0000616667	0.129	0.013	0.129	0.013	
181	.	.	.	.	.	3 0.0000616667	0.129	0.013	0.129	0.013	
182	.	.	.	.	.	3 0.0000616667	0.129	0.013	0.129	0.013	
183	.	.	.	.	.	3 0.0000616667	0.129	0.013	0.129	0.013	
184	.	.	.	.	.	3 0.0000616667	0.129	0.013	0.129	0.013	
185	.	.	.	.	.	3 0.0000616667	0.129	0.013	0.129	0.013	
186	.	.	.	.	.	3 0.0000616667	0.129	0.013	0.129	0.013	
187	.	.	.	.	.	3 0.0000616667	0.129	0.013	0.129	0.013	
188	.	.	.	.	.	3 0.0000616667	0.129	0.013	0.129	0.013	
189	.	.	.	.	.	3 0.0000616667	0.129	0.013	0.129	0.013	
190	.	.	.	.	.	3 0.0000616667	0.129	0.013	0.129	0.013	
191	(Ejecta under catcher, total 0.0033 g)						15 0.00018	0.098	0.008	0.098	0.008
192	(average of 5)						15 0.00018	0.098	0.008	0.098	0.008
193	.	.	.	.	.	15 0.00018	0.098	0.008	0.098	0.008	
194	.	.	.	.	.	15 0.00018	0.098	0.008	0.098	0.008	
195	.	.	.	.	.	15 0.00018	0.098	0.008	0.098	0.008	
196	.	.	.	.	.	2 0.00006	0.156	0.019	0.156	0.019	
197	.	.	.	.	.	2 0.00006	0.156	0.019	0.156	0.019	
198	.	.	.	.	.	2 0.00006	0.156	0.019	0.156	0.019	
199	.	.	.	.	.	2 0.00006	0.156	0.019	0.156	0.019	
200	.	.	.	.	.	2 0.00006	0.156	0.019	0.156	0.019	
201	.	.	.	.	.	2 0.00006	0.156	0.019	0.156	0.019	
202	.	.	.	.	.	2 0.00006	0.156	0.019	0.156	0.019	
203	.	.	.	.	.	2 0.00006	0.156	0.019	0.156	0.019	
204	.	.	.	.	.	2 0.00006	0.156	0.019	0.156	0.019	
205	.	.	.	.	.	2 0.00006	0.156	0.019	0.156	0.019	
206	.	.	.	.	.	2 0.00006	0.156	0.019	0.156	0.019	
207	.	.	.	.	.	2 0.00006	0.156	0.019	0.156	0.019	
208	.	.	.	.	.	2 0.00006	0.156	0.019	0.156	0.019	
209	.	.	.	.	.	2 0.00006	0.156	0.019	0.156	0.019	
210	.	.	.	.	.	2 0.00006	0.156	0.019	0.156	0.019	
211	.	.	.	.	.	2 0.00006	0.156	0.019	0.156	0.019	
212	.	.	.	.	.	2 0.00006	0.156	0.019	0.156	0.019	
213	.	.	.	.	.	2 0.00006	0.156	0.019	0.156	0.019	
214	.	.	.	.	.	2 0.00006	0.156	0.019	0.156	0.019	
215	.	.	.	.	.	2 0.00006	0.156	0.019	0.156	0.019	
216	.	.	.	.	.	2 0.00006	0.156	0.019	0.156	0.019	
217	.	.	.	.	.	2 0.00006	0.156	0.019	0.156	0.019	

Measured Values

Calculated Values

Particle No.	X location of impact (origin at e)	Y location of impact (origin at e)	Z location of impact (origin at e)	Penetration Depth	Length of Particle	Mass	R location of impact (origin at ee)	Theta location of impact (origin at ee)	Phi location of impact (origin at ee)	Diameter Ave. Area
	mm	mm	mm	mm	mm	gms	mm	Degrees	Degrees	mm squared
130	.	.	.	0.0000616667	3	0.0000616667	0.129	0.013	0.129	0.013
131	.	.	.	0.0000616667	3	0.0000616667	0.129	0.013	0.129	0.013
132	.	.	.	0.0000616667	3	0.0000616667	0.129	0.013	0.129	0.013
133	.	.	.	0.0000616667	3	0.0000616667	0.129	0.013	0.129	0.013
134	.	.	.	0.0000616667	3	0.0000616667	0.129	0.013	0.129	0.013
135	.	.	.	0.0000616667	3	0.0000616667	0.129	0.013	0.129	0.013
136	.	.	.	0.0000616667	3	0.0000616667	0.129	0.013	0.129	0.013
137	.	.	.	0.0000616667	3	0.0000616667	0.129	0.013	0.129	0.013
138	.	.	.	0.0000616667	3	0.0000616667	0.129	0.013	0.129	0.013
139	.	.	.	0.0000616667	3	0.0000616667	0.129	0.013	0.129	0.013
140	.	.	.	0.0000616667	3	0.0000616667	0.129	0.013	0.129	0.013
141	.	.	.	0.0000616667	3	0.0000616667	0.129	0.013	0.129	0.013
142	.	.	.	0.0000616667	3	0.0000616667	0.129	0.013	0.129	0.013
143	.	.	.	0.0000616667	3	0.0000616667	0.129	0.013	0.129	0.013
144	.	.	.	0.0000616667	3	0.0000616667	0.129	0.013	0.129	0.013
145	.	.	.	0.0000616667	3	0.0000616667	0.129	0.013	0.129	0.013
146	.	.	.	0.0000616667	3	0.0000616667	0.129	0.013	0.129	0.013
147	.	.	.	0.0000616667	3	0.0000616667	0.129	0.013	0.129	0.013
148	.	.	.	0.0000616667	3	0.0000616667	0.129	0.013	0.129	0.013
149	.	.	.	0.0000616667	3	0.0000616667	0.129	0.013	0.129	0.013
150	.	.	.	0.0000616667	3	0.0000616667	0.129	0.013	0.129	0.013
151	.	.	.	0.0000616667	3	0.0000616667	0.129	0.013	0.129	0.013
152	.	.	.	0.0000616667	3	0.0000616667	0.129	0.013	0.129	0.013
153	.	.	.	0.0000616667	3	0.0000616667	0.129	0.013	0.129	0.013
154	.	.	.	0.0000616667	3	0.0000616667	0.129	0.013	0.129	0.013
155	.	.	.	0.0000616667	3	0.0000616667	0.129	0.013	0.129	0.013
156	.	.	.	0.0000616667	3	0.0000616667	0.129	0.013	0.129	0.013
157	.	.	.	0.0000616667	3	0.0000616667	0.129	0.013	0.129	0.013
158	.	.	.	0.0000616667	3	0.0000616667	0.129	0.013	0.129	0.013
159	.	.	.	0.0000616667	3	0.0000616667	0.129	0.013	0.129	0.013
160	.	.	.	0.0000616667	3	0.0000616667	0.129	0.013	0.129	0.013
161	.	.	.	0.0000616667	3	0.0000616667	0.129	0.013	0.129	0.013
162	.	.	.	0.0000616667	3	0.0000616667	0.129	0.013	0.129	0.013
163	.	.	.	0.0000616667	3	0.0000616667	0.129	0.013	0.129	0.013
164	.	.	.	0.0000616667	3	0.0000616667	0.129	0.013	0.129	0.013
165	.	.	.	0.0000616667	3	0.0000616667	0.129	0.013	0.129	0.013
166	.	.	.	0.0000616667	3	0.0000616667	0.129	0.013	0.129	0.013
167	.	.	.	0.0000616667	3	0.0000616667	0.129	0.013	0.129	0.013
168	.	.	.	0.0000616667	3	0.0000616667	0.129	0.013	0.129	0.013
169	.	.	.	0.0000616667	3	0.0000616667	0.129	0.013	0.129	0.013
170	.	.	.	0.0000616667	3	0.0000616667	0.129	0.013	0.129	0.013
171	.	.	.	0.0000616667	3	0.0000616667	0.129	0.013	0.129	0.013
172	.	.	.	0.0000616667	3	0.0000616667	0.129	0.013	0.129	0.013
173	.	.	.	0.0000616667	3	0.0000616667	0.129	0.013	0.129	0.013

Measured Values

Calculated Values

Particle No.	Measured Values				Calculated Values						
	X location of impact (origin at *)	Y location of impact (origin at *)	Z location of impact (origin at *)	Penetration Depth	Length of Particle	Mass	R location of impact (origin at *)	Theta location of impact (origin at *)	Phi location of impact (origin at *)	Ave. Diameter	Ave. Area
	mm	mm	mm	mm	mm	gms	mm	Degrees	Degrees	mm	mm squared
261	.	.	.	.	3	0.0001	0.164	0.021	0.164	0.021	0.164
262	.	.	.	.	3	0.0001	0.164	0.021	0.164	0.021	0.164
263	.	.	.	.	3	0.0001	0.164	0.021	0.164	0.021	0.164
264	.	.	.	.	3	0.0001	0.164	0.021	0.164	0.021	0.164
265	.	.	.	.	3	0.0001	0.164	0.021	0.164	0.021	0.164
266	.	.	.	.	3	0.0001	0.164	0.021	0.164	0.021	0.164
267	.	.	.	.	3	0.0001	0.164	0.021	0.164	0.021	0.164
268	.	.	.	.	3	0.0001	0.164	0.021	0.164	0.021	0.164
269	.	.	.	.	3	0.0001	0.164	0.021	0.164	0.021	0.164
270	.	.	.	.	3	0.0001	0.164	0.021	0.164	0.021	0.164
271	.	.	.	.	3	0.0001	0.164	0.021	0.164	0.021	0.164
272	.	.	.	.	3	0.0001	0.164	0.021	0.164	0.021	0.164
273	.	.	.	.	3	0.0001	0.164	0.021	0.164	0.021	0.164
274	.	.	.	.	3	0.0001	0.164	0.021	0.164	0.021	0.164
275	.	.	.	.	3	0.0001	0.164	0.021	0.164	0.021	0.164
276	.	.	.	.	3	0.0001	0.164	0.021	0.164	0.021	0.164
277	.	.	.	.	3	0.0001	0.164	0.021	0.164	0.021	0.164
278	.	.	.	.	3	0.0001	0.164	0.021	0.164	0.021	0.164
279	.	.	.	.	3	0.0001	0.164	0.021	0.164	0.021	0.164
280	.	.	.	.	3	0.0001	0.164	0.021	0.164	0.021	0.164
281	.	.	.	.	3	0.0001	0.164	0.021	0.164	0.021	0.164
Total Ejecta						0.039					

SPALL (total less spall behind & in catcher = .0447 g)

1 (Loose on Bottom)	0.0447	0.191	0.029
2	0.0034	0.217	0.037
3	0.0035	0.201	0.032
4	0.0016	0.124	0.012
5	0.0008	0.053	0.002
6	0.0001	0.156	0.019
7	0.0009	0.182	0.026
8	0.0016	0.083	0.005
9	0.0005	0.088	0.006
10	0.0005	0.189	0.028
11	0.0003	0.083	0.005
12	0.0004	0.095	0.007
13 (average of 6)	0.0007333333	0.151	0.018
14	0.0007333333	0.151	0.018
15	0.0007333333	0.151	0.018
16	0.0007333333	0.151	0.018
17	0.0007333333	0.151	0.018
18	0.0007333333	0.151	0.018
19 (average of 17)	0.0003	0.119	0.011



Measured Values

Calculated Values

Particle No.	X location of impact (origin at s)	Y location of impact (origin at s)	Z location of impact (origin at s)	Penetration Depth	Length of Particle	Mass	R location of impact (origin at ss)	Theta location of impact (origin at ss)	Phi location of impact (origin at ss)	Diameter Ave. Area
	mm	mm	mm	mm	mm	gms	mm	Degrees	Degrees	mm squared
218	.	.	.	.	.	2	0.00006			0.156
219	.	.	.	.	.	2	0.00006			0.156
220	.	.	.	.	.	2	0.00006			0.156
221	.	.	.	.	.	2	0.00006			0.156
222	.	.	.	.	.	2	0.00006			0.156
223	.	.	.	.	.	2	0.00006			0.156
224	.	.	.	.	.	2	0.00006			0.156
225	.	.	.	.	.	2	0.00006			0.156
226	.	.	.	.	.	2	0.00006			0.156
227	.	.	.	.	.	2	0.00006			0.156
228	.	.	.	.	.	2	0.00006			0.156
229	.	.	.	.	.	2	0.00006			0.156
230	.	.	.	.	.	2	0.00006			0.156
231	.	.	.	.	.	2	0.00006			0.156
232	.	.	.	.	.	2	0.00006			0.156
233	.	.	.	.	.	2	0.00006			0.156
234	.	.	.	.	.	2	0.00006			0.156
235	.	.	.	.	.	2	0.00006			0.156
Ejecta in catcher (170 x 165 mm) origin at lower left looking at catcher										
236	88	124	100			52	0.0025			0.197
237	.	.	.			3	0.0001	108.31	1.72	0.030
238	.	.	.			3	0.0001		22.54	0.021
239	.	.	.			3	0.0001			0.164
240	.	.	.			3	0.0001			0.164
241	.	.	.			3	0.0001			0.164
242	.	.	.			3	0.0001			0.164
243	.	.	.			3	0.0001			0.164
244	.	.	.			3	0.0001			0.164
245	.	.	.			3	0.0001			0.164
246	.	.	.			3	0.0001			0.164
247	.	.	.			3	0.0001			0.164
248	.	.	.			3	0.0001			0.164
249	.	.	.			3	0.0001			0.164
250	.	.	.			3	0.0001			0.164
251	.	.	.			3	0.0001			0.164
252	.	.	.			3	0.0001			0.164
253	.	.	.			3	0.0001			0.164
254	.	.	.			3	0.0001			0.164
255	.	.	.			3	0.0001			0.164
256	.	.	.			3	0.0001			0.164
257	.	.	.			3	0.0001			0.164
258	.	.	.			3	0.0001			0.164
259	.	.	.			3	0.0001			0.164
260	.	.	.			3	0.0001			0.164

Particle No.	Measured Values					Calculated Values				
	X location of impact (origin at e)	Y location of impact (origin at e)	Z location of impact (origin at e)	Penetration Depth	Length of Particle	Mass	R location of impact (origin at es)	Theta location of impact (origin at es)	Phi location of impact (origin at es)	Diameter Ave. Area
	mm	mm	mm	mm	mm	gms	mm	Degrees	Degrees	mm squared
64	.	.	.	0.0006625	4	0.0006625	0.116	0.010	0.010	0.010
65	.	.	.	0.0006625	4	0.0006625	0.116	0.010	0.010	0.010
66	.	.	.	0.0006625	4	0.0006625	0.116	0.010	0.010	0.010
67	.	.	.	0.0006625	4	0.0006625	0.116	0.010	0.010	0.010
68	.	.	.	0.0006625	4	0.0006625	0.116	0.010	0.010	0.010
69	.	.	.	0.0006625	4	0.0006625	0.116	0.010	0.010	0.010
70	.	.	.	0.0006625	4	0.0006625	0.116	0.010	0.010	0.010
71	.	.	.	0.0006625	4	0.0006625	0.116	0.010	0.010	0.010
72	.	.	.	0.0006625	4	0.0006625	0.116	0.010	0.010	0.010
73	.	.	.	0.0006625	4	0.0006625	0.116	0.010	0.010	0.010
74	.	.	.	0.0006625	4	0.0006625	0.116	0.010	0.010	0.010
75	.	.	.	0.0006625	4	0.0006625	0.116	0.010	0.010	0.010
76	.	.	.	0.0006625	4	0.0006625	0.116	0.010	0.010	0.010
77	.	.	.	0.0006625	4	0.0006625	0.116	0.010	0.010	0.010
78	.	.	.	0.0006625	4	0.0006625	0.116	0.010	0.010	0.010
79	.	.	.	0.0006625	4	0.0006625	0.116	0.010	0.010	0.010
80	.	.	.	0.0006625	4	0.0006625	0.116	0.010	0.010	0.010
81	.	.	.	0.0006625	4	0.0006625	0.116	0.010	0.010	0.010
82	.	.	.	0.0006625	4	0.0006625	0.116	0.010	0.010	0.010
83	.	.	.	0.0006625	4	0.0006625	0.116	0.010	0.010	0.010
84	.	.	.	0.0006625	4	0.0006625	0.116	0.010	0.010	0.010
85	.	.	.	0.0006625	4	0.0006625	0.116	0.010	0.010	0.010
86	.	.	.	0.0006625	4	0.0006625	0.116	0.010	0.010	0.010
87	.	.	.	0.0006625	4	0.0006625	0.116	0.010	0.010	0.010
88	.	.	.	0.0006625	4	0.0006625	0.116	0.010	0.010	0.010
89	.	.	.	0.0006625	4	0.0006625	0.116	0.010	0.010	0.010
90	.	.	.	0.0006625	4	0.0006625	0.116	0.010	0.010	0.010
91	.	.	.	0.0006625	4	0.0006625	0.116	0.010	0.010	0.010
92	.	.	.	0.0006625	4	0.0006625	0.116	0.010	0.010	0.010
93	.	.	.	0.0006625	4	0.0006625	0.116	0.010	0.010	0.010
94	.	.	.	0.0006625	4	0.0006625	0.116	0.010	0.010	0.010
95	.	.	.	0.0006625	4	0.0006625	0.116	0.010	0.010	0.010
96	.	.	.	0.0006625	4	0.0006625	0.116	0.010	0.010	0.010
97	.	.	.	0.0006625	4	0.0006625	0.116	0.010	0.010	0.010
98	.	.	.	0.0006625	4	0.0006625	0.116	0.010	0.010	0.010
99	.	.	.	0.0006625	4	0.0006625	0.116	0.010	0.010	0.010
100	.	.	.	0.0006625	4	0.0006625	0.116	0.010	0.010	0.010
101	.	.	.	0.0006625	4	0.0006625	0.116	0.010	0.010	0.010
102	.	.	.	0.0006625	4	0.0006625	0.116	0.010	0.010	0.010
103	.	.	.	0.0006625	4	0.0006625	0.116	0.010	0.010	0.010
104	.	.	.	0.0006625	4	0.0006625	0.116	0.010	0.010	0.010
105	.	.	.	0.0006625	4	0.0006625	0.116	0.010	0.010	0.010
106	.	.	.	0.0006625	4	0.0006625	0.116	0.010	0.010	0.010
107	.	.	.	0.0006625	4	0.0006625	0.116	0.010	0.010	0.010

Measured Values

Calculated Values

Particle No.	Measured Values				Calculated Values						
	X location of impact (origin at s)	Y location of impact (origin at s)	Z location of impact (origin at s)	Penetration Depth	Length of Particle	Mass	R location of impact (origin at ss)	Theta location of impact (origin at ss)	Phi location of impact (origin at ss)	Diameter Ave. Area	
20	..	..	..	..	..	0.0003	..	..	..	0.119	0.011
21	..	..	..	..	..	0.0003	..	..	..	0.119	0.011
22	..	..	..	..	..	0.0003	..	..	..	0.119	0.011
23	..	..	..	..	..	0.0003	..	..	..	0.119	0.011
24	..	..	..	..	..	0.0003	..	..	..	0.119	0.011
25	..	..	..	..	..	0.0003	..	..	..	0.119	0.011
26	..	..	..	..	..	0.0003	..	..	..	0.119	0.011
27	..	..	..	..	..	0.0003	..	..	..	0.119	0.011
28	..	..	..	..	..	0.0003	..	..	..	0.119	0.011
29	..	..	..	..	..	0.0003	..	..	..	0.119	0.011
30	..	..	..	..	..	0.0003	..	..	..	0.119	0.011
31	..	..	..	..	..	0.0003	..	..	..	0.119	0.011
32	..	..	..	..	..	0.0003	..	..	..	0.119	0.011
33	..	..	..	..	..	0.0003	..	..	..	0.119	0.011
34	..	..	..	..	..	0.0003	..	..	..	0.119	0.011
35	..	..	..	..	..	0.0003	..	..	..	0.119	0.011
36	..	..	..	..	..	0.0006625	..	..	..	0.116	0.010
37	..	..	..	..	..	0.0006625	..	..	..	0.116	0.010
38	..	..	..	..	..	0.0006625	..	..	..	0.116	0.010
39	..	..	..	..	..	0.0006625	..	..	..	0.116	0.010
40	..	..	..	..	..	0.0006625	..	..	..	0.116	0.010
41	..	..	..	..	..	0.0006625	..	..	..	0.116	0.010
42	..	..	..	..	..	0.0006625	..	..	..	0.116	0.010
43	..	..	..	..	..	0.0006625	..	..	..	0.116	0.010
44	..	..	..	..	..	0.0006625	..	..	..	0.116	0.010
45	..	..	..	..	..	0.0006625	..	..	..	0.116	0.010
46	..	..	..	..	..	0.0006625	..	..	..	0.116	0.010
47	..	..	..	..	..	0.0006625	..	..	..	0.116	0.010
48	..	..	..	..	..	0.0006625	..	..	..	0.116	0.010
49	..	..	..	..	..	0.0006625	..	..	..	0.116	0.010
50	..	..	..	..	..	0.0006625	..	..	..	0.116	0.010
51	..	..	..	..	..	0.0006625	..	..	..	0.116	0.010
52	..	..	..	..	..	0.0006625	..	..	..	0.116	0.010
53	..	..	..	..	..	0.0006625	..	..	..	0.116	0.010
54	..	..	..	..	..	0.0006625	..	..	..	0.116	0.010
55	..	..	..	..	..	0.0006625	..	..	..	0.116	0.010
56	..	..	..	..	..	0.0006625	..	..	..	0.116	0.010
57	..	..	..	..	..	0.0006625	..	..	..	0.116	0.010
58	..	..	..	..	..	0.0006625	..	..	..	0.116	0.010
59	..	..	..	..	..	0.0006625	..	..	..	0.116	0.010
60	..	..	..	..	..	0.0006625	..	..	..	0.116	0.010
61	..	..	..	..	..	0.0006625	..	..	..	0.116	0.010
62	..	..	..	..	..	0.0006625	..	..	..	0.116	0.010
63	..	..	..	..	..	0.0006625	..	..	..	0.116	0.010

JSC Shot No. 894

(Thin Plate) 12/17/85

Measured Values

Calculated Values

Particle No.	X location of impact (origin at e) (origin at e)	Y location of impact (origin at e) (origin at e)	Z location of impact (origin at e) (origin at e)	Penetration Depth	Length of Particle	Mass	R location of impact (origin at ee) (origin at ee)	Theta location of impact (origin at ee) (origin at ee)	Phi location of impact (origin at ee) (origin at ee)	Diameter	Ave. Area
	mm	mm	mm	mm	mm	gms	mm	Degrees	Degrees	mm	mm squared
152	.	.	.	.	.	4 0.00006625	mm	Degrees	Degrees	mm	mm squared
153	.	.	.	.	.	4 0.00006625	mm	Degrees	Degrees	mm	mm squared
154	.	.	.	.	.	4 0.00006625	mm	Degrees	Degrees	mm	mm squared
155	.	.	.	.	.	4 0.00006625	mm	Degrees	Degrees	mm	mm squared
156	.	.	.	.	.	4 0.00006625	mm	Degrees	Degrees	mm	mm squared
157	.	.	.	.	.	4 0.00006625	mm	Degrees	Degrees	mm	mm squared
158	.	.	.	.	.	4 0.00006625	mm	Degrees	Degrees	mm	mm squared
159	.	.	.	.	.	4 0.00006625	mm	Degrees	Degrees	mm	mm squared
160	.	.	.	.	.	4 0.00006625	mm	Degrees	Degrees	mm	mm squared
161	.	.	.	.	.	4 0.00006625	mm	Degrees	Degrees	mm	mm squared
162	.	.	.	.	.	4 0.00006625	mm	Degrees	Degrees	mm	mm squared
163	.	.	.	.	.	4 0.00006625	mm	Degrees	Degrees	mm	mm squared
164	.	.	.	.	.	4 0.00006625	mm	Degrees	Degrees	mm	mm squared
165	.	.	.	.	.	4 0.00006625	mm	Degrees	Degrees	mm	mm squared
166	.	.	.	.	.	4 0.00006625	mm	Degrees	Degrees	mm	mm squared
167	.	.	.	.	.	4 0.00006625	mm	Degrees	Degrees	mm	mm squared
168	.	.	.	.	.	4 0.00006625	mm	Degrees	Degrees	mm	mm squared
169	.	.	.	.	.	4 0.00006625	mm	Degrees	Degrees	mm	mm squared
170	.	.	.	.	.	4 0.00006625	mm	Degrees	Degrees	mm	mm squared
171	.	.	.	.	.	4 0.00006625	mm	Degrees	Degrees	mm	mm squared
172	.	.	.	.	.	4 0.00006625	mm	Degrees	Degrees	mm	mm squared
173	.	.	.	.	.	4 0.00006625	mm	Degrees	Degrees	mm	mm squared
174	.	.	.	.	.	4 0.00006625	mm	Degrees	Degrees	mm	mm squared
175	.	.	.	.	.	4 0.00006625	mm	Degrees	Degrees	mm	mm squared
176	.	.	.	.	.	4 0.00006625	mm	Degrees	Degrees	mm	mm squared
177	.	.	.	.	.	4 0.00006625	mm	Degrees	Degrees	mm	mm squared
178	.	.	.	.	.	4 0.00006625	mm	Degrees	Degrees	mm	mm squared
179	.	.	.	.	.	4 0.00006625	mm	Degrees	Degrees	mm	mm squared
180	.	.	.	.	.	4 0.00006625	mm	Degrees	Degrees	mm	mm squared
181	.	.	.	.	.	4 0.00006625	mm	Degrees	Degrees	mm	mm squared
182	.	.	.	.	.	4 0.00006625	mm	Degrees	Degrees	mm	mm squared
183	.	.	.	.	.	4 0.00006625	mm	Degrees	Degrees	mm	mm squared
184	.	.	.	.	.	4 0.00006625	mm	Degrees	Degrees	mm	mm squared
185	.	.	.	.	.	4 0.00006625	mm	Degrees	Degrees	mm	mm squared
186	.	.	.	.	.	4 0.00006625	mm	Degrees	Degrees	mm	mm squared
187	.	.	.	.	.	4 0.00006625	mm	Degrees	Degrees	mm	mm squared
188	.	.	.	.	.	4 0.00006625	mm	Degrees	Degrees	mm	mm squared
189	.	.	.	.	.	4 0.00006625	mm	Degrees	Degrees	mm	mm squared
190	.	.	.	.	.	4 0.00006625	mm	Degrees	Degrees	mm	mm squared
191	.	.	.	.	.	4 0.00006625	mm	Degrees	Degrees	mm	mm squared
192	.	.	.	.	.	4 0.00006625	mm	Degrees	Degrees	mm	mm squared
193	.	.	.	.	.	4 0.00006625	mm	Degrees	Degrees	mm	mm squared
194	.	.	.	.	.	4 0.00006625	mm	Degrees	Degrees	mm	mm squared
195	.	.	.	.	.	4 0.00006625	mm	Degrees	Degrees	mm	mm squared

Measured Values

Calculated Values

Particle No.	X location of impact (origin at e)	Y location of impact (origin at e)	Z location of impact (origin at e)	Penetration Depth	Length of Particle	Mass	R location of impact (origin at ee)	Theta location of impact (origin at ee)	Phi location of impact (origin at ee)	Diameter Ave. Area
	mm	mm	mm	mm	mm	gms	mm	Degrees	Degrees	mm squared
414	.	.	.	.	.	4	0.0001			0.142
415	.	.	.	.	.	4	0.0001			0.016
416	.	.	.	.	.	4	0.0001			0.142
417	.	.	.	.	.	4	0.0001			0.016
418	.	.	.	.	.	4	0.0001			0.142
419	.	.	.	.	.	4	0.0001			0.016
420	.	.	.	.	.	4	0.0001			0.142
421	.	.	.	.	.	1	0.00025			0.016
422	.	.	.	.	.	1	0.00025			0.142
423	.	.	.	.	.	1	0.00025			0.016
424	.	.	.	.	.	1	0.00025			0.142
425	.	.	.	.	.	1	0.00025			0.016
426	.	.	.	.	.	1	0.00025			0.142
427	.	.	.	.	.	1	0.00025			0.016
428	.	.	.	.	.	1	0.00025			0.142
429	.	.	.	.	.	1	0.00025			0.016
430	.	.	.	.	.	1	0.00025			0.142
431	.	.	.	.	.	1	0.00025			0.016
432	.	.	.	.	.	1	0.00025			0.142
433	.	.	.	.	.	1	0.00025			0.016
434	.	.	.	.	.	1	0.00025			0.142
435	.	.	.	.	.	1	0.00025			0.016
436	.	.	.	.	.	1	0.00025			0.142
437	.	.	.	.	.	1	0.00025			0.016
438	.	.	.	.	.	1	0.00025			0.142
439	.	.	.	.	.	1	0.00025			0.016
440	.	.	.	.	.	1	0.00025			0.142
441	.	.	.	.	.	1	0.00025			0.016
442	.	.	.	.	.	1	0.00025			0.142
443	.	.	.	.	.	1	0.00025			0.016
444	.	.	.	.	.	1	0.00025			0.142
445	.	.	.	.	.	1	0.00025			0.016
446	.	.	.	.	.	1	0.00025			0.142
447	.	.	.	.	.	1	0.00025			0.016
448	.	.	.	.	.	1	0.00025			0.142
449	.	.	.	.	.	1	0.00025			0.016
450	.	.	.	.	.	1	0.00025			0.142
451	.	.	.	.	.	1	0.00025			0.016
452	.	.	.	.	.	1	0.00025			0.142
453	.	.	.	.	.	1	0.00025			0.016
454	.	.	.	.	.	1	0.00025			0.142
455	.	.	.	.	.	1	0.00025			0.016
456	.	.	.	.	.	1	0.00025			0.142
457	.	.	.	.	.	1	0.00025			0.016

Measured Values

Calculated Values

Particle No.	Measured Values					Calculated Values				
	X location of impact (origin at e)	Y location of impact (origin at e)	Z location of impact (origin at e)	Penetration Depth	Length of Particle	Mass	R location of impact (origin at ee)	Theta location of impact (origin at ee)	Phi location of impact (origin at ee)	Diameter Ave. Area
	mm	mm	mm	mm	mm	gms	mm	Degrees	Degrees	mm squared
283	.	.	.	.	.	3 0.0001233333	0.182	0.076	0.182	0.076
284	.	.	.	.	.	3 0.0001233333	0.182	0.076	0.182	0.076
285	.	.	.	.	.	3 0.0001233333	0.182	0.076	0.182	0.076
286	.	.	.	.	.	3 0.0001233333	0.182	0.076	0.182	0.076
287	.	.	.	.	.	3 0.0001233333	0.182	0.076	0.182	0.076
288	.	.	.	.	.	3 0.0001233333	0.182	0.076	0.182	0.076
289	.	.	.	.	.	3 0.0001233333	0.182	0.076	0.182	0.076
290	.	.	.	.	.	3 0.0001233333	0.182	0.076	0.182	0.076
291	.	.	.	.	.	3 0.0001233333	0.182	0.076	0.182	0.076
292	.	.	.	.	.	3 0.0001233333	0.182	0.076	0.182	0.076
293	.	.	.	.	.	3 0.0001233333	0.182	0.076	0.182	0.076
294	.	.	.	.	.	3 0.0001233333	0.182	0.076	0.182	0.076
295	.	.	.	.	.	3 0.0001233333	0.182	0.076	0.182	0.076
296	.	.	.	.	.	3 0.0001233333	0.182	0.076	0.182	0.076
297	.	.	.	.	.	3 0.0001233333	0.182	0.076	0.182	0.076
298	.	.	.	.	.	3 0.0001233333	0.182	0.076	0.182	0.076
299	.	.	.	.	.	3 0.0001233333	0.182	0.076	0.182	0.076
300	.	.	.	.	.	3 0.0001233333	0.182	0.076	0.182	0.076
301	.	.	.	.	.	3 0.0001233333	0.182	0.076	0.182	0.076
302	.	.	.	.	.	3 0.0001233333	0.182	0.076	0.182	0.076
303	.	.	.	.	.	3 0.0001233333	0.182	0.076	0.182	0.076
304	.	.	.	.	.	3 0.0001233333	0.182	0.076	0.182	0.076
305	.	.	.	.	.	3 0.0001233333	0.182	0.076	0.182	0.076
306	.	.	.	.	.	3 0.0001233333	0.182	0.076	0.182	0.076
307	.	.	.	.	.	3 0.0001233333	0.182	0.076	0.182	0.076
308	.	.	.	.	.	3 0.0001233333	0.182	0.076	0.182	0.076
309	.	.	.	.	.	3 0.0001233333	0.182	0.076	0.182	0.076
310	.	.	.	.	.	3 0.0001233333	0.182	0.076	0.182	0.076
311	.	.	.	.	.	3 0.0001233333	0.182	0.076	0.182	0.076
312	.	.	.	.	.	3 0.0001233333	0.182	0.076	0.182	0.076
313	.	.	.	.	.	3 0.0001233333	0.182	0.076	0.182	0.076
314	.	.	.	.	.	3 0.0001233333	0.182	0.076	0.182	0.076
315	.	.	.	.	.	3 0.0001233333	0.182	0.076	0.182	0.076
316	.	.	.	.	.	3 0.0001233333	0.182	0.076	0.182	0.076
317	.	.	.	.	.	3 0.0001233333	0.182	0.076	0.182	0.076
318	.	.	.	.	.	3 0.0001233333	0.182	0.076	0.182	0.076
319	.	.	.	.	.	3 0.0001233333	0.182	0.076	0.182	0.076
320	.	.	.	.	.	3 0.0001233333	0.182	0.076	0.182	0.076
321	.	.	.	.	.	3 0.0001233333	0.182	0.076	0.182	0.076
322	.	.	.	.	.	3 0.0001233333	0.182	0.076	0.182	0.076
323	.	.	.	.	.	3 0.0001233333	0.182	0.076	0.182	0.076
324	.	.	.	.	.	3 0.0001233333	0.182	0.076	0.182	0.076
325	.	.	.	.	.	3 0.0001233333	0.182	0.076	0.182	0.076
326	.	.	.	.	.	3 0.0001233333	0.182	0.076	0.182	0.076



JSC Shot No. 894

(Thin Plate) 12/17/85

Measured Values

Calculated Values

Particle No.	Measured Values					Calculated Values				
	X location of impact (origin at s)	Y location of impact (origin at s)	Z location of impact (origin at s)	Penetration Depth	Length of Particle	Mass	R location of impact (origin at ss)	Theta location of impact (origin at ss)	Phi location of impact (origin at ss)	Diameter Ave. Area
	mm	mm	mm	mm	mm	gms	mm	Degrees	Degrees	mm squared
327	.	.	.	.	.	3 0.0001233333	0.182			0.026
328	.	.	.	.	.	3 0.0001233333	0.182			0.026
329	.	.	.	.	.	3 0.0001233333	0.182			0.026
330	.	.	.	.	.	3 0.0001233333	0.182			0.026
331	.	.	.	.	.	3 0.0001233333	0.182			0.026
332	.	.	.	.	.	3 0.0001233333	0.182			0.026
333	.	.	.	.	.	3 0.0001233333	0.182			0.026
334	.	.	.	.	.	3 0.0001233333	0.182			0.026
335	.	.	.	.	.	3 0.0001233333	0.182			0.026
336	.	.	.	.	.	3 0.0001233333	0.182			0.026
337	.	.	.	.	.	3 0.0001233333	0.182			0.026
338	.	.	.	.	.	3 0.0001233333	0.182			0.026
339	.	.	.	.	.	3 0.0001233333	0.182			0.026
340	.	.	.	.	.	3 0.0001233333	0.182			0.026
341	.	.	.	.	.	3 0.0001233333	0.182			0.026
342	.	.	.	.	.	3 0.0001233333	0.182			0.026
343	.	.	.	.	.	3 0.0001233333	0.182			0.026
344	.	.	.	.	.	3 0.0001233333	0.182			0.026
345	.	.	.	.	.	3 0.0001233333	0.182			0.026
346	.	.	.	.	.	3 0.0001233333	0.182			0.026
347	.	.	.	.	.	3 0.0001233333	0.182			0.026
348	.	.	.	.	.	3 0.0001233333	0.182			0.026
349	.	.	.	.	.	3 0.0001233333	0.182			0.026
350	.	.	.	.	.	3 0.0001233333	0.182			0.026
351	.	.	.	.	.	3 0.0001233333	0.182			0.026
352	.	.	.	.	.	3 0.0001233333	0.182			0.026
353	.	.	.	.	.	3 0.0001233333	0.182			0.026
354	.	.	.	.	.	3 0.0001233333	0.182			0.026
355	.	.	.	.	.	3 0.0001233333	0.182			0.026
356	.	.	.	.	.	3 0.0001233333	0.182			0.026
357	.	.	.	.	.	3 0.0001233333	0.182			0.026
358	.	.	.	.	.	3 0.0001233333	0.182			0.026
359	.	.	.	.	.	3 0.0001233333	0.182			0.026
360	.	.	.	.	.	3 0.0001233333	0.182			0.026
361	.	.	.	.	.	3 0.0001233333	0.182			0.026
362	.	.	.	.	.	3 0.0001233333	0.182			0.026
363	.	.	.	.	.	3 0.0001233333	0.182			0.026
364	.	.	.	.	.	3 0.0001233333	0.182			0.026
365	.	.	.	.	.	3 0.0001233333	0.182			0.026
366	.	.	.	.	.	3 0.0001233333	0.182			0.026
Spall in catcher (160 x 170 mm) origin at lower left looking at catcher										
367	153	89	95	95	62	0.0026	119.87	-37.54	2.41	0.184
368	92	0	95	95	72	0.0005	178.04	-7.20	-41.82	0.135
369	155	50	95	95	5	0.001	176.00	-38.29	-20.22	0.402



## Measured Values

## Calculated Values

Particle No.	Measured Values				Calculated Values					
	X location of impact (origin at e)	Y location of impact (origin at e)	Z location of impact (origin at e)	Penetration Depth	Length of Particle	Mass	R location of impact (origin at ee)	Theta location of impact (origin at ee)	Phi location of impact (origin at ee)	Diameter Ave. Area
370	mm	mm	mm	mm	mm	gms	mm	Degrees	Degrees	mm squared
371	.	.	.	periphery - outer 40 mm (approx. 50)	mm	4	0.0001			0.142
372	.	.	.	.	mm	4	0.0001			0.142
373	.	.	.	.	mm	4	0.0001			0.142
374	.	.	.	.	mm	4	0.0001			0.142
375	.	.	.	.	mm	4	0.0001			0.142
376	.	.	.	.	mm	4	0.0001			0.142
377	.	.	.	.	mm	4	0.0001			0.142
378	.	.	.	.	mm	4	0.0001			0.142
379	.	.	.	.	mm	4	0.0001			0.142
380	.	.	.	.	mm	4	0.0001			0.142
381	.	.	.	.	mm	4	0.0001			0.142
382	.	.	.	.	mm	4	0.0001			0.142
383	.	.	.	.	mm	4	0.0001			0.142
384	.	.	.	.	mm	4	0.0001			0.142
385	.	.	.	.	mm	4	0.0001			0.142
386	.	.	.	.	mm	4	0.0001			0.142
387	.	.	.	.	mm	4	0.0001			0.142
388	.	.	.	.	mm	4	0.0001			0.142
389	.	.	.	.	mm	4	0.0001			0.142
390	.	.	.	.	mm	4	0.0001			0.142
391	.	.	.	.	mm	4	0.0001			0.142
392	.	.	.	.	mm	4	0.0001			0.142
393	.	.	.	.	mm	4	0.0001			0.142
394	.	.	.	.	mm	4	0.0001			0.142
395	.	.	.	.	mm	4	0.0001			0.142
396	.	.	.	.	mm	4	0.0001			0.142
397	.	.	.	.	mm	4	0.0001			0.142
398	.	.	.	.	mm	4	0.0001			0.142
399	.	.	.	.	mm	4	0.0001			0.142
400	.	.	.	.	mm	4	0.0001			0.142
401	.	.	.	.	mm	4	0.0001			0.142
402	.	.	.	.	mm	4	0.0001			0.142
403	.	.	.	.	mm	4	0.0001			0.142
404	.	.	.	.	mm	4	0.0001			0.142
405	.	.	.	.	mm	4	0.0001			0.142
406	.	.	.	.	mm	4	0.0001			0.142
407	.	.	.	.	mm	4	0.0001			0.142
408	.	.	.	.	mm	4	0.0001			0.142
409	.	.	.	.	mm	4	0.0001			0.142
410	.	.	.	.	mm	4	0.0001			0.142
411	.	.	.	.	mm	4	0.0001			0.142
412	.	.	.	.	mm	4	0.0001			0.142
413	.	.	.	.	mm	4	0.0001			0.142



Measured Values

Calculated Values

Particle No.	X location of impact (origin at s)	Y location of impact (origin at s)	Z location of impact (origin at s)	Penetration Depth	Length of Particle	Mass	R location of impact (origin at ss)	Theta location of impact (origin at ss)	Phi location of impact (origin at ss)	Area
	mm	mm	mm	mm	mm	gms	mm	Degrees	Degrees	mm squared
240	.	.	.	.	4	0.00006625	0.116	0.010	0.010	0.010
241	.	.	.	.	4	0.00006625	0.116	0.010	0.010	0.010
242	.	.	.	.	4	0.00006625	0.116	0.010	0.010	0.010
243	.	.	.	.	4	0.00006625	0.116	0.010	0.010	0.010
244	.	.	.	.	4	0.00006625	0.116	0.010	0.010	0.010
245	.	.	.	.	4	0.00006625	0.116	0.010	0.010	0.010
246	.	.	.	.	4	0.00006625	0.116	0.010	0.010	0.010
247	.	.	.	.	4	0.00006625	0.116	0.010	0.010	0.010
248	.	.	.	.	4	0.00006625	0.116	0.010	0.010	0.010
249	.	.	.	.	4	0.00006625	0.116	0.010	0.010	0.010
250	.	.	.	.	4	0.00006625	0.116	0.010	0.010	0.010
251	.	.	.	.	4	0.00006625	0.116	0.010	0.010	0.010
252	.	.	.	.	4	0.00006625	0.116	0.010	0.010	0.010
253	.	.	.	.	4	0.00006625	0.116	0.010	0.010	0.010
254	.	.	.	.	4	0.00006625	0.116	0.010	0.010	0.010
255	.	.	.	.	4	0.00006625	0.116	0.010	0.010	0.010
256	.	.	.	.	4	0.00006625	0.116	0.010	0.010	0.010
257	.	.	.	.	4	0.00006625	0.116	0.010	0.010	0.010
258	.	.	.	.	4	0.00006625	0.116	0.010	0.010	0.010
259	.	.	.	.	4	0.00006625	0.116	0.010	0.010	0.010
260	.	.	.	.	4	0.00006625	0.116	0.010	0.010	0.010
261	.	.	.	.	4	0.00006625	0.116	0.010	0.010	0.010
262	.	.	.	.	4	0.00006625	0.116	0.010	0.010	0.010
263	.	.	.	.	4	0.00006625	0.116	0.010	0.010	0.010
264	.	.	.	.	4	0.00006625	0.116	0.010	0.010	0.010
265	.	.	.	.	4	0.00006625	0.116	0.010	0.010	0.010
266	.	.	.	.	4	0.00006625	0.116	0.010	0.010	0.010
267	.	.	.	.	4	0.00006625	0.116	0.010	0.010	0.010
268	.	.	.	.	4	0.00006625	0.116	0.010	0.010	0.010
269	.	.	.	.	4	0.00006625	0.116	0.010	0.010	0.010
270	.	.	.	.	4	0.00006625	0.116	0.010	0.010	0.010
271	.	.	.	.	4	0.00006625	0.116	0.010	0.010	0.010
272	.	.	.	.	4	0.00006625	0.116	0.010	0.010	0.010
273	.	.	.	.	4	0.00006625	0.116	0.010	0.010	0.010
274	.	.	.	.	4	0.00006625	0.116	0.010	0.010	0.010
275	.	.	.	.	4	0.00006625	0.116	0.010	0.010	0.010
Spall Dust Loose on Bottom										
276 Spall under catcher										
277	.	.	.	.	27	0.0004	0.109	0.009	0.009	0.009
278	.	.	.	.	3	0.0001233333	0.182	0.026	0.026	0.026
279	.	.	.	.	3	0.0001233333	0.182	0.026	0.026	0.026
280	.	.	.	.	3	0.0001233333	0.182	0.026	0.026	0.026
281	.	.	.	.	3	0.0001233333	0.182	0.026	0.026	0.026
282	.	.	.	.	3	0.0001233333	0.182	0.026	0.026	0.026
average of approx. 90 (less dust)										



Measured Values

Calculated Values

Particle No.	Measured Values				Calculated Values									
	X location of impact (origin at s)	Y location of impact (origin at s)	Z location of impact (origin at s)	Penetration Depth	Length of Particle	Mass	R location of impact (origin at ss)	Theta of impact (origin at ss)	Phi of impact (origin at ss)	Cone Angle (from normal to surface) (origin at ss)	Average Diameter	Average Area	Velocity	
88	00	00	00	00	0	5 0.0002418182	00	-90.00	-90.00	0	0.20	0.03	0.00	
89	00	00	00	00	0	5 0.0002418182	00	-90.00	-90.00	0	0.20	0.03	0.00	
90	00	00	00	00	0	5 0.0002418182	00	-90.00	-90.00	0	0.20	0.03	0.00	
91	00	00	00	00	0	5 0.0002418182	00	-90.00	-90.00	0	0.20	0.03	0.00	
92	00	00	00	00	0	5 0.0002418182	00	-90.00	-90.00	0	0.20	0.03	0.00	
93	00	00	00	00	0	5 0.0002418182	00	-90.00	-90.00	0	0.20	0.03	0.00	
94	00	00	00	00	0	5 0.0002418182	00	-90.00	-90.00	0	0.20	0.03	0.00	
95	00	00	00	00	0	5 0.0002418182	00	-90.00	-90.00	0	0.20	0.03	0.00	
96	00	00	00	00	0	5 0.0002418182	00	-90.00	-90.00	0	0.20	0.03	0.00	
97	00	00	00	00	0	5 0.0002418182	00	-90.00	-90.00	0	0.20	0.03	0.00	
98	00	00	00	00	0	5 0.0002418182	00	-90.00	-90.00	0	0.20	0.03	0.00	
99	00	00	00	00	0	5 0.0002418182	00	-90.00	-90.00	0	0.20	0.03	0.00	
100	00	00	00	00	0	5 0.0002418182	00	-90.00	-90.00	0	0.20	0.03	0.00	
101	00	00	00	00	0	5 0.0002418182	00	-90.00	-90.00	0	0.20	0.03	0.00	
102	00	00	00	00	0	5 0.0002418182	00	-90.00	-90.00	0	0.20	0.03	0.00	
103	00	00	00	00	0	5 0.0002418182	00	-90.00	-90.00	0	0.20	0.03	0.00	
104	00	00	00	00	0	5 0.0002418182	00	-90.00	-90.00	0	0.20	0.03	0.00	
105	00	00	00	00	0	5 0.0002418182	00	-90.00	-90.00	0	0.20	0.03	0.00	
106	00	00	00	00	0	5 0.0002418182	00	-90.00	-90.00	0	0.20	0.03	0.00	
107	00	00	00	00	0	5 0.0002418182	00	-90.00	-90.00	0	0.20	0.03	0.00	
108	00	00	00	00	0	5 0.0002418182	00	-90.00	-90.00	0	0.20	0.03	0.00	
109	00	00	00	00	0	5 0.0002418182	00	-90.00	-90.00	0	0.20	0.03	0.00	
110	00	00	00	00	0	5 0.0002418182	00	-90.00	-90.00	0	0.20	0.03	0.00	
111	00	00	00	00	0	5 0.0002418182	00	-90.00	-90.00	0	0.20	0.03	0.00	
112	00	00	00	00	0	5 0.0002418182	00	-90.00	-90.00	0	0.20	0.03	0.00	
113	00	00	00	00	0	5 0.0002418182	00	-90.00	-90.00	0	0.20	0.03	0.00	
114	00	00	00	00	0	5 0.0002418182	00	-90.00	-90.00	0	0.20	0.03	0.00	
115	00	00	00	00	0	5 0.0002418182	00	-90.00	-90.00	0	0.20	0.03	0.00	
116	00	00	00	00	0	5 0.0002418182	00	-90.00	-90.00	0	0.20	0.03	0.00	
117	00	00	00	00	0	5 0.0002418182	00	-90.00	-90.00	0	0.20	0.03	0.00	
118	00	00	00	00	0	5 0.0002418182	00	-90.00	-90.00	0	0.20	0.03	0.00	
119	00	00	00	00	0	5 0.0002418182	00	-90.00	-90.00	0	0.20	0.03	0.00	
120	00	00	00	00	0	5 0.0002418182	00	-90.00	-90.00	0	0.20	0.03	0.00	
121	00	00	00	00	0	5 0.0002418182	00	-90.00	-90.00	0	0.20	0.03	0.00	
122	00	00	00	00	0	5 0.0002418182	00	-90.00	-90.00	0	0.20	0.03	0.00	
123	00	00	00	00	0	5 0.0002418182	00	-90.00	-90.00	0	0.20	0.03	0.00	
124	00	00	00	00	0	5 0.0002418182	00	-90.00	-90.00	0	0.20	0.03	0.00	
125	00	00	00	00	0	5 0.0002418182	00	-90.00	-90.00	0	0.20	0.03	0.00	
126	00	00	00	00	0	5 0.0002418182	00	-90.00	-90.00	0	0.20	0.03	0.00	
127	00	00	00	00	0	5 0.0002418182	00	-90.00	-90.00	0	0.20	0.03	0.00	
128	00	00	00	00	0	5 0.0002418182	00	-90.00	-90.00	0	0.20	0.03	0.00	
129	00	00	00	00	0	5 0.0002418182	00	-90.00	-90.00	0	0.20	0.03	0.00	
130	00	00	00	00	0	5 0.0002418182	00	-90.00	-90.00	0	0.20	0.03	0.00	
131 (3 large loose particles)	00	00	00	00	0	8 0.0012	00	-90.00	-90.00	0	0.35	0.10	0.00	

JSC Shot No. 883

12/23/85

Particle No.	Measured Values					Calculated Values							
	X location of impact (origin at e)	Y location of impact (origin at e)	Z location of impact (origin at e)	Penetration Depth	Length of Particle	Mass	R location of impact (origin at ee)	Theta location of impact (origin at ee)	Phi location of impact (origin at ee)	Cone Angle (from normal to surface) (origin at ee)	Average Diameter	Average Area	Velocity
	ee	ee	ee	ee	ee	gas	ee	Degrees	Degrees	ee	ee	ee squared	ee/sec
	Origin e, at lower left hand corner of box on the open end.												
	Origin ee, at center of open end - ie. at the impact point.												
	X, ee	Y, ee	Z, ee		Combined Measured	0.0352							
	71	74	0		Total from mass of target before & after	0.11							
					Total calc. small particles (dust)	0.07391							Percent of total
													67.192

Shear Strength (Estimated) used in velocity calculation, N Pascals

55

Measured Values

Calculated Values

Particle No.	X location of impact (origin at s)	Y location of impact (origin at s)	Z location of impact (origin at s)	Penetration Depth	Length of Particle	Mass	gas	R location of impact (origin at es)	Theta location of impact (origin at es)	Phi location of impact (origin at es)	Area Diameter Ave.
	mm	mm	mm	mm	mm	gms		mm	Degrees	Degrees	mm squared
458	.	.	.			0.000025	1	0.142			0.016
459	.	.	.			0.000025	1	0.142			0.016
460	.	.	.			0.000025	1	0.142			0.016
461	.	.	.			0.000025	1	0.142			0.016
462	.	.	.			0.000025	1	0.142			0.016
463	.	.	.			0.000025	1	0.142			0.016
464	.	.	.			0.000025	1	0.142			0.016
465	.	.	.			0.000025	1	0.142			0.016
466	.	.	.			0.000025	1	0.142			0.016
467	.	.	.			0.000025	1	0.142			0.016
468	.	.	.			0.000025	1	0.142			0.016
469	.	.	.			0.000025	1	0.142			0.016
Total Spall						0.06655		63.1%	Percent Spall		

Target mass before	85.92
Target mass after	85.79
Total expected Ejecta/Spall	0.13
Measured Ejecta	0.039
Measured Spall	0.06655
Total measured Ejecta/Spall	0.10555
Unaccounted (Dust)	0.02445
Compensated Ejecta Mass	0.04803
Compensated Spall Mass	0.08197
Total Compensated Mass	0.13

36.9% Percent Ejecta  
63.1% Percent Spall

18.8% Percent Dust

36.9% Percent Ejecta  
63.1% Percent Spall

JSC Shot No. 917  
 (Thin Plate with Cloth)  
 1/17/86

Measured Values

Calculated Values

Particle No.	X location of impact (origin at e)		Y location of impact (origin at e)		Z location of impact (origin at e)		Penetration Depth	Length of Particle	Mass	R location of impact (origin at e)		Theta location of impact (origin at e)		Phi location of impact (origin at e)		Cone Angle (angle from Diameter to surf normal)	Average Diameter	Average Area	Velocity
	mm	mm	mm	mm	mm	mm				mm	mm	mm	mm	mm	mm				
44	78	71	113	0.5	1	0.000046667	115.40	11.02	4.05	11.70	0.19	0.03	0.63						
45	57	78	113	0.5	1	0.000046667	114.00	0.51	7.56	7.58	0.19	0.03	0.63						
46	30	95	113	1	1	0.000046667	120.29	-12.96	15.81	20.05	0.19	0.03	1.23						
47	125	78	113	0.5	1.5	0.000046667	135.25	31.41	7.56	32.00	0.16	0.02	0.56						
48	94	33	113	2	1.5	0.000046667	122.93	18.59	-14.87	23.19	0.16	0.02	2.19						
49	106	107	113	2	2	0.000046667	131.17	23.87	21.27	30.52	0.14	0.01	2.03						
50	82	95	113	2	2	0.000046667	120.29	12.96	15.81	20.05	0.14	0.01	2.03						
51	74	91	113	2	1	0.000046667	117.80	9.05	13.92	16.41	0.19	0.03	2.43						
52	98	116	113	1	1	0.000046667	131.69	20.39	25.13	30.90	0.19	0.03	1.23						
53	36	69	113	1	1	0.000046667	114.91	-10.04	3.04	10.47	0.19	0.03	1.23						
54	55	0	22	0.5	1	0.00004	66.74	-2.60	-70.75	70.75	0.18	0.03	0.65						
55	3	0	85	0.5	1	0.00004	118.33	-31.94	-36.54	44.09	0.18	0.03	0.65						
56	85	0	24	1	1	0.00004	73.37	50.39	-69.15	70.91	0.18	0.03	1.27						
57	53	0	41	1.5	1.5	0.00004	75.23	-4.18	-56.94	56.97	0.15	0.02	1.71						
58	30	0	98	0.5	1	0.00004	119.37	-14.86	-32.74	34.82	0.18	0.03	0.65						
59	71	0	68	1	1.5	0.00004	93.90	12.44	-42.81	43.60	0.15	0.02	1.15						
60	76	0	111	1	1	0.00004	129.19	10.21	-29.58	30.77	0.18	0.03	1.27						
61	78	0	63	2	2	0.00004	91.77	19.25	-45.00	46.65	0.13	0.01	2.11						
62	76	0	110	0.5	1	0.00004	128.33	10.30	-29.80	31.00	0.18	0.03	0.65						
63	82	0	20	1	1.5	0.00004	71.03	52.43	-72.39	73.65	0.15	0.02	1.15						
64	Loose on bottom				9	0.0035	0.00	-90	-90	0	0.56	0.25	0.00						
65					8	0.0065	0.00	-90	-90	0	0.22	0.04	0.00						
66					9	0.0065	0.00	-90	-90	0	0.21	0.04	0.00						
67					6	0.0065	0.00	-90	-90	0	0.26	0.05	0.00						
68					7	0.0063	0.00	-90	-90	0	0.19	0.03	0.00						
69					7	0.0064	0.00	-90	-90	0	0.21	0.04	0.00						
70					7	0.0064	0.00	-90	-90	0	0.21	0.04	0.00						
71					5	0.0023	0.00	-90	-90	0	0.61	0.29	0.00						
72					7	0.0014	0.00	-90	-90	0	0.40	0.13	0.00						
73					5	0.0068	0.00	-90	-90	0	0.36	0.10	0.00						
74					6	0.0035	0.00	-90	-90	0	0.69	0.37	0.00						
75					8	0.0065	0.00	-90	-90	0	0.22	0.04	0.00						
76					6	0.0067	0.00	-90	-90	0	0.31	0.07	0.00						
77					6	0.0064	0.00	-90	-90	0	0.23	0.04	0.00						
78					6	0.0025	0.00	-90	-90	0	0.18	0.03	0.00						
79					6	0.0025	0.00	-90	-90	0	0.18	0.03	0.00						
80					6	0.0025	0.00	-90	-90	0	0.18	0.03	0.00						
81					6	0.0025	0.00	-90	-90	0	0.18	0.03	0.00						
82					6	0.0025	0.00	-90	-90	0	0.18	0.03	0.00						
83					6	0.0025	0.00	-90	-90	0	0.18	0.03	0.00						
84					4	0.002642857	0.00	-90	-90	0	0.23	0.04	0.00						
85					4	0.002642857	0.00	-90	-90	0	0.23	0.04	0.00						
86					4	0.002642857	0.00	-90	-90	0	0.23	0.04	0.00						
87					4	0.002642857	0.00	-90	-90	0	0.23	0.04	0.00						



Measured Values

Calculated Values

Particle No.	X location of impact (origin at +)		Y location of impact (origin at +)		Z location of impact (origin at +)		Penetration Depth	Length of Particle	Mass	R location of impact (origin at +)	Theta location of impact (origin at +)		Phi location of impact (origin at +)		Cone Angle (angle from impact pt. to surf norm)	Average Diameter	Average Area	Velocity
	mm	mm	mm	mm	mm	mm					mm	mm	mm	mm				
1	0	0	66	80	3	0.0002	4	97.70	-34.99	2.15	35.03	0.20	0.03	1.78				
2	0	0	0	4	0.01	0.0001	2	84.39	-85.91	-86.37	87.28	0.20	0.03	0.02				
3	0	0	56	81	2	0.0001	2	98.72	-34.66	-4.94	34.87	0.20	0.03	1.69				
4	0	0	6	101	0.01	0.0001	2	128.79	-29.01	-29.44	38.35	0.20	0.03	0.02				
5	0	0	129	83	2	0.0002	3	119.92	-34.01	38.49	46.20	0.23	0.04	1.28				
6	0	0	83	67	5	0.0008	5	89.58	-39.89	16.62	41.59	0.36	0.10	1.99				
7	0	0	58	56	0.5	0.0007	4	79.35	-45.00	-5.10	45.11	0.38	0.11	0.23				
8	0	0	10	91	3	0.0001	2	119.27	-31.61	-30.22	40.27	0.20	0.03	2.52				
9	0	0	142	97	4	0.0001	3	137.06	-30.00	39.16	44.95	0.16	0.02	3.03				
10	0	0	87	87	0.5	0.0005	1	106.21	-32.77	15.42	35.00	0.20	0.03	0.62				
11	0	0	22	80	2	0.0001	2	105.91	-34.99	-27.14	40.94	0.20	0.03	1.69				
12	0	0	92	58	2	0.0001	4	85.68	-43.99	26.57	47.39	0.14	0.02	1.41				
13	0	0	6	86	1	0.0001	3	117.39	-33.07	-33.54	42.90	0.16	0.02	0.77				
14	20	137	33	87	0.5	0.0001	2	88.66	-47.49	65.97	68.15	0.20	0.03	0.44				
15	81	137	87	87	3	0.0001	2	116.92	16.03	40.38	41.92	0.20	0.03	2.52				
16	116	118	93	93	2	0.0002	4	123.59	32.83	30.60	41.19	0.20	0.03	1.19				
17	116	74	94	94	4	0.0001	5	112.06	32.55	6.67	32.98	0.13	0.01	2.66				
18	116	77	69	69	2	0.0001	1	92.50	41.01	11.47	41.76	0.28	0.06	2.02				
19	116	102	109	109	2	0.0001	2	130.39	28.83	19.69	33.29	0.20	0.03	1.67				
20	116	4	70	70	0.5	0.0001	1	109.46	40.60	-40.13	50.24	0.28	0.06	0.53				
21	116	56	81	81	2	0.00025	1.5	101.04	36.53	-4.94	36.71	0.12	0.01	2.55				
22	116	78	93	93	1	0.00025	2	111.69	32.83	9.16	33.62	0.10	0.01	1.19				
23	116	80	79	79	3	0.00025	2	100.65	37.22	12.14	38.29	0.10	0.01	3.55				
24	116	67	75	75	1	0.00025	1	96.23	38.66	4.57	38.80	0.14	0.02	1.43				
25	29	32	113	113	1	0.0009	2	120.25	-13.44	-15.34	19.99	0.60	0.29	0.52				
26	39	7	113	113	0.5	0.0002	2	127.26	-8.56	-26.36	27.38	0.28	0.06	0.37				
27	61	12	113	113	0.5	0.0001	1.5	124.08	2.53	-24.29	24.39	0.23	0.04	0.47				
28	85	88	113	113	4	0.0003	4	119.31	14.39	12.48	18.72	0.25	0.05	2.15				
29	107	106	113	113	0.5	0.0004	4	131.22	24.29	20.83	30.56	0.28	0.06	0.26				
30	108	100	113	113	5	0.0002	3	129.78	24.71	18.13	29.46	0.23	0.04	3.18				
31	11	89	113	113	0.5	0.0001	3	124.38	-21.71	12.96	24.70	0.16	0.02	0.39				
32	35	95	113	113	1	0.0002	2	119.31	-10.53	15.81	18.71	0.28	0.06	0.73				
33	6	31	113	113	2	0.0001	1	127.64	-23.87	-15.81	27.71	0.28	0.06	2.02				
34	66	75	113	113	1	0.0001	2	114.07	5.06	6.06	7.87	0.20	0.03	0.85				
35	107	66	113	113	0.5	0.0001	1	124.01	24.29	1.52	24.33	0.28	0.06	0.53				
36	107	83	113	113	2	0.0002	3	125.58	24.29	10.04	25.86	0.23	0.04	1.28				
37	118	115	113	113	0.5	0.0001	3	138.99	28.75	24.71	35.61	0.16	0.02	0.39				
38	87	38	113	113	2	0.0002	2.5	119.81	15.34	-12.48	19.41	0.25	0.05	1.35				
39	1	28	113	113	0.5	0.000466667	1	130.46	-25.95	-17.21	29.98	0.19	0.03	0.63				
40	7	30	113	113	0.5	0.000466667	1	127.51	-23.44	-16.28	27.60	0.19	0.03	0.63				
41	73	16	113	113	1	0.000466667	1	121.56	8.56	-22.58	23.86	0.19	0.03	1.23				
42	24	60	113	113	0.5	0.000466667	1	117.48	-15.81	-1.52	15.88	0.19	0.03	0.63				
43	63	78	113	113	0.5	0.000466667	1.5	114.21	3.54	7.56	8.33	0.16	0.02	0.56				



Measured Values

Calculated Values

Particle No.	Measured Values				Calculated Values								
	X location of impact (origin at e)	Y location of impact (origin at e)	Z location of impact (origin at e)	Penetration Depth	Length of Particle	Mass	R location of impact (origin at ee)	Theta location of impact (origin at ee)	Phi location of impact (origin at ee)	Cone Angle (angle from impact pt. to surf norm)	Average Diameter	Average Area	Velocity
	mm	mm	mm	mm	mm	gms	mm	Degrees	Degrees	Degrees	mm	mm squared	mm/sec
88	.	.	.	.	.	4 0.0002642857	0.00	-90	-90	0	0.23	0.04	0.00
89	.	.	.	.	.	4 0.0002642857	0.00	-90	-90	0	0.23	0.04	0.00
90	.	.	.	.	.	4 0.0002642857	0.00	-90	-90	0	0.23	0.04	0.00
91	.	.	.	.	.	4 0.0002642857	0.00	-90	-90	0	0.23	0.04	0.00
92	.	.	.	.	.	4 0.0002642857	0.00	-90	-90	0	0.23	0.04	0.00
93	.	.	.	.	.	4 0.0002642857	0.00	-90	-90	0	0.23	0.04	0.00
94	.	.	.	.	.	4 0.0002642857	0.00	-90	-90	0	0.23	0.04	0.00
95	.	.	.	.	.	4 0.0002642857	0.00	-90	-90	0	0.23	0.04	0.00
96	.	.	.	.	.	4 0.0002642857	0.00	-90	-90	0	0.23	0.04	0.00
97	.	.	.	.	.	4 0.0002642857	0.00	-90	-90	0	0.23	0.04	0.00
98	.	.	.	.	.	3 0.0001363636	0.00	-90	-90	0	0.19	0.03	0.00
99	.	.	.	.	.	3 0.0001363636	0.00	-90	-90	0	0.19	0.03	0.00
100	.	.	.	.	.	3 0.0001363636	0.00	-90	-90	0	0.19	0.03	0.00
101	.	.	.	.	.	3 0.0001363636	0.00	-90	-90	0	0.19	0.03	0.00
102	.	.	.	.	.	3 0.0001363636	0.00	-90	-90	0	0.19	0.03	0.00
103	.	.	.	.	.	3 0.0001363636	0.00	-90	-90	0	0.19	0.03	0.00
104	.	.	.	.	.	3 0.0001363636	0.00	-90	-90	0	0.19	0.03	0.00
105	.	.	.	.	.	3 0.0001363636	0.00	-90	-90	0	0.19	0.03	0.00
106	.	.	.	.	.	3 0.0001363636	0.00	-90	-90	0	0.19	0.03	0.00
107	.	.	.	.	.	3 0.0001363636	0.00	-90	-90	0	0.19	0.03	0.00
108	.	.	.	.	.	3 0.0001363636	0.00	-90	-90	0	0.19	0.03	0.00
109	.	.	.	.	.	3 0.0001363636	0.00	-90	-90	0	0.19	0.03	0.00
110	.	.	.	.	.	3 0.0001363636	0.00	-90	-90	0	0.19	0.03	0.00
111	.	.	.	.	.	3 0.0001363636	0.00	-90	-90	0	0.19	0.03	0.00
112	.	.	.	.	.	3 0.0001363636	0.00	-90	-90	0	0.19	0.03	0.00
113	.	.	.	.	.	3 0.0001363636	0.00	-90	-90	0	0.19	0.03	0.00
114	.	.	.	.	.	3 0.0001363636	0.00	-90	-90	0	0.19	0.03	0.00
115	.	.	.	.	.	3 0.0001363636	0.00	-90	-90	0	0.19	0.03	0.00
116	.	.	.	.	.	3 0.0001363636	0.00	-90	-90	0	0.19	0.03	0.00
117	.	.	.	.	.	3 0.0001363636	0.00	-90	-90	0	0.19	0.03	0.00
118	.	.	.	.	.	3 0.0001363636	0.00	-90	-90	0	0.19	0.03	0.00
119	.	.	.	.	.	3 0.0001363636	0.00	-90	-90	0	0.19	0.03	0.00
120	.	.	.	.	.	1.5 0.000105	0.00	-90	-90	0	0.24	0.04	0.00
121	.	.	.	.	.	1.5 0.000105	0.00	-90	-90	0	0.24	0.04	0.00
122	.	.	.	.	.	1.5 0.000105	0.00	-90	-90	0	0.24	0.04	0.00
123	.	.	.	.	.	1.5 0.000105	0.00	-90	-90	0	0.24	0.04	0.00
124	.	.	.	.	.	1.5 0.000105	0.00	-90	-90	0	0.24	0.04	0.00
125	.	.	.	.	.	1.5 0.000105	0.00	-90	-90	0	0.24	0.04	0.00
126	.	.	.	.	.	1.5 0.000105	0.00	-90	-90	0	0.24	0.04	0.00
127	.	.	.	.	.	1.5 0.000105	0.00	-90	-90	0	0.24	0.04	0.00
128	.	.	.	.	.	1.5 0.000105	0.00	-90	-90	0	0.24	0.04	0.00
129	.	.	.	.	.	1.5 0.000105	0.00	-90	-90	0	0.24	0.04	0.00
130	.	.	.	.	.	1.5 0.000105	0.00	-90	-90	0	0.24	0.04	0.00
131	.	.	.	.	.	1.5 0.000105	0.00	-90	-90	0	0.24	0.04	0.00





JSC Shot No. 917  
 (Thin Plate with Cloth) 1/17/86

Measured Values

Calculated Values

Particle No.	X location of impact (origin at s)	Y location of impact (origin at s)	Z location of impact (origin at s)	Penetration Depth	Length of Particle	Mass	R location of impact (origin at s)	Theta location of impact (origin at s)	Phi location of impact (origin at s)	Cone Angle (angle from impact pt. to surf norm)	Average Diameter	Average Area	Velocity
	mm	mm	mm	mm	mm	gms	mm	Degrees	Degrees	Degrees	mm	mm squared	km/sec
Ejecta Origin s, At lower right corner facing target (at target surface)				Total from mass of target before & after		0.25							
Origin ss, At impact point on target surface				Corrected Ejecta Mass =		0.075164	30.07 percent Ejecta						
I, mm	Y, mm	Z, mm		Corrected Spall Mass =		0.174036	69.93 percent Spall						
	56	63	0	Calc. Ejecta Dust =		0.028196							
				Calc. Spall Dust =		0.065586							
Shear Strength (est.) used in velocity calculation, M Pascals			55	Total Calc. Dust =		0.093782	37.51 percent Dust						

Measured Values

Calculated Values

Particle No.	X location of impact (origin at s)	Y location of impact (origin at s)	Z location of impact (origin at s)	Penetration Depth	Length of Particle	Mass	R location of impact (origin at s)	Theta location of impact (origin at s)	Phi location of impact (origin at s)	Cone Angle (angle from impact pt. to surf norm)	Average Diameter	Average Area	Velocity
	mm	mm	mm	mm	mm	gms	mm	Degrees	Degrees	Degrees	mm	mm squared	Km/sec
264	.	.	.	.	.	0.5 0.000081875	0.00	-90	-90	0	0.36	0.10	0.00
265	.	.	.	.	.	0.5 0.000081875	0.00	-90	-90	0	0.36	0.10	0.00
266	.	.	.	.	.	0.5 0.000081875	0.00	-90	-90	0	0.36	0.10	0.00
267	.	.	.	.	.	0.5 0.000081875	0.00	-90	-90	0	0.36	0.10	0.00
268	.	.	.	.	.	0.5 0.000081875	0.00	-90	-90	0	0.36	0.10	0.00
269	.	.	.	.	.	0.5 0.000081875	0.00	-90	-90	0	0.36	0.10	0.00
270	.	.	.	.	.	0.5 0.000081875	0.00	-90	-90	0	0.36	0.10	0.00
271	.	.	.	.	.	0.5 0.000081875	0.00	-90	-90	0	0.36	0.10	0.00
272	.	.	.	.	.	0.5 0.000081875	0.00	-90	-90	0	0.36	0.10	0.00
273	.	.	.	.	.	0.5 0.000081875	0.00	-90	-90	0	0.36	0.10	0.00
274	.	.	.	.	.	0.5 0.000081875	0.00	-90	-90	0	0.36	0.10	0.00
275	.	.	.	.	.	0.5 0.000081875	0.00	-90	-90	0	0.36	0.10	0.00
276	.	.	.	.	.	0.5 0.000081875	0.00	-90	-90	0	0.36	0.10	0.00
277	.	.	.	.	.	0.5 0.000081875	0.00	-90	-90	0	0.36	0.10	0.00
278	.	.	.	.	.	0.5 0.000081875	0.00	-90	-90	0	0.36	0.10	0.00
279	.	.	.	.	.	0.5 0.000081875	0.00	-90	-90	0	0.36	0.10	0.00
280	.	.	.	.	.	0.5 0.000081875	0.00	-90	-90	0	0.36	0.10	0.00
281	.	.	.	.	.	0.5 0.000081875	0.00	-90	-90	0	0.36	0.10	0.00
282	.	.	.	.	.	0.5 0.000081875	0.00	-90	-90	0	0.36	0.10	0.00
283	.	.	.	.	.	0.5 0.000081875	0.00	-90	-90	0	0.36	0.10	0.00
284	.	.	.	.	.	0.5 0.000081875	0.00	-90	-90	0	0.36	0.10	0.00
285	.	.	.	.	.	0.5 0.000081875	0.00	-90	-90	0	0.36	0.10	0.00
286	.	.	.	.	.	0.5 0.000081875	0.00	-90	-90	0	0.36	0.10	0.00
287	.	.	.	.	.	0.5 0.000081875	0.00	-90	-90	0	0.36	0.10	0.00
288	.	.	.	.	.	0.5 0.000081875	0.00	-90	-90	0	0.36	0.10	0.00
289	.	.	.	.	.	0.5 0.000081875	0.00	-90	-90	0	0.36	0.10	0.00
290	.	.	.	.	.	0.5 0.000081875	0.00	-90	-90	0	0.36	0.10	0.00
291	.	.	.	.	.	0.5 0.000081875	0.00	-90	-90	0	0.36	0.10	0.00
292	.	.	.	.	.	0.5 0.000081875	0.00	-90	-90	0	0.36	0.10	0.00
293	.	.	.	.	.	0.5 0.000081875	0.00	-90	-90	0	0.36	0.10	0.00
294	.	.	.	.	.	0.5 0.000081875	0.00	-90	-90	0	0.36	0.10	0.00
295	.	.	.	.	.	0.5 0.000081875	0.00	-90	-90	0	0.36	0.10	0.00
296	.	.	.	.	.	0.5 0.000081875	0.00	-90	-90	0	0.36	0.10	0.00
297	.	.	.	.	.	0.5 0.000081875	0.00	-90	-90	0	0.36	0.10	0.00
298	.	.	.	.	.	0.5 0.000081875	0.00	-90	-90	0	0.36	0.10	0.00
299	.	.	.	.	.	0.5 0.000081875	0.00	-90	-90	0	0.36	0.10	0.00

Total Ejecta = 0.046968  
 Total measured ejecta = 0.0465  
 Total Spall = 0.10925  
 Total Mass = 0.156210

Measured Values

Calculated Values

Particle No.	X location of impact (origin at e)			Y location of impact (origin at e)			Z location of impact (origin at e)			Penetration Depth	Length of Particle	Mass	gms	Theta location of impact (origin at ee)		Phi location of impact (origin at ee)		Cone Angle (angle from impact pt. to surf norm)	Average Diameter	Average Area	Velocity
	mm	mm	mm	mm	mm	mm	mm	mm	mm					mm	mm	mm	mm				
44	122	14	82	115.30	37.53	-31.88	44.67	0.16	0.02	0.94											
45	122	87	91	112.85	34.70	13.59	36.25	0.16	0.02	0.48											
46	122	120	62	104.11	45.46	41.58	53.45	0.16	0.02	0.48											
47	122	106	76	106.89	39.66	28.35	44.68	0.16	0.02	2.79											
48	122	60	108	125.13	30.26	-2.85	30.33	0.16	0.02	1.86											
49	122	44	57	87.52	47.86	-20.22	49.36	0.26	0.05	0.21											
50	122	30	111	132.34	29.58	-17.50	32.99	0.20	0.03	0.85											
51	122	57	64	90.16	44.55	-7.13	44.78	0.24	0.05	0.42											
52	122	58	112	128.69	29.36	-3.58	29.51	0.28	0.06	0.73											
53	122	56	100	118.53	32.21	-5.14	32.47	0.20	0.03	1.69											
54	122	147	113	153.17	29.14	35.97	42.46	0.20	0.03	0.85											
55	122	106	75	106.18	40.03	28.66	45.06	0.16	0.02	1.52											
56	85	15	116	128.97	12.63	-23.32	23.91	0.21	0.04	1.73											
57	78	15	116	127.74	9.30	-23.32	24.75	0.20	0.03	0.97											
58	70	8	116	129.72	5.42	-26.17	26.59	0.23	0.04	1.34											
59	78	11	116	129.36	9.30	-24.96	26.27	0.25	0.05	1.89											
60	75	6	116	131.12	7.85	-26.96	27.79	0.20	0.03	1.69											
61	26	28	116	126.15	-15.88	-17.69	23.14	0.43	0.14	0.43											
62	53	48	116	117.39	-2.96	-8.34	8.83	0.28	0.06	1.43											
63	66	57	116	116.49	3.45	-3.95	5.24	0.84	0.32	1.91											
64	68	58	116	116.56	4.44	-3.45	5.61	0.28	0.06	2.83											
65	26	76	116	121.10	-15.88	5.42	16.69	0.37	0.11	0.27											
66	68	57	116	116.62	4.44	-3.95	5.93	0.28	0.06	3.53											
67	30	110	116	127.76	-14.04	21.20	24.77	0.67	0.35	0.95											
68	112	62	116	127.57	24.56	-1.48	24.59	0.22	0.04	0.21											
69	62	103	116	122.10	1.48	18.14	18.19	0.28	0.06	0.37											
70	62	73	116	116.31	1.48	3.95	4.21	0.20	0.03	1.69											
71	112	100	116	132.25	24.56	16.79	28.70	0.20	0.03	0.44											
72	97	125	116	136.01	18.14	27.35	31.48	0.16	0.02	0.39											
73	56	4	116	131.10	-1.48	-27.74	27.77	0.23	0.04	0.41											
74	61	15	116	126.33	0.99	-23.32	23.33	0.32	0.08	0.97											
75	32	57	116	119.37	-13.10	-3.95	13.65	0.32	0.08	0.97											
76	18	61	116	123.10	-19.47	-1.97	19.55	0.32	0.08	0.97											
77	19	60	116	122.80	-19.03	-2.47	19.16	0.32	0.08	0.97											
78	22	70	116	121.86	-17.69	2.47	17.84	0.32	0.08	0.50											
79	31	62	116	119.37	-13.57	-1.48	13.65	0.32	0.08	0.97											
80	55	60	116	116.18	-1.97	-2.47	3.16	0.32	0.08	1.90											
81	47	76	116	117.14	-5.91	5.42	7.99	0.32	0.08	0.97											
82	80	64	116	117.89	10.26	-4.49	10.27	0.19	0.03	1.43											
83	105	40	116	127.27	21.63	-12.16	24.29	0.23	0.04	1.59											
84	115	18	116	137.12	25.77	-22.06	32.22	0.23	0.04	0.41											
85	108	116	116	126.59	22.90	6.39	23.61	0.23	0.04	3.16											
86	80	78	116	116.40	10.26	6.39	12.02	0.32	0.08	1.90											
87	50	10	116	128.69	-4.44	-25.37	25.66	0.32	0.08	0.97											





Measured Values

Calculated Values

Particle No.	X location of impact (origin at e)			Y location of impact (origin at e)			Z location of impact (origin at e)			Penetration Depth	Length of Particle	Mass	R location of impact (origin at ee)	Theta location of impact (origin at ee)	Phi location of impact (origin at ee)	Cone Angle (angle from impact pt. to surf norm)	Average Diameter	Average Area	Velocity
	mm	mm	mm	mm	mm	mm	mm	mm	mm										
132											6	0.000344	0.00	-90.00	-90.00	0	0.22	0.04	0.00
133											6	0.000344	0.00	-90.00	-90.00	0	0.22	0.04	0.00
134											6	0.000344	0.00	-90.00	-90.00	0	0.22	0.04	0.00
135											6	0.000344	0.00	-90.00	-90.00	0	0.22	0.04	0.00
136											6	0.000344	0.00	-90.00	-90.00	0	0.22	0.04	0.00
137											6	0.000344	0.00	-90.00	-90.00	0	0.22	0.04	0.00
138											6	0.000344	0.00	-90.00	-90.00	0	0.22	0.04	0.00
139											6	0.000344	0.00	-90.00	-90.00	0	0.22	0.04	0.00
140											6	0.000344	0.00	-90.00	-90.00	0	0.22	0.04	0.00
141											6	0.000344	0.00	-90.00	-90.00	0	0.22	0.04	0.00
142											6	0.000344	0.00	-90.00	-90.00	0	0.22	0.04	0.00
143											6	0.000344	0.00	-90.00	-90.00	0	0.22	0.04	0.00
144											6	0.000344	0.00	-90.00	-90.00	0	0.22	0.04	0.00
145											6	0.000344	0.00	-90.00	-90.00	0	0.22	0.04	0.00
146											6	0.000344	0.00	-90.00	-90.00	0	0.22	0.04	0.00
147											6	0.000344	0.00	-90.00	-90.00	0	0.22	0.04	0.00
148											6	0.000344	0.00	-90.00	-90.00	0	0.22	0.04	0.00
149											6	0.000344	0.00	-90.00	-90.00	0	0.22	0.04	0.00
150											6	0.000344	0.00	-90.00	-90.00	0	0.22	0.04	0.00
151											6	0.000344	0.00	-90.00	-90.00	0	0.22	0.04	0.00
152											6	0.000344	0.00	-90.00	-90.00	0	0.22	0.04	0.00
153											6	0.000344	0.00	-90.00	-90.00	0	0.22	0.04	0.00
154											6	0.000344	0.00	-90.00	-90.00	0	0.22	0.04	0.00
155											6	0.000344	0.00	-90.00	-90.00	0	0.22	0.04	0.00
156											6	0.000344	0.00	-90.00	-90.00	0	0.22	0.04	0.00
157											6	0.000344	0.00	-90.00	-90.00	0	0.22	0.04	0.00
158											6	0.000344	0.00	-90.00	-90.00	0	0.22	0.04	0.00
159											6	0.000344	0.00	-90.00	-90.00	0	0.22	0.04	0.00
160											6	0.000344	0.00	-90.00	-90.00	0	0.22	0.04	0.00
161											6	0.000344	0.00	-90.00	-90.00	0	0.22	0.04	0.00
162											6	0.000344	0.00	-90.00	-90.00	0	0.22	0.04	0.00
163											6	0.000344	0.00	-90.00	-90.00	0	0.22	0.04	0.00
164											6	0.000344	0.00	-90.00	-90.00	0	0.22	0.04	0.00
165											6	0.000344	0.00	-90.00	-90.00	0	0.22	0.04	0.00
166											6	0.000344	0.00	-90.00	-90.00	0	0.22	0.04	0.00
167											6	0.000344	0.00	-90.00	-90.00	0	0.22	0.04	0.00
168											6	0.000344	0.00	-90.00	-90.00	0	0.22	0.04	0.00
169											6	0.000344	0.00	-90.00	-90.00	0	0.22	0.04	0.00
170											6	0.000344	0.00	-90.00	-90.00	0	0.22	0.04	0.00
171											6	0.000344	0.00	-90.00	-90.00	0	0.22	0.04	0.00
172											6	0.000344	0.00	-90.00	-90.00	0	0.22	0.04	0.00
173											6	0.000344	0.00	-90.00	-90.00	0	0.22	0.04	0.00
174											6	0.000344	0.00	-90.00	-90.00	0	0.22	0.04	0.00
175											6	0.000344	0.00	-90.00	-90.00	0	0.22	0.04	0.00

Measured Values

Calculated Values

Particle No.	Measured Values										Calculated Values									
	X location of impact (origin at *)	Y location of impact (origin at *)	Z location of impact (origin at *)	Penetration Depth	Length of Particle	Mass	gms	R location of impact (origin at *)	Theta location of impact (origin at *)	Phi location of impact (origin at *)	Cone Angle (angle from Diameter to surf norm)	Average Diameter	Average Area	Velocity						
88	55	111	116	2	2	0.000128	2	124.85	-1.97	21.63	21.70	0.23	0.04	1.59						
89	52	90	116	2	2	0.000128	2	118.87	-3.45	12.16	12.62	0.23	0.04	1.59						
90	100	50	116	1	1	0.000128	1	123.94	19.47	-7.37	20.62	0.32	0.08	0.27						
91	97	0	6	0.5	7	0.000200	7	75.53	81.03	-84.73	85.44	0.15	0.02	0.27						
92	21	0	42	2	4	0.000500	4	86.21	-42.14	-57.13	60.85	0.32	0.08	0.96						
93	64	0	43	0.5	4	0.000600	4	78.10	6.63	-56.51	56.59	0.35	0.10	0.24						
94	27	0	50	3	7	0.000100	7	88.03	-32.62	-52.43	55.39	0.11	0.01	1.84						
95	92	0	50	2	5	0.000700	5	88.40	33.42	-52.43	55.55	0.34	0.09	0.83						
96	57	0	15	2	3	0.000200	3	66.74	-7.59	-77.01	77.01	0.23	0.04	1.28						
97	53	0	78	1	3	0.000100	3	101.71	-4.40	-39.81	39.93	0.16	0.02	0.77						
98	27	0	51	2	3	0.000100	3	88.60	-32.11	-51.88	54.86	0.16	0.02	1.52						
99	5	0	57	2	2	0.000200	2	101.93	-43.45	-48.75	56.00	0.28	0.06	1.43						
100	64	0	39	2	3	0.000200	3	75.97	7.31	-59.04	59.11	0.23	0.04	1.28						
101	28	0	61	1	2	0.000100	2	94.38	-26.94	-46.82	49.73	0.20	0.03	0.85						
102	56	0	33	2	3	0.000200	3	72.96	-5.19	-63.08	63.11	0.23	0.04	1.28						
103	25	0	80	0.5	1	0.000100	1	108.54	-23.03	-39.09	42.52	0.28	0.06	0.53						
104	Loose on bottom				10	0.003400	10	0.00	-90.00	-90.00	0	0.66	0.34	0.00						
105					9	0.000700	9	0.00	-90.00	-90.00	0	0.25	0.05	0.00						
106					10	0.000900	10	0.00	-90.00	-90.00	0	0.27	0.06	0.00						
107					10	0.000800	10	0.00	-90.00	-90.00	0	0.25	0.05	0.00						
108					7	0.001500	7	0.00	-90.00	-90.00	0	0.42	0.14	0.00						
109					7	0.001100	7	0.00	-90.00	-90.00	0	0.36	0.10	0.00						
110					7	0.000700	7	0.00	-90.00	-90.00	0	0.28	0.06	0.00						
111					7	0.000800	7	0.00	-90.00	-90.00	0	0.30	0.07	0.00						
112					7	0.000775	7	0.00	-90.00	-90.00	0	0.30	0.07	0.00						
113					7	0.000775	7	0.00	-90.00	-90.00	0	0.30	0.07	0.00						
114					7	0.000775	7	0.00	-90.00	-90.00	0	0.30	0.07	0.00						
115					7	0.000775	7	0.00	-90.00	-90.00	0	0.30	0.07	0.00						
116					7	0.000775	7	0.00	-90.00	-90.00	0	0.30	0.07	0.00						
117					7	0.000775	7	0.00	-90.00	-90.00	0	0.30	0.07	0.00						
118					7	0.000775	7	0.00	-90.00	-90.00	0	0.30	0.07	0.00						
119					7	0.000775	7	0.00	-90.00	-90.00	0	0.30	0.07	0.00						
120					7	0.000775	7	0.00	-90.00	-90.00	0	0.30	0.07	0.00						
121					7	0.000775	7	0.00	-90.00	-90.00	0	0.30	0.07	0.00						
122					7	0.000775	7	0.00	-90.00	-90.00	0	0.30	0.07	0.00						
123					7	0.000775	7	0.00	-90.00	-90.00	0	0.30	0.07	0.00						
124					7	0.000775	7	0.00	-90.00	-90.00	0	0.30	0.07	0.00						
125					7	0.000775	7	0.00	-90.00	-90.00	0	0.30	0.07	0.00						
126					7	0.000775	7	0.00	-90.00	-90.00	0	0.30	0.07	0.00						
127					7	0.000775	7	0.00	-90.00	-90.00	0	0.30	0.07	0.00						
128					6	0.000344	6	0.00	-90.00	-90.00	0	0.22	0.04	0.00						
129					6	0.000344	6	0.00	-90.00	-90.00	0	0.22	0.04	0.00						
130					6	0.000344	6	0.00	-90.00	-90.00	0	0.22	0.04	0.00						
131					6	0.000344	6	0.00	-90.00	-90.00	0	0.22	0.04	0.00						

JSC Shot No. 917  
1/17/86

(Thin Plate with Cloth)

Measured Values

Calculated Values

Particle No.	X location of impact (origin at e)			Y location of impact (origin at e)			Z location of impact (origin at e)			Penetration Depth	Length of Particle	Mass	R location of impact (origin at es)	Theta location of impact (origin at es)		Phi location of impact (origin at es)		Cone Angle (angle from impact pt. to surf norm)	Average Diameter	Average Area	Velocity
	mm	mm	mm	mm	mm	mm	mm	mm	mm					mm	mm	mm	mm				
220											4	0.000219	0.00	-90.00	-90.00	0	0.21	0.03	0.00	0.00	
221											4	0.000219	0.00	-90.00	-90.00	0	0.21	0.03	0.00	0.00	
222											4	0.000219	0.00	-90.00	-90.00	0	0.21	0.03	0.00	0.00	
223											4	0.000219	0.00	-90.00	-90.00	0	0.21	0.03	0.00	0.00	
224											4	0.000219	0.00	-90.00	-90.00	0	0.21	0.03	0.00	0.00	
225											4	0.000219	0.00	-90.00	-90.00	0	0.21	0.03	0.00	0.00	
226											4	0.000219	0.00	-90.00	-90.00	0	0.21	0.03	0.00	0.00	
227											4	0.000219	0.00	-90.00	-90.00	0	0.21	0.03	0.00	0.00	
228											4	0.000219	0.00	-90.00	-90.00	0	0.21	0.03	0.00	0.00	
229											4	0.000219	0.00	-90.00	-90.00	0	0.21	0.03	0.00	0.00	
230											4	0.000219	0.00	-90.00	-90.00	0	0.21	0.03	0.00	0.00	
231											4	0.000219	0.00	-90.00	-90.00	0	0.21	0.03	0.00	0.00	
232											4	0.000219	0.00	-90.00	-90.00	0	0.21	0.03	0.00	0.00	
233											4	0.000219	0.00	-90.00	-90.00	0	0.21	0.03	0.00	0.00	
234											4	0.000219	0.00	-90.00	-90.00	0	0.21	0.03	0.00	0.00	
235											4	0.000750	0.00	-90.00	-90.00	0	0.39	0.12	0.00	0.00	
236											4	0.000750	0.00	-90.00	-90.00	0	0.39	0.12	0.00	0.00	
237											4	0.000750	0.00	-90.00	-90.00	0	0.39	0.12	0.00	0.00	
238											4	0.000750	0.00	-90.00	-90.00	0	0.39	0.12	0.00	0.00	
239											2	0.000216	0.00	-90.00	-90.00	0	0.30	0.07	0.00	0.00	
240											2	0.000216	0.00	-90.00	-90.00	0	0.30	0.07	0.00	0.00	
241											2	0.000216	0.00	-90.00	-90.00	0	0.30	0.07	0.00	0.00	
242											2	0.000216	0.00	-90.00	-90.00	0	0.30	0.07	0.00	0.00	
243											2	0.000216	0.00	-90.00	-90.00	0	0.30	0.07	0.00	0.00	
244											2	0.000216	0.00	-90.00	-90.00	0	0.30	0.07	0.00	0.00	
245											2	0.000216	0.00	-90.00	-90.00	0	0.30	0.07	0.00	0.00	
246											2	0.000216	0.00	-90.00	-90.00	0	0.30	0.07	0.00	0.00	
247											2	0.000216	0.00	-90.00	-90.00	0	0.30	0.07	0.00	0.00	
248											2	0.000216	0.00	-90.00	-90.00	0	0.30	0.07	0.00	0.00	
249											2	0.000216	0.00	-90.00	-90.00	0	0.30	0.07	0.00	0.00	
250											2	0.000216	0.00	-90.00	-90.00	0	0.30	0.07	0.00	0.00	
251											2	0.000216	0.00	-90.00	-90.00	0	0.30	0.07	0.00	0.00	
252											2	0.000216	0.00	-90.00	-90.00	0	0.30	0.07	0.00	0.00	
253											2	0.000216	0.00	-90.00	-90.00	0	0.30	0.07	0.00	0.00	
254											2	0.000216	0.00	-90.00	-90.00	0	0.30	0.07	0.00	0.00	
255											2	0.000216	0.00	-90.00	-90.00	0	0.30	0.07	0.00	0.00	
256											2	0.000216	0.00	-90.00	-90.00	0	0.30	0.07	0.00	0.00	
257											2	0.000216	0.00	-90.00	-90.00	0	0.30	0.07	0.00	0.00	
258											2	0.000216	0.00	-90.00	-90.00	0	0.30	0.07	0.00	0.00	
259											2	0.000216	0.00	-90.00	-90.00	0	0.30	0.07	0.00	0.00	
260											2	0.000216	0.00	-90.00	-90.00	0	0.30	0.07	0.00	0.00	
261											2	0.000216	0.00	-90.00	-90.00	0	0.30	0.07	0.00	0.00	
262											2	0.000216	0.00	-90.00	-90.00	0	0.30	0.07	0.00	0.00	
263											2	0.000216	0.00	-90.00	-90.00	0	0.30	0.07	0.00	0.00	

Measured Values

Calculated Values

Particle No.	Location of impact (origin at *)				Penetration Depth	Length of Particle	Mass	Location of impact (origin at **)				Average Diameter	Average Area	Velocity
	X	Y	Z	Phi				Theta	Phi	Theta	Cone Angle			
176	0.00	0.00	0.00	-90.00	0.00	6	0.000344	0.00	-90.00	-90.00	0	0.22	0.04	0.00
177	0.00	0.00	0.00	-90.00	0.00	6	0.000344	0.00	-90.00	-90.00	0	0.22	0.04	0.00
178	0.00	0.00	0.00	-90.00	0.00	6	0.000344	0.00	-90.00	-90.00	0	0.22	0.04	0.00
179	0.00	0.00	0.00	-90.00	0.00	6	0.000344	0.00	-90.00	-90.00	0	0.22	0.04	0.00
180	0.00	0.00	0.00	-90.00	0.00	6	0.000344	0.00	-90.00	-90.00	0	0.22	0.04	0.00
181	0.00	0.00	0.00	-90.00	0.00	6	0.000344	0.00	-90.00	-90.00	0	0.22	0.04	0.00
182	0.00	0.00	0.00	-90.00	0.00	6	0.000344	0.00	-90.00	-90.00	0	0.22	0.04	0.00
183	0.00	0.00	0.00	-90.00	0.00	6	0.000344	0.00	-90.00	-90.00	0	0.22	0.04	0.00
184	0.00	0.00	0.00	-90.00	0.00	6	0.000344	0.00	-90.00	-90.00	0	0.22	0.04	0.00
185	0.00	0.00	0.00	-90.00	0.00	6	0.000344	0.00	-90.00	-90.00	0	0.22	0.04	0.00
186	0.00	0.00	0.00	-90.00	0.00	6	0.000344	0.00	-90.00	-90.00	0	0.22	0.04	0.00
187	0.00	0.00	0.00	-90.00	0.00	4	0.000219	0.00	-90.00	-90.00	0	0.21	0.03	0.00
188	0.00	0.00	0.00	-90.00	0.00	4	0.000219	0.00	-90.00	-90.00	0	0.21	0.03	0.00
189	0.00	0.00	0.00	-90.00	0.00	4	0.000219	0.00	-90.00	-90.00	0	0.21	0.03	0.00
190	0.00	0.00	0.00	-90.00	0.00	4	0.000219	0.00	-90.00	-90.00	0	0.21	0.03	0.00
191	0.00	0.00	0.00	-90.00	0.00	4	0.000219	0.00	-90.00	-90.00	0	0.21	0.03	0.00
192	0.00	0.00	0.00	-90.00	0.00	4	0.000219	0.00	-90.00	-90.00	0	0.21	0.03	0.00
193	0.00	0.00	0.00	-90.00	0.00	4	0.000219	0.00	-90.00	-90.00	0	0.21	0.03	0.00
194	0.00	0.00	0.00	-90.00	0.00	4	0.000219	0.00	-90.00	-90.00	0	0.21	0.03	0.00
195	0.00	0.00	0.00	-90.00	0.00	4	0.000219	0.00	-90.00	-90.00	0	0.21	0.03	0.00
196	0.00	0.00	0.00	-90.00	0.00	4	0.000219	0.00	-90.00	-90.00	0	0.21	0.03	0.00
197	0.00	0.00	0.00	-90.00	0.00	4	0.000219	0.00	-90.00	-90.00	0	0.21	0.03	0.00
198	0.00	0.00	0.00	-90.00	0.00	4	0.000219	0.00	-90.00	-90.00	0	0.21	0.03	0.00
199	0.00	0.00	0.00	-90.00	0.00	4	0.000219	0.00	-90.00	-90.00	0	0.21	0.03	0.00
200	0.00	0.00	0.00	-90.00	0.00	4	0.000219	0.00	-90.00	-90.00	0	0.21	0.03	0.00
201	0.00	0.00	0.00	-90.00	0.00	4	0.000219	0.00	-90.00	-90.00	0	0.21	0.03	0.00
202	0.00	0.00	0.00	-90.00	0.00	4	0.000219	0.00	-90.00	-90.00	0	0.21	0.03	0.00
203	0.00	0.00	0.00	-90.00	0.00	4	0.000219	0.00	-90.00	-90.00	0	0.21	0.03	0.00
204	0.00	0.00	0.00	-90.00	0.00	4	0.000219	0.00	-90.00	-90.00	0	0.21	0.03	0.00
205	0.00	0.00	0.00	-90.00	0.00	4	0.000219	0.00	-90.00	-90.00	0	0.21	0.03	0.00
206	0.00	0.00	0.00	-90.00	0.00	4	0.000219	0.00	-90.00	-90.00	0	0.21	0.03	0.00
207	0.00	0.00	0.00	-90.00	0.00	4	0.000219	0.00	-90.00	-90.00	0	0.21	0.03	0.00
208	0.00	0.00	0.00	-90.00	0.00	4	0.000219	0.00	-90.00	-90.00	0	0.21	0.03	0.00
209	0.00	0.00	0.00	-90.00	0.00	4	0.000219	0.00	-90.00	-90.00	0	0.21	0.03	0.00
210	0.00	0.00	0.00	-90.00	0.00	4	0.000219	0.00	-90.00	-90.00	0	0.21	0.03	0.00
211	0.00	0.00	0.00	-90.00	0.00	4	0.000219	0.00	-90.00	-90.00	0	0.21	0.03	0.00
212	0.00	0.00	0.00	-90.00	0.00	4	0.000219	0.00	-90.00	-90.00	0	0.21	0.03	0.00
213	0.00	0.00	0.00	-90.00	0.00	4	0.000219	0.00	-90.00	-90.00	0	0.21	0.03	0.00
214	0.00	0.00	0.00	-90.00	0.00	4	0.000219	0.00	-90.00	-90.00	0	0.21	0.03	0.00
215	0.00	0.00	0.00	-90.00	0.00	4	0.000219	0.00	-90.00	-90.00	0	0.21	0.03	0.00
216	0.00	0.00	0.00	-90.00	0.00	4	0.000219	0.00	-90.00	-90.00	0	0.21	0.03	0.00
217	0.00	0.00	0.00	-90.00	0.00	4	0.000219	0.00	-90.00	-90.00	0	0.21	0.03	0.00
218	0.00	0.00	0.00	-90.00	0.00	4	0.000219	0.00	-90.00	-90.00	0	0.21	0.03	0.00
219	0.00	0.00	0.00	-90.00	0.00	4	0.000219	0.00	-90.00	-90.00	0	0.21	0.03	0.00

Measured Values

Calculated Values

Particle No.	X location of impact (origin at e)			Y location of impact (origin at e)			Z location of impact (origin at e)			Penetration Depth	Length of Particle	Mass	R location of impact (origin at e)			Theta location of impact (origin at e)			Phi location of impact (origin at e)			Cone Angle (angle from impact pt. to surf norm)	Average Diameter	Average Area	Velocity
	mm	mm	mm	mm	mm	mm	mm	mm	mm				mm	mm	mm	mm	mm	mm	mm	mm	mm				
308	.	.	.	.	.	.	.	.	.	.	2	0.000216	0.00	-90.00	-90.00	-90.00	0	0.30	0.07	0.00					
309	.	.	.	.	.	.	.	.	.	.	2	0.000216	0.00	-90.00	-90.00	-90.00	0	0.30	0.07	0.00					
310	.	.	.	.	.	.	.	.	.	.	2	0.000216	0.00	-90.00	-90.00	-90.00	0	0.30	0.07	0.00					
311	.	.	.	.	.	.	.	.	.	.	2	0.000216	0.00	-90.00	-90.00	-90.00	0	0.30	0.07	0.00					
312	.	.	.	.	.	.	.	.	.	.	2	0.000216	0.00	-90.00	-90.00	-90.00	0	0.30	0.07	0.00					
313	.	.	.	.	.	.	.	.	.	.	2	0.000216	0.00	-90.00	-90.00	-90.00	0	0.30	0.07	0.00					
314	.	.	.	.	.	.	.	.	.	.	2	0.000216	0.00	-90.00	-90.00	-90.00	0	0.30	0.07	0.00					
315	.	.	.	.	.	.	.	.	.	.	2	0.000216	0.00	-90.00	-90.00	-90.00	0	0.30	0.07	0.00					
316	.	.	.	.	.	.	.	.	.	.	2	0.000216	0.00	-90.00	-90.00	-90.00	0	0.30	0.07	0.00					
317	.	.	.	.	.	.	.	.	.	.	2	0.000216	0.00	-90.00	-90.00	-90.00	0	0.30	0.07	0.00					
318	.	.	.	.	.	.	.	.	.	.	2	0.000216	0.00	-90.00	-90.00	-90.00	0	0.30	0.07	0.00					
319	.	.	.	.	.	.	.	.	.	.	2	0.000216	0.00	-90.00	-90.00	-90.00	0	0.30	0.07	0.00					
320	.	.	.	.	.	.	.	.	.	.	2	0.000216	0.00	-90.00	-90.00	-90.00	0	0.30	0.07	0.00					
321	.	.	.	.	.	.	.	.	.	.	2	0.000216	0.00	-90.00	-90.00	-90.00	0	0.30	0.07	0.00					
322	.	.	.	.	.	.	.	.	.	.	2	0.000216	0.00	-90.00	-90.00	-90.00	0	0.30	0.07	0.00					
323	.	.	.	.	.	.	.	.	.	.	2	0.000216	0.00	-90.00	-90.00	-90.00	0	0.30	0.07	0.00					
324	.	.	.	.	.	.	.	.	.	.	2	0.000216	0.00	-90.00	-90.00	-90.00	0	0.30	0.07	0.00					
325	.	.	.	.	.	.	.	.	.	.	2	0.000216	0.00	-90.00	-90.00	-90.00	0	0.30	0.07	0.00					
326	.	.	.	.	.	.	.	.	.	.	2	0.000216	0.00	-90.00	-90.00	-90.00	0	0.30	0.07	0.00					
327	.	.	.	.	.	.	.	.	.	.	2	0.000216	0.00	-90.00	-90.00	-90.00	0	0.30	0.07	0.00					
328	.	.	.	.	.	.	.	.	.	.	2	0.000216	0.00	-90.00	-90.00	-90.00	0	0.30	0.07	0.00					
329	.	.	.	.	.	.	.	.	.	.	2	0.000216	0.00	-90.00	-90.00	-90.00	0	0.30	0.07	0.00					
330	.	.	.	.	.	.	.	.	.	.	2	0.000216	0.00	-90.00	-90.00	-90.00	0	0.30	0.07	0.00					
331	.	.	.	.	.	.	.	.	.	.	2	0.000216	0.00	-90.00	-90.00	-90.00	0	0.30	0.07	0.00					
332	.	.	.	.	.	.	.	.	.	.	2	0.000216	0.00	-90.00	-90.00	-90.00	0	0.30	0.07	0.00					
333	.	.	.	.	.	.	.	.	.	.	2	0.000216	0.00	-90.00	-90.00	-90.00	0	0.30	0.07	0.00					
334	.	.	.	.	.	.	.	.	.	.	2	0.000216	0.00	-90.00	-90.00	-90.00	0	0.30	0.07	0.00					
335	.	.	.	.	.	.	.	.	.	.	2	0.000216	0.00	-90.00	-90.00	-90.00	0	0.30	0.07	0.00					
336	.	.	.	.	.	.	.	.	.	.	2	0.000216	0.00	-90.00	-90.00	-90.00	0	0.30	0.07	0.00					
337	.	.	.	.	.	.	.	.	.	.	2	0.000216	0.00	-90.00	-90.00	-90.00	0	0.30	0.07	0.00					
338	.	.	.	.	.	.	.	.	.	.	2	0.000216	0.00	-90.00	-90.00	-90.00	0	0.30	0.07	0.00					
339	.	.	.	.	.	.	.	.	.	.	2	0.000216	0.00	-90.00	-90.00	-90.00	0	0.30	0.07	0.00					
340	.	.	.	.	.	.	.	.	.	.	2	0.000216	0.00	-90.00	-90.00	-90.00	0	0.30	0.07	0.00					
341	.	.	.	.	.	.	.	.	.	.	2	0.000216	0.00	-90.00	-90.00	-90.00	0	0.30	0.07	0.00					
342	.	.	.	.	.	.	.	.	.	.	2	0.000216	0.00	-90.00	-90.00	-90.00	0	0.30	0.07	0.00					
343	.	.	.	.	.	.	.	.	.	.	2	0.000216	0.00	-90.00	-90.00	-90.00	0	0.30	0.07	0.00					
344	.	.	.	.	.	.	.	.	.	.	2	0.000216	0.00	-90.00	-90.00	-90.00	0	0.30	0.07	0.00					
345	.	.	.	.	.	.	.	.	.	.	2	0.000216	0.00	-90.00	-90.00	-90.00	0	0.30	0.07	0.00					
346	.	.	.	.	.	.	.	.	.	.	2	0.000216	0.00	-90.00	-90.00	-90.00	0	0.30	0.07	0.00					
347	.	.	.	.	.	.	.	.	.	.	2	0.000216	0.00	-90.00	-90.00	-90.00	0	0.30	0.07	0.00					
348	.	.	.	.	.	.	.	.	.	.	2	0.000216	0.00	-90.00	-90.00	-90.00	0	0.30	0.07	0.00					
349	.	.	.	.	.	.	.	.	.	.	2	0.000216	0.00	-90.00	-90.00	-90.00	0	0.30	0.07	0.00					
350	.	.	.	.	.	.	.	.	.	.	2	0.000216	0.00	-90.00	-90.00	-90.00	0	0.30	0.07	0.00					
351	.	.	.	.	.	.	.	.	.	.	2	0.000216	0.00	-90.00	-90.00	-90.00	0	0.30	0.07	0.00					



JSC Shot No. 923  
 (Thin Plate with no Cloth)  
 1/17/86  
 (Impact at -30 deg. phi from normal on ejecta side)

Measured Values

Calculated Values

Particle No.	X location of impact (origin at e)			Y location of impact (origin at e)			Z location of impact (origin at e)			Penetration Depth	Length of Particle	Mass	R location of impact (origin at ee)	Theta location of impact (origin at ee)			Phi location of impact (origin at ee)			Cone Angle (angle from normal)	Average Diameter	Average Area	Velocity
	no	no	no	no	no	no	no	no	no					no	no	no	no	no	no				
1	0	0	136	72	4	0.000100	109.16	-76.90	80.97	82.53	0.14	0.02	0.71										
2	29	36	136	58	0.5	0.000100	104.93	-50.56	74.73	75.47	0.13	0.01	0.34										
3	36	0	136	66	3	0.000300	97.67	-52.19	78.14	78.55	0.15	0.02	1.25										
4	0	0	118	118	3	0.000600	88.15	-56.10	-50.05	62.38	0.28	0.06	1.23										
5	0	0	102	114	5	0.001300	89.50	-48.90	-35.66	53.52	0.26	0.05	1.31										
6	0	0	114	114	14	0.000400	80.71	-57.86	-43.51	61.65	0.19	0.03	0.33										
7	0	0	114	114	5	0.002700	83.94	-56.21	-44.92	60.90	0.16	0.02	0.73										
8	0	0	110	110	17	0.000500	77.39	-57.88	-36.49	60.34	0.15	0.02	0.33										
9	0	0	109	109	14	0.000300	78.21	-56.97	-35.88	59.53	0.13	0.01	0.78										
10	0	0	112	112	3	0.000800	76.92	-59.06	-38.73	61.62	0.12	0.01	0.69										
11	0	0	107	107	4	0.001400	77.08	-56.82	-32.17	58.84	0.19	0.03	0.86										
12	0	0	111	111	2	0.000600	77.72	-58.13	-38.05	60.79	0.14	0.02	0.57										
13	0	0	123	123	3	0.000100	127.12	-29.20	11.89	30.85	0.16	0.02	0.77										
14	0	0	129	129	1	0.000100	118.95	-32.18	18.32	35.41	0.20	0.03	0.85										
15	0	0	142	142	3	0.000100	113.77	-32.52	4.94	32.76	0.20	0.03	2.52										
16	0	0	150	150	3	0.000100	104.13	-36.23	9.41	36.91	0.16	0.02	2.27										
17	0	0	144	144	2	0.000275	107.97	-35.05	12.58	36.36	0.27	0.06	1.19										
18	0	0	143	143	3	0.000275	115.15	-33.09	16.58	35.62	0.24	0.04	1.65										
19	0	0	151	151	2	0.000275	102.46	-38.21	19.73	40.86	0.33	0.09	0.67										
20	0	0	161	161	4	0.000275	99.92	-40.77	26.61	44.92	0.28	0.04	1.65										
21	0	0	164	164	5	0.000100	99.03	-41.73	28.77	46.33	0.13	0.01	0.67										
22	0	0	169	169	4	0.000150	99.87	-42.42	32.41	48.05	0.17	0.02	0.65										
23	0	0	189	189	4	0.000150	100.97	-47.95	46.85	56.98	0.17	0.02	0.65										
24	0	0	197	197	3	0.000150	105.37	-48.68	51.38	59.41	0.20	0.03	0.70										
25	0	0	192	192	2	0.000150	121.73	-39.06	44.47	51.86	0.25	0.05	1.53										
26	0	0	205	205	1	0.000150	123.85	-38.79	45.24	52.20	0.17	0.02	0.65										
27	0	0	109	109	2	0.000150	101.78	-58.02	62.13	68.02	0.17	0.02	1.28										
28	0	0	12	12	2	0.000150	89.28	-46.01	-25.42	48.74	0.14	0.02	1.15										
29	0	0	20	106	2	0.000150	79.60	-54.97	-33.27	57.51	0.17	0.02	1.28										
30	0	0	69	50	2	0.000150	99.87	-42.42	32.41	48.05	0.16	0.02	1.21										
31	0	0	83	56	1	0.000150	96.70	-48.19	43.35	55.65	0.17	0.02	0.65										
32	0	0	74	53	3	0.000200	97.81	-44.69	36.25	50.92	0.18	0.03	1.68										
33	0	0	20	10	6	0.000500	141.31	-25.85	9.00	27.01	0.20	0.03	2.25										
34	0	0	23	102	0.5	0.000200	79.19	-53.75	-27.68	55.62	0.15	0.02	0.27										
35	0	0	66	45	4	0.000400	103.81	-40.04	30.22	45.64	0.28	0.06	2.00										
36	0	0	21	114	0.5	0.000200	77.08	-59.92	-41.44	62.72	0.18	0.03	0.29										
37	0	0	39	34	1	0.000067	116.01	-32.54	14.32	34.50	0.16	0.02	0.94										
38	0	0	33	20	0.5	0.000067	129.11	-28.85	13.31	30.94	0.16	0.02	0.48										
39	0	0	51	56	0.5	0.000067	96.26	-40.85	18.63	42.86	0.16	0.02	0.48										
40	0	0	50	55	0.5	0.000067	97.17	-40.30	18.04	42.26	0.16	0.02	0.48										
41	0	0	10	114	0.5	0.000067	83.94	-56.21	-44.92	60.90	0.12	0.01	0.40										
42	0	0	114	114	2	0.000067	86.64	-54.93	-45.89	60.38	0.07	0.00	1.24										
43	0	0	7	105	3	0.000067	87.98	-50.59	-37.75	55.27	0.13	0.01	0.85										

SPALL



Measured Values

Calculated Values

Particle No.	X location of impact (origin at *)	Y location of impact (origin at *)	Z location of impact (origin at *)	Penetration Depth	Length of Particle	Mass	R location of impact (origin at *)	Theta location of impact (origin at *)	Phi location of impact (origin at *)	Cone Angle (to surf norm)	Average Diameter	Average Area	Velocity
	mm	mm	mm	mm	mm	gms	mm	Degrees	Degrees	Degrees	mm	mm squared	km/sec
352	.	.	.			2 0.000216	0.00	-90.00	-90.00	0	0.30	0.07	0.00
353	.	.	.			2 0.000216	0.00	-90.00	-90.00	0	0.30	0.07	0.00
354	.	.	.			2 0.000216	0.00	-90.00	-90.00	0	0.30	0.07	0.00
355	.	.	.			2 0.000216	0.00	-90.00	-90.00	0	0.30	0.07	0.00
356	.	.	.			2 0.000216	0.00	-90.00	-90.00	0	0.30	0.07	0.00
357	.	.	.			2 0.000216	0.00	-90.00	-90.00	0	0.30	0.07	0.00
358	.	.	.			2 0.000216	0.00	-90.00	-90.00	0	0.30	0.07	0.00

Total Spall Mass = 0.10925  
Total measured Spall = 0.1081

Total Ejecta Mass = 0.046968  
Total Mass = 0.156218

Total from mass of target before & after = 0.25

Corrected Ejecta Mass = 0.075164 (30.07 percent Ejecta)  
Corrected Spall Mass = 0.174836 (69.93 percent Spall)

Calc. Ejecta Dust = 0.028196  
Calc. Spall Dust = 0.065586

Total Calc. Dust = 0.093782 (37.51 percent Dust)

Spall Origin \*, At lower left corner facing target (at target surface)

Origin \*\*, At impact point on target surface

X, mm 59 Y, mm 65 Z, mm 0

Shear Strength (est.) used in velocity calculation, N Pascals 55



JSC Shot No. 923  
 1/17/86  
 (Thin Plate with no Cloth)  
 (Impact at -30 deg. phi from normal on ejecta side)

Measured Values

Calculated Values

Particle No.	X location of impact (origin at e)			Y location of impact (origin at e)			Z location of impact (origin at e)			Penetration Depth	Length of Particle	Mass	R location of impact (origin at e)	Theta location of impact (origin at e)		Phi location of impact (origin at e)		Cone Angle (angle from normal)	Average Diameter	Average Area	Velocity
	mm	mm	mm	mm	mm	mm	mm	mm	mm					mm	mm	mm	mm				
44	0	0	48	51	0.5	2	0.000067	100.59	-38.61	17.23	60.59	0.16	0.02	0.48							
45	0	0	47	31	2	0.000067	116.93	-32.92	19.21	36.33	0.16	0.02	1.86								
46	0	0	52	43	2	0.000067	106.32	-36.88	20.97	40.11	0.16	0.02	1.86								
47	0	0	72	51	1	0.000067	99.22	-43.45	34.64	49.54	0.13	0.01	0.85								
48	0	0	102	57	1	0.000067	101.12	-54.08	56.77	64.09	0.16	0.02	0.94								
49	0	0	133	97	0.5	0.000067	96.32	-84.43	85.42	93.54	0.16	0.02	0.48								
50	0	0	22	100	3	0.000067	80.43	-52.41	-26.42	54.29	0.09	0.01	2.11								
51	0	0	3	109	2	0.000067	89.72	-31.42	-42.30	57.16	0.16	0.02	1.86								
52	118	121	42	42	6	0.001500	117.81	50.09	62.45	66.13	0.19	0.03	1.27								
53	118	140	35	35	20	0.003200	132.70	52.18	68.33	70.52	0.21	0.04	3.04								
54	118	130	0	0	1	0.002000	155.01	35.62	56.30	59.12	0.14	0.02	0.50								
55	118	124	53	53	12	0.003600	111.48	57.26	67.50	70.80	0.26	0.05	1.91								
56	118	127	56	56	25	0.004100	111.08	60.27	70.03	72.96	0.23	0.04	3.49								
57	118	116	55	55	5	0.001000	106.10	55.67	64.22	68.48	0.23	0.04	1.42								
58	118	125	69	69	6	0.002300	101.83	68.63	74.68	77.35	0.24	0.04	1.14								
59	118	125	66	66	2	0.002000	112.00	57.61	67.98	71.17	0.15	0.01	0.90								
60	118	120	66	66	2	0.006000	100.84	64.33	70.77	74.24	0.15	0.02	0.59								
61	118	115	53	53	1	0.003000	107.04	54.17	62.98	67.39	0.13	0.01	0.40								
62	118	109	62	58	6	0.002000	100.83	55.06	61.39	66.74	0.16	0.02	1.71								
63	118	112	54	54	2	0.002000	104.98	53.75	61.70	66.54	0.15	0.02	1.03								
64	118	112	64	63	3	0.005000	105.69	53.19	61.36	66.20	0.16	0.02	1.19								
65	118	116	63	63	3	0.003000	100.69	60.69	67.33	71.47	0.16	0.02	1.31								
66	118	111	60	60	2	0.003000	100.32	56.95	63.30	68.30	0.17	0.02	0.91								
67	118	121	50	50	3	0.003000	112.03	54.44	65.00	68.67	0.12	0.01	1.91								
68	118	109	61	57	7	0.005000	101.54	54.48	61.04	66.38	0.18	0.03	2.50								
69	118	112	61	61	2	0.006000	100.10	57.92	64.27	69.09	0.22	0.04	0.72								
70	118	122	61	61	3	0.006000	111.13	55.95	66.19	69.72	0.19	0.03	1.40								
71	118	111	61	61	2	0.000100	99.64	57.56	63.69	68.68	0.11	0.01	1.23								
72	118	121	58	58	0.5	0.000100	106.54	59.31	67.93	71.49	0.13	0.01	0.34								
73	118	118	60	60	4	0.000300	103.67	59.49	67.17	71.09	0.16	0.02	1.75								
74	118	122	51	51	3	0.000200	111.83	55.36	65.83	69.38	0.13	0.01	1.45								
75	118	121	46	46	15	0.001100	114.89	52.20	63.69	67.36	0.20	0.03	3.73								
76	118	124	53	53	7	0.000600	111.48	57.26	67.50	70.80	0.22	0.04	2.50								
77	118	147	5	5	7	0.000400	158.87	40.51	63.26	65.17	0.12	0.01	2.27								
78	118	112	53	53	2	0.000400	105.69	53.19	61.36	66.20	0.25	0.05	0.95								
79	118	112	56	56	5	0.000100	103.56	54.90	62.40	67.24	0.09	0.01	2.87								
80	118	119	47	47	2	0.000100	99.68	64.63	70.70	74.27	0.14	0.02	1.41								
81	118	108	47	47	3	0.000100	108.46	48.83	57.30	62.44	0.09	0.01	1.68								
82	118	36	53	53	3	0.000100	99.53	35.25	8.67	35.87	0.16	0.02	2.27								
83	118	40	51	51	4	0.000200	99.96	35.34	11.78	36.47	0.20	0.03	2.37								
84	118	26	11	11	0.5	0.000200	136.92	25.04	11.42	26.97	0.28	0.06	0.37								
85	118	24	24	24	1	0.000200	114.39	29.99	5.15	30.29	0.28	0.06	0.73								
86	118	42	58	58	1	0.000200	94.08	37.86	11.56	38.79	0.28	0.06	0.73								
87	118	39	61	61	0.5	0.000200	92.65	38.28	8.58	38.78	0.28	0.06	0.37								





JSC Shot No. 923 1/17/86  
 (Thin Plate with no Cloth)  
 (Impact at -30 deg. phi from normal on ejecta side)

Measured Values

Calculated Values

Particle No.	I location of impact (origin at s)			Y location of impact (origin at s)			Z location of impact (origin at s)			Penetration Depth	Length of Particle	Mass	R location of impact (origin at s)	Theta of impact (origin at s)	Phi location of impact (origin at s)	Cone Angle (angle from surf. normal)	Average Diameter	Average Area	Velocity
	mm	mm	mm	mm	mm	mm	mm	mm	mm										
264	.	.	.	.	.	.	0.00	-90.00	-90.00	0.00	0.00	0.00	0.00	0.00	0.00	0.23	0.04	0.00	
265	.	.	.	.	.	.	0.00	-90.00	-90.00	0.00	0.00	0.00	0.00	0.00	0.00	0.23	0.04	0.00	
266	.	.	.	.	.	.	0.00	-90.00	-90.00	0.00	0.00	0.00	0.00	0.00	0.00	0.23	0.04	0.00	
267	.	.	.	.	.	.	0.00	-90.00	-90.00	0.00	0.00	0.00	0.00	0.00	0.00	0.23	0.04	0.00	
268	.	.	.	.	.	.	0.00	-90.00	-90.00	0.00	0.00	0.00	0.00	0.00	0.00	0.23	0.04	0.00	
269	.	.	.	.	.	.	0.00	-90.00	-90.00	0.00	0.00	0.00	0.00	0.00	0.00	0.23	0.04	0.00	
270	.	.	.	.	.	.	0.00	-90.00	-90.00	0.00	0.00	0.00	0.00	0.00	0.00	0.23	0.04	0.00	
271	.	.	.	.	.	.	0.00	-90.00	-90.00	0.00	0.00	0.00	0.00	0.00	0.00	0.23	0.04	0.00	
272	.	.	.	.	.	.	0.00	-90.00	-90.00	0.00	0.00	0.00	0.00	0.00	0.00	0.23	0.04	0.00	
273	.	.	.	.	.	.	0.00	-90.00	-90.00	0.00	0.00	0.00	0.00	0.00	0.00	0.23	0.04	0.00	
274	.	.	.	.	.	.	0.00	-90.00	-90.00	0.00	0.00	0.00	0.00	0.00	0.00	0.23	0.04	0.00	
275	.	.	.	.	.	.	0.00	-90.00	-90.00	0.00	0.00	0.00	0.00	0.00	0.00	0.23	0.04	0.00	
276	.	.	.	.	.	.	0.00	-90.00	-90.00	0.00	0.00	0.00	0.00	0.00	0.00	0.23	0.04	0.00	
277	.	.	.	.	.	.	0.00	-90.00	-90.00	0.00	0.00	0.00	0.00	0.00	0.00	0.23	0.04	0.00	
278	.	.	.	.	.	.	0.00	-90.00	-90.00	0.00	0.00	0.00	0.00	0.00	0.00	0.23	0.04	0.00	
279	.	.	.	.	.	.	0.00	-90.00	-90.00	0.00	0.00	0.00	0.00	0.00	0.00	0.23	0.04	0.00	
280	.	.	.	.	.	.	0.00	-90.00	-90.00	0.00	0.00	0.00	0.00	0.00	0.00	0.23	0.04	0.00	
281	.	.	.	.	.	.	0.00	-90.00	-90.00	0.00	0.00	0.00	0.00	0.00	0.00	0.23	0.04	0.00	
282	.	.	.	.	.	.	0.00	-90.00	-90.00	0.00	0.00	0.00	0.00	0.00	0.00	0.23	0.04	0.00	
283	.	.	.	.	.	.	0.00	-90.00	-90.00	0.00	0.00	0.00	0.00	0.00	0.00	0.23	0.04	0.00	
284	.	.	.	.	.	.	0.00	-90.00	-90.00	0.00	0.00	0.00	0.00	0.00	0.00	0.23	0.04	0.00	
285	.	.	.	.	.	.	0.00	-90.00	-90.00	0.00	0.00	0.00	0.00	0.00	0.00	0.23	0.04	0.00	
286	.	.	.	.	.	.	0.00	-90.00	-90.00	0.00	0.00	0.00	0.00	0.00	0.00	0.23	0.04	0.00	
287	.	.	.	.	.	.	0.00	-90.00	-90.00	0.00	0.00	0.00	0.00	0.00	0.00	0.23	0.04	0.00	
288	.	.	.	.	.	.	0.00	-90.00	-90.00	0.00	0.00	0.00	0.00	0.00	0.00	0.23	0.04	0.00	
289	.	.	.	.	.	.	0.00	-90.00	-90.00	0.00	0.00	0.00	0.00	0.00	0.00	0.23	0.04	0.00	
290	.	.	.	.	.	.	0.00	-90.00	-90.00	0.00	0.00	0.00	0.00	0.00	0.00	0.23	0.04	0.00	
291	.	.	.	.	.	.	0.00	-90.00	-90.00	0.00	0.00	0.00	0.00	0.00	0.00	0.23	0.04	0.00	
292	.	.	.	.	.	.	0.00	-90.00	-90.00	0.00	0.00	0.00	0.00	0.00	0.00	0.23	0.04	0.00	
293	.	.	.	.	.	.	0.00	-90.00	-90.00	0.00	0.00	0.00	0.00	0.00	0.00	0.23	0.04	0.00	
294	.	.	.	.	.	.	0.00	-90.00	-90.00	0.00	0.00	0.00	0.00	0.00	0.00	0.23	0.04	0.00	
295	.	.	.	.	.	.	0.00	-90.00	-90.00	0.00	0.00	0.00	0.00	0.00	0.00	0.23	0.04	0.00	
296	.	.	.	.	.	.	0.00	-90.00	-90.00	0.00	0.00	0.00	0.00	0.00	0.00	0.23	0.04	0.00	
297	.	.	.	.	.	.	0.00	-90.00	-90.00	0.00	0.00	0.00	0.00	0.00	0.00	0.23	0.04	0.00	
298	.	.	.	.	.	.	0.00	-90.00	-90.00	0.00	0.00	0.00	0.00	0.00	0.00	0.23	0.04	0.00	
299	.	.	.	.	.	.	0.00	-90.00	-90.00	0.00	0.00	0.00	0.00	0.00	0.00	0.26	0.05	0.00	
300	.	.	.	.	.	.	0.00	-90.00	-90.00	0.00	0.00	0.00	0.00	0.00	0.00	0.26	0.05	0.00	
301	.	.	.	.	.	.	0.00	-90.00	-90.00	0.00	0.00	0.00	0.00	0.00	0.00	0.26	0.05	0.00	
302	.	.	.	.	.	.	0.00	-90.00	-90.00	0.00	0.00	0.00	0.00	0.00	0.00	0.26	0.05	0.00	
303	.	.	.	.	.	.	0.00	-90.00	-90.00	0.00	0.00	0.00	0.00	0.00	0.00	0.26	0.05	0.00	
304	.	.	.	.	.	.	0.00	-90.00	-90.00	0.00	0.00	0.00	0.00	0.00	0.00	0.26	0.05	0.00	
305	.	.	.	.	.	.	0.00	-90.00	-90.00	0.00	0.00	0.00	0.00	0.00	0.00	0.26	0.05	0.00	
306	.	.	.	.	.	.	0.00	-90.00	-90.00	0.00	0.00	0.00	0.00	0.00	0.00	0.26	0.05	0.00	
307	.	.	.	.	.	.	0.00	-90.00	-90.00	0.00	0.00	0.00	0.00	0.00	0.00	0.26	0.05	0.00	



JSC Shot No. 923 1/17/86  
 (Thin Plate with no Cloth)  
 (Impact at -30 deg. phi from normal on ejecta side)

Measured Values

Calculated Values

Particle No.	Location of impact (origin at *)			Penetration Depth	Length of Particle	Mass	Location of impact (origin at ee)			Cone Angle (angle from normal)	Average Diameter	Average Area	Velocity
	X	Y	Z				Phi	Theta	R				
352	.	.	.	00	00	00	00	00	00	00	00	00	00
353	.	.	.	00	00	00	00	00	00	00	00	00	00
354	.	.	.	00	00	00	00	00	00	00	00	00	00
355	.	.	.	00	00	00	00	00	00	00	00	00	00
356	.	.	.	00	00	00	00	00	00	00	00	00	00
357	.	.	.	00	00	00	00	00	00	00	00	00	00
358	.	.	.	00	00	00	00	00	00	00	00	00	00
359	.	.	.	00	00	00	00	00	00	00	00	00	00
360	.	.	.	00	00	00	00	00	00	00	00	00	00
361	.	.	.	00	00	00	00	00	00	00	00	00	00
362	.	.	.	00	00	00	00	00	00	00	00	00	00
363	.	.	.	00	00	00	00	00	00	00	00	00	00
364	.	.	.	00	00	00	00	00	00	00	00	00	00
365	.	.	.	00	00	00	00	00	00	00	00	00	00
366	.	.	.	00	00	00	00	00	00	00	00	00	00
367	.	.	.	00	00	00	00	00	00	00	00	00	00
368	.	.	.	00	00	00	00	00	00	00	00	00	00
369	.	.	.	00	00	00	00	00	00	00	00	00	00
370	.	.	.	00	00	00	00	00	00	00	00	00	00
371	.	.	.	00	00	00	00	00	00	00	00	00	00
372	.	.	.	00	00	00	00	00	00	00	00	00	00
373	.	.	.	00	00	00	00	00	00	00	00	00	00
374	.	.	.	00	00	00	00	00	00	00	00	00	00
375	.	.	.	00	00	00	00	00	00	00	00	00	00
376	.	.	.	00	00	00	00	00	00	00	00	00	00
377	.	.	.	00	00	00	00	00	00	00	00	00	00
378	.	.	.	00	00	00	00	00	00	00	00	00	00
379	.	.	.	00	00	00	00	00	00	00	00	00	00
380	.	.	.	00	00	00	00	00	00	00	00	00	00
381	.	.	.	00	00	00	00	00	00	00	00	00	00
382	.	.	.	00	00	00	00	00	00	00	00	00	00
383	.	.	.	00	00	00	00	00	00	00	00	00	00
384	.	.	.	00	00	00	00	00	00	00	00	00	00
385	.	.	.	00	00	00	00	00	00	00	00	00	00
386	.	.	.	00	00	00	00	00	00	00	00	00	00
387	.	.	.	00	00	00	00	00	00	00	00	00	00
388	.	.	.	00	00	00	00	00	00	00	00	00	00
389	.	.	.	00	00	00	00	00	00	00	00	00	00
390	.	.	.	00	00	00	00	00	00	00	00	00	00
391	.	.	.	00	00	00	00	00	00	00	00	00	00
392	.	.	.	00	00	00	00	00	00	00	00	00	00
393	.	.	.	00	00	00	00	00	00	00	00	00	00
394	.	.	.	00	00	00	00	00	00	00	00	00	00
395	.	.	.	00	00	00	00	00	00	00	00	00	00



JSC Shot No. 923 1/17/86  
 (Thin Plate with no Cloth)  
 (Impact at -30 deg. phi from normal on ejecta side)

Particle No.	Measured Values										Calculated Values									
	X location of impact (origin at s)	Y location of impact (origin at s)	Z location of impact (origin at s)	Penetration Depth	Length of Particle	Mass	gas	R location of impact (origin at s)	Theta of impact (origin at s)	Phi location of impact (origin at s)	Cone Angle (angle from normal) (origin at s)	Average Diameter	Average Area	Velocity						
308	.	.	.	.	.	1.5	0.000121	0.00	-90.00	-90.00	0.00	0.26	0.05	0.00						
309	.	.	.	.	.	1.5	0.000121	0.00	-90.00	-90.00	0.00	0.26	0.05	0.00						
310	.	.	.	.	.	1.5	0.000121	0.00	-90.00	-90.00	0.00	0.26	0.05	0.00						
311	.	.	.	.	.	1.5	0.000121	0.00	-90.00	-90.00	0.00	0.26	0.05	0.00						
312	.	.	.	.	.	1.5	0.000121	0.00	-90.00	-90.00	0.00	0.26	0.05	0.00						
313	.	.	.	.	.	1.5	0.000121	0.00	-90.00	-90.00	0.00	0.26	0.05	0.00						
314	.	.	.	.	.	1.5	0.000121	0.00	-90.00	-90.00	0.00	0.26	0.05	0.00						
315	.	.	.	.	.	1.5	0.000121	0.00	-90.00	-90.00	0.00	0.26	0.05	0.00						
316	.	.	.	.	.	1.5	0.000121	0.00	-90.00	-90.00	0.00	0.26	0.05	0.00						
317	.	.	.	.	.	1.5	0.000121	0.00	-90.00	-90.00	0.00	0.26	0.05	0.00						
318	.	.	.	.	.	1.5	0.000121	0.00	-90.00	-90.00	0.00	0.26	0.05	0.00						
319	.	.	.	.	.	1.5	0.000121	0.00	-90.00	-90.00	0.00	0.26	0.05	0.00						
320	.	.	.	.	.	1.5	0.000121	0.00	-90.00	-90.00	0.00	0.26	0.05	0.00						
321	.	.	.	.	.	1.5	0.000121	0.00	-90.00	-90.00	0.00	0.26	0.05	0.00						
322	.	.	.	.	.	1.5	0.000121	0.00	-90.00	-90.00	0.00	0.26	0.05	0.00						
323	.	.	.	.	.	1.5	0.000121	0.00	-90.00	-90.00	0.00	0.26	0.05	0.00						
324	.	.	.	.	.	1.5	0.000121	0.00	-90.00	-90.00	0.00	0.26	0.05	0.00						
325	.	.	.	.	.	1.5	0.000121	0.00	-90.00	-90.00	0.00	0.26	0.05	0.00						
326	.	.	.	.	.	1.5	0.000121	0.00	-90.00	-90.00	0.00	0.26	0.05	0.00						
327	.	.	.	.	.	1.5	0.000121	0.00	-90.00	-90.00	0.00	0.26	0.05	0.00						
328	.	.	.	.	.	1.5	0.000121	0.00	-90.00	-90.00	0.00	0.26	0.05	0.00						
329	.	.	.	.	.	1.5	0.000121	0.00	-90.00	-90.00	0.00	0.26	0.05	0.00						
330	.	.	.	.	.	1.5	0.000121	0.00	-90.00	-90.00	0.00	0.26	0.05	0.00						
331	.	.	.	.	.	1.5	0.000121	0.00	-90.00	-90.00	0.00	0.26	0.05	0.00						
332	.	.	.	.	.	1.5	0.000121	0.00	-90.00	-90.00	0.00	0.26	0.05	0.00						
333	.	.	.	.	.	1.5	0.000121	0.00	-90.00	-90.00	0.00	0.26	0.05	0.00						
334	.	.	.	.	.	1.5	0.000121	0.00	-90.00	-90.00	0.00	0.26	0.05	0.00						
335	.	.	.	.	.	1.5	0.000121	0.00	-90.00	-90.00	0.00	0.26	0.05	0.00						
336	.	.	.	.	.	1.5	0.000121	0.00	-90.00	-90.00	0.00	0.26	0.05	0.00						
337	.	.	.	.	.	1.5	0.000121	0.00	-90.00	-90.00	0.00	0.26	0.05	0.00						
338	.	.	.	.	.	1.5	0.000121	0.00	-90.00	-90.00	0.00	0.26	0.05	0.00						
339	.	.	.	.	.	1.5	0.000121	0.00	-90.00	-90.00	0.00	0.26	0.05	0.00						
340	.	.	.	.	.	1.5	0.000121	0.00	-90.00	-90.00	0.00	0.26	0.05	0.00						
341	.	.	.	.	.	1.5	0.000121	0.00	-90.00	-90.00	0.00	0.26	0.05	0.00						
342	.	.	.	.	.	1.5	0.000121	0.00	-90.00	-90.00	0.00	0.26	0.05	0.00						
343	.	.	.	.	.	1.5	0.000121	0.00	-90.00	-90.00	0.00	0.26	0.05	0.00						
344	.	.	.	.	.	1.5	0.000121	0.00	-90.00	-90.00	0.00	0.26	0.05	0.00						
345	.	.	.	.	.	1.5	0.000121	0.00	-90.00	-90.00	0.00	0.26	0.05	0.00						
346	.	.	.	.	.	1.5	0.000121	0.00	-90.00	-90.00	0.00	0.26	0.05	0.00						
347	.	.	.	.	.	1.5	0.000121	0.00	-90.00	-90.00	0.00	0.26	0.05	0.00						
348	.	.	.	.	.	1.5	0.000121	0.00	-90.00	-90.00	0.00	0.26	0.05	0.00						
349	.	.	.	.	.	1.5	0.000121	0.00	-90.00	-90.00	0.00	0.26	0.05	0.00						
350	.	.	.	.	.	1.5	0.000121	0.00	-90.00	-90.00	0.00	0.26	0.05	0.00						
351	.	.	.	.	.	1.5	0.000121	0.00	-90.00	-90.00	0.00	0.26	0.05	0.00						

JSC Shot No. 923 1/17/86  
 (Thin Plate with no Cloth)  
 (Impact at -30 deg. phi from normal on ejecta side)

Measured Values

Calculated Values

Particle No.	X location of impact (origin at s)	Y location of impact (origin at s)	Z location of impact (origin at s)	Penetration Depth	Length of Particle	Mass	R location of impact (origin at s)	Theta location of impact (origin at s)	Phi location of impact (origin at s)	Cone Angle (angle from normal)	Average Diameter	Average Area	Velocity
	mm	mm	mm	mm	mm	gms	mm	Degrees	Degrees	Degrees	mm	mm squared	Ka/sec
Origin s, At impact point on target surface													
X, mm	61	65.67	129			0.15593	62.37%	percent Spall					
Y, mm		Z, mm				0.09407	37.63%	percent Ejecta					
						0.03559							
						0.02147							
						0.057064	22.83%	percent Dust					
Total Calc. Dust =													
Shear Strength (Estimated) used in velocity calculation, N Pascals 55													

JSC Shot No. 923  
 (Thin Plate with no Cloth)  
 (Impact at +30 deg Phi)

1/28/86

Measured Values

Calculated Values

Particle No.	Y location of impact (origin at e)			Z location of impact (origin at e)			Penetration Depth	Length of Particle	Mass	R location of impact (origin at e)	Theta location of impact (origin at e)			Phi location of impact (origin at e)			Average Diameter	Average Area	Velocity
	mm	mm	mm	mm	mm	mm					mm	mm	mm	mm	mm	mm			
1	0	21	69	63	0.0019	89.51	-81.47	-81.71	84.03	0.16	0.02	0.51							
2	0	23	70	62	0.0029	87.94	-81.34	-81.30	83.84	0.19	0.03	0.92							
3	0	21	71	40	0.0006	88.63	-83.04	-83.13	85.10	0.11	0.01	1.26							
4	0	18	72	29	0.0003	89.97	-85.20	-85.42	86.68	0.09	0.01	2.27							
5	0	24	65	11	0.0003	89.74	-85.04	-77.30	80.85	0.15	0.02	2.07							
6	0	22	74	9	0.0001	86.81	-84.95	-84.83	86.39	0.09	0.01	0.29							
7	0	22	69	12	0.0002	88.95	-81.01	-81.16	83.67	0.12	0.01	1.80							
8	0	32	54	6	0.0001	91.89	-65.85	-65.80	72.39	0.12	0.02	1.28							
9	0	28	61	3	0.0001	89.75	-72.35	-72.30	77.30	0.16	0.02	0.39							
10	0	23	41	3	0.0001	104.10	-60.87	-65.60	70.62	0.16	0.02	0.39							
11	0	112	47	3	0.0001	96.51	-40.01	3.04	40.07	0.16	0.02	0.77							
12	0	111	45	4	0.0001	97.40	-39.55	1.57	39.56	0.14	0.02	1.41							
13	0	123	42	4	0.0001	104.72	-36.53	7.45	36.96	0.14	0.02	1.41							
14	0	30	63	4	0.000571429	87.73	-72.96	-72.18	77.49	0.11	0.01	0.82							
15	0	46	50	3	0.000571429	89.35	-58.32	-53.52	64.65	0.12	0.01	0.88							
16	0	25	25	5	0.000571429	114.36	-51.45	-59.06	64.40	0.10	0.01	0.39							
17	0	35	23	1	0.000571429	112.18	-47.84	-53.10	59.97	0.11	0.01	0.82							
18	0	58	16	3	0.000571429	112.61	-40.07	-38.36	49.12	0.12	0.01	0.88							
19	0	92	43	3	0.000571429	92.81	-42.64	-12.88	43.50	0.12	0.01	0.88							
20	0	49	52	2	0.000571429	87.22	-58.48	-51.69	64.15	0.15	0.02	0.50							
21	58	131	95	4	0.0001	61.09	-5.47	46.72	48.84	0.14	0.02	1.41							
22	59	131	97	6	0.0003	60.60	-4.28	48.56	48.63	0.20	0.03	0.97							
23	58	131	101	6	0.0005	60.00	-6.24	52.42	52.42	0.26	0.05	0.86							
24	50	131	29	0.5	2.000022222	100.32	-6.92	6.56	9.49	0.09	0.01	0.42							
25	68	131	98	3	0.000022222	60.63	8.70	49.50	49.74	0.08	0.00	1.11							
26	56	131	100	0.5	1.5	60.30	-9.10	51.37	51.60	0.11	0.01	0.67							
27	53	131	102	0.5	1	60.41	-14.14	53.27	53.75	0.13	0.01	0.75							
28	104	131	86	1	4	76.24	40.27	38.81	49.43	0.07	0.00	1.03							
29	56	131	82	2	2	65.46	-6.45	35.53	35.87	0.09	0.01	2.44							
30	55	131	81	2	3	65.97	-7.40	34.73	35.20	0.16	0.02	1.52							
31	31	131	92	1	1	69.06	-34.93	44.01	50.01	0.13	0.01	1.47							
32	56	131	16	1	1	110.47	-3.12	2.53	4.01	0.13	0.01	1.47							
33	97	131	43	2	2	95.40	21.96	11.95	24.48	0.09	0.01	2.44							
34	116	12	32	3	0.0001	111.38	55.69	-67.78	70.68	0.28	0.02	0.39							
35	116	78	20	0.5	1	104.29	33.94	-25.93	39.70	0.16	0.06	0.53							
36	116	85	32	3	0.0001	94.99	36.36	-20.18	39.45	0.16	0.02	1.52							
37	116	90	30	1	0.0001	97.43	34.84	-16.94	37.23	0.16	0.02	0.77							
38	116	105	15	2	0.0001	113.41	28.84	-10.48	30.15	0.20	0.03	1.69							
39	116	84	53	0.5	3	78.76	44.65	-17.59	46.06	0.16	0.02	0.39							
40	116	95	33	1	2	96.10	34.87	-12.94	36.27	0.13	0.01	1.06							
41	116	107	24	0.5	2	106.72	30.61	-7.43	31.21	0.13	0.01	0.54							
42	116	115	35	1	2	101.34	32.20	0.35	32.20	0.13	0.01	1.06							
43	116	84	50	1	1	80.93	43.32	-18.20	44.96	0.18	0.03	1.27							



JSC Shot No. 923  
 1/28/86  
 (Thin Plate with no Cloth)  
 (Impact at +30 deg Phi)

Measured Values

Calculated Values

Particle No.	X location of impact (origin at *)			Y location of impact (origin at *)			Z location of impact (origin at *)			Penetration Depth	Length of Particle	Mass	R location of impact (origin at *)	Theta of impact (origin at *)	Phi of impact (origin at *)	Location of impact (angle from cone axis)	Cone Angle (angle from impact pt. to surf. norm.)	Average Diameter	Average Area	Velocity
	mm	mm	mm	mm	mm	mm	mm	mm	mm											
88	.	.	.	.	.	.	.	.	.	.	45	0.0012	0.00	-90	-90	-90	0	0.15	0.02	0.00
89	.	.	.	.	.	.	.	.	.	.	20	0.0015	0.00	-90	-90	-90	0	0.25	0.05	0.00
90	.	.	.	.	.	.	.	.	.	.	20	0.0009	0.00	-90	-90	-90	0	0.19	0.03	0.00
91	.	.	.	.	.	.	.	.	.	.	24	0.0006	0.00	-90	-90	-90	0	0.14	0.02	0.00
92	.	.	.	.	.	.	.	.	.	.	18	0.0008	0.00	-90	-90	-90	0	0.19	0.03	0.00
93	.	.	.	.	.	.	.	.	.	.	18	0.0005	0.00	-90	-90	-90	0	0.15	0.02	0.00
94	.	.	.	.	.	.	.	.	.	.	18	0.0003	0.00	-90	-90	-90	0	0.12	0.01	0.00
95	.	.	.	.	.	.	.	.	.	.	20	0.0003	0.00	-90	-90	-90	0	0.11	0.01	0.00
96	.	.	.	.	.	.	.	.	.	.	13	0.0003	0.00	-90	-90	-90	0	0.14	0.01	0.00
97	.	.	.	.	.	.	.	.	.	.	16	0.0002	0.00	-90	-90	-90	0	0.10	0.01	0.00
98	.	.	.	.	.	.	.	.	.	.	14	0.0005	0.00	-90	-90	-90	0	0.05	0.00	0.00
99	.	.	.	.	.	.	.	.	.	.	14	0.0005	0.00	-90	-90	-90	0	0.05	0.00	0.00
100	.	.	.	.	.	.	.	.	.	.	14	0.0005	0.00	-90	-90	-90	0	0.05	0.00	0.00
101	.	.	.	.	.	.	.	.	.	.	14	0.0005	0.00	-90	-90	-90	0	0.05	0.00	0.00
102	.	.	.	.	.	.	.	.	.	.	14	0.0005	0.00	-90	-90	-90	0	0.05	0.00	0.00
103	.	.	.	.	.	.	.	.	.	.	14	0.0005	0.00	-90	-90	-90	0	0.05	0.00	0.00
104	.	.	.	.	.	.	.	.	.	.	14	0.0005	0.00	-90	-90	-90	0	0.05	0.00	0.00
105	.	.	.	.	.	.	.	.	.	.	14	0.0005	0.00	-90	-90	-90	0	0.05	0.00	0.00
106	.	.	.	.	.	.	.	.	.	.	14	0.0005	0.00	-90	-90	-90	0	0.05	0.00	0.00
107	.	.	.	.	.	.	.	.	.	.	14	0.0005	0.00	-90	-90	-90	0	0.05	0.00	0.00
108	.	.	.	.	.	.	.	.	.	.	14	0.0005	0.00	-90	-90	-90	0	0.05	0.00	0.00
109	.	.	.	.	.	.	.	.	.	.	14	0.0005	0.00	-90	-90	-90	0	0.05	0.00	0.00
110	.	.	.	.	.	.	.	.	.	.	14	0.0005	0.00	-90	-90	-90	0	0.05	0.00	0.00
111	.	.	.	.	.	.	.	.	.	.	5	0.0004666667	0.00	-90	-90	-90	0	0.27	0.06	0.00
112	.	.	.	.	.	.	.	.	.	.	5	0.0004666667	0.00	-90	-90	-90	0	0.27	0.06	0.00
113	.	.	.	.	.	.	.	.	.	.	4	0.0009	0.00	-90	-90	-90	0	0.43	0.14	0.00
114	.	.	.	.	.	.	.	.	.	.	4	0.0006	0.00	-90	-90	-90	0	0.35	0.10	0.00
115	.	.	.	.	.	.	.	.	.	.	4	0.0005	0.00	-90	-90	-90	0	0.32	0.08	0.00
116	.	.	.	.	.	.	.	.	.	.	2.5	0.0002	0.00	-90	-90	-90	0	0.25	0.05	0.00
117	.	.	.	.	.	.	.	.	.	.	10	0.00022	0.00	-90	-90	-90	0	0.13	0.01	0.00
118	.	.	.	.	.	.	.	.	.	.	10	0.00022	0.00	-90	-90	-90	0	0.13	0.01	0.00
119	.	.	.	.	.	.	.	.	.	.	10	0.00022	0.00	-90	-90	-90	0	0.13	0.01	0.00
120	.	.	.	.	.	.	.	.	.	.	10	0.00022	0.00	-90	-90	-90	0	0.13	0.01	0.00
121	.	.	.	.	.	.	.	.	.	.	10	0.00022	0.00	-90	-90	-90	0	0.13	0.01	0.00
122	.	.	.	.	.	.	.	.	.	.	10	0.0003333333	0.00	-90	-90	-90	0	0.05	0.00	0.00
123	.	.	.	.	.	.	.	.	.	.	10	0.0003333333	0.00	-90	-90	-90	0	0.05	0.00	0.00
124	.	.	.	.	.	.	.	.	.	.	10	0.0003333333	0.00	-90	-90	-90	0	0.05	0.00	0.00
125	.	.	.	.	.	.	.	.	.	.	10	0.0003333333	0.00	-90	-90	-90	0	0.05	0.00	0.00
126	.	.	.	.	.	.	.	.	.	.	10	0.0003333333	0.00	-90	-90	-90	0	0.05	0.00	0.00
127	.	.	.	.	.	.	.	.	.	.	10	0.0003333333	0.00	-90	-90	-90	0	0.05	0.00	0.00
128	.	.	.	.	.	.	.	.	.	.	7	0.0001	0.00	-90	-90	-90	0	0.11	0.01	0.00
129	.	.	.	.	.	.	.	.	.	.	7	0.0001	0.00	-90	-90	-90	0	0.11	0.01	0.00
130	.	.	.	.	.	.	.	.	.	.	7	0.0001	0.00	-90	-90	-90	0	0.11	0.01	0.00
131	.	.	.	.	.	.	.	.	.	.	7	0.0001	0.00	-90	-90	-90	0	0.11	0.01	0.00

JSC Shot No. 923  
 (This Plate with no Cloth)  
 (Impact at +30 deg Phi)  
 1/28/86

Measured Values

Calculated Values

Particle No.	Measured Values				Calculated Values									
	X location of impact (origin at e)	Y location of impact (origin at e)	Z location of impact (origin at e)	Penetration Depth	Length of Particle	Mass	R location of impact (origin at e)	Theta of impact (origin at e)	Phi location of impact (origin at e)	Cone Angle (angle from impact pt. to surf. norm.)	Average Diameter	Average Area	Velocity	
220						2	0.0000475	-90	-90	0	0.14	0.02	0.00	
221						2	0.0000475	-90	-90	0	0.14	0.02	0.00	
222						2	0.0000475	-90	-90	0	0.14	0.02	0.00	
223						2	0.0000475	-90	-90	0	0.14	0.02	0.00	
224						2	0.0000475	-90	-90	0	0.14	0.02	0.00	
225						2	0.0000475	-90	-90	0	0.14	0.02	0.00	
226						2	0.0000475	-90	-90	0	0.14	0.02	0.00	
227						2	0.0000475	-90	-90	0	0.14	0.02	0.00	
228						2	0.0000475	-90	-90	0	0.14	0.02	0.00	
229						2	0.0000475	-90	-90	0	0.14	0.02	0.00	
230						2	0.0000475	-90	-90	0	0.14	0.02	0.00	
231						2	0.0000475	-90	-90	0	0.14	0.02	0.00	
232						2	0.0000475	-90	-90	0	0.14	0.02	0.00	
233						2	0.0000475	-90	-90	0	0.14	0.02	0.00	
234						1	0.0000591667	-90	-90	0	0.22	0.04	0.00	
235						1	0.0000591667	-90	-90	0	0.22	0.04	0.00	
236						1	0.0000591667	-90	-90	0	0.22	0.04	0.00	
237						1	0.0000591667	-90	-90	0	0.22	0.04	0.00	
238						1	0.0000591667	-90	-90	0	0.22	0.04	0.00	
239						1	0.0000591667	-90	-90	0	0.22	0.04	0.00	
240						1	0.0000591667	-90	-90	0	0.22	0.04	0.00	
241						1	0.0000591667	-90	-90	0	0.22	0.04	0.00	
242						1	0.0000591667	-90	-90	0	0.22	0.04	0.00	
243						1	0.0000591667	-90	-90	0	0.22	0.04	0.00	
244						1	0.0000591667	-90	-90	0	0.22	0.04	0.00	
245						1	0.0000591667	-90	-90	0	0.22	0.04	0.00	
246						1	0.0000591667	-90	-90	0	0.22	0.04	0.00	
247						1	0.0000591667	-90	-90	0	0.22	0.04	0.00	
248						1	0.0000591667	-90	-90	0	0.22	0.04	0.00	
249						1	0.0000591667	-90	-90	0	0.22	0.04	0.00	
250						1	0.0000591667	-90	-90	0	0.22	0.04	0.00	
251						1	0.0000591667	-90	-90	0	0.22	0.04	0.00	
252						1	0.0000591667	-90	-90	0	0.22	0.04	0.00	
253						1	0.0000591667	-90	-90	0	0.22	0.04	0.00	
254						1	0.0000591667	-90	-90	0	0.22	0.04	0.00	
255						1	0.0000591667	-90	-90	0	0.22	0.04	0.00	
256						1	0.0000591667	-90	-90	0	0.22	0.04	0.00	
257						1	0.0000591667	-90	-90	0	0.22	0.04	0.00	
258						1	0.0000591667	-90	-90	0	0.22	0.04	0.00	
259						1	0.0000591667	-90	-90	0	0.22	0.04	0.00	
260						1	0.0000591667	-90	-90	0	0.22	0.04	0.00	
261						1	0.0000591667	-90	-90	0	0.22	0.04	0.00	
262						1	0.0000591667	-90	-90	0	0.22	0.04	0.00	
263						1	0.0000591667	-90	-90	0	0.22	0.04	0.00	











JSC Shot No. 923 1/17/86  
 (Thin Plate with no Cloth)  
 (Impact at -30 deg. phi from normal on ejecta side)

Measured Values

Calculated Values

Particle No.	X location of impact (origin at *)	Y location of impact (origin at *)	Z location of impact (origin at *)	Penetration Depth	Length of Particle	Mass	gas	R location of impact (origin at *)	Theta location of impact (origin at *)	Phi location of impact (origin at *)	Cone Angle (angle from normal)	Average Diameter	Average Area	Velocity
	mm	mm	mm	mm	mm	mm	mm	mm	Degrees	Degrees	Degrees	mm	mm squared	Km/sec
396	.	.	.	.	.	1.5	0.000121	0.00	-90.00	-90.00	0.00	0.26	0.05	0.00
397	.	.	.	.	.	1.5	0.000121	0.00	-90.00	-90.00	0.00	0.26	0.05	0.00
398	.	.	.	.	.	1.5	0.000121	0.00	-90.00	-90.00	0.00	0.26	0.05	0.00
399	.	.	.	.	.	1.5	0.000121	0.00	-90.00	-90.00	0.00	0.26	0.05	0.00
400	.	.	.	.	.	1.5	0.000121	0.00	-90.00	-90.00	0.00	0.26	0.05	0.00
401	.	.	.	.	.	1.5	0.000121	0.00	-90.00	-90.00	0.00	0.26	0.05	0.00
402	.	.	.	.	.	1.5	0.000121	0.00	-90.00	-90.00	0.00	0.26	0.05	0.00
403	.	.	.	.	.	1.5	0.000121	0.00	-90.00	-90.00	0.00	0.26	0.05	0.00
404	.	.	.	.	.	1.5	0.000121	0.00	-90.00	-90.00	0.00	0.26	0.05	0.00
405	.	.	.	.	.	1.5	0.000121	0.00	-90.00	-90.00	0.00	0.26	0.05	0.00
406	.	.	.	.	.	1.5	0.000121	0.00	-90.00	-90.00	0.00	0.26	0.05	0.00
407	.	.	.	.	.	1.5	0.000121	0.00	-90.00	-90.00	0.00	0.26	0.05	0.00
408	.	.	.	.	.	1.5	0.000121	0.00	-90.00	-90.00	0.00	0.26	0.05	0.00
409	.	.	.	.	.	1.5	0.000121	0.00	-90.00	-90.00	0.00	0.26	0.05	0.00
410	.	.	.	.	.	1.5	0.000121	0.00	-90.00	-90.00	0.00	0.26	0.05	0.00
411	.	.	.	.	.	1.5	0.000121	0.00	-90.00	-90.00	0.00	0.26	0.05	0.00
412	.	.	.	.	.	1.5	0.000121	0.00	-90.00	-90.00	0.00	0.26	0.05	0.00
413	.	.	.	.	.	1.5	0.000121	0.00	-90.00	-90.00	0.00	0.26	0.05	0.00
414	.	.	.	.	.	1.5	0.000121	0.00	-90.00	-90.00	0.00	0.26	0.05	0.00
415	.	.	.	.	.	1.5	0.000121	0.00	-90.00	-90.00	0.00	0.26	0.05	0.00
416	.	.	.	.	.	1.5	0.000121	0.00	-90.00	-90.00	0.00	0.26	0.05	0.00
417	.	.	.	.	.	1.5	0.000121	0.00	-90.00	-90.00	0.00	0.26	0.05	0.00
418	.	.	.	.	.	1.5	0.000121	0.00	-90.00	-90.00	0.00	0.26	0.05	0.00
419	.	.	.	.	.	1.5	0.000121	0.00	-90.00	-90.00	0.00	0.26	0.05	0.00
420	.	.	.	.	.	1.5	0.000121	0.00	-90.00	-90.00	0.00	0.26	0.05	0.00
421	.	.	.	.	.	1.5	0.000121	0.00	-90.00	-90.00	0.00	0.26	0.05	0.00
422	.	.	.	.	.	1.5	0.000121	0.00	-90.00	-90.00	0.00	0.26	0.05	0.00
423	.	.	.	.	.	1.5	0.000121	0.00	-90.00	-90.00	0.00	0.26	0.05	0.00
424	.	.	.	.	.	1.5	0.000121	0.00	-90.00	-90.00	0.00	0.26	0.05	0.00
425	.	.	.	.	.	1.5	0.000121	0.00	-90.00	-90.00	0.00	0.26	0.05	0.00
426	.	.	.	.	.	1.5	0.000121	0.00	-90.00	-90.00	0.00	0.26	0.05	0.00
427	.	.	.	.	.	1.5	0.000121	0.00	-90.00	-90.00	0.00	0.26	0.05	0.00
428	.	.	.	.	.	1.5	0.000121	0.00	-90.00	-90.00	0.00	0.26	0.05	0.00
429	.	.	.	.	.	1.5	0.000121	0.00	-90.00	-90.00	0.00	0.26	0.05	0.00

Total Spall Mass = 0.120336

Total Ejecta Mass = 0.0726

Total Mass = 0.192936

Total from mass of target before & after = 0.25

Spall Origin is At lower right hand corner of back styrofoam surface facing surface.

JSC Shot No. 923  
 (Thin Plate with no Cloth)  
 (Impact at +30 deg Phi)

1/28/86

Measured Values

Calculated Values

Particle No.	X location of impact (origin at +)			Y location of impact (origin at +)			Z location of impact (origin at +)			Penetration Depth	Length of Particle	Mass	R location of impact (origin at +)			Theta location of impact (origin at +)			Phi location of impact (origin at +)			Cone Angle (angle from normal to surf. norm.)	Average Diameter	Average Area	Velocity Km/sec
	mm	mm	mm	mm	mm	mm	mm	mm	mm				mm	mm	mm	mm	mm	mm	mm	mm	mm				
44	116	103	67	0.00004	75.24	46.06	6.72	46.24	0.13	0.01	1.06														
45	116	130	95	0.0002	80.71	52.80	46.50	59.23	0.23	0.04	1.28														
46	116	101	63	0.0001	76.76	44.74	2.52	44.76	0.20	0.03	1.69														
47	0	38	0	0.0002	129.84	-38.64	-47.17	53.32	0.15	0.02	1.55														
48	2	40	0	0.0001	128.39	-37.37	-46.29	52.27	0.16	0.02	1.52														
49	5	28	0	0.00006	130.53	-38.15	-51.84	56.23	0.16	0.02	0.96														
50	31	50	0	0.00006	115.38	-20.35	-41.25	43.59	0.16	0.02	0.96														
51	53	95	0	0.00006	111.83	-4.85	-17.92	18.49	0.16	0.02	0.96														
52	24	118	0	0.00006	124.38	-17.91	-6.97	19.07	0.16	0.02	1.91														
53	26	118	0	0.00006	123.79	-17.03	-6.97	18.25	0.14	0.02	0.91														
54	95	110	0	0.00006	120.16	16.20	-10.43	19.08	0.16	0.02	0.49														
55	112	54	0	0.00006	121.22	30.36	-39.21	45.10	0.22	0.04	1.16														
56	105	115	0	0.00006	124.93	20.33	-8.32	21.72	0.22	0.04	2.28														
57	102	93	0	0.00006	118.05	20.86	-18.93	27.13	0.13	0.01	0.87														
58	51	92	0	0.00006	111.42	-6.01	-19.44	20.22	0.22	0.04	1.16														
59	122	108	0	0.0002	129.62	28.06	-11.57	29.73	0.20	0.03	2.37														
60	80	122	0	0.0002	121.40	8.56	-5.22	9.99	0.28	0.06	0.37														
61	97	131	113	0.0003	69.00	53.18	63.86	67.68	0.32	0.08	0.35														
62	105	131	118	0.0001	73.82	63.04	68.63	72.77	0.11	0.01	0.31														
63	76	131	124	0.0002	62.77	40.02	74.19	74.60	0.15	0.02	1.03														
64	78	131	127	0.0003	64.03	48.66	76.88	77.30	0.13	0.01	0.78														
65	85	131	124	0.0002	65.37	54.06	74.19	75.22	0.13	0.01	0.24														
66	73	131	124	0.0001	62.17	33.42	74.19	74.45	0.14	0.02	0.36														
67	75	131	116	0.0001	61.14	28.85	66.73	67.29	0.13	0.01	0.67														
68	83	131	130	0.0002	66.34	61.34	79.49	80.04	0.18	0.03	0.29														
69	103	131	107	0.0003	72.14	52.56	58.07	64.20	0.11	0.01	0.58														
70	72	131	122	0.00003	61.55	28.52	72.36	72.60	0.11	0.01	2.27														
71	92	131	109	0.0003	66.48	45.32	60.00	63.50	0.11	0.01	0.58														
72	96	131	114	0.0003	68.56	53.31	64.82	68.32	0.11	0.01	0.58														
73	89	131	130	0.0003	68.48	66.97	79.49	80.35	0.11	0.01	0.58														
74	73	131	122	0.0003	61.72	30.87	72.36	72.65	0.09	0.01	3.06														
75	77	131	106	0.0003	61.27	24.94	57.11	58.23	0.11	0.01	2.27														
76	83	131	122	0.0003	64.76	48.77	72.36	73.36	0.16	0.02	1.36														
77	53	131	144	0.0003	69.47	-85.88	89.46	90.53	0.11	0.01	2.27														
78	105	123	105	0.0003	67.08	55.89	55.54	64.26	0.11	0.01	2.27														
79	116	120	102	0.0003	60.76	51.76	65.47	75.07	0.15	0.02	0.83														
80	116	122	116	0.0021	74.15	70.52	67.92	75.07	0.25	0.05	2.62														
81	116	127	124	0.0012	74.80	74.80	75.17	79.26	0.19	0.03	0.24														
82	116	123	122	0.0007	75.63	75.63	74.21	79.02	0.17	0.02	0.30														
83	116	126	118	0.0004	77.13	70.27	69.41	75.46	0.18	0.03	1.58														
84	116	122	112	0.0001	73.88	67.32	63.41	72.22	0.16	0.02	0.39														
85	58	0	62	0.0001	85.80	-39.42	-86.75	86.75	0.14	0.02	0.71														
86	58	0	62	0.0176	0.00	-90	-90	0	0.41	0.02	0.00														
87	58	0	62	0.0013	0.00	-90	-90	0	0.17	0.02	0.00														

LOOSE ON BOTTOM





JSC Shot No. 923 1/28/86  
 (Thin Plate with no Cloth)  
 (Impact at +30 deg Phi)

Measured Values

Calculated Values

Particle No.	X location of impact (origin at e)	Y location of impact (origin at e)	Z location of impact (origin at e)	Penetration Depth	Length of Particle	Mass	R location of impact (origin at ee)	Theta location of impact (origin at ee)	Phi location of impact (origin at ee)	Cone Angle (angle from impact pt. to surf. norm.)	Average Diameter	Average Area	Velocity
	mm	mm	mm	mm	mm	gms	mm	Degrees	Degrees	Degrees	mm	mm squared	ft/sec
352	.	.	.			0.0000591667	0.00	-90	-90	0	0.22	0.04	0.00
353	.	.	.			0.0000591667	0.00	-90	-90	0	0.22	0.04	0.00

Total Ejecta Mass = 0.0726

Total Spall Mass = 0.120336

Total Mass = 0.192936

Total from mass of target before & after = 0.25

Corrected Ejecta Mass = 0.09407 37.63 percent Ejecta

Corrected Spall Mass = 0.15593 62.37 percent Spall

Calc. Ejecta Dust = 0.02147

Calc. Spall Dust = 0.03559

Total Calc. Dust = 0.057064 22.83 percent Dust

Ejecta Origin ee, At lower left hand corner of back styrofoam surface (facing surface).

Origin ee, At impact point on target surface

X, mm Y, mm Z, mm

62 71.674337148 109

Shear Strength (estimated) used in velocity calculation, N Pascals 55

ORIGINAL PAGE IS OF POOR QUALITY

Particle No.	Measured Values										Calculated Values														
	X location of impact (origin at e)	Y location of impact (origin at e)	Z location of impact (origin at e)	Penetration Depth	Length of Particle	Mass	R location of impact (origin at e)	Theta location of impact (origin at e)	Phi location of impact (origin at e)	Cone Angle (Angle from surface normal to particle)	Average Diameter	Average Area	Velocity	X location of impact (origin at e)	Y location of impact (origin at e)	Z location of impact (origin at e)	Penetration Depth	Length of Particle	Mass	R location of impact (origin at e)	Theta location of impact (origin at e)	Phi location of impact (origin at e)	Cone Angle (Angle from surface normal to particle)	Average Diameter	Average Area
422	68	136	58	0.5	0.1	0.00001	80.68	-2.96	43.99	44.04	0.265	0.055	1.316												
442	68	136	65	1	0.1	0.00001	85.85	-2.64	40.75	40.79	0.265	0.055	2.553												
462	68	136	72	1	0.1	0.00001	91.26	-2.39	37.87	37.91	0.265	0.055	2.553												
482	68	136	77	1	0.1	0.00001	95.26	-2.23	36.03	36.07	0.265	0.055	2.553												
502	68	136	80	1	0.1	0.00001	97.70	-2.15	34.99	35.03	0.265	0.055	2.553												
522	65	136	80	2	0.1	0.00001	97.65	0.00	34.99	34.99	0.265	0.055	5.027												
542	75	136	80	2	0.1	0.00001	98.16	-7.13	34.99	35.42	0.265	0.055	5.027												
562	65	136	84	3	0.1	0.00001	100.96	0.00	33.69	33.69	0.265	0.055	7.499												
582	75	136	84	3	0.1	0.00001	101.45	-6.79	33.69	34.11	0.265	0.055	7.499												
602	57	136	85	1	0.1	0.00001	102.10	5.38	33.38	33.64	0.265	0.055	2.553												
622	82	136	85	1	0.1	0.00001	103.20	-11.31	33.38	34.55	0.265	0.055	2.553												
642	48	136	90	1	0.1	0.00001	107.35	10.70	31.89	33.03	0.265	0.055	2.553												
662	88	136	90	1	0.1	0.00001	108.47	-14.34	31.89	31.89	0.265	0.055	2.553												
682	38	136	95	0.5	0.1	0.00001	113.53	15.87	30.52	33.20	0.265	0.055	1.316												
702	78	136	95	0.5	0.1	0.00001	111.04	-7.79	30.52	31.18	0.265	0.055	1.316												
722	23	58	108	12	2	0.00071	117.95	21.25	-11.51	23.70	0.409	0.131	5.370												
723	24	77	108	12	1.5	0.00053	115.56	20.79	-1.59	20.84	0.409	0.131	6.200												
724	36	94	108	12	1.5	0.00053	112.70	15.03	7.39	16.60	0.409	0.131	6.200												
725	66	0	75	0.5	0.1	0.00001	109.66	-0.76	-46.85	46.85	0.265	0.055	1.316												
745	68	0	88	1	0.1	0.00001	118.97	-1.95	-42.27	42.29	0.265	0.055	2.553												
765	68	0	95	1.5	0.1	0.00001	124.23	-1.81	-40.10	40.12	0.265	0.055	3.790												
785	69	0	101	2	0.1	0.00001	128.91	-2.27	-38.38	38.42	0.265	0.055	5.027												
805	60	0	102	3	0.1	0.00001	129.73	2.81	-38.11	38.16	0.265	0.055	7.499												
825	58	0	106	1	0.1	0.00001	132.98	3.78	-37.04	37.15	0.265	0.055	2.553												
845	50	0	110	1	0.1	0.00001	136.84	7.77	-36.03	36.50	0.265	0.055	2.553												
865	42	0	115	0.5	0.1	0.00001	141.96	11.31	-34.82	35.90	0.265	0.055	1.316												
885	77	0	101	1	0.1	0.00001	129.40	-6.78	-38.38	38.69	0.265	0.055	2.553												
905	53	0	102	1	0.1	0.00001	130.18	6.71	-38.11	38.42	0.265	0.055	2.553												
925	90	0	105	0.5	0.1	0.00001	134.35	-13.39	-37.30	38.60	0.265	0.055	1.316												
945	99	0	110	0.5	0.1	0.00001	140.20	-17.18	-36.03	38.32	0.265	0.055	1.316												
965	Loose on Bottom					0.00020	0.00	-90.00	-90.00	0.00	0.164	0.021	0.000												
966	"					0.00130	0.00	-90.00	-90.00	0.00	0.494	0.071	0.000												
967	"					0.00150	0.00	-90.00	-90.00	0.00	0.593	0.277	0.000												
Ejecta Origin e, At lower left corner				Total Ejecta Mass		0.01760	28.81																		
Spall Origin e, At lower right corner				Total Spall Mass		0.04350	71.19																		
Spall Origin e, At lower right corner facing target (at target surface)				Total Spall & Ejecta		0.06110																			
Origin ee, At impact point on target surface				Total from mass of target before & after		0.12																			
Origin ee, At impact point on target surface				Corrected Ejecta Mass		0.03457																			
Origin ee, At impact point on target surface				Corrected Spall Mass		0.02653																			



**Appendix C - Single Frame Photography Data**



## Appendix C - Single Frame Photography Data

The following three photographs were taken shortly after the impact of hypervelocity projectiles on composite targets. Due to various problems with time measurement and scaling, only approximate velocity data can be derived from these photos. They still provide useful information however, and are therefore documented here.

### Shot # 873

5 mg nylon projectile, 6.32 km/sec velocity

.416 inch thick composite plate from Hercules (generic graphite/epoxy plate)

Photo is of ejecta approximately 15 microseconds after impact

Scaling - 16 threads per inch in photo = .15875 cm/thread

Threads are 10 inches from camera. Centerline of shot is 12 inches. Therefore Real Distance = 1.2 x Measured from thread.

Therefore scaling for shot centerline is  $1.2 \times .1575 = .1905$  cm/thread.

The furthest particles from the target are roughly 19 threads out, assuming they are on the centerline.  $19 \times .1905 = 3.62$  cm.

$3.62 \text{ cm} / 15 \text{ microseconds} = .0362 \text{ m} / .000015 \text{ sec} = 2.41 \text{ km/sec}$

Therefore the highest velocity ejecta appears to be traveling in the range of 2.4 km/sec, which agrees with calculated and other data measured with the high speed movie camera.

### Shot # 917

See section 3.2.3 for more discussion of this shot.

5 mg nylon projectile, 5.99 km/sec velocity

.127 inch thick graphite epoxy target (JSC-03A-003) with cloth covering on both sides.

Photo was taken of spall an estimated 20 to 50 microseconds after impact.

A couple of threads are visible in the photo. As calculated above, 1 thread = .1905 cm.

The fastest particles are roughly 15 threads out.  $15 \times .1905 = 2.86$  cm.

JSC Shot No. 933 2/10/86  
 (Thin 6061-T6 Aluminum Plate)

Measured Values

Calculated Values

Particle No.	X location of impact (origin at e)	Y location of impact (origin at e)	Z location of impact (origin at e)	Penetration Depth	Length of Particle	Mass	R location of impact (origin at e)	Theta location of impact (origin at e)	Phi location of impact (origin at e)	Cone Angle (Angle from surface normal to particle)	Average Diameter	Average Area	Velocity
	mm	mm	mm	mm	mm	gms	mm	Degrees	Degrees	Degrees	mm	mm squared	Km/sec
Shear Strength (est.) used in calculation, M Pascals			55			0.01697							
Calc. Ejecta Dust						0.04193							
Calc. Spall Dust						0.0589							
Total Calc. Dust						49.08 X Dust							

$2.86 \text{ cm} / 20 \text{ microseconds} = .0286 \text{ m} / .000020 \text{ sec.} = 1.43 \text{ km/sec}$

$2.86 \text{ cm} / 50 \text{ microseconds} = .0286 \text{ m} / .000050 \text{ sec.} = .57 \text{ km/sec}$

The one high speed camera shot (#990) for a .111 inch thick, cloth covered graphite/epoxy sample (JSC-02A-003), at a 30 deg. angle, indicated a maximum spall velocity of .75 km/sec.

#### **Shot #894**

See section 3.2.2 for more discussion of this shot.

4.94 mg nylon projectile, 4.75 km/sec velocity.

Target - .093 inch thick graphite/epoxy with no cloth covering (JSC-02B-003).

Photo shows ejecta (on the right) and spall (on the left) approx. 30 to 35 microseconds after impact.

No good scaling parameter is available in this shot. The thickness of the sample could be used, but appears to be uncertain due to angle and depth by a factor of 1.5 to 2. The extent of the ejecta and spall clouds are also off the photo, adding to the uncertainty in calculating fastest particle velocity. Nevertheless, using the same scale as the other two photos, the ejecta cloud is estimated to extend 16 threads or  $16 \times .1905 = 3.05 \text{ cm}$ .

$3.05 \text{ cm} / 32 \text{ microseconds} = .0305 \text{ m} / .000032 \text{ sec.} = .953 \text{ km/sec}$

This velocity does not agree well with high speed camera numbers of 2 to 5 km/sec, but the uncertainty in this measurement is high.

